I. A Total Synthesis of (−)-Virosaine A
and
II. A Direct Approach for the Synthesis of 1,3-Disubstituted Bicyclo[1.1.1]pentan-1-amines

BY

JONATHAN M. E. HUGHES

Department of Chemistry, McGill University

December 2017

A thesis submitted to McGill University in partial fulfillment of the requirements of the degree of Doctor of Philosophy

TABLE OF CONTENTS

ABSTRACT

Part I

The *Securinega* alkaloids are a fascinating class of bridged tetracyclic natural products that are produced exclusively by plants of the Phyllanthaceae family. These plants have a rich history in traditional folk medicine and the *Securinega* alkaloids themselves have been associated with a wide range of biological activities. Virosaine A, which was isolated in 2012 from the twigs and leaves of *Flueggea virosa* in China, is arguably the most structurally complex monomeric member of this alkaloid family. Specifically, it features an unprecedented caged pentacyclic skeleton that is comprised of a 7-oxa-1-azabicyclo[3.2.1]octane ring system, multiple bridged bicycles, and an isoxazolidine ring. The latter feature is a very rare structural motif in natural products and has been suggested to form *via* a biosynthetic [3+2] nitrone cycloaddition.

The intriguing structural features and unique biosynthetic origin of virosaine A inspired us to pursue its total synthesis and Part I of this thesis details our efforts in accomplishing this goal. A novel bio-inspired cascade reaction sequence, involving sequential epoxide opening/[3+2] nitrone cycloaddition, was programmed into the synthesis as a strategy to rapidly construct the complex virosaine core. A robust route was developed to prepare the pivotal cascade precursor in enantiopure form, beginning with an enantioselective Diels-Alder reaction between furan and 2-bromoacrolein. Subsequent implementation of the key cascade reaction sequence facilitated access to the core of virosaine A in a total of only 5 steps.

Several methods for C-H functionalization were applied to the virosaine core, including carbene and nitrene insertions as well as radical hydrogen atom abstractions. These studies led to the formation of a diverse set of novel complex polycycles and provided valuable information on the differences in reactivity between several positions. Finally, a combination of NMR and computational analyses laid the groundwork for a successful directed lithiation/bromination strategy to selectively functionalize the desired position on the caged core. This selective late-stage functionalization enabled the total synthesis of virosaine A in a total of 10 steps and 9% overall yield.

Part II

The bicyclo[1.1.1]pentane (BCP) motif is a unique bioisostere used in drug discovery for the replacement of phenyl rings, *tert*-butyl groups, and internal alkynes. Its incorporation into lead compounds has been shown to impart favorable physicochemical properties while also creating novel chemical space in the extremely competitive intellectual property landscape. Despite their utility, the synthesis of BCP-containing building blocks is, in many cases, quite challenging. This limits their potential use in drug discovery and highlights an important need to develop efficient methods for their preparation. While significant advances have recently been made in this area, there are currently no methods available to directly access 1,3-disubstituted bicyclo[1.1.1]pentan-1-amines.

A collaboration between our group and Inception Sciences prompted the development of a novel approach for the synthesis of 3-alkyl bicyclo[1.1.1]pentan-1-amines, which is detailed in Part II of this thesis. This goal was motivated by their specific need to prepare a 1,3-disubstituted BCP building block for the preparation of a lead oncology clinical candidate. An efficient difunctionalization of [1.1.1]propellane was developed to access 3-allyl-*N*,*N*-dibenzylbicyclo[1.1.1]pentan-1-amine *via* a one-pot amination/allylation protocol. This reaction represented the first example of a 3-alkyl bicyclo[1.1.1]pentan-1-amine substrate being prepared from [1.1.1]propellane in a single step and its utilization enabled an efficient synthesis of Inception Sciences' building block. Finally, the scope of this reaction was extended to include the use of several alkyl iodide electrophiles. This enabled the synthesis of a diverse set of 3-alkyl bicyclo[1.1.1]pentan-1-amines, which are expected to serve as valuable building blocks in future drug discovery efforts.

RÉSUMÉ

Première partie

Les alcaloïdes de type *Securinega* forment une classe fascinante de composés naturels tétracycliques pontés produits exclusivement par les plantes de la famille des Phyllantacées. Ces plantes font historiquement partie de la médecine traditionnelle populaire et les alcaloïdes Securigena ont eux-même été associés à un large éventail d'activités biologiques. La virosaïne A, isolée en 2012 en Chine à partir de branches ou de feuilles de Fluegga virosa, est sans doute l'un des composés monomériques de cette famille possédant la structure la plus complexe. Plus spécifiquement, elle présente un squelette pentacyclique en forme de cage comprenant un système annulaire de type oxa-1-azabicyclo[3.2.1]octane, de multiples bicycles pontés et un cycle de type isoxazolidine. Ce dernier motif structural est très rarement observé dans les composés naturels et il a été proposé que sa biosynthèse procède via une cyclo-addition de type nitrone [3+2].

Les caractéristiques intrigantes de la virosaïne A et sa biosynthèse exceptionnelle nous ont poussé à accomplir sa synthèse totale ; la première partie de cette thèse détaille nos efforts dans ce sens. Une nouvelle réaction en cascade bio-inspirée, impliquant une ouverture d'époxyde suivie d'une cyclo-addition de type nitrone [3+2], a été incluse dans la synthèse de manière à construire rapidement le noyau complexe de la virosaïne A. Dans le but de préparer le précurseur de la cascade cruciale dans sa forme énantiopure, une route robuste a été développée, commençant par une réaction de Diels-Alder énantiosélective entre le furane et la 2-bromoacroléine. L'étape cascade clé réalisée par la suite a permis l'accès au noyau de la virosaïne A en seulement 5 étapes.

Plusieurs méthodes de fonctionnalisation de liaisons C-H ont été appliquées au noyau, incluant des insertions de carbènes et nitrènes ainsi que des abstractions d'hydrogène radicalaires. Ces études ont permis la formation d'un ensemble varié de nouvelles molécules polycycliques complexes et ont fourni des informations précieuses sur les différences de réactivité entre les diverses positions. Enfin, la combinaison d'analyses RMN et computationelles a établi les fondations d'une stratégie de lithiation/bromation pour fonctionnaliser sélectivement les positions du noyau. Cette fonctionnalisation tardive a permis la synthèse totale de la virosaïne A en un total de 10 étapes et un rendement global de 9%.

Deuxième partie

Le motif bicyclo[1.1.1]pentane (BCP) est un bioisostère exceptionnel en recherche pharmaceutique où il peut remplacer des groupements phényles, *tert*-butyles ou des alcynes internes. Son incorporation dans des composés prometteurs a montré un impact favorable sur leurs propriétés physicochimiques tout en créant un nouvel espace dans un paysage extrêmement compétitif en propriété intellectuelle. Malgré leur utilité, la synthèse de blocs basiques comprenant un groupe BCP reste souvent délicate. Ceci limite leur usage potentiel en pharmaceutique et souligne le besoin de développer des méthodes efficaces pour les préparer. Bien que des progrès significatifs ont été faits dans ce domaine, aucune méthode n'est disponible actuellement pour accéder directement aux bicyclo[1.1.1]pentyl-1-amines 1,3-disubstituées.

La collaboration entre notre groupe et Inception Sciences a conduit au développement d'une nouvelle approche pour la synthèse de 3-alkyl-bicyclo[1.1.1]pentyl-1-amines, détaillée dans la deuxième partie de cette thèse. Cet objectif a été motivé par leur besoin de préparer un bloc de base présentant un groupement BCP 1,3-disubstitué pour la préparation d'un composé lead en oncologie clinique. Une di-fonctionnalisation efficace du [1.1.1]propellane a été développée afin d'accéder à la 3-allyl-N,N-dibenzylcyclo[1.1.1]pentyl-1-amine *via* un protocole d'amination/allylation tout en un. Cette réaction représente le tout premier exemple d'une 3-alkyl bicyclo[1 .1.1]pentyl-1-amine préparée à partir de propellane en une seule étape et son utilisation a permis la synthèse efficace du bloc de base demandé par Inception Sciences. Enfin, la portée de cette réaction a été étendue pour inclure l'usage de plusieurs iodures d'alkyle, ce qui a conduit à la synthèse d'un ensemble varié de 3-alkyl bicyclo[1.1.1]pentyl-1-amines, qui constitueront des blocs de base précieux en recherche pharmaceutique.

ACKNOWLEDGEMENTS

I would like to thank my supervisor, Dr. Jim Gleason, for giving me the opportunity to join his group and for providing an exceptional environment in which to learn and do research. His knowledge and passion for chemistry was an inspiration to me and I am proud to have had him as a mentor. I appreciated his constant guidance and support throughout the ups and downs of a challenging total synthesis project and I will leave his lab a better chemist than I ever thought I could be – for that I am very grateful.

There were many educators throughout my high school and post-secondary education that motivated me to pursue a career in science. First and foremost I need to thank Mr. Dev Prakhya for his ability to inspire and educate high school students and for teaching me the joys of chemistry very early on in my life. I also want to thank all of my undergraduate chemistry professors at the University of Regina for their superb teaching abilities and contagious passion for chemistry. I am grateful to have had Henry Yee as my first organic chemistry professor. He is both an outstanding educator and friend. I am very fortunate to have conducted undergraduate research under the mentorship of Dr. Andrew Wee, from whom I learned the skills and perseverance necessary to succeed in graduate school. I am also grateful to Dr. Krishna Annadi for all of his guidance during my time as an undergraduate researcher.

I would like to acknowledge Dr. Fred Morin and Dr. Robin Stein for their assistance in the McGill NMR facility as well as Dr. Nadim Saade and Dr. Alex Wahba for their tireless efforts in the McGill mass spectrometry facility. I am grateful to the administrative staff in the McGill Department of Chemistry, who always kept things running smoothly. In particular, I want to thank Sandra Aerssen and Jennifer Marleau for their help in administrative duties for the MCSILS. A special thanks goes to Chantal Marotte for always having an open door and for always ensuring that our deadlines are met and our paperwork is completed.

I am grateful to Dr. Jason Burch and Dr. Austin Chen (Inception Sciences) for recently providing an opportunity to work on a very interesting and rewarding project. It has been a pleasure collaborating with them. I am also grateful to NSERC, the Walter C.

Sumner Foundation, and the Department of Chemistry at McGill University for generous funding throughout the years.

Since joining the Gleason lab, I have had the opportunity to work alongside many people who were not only outstanding scientists but also great friends. I want to thank the newer members of the lab, Ryan Barrett, Josie Warnica, Ali Monsour, Donald Campbell, June Jun, David Scarlata, and Yufei Wang, as well as former post-doctoral researchers, Dr. Florent Larnaud and Dr. Nicolas De Rycke for everything they taught me and for all of the good times we shared. I am particularly grateful to Dr. Rodrigo Mendoza-Sanchez for being a great friend and mentor, from the first day that I joined the lab, as well as to Dr. Daniel Rivalti for his friendship, knowledge, and for being the hardest working chemist I have ever seen. Thank you to Marx Ruiz-Wilson, Chris Doyle, Shuo Xing, and Ben Williams for always keeping things entertaining with "questions of the day", to Nicklas Häggman for keeping the coffee schedule tight and continually pushing the limits of what a human can consume in one meal, to Sam (the King of peanuts and cheese) for always having a positive attitude in the lab, to Dr. Dainis Kaldre for demonstrating the importance of balancing lab work with good fitness – Latvian Horse never break, and to Adam Elmehriki for being a great friend and labmate, for always lending an ear when needed, and for proof-reading this thesis. Finally, it was a privilege to work alongside Anthony Palermo, who is not only a talented chemist but is also an incredible friend. He taught me much about chemistry, life, and goats, and I am certain he will continue to achieve great things.

I must acknowledge Dr. Fabien Hammerer for being a top-notch intramural hockey coach and friend as well as for translating my thesis abstract. Thank you to Tim Mack and Jack Cheong for being great friends and for helping to make my years in Montreal so enjoyable and thank you to the many people I have met in Montreal whom I have not specifically mentioned by name – I am lucky to have made so many new friends along the way. I am also grateful to my friends in Regina (the Dippers) for their continued support and friendship, you guys are the craziest and best group of friends I could ask for.

Thank you to my family, for always loving and supporting me throughout both my research career and my entire life. I am grateful for the important lessons they taught

me, such as to always work hard, to have integrity in everything I do, and to never give up. Their unending encouragement for me to pursue any ambition in life has always been so appreciated and I am lucky to have them.

Most importantly, I thank my wife, Lindsey. She gave up everything to come to Montreal and be with me and has always been the most supportive person during both the good times and the bad. She is always a continual source of inspiration, which has made me strive to be a better chemist and, more importantly, a better person. Her unconditional love and support as well as her unwavering encouragement to pursue my dreams have given me the strength and motivation that I consistently needed to push through. Lindsey, you must have studied that "Caring for a Loved One in Graduate School" pamphlet from cover to cover because you not only helped make this journey a successful one but you made it incredibly fun and unforgettable, as well. I will forever be grateful.

LIST OF FIGURES

LIST OF SCHEMES

LIST OF TABLES

LIST OF SPECTRA

LIST OF ABBREVIATIONS

Å	angstrom
Ac	acetyl
AD	asymmetric dihydroxylation
AIBN	2,2'-azobisisobutyronitrile
APCI	atomospheric pressure chemical-ionization
aq.	aqueous
Ar	argon/aryl
atm	atmosphere
BCP	bicyclo[1.1.1]pentane
Bn	benzyl
Boc	*tert*-butoxycarbonyl
Bu	butyl
Bn	benzyl
Bz	benzoyl
^{o}C	degrees Celcius
CDI	carbonyl diimidazole
CD_{50}	median convulsive dose
cm	centimeter
cm^{-1}	wavenumber
COSY	correlation spectroscopy
CSA	10-camphorsulfonic acid
δ	chemical shift/partial charge
d	deuterium
d	doublet
DBU	1,8-diazobicyclo[5.4.0]undec-7-ene
DCC	*N*,*N*'-dicyclohexylcarbodiimide
DCE	1,2-dichloroethane
decomp	decomposition
DIAD	diisopropyl azodicarboxylate

DIBAL	diisobutylaluminum hydride
DIPEA	*N,N*-diisopropylethylamine
DMAP	4-(dimethylamino)pyridine
DMF	*N,N*-dimethylformamide
DMP	Dess-Martin periodinane
DMSO	dimethylsulfoxide
Dppf	1-1'-bis(diphenylphosphino)ferrocene
d.r.	diastereomeric ratio
E^+	electrophile
EC_{50}	half maximum effective concentration
ee	enantiomeric excess
ent	enantiomer
equiv	equivalent
ESI	electrospray ionization
Et	ethyl
Et_3N	triethylamine
EtOAc	ethyl acetate
EtOH	ethanol
g	gram
[H]	reduction
h	hour
HMBC	heteronuclear multiple-bond correlation
HMPA	hexamethylphosphoramide
HOMO	highest occupied molecular orbital
HPLC	high-performance liquid chromatography
HRMS	high-resolution mass spectroscopy
HSQC	heteronuclear single quantum correlation
Hz	hertz
i	iso
imid.	imidazole
i-PrOH	*iso*-propanol

IC_{50}	half maximum inhibition concentration
IR	infrared
J	coupling constant
kcal	kilocalorie
KHMDS	potassium hexamethyldisilazide
K-Selectride	tri-sec-butylborohydride
L	litre/ligand
LD_{50}	median lethal dose
LDA	lithium diisopropylamide
LiDBB	di-*tert*-butylbiphenylide
m/z	mass to charge ratio
M	molar/metal
$[M]^+$	molecular ion
m	meta
m	multiplet
m-CPBA	*meta*-chloroperoxybenzoic acid
Me	methyl
MeOH	methanol
Mes	mesityl
mg	milligram
$M+H^+$	protonated parent mass
MeCN	acetonitrile
MHz	megahertz
min	minutes
mL	milliliter
MOM	methoxymethyl
µg	microgram
µL	microliter
µM	micromolar
mmol	millimole
mol	mole

$M+Na^+$	sodiated parent mass
Ms	methanesulfonyl
MS	mass spectrometry
mW	mega watt
MW	microwave
n	non-bonding electrons/number of groups
NBO	natural bond orbital
NBS	*n*-bromosuccinimide
nd	not determined
NaHMDS	sodium hexamethyldisilazide
nm	nanometer
nM	nanomolar
NMR	nuclear magnetic resonance
nOe	nuclear Overhauser effect
NOESY	nuclear Oherhauser effect spectroscopy
NPA	natural population analysis
[O]	oxidation
o	ortho
Oxone	$2KHSO_5 \bullet KHSO_4 \bullet K_2SO_4$
π	pi
p	para
p-TSA	*para*-toluenesulfonic acid
Pc	phthalocyanine
pH	hydrogen ion concentration
Ph	phenyl
PhMe	toluene
pin	pinacolato
PMB	*para*-methoxybenzyl
PMP	*para*-methoxyphenyl
PNB	*para*-nitrobenzyl
ppm	parts per million

PPTS	*para*-toluenesulfonic acid
Pr	propyl
pyr	pyridine
q	quartet
quant.	quantitative
R	generic group (typically carbon-based)
R	rectus
recryst.	recrystallization
R_f	retention factor
rt	room temperature
rsm	recovered starting material
σ*	antibonding sigma orbital
s	second/singlet
s	sec
S	sinister
S_N1	substitution nucleophilic unimolecular
S_N2	substitution nucleophilic bimolecular
‡	transition state
t	triplet
t	tert
TBAF	tetra-*n*-butylammonium fluoride
TBAI	tetra-*n*-butylammonium iodide
TBDPS	*tert*-butyldiphenylsilyl
TBS	*tert*-butyldimethylsilyl
Tf	trifluoromethansulfonyl
TFA	trifluoroacetic acid
THF	tetrahydrofuran
TIPS	triisopropylsilyl
TLC	thin layer chromatography
TMEDA	tetramethylethylenediamine
TMS	trimethylsilyl

Ts	*para*-toluenesulfonyl
W	watt
X	generic group (typically a heteroatom or halogen)

PART I

A Total Synthesis of (−)-Virosaine A

CHAPTER 1

The *Securinega* Alkaloids and Virosaine A

1.1 Introduction

1.1.1 The *Securinega* Alkaloids

The *Securinega* alkaloids are a fascinating class of natural products that have been known for over 60 years.[1] This class of secondary metabolites is produced exclusively in plants of the Phyllanthaceae family, specifically in the *Securinega*, *Phyllanthus*, *Breynia*, *Margaritaria*, and *Flueggea* genera. It is worth noting that Hoffmann et al. classified the Phyllanthaceae plant family as a segregate of the Euphorbiaceae family in 2006.[2] However, despite this, the *Securinega* alkaloids are often still assigned to the Euphorbiaceae family in the contemporary literature. Plants of the Phyllanthaceae family are mainly distributed in the tropical/subtropical regions of Asia, Africa, and the Americas and have a well-documented history in traditional medicine. For example, the species *Securinega suffruticosa* and *Flueggea virosa* have been used in Chinese folk medicine to treat ailments such as infantile paralysis, rheumatic disease, impotence, eczema, and allergic dermatitis, among others.[3] In traditional Senegalese medicine, a decoction of the roots of *Flueggea virosa* was applied for troubles involving the liver, gall bladder, kidneys, bladder, and genitals and, in India, seeds of the same plant were used to treat diabetes.[4] The species *Margaritaria discoidea* is well known for its use in traditional Guinean medicine for treating helminthiases, wounds, diarrhea, malaria and gastric disorders.[5] In addition, *Phyllanthus niruri* has been used medicinally to treat diabetes, kidney stones, eczema, and malaryia in India, China, and Africa.[6]

The intriguing biological activities of these plants have stimulated significant interest in the isolation of natural products from them and, to date, nearly 80 different *Securinega* alkaloids have been reported. In 1956, securinine (**1.1**) was isolated from the leaves of *Securinega suffruticosa* in Russia, as both the inaugural and most abundant member of this family (Figure 1.1).[7] Its structure was elucidated independently in 1962 by two separate groups and was later confirmed by X-ray crystallography.[8,9] Securinine (**1.1**) is comprised of a bridged tetracyclic scaffold containing an interesting α,β,γ,δ-unsaturated lactone, structural features that define this alkaloid class. The *Securinega* alkaloids are divided into four subgroups based on differences in their bridged core structures, although every member of this family maintains a characteristic butenolide D-ring. Securinine (**1.1**) belongs to the securinane group, which contains a piperidine A-ring

and an azabicyclo[3.2.1]octene ring system (B- and C-rings). The norsecurinane-type alkaloids differ only in their A-ring, which is composed of a 5-membered pyrrolidine, and is represented by norsecurinine (**1.2**). The numbering system for the securinane and norsecurinane skeletons is identical except that C6 is omitted in the latter. The neosecurinane- and neonorsecurinane *Securinega* alkaloids are typified by an azabicyclo[2.2.2]octane B/C-ring core, where the former group possesses a piperidine-derived A-ring and the latter contains a pyrrolidine-derived A-ring. Securinol A (**1.3**) and epibubbialine (**1.4**) are representative members of the neosecurinane and neonorsecurinane classes, respectively.

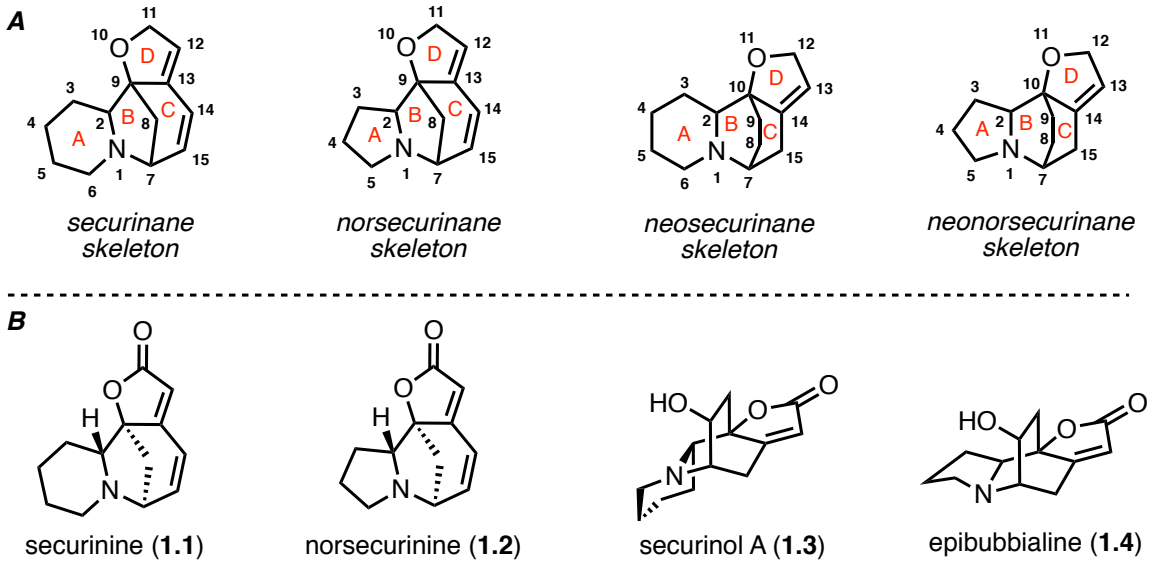

Figure 1.1. (A) The *Securinega* alkaloid skeletal classes and (B) representative natural products.

Besides the four main *Securinega* alkaloid subgroups, there is also an oligomeric group comprised of dimeric, trimeric, tetrameric, and even pentameric members.[10] Interestingly, all of these oligomeric alkaloids were isolated from a single plant species, namely *F. virosa*. The dimeric members are quite diverse in both their subunit composition and mode of connectivity (Figure 1.2). The norsecurinane skeleton is the most commonly occurring monomeric subunit and constitutes several homo- and heterodimers of this class, although the securinane and neosecurinane skeletal types are also found. To date, no *Securinega* alkaloid oligomer has been isolated that contains a

neonorsecurinane-type skeleton. Many of these dimeric alkaloids are forged *via* a single C-C bond linkage, which occurs between varying positions such as C14-C15' (flueggenine A (**1.5**) and C (**1.7**))[10a,d] and C12-C15' (flueggenine D (**1.8**) and flueggine B (**1.12**))[10b,d]. However, there are several dimers that contain two points of connectivity, such as flueggenine B (**1.6**),[10a] flueggine A (**1.11**),[10b] and flueggedine (**1.13**).[10e] There are also dimers that have been linked *via* a heteroatom, such as flueggether A (**1.9**) and norsecurinamine B (**1.10**), which are connected by an ether and amine tether, respectively.[10g,i] Interestingly, **1.10** is the only known *NH*-linked *Securinega* alkaloid dimer. Finally, while almost every dimeric *Securinega* alkaloid is comprised of two subunits belonging to the four main skeletal types found in Figure 1.1, flueggine A (**1.11**) represents a rare example where one of its subunits (right-hand side) does not. This intriguing discrepancy will be discussed further in Section 1.2.

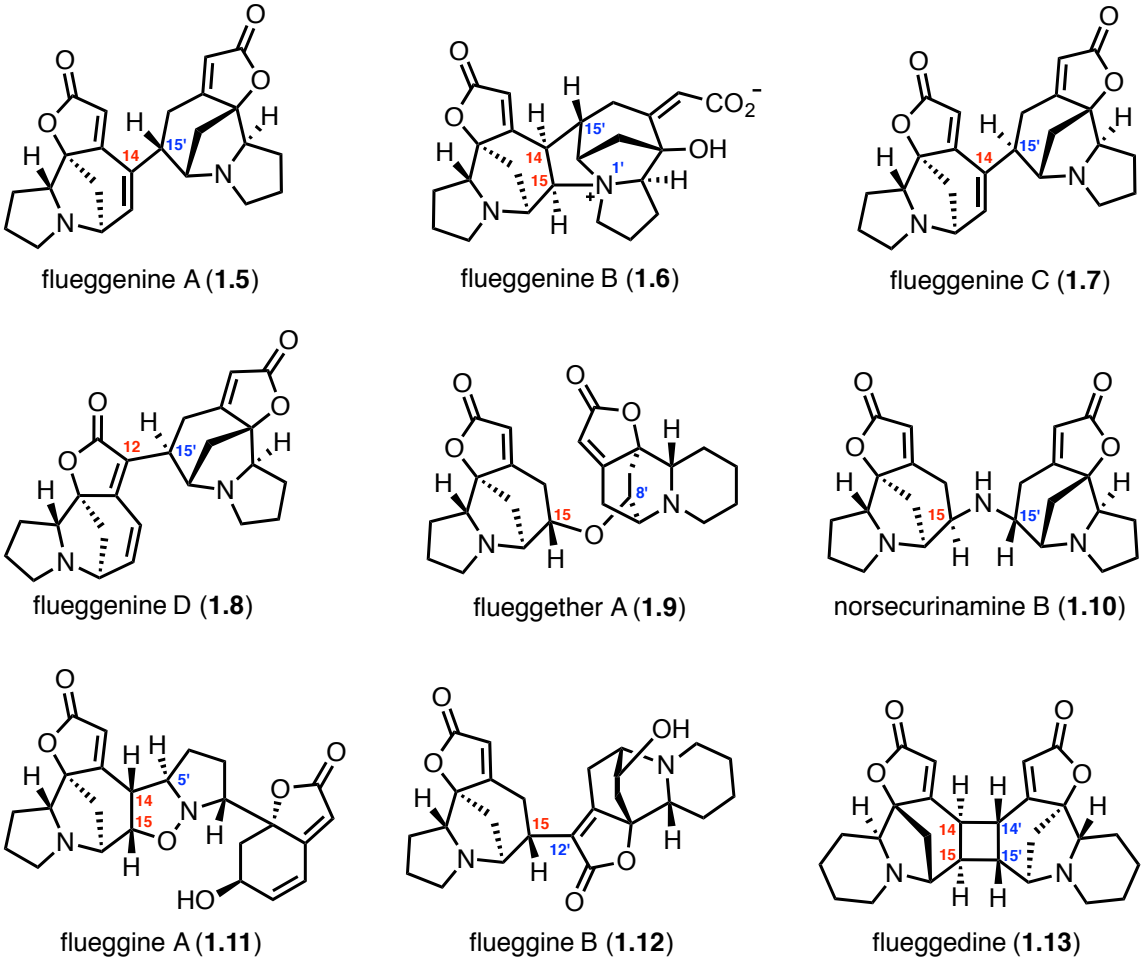

Figure 1.2. Examples of dimeric *Securinega* alkaloids.

Similar to their dimeric counterparts, the tri-, tetra-, and pentameric *Securinega* alkaloids are mainly comprised of linked norsecurinane-type monomers (Scheme 1.3). However, there are several oligomeric members that possess other structural subunits, as well. For example, fluevirosine B (**1.15**) contains one securinane- and two norsecurinane-

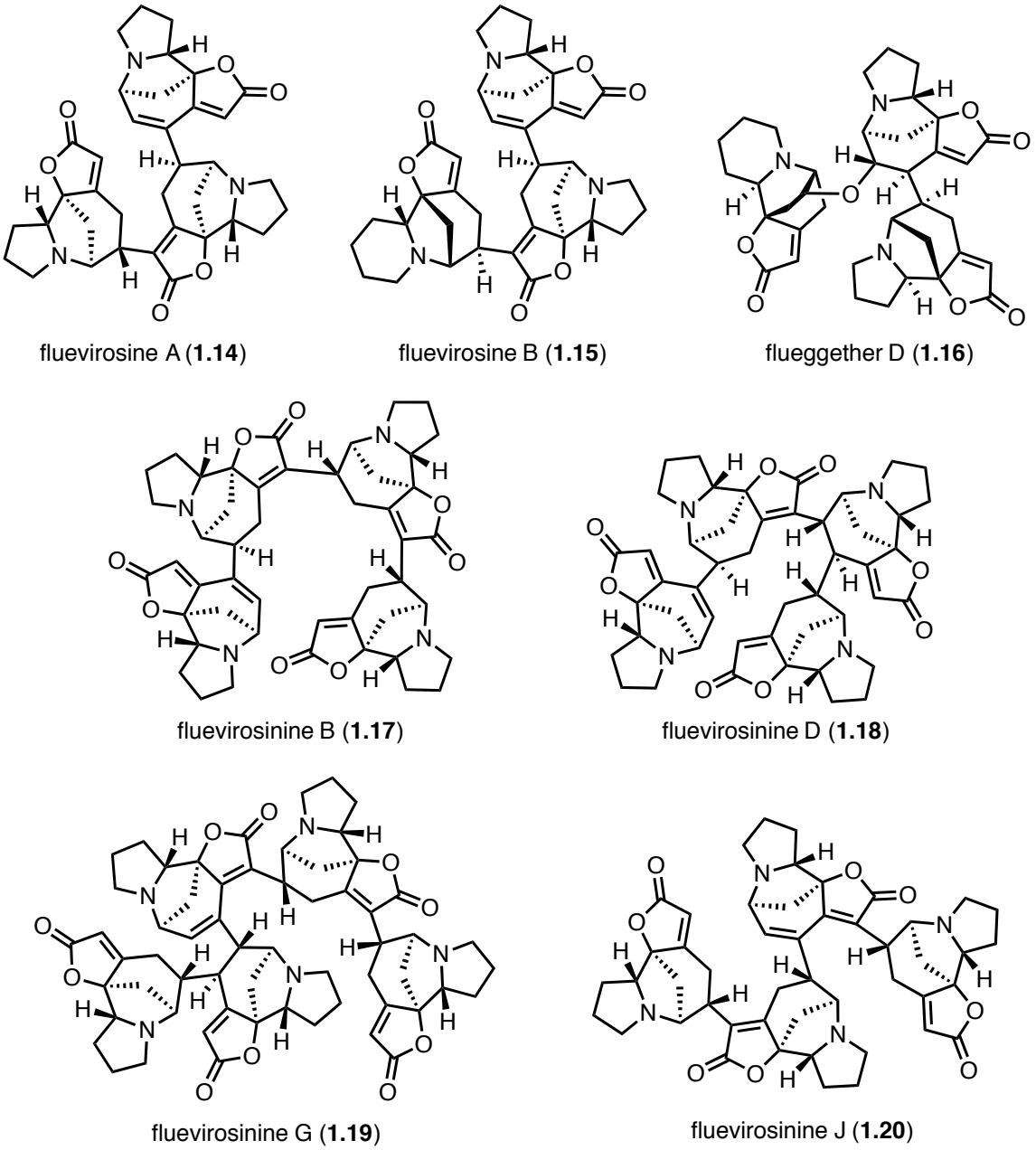

Figure 1.3. Examples of tri-, tetra-, and pentameric *Securinega* alkaloids.

type subunits, while flueggether D (**1.16**) is comprised of one neosecurinane- and two norsecurinane-type subunits.[10c,h] Given the vast set of possible connectivity permutations

in these oligomers, there is a significant amount of structural diversity found among them. Accordingly, it seems very likely that new *Securinega* alkaloid oligomers will continue to be isolated with unprecedented levels of structural complexity.

In addition to the four main structural subgroups, and the oligomers from which they are derived, several *Securinega* alkaloids have been identified that contain unprecedented structures due to additional skeletal oxidation and/or rearrangement and therefore do not fit into these main categories. Phyllantidine (**1.21**), which was initially isolated from the rootbarks of *Phyllanthus discoides* in Congo, contains an expanded securinane-type B-ring (Figure 1.4).[11] Structural elucidation helped identify the presence of an additional oxygen atom situated between N1 and C7 resulting in a tetrahydro-1,2-oxazine ring and an oxazabicyclo[3.3.1]nonene B/C-ring core. Investigation of the chemical constituents isolated from the twigs and leaves of a Japanese *Securinega suffruticosa* var *amamiensis* species led to the isolation of the novel alkaloid secu'amamine A (**1.22**).[12] This secondary metabolite contains an extended B-ring with an additional hydroxylated-carbon situated between C2 and C9 and makes it the only *Securinega* alkaloid with an azabicyclo[3.3.1]nonene B/C-ring core. In 1986, Cordell et al. isolated nirurine (**1.23**) from *Phyllanthus niruri* and confirmed its structure using X-ray crystallographic analysis. Interestingly, **1.23** was found to contain a novel pentacyclic scaffold due to the presence of an oxazolidine ring forged by a C5-O-C8 bridge on a neonorsecurinine scaffold.[13]

1.1.2 Virosaine A and B

Virosaine A (**1.24**) and virosaine B (**1.25**) were recently isolated from the twigs and leaves of *Flueggea virosa* in China and are arguably the most complex monomeric *Securinega* alkaloids identified to date.[14] They each feature an unprecedented caged pentacyclic skeleton that is comprised of a 7-oxa-1-azabicyclo[3.2.1]octane ring system, multiple bridged bicycles, and an isoxazolidine ring. The latter is particularly noteworthy, as it is an extremely rare structural motif in natural products and has intriguing biosynthetic origins that will be discussed in Section 1.2.[15] Another fascinating feature of the virosaines is that they are pseudoenantiomers. More specifically, each of the six stereocenters present in **1.24** is inverted in **1.25** with the exception of that at C8, which

has an *R*-configuration in both alkaloids. The remarkable structures of **1.24** and **1.25** make them almost unrecognizable as *Securinega* alkaloids. However, they maintain several characteristic features of this class, such as the presence of both a butenolide and a pyrrolidine ring.

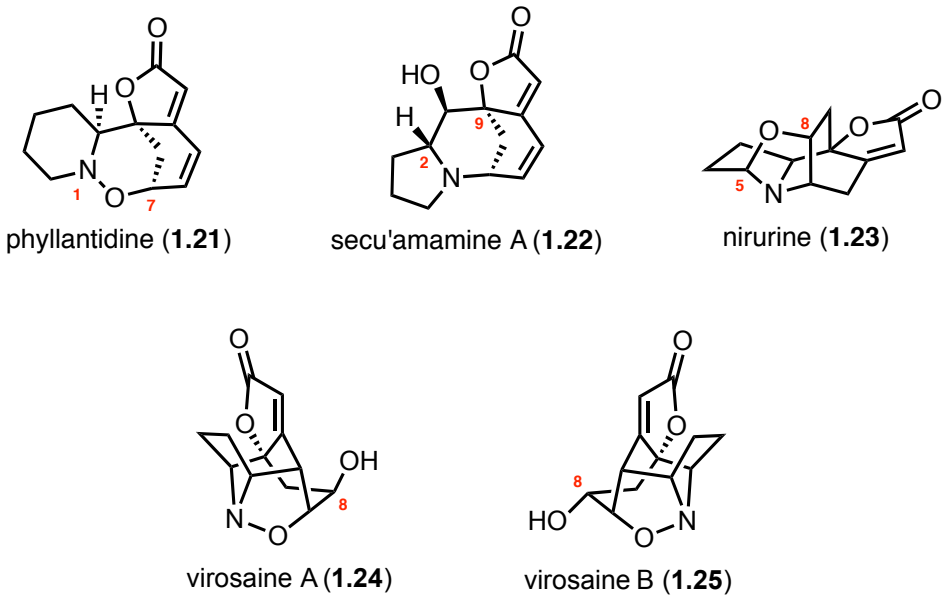

Figure 1.4. Examples of *Securinega* alkaloids with unique skeletal cores.

The apparent breadth of structural complexity found among the *Securinega* alkaloids has captivated chemists since securinine (**1.1**) was first isolated in 1956. Following a period of latency between the 1970s and late 1990s, there has been a resurgence of interest in this natural product class by both isolation and synthetic chemists. As a result, a large majority of the known *Securinega* alkaloids were isolated within the last two decades alone. Moreover, countless synthetic efforts and total syntheses have been published within the same timeframe.

1.2 Biosynthetic Origins of the *Securinega* Alkaloids

The unique composition of the *Securinega* alkaloid tetracyclic cores made comparison of their biosynthetic pathways to other known alkaloid classes impossible. Given its high natural abundance, securinine (**1.1**) was the focus of the first studies dedicated to delineating the biosynthetic origins of the *Securinega* alkaloid core. The methodology used for this purpose mainly involved feeding experiments, where

radiolabelled precursors were administered to *Securinega suffruticosa* by the cotton wick method. After a cultivation period, the leaves of the plant were harvested and the alkaloid extracts purified. Finally, quantification of radiolabelled atom incorporation was achieved *via* degradation studies. Prior work on the biosynthesis of piperidine alkaloids suggested that the piperidine A-ring of **1.1** was derived from L-lysine (**1.26**) *via* cadaverine (**1.27**) and Δ^1-piperideine (**1.28**) (Scheme 1.1).[16] This hypothesis was corroborated by preliminary work done by Parry and Yamasaki, where both radiolabelled ^{14}C-lysine and

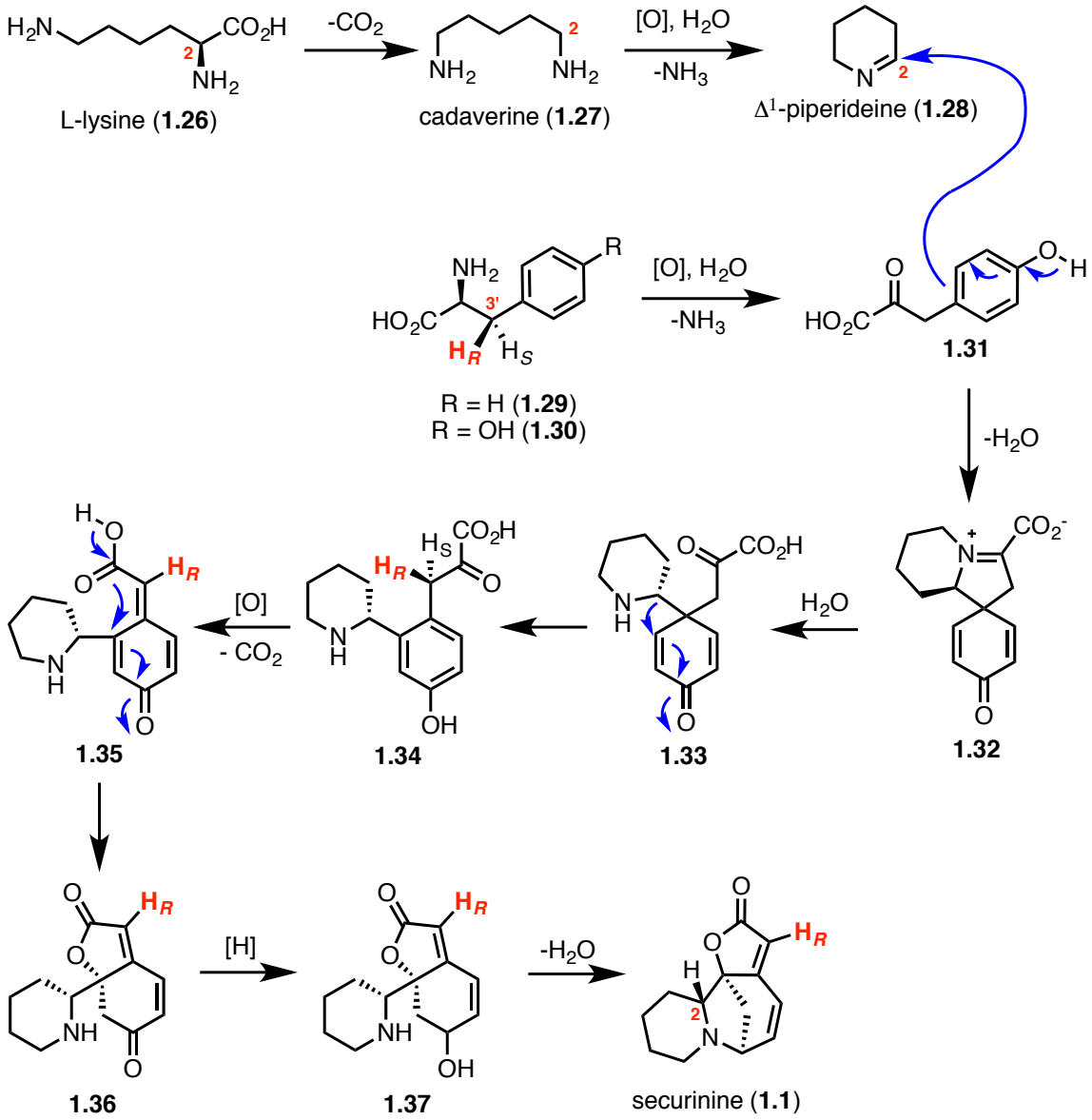

Scheme 1.1. Originally proposed biosynthesis of securinine (**1.1**).

(1,5-^{14}C)-cadaverine were incorporated into **1.1**.[17,18] Moreover, Spenser and co-workers identified the mode of lysine incorporation to be unsymmetrical in nature, where administration of either (2-^{14}C)-lysine or (2-^{14}C)-Δ^1-piperideine resulted in exclusive labeling at the C2 position of securinine (**1.1**).[19] This unsymmetrical mode of lysine incorporation is also observed in the biosyntheses of other piperidine alkaloids, such as anabasine, sedamine, and *N*-methylpelletierine, and suggests the intermediacy of an unsymmetrical cadaverine-pyridoxal phosphate adduct *en route* to **1.28**.[20] The origin of the remaining eight carbon atoms in **1.1** (C/D rings) was more of a mystery than that of the piperidine A-ring and Parry proposed that this portion might be derived from an aromatic amino acid, such as phenylalanine (**1.29**) or tyrosine (**1.30**). However, feeding experiments revealed that only radiolabelled tyrosine (**1.30**) was incorporated into securinine (**1.1**), while phenylalanine (**1.29**) was not.[17] Furthermore, the C1-carboxyl group of tyrosine (**1.30**) is lost during its incorporation. Yamasaki observed similar results, providing further evidence to support the tyrosine-based origin of the securinine C/D ring system.[18]

While the specific details involved in the coupling of lysine (**1.26**) and tyrosine (**1.30**) are not fully understood, a plausible biosynthetic pathway was put forth on the basis of the combined efforts of Parry, Yamasaki, and Spenser and is presented in Scheme 1.1.[17-21] Amino acids **1.26** and **1.30** produce Δ^1-piperideine (**1.28**) and aryl pyruvic acid **1.31**, respectively. Electrophilic aromatic addition of **1.31** onto cyclic imine **1.28** and iminium ion formation might produce spirocycle **1.32**.[22] Hydrolysis of **1.32** followed by a 1,2-alkyl migration/aromatization of intermediate **1.33** would then provide **1.34**. Two oxidative events and a decarboxylation on **1.34** would produce *para*-quinone methide **1.35**, which was proposed to undergo subsequent cyclization to yield tricycle **1.36**. Finally, C7-ketone reduction of **1.36** and subsequent annulation of **1.37** would produce securinine (**1.1**). Parry also established that the pro-*R* hydrogen atom at C3' in tyrosine (**1.30**) is exclusively retained in **1.1**, which indicated stereospecific removal of the pro-*S* hydrogen during phenol oxidation to produce **1.35**.[23]

Interestingly, bicyclic lactones menisdaurilide (**1.38**) and aquilegiolide (**1.39**) have also been isolated from plants of the *Securinega* and *Phyllanthus* genera (Scheme 1.2).[24] Given their notable resemblance to the C/D ring system of the *Securinega*

alkaloids, it is conceivable that they might serve as biosynthetic building blocks for this alkaloid family by reaction with Δ^1-piperideine (**1.28**) to produce **1.37** directly. However, there are currently no experimental studies that definitively support this hypothesis.

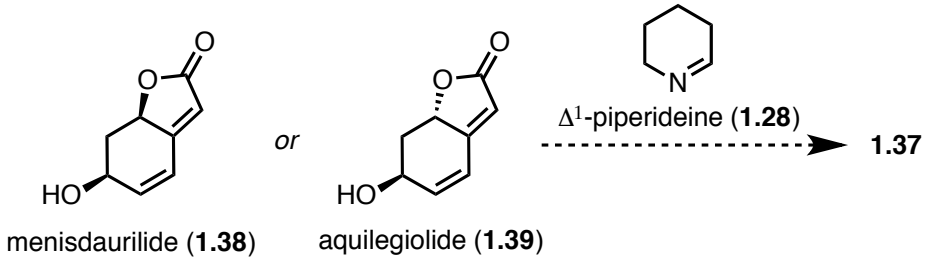

Scheme 1.2. Plausible alternative biosynthesis of **1.37** from menisdaurilide (**1.38**) or aquilegiolide (**1.39**).

The biosynthesis of norsecurinane-type *Securinega* alkaloids, such as norsecurinine (**1.2**), has not been studied in detail but likely mirrors that of securinine (**1.1**) (Scheme 1.3). The only necessary difference in the formation of the norsecurinane-type alkaloids is the origin of the pyrrolidine A-ring, which likely arises from L-ornithine (**1.40**) *via* Δ^1-pyrroline (**1.41**). Previous work on the biosynthesis of other pyrrolidine alkaloids supports this hypothesis.[25]

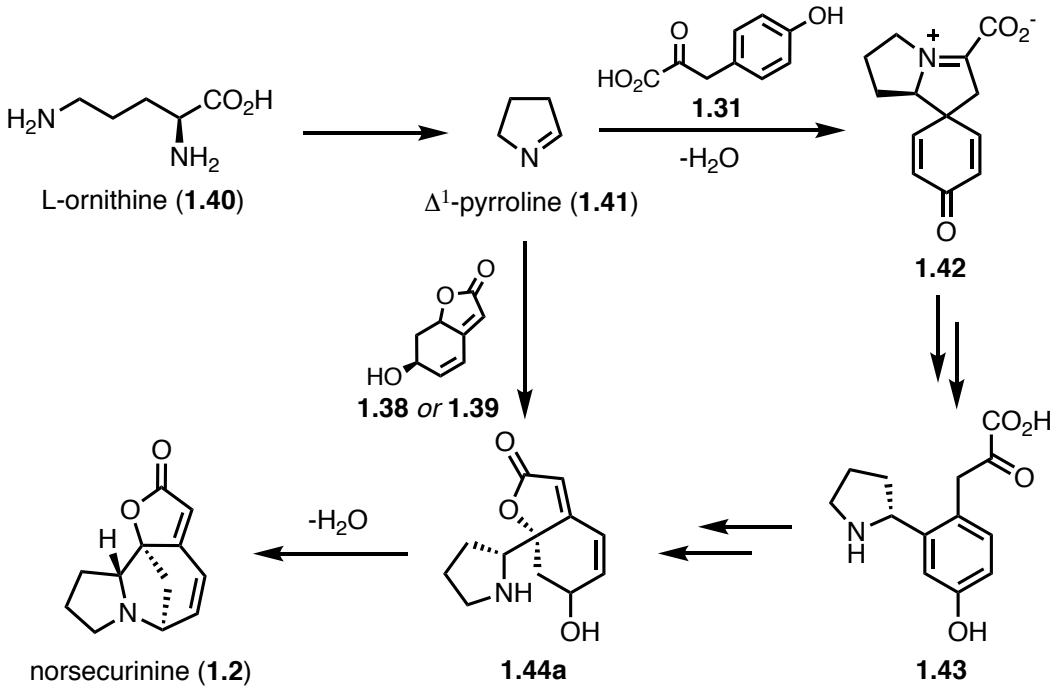

Scheme 1.3. Plausible biosynthesis of norsecurinine (**1.2**).

Neosecurinane and neonorsecurinane *Securinega* alkaloids are suggested to be biosynthesized *via* an intramolecular conjugate 1,6-addition of intermediate **1.45** to forge the azabicyclo[2.2.2]octane B/C ring system (Scheme 1.4). Interestingly, it has been proposed that these neo(nor)securinane-type alkaloids may in fact be biosynthetic intermediates *en route* to their (nor)securinane relatives *via* dehydrative skeletal rearrangement. This linear biosynthetic relationship contradicts the alternative, divergent biosynthetic pathway, which involves dehydration of **1.45** to access the azabicyclo[3.2.1]octene core of the (nor)securinane-type alkaloids (*vide supra*). Magnus and coworkers first suggested this linear biosynthetic hypothesis in 1993 when they successfully converted (±)-niruroidine (**1.46**) to (±)-norsecurinane (**1.2**) upon activation

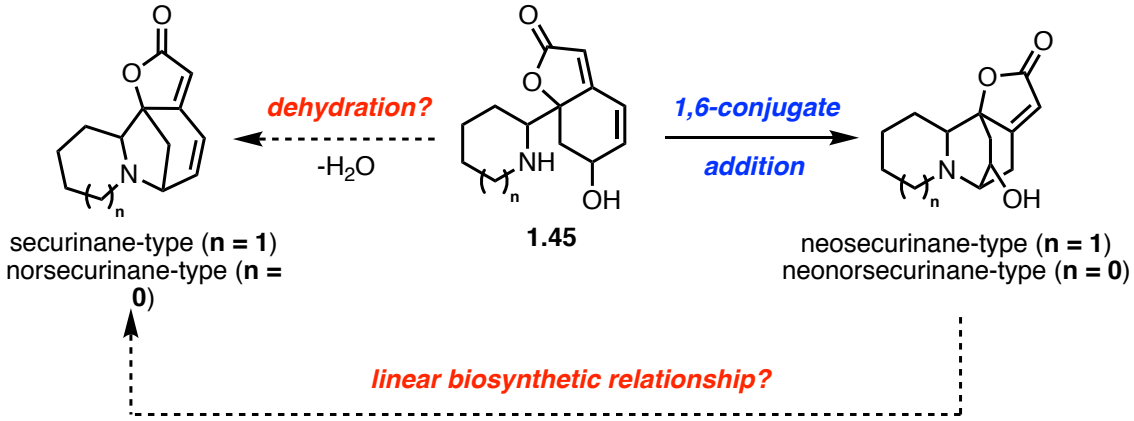

Scheme 1.4. Proposed linear biosynthetic relationship between neo(nor)securinane- and (nor)securinane-type *Securinega* alkaloids.

with methanesulfonyl chloride (Scheme 1.5).[26] Ye and Jang et al. corroborated this result in 2014 by converting (−)-**1.46** to (−)-**1.2** upon treatment with Ph_3P and DIAD.[27] They went on to propose a mechanism for the rearrangement, which involved formation of aziridinium intermediate **1.48** followed by β-elimination. Additional evidence to support this biosynthetic hypothesis was recently reported by Gademann and coworkers, where they successfully converted bubbialidine (**1.49**) and secu'amamine E (**1.50**) to their rearranged counterparts, (−)-allonorsecurinine (**1.51**) and allosecurinine (**1.52**), respectively.[28] Interestingly, when they attempted to induce the same reaction of bubbialine (**1.53**), only mesylate **1.54** was isolated. Furthermore, rearrangement of **1.54** to (+)-allonorsecurinine (**1.55**) only occurred under forcing conditions (100 ^{o}C,

microwave) and in very low yield (21%). This observation was attributed to the synperiplanar arrangement of the amine and mesylate moieties in **1.54**, which prevents an intramolecular S_N2-type displacement to generate an aziridinium intermediate, similar to **1.48**. An alternative S_N1 mechanism, with a higher activation barrier, might have therefore been operative in this case and thus might explain the need for such forcing conditions. Based on the collective results of these studies, a linear biosynthetic relationship between neo(nor)securinane-type and (nor)securinane-type *Securinega* alkaloids seems highly feasible.

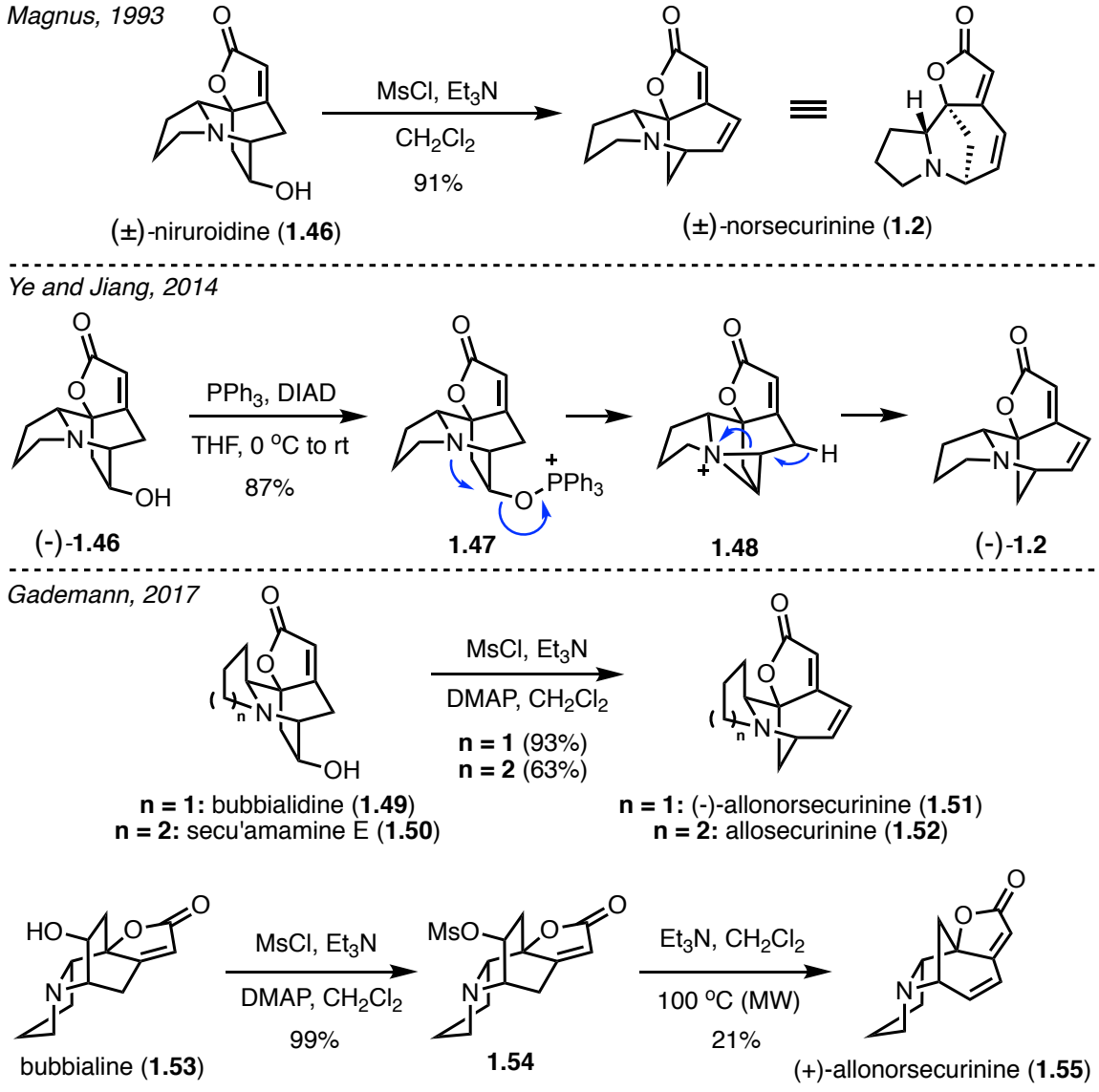

Scheme 1.5. Dehydrative rearrangements of neo(nor)securinane-type *Securinega* alkaloids to their (nor)securinane-type counterparts.

A fascinating feature of the *Securinega* alkaloid family is that, in many cases, every possible stereoisomer of the monomeric members has been isolated as distinct natural products. For example, the three stereoisomers of securinine (**1.1**) have all been isolated from natural sources and were named virosecurinine (**1.56**), allosecurinine (**1.52**), and viroallosecurinine (**1.57**) (Figure 1.5). This feature is quite unique since the majority of chiral natural products are produced in optically pure form and as a single enantiomer by the producing organism.[29] In fact, enantiomeric natural products are estimated to represent less than 1% of the entire biosphere's metabolome. The biosynthetic implications of these rare occurrences are of great interest to chemists and biologists alike and, while a significant amount of research has been done to understand them, many puzzles remain unsolved. Enantiomeric natural products are commonly produced by different genera or species, where one organism produces one isomer while another organism produces its antipode and this is typically the case among the *Securinega* alkaloids.[1,29] However, there are instances where a single organism produces both enantiomers, either as a racemic or scalemic mixture. Yue et al. recently disclosed a remarkable example of this, where they isolated all eight stereoisomers of securinol A (**1.3**) from *Flueggea virosa*.[30] Several different mechanisms by which biosynthetic stereodivergence can occur have been identified. For example, a simple precursor might give rise to two separate enantiomeric forms (or a mixture of enantiomers) in the initial step of a biosynthetic pathway, depending on the specific enzyme involved. Alternatively, the stereodivergent step may occur further downstream the biosynthetic pathway. In the biosynthesis of securinine (**1.1**) and its three stereoisomers, two stereodivergent steps dictate which metabolite is produced in the pathway depicted in Scheme 1.1: (1) enantioselective addition of **1.31** onto **1.28** to set the stereochemistry at C2 and (2) diastereoselective intramolecular cyclization of **1.35** (or *ent*-**1.35**) to set the C9 stereochemistry. Alternatively, if menisdaurilide (**1.38**) and/or aquilegiolide (**1.39**) serve as biosynthetic precursors to **1.1** (Scheme 1.2), a single stereodetermining event would simultaneously set both the C2 and C9 stereochemistry.

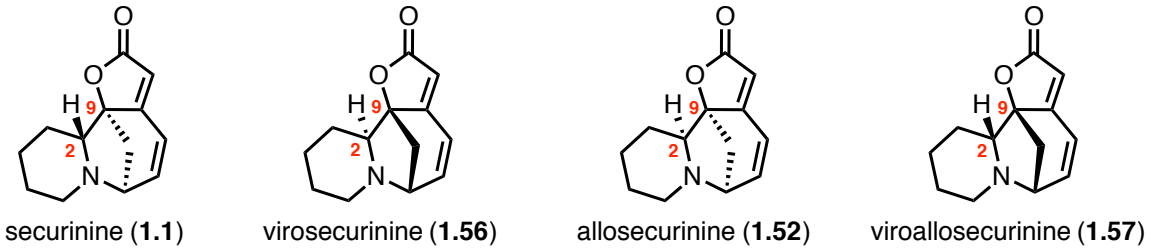

Figure 1.5. Naturally-occurring stereoisomers of securinine (**1.1**).

Since the *Securinega* alkaloids displayed in Figure 1.4 (*vide supra*) do not fit into any of the four characteristic structural classes of this family, their unique biosynthetic origins warrant discussion. The complete biosynthetic pathway to phyllantidine (**1.21**) has not been reported. However, experimental evidence suggests that allosecurinine (**1.52**) might serve as its natural precursor (Scheme 1.6). Nakano et al. demonstrated that treating virosecurinine (**1.56**) with monoperphthalic acid led to the formation of *O*-alkylhydroxylamines **1.58** and **1.59** in a 5.5:1 ratio.[31] Notably, **1.59** represents a stereoisomer of phyllantidine (**1.21**) that has not (yet) been isolated from a natural source.

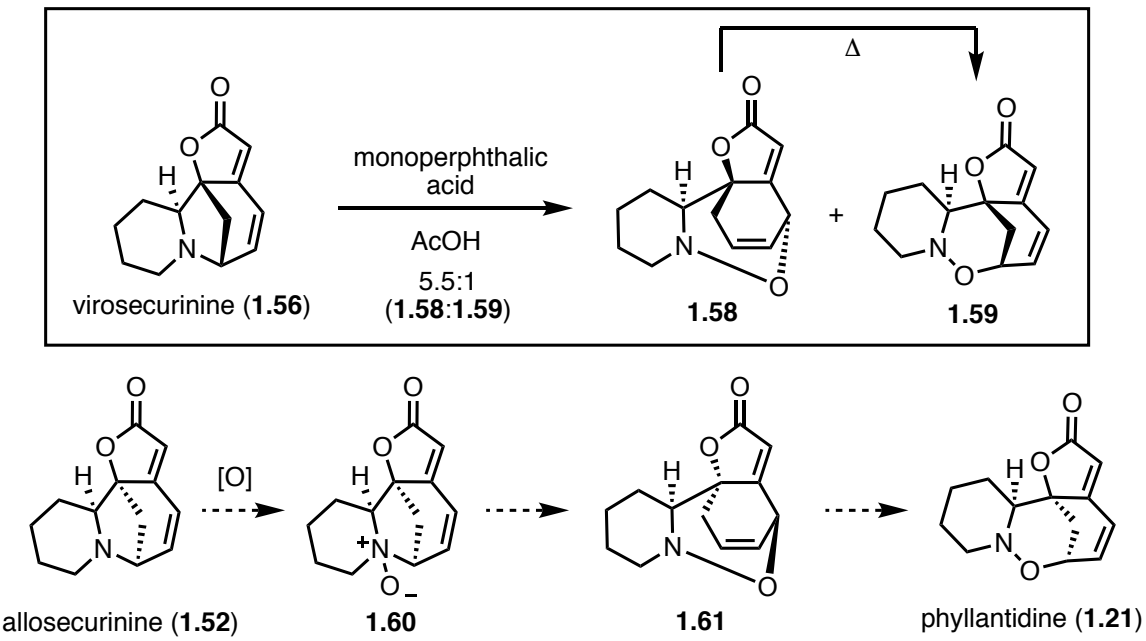

Scheme 1.6. Experimental evidence to support a plausible biosynthesis of phyllantidine (**1.21**).

Heating **1.58** resulted in rearrangement to **1.59**, while the reverse reaction was found not occur. Thus, it appeared that the phyllantidine-like structure **1.59** was the thermodynamically more stable species. Based on these experimental results, a plausible hypothesis for the biosynthesis of phyllantidine (**1.21**) can be proposed. Oxidation of allosecurinine (**1.52**) to the corresponding *N*-oxide **1.60** might be followed by a [2,3]-Meisenheimer rearrangement to provide **1.61**.[32] Stepwise rearrangement of **1.61** might then occur to produce the natural product **1.21**.

Secu'amamine A (**1.22**) is unique due to its unprecedented hydroxylated B-ring and azabicyclo[3.3.1]nonene B/C-ring system. Magnus et al. proposed that **1.22** is also biosynthetically derived from allosecurinine (**1.52**), according to the pathway depicted in Scheme 1.7.[33] They suggested that a C3-hydroxylated derivative of allosecurinine might serve as a precursor to an aziridinium intermediate **1.63** *via* intramolecular S_N2 displacement. Moreover, hydrative aziridinium opening at C2 would generate secu'amamine A (**1.22**). They were able to support this hypothesis experimentally using indolizidine model substrate **1.64**. Specifically, when **1.64** was allowed to react with NaOAc in refluxing AcOH, rearranged product **1.65** could be detected alongside transesterification product **1.66**. The deuterium migration that occurs during the conversion of **1.64** to **1.65** is fully consistent with the intermediacy of an aziridinium ion.

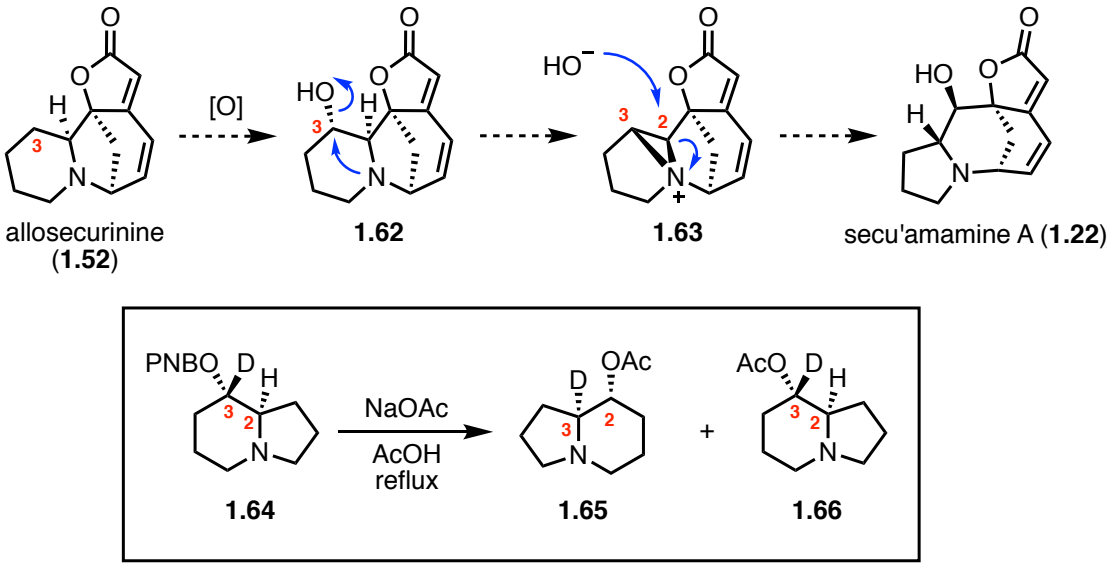

Scheme 1.7. Proposed biosynthesis of secu'amamine A (**1.22**).

Furthermore, the presence of **1.66** in the reaction mixture suggests that aziridinium opening at C3 may be a competing pathway. While these experiments provide compelling evidence to support this biosynthetic proposal, it is worth mentioning that a C3-hydroxylated *Securinega* alkaloid, such as **1.62**, has yet to be isolated from a natural source. Thus, the identification of a naturally occurring C3-hydroxylated securinane-type alkaloid would offer additional evidence to support this proposal.

Nirurine (**1.23**), which is the only *Securinega* alkaloid to possess an oxazolidine ring, bears a striking structural resemblance to epibubbialine (**1.4**). Given that both **1.23** and **1.4** are produced by *Phyllanthus niruri*, it is feasible that the latter serves as a biosynthetic precursor to the former.[13] Specifically, C5 oxidation of **1.4** might occur to produce iminium **1.67**, which can undergo intramolecular cyclization to give **1.23** (Scheme 1.8). Magnus and coworkers attempted to mimic this putative biosynthetic oxidation in their synthesis of **1.23** but found that it was not as straightforward as one might expect.[26,34] While most oxidants failed to produce any detectable amounts of **1.23**, treatment of **1.4** with *m*-CPBA resulted in the formation of minor amounts of **1.23** (*ca.* 10%). Thus, while this proposal appears feasible, its credibility would benefit from additional studies.

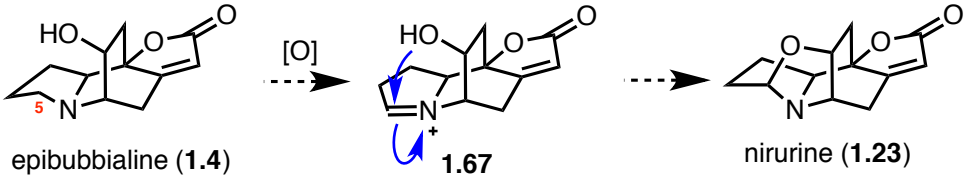

Scheme 1.8. Proposed biosynthetic oxidation of epibubbialine (**1.4**) into nirurine (**1.23**).

As stated in Section 1.1.1, virosaine A (**1.24**) and B (**1.25**) possess several intriguing structural features that set them apart from other monomeric *Securinega* alkaloids. These differences are believed to be the outcome of a unique biosynthetic pathway, which is proposed to originate from tyrosine (**1.30**) and ornithine (**1.40**) (Scheme 1.9). In their isolation report, Zhao et al. suggested that amino acids **1.30** and **1.40** combine to form amino alcohols **1.68** and **1.69**, according to the accepted biosynthetic pathway for the (neo)norsecurinane-type alkaloids (*vide supra*).[14] However, in contrast to the (neo)norsecurinane pathway, they suggested that amines **1.68** and **1.69**

undergo oxidation to nitrones **1.70** and **1.71**, respectively. These nitrones are then proposed to undergo subsequent intramolecular [3+2] cycloaddition (1,3-dipolar cycloaddition) to produce virosaine A (**1.24**) and B (**1.25**). Biosynthetic [3+2] nitrone cycloadditions are exceedingly rare but evidence to support their feasibility has mounted in recent years *via* both computational studies and biomimetic syntheses.[35,36,37] Of note, Tantillo and coworkers reported density functional theory (DFT) calculations which suggest that the energy barriers required for the putative cycloadditions of nitrones **1.70** and **1.71** are low enough such that enzymatic intervention is not required.[35b] Interestingly, Leys et al. also recently reported the first example of an enzyme shown to catalyze a 1,3-dipolar cycloaddition.[38,39]

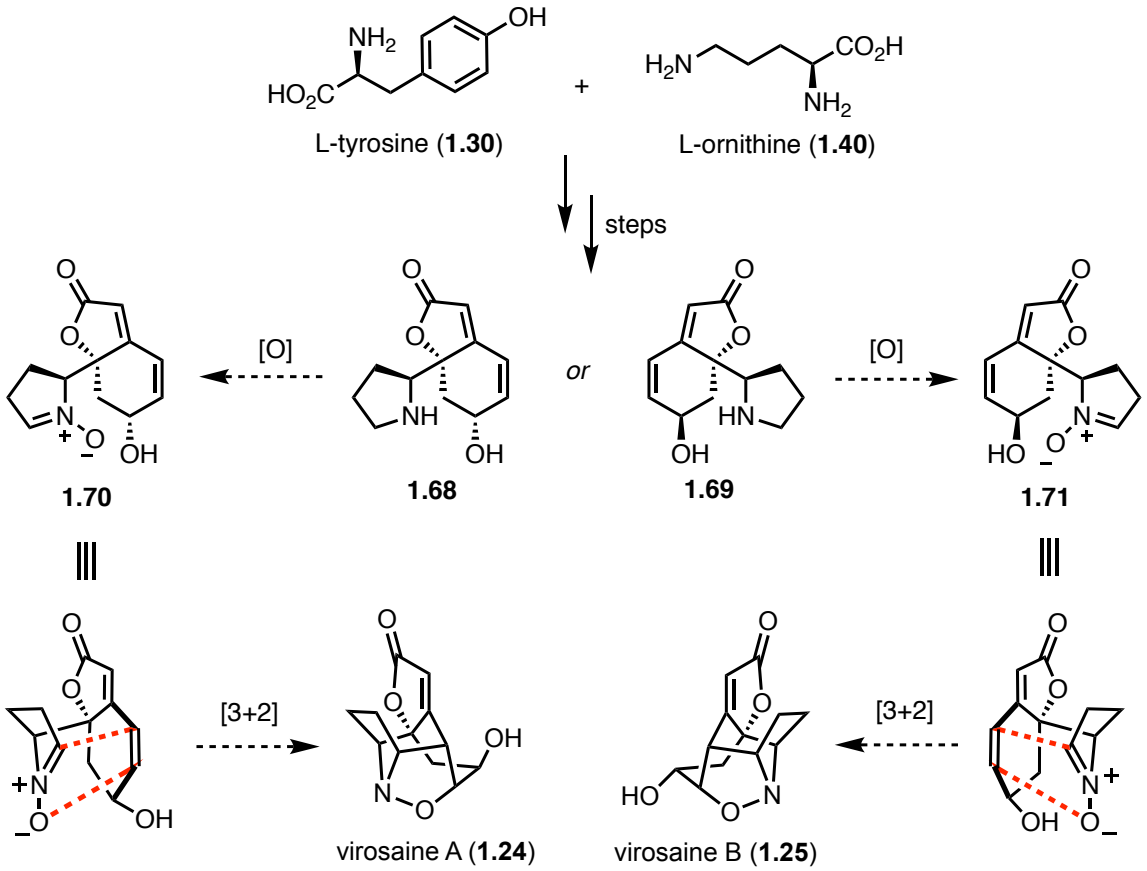

Scheme 1.9. Zhao et al.'s proposed biosynthesis of virosaine A (**1.24**) and B (**1.25**).

While the original biosynthetic proposal put forth by Zhao et al. for virosaine A (**1.24**) and B (**1.25**) is feasible, synthetic studies suggest that their biosynthesis may involve the intermediacy of other *Securinega* alkaloids. Specifically, Gademann

demonstrated that virosaine A (**1.24**) could be accessed from the bubbialidine core and Yang and Li showed that virosaine B (**1.25**) could be accessed from (+)-allonorsecurinine (**1.55**) in a similar fashion.[36a,b] While these synthetic studies will be discussed in greater detail in Section 1.4, their potential biosynthetic implications are shown in Scheme 1.10.

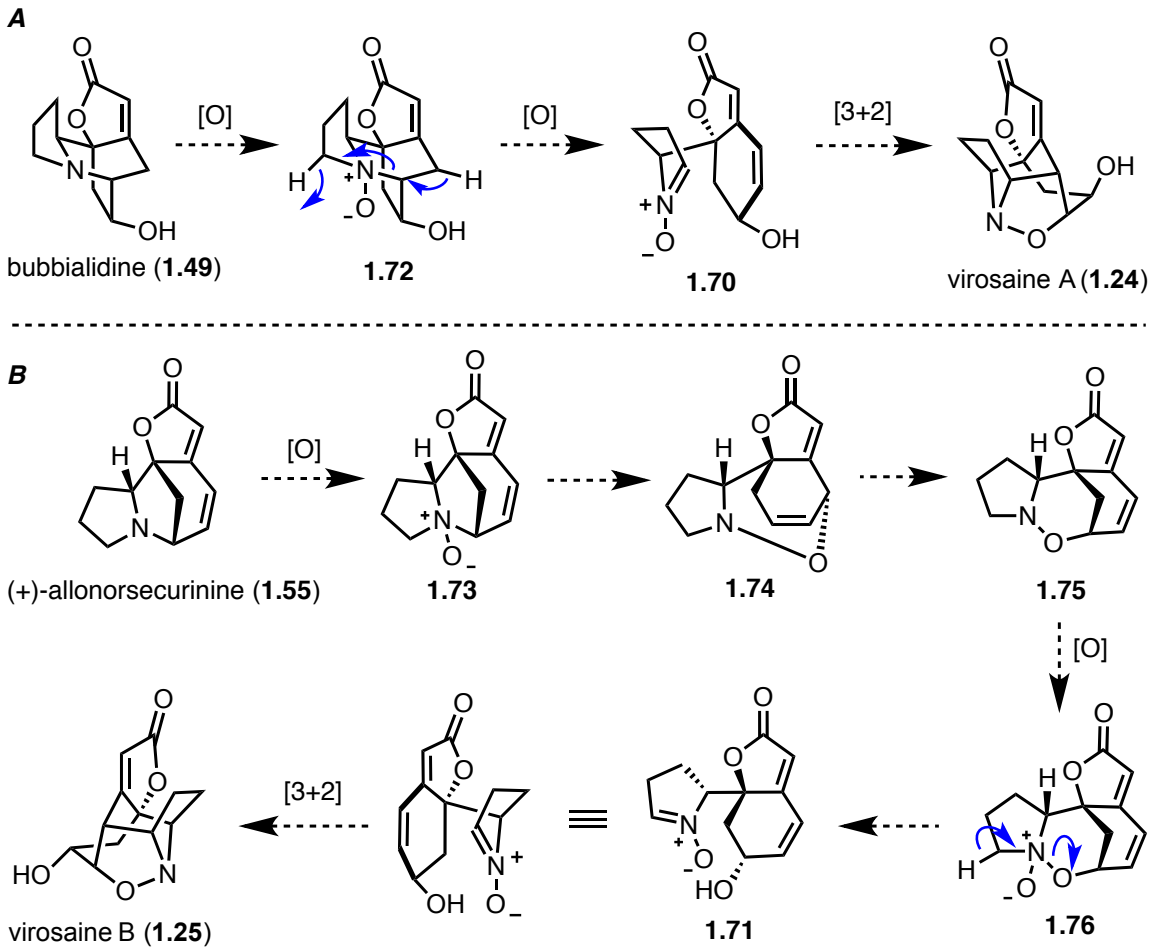

Scheme 1.10. Plausible biosynthetic relationship between: (A) bubbialidine and virosaine A and (B) (+)-allonorsecurinine and virosaine B.

In the case of virosaine A (**1.24**), bubbialidine (**1.49**) might initially be oxidized to *N*-oxide **1.72**. Subsequent elimination/oxidation of **1.72** might then occur to produce nitrone **1.70**, the immediate precursor to **1.24** (Scheme 1.10 A). Similarly, (+)-allonorsecurinine (**1.55**) might be oxidized to *N*-oxide **1.73**.[40] Then, in a sequence analogous to that proposed for the biosynthesis of phyllantidine (**1.21**) (see Scheme 1.6), *N*-oxide **1.73** might undergo [2,3]-Meisenheimer rearrangement/[1,3]-rearrangement to produce tetracyclic oxazine **1.75**.[32] Finally, an oxidation/elimination sequence might

produce nitrone **1.71**, which can undergo the putative [3+2] cycloaddition to give **1.25** (Scheme 1.10 B).

While there are no reported biosynthetic studies for any of the oligomeric *Securinega* alkaloids, the pathways that have been proposed will be briefly discussed. As previously stated, besides a few exceptions, these oligomers are predominantly comprised of norsecurinane-type monomers. Furthermore, each contains at least one anchoring bond at the C15 position of a (nor)securinane skeletal subunit. This feature is not surprising since the C15 position is highly electrophilic due to conjugation into the butenolide D-ring.

Flueggenines A-D (**1.5**-**1.8**) are all true norsecurinine homodimers and their biosyntheses have been proposed to involve a self-catalyzing Baylis-Hillman reaction (Scheme 1.11).[10a,d] According to this proposal, conjugate addition of the norsecurinine amine lone pair onto the C15 position of another norsecurinine molecule would initially provide the ylide intermediate **1.77**. There are then several potential fates of **1.77**, each leading to a different *Securinega* dimer. The first possibility (path a) is that **1.77** undergoes intramolecular conjugate addition, forging an additional bond between C14 and C15' to generate intermediate **1.78**. β-Elimination of the quaternary ammonium would then produce flueggenine A (**1.5**) (path a'), whereas flueggenine B (**1.6**) would be produced *via* saponification (path a"). Flueggenine C (**1.7**), which is the C14' epimer of flueggenine B (**1.6**), is likely produced from **1.77** *via* intermolecular C14 addition onto C15' of a third norsecurinine subunit (path b). This would generate the trimeric ammonium intermediate **1.79**, which might then undergo β-elimination of norsecurinine (**1.2**) to reveal **1.7**. Lastly, flueggenine D (**1.8**) might arise *via* intermolecular conjugate addition from C12 of **1.77** onto C15' of a third norsecurinine subunit (path c). This would produce ammonium intermediate **1.80**, which might then undergo elimination of norsecurinine (**1.2**) to generate dimer **1.8**.

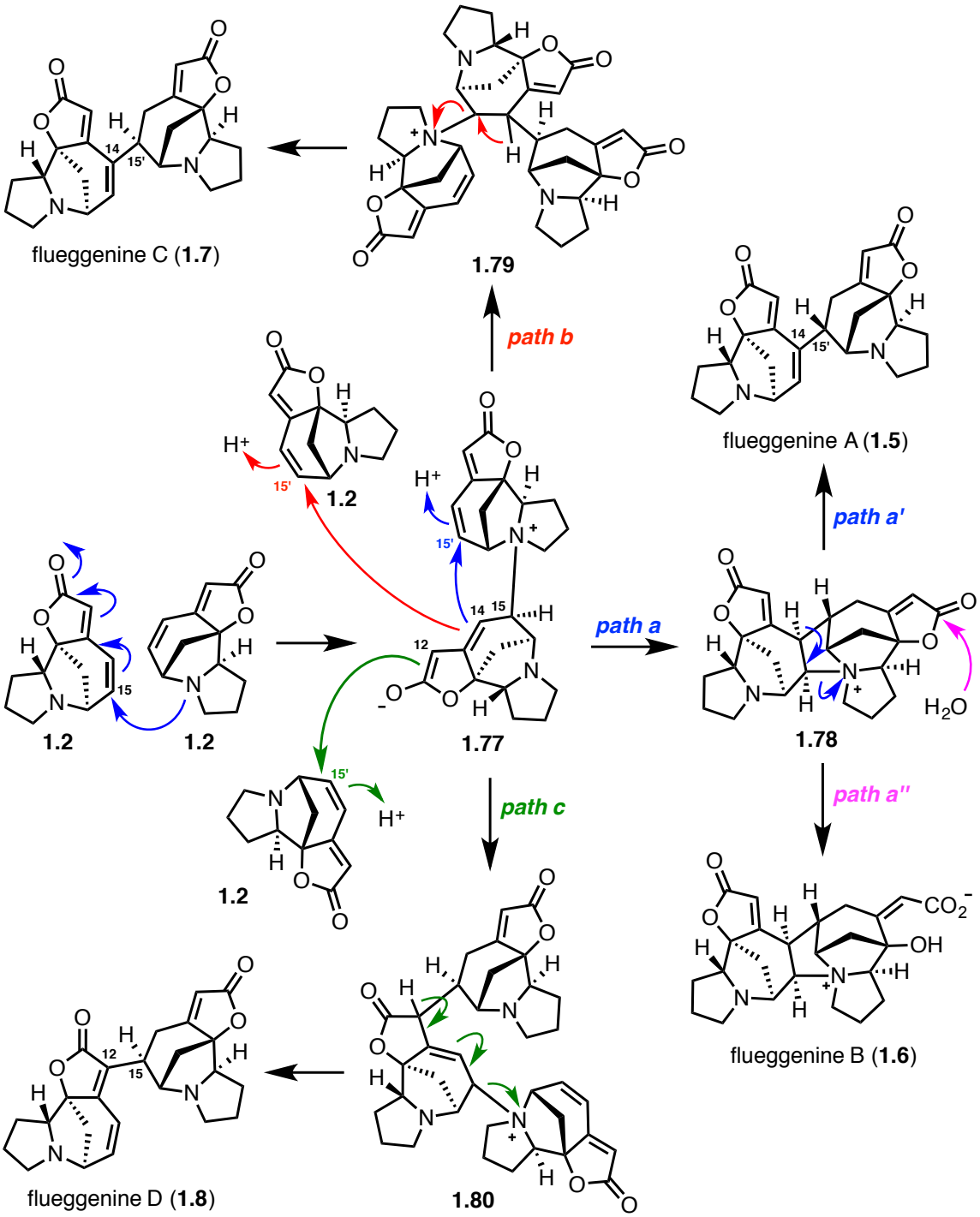

Scheme 1.11. Proposed biosyntheses of flueggenines A-D.

Several other *Securinega* alkaloid dimers appear to have also arisen *via* 1,6-conjugate addition onto C15 of norsecurinine (**1.2**). As examples, flueggether A (**1.9**) is

likely produced *via* *O*-alkylation of virosine A (**1.81**) onto **1.2**, while flueggine B (**1.12**) appears to be the C15-C12' dimer of securinol A (**1.82**) and **1.2** (Scheme 1.12).[10b,g]

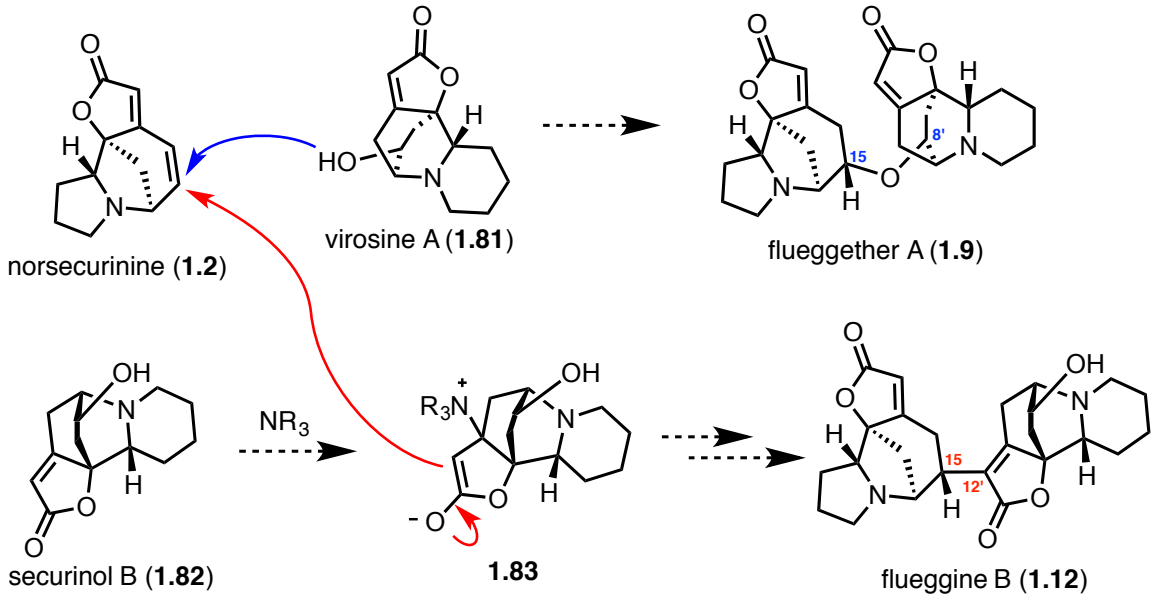

Scheme 1.12. Plausible biosyntheses of flueggether A and flueggine B.

Interestingly, flueggedine (**1.13**) is the only dimeric *Securinega* alkaloid to possess a securinane-type skeleton and is an apparent homodimer of virosecurinine (**1.56**). Furthermore, it is also the only member of this family to possess a cyclobutane ring. The latter suggests that **1.13** is produced *via* [2+2] cycloaddition of **1.56**, which is a reasonable hypothesis given that these two alkaloids were isolated from the same plant.[10e] Zhu and Ye et al. supported this hypothesis experimentally by producing **1.13** upon exposure of **1.56** to ultraviolet light (Scheme 1.13). Remarkably, **1.13** was produced as the sole product of the reaction and as a single diastereomer, accompanied only by unreacted **1.56**.

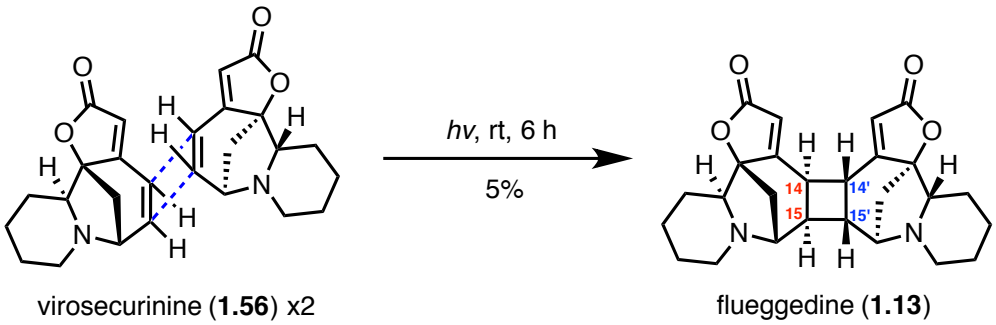

Scheme 1.13. Experimental evidence to support the plausible biosynthesis of flueggedine.

Among the dimeric *Securinega* alkaloids, flueggine A (**1.11**) stands out because one of its monomeric units does not directly correspond to any of the four main *Securinega* alkaloid skeletal classes. Moreover, **1.11** contains an isoxazolidine ring, similar to that found within virosaine A (**1.24**) and B (**1.25**) (*vide supra*). Ye et al. proposed that flueggine A (**1.11**) is derived from norsecurinine (**1.2**) according to the pathway outlined in Scheme 1.14.[10b] Specifically, they suggested that oxidation of **1.2** occurs to give *N*-oxide **1.84**. This species might then undergo further oxidation/ rearrangement to give nitrone **1.85**. Interestingly, in contrast to the biosyntheses of the virosaines (**1.24** and **1.25**), nitrone **1.85** does not undergo an intramolecular [3+2] cycloaddition, presumably due to increased strain in the resulting cycloadduct **1.86**. Instead, **1.85** is proposed to react with norsecurinine (**1.2**) in an intermolecular [3+2] cycloaddition to produce the dimer flueggine A (**1.11**). DFT calculations support the feasibility of an uncatalyzed reaction between nitrone **1.85** and norsecurinine (**1.2**) and indicate that enzymatic intervention is not required to control diastereoselectivity in the cycloaddition.[35b] These assertions have also been supported experimentally by Yang and Li et al. and Ye and Jang et al., where the cycloaddition of **1.85** with **1.2** generated flueggine A (**1.11**) in 77% and 66% yield, respectively, and as a single diastereomer.[27,36b]

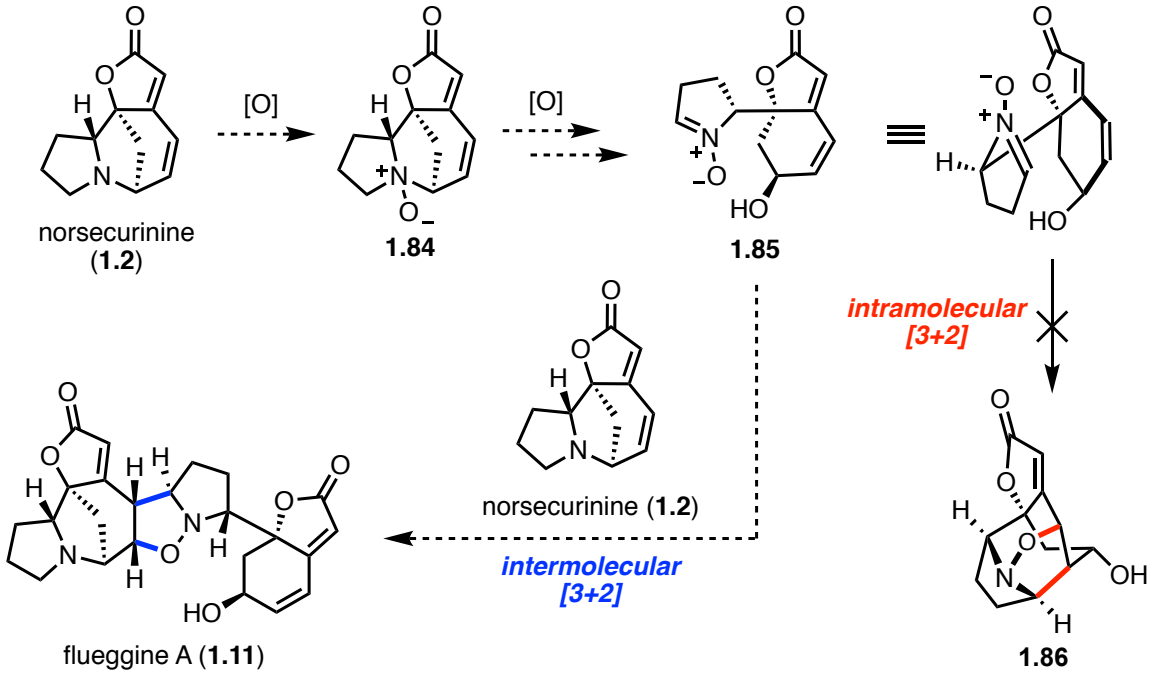

Scheme 1.14. Proposed biosynthesis of flueggine A.

The *Securinega* alkaloid trimers, tetramers, and pentamers have all been proposed to arise from flueggenine A (**1.5**), C (**1.7**), and D (**1.8**) *via* further iteration of the reactions shown in Scheme 1.11. For example, the trimeric alkaloids fluevirosine A (**1.14**) and B (**1.15**) are likely derived from a combination of flueggenine A (**1.5**) with norsecurinine (**1.2**) and viroallosecurinine (**1.57**), respectively.[10c] Several tetra- and pentameric members can also be distinctly traced back to other *Securinega* oligomers. For instance, careful analysis of fluevirosinine D (**1.18**) suggests that it is the heterodimer of flueggenine A (**1.5**) and C (**1.7**). Importantly, given the absence of studies that are focused on these biosynthetic pathways, the ordering in which each structural unit is installed to construct the tetra- and pentameric *Securinega* alkaloids remains speculative in many cases. Therefore, future studies in this area would likely provide valuable insight into the biosyntheses of these fascinating metabolites.

1.3 Biological Activity of the *Securinega* Alkaloids

Given the well-documented use of Phyllanthaceae plant species in traditional folk medicines, it is not surprising that their *Securinega* alkaloid metabolites have been thoroughly probed for potential biological activities. As a result, many *Securinega*

alkaloids have been found to exhibit interesting pharmacological profiles. Regardless of this fact, connections between the medicinal properties of the plants and their individual *Securinega* alkaloid metabolites have not been established, in most cases. While numerous pharmacological studies of many different *Securinega* alkaloids have been published, this discussion will mainly focus on those of securinine (**1.1**), which has been the most extensively studied member of this family. Moreover, this section is by no means a comprehensive review of these pharmacological studies but is instead intended to provide the reader with a broad overview of the area.[41]

1.3.1 Central Nervous System (CNS) Activity

The *Securinega suffruticosa* plant, from which securinine (**1.1**) was first isolated, had been used in traditional Chinese medicine as a stimulant to treat infantile paralysis, neurasthenia, and neuroparalysis. Consequently, initial biological studies on **1.1** were largely focused on its central nervous system (CNS) activity. In 1956, Soviet scientists reported that an ethanolic leaf extract from *Securinega suffruticosa* induced tachycardia and motor excitement in cats.[42] This CNS stimulant activity was ultimately linked to securinine (**1.1**), which caused similar effects in both frogs and mice.

Securinine's pharmacological properties were promptly recognized as being similar to those of strychnine.[43] Importantly, **1.1** was found to be approximately ten times less toxic than strychnine and therefore had a higher therapeutic index. Following its approval in the USSR as an imported strychnine substitute, securinine nitrate became a marketed drug in that country until the early 1990's for its stimulant and antiplasmodic effects.[44,45]

Beutler et al. revealed securinine's mechanism of action in 1985 by showing that it was a selective γ-aminobutyric acid (GABA) receptor antagonist.[46] Both **1.1** and 14,15-dihydrosecurinine demonstrated significant binding activity to [^{3}H]GABA receptors in rat brain membranes, with IC_{50} values of 57 ± 7 μM and 49 ± 8 μM, respectively. This was approximately seven times less potent than the reference compound, bicuculline (IC_{50} = 7 ± 0.4 μM). Interestingly, securinine's enantiomer and C2-epimer, virosecurinine (**1.56**) and allosecurinine (**1.52**), respectively, demonstrated significantly lower affinities to GABA receptors. Wermuth and coworkers elucidated securinine's mode of binding to

$GABA_A$ receptors by performing *ab initio* molecular orbital calculations using **1.1**'s crystal structure atomic coordinates.[47] They determined that the pharmacophores responsible for securinine's activity were its lactone (acting as an anionic binding site) and protonated amine (cationic binding site). Furthermore, its mode of binding appeared to be stereospecific, which helps explain the lack of GABA binding activity observed with virosecurinine (**1.56**) and allonorsecurinine (**1.52**).

Securinine (**1.1**) and 14,15-dihydrosecurinine also exhibited significant convulsant activity in mice (CD_{50} = 28 ± 3 μM and 11 ± 0.4 μM, respectively), which was comparable to the potency displayed by bicuculline (CD_{50} = 8 ± 4 μM).[46] Subsequent studies confirmed and expanded upon these results and, eventually, **1.1** was used clinically as a GABA receptor inhibitor.[41] **1.1** was also studied clinically as a CNS stimulant to treat paralysis following both Bell's palsy and infantile paralysis as well as for alleviating symptoms of amyotrophic lateral sclerosis (ALS) and chronic aplastic anemia.[48,49]

Intriguingly, Lin and Jun-tian demonstrated that cognitive deficits and neurodegeneration induced by β-amyloid protein (βAP) in rats could be reversed by daily oral administration of **1.1**.[50] The same study revealed that **1.1** increased acetylcholine (Ach) concentrations in the brain as a result of acetylcholinesterase (AchE) inhibition, with no noticeable effect on acetylcholinetransferase (ChAT) activity. Moreover, **1.1** reduced glial inflammatory responses induced by βAP. Recently, another study showed that **1.1** significantly suppressed nitric oxide production in microglia and astrocyte cultures in a dose-dependent manner.[51] These neuroprotective properties were suggested to be the result of securinine's inhibition of the p38 mitogen-activated protein (MAP) kinase-NF-κB pathway. The results of these studies hold particular significance for securinine's potential in the treatment of neurodegenerative diseases, such as Alzheimer's and Parkinson's diseases. Securinine's potential in this regard might stem from its ability to block GABA receptors and their corresponding cholinergic mechanisms.[41,52]

1.3.2 Oncological Activity

Many of the *Securinega* alkaloids have been probed for their cytotoxic effects on several different cancer cell lines. Of those studied, only securinine (**1.1**), 4-

epiphyllanthine (**1.87**), flueggine A (**1.11**), flueggine B (**1.12**), and flueggenine A (**1.5**) showed promising activities (Table 1). Wald et al. initially discovered that **1.1** killed HCT116 p53 cells at moderate to low micromolar concentrations (entries 1 and 2).[53] Recently, **1.1** was also found to induce apoptosis in human leukemia HL60 cells in a time- and concentration-dependent manner by modulating PI3K/AKT/mTOR pathway gene expression (entries 6-9).[54,55] These results indicated the potential usefulness of **1.1** for the developement of antitumor agents. Interestingly, Ohsaki and coworkers found that 4-epiphyllanthine (**1.87**) (Figure 1.6) exhibited promising cytotoxicity against human epidermoid carcinoma KB cells and murine lymphoma L1210 cells, at comparable levels to those exhibited by securinine (**1.1**) (compare entries 4 and 5 to entries 10 and 11, respectively).[56] Dimers flueggine A (**1.11**) and B (**1.12**) were evaluated against three different human breast cancer cell lines (entries 12-17).[10b] While **1.11** demonstrated only modest activities in all three cell lines, **1.12** exhibited nM inhibitory activity on the growth of both MCF-7 and MDA-MB-231 cells (entries 15 and 16).

No extensive structure-activity relationship (SAR) studies have been conducted on the *Securinega* alkaloids with regards to their cytotoxic properties. However, a comparative analysis of the cytotoxicity of several *Securinega* alkaloids and their saturated derivatives led Tatematsu et al. to propose that the highly strained α,β,γ,δ-unsaturated lactone moiety is necessary for activity.[57] Interestingly, bicyclic lactones menisdaurilide (**1.38**) and aquilegiolide (**1.39**), which also contain this structural feature, were found to induce apoptosis in Jurkat human T-cell lymphoma and HT29 human colon cancer cells.[58] A lack of cytotoxic activity in several structurally distinct *Securinega* alkaloids, such as virosaines A (**1.24**) and B (**1.25**), has led others to propose that an indolizidine core (A/B rings) is essential for oncological activity.[14] Notably, flueggine B (**1.12**) does not possess an α,β,γ,δ-unsaturated lactone or an indolizidine moiety and still exhibits significant cytotoxicity against breast cancer cells. Thus, additional SAR studies are necessary to fully understand the structural requirements for oncological activity in this alkaloid family.

Table 1. Cytotoxic activities of some *Securinega* alkaloids.[59]

Entry	Compound	Cell Line	LD_{50} (μM)
1[53]	securinine (**1.1**)	HCT116 p53 – (human colon cancer)	17.5
2[53]		HCT116 p53 + (human colon cancer) wild type p53 expressing	50
	Compound	**Cell Line**	**IC_{50} (μM)**
3[60]	securinine (**1.1**)	SW480 (human colon cancer)	19.1
4[56]		KB (human epidermoid carcinoma)	10
5[56]		L1210 (murine lymphomia)	8.8
6[54]		HL60 (human leukemia)	124 (12 h)
7[55]		HL60 (human leukemia)	47.9 (24 h)
8[55]		HL60 (human leukemia)	23.8 (48 h)
9[55]		HL60 (human leukemia)	18.9 (72 h)
10[56]	4-epiphyllanthine (**1.87**)	KB (human epidermoid carcinoma)	12
11[56]		L1210 (murine lymphomia)	15
12[10b]	flueggine A (**1.11**)	MCF-7 (human breast cancer) estrogen-dependent phenotype	60 ± 4
13[10b]		MDA-MD-231 (human breast cancer) estrogen-independent phenotype	86 ± 9
14[10b]		MCF-7/ADR (doxorubicin-induced multidrug resistant phenotype)	68 ± 7
15[10b]	flueggine B (**1.12**)	MCF-7 (human breast cancer) estrogen-dependent phenotype	135 ± 5 (nM)
16[10b]		MDA-MD-231 (human breast cancer) estrogen-independent phenotype	147 ± 3 (nM)
17[10b]		MCF-7/ADR (doxorubicin-induced multidrug resistant phenotype)	19 ± 3
18[10a]	flueggenine A (**1.5**)	P-388 (murine leukemia)	51.5

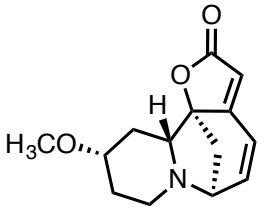

4-epiphyllanthine (**1.87**)

Figure 1.6. Structure of 4-epiphyllanthine.

Recently, synthetic securinine derivatives bearing a β'-hydroxy-α,β,γ,δ-unsaturated lactone moiety were evaluated as DNA topoisomerase I (Topo I) inhibitors and antitumor agents (Figure 1.7).[61] Several of these demonstrated significant Topo I inhibitory activity as well as cytotoxicity against several cancer cell lines. Notably, every synthetic derivative was more effective than **1.1** in terms of both Topo I inhibition and cytoxicity. Mechanistic and docking studies revealed that these new compounds inhibited Topo I in a different manner than current well-known inhibitors and, as a result, possessed relatively lower toxicity profiles. Several cytotoxic SAR studies on arylated securinine derivatives have also recently been disclosed with promising results.[62] These findings support the feasibility of using a securinine-based template in the search for novel anticancer drugs.

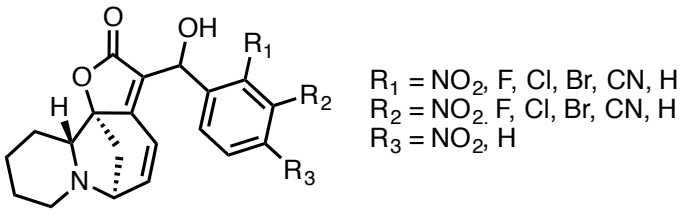

1.88

Figure 1.7. General structure of novel Topo I inhibitors and antitumor agents derived from securinine.

1.3.3 Antimalarial Activity

Weenen et al. reported that securinine (**1.1**) exhibited *in vitro* antimalarial activity with an IC_{50} of 5.35 μg/mL.[63] Two other α,β-unsaturated carbonyl compounds also exhibited significant antimalarial activity in the same study and led the authors to propose a preliminary mechanism of action. They suggested that the observed activity might be

the result of conjugate addition of the nucleic acids of the malarial parasites onto the unsaturated carbonyl moiety. In a recent study, *ent*-norsecurinine (*ent*-**1.2**) and (+)-allonorsecurinine (**1.55**) exhibited moderate antiplasmodial activity against the chloroquine-resistant (W2) strain of *Plasmodium falciparum*, with IC_{50} values of 1.14 ± 0.32 and 2.57 ± 0.53 μM, respectively.**Error! Bookmark not defined.**

1.3.4 Antimicrobial Activity

Securinine (**1.1**) and virosecurinine (**1.56**) have exhibited antibacterial activities against several bacterial strains, including *Escherichia coli, Enterococcus faecium, Myobacterium smegmatis, Pseudomonas aeruginosa,* and *Staphyloccocus aureus*.[64] The minimal inhibitory concentration (MIC) of **1.1** was 0.500 mg/mL for *E. coli, Staph. aureus,* and *Myc. smegmatis*. Additionally, **1.56** exhibited a MIC of 0.48 μg/mL for *Ps. aeruginosa* and *Staph. aureus*, which led to its designation as being bactericidal.

Antifungal activities have been reported for *ent*-norsecurinine (*ent*-**1.2**), where it was found to inhibit spore germination on *Alternaria brassicae, Curvularia penniseti, Curvularia* spp., *Erysiphe pisi, Fusarium udam,* and *Helminthosporium frumentacei* at a concentration of approximately 10 μM.[65] Moreover, norsecurinine (**1.2**) was found to be a highly effective antifungal agent against several phytopathogenic and saprophytic fungi and was suggested as a possible substitute to synthetic fungicides.[66]

1.3.5 Anti-HIV Activity

Several reports have recently emerged on the anti-HIV activity of newly isolated *Securinega* alkaloids.[67] While interesting, the activities reported are generally modest at best. Of the alkaloids studied, flueggenine D (**1.18**) exhibited the best anti-HIV activity when tested on HIV-1 NL 4-3 infected MT4 cells, with an EC_{50} value of 7.8 ± 0.8 μM.[67a]

1.4 Total Syntheses of the *Securinega* Alkaloids

The fascinating structural features and potent bioactivities of the *Securinega* alkaloids have spurred significant interest from the synthetic chemistry community, leading to many elegant total syntheses. This section is not a comprehensive review of these synthetic efforts and, if interested, the reader is directed to the excellent reviews

that have already been published on the subject.[68] Moreover, while certain notable synthetic milestones are presented, this section is mainly focused on the syntheses of virosaine A (**1.24**), virosaine B (**1.25**), and flueggine A (**1.11**).

1.4.1 Horii's Racemic Synthesis of Securinine/Virosecurinine

The first total synthesis of a *Securinega* alkaloid was accomplished by Horii and coworkers in 1967, where they prepared a racemic sample of securinine (**1.1**) (i.e. a 1:1 mixture of **1.1** and virosecurinine (**1.56**)).[69] Their synthesis began with the addition of 2-lithio pyridine to ketone **1.89,** providing alcohol **1.90** in 66% yield. Reduction of the pyridine ring was followed by sequential acid-mediated ketal hydrolysis and amine acetylation to provide a mixture of ketone intermediates **1.91** and **1.92**, which were separated by flash chromatography. Bromination of **1.92** produced a diastereomeric mixture of α-brominated ketone **1.93** in 75% yield. Treatment of **1.93** with $LiBr/Li_2CO_3$ effected elimination to the corresponding α,β-unsaturated ketone. Addition of lithium ethoxyacetylene (**1.94**) to this intermediate was followed by acidic hydrolysis to provide the tricyclic α,β,γ,δ-unsaturated lactone **1.95** in 49% yield, over two steps. At this stage, the amine protecting group was converted to a formamide in order to facilitate milder deprotection at a later stage. In the event, treatment of **1.95** with concentrated HCl provided an intermediate amine which was subsequently reacted with formic acid/Ac_2O to give formamide **1.96** in good yield. Allylic bromination of **1.96** was achieved upon treatment with NBS/catalytic benzoyl peroxide ($(BzO)_2$). Finally, formamide removal (20% aq. HCl, reflux) and K_2CO_3-mediated annulation yielded *rac*-securinine (i.e. a 1:1 mixture of **1.1** to **1.56**). The racemic material was readily resolved into pure securinine (**1.1**) and virosecurinine (**1.56)** *via* recrystallization of their D-camphorsulfonate salts from hot acetone.

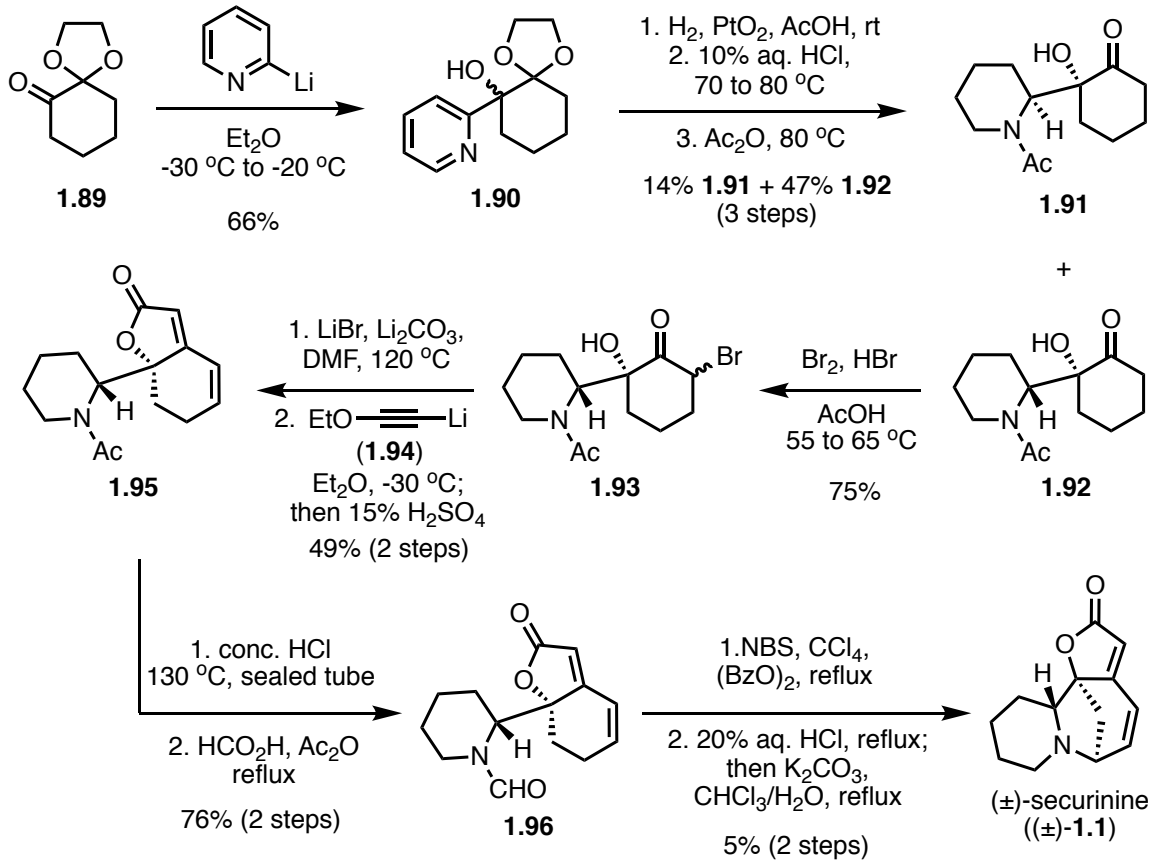

Scheme 1.15. Horii's racemic synthesis of securinine/virosecurinine.

1.4.2 Jacobi's Enantiospecific Synthesis of Norsecurinine

Surprisingly, following Horii's inaugural synthesis of (±)-**1.1**, the area of *Securinega* alkaloid total synthesis remained dormant for twenty years. In 1987, Heathcock et al. followed up with the first total synthesis of racemic norsecurinine ((±)-**1.2**).[70] Several years later, Jacobi and coworkers published the first non-racemic synthesis of a *Securinega* alkaloid. Their approach enabled them to prepare either (−)- or (+)-norsecurinine (**1.2**) in an enantiospecific fashion from either D- or L-proline, respectively.[71] Their synthesis of (−)-norsecurinine (**1.2**) is shown in Scheme 1.16.

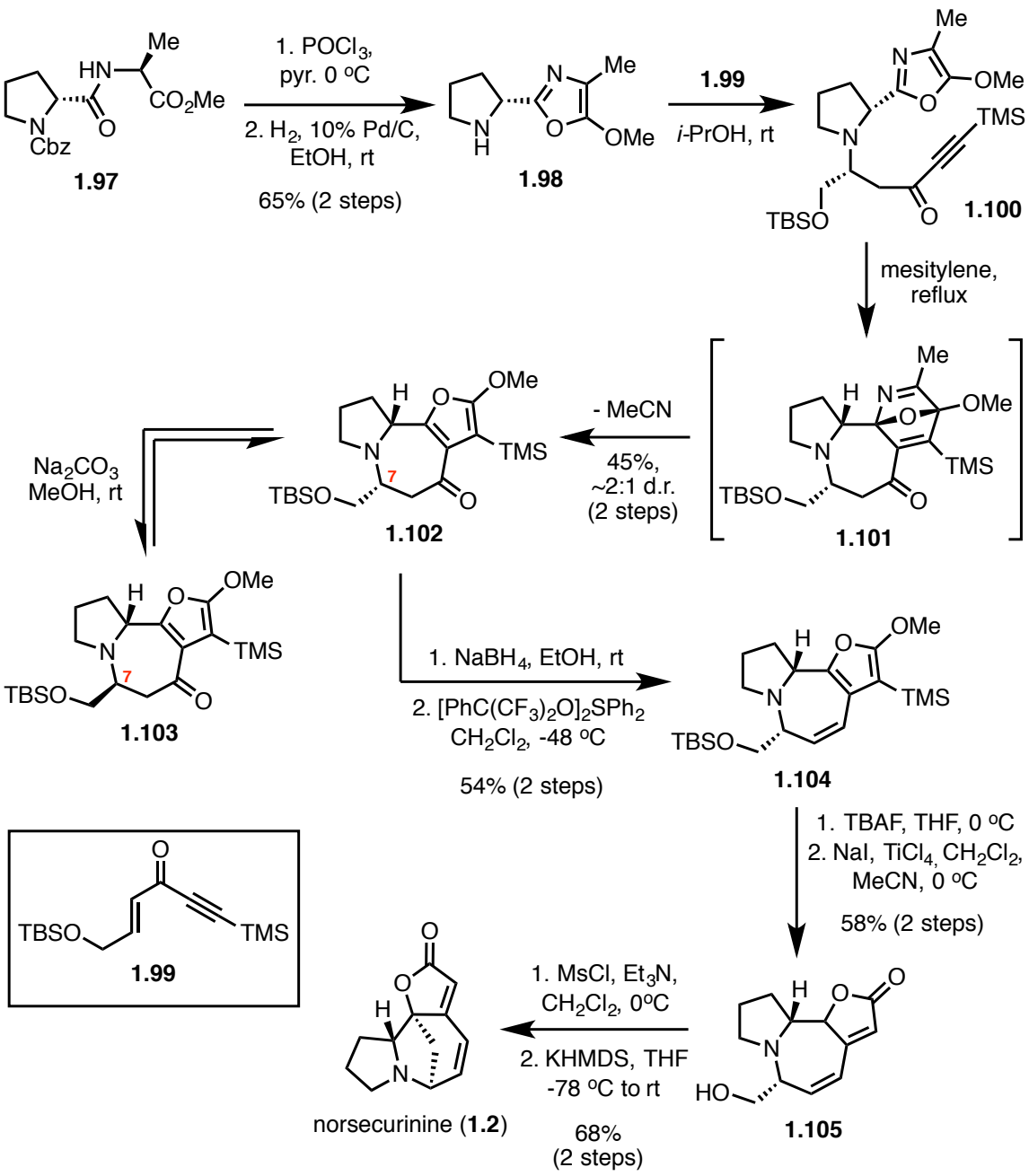

Scheme 1.16. Jacobi's enantiospecific synthesis of norsecurinine.

Jacobi's synthesis began with protected dipeptide **1.97**, which is readily prepared from D-proline.[72] Sequential cyclodehydration and amine deprotection of **1.97** provided oxazole **1.98** in 65% yield, over two steps. Conjugate 1,4-addition of **1.98** onto enone **1.99** then proceeded rapidly to provide **1.100** as a mixture of diastereomers. Without further purification, acetylenic ketone **1.100** was refluxed in mesitylene to induce an

intramolecular Diels-Alder reaction to provide furano ketone **1.102** *via* loss of acetonitrile from the [4+2] cycloadduct **1.101**. The desired product **1.102** was formed as the major product alongside its C7 epimer **1.103** (~2:1 d.r.). These diastereomers were found to be separable and, after purification, **1.103** could be epimerized to **1.102** under basic conditions *via* a β-elimination/conjugate addition sequence. Sodium borohydride reduction of ketone **1.102** followed by dehydration of the resultant secondary alcohol using Martin's sulfurane provided alkene **1.104**. Silyl deprotection of **1.104** was achieved with TBAF and then the methoxyfuran moiety was converted to the corresponding α,β,γ,δ-unsaturated lactone **1.105** by treating with NaI/$TiCl_4$. With **1.105** in hand, a final displacement sequence was employed to access the natural product. The primary alcohol of **1.105** was activated using MsCl and then the resulting mesylate was treated with KHMDS to effect transannular alkylation to provide norsecurinine (**1.2**) in good yield.

1.4.3 *Securinega* Alkaloid Total Syntheses of the 21st Century

Only one additional total synthesis of a *Securinega* alkaloid was published before the end of the 20th century, where Magnus et al. reported a synthesis of racemic norsecurinine (**1.2**) as well as the first and only racemic synthesis of nirurine (**1.23**).[26,34] Interest in the *Securinega* alkaloids began to spike drastically in the year 2000 and, since then, more than two-dozen new total syntheses of various members have appeared in the literature. These reports are mainly limited to syntheses of securinine (**1.1**), norsecurinine (**1.2**), their diastereomers, and saturated analogues.[27,28,36a,b,73] Notable exceptions include the first and only total synthesis of phyllantidine (**1.21**), reported by Kerr et al. in 2006,[74] as well as the first total synthesis of secu'amamine A (**1.22**) by Weinreb et al. in 2008.[75] Smith recently reported the only other synthesis of **1.22**.[76] Moreover, Bélanger and coworkers disclosed the first and only total synthesis of virosine A (**1.81**) in 2012.[77] Recently, Gademann et al. published the first and only total syntheses of secu'amamine E (**1.50**) and bubbialine (**1.53**) and Han completed the first and only total synthesis of flueggenine C (**1.7**).[28,78]

1.4.3.1 Gademann's Total Synthesis of Bubbialidine and Virosaine A

Beginning in 2013, several of the most structurally complex and synthetically challenging *Securinega* alkaloids started to succumb to total synthesis. In that year, Gademann et al. reported the first enantioselective total syntheses of both bubbialidine (**1.49**) and virosaine A (**1.24**).[36a] Moreover, their synthesis of **1.24** was inspired by the putative biosynthetic [3+2] nitrone cycloaddition proposed by Zhao et al. (*vide supra*). The preparation of **1.49** and **1.24** began by converting 1,4-cyclohexadiene (**1.106**) to the TBDPS-protected (+)-aquilegiolide intermediate **1.112** (Scheme 1.17). A three-step sequence involving mono-epoxidation of **1.106**, epoxide opening with cyanomethyllithium and acetylation provided **1.107**, as a racemic mixture, in 22% yield. Kinetic enzymatic resolution of **1.107** using lipase AK(amano) provided acetate **1.108** in 40% yield (96% *ee*) and the desired alcohol **1.109** in 38% yield (94.6% *ee*). Base-mediated nitrile hydrolysis of **1.109** was followed by acid-mediated lactonization to give lactone **1.110** in good yield over two steps. A two-step sequence involving phenylselenation and oxidative elimination was employed to generate butenolide **1.111**.

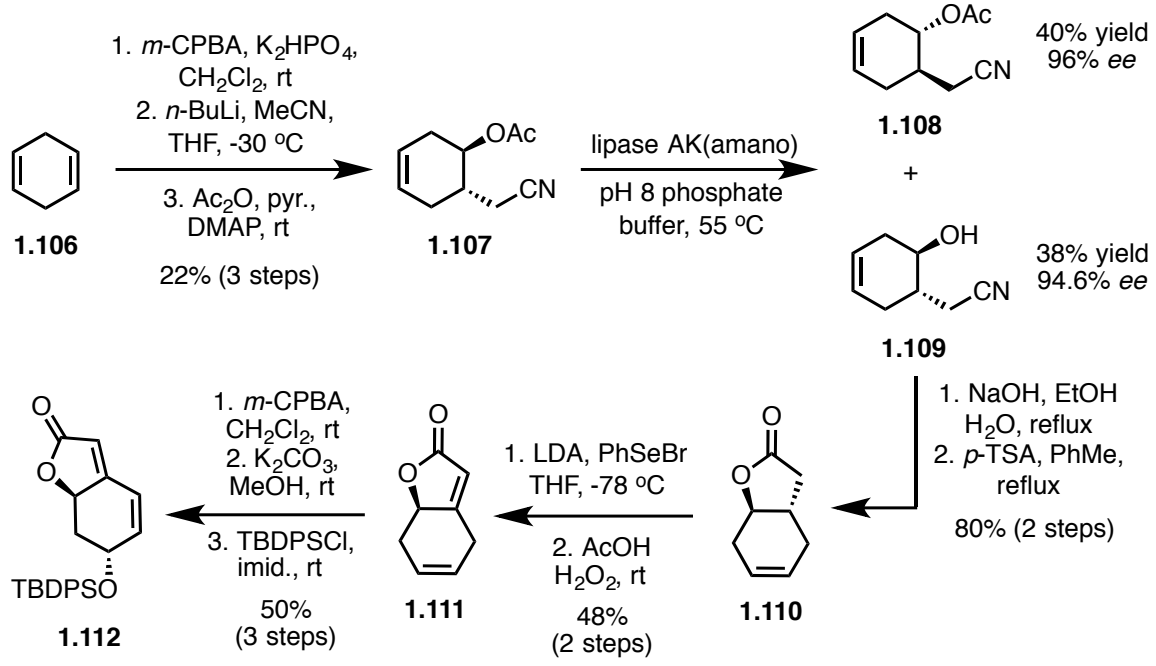

Scheme 1.17. Gademann's synthesis of TBDPS-protected (+)-aquilegiolide.

Diastereoselective epoxidation of the more electron-rich olefin in **1.111** was followed by an elimination/silyl protection sequence to provide **1.112** in 50% yield over three steps.

Notably, the same group recently published a shorter and more efficient route to access the α,β,γ,δ-unsaturated lactone intermediate **1.112**.[28]

With a route to **1.112** in place, Gademann and coworkers proceeded to install the remaining carbon framework of the natural products. A vinylogous Mannich addition was achieved by first treating **1.112** with TIPSOTf/Et_3N to produce a 2-siloxyfuran intermediate (not shown), which was then allowed to react with hemiaminal **1.113** in the presence of TIPSOTf (Scheme 1.18). The reaction generated two diastereomers in a 1:1 ratio, from which the desired product **1.114** was isolated in 45% yield. The Boc protecting group was removed under acidic conditions to provide the corresponding amine as its hydrochloride salt. Treatment of this species under mild basic conditions at 75 ^oC effected a conjugate 1,6-addition to provide bridged tetracycle **1.115** in excellent yield. Silyl deprotection of **1.115** using HF•pyridine produced bubbialidine (**1.49**) in 92% yield. This concluded the first and only total synthesis of **1.49** in 16 steps and 0.6% overall yield.

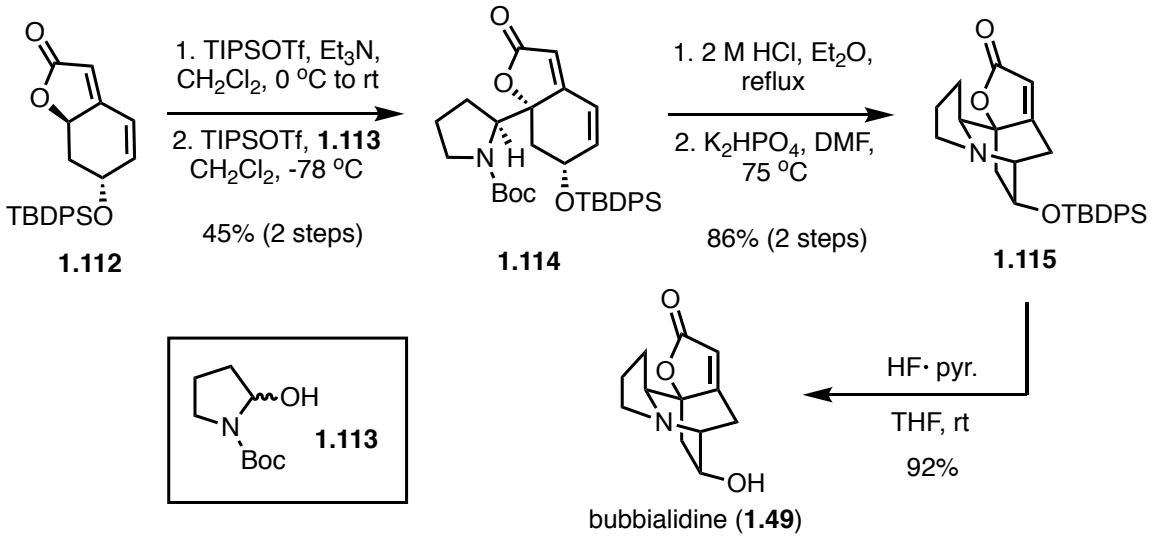

Scheme 1.18. Gademann's synthesis of bubbialidine.

For the synthesis of **1.24**, Gademann et al. conducted a chemoselective amine oxidation of **1.115** with *m*-CPBA to afford the corresponding *N*-oxide **1.116**, which underwent facile elimination on silica gel to provide hydroxylamine **1.117** (Scheme 1.19). Regioselective oxidation of the hydroxylamine moiety using *N-tert-*

butylbenzenesulfinimidoyl chloride/DBU provided nitrone **1.118** which underwent rapid intramolecular [3+2] cycloaddition to provide the protected-virosaine A skeleton **1.119** in an excellent 92% yield. Finally, silyl deprotection afforded the natural product, virosaine A (**1.24**) in a total of 18 steps and 0.4% overall yield. Not only was this the first total synthesis of **1.24**, but it elegantly demonstrated the viability of the proposed biosynthetic nitrone cycloaddition and also established a potential relationship between **1.49** and **1.24**.

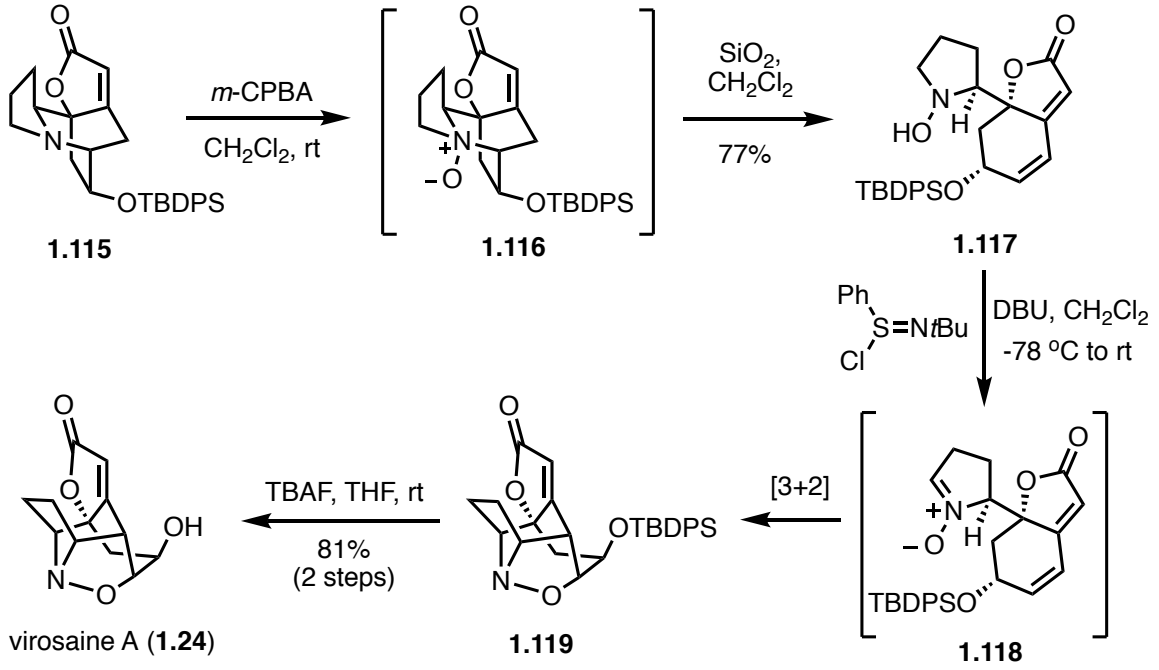

Scheme 1.19. Gademann's synthesis of virosaine A.

1.4.3.2 Yang and Li's Total Synthesis of (+)-Allonorsecurinine, Norsecurinine, Virosaine B, and Flueggine A

In the same year, Yang and Li published the first total syntheses of both virosaine B (**1.25**) and flueggine A (**1.11**).[36b] Their strategy was also biomimetic in nature and utilized the proposed [3+2] nitrone cycloaddition to furnish the isoxazolidine moieties of these targets. Moreover, they prepared **1.25** and **1.11** from (+)-allonorsecurinine (**1.55**) and norsecurinine (**1.2**), respectively, which suggested that there might be a biosynthetic relationship between the two pairs (*vide supra*).

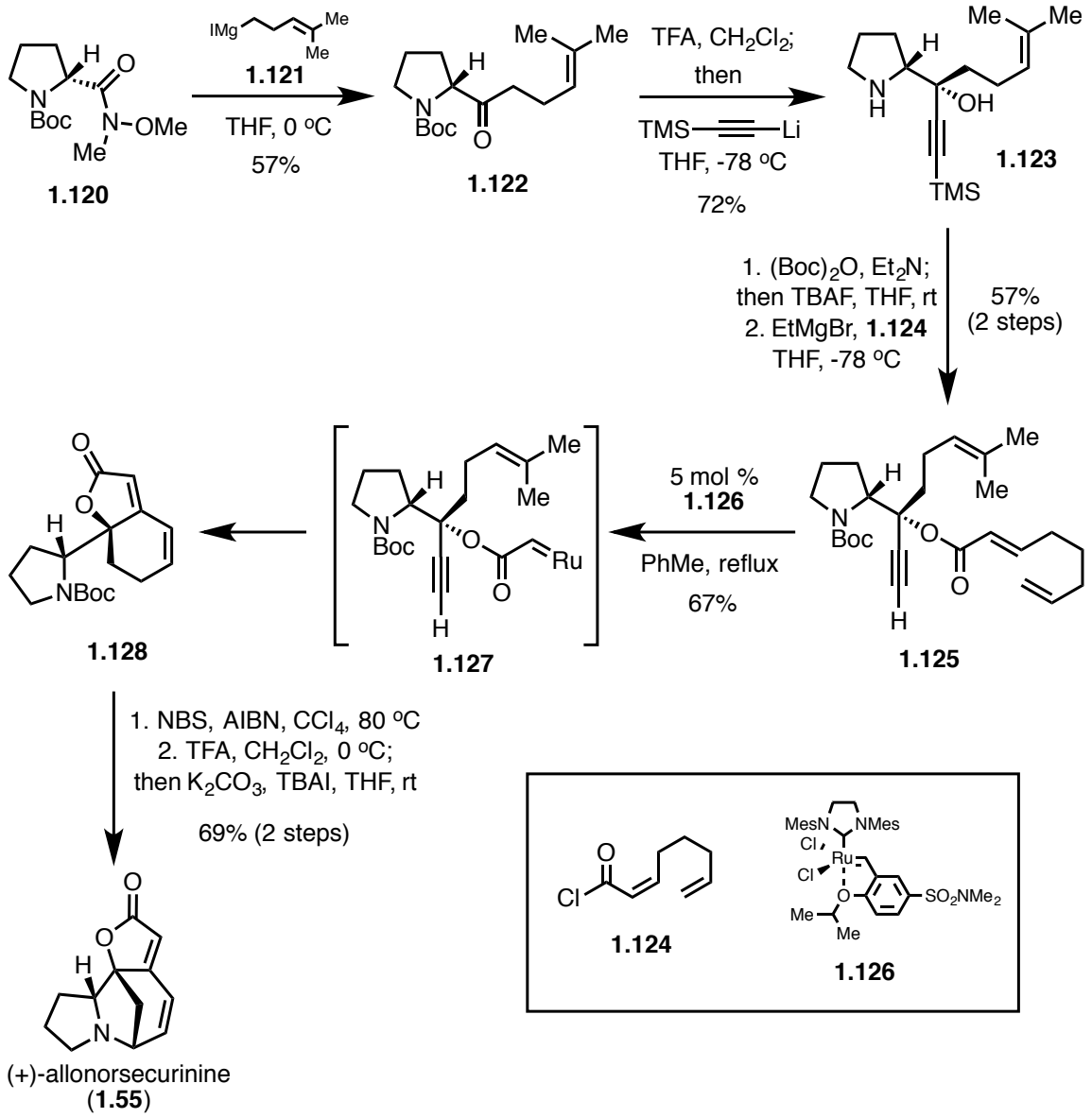

Scheme 1.20. Yang and Li's synthesis of (+)-allonorsecurinine.

The synthesis of virosaine B (**1.25**) commenced by preparing (+)-allonorsecurinine (**1.55**) from commercially available Weinreb amide **1.120** (Scheme 1.20). Addition of Grignard reagent **1.121** gave ketone **1.122** in 57% yield. Boc deprotection of **1.122** followed by *in situ* chelation-controlled addition of lithium trimethylsilylacetylide provided alcohol **1.123**. A three-step sequence involving Boc-protection of the amine, silyl deprotection, and acetylation with **1.124** provided trienyne **1.125** in 57% yield. With **1.125** in hand, a relay ring-closing metathesis (RRCM) reaction

was employed in order to construct the A/B rings of (+)-allonorsecurinine (**1.55**). In the event, **1.125** was reacted with 5 mol % of the Zhan-1b catalyst **1.126** to provide α,β,γ,δ-unsaturated lactone **1.128** in 67% yield. Presumably, this reaction proceeds *via* ruthenium acyl-carbenoid complex **1.127**, which can undergo sequential enyne/diene RCM. To complete the total synthesis of (+)-allonorsecurinine (**1.55**), **1.128** was submitted to a final two-step annulation procedure. Allylic bromination of **1.128** was followed by a one-pot Boc-deprotection/cyclization to yield **1.55** in a total of 7 steps and 11% overall yield.

With **1.55** in hand, elaboration to virosaine B (**1.25**) only required a short sequence of oxidations/rearrangements (Scheme 1.21). Chemoselective oxidation of **1.55** yielded the corresponding *n*-oxide **1.73** which, upon refluxing in xylene underwent [2,3]-Meisenheimer rearrangement/[1,3]-rearrangement to provide *O*-alkylhydroxylamine **1.75** in excellent yield. Lastly, oxidation of **1.75** with *m*-CPBA in the presence of acetic acid furnished virosaine B (**1.25**) in 76% yield, presumably *via* intramolecular [3+2] cycloaddition of nitrone **1.71**. This completed the first and only total synthesis of **1.25** in 10 steps (7% overall yield) and serves as additional evidence to support the proposed biosynthetic nitrone cycloaddition step.

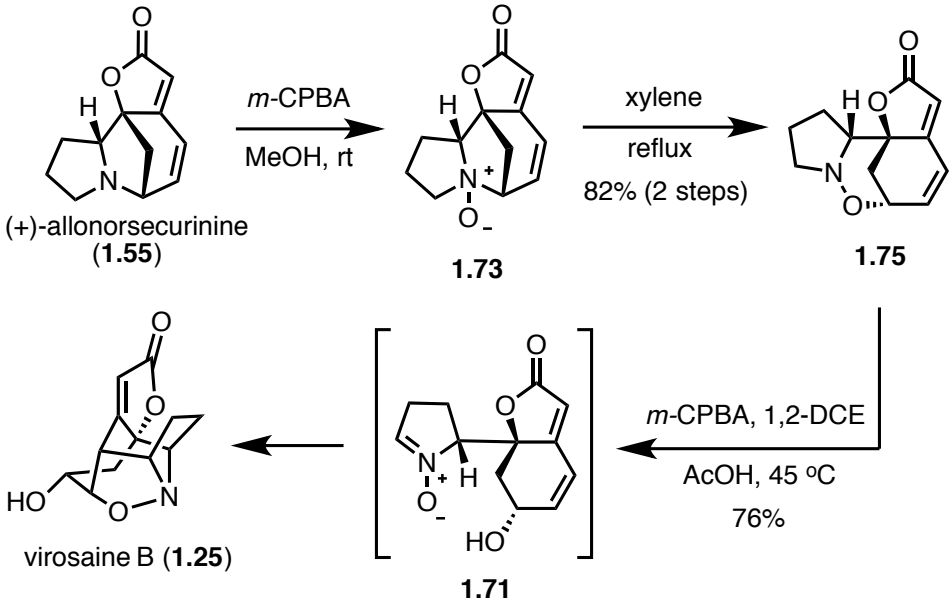

Scheme 1.21. Yang and Li's synthesis of virosaine B.

Yang and Li prepared norsecurinine (**1.2**) using a similar sequence to that used to prepare **1.55** (Scheme 1.22). The major difference between the two routes was that, in the synthesis of **1.2**, initial Felkin-Anh addition of lithium trimethylsilylacetylide to ketone **1.122** was employed to provide alcohol **1.129** in 81% yield. Notably, **1.129** is simply the epimer of alcohol **1.123** (*vide supra*). Elaboration of **1.129** to **1.2** was then achieved in an additional 5 steps. Overall, this route enabled the preparation of **1.2** in a total of 7 steps and 10% overall yield.

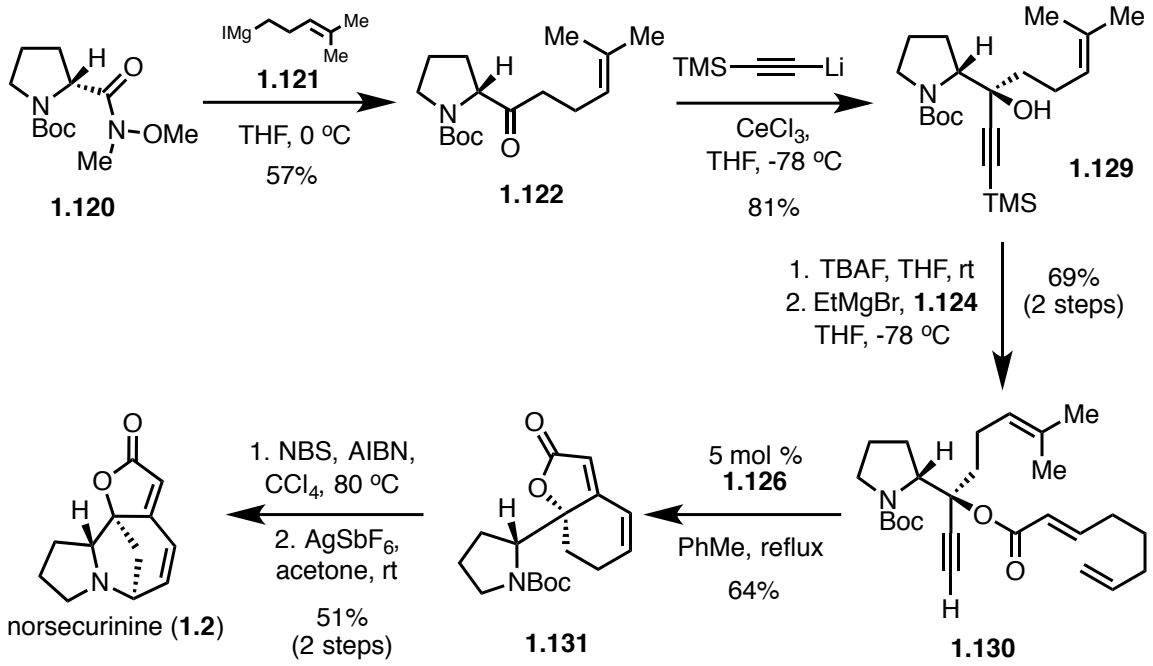

Scheme 1.22. Yang and Li's synthesis of norsecurinine.

With norsecurinine (**1.2**) in hand, flueggine A (**1.11**) was prepared following the biomimetic reaction sequence shown in Scheme 1.23. Oxidation of **1.2** to *N*-oxide **1.84** was followed by a thermally-induced [2,3]-Meisenheimer rearrangement/[1,3]-rearrangement to generate *O*-alkylhydroxylamine **1.132**. Oxidative elimination of **1.132** was effected with *m*-CPBA to yield nitrone **1.85**, which was isolated in 87% yield. Finally, nitrone **1.85** was allowed to react with **1.2** in refluxing toluene to provide flueggine A (**1.11**) in 77% yield, *via* intermolecular dipolar cycloaddition. Overall, the synthesis of **1.11** proceeded in 11 steps and 6% overall yield.

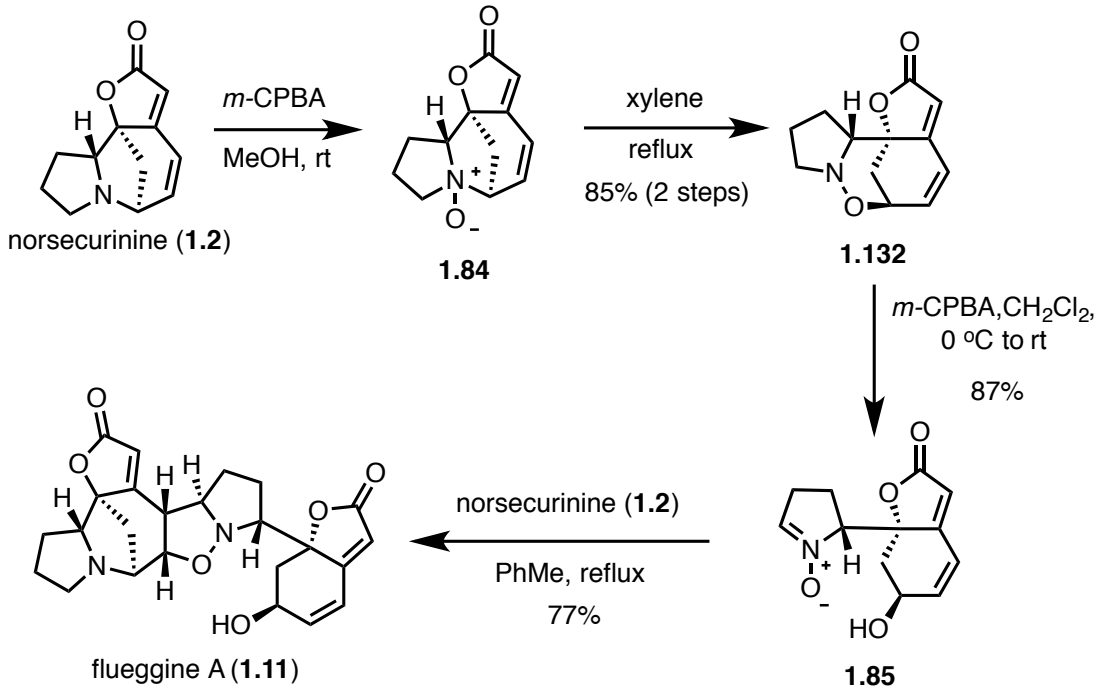

Scheme 1.23. Yang and Li's synthesis of flueggine A.

1.4.3.3 Ye and Jiang's Total Synthesis of Norsecurinine, Niruroidine, and Flueggine A

The only other synthesis of flueggine A (**1.11**) was reported by Ye and Jiang et al. in 2014.[27] Their synthesis maintained several features of the Yang/Li approach, including the use of norsecurinine (**1.2**) to access nitrone **1.85** and the implementation of the biomimetic nitrone cycloaddition. However, a novel feature of Ye/Jiang's approach involved preparing nitrone **1.85** from **1.2** *via* niruroidine (**1.46**), a structurally related *Securinega* alkaloid. Thus, this synthesis established a potential biosynthetic relationship between these three natural products.

Their synthesis of **1.2** began with the addition of 3-butenylmagnesium bromide (**1.133**) to Weinreb amide **1.120** to provide ketone **1.134** in excellent yield (Scheme 1.24). Sequential methoxyallene addition/hydrolysis gave dienone **1.135** in 70% yield. RCM using Grubbs' second-generation catalyst smoothly generated cyclohexenone **1.136**, which was brominated using NBS/AIBN to provide **1.137** in 57% yield over two steps. B-ring formation was achieved *via* acid-mediated Boc deprotection and Et_3N-induced annulation. DCC-mediated coupling with diethylphosphonoacetic acid (**1.138**)

provided **1.139**, which underwent Horner-Wadsworth-Emmons reaction upon treatment with NaH to provide norsecurinine (**1.2**) in 39% yield (three steps).

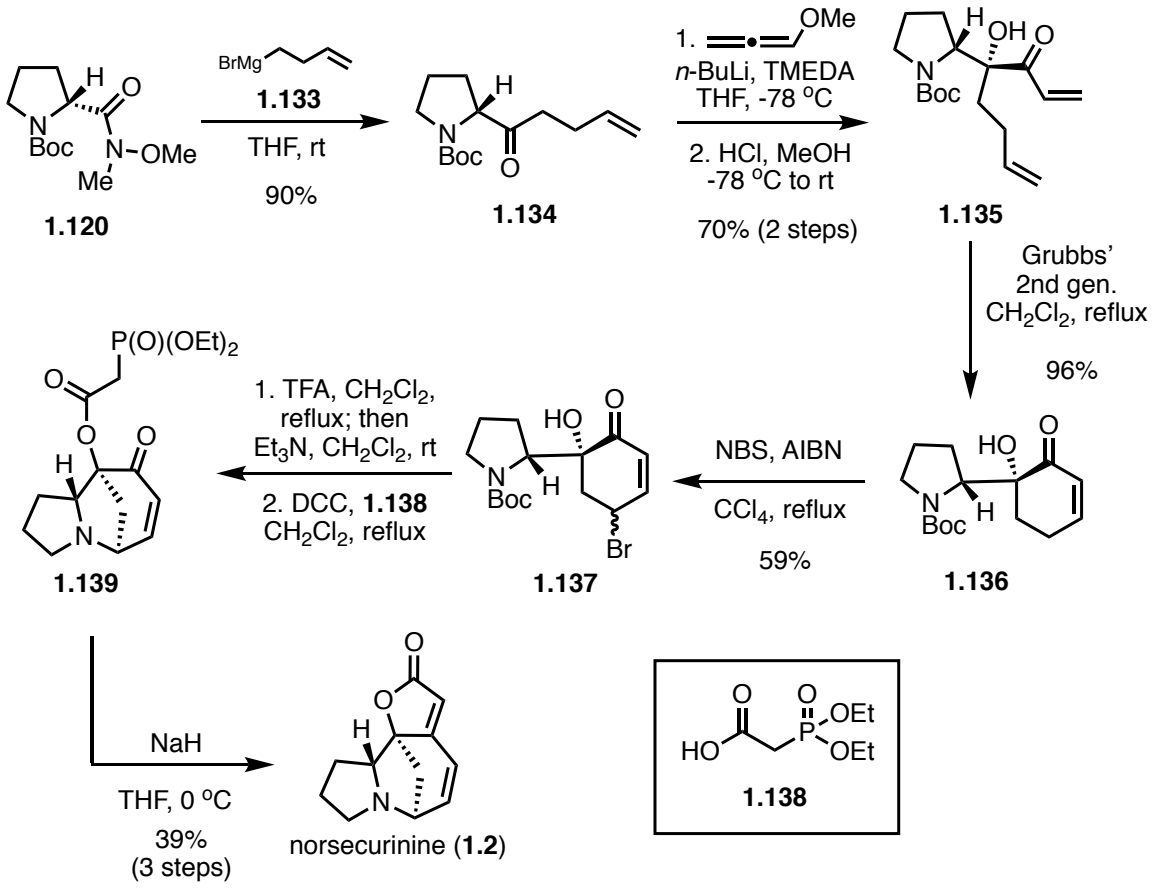

Scheme 1.24. Ye and Jiang's synthesis of norsecurinine.

With **1.2** in hand, they proceeded to prepare niruroidine (**1.46**) according to the route depicted in Scheme 1.25. Treating **1.2** with 2,2,2-trichloroethyl chloroformate (**1.140**) and K_2CO_3 smoothly generated tricyclic intermediate **1.141**, whose structure was unambiguously confirmed by X-ray crystallographic analysis. Allylic substitution of **1.141** was effected using $AgBF_4$ in acetone/H_2O to provide allylic alcohol **1.142** in 75% yield. Reductive removal of the carbamate protecting group with Zn dust in AcOH/H_2O followed by treatment with NH_3•H_2O effected 1,6-conjugate addition to provide niruroidine (**1.46**) in moderate yield. Notably, this is the only total synthesis of **1.46** reported to date.

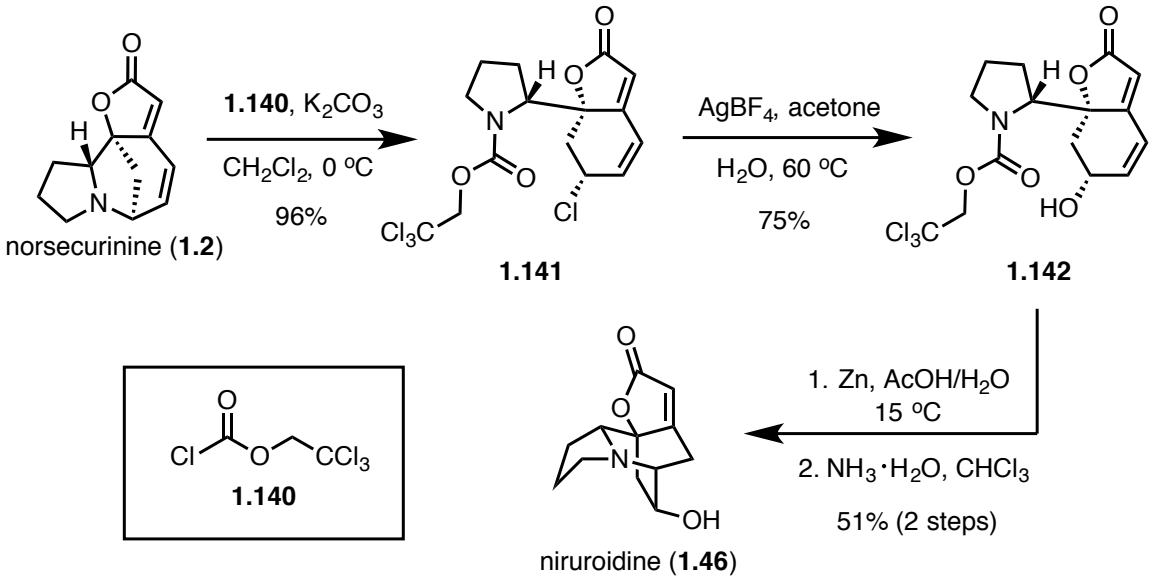

Scheme 1.25. Ye and Jiang's synthesis of niruroidine.

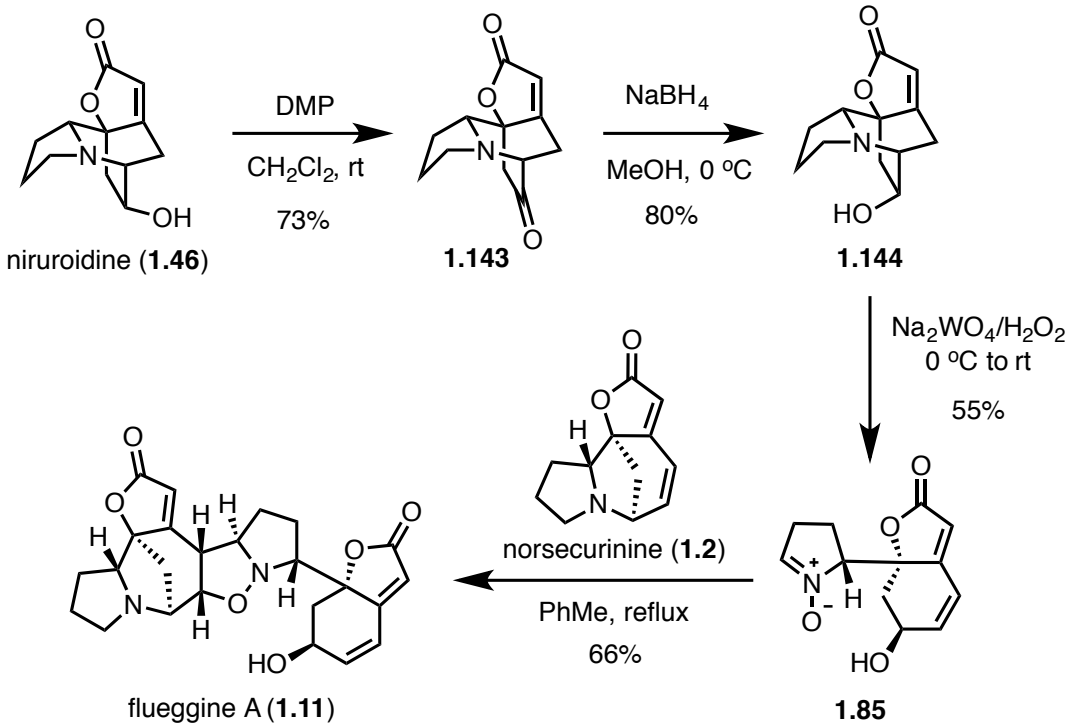

Scheme 1.26. Ye and Jiang's synthesis of flueggine A.

Finally, with **1.46** in hand, elaboration to nitrone **1.85** and completion of the flueggine A (**1.11**) synthesis was within reach. Inversion of the secondary alcohol in **1.46** was accomplished using a two-step protocol involving Dess-Martin oxidation and $NaBH_4$

reduction to provide alcohol **1.144** in 58% overall yield (Scheme 1.25). Oxidation of **1.144** to nitrone **1.85** was achieved using Na_2WO_4/H_2O_2 and then cycloaddition between **1.85** and norsecurinine (**1.2**) produced flueggine A (**1.11**) in a comparable yield to that reported by Yang/Li. Overall, the three putative relatives, norsecurinine (**1.2**), niruroidine (**1.46**), and flueggine A (**1.11**) were generated in 8, 12, and 16 steps and 14%, 5%, and 1% yield, respectively.

The renaissance of interest in the *Securinega* alkaloids over the past several decades has resulted in numerous elegant total syntheses, a trend that does not appear to be slowing down any time soon. The structural intricacies found in this natural product class continue to challenge synthetic chemists while also providing them with a platform for novel reaction development and biosynthetic investigation. Undoubtedly, if this interest persists, novel members of this family will continue to be isolated from natural sources and will serve as additional inspiration to the synthetic chemistry community.

References

(1) For general reviews on the *Securinega* alkaloids, see: (a) Snieckus, V.; The *Securinega* Alkaloids. In *The Alkaloids*; Manske, R. H. F., Ed.; Academic Press: New York, 1973; Vol. 14, pp. 425-506. (b) Chirkin E.; Atkatlian W.; Porée, F.-H.; The *Securinega* Alkaloids. In *The Alkaloids*; Knölker, H.-J., Ed.; Academic Press: New York, 2015; Vol. 74, pp. 1-120. (c) Wehlauch, R.; Gademann, K. *Asian J. Org. Chem.* **2017**, *6*, 1146.

(2) Hoffmann, P.; Kathriarachchi, H.; Wurdack, K. J. *Kew Bull.* **2006**, *61*, 37.

(3) (a) Bingtao, L.; Gilbert, M. G. Flueggea Willdenow. In *Flora of China*; An Editorial Committee, Eds.; Science Press: Beijing, 2008; Vol. 11, pp. 177-179. (b) Raj, D.; Łuczkiewicz, M. *Fitoterapia*, **2008**, *79*, 419. (c) Qin, S.; Liang, J.-Y.; Guo, Y.-W. *Helv. Chim. Acta* **2009**, *92*, 399, and references therein.

(4) Oliver-Bever, B. *J. Ethnopharaclogy* **1983**, *7*, 1.

(5) Diallo, M. S. T.; Baldé, M. A.; Camara, A.; Traoré, M. S.; Bah, M. L.; Diallo, A. S.; Camara, A. K.; Laurent, S.; Roch, A.; Muller, R. N.; Maes, L.; Pieters, L.; Baldé, A. M. *J. Plant Sci.* **2015**, *3*(1-2), 40, and references therein.

(6) (a) Zhou, M.; Zhu, H.; Wang, K.; Wei, W.; Zhang, Y. *Nat. Prod. Res.* **2012**, *26*, 762. (b) Babady-Bila; Gedris, T. E.; Herz, W. *Phytochemistry* **1996**, *41*, 1441. (c) Kaur, N.; Kaur, B.; Sirhindi, G. *Phytotherapy Res.* **2017**, *31*, 980, and references therein.

(7) Murav'eva, V. I.; Ban'kovskii, A. I. *Dokl. Akad. Nauk SSSR* **1956**, *110*, 998.

(8) (a) Saito, S.; Kotera, K.; Sugimoto, N.; Horii, Z.; Tamura Y. *Chem. Ind.* **1962**, 1652. (b) Satoda, I.; Murayama, M.; Tsuji, J.; Yoshii, E. *Tetrahedron Lett.* **1962**, *3*, 1199.

(9) Imado, S.; Shiro, M.; Horii, Z.-i. *Chem. Pharm. Bull.* **1965**, *13*, 643.

(10) (a) Gan, L.-S.; Fan, C.-Q.; Yang, S.-P.; Wu, Y.; Lin, L.-P.; Ding, J.; Yue, J.-M. *Org. Lett.* **2006**, *8*, 2285. (b) Zhao, B.-X.; Wang, Y.; Zhang, D.-M.; Jiang, R.-W.; Wang, G.-C.; Shi, J.-M.; Huang, X.-J.; Chen, W.-M.; Che, C.-T.; Ye, W.-C. *Org. Lett.* **2011**, *13*, 3888. (c) Zhang, H.; Zhang, C.-R.; Zhu, K.-K.; Gao, A.-H.; Luo, C.; Li, J.; Yue, J.-M. *Org. Lett.* **2013**, *15*, 120. (d) Zhang, H.; Wei, W.; Yue, J.-M.

Tetrahedron **2013**, *69*, 3942. (e) Zhao, B.-X.; Wang, Y.; Li, C.; Wang, G.-C.; Huang, X.-J.; Fan, C.-L.; Li, Q.-M.; Zhu, H.-J.; Chen, W.-M.; Ye, W.-C. *Tetrahedron Lett.* **2013**, *54*, 4708. (f) Zhang, H.; Han, Y.-S.; Wainberg, M. A.; Yue, J.-M. *Tetrahedron* **2015**, *71*, 3671. (g) Zhang, H.; Zhu, K.-K.; Han, Y.-S.; Luo, C.; Wainberg, M. A.; Yue, J.-M. *Org. Lett.* **2015**, *17*, 6274. (h) Zhang, H.; Han, Y.-S.; Wainberg, M. A.; Yue, J.-M. *Tetrahedron Lett.* **2016**, *57*, 1798. (i) Wang, G.-Y.; Wang, A.-T.; Zhao, B.-X.; Lei, X.-P.; Zhang, D.-M.; Jiang, R.-W.; Wang, Y.; Ye, W.-C. *Tetrahedron Lett.* **2016**, *57*, 3810.

(11) (a) Parello, J.; Munavalli, S. *C. R. Hebd. Seances Acad. Sci.* **1965**, *260*, 337. (b) Horii, Z.; Imanishi, T.; Yamauchi, M.; Hanaoka, M.; Parello, J.; Munavalli, S. *Tetrahedron Lett.* **1972**, *19*, 1877.

(12) Ohsaki, A.; Ishiyama, H.; Yoneda, K.; Kobayashi, J. *Tetrahedron Lett.* **2003**, *44*, 3097.

(13) Petchnaree, P.; Bunyapraphatsara, N.; Cordell, G. A.; Cowe, H. J.; Cox, P. J.; Howie, R. A.; Patt, S. L. *J. Chem. Soc. Perkin Trans 1*. **1986**, 1551.

(14) Zhao, B.-X.; Wang, Y.; Zhang, D.-M.; Huang, X.-J.; Bai, L.-L.; Yan, Y.; Chen, J.-M.; Lu, T.-B.; Wang, Y.-T.; Zhang, Q.-W.; Ye, W.-C. *Org. Lett.* **2012**, *14*, 3096.

(15) For the occurrence of the isoxazolidine moiety in natural products, see: (a) Berthet, M.; Cheviet, T.; Dujardin G.; Parrot, I.; Martinez, J. *Chem. Rev.* **2016**, *116*, 15235, and references therein. (b) Nge, C.-E.; Sim, K.-S.; Lim, S.-H.; Thomas, N. F.; Low, Y.-Y.; Kam, T.-S. *J. Nat. Prod.* **2016**, *79*, 2709.

(16) Spenser, I. D.; The Biosynthesis of Alkaloids and of Other Nitrogenous Secondary Metabolites. In *Comprehensive Biochemistry*; Florkin, M. and Stotz, E. H., Eds.; Elsevier Publishing Co.: Amsterdam, 1968; Vol. 20, p. 231.

(17) Parry, R. J. *Tetrahedron Lett.* **1974**, *15*, 307.

(18) Sankawa, U.; Yamasaki, K.; Ebizuka, Y. *Tetrahedron Lett.* **1974**, *15*, 1867.

(19) Golebiewski, W. M.; Horsewood, P.; Spenser, I. D. *J. Chem. Soc., Chem. Commun.* **1976**, 217.

(20) Leistner, E.; Spenser, I. D. *J. Am. Chem. Soc.* **1973**, *95*, 4715.

(21) (a) Sankawa, U.; Ebizuka, Y.; Yamasaki, K. *Phytochemistry* **1977**, *16*, 561. (b) Parry, R. J. *Bioorg. Chem.* **1978**, *7*, 277.

(22) Iminium intermediate **1.32** was proposed in ref. 21b. Alternatively, addition of **1.31** onto **1.28** might produce amine **1.33** directly.

(23) Parry, R. J. *J. Chem. Soc., Chem. Commun.* **1975**, 144.

(24) (a) Guerriero, A.; Pietra, F. *Phytochemistry* **1984**, *23*, 2394. (b) Bachman, T. L.; Ghia, F.; Torssell, K. B. G. *Phytochemistry* **1993**, *33*, 189. (c) Kuster, R. M.; Mors, W. B.; Wagner, H. *Biochem. Syst. Ecol.* **1997**, *25*, 675. (d) Youkwan, J.; Srisomphot, P.; Sutthivaiyakit, S. *J. Nat. Prod.* **2005**, *68*, 1006.

(25) For the biosynthetic origin of the pyrrolidine ring of nicotine, see: (a) Leete, E.; Siegfried, K. J. *J. Am. Chem. Soc.* **1957**, *79*, 4529. (b) Lamberts, B. L.; Dewey, L. J.; Byerrum, R. U. *Biochem. et Biophys. Acta* **1959**, *33*, 22. (c) Leete, E.; Gros, E. G.; Gilbertson, T. J. *Tetrahedron Lett.* **1964**, *11*, 587.

(26) Magnus, P.; Ródriguez-López, J.; Mulholland, K.; Matthews, I. *Tetrahedron* **1993**, *49*, 8059.

(27) Ma, N.; Yao, Y.; Zhao, B.-X.; Wang, Y.; Ye, W.-C.; Jiang, S. *Chem. Commun.* **2014**, *50*, 9284.

(28) Wehlauch, R.; Grendelmeier, S. M.; Miyatake-Ondozabal, H.; Sandtorv, A. H.; Scherer, M.; Gademann, K. *Org. Lett.* **2017**, *19*, 548.

(29) Finefield, J. M.; Sherman, D. H.; Kreitman, M.; Williams, R. M. *Angew. Chem. Int. Ed.* **2012**, *51*, 4802 and references therein.

(30) Zhang, H.; Zhu, K.-K.; Gao, X.-H.; Yue, J.-M. *Tetrahedron* **2017**, *73*, 4692.

(31) Nakano, T.; Terao, S.; Lee, K. H.; Saeki, Y.; Durham, L. J. *J. Org. Chem.* **1966**, *31*, 2274.

(32) Wang, Z.; Meisenheimer Rearrangement. In *Comprehensive Organic Name Reactions and Reagents*; John Wiley & Sons, Inc., 2010; pp. 1889-1892 and references therein.

(33) Magnus, P.; Padilla, A. I. *Org. Lett.* **2006**, *8*, 3569.

(34) Magnus, P.; Rodríguez-López, J.; Mulholland, K.; Matthews, I. *J. Am. Chem. Soc.* **1992**, *114*, 382.

(35) For computational studies of biosynthetic [3+2] nitrone cycloadditions, see: (a) Krenske, E. H.; Patel, A.; Houk, K. N. *J. Am. Chem. Soc.* **2013**, *135*, 17638. (b) Painter, P. P.; Pemberton, R. P.; Wong, B. M.; Ho, K. C.; Tantillo, D. J. *J. Org. Chem.* **2014**, *79*, 432.

(36) For recent total syntheses employing biomimetic [3+2] nitrone cycloadditions, see Ref 27 and: (a) Miyatake-Ondozabal, H.; Bannwart, L. M.; Gademann, K. *Chem. Commun.* **2013**, *125*, 648. (b) Wei, H.; Qiao, C.; Liu, G.; Yang, Z.; Li, C.-C. *Angew. Chem. Int. Ed.* **2013**, *52*, 620. (c) Hong, A. Y.; Vanderwal, C. D. *J. Am. Chem. Soc.* **2015**, *137*, 7306. (d) Hong, A. Y.; Vanderwal, C. D. *Tetrahedron* **2016**, *73*, 4160.

(37) For synthetic studies towards pyridomacrolidin employing a biomimetic [3+2] nitrone cycloaddition, see: (a) Irlapati, N. R.; Baldwin, J. E.; Adlington, R. M.; Pritchard, G. J. *Org. Lett.* **2003**, *5*, 2351. (b) Irlapati, N. R.; Baldwin, J. E.; Adlington, R. M.; Pritchard, G. J.; Cowley, A. R. *Tetrahedron* **2006**, *62*, 4603.

(38) (a) Payne, K. A. P.; White, M. D.; Fisher, K.; Khara, B.; Bailey, S. S.; Parker, D.; Rattray, N. J. W.; Trivedi, D. K.; Goodacre, R.; Beveridge, R.; Barran, P.; Rigby, S. E. J.; Scrutton, N. S.; Hay, S.; Leys, D. *Nature*, **2015**, *522*, 497. (b) White, M. D.; Payne, K. A. P.; Fisher, K.; Marshall, S. A.; Parker, D.; Rattray, N. J. W.; Trivedi, D. K.; Goodacre, R.; Rigby, S. E. J.; Scrutton, N. S.; Hay, S.; Leys, D. *Nature*, **2015**, *522*, 502.

(39) Ferguson, K. L.; Eschweiler, J. D.; Ruotolo, B. T.; Marsh, E. N. G. *J. Am. Chem. Soc.* **2017**, *139*, 10972.

(40) The first known natural sample of (+)-allonorsecurinine was recently isolated from *Phyllanthus fraternus*: Komlaga, G.; Genta-Jouve, G.; Cojean S.; Dickson, R. A.; Mensah, M. L. K.; Loiseau, P. M.; Champy, P.; Beniddir, M. A. *Tetrahedron Lett.* **2017**, *58*, 3754.

(41) For discussions of the biological activities of securinine, see Ref. 1 and: Zhang, W.; Li, J.-Y.; Lan, P.; Sun, P.-H.; Wang, Y.; Ye, W.-C.; Chen, W.-M. *J. Chin. Pharm. Sci.* **2011**, *20*, 203, and references therein.

(42) Turova, A. D.; Aleshkina, Y. A. *Farmakol. I Toksikol* **1956**, *19*, 11.

(43) Friess, S. L.; Durant, R. C.; Whitcomb, E. R.; Reber, L. J.; Thommesen, W. C. *Toxicol. Appl. Pharmacol.* **1961**, *3*, 347.

(44) *Gosudarstvennaya Farmakopeja SSSR*, 10th ed.; Moscow Medicina, 1968; pp 612–614.

(45) Mashkovskii, M. D.; *Lekarstvennye Sredstva*, 14th ed.; Moscow Novaya Volna: 2002, Vols. 1 and 2.

(46) Beutler, J. A.; Karbon, E. W.; Brubaker, A. N.; Malik, R.; Curtis, D. R.; Enna, S. J. *Brain Res.* **1985**, *330*, 135.

(47) Rognan, D.; Boulanger, T.; Hoffmann, R.; Vercauteren, D. P.; Andre, J.-M.; Durant, F.; Wermuth, C.-G. *J. Med. Chem.* **1992**, *35*, 1969.

(48) Beutler, J. A.; Brubaker, A. N. *Drugs Fut.* **1987**, *12*, 957.

(49) Copperman, R.; Copperman, G.; Der Marderosian, A. *Pennsylvania Med.* **1973**, *76*, 36.

(50) Lin, X.; Jun-tian, Z. *Neurological Res.* **2004**, *26*, 792.

(51) Leonoudakis, D.; Rane, A.; Angeli, S.; Lithgow, G. J.; Andersen, J. K.; Chinta, S. J. *Mediators of Inflammation* **2017**, 8302636.

(52) Marczynski, T. J. *Brain Res. Bull.* **1998**, *45*, 341.

(53) Rana, S.; Gupta, K.; Gomez, J.; Matsuyama, S.; Chakrabarti, A.; Agarwal, M. L.; Agarwal, A.; Agarwal, M. K.; Wald, D. N. *Faseb J.* **2010**, *24*, 2126.

(54) Dong, N. Z.; Gu, Z.-L.; Chou, W.-H.; Kwok, C.-Y. *Acta Pharm. Sin.* **1999**, *20*, 267.

(55) Han, S.; Zhang, G.; Li, M.; Chen, D.; Wang, Y.; Ye, W.; Ji, Z. *Oncol. Rep.* **2014**, *31*, 2245.

(56) Ohsaki, A.; Kobayashi, Y.; Yoneda, K.; Kishida, A.; Ishiyama, H. *J. Nat. Prod.* **2007**, *70*, 2003.

(57) Tatematsu, H.; Mori, M.; Yang, T.-H.; Chang, J.-J.; Lee, T. T.-Y.; Lee, K.-H. *J. Pharm. Sci.* **1991**, *80*, 325.

(58) McNulty, J.; Poloczek, J.; Larichev, V.; Werstiuk, N. H.; Griffin, C.; Pandey, S. *Planta Med.* **2007**, *73*, 1543.

(59) Reproduced in part from Ref. 1b.

(60) Chen, C.-R.; Xia, Y.-H.; Yao, S.-Y.; Zhang, Q.; Wang, Y.; Ji, Z.-N. *Pharmazie* **2012**, *67*, 351.

(61) Hou, W.; Wang, Z.-Y.; Peng, C.-K.; Lin, J.; Liu, X.; Chang, Y.-Q.; Xu, J.; Jiang, R.-W.; Lin, H.; Sun, P.-H.; Chen, W.-M. *Eur. J. Med. Chem.* **2016**, *122*, 149.

(62) (a) Perez, M.; Ayad, T.; Maillos, P.; Poughon, V.; Fahy, J.; Ratovelomanana-Vidal, V. *Synlett* **2016**, *27*, 1077. (b) Perez, M.; Ayad, T.; Maillos, P.; Poughon, V.; Fahy, J.; Ratovelomanana-Vidal, V. *Eur. J. Org. Chem.* **2016**, *109*, 287. (c) Perez, M.; Ayad, T.; Maillos, P.; Poughon, V. Fahy, J.; Ratovelomanana-Vidal, V. *ACS Med. Chem. Lett.* **2016**, *7*, 403.

(63) Weenen, H.; Nkunya, M. H. H.; Bray, D. H.; Mwasumbi, L. B.; Kinabo, L. S.; Kilimali, V. A. E. B.; Wijnberg, J. B. P. A. *Planta Med.* **1990**, *56*, 371.

(64) Mensah, J. L.; Lagarde, I.; Ceschin-Roques, C.; Michel, G.; Gleye, J.; Fouraste, I. *J. Ethnopharmacol.* **1990**, *28*, 129.

(65) Goel, M.; Maurya, S.; Pandey V. B.; Singh, V. P.; Singh, A. K.; Singh, U. P. *Mycobiology* **2002**, *30*, 225.

(66) Sahni, S.; Maurya, S.; Singh, U. P. Singh, A. K.; Singh, V. P.; Pandey, V. B. *Mycobiology* **2005**, *33*, 97.

(67) (a) Zhang, H.; Zhang, C.-R.; Han, Y.-S.; Wainberg, M. A.; Yue, J.-M. *RSC Adv.* **2015**, *5*, 107045. (b) Zhang, H.; Han, Y.-S.; Wainberg, M. A.; Yue, J.-M. *Tetrahedron*, **2015**, *71*, 3671. (c) Zhang, H.; Zhu, K.-K.; Han, Y.-S.; Luo, C.; Wainberg, M. A.; Yue, J.-M. *Org. Lett.* **2015**, *17*, 6274. (d) Zhang, H.; Han, Y.-S.; Wainberg, M. A.; Yue, J.-M. *Tetrahedron Lett.* **2016**, *57*, 1798.

(68) For reviews on the syntheses of *Securinega* alkaloids, see Refs. 1, 41 and: Jeon, S.; Park, J.; Han, S. *Synlett* **2017**, *28*, 2353.

(69) Horii, Z.; Yamawaki, Y.; Tamura, Y. *Tetrahedron*, **1967**, *23*, 1165.

(70) Heathcock, C. H.; vin Geldern, T. W. *Heterocycles* **1987**, *25*, 75.

(71) Jacobi, P. A.; Blum, C. A.; DeSimone, R. W.; Udodong, U. E. S. *J. Am. Chem. Soc.* **1991**, *113*, 5384.

(72) Savige, W. E. *Aust. J. Chem.* **1961**, *14*, 664.

(73) (a) Han, G.; LaPorte, M. G.; Folmer, J. J.; Werner, K. M.; Weinreb, S. M. *Angew. Chem. Int. Ed.* **2000**, *39*, 237. (b) Han, G.; LaPorte, M. G.; Folmer, J. J.; Werner, K. M.; Weinreb, S. M. *J. Org. Chem.* **2000**, *65*, 6293. (c) Honda, T.; Namiki, H.; Kudoh, M.; Watanabe, N.; Nagase, H.; Mizutani, H. *Tetrahedron Lett.* **2000**, *41*, 5927. (d) Liras, S.; Davoren, J. E.; Bordner, J. *Org. Lett.* **2001**, *3*, 703. (e) Honda, T.; Namiki, H.; Watanabe, M.; Mizutani, H. *Tetrahedron Lett.* **2004**, *45*, 5211. (f) Alibés, R.; Ballbé, M.; Busqué, F. de March, P.; Elias, L.; Figueredo, M.; Font, J. *Org. Lett.* **2004**, *6*, 1813. (g) Honda, T.; Namiki, H.; Watanabe, M.; Mizutani, H. *Org. Lett.* **2004**, *6*, 87. (h) Alibé, R.; Bayón, P.; de March, P.; Figuerdo, M.; Font, J.; Garciá-Garciá, E.; González-Gálvez, D. *Org. Lett.* **2005**, *7*, 5107. (i) Bardají, G. G.; Cantó, M.; Alibés, R.; Bayón, P.; Busqué, F.; de March, P.; Figuerdo, M.; Font, J. *J. Org. Chem.* **2008**, *73*, 7657. (j) Leduc, A. B.; Kerr, M. A. *Angew. Chem. Int. Ed.* **2008**, *47*, 7945. (k) Dhudshia, B.; Cooper, B. F. T.; Macdonald, C. L. B.; Thadani, A. N. *Chem. Commun.* **2009**, 463. (l) González-Gálvez, D.; Garciá-Garciá, E.; Alibé, R.; Bayón, P.; de March, P.; Figuerdo, M.; Font, J. *J. Org. Chem.* **2009**, *74*, 6199. (m) Medeiros, M. R.; Wood, J. L. *Tetrahedron* **2010**, *66*, 4701. (n) Sathish Reddy, A.; Srihari, P. *Tetrahedron Lett.* **2012**, *53*, 5926. (o) Chen, J.-H.; Levine, S. R.; Buergler, J. F.; McMahon, T. C.; Medeiros, M. R.; Wood, J. L. *Org. Lett.* **2012**, *14*, 4531. (p) Zheng, X.; Liu, J.; Ye, C.-X.; Wang, A.; Wang, A.-E.; Huang, P.-Q. *J. Org. Chem.* **2015**, *80*, 1034.

(74) Carson, C. A.; Kerr, M. A. *Angew. Chem. Int. Ed.* **2006**, *45*, 6560.

(75) Liu, P.; Hong, S.; Weinreb, S. M. *J. Am. Chem. Soc.* **2008**, *130*, 7562.

(76) Han, H.; Smith, III, A. B. *Org. Lett.* **2015**, *17*, 4232.

(77) Bélanger, G.; Dupuis, M.; Larouche-Gauthier, R. *J. Org. Chem.* **2012**, *77*, 3215.

(78) Jeon, S.; Han, S. *J. Am. Chem. Soc.* **2017**, *139*, 6302.

CHAPTER 2

Retrosynthetic Analysis of Virosaine A and Enantioselective Synthesis of the Virosaine Core

2.1 Introduction

Virosaine A (**1.24**) contains several structural characteristics that make it a remarkably complex natural product (Figure 2.1).[1] Despite the fact that **1.24** only contains 12 carbon atoms, it possesses a densely functionalized caged pentacyclic core that is comprised of multiple bridged bicycles, 6 stereocenters, and an isoxazolidine ring. Interestingly, the latter is a rare motif in natural products and its presence in **1.24** was proposed to be the result of a unique biosynthetic [3+2] nitrone cycloaddition.[1] Collectively, these features make **1.24** a challenging target for total synthesis and offer an excellent opportunity for novel reaction development. Intrigued by its fascinating structural features and putative biosynthetic origin, we initiated a project with the aim of completing a total synthesis of **1.24**. Moreover, we set a goal to develop efficient and strategic bond-forming reaction sequences that would not only allow us to prepare such an intricate molecule, but would enable us to do so in a concise manner. Chapter 2 describes our retrosynthetic analysis of **1.24** and the enantioselective synthesis of its core structure. The development of a one-pot procedure to access a highly functionalized bromohydrin intermediate and the implementation of a novel cascade reaction sequence were crucial to both the success and efficiency of the approach described herein.[2]

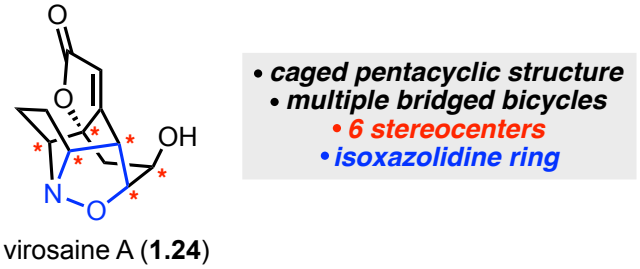

Figure 2.1. Notable structural features of virosaine A.

2.2 Retrosynthetic Analysis of Virosaine A

At the time we began our studies, the putative biosynthetic [3+2] nitrone cycloaddition to generate virosaine A (**1.24**) had not been investigated synthetically. However, we felt that successful incorporation of this step into a synthesis of **1.24** would not only provide evidence to support its occurrence in nature but would also greatly simplify the assembly of the congested virosaine core.[3,4] Indeed, retrosynthetic analysis of **1.24** revealed that a late-stage biomimetic [3+2] cycloaddition of nitrone **1.70** would

markedly simplify the target structure (Scheme 2.1). In particular, this disconnection reduces the number of rings in the molecule from 5 to 3 as well as the number of stereocenters from 6 to 3. However, cycloaddition precursor **1.70** displayed its own set of challenging structural features. Specifically, both the nitrone and α,β,γ,δ-unsaturated lactone are highly reactive groups that might serve as potential liabilities in the synthesis if they are generated prior to the final step. Moreover, the C8 hydroxyl group would likely also require protection throughout the synthesis in order to prevent unwanted participation in other reactions. In light of these concerns, we identified lactone **2.1** as an alternative precursor to **1.24** *via* a β-elimination. Importantly, this retrosynthetic maneuver effectively masked both the butenolide and C8 hydroxyl of **1.24**.

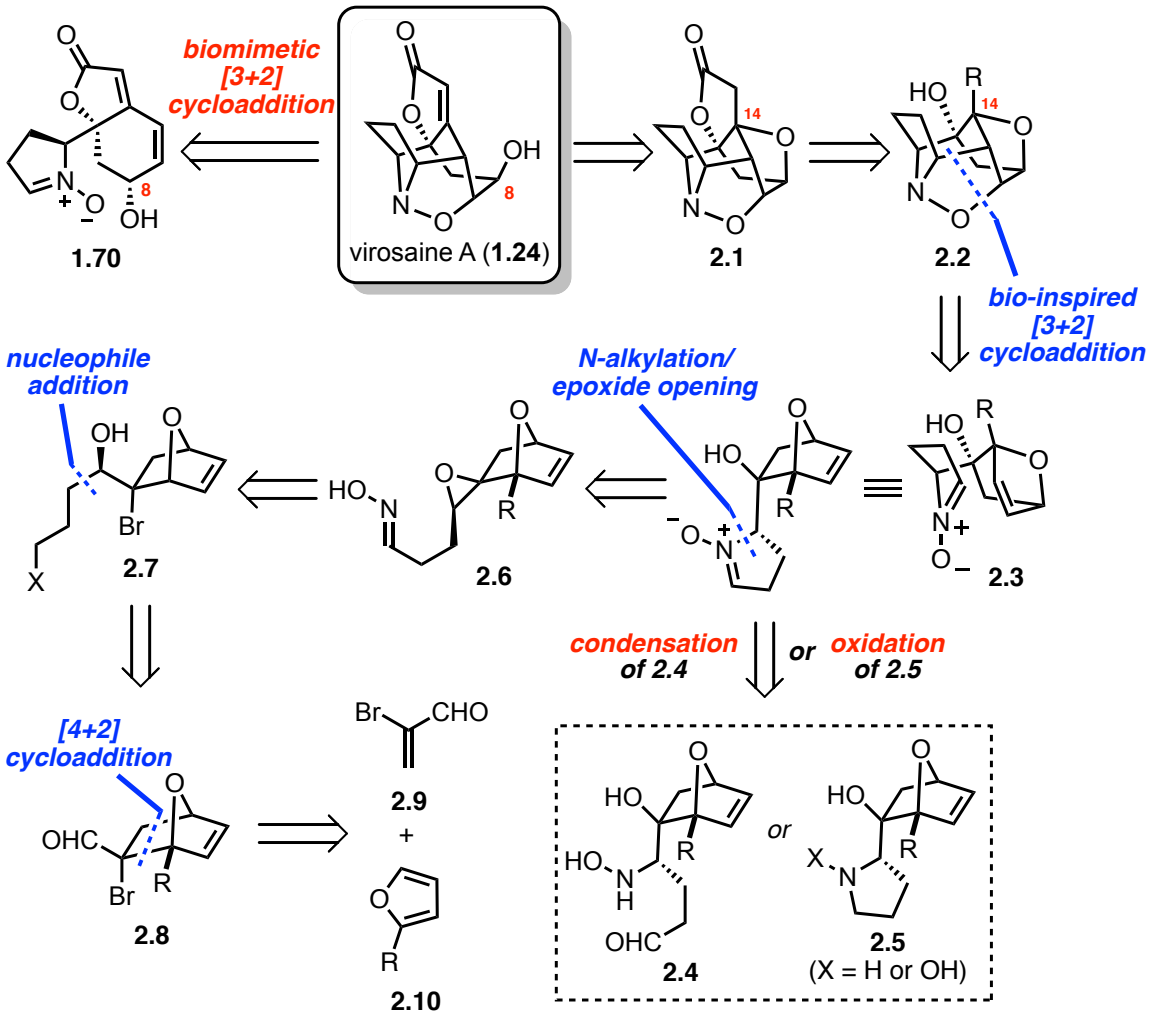

Scheme 2.1. Retrosynthetic analysis of virosaine A.

Hexacycle **2.1** was simplified to pentacycle **2.2**, with an unspecified R group at C14 that could eventually be elaborated into the butanolide in **2.1.** Furthermore, we hypothesized that pentacycle **2.2** might arise *via* a bio-inspired [3+2] nitrone cycloaddition of **2.3**. Analogous to the biomimetic cycloaddition described above, this transformation would not only assemble the caged core of the natural product but would also serve to set 3 of its 6 stereocenters in a single step. We then considered several different strategies that might be used to install the requisite nitrone in **2.3**, including either intramolecular condensation of aldehyde **2.4** or oxidation of **2.5**. However, these two approaches were deemed to be unsatisfactory for several reasons. In particular, the condensation strategy would require stereoselective installation of the hydroxylamine moiety in **2.4**, which would likely require several undesired functional group manipulations/protections. Moreover, oxidation of **2.5** might lead to the formation of the regioisomeric nitrone product. Alternatively, we identified a more attractive strategy that involved intramolecular opening of a trisubstituted epoxide with a pendant oxime, leading back to **2.6**. The advantage of this method is that it would efficiently install the nitrone in a stereospecific fashion and would eliminate any need for an oxidation event. Furthermore, our goal was to implement this epoxide-opening step in tandem with the subsequent nitrone cycloaddition (**2.6**→**2.3**→**2.2**). The successful development of this cascade reaction sequence would enable efficient and rapid entry into the complex virosaine core and would provide a foundation for a concise total synthesis of **1.24**. The proposed cascade precursor **2.6** should be accessible from bromohydrin **2.7**, which in turn might arise from the diastereoselective addition of a suitable nucleophile onto α-bromo aldehyde **2.8**. Finally, aldehyde **2.8** might be generated *via* Diels-Alder cycloaddition of 2-bromoacrolein (**2.9**) and substituted furan **2.10**.[5]

2.3 Model Cascade Reaction Sequence

Given that the proposed bio-inspired cascade reaction sequence to access the caged pentacycle **2.2** was a focal point of the synthetic plan, we initially pursued a model study to assess the feasibility of this approach. Cascade reactions involving sequential nitrone formation/[3+2] nitrone cycloaddition (1,3-dipolar cycloaddition) have provided a platform for rapid complexity generation and have found use in several recent total

syntheses.[6,7] A commonly employed approach for nitrone formation in these cascade reaction sequences has been conjugate addition of an oxime onto a Michael acceptor. Of note, Stockman and Fuchs developed an intramolecular conjugate addition/nitrone cycloaddition strategy to access the cores of both histrionicotoxin (**2.15**) and perhydrohistrionicotoxin (**2.16**) (Scheme 2.2).[7a,b] Specifically, they found that heating ketone **2.11** with hydroxylamine generated an oxime intermediate (not shown) that underwent spontaneous conjugate addition onto one of the α,β-unsaturated nitrile moieties to deliver nitrone **2.12a**. This nitrone intermediate proceeded to undergo a subsequent [3+2] cycloaddition to give tricyclic isoxazolidine **2.13** in 89% yield in one pot. Heating **2.13** (180 °C, sealed tube) provided the bridged isoxazolidine **2.14**, which represents the core structure of both **2.15** and **2.16**, in 95% yield. This transformation likely proceeds *via* sequential retro-[3+2] of isoxazolidine **2.13**/[3+2] cycloaddition of nitrone conformer **2.12b**.

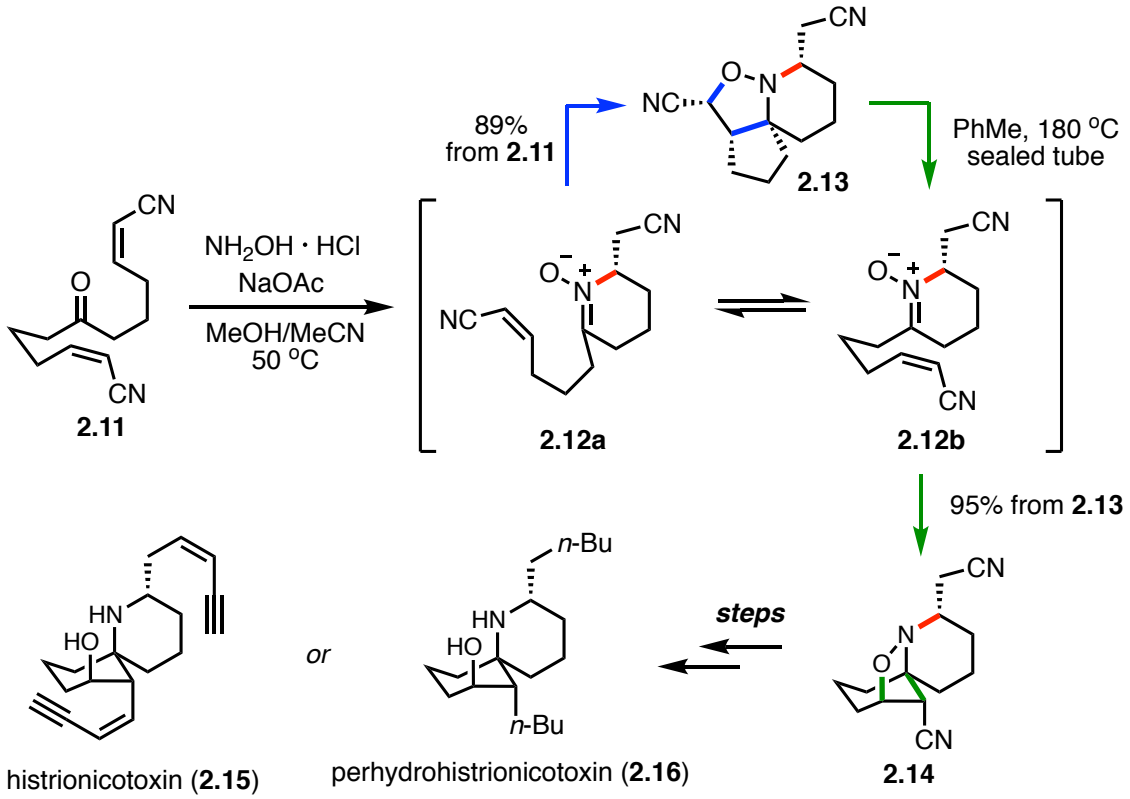

Scheme 2.2. Stockman and Fuchs' conjugate addition/[3+2] nitrone cycloaddition cascade strategy for the total synthesis of histrionicotoxin and perhydrohistrionicotoxin.

Padwa and coworkers utilized a similar strategy in their total syntheses of 2,7,8-*epi*-perhydrohistrionicotoxin (**2.22**), cylindricine C (**2.25**), and yohimbenone (**2.28**) (Scheme 2.3).[7c,e,f] However, instead of intramolecular conjugate addition, the nitrone intermediates were generated *via* intermolecular conjugate addition of an oxime onto 2,3-bis(phenylsulfonyl)-1,3-butadiene (**2.18**). Subsequent intramolecular [3+2] cycloaddition produced the cascade products in good yields. The same group applied this methodology for the formal synthesis of the halichlorine core.[7g]

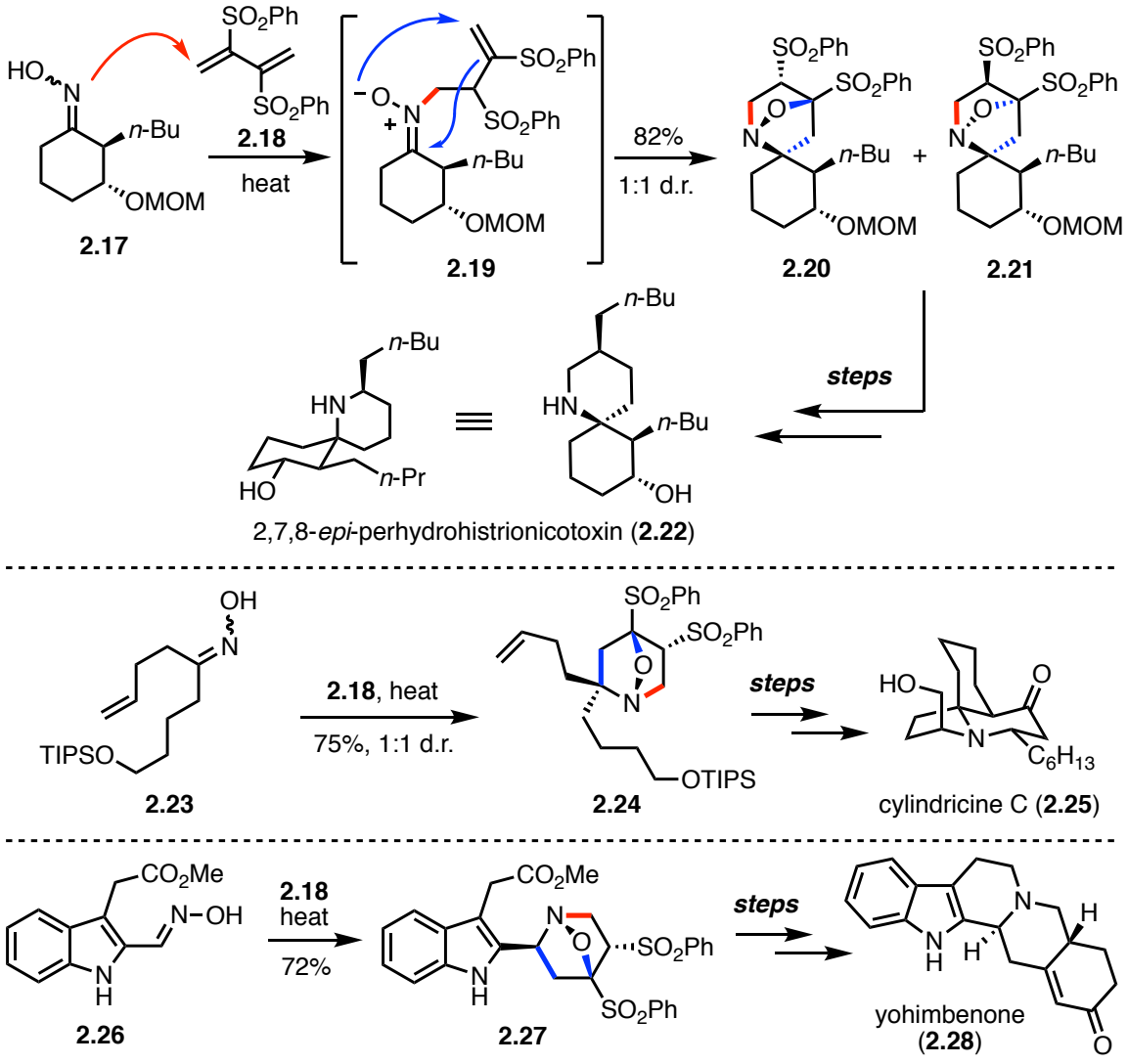

Scheme 2.3. Padwa's intermolecular conjugate addition/[3+2] nitrone cycloaddition strategy for the total syntheses of 2,7,8-*epi*-perhydrohistrionicotoxin, cylindricine C, and yohimbenone.

An alternative but related strategy was employed by Burrell and Coldham et al. in their total synthesis of myrioxazine A (**2.32**) (Scheme 2.4).[7d] In this case, formation of nitrone intermediate **2.30** was achieved *via* intramolecular alkylation of an *in situ* generated oxime derived from aldehyde **2.29**. Subsequent intramolecular cycloaddition provided the fused tricyclic product **2.31** in 77% yield from **2.29**.

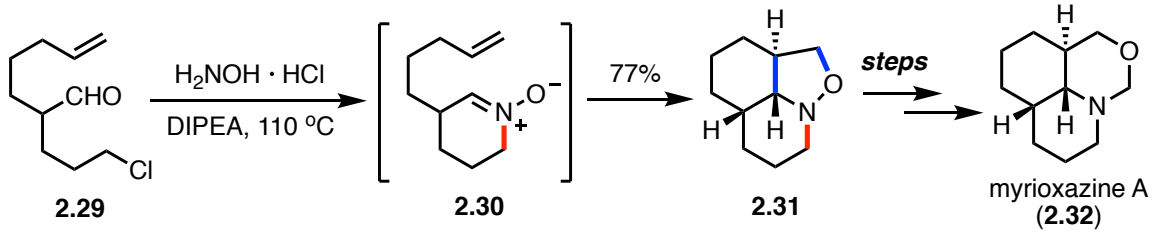

2.29 **2.30** **2.31**

Scheme 2.4. Burrell and Coldham's sequential intramolecular alkylation/[3+2] nitrone cycloaddition strategy for the total synthesis of myrioxazine A.

While these elegant examples offer valuable insight into the potential of such a transformation, there is limited literature precedent for cascades that specifically involve an intramolecular epoxide opening/intramolecular nitrone cycloaddition, with only one reported example prior to our work. Specifically, Grigg and coworkers demonstrated that heating oxime **2.33** resulted in *N*-alkylative epoxide opening to generate nitrone **2.34**, which underwent a subsequent [3+2] cycloaddition to yield the angularly fused tricycle **2.35** (Scheme 2.5 A).[6f] However, to the best of our knowledge, there were no examples of such a cascade to access bridged systems similar to that found in the virosaine core. As such, we identified acyclic epoxy oxime **2.36** as a simplified model substrate with which we could probe the feasibility of our proposed cascade transformation (Scheme 2.5 B).

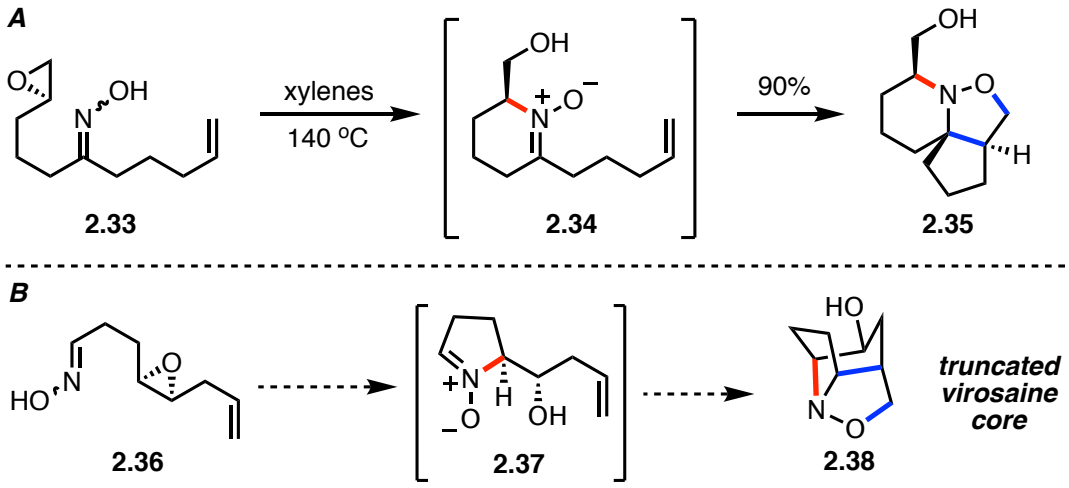

Scheme 2.5. (A) Grigg's intramolecular epoxide opening/[3+2] nitrone cycloaddition cascade reaction sequence and (B) proposed cascade reaction sequence to access truncated virosaine core **2.38**.

2.3.1 Synthesis of the Model Cascade Precursor

The synthesis of oxime **2.36** commenced with sequential silyl protection and allylation of 4-pentyn-1-ol (**2.39**) to provide enyne **2.40** in excellent yield over two steps (Scheme 2.6). With enyne **2.40** in hand, stereoselective semi-hydrogenation to the corresponding *cis* skipped diene **2.41** was studied. However, this transformation proved to be more challenging than originally anticipated due to the susceptibility of diene **2.41** to over-reduction. As a result, the undesired alkene **2.42** was always generated alongside the desired product **2.41**.

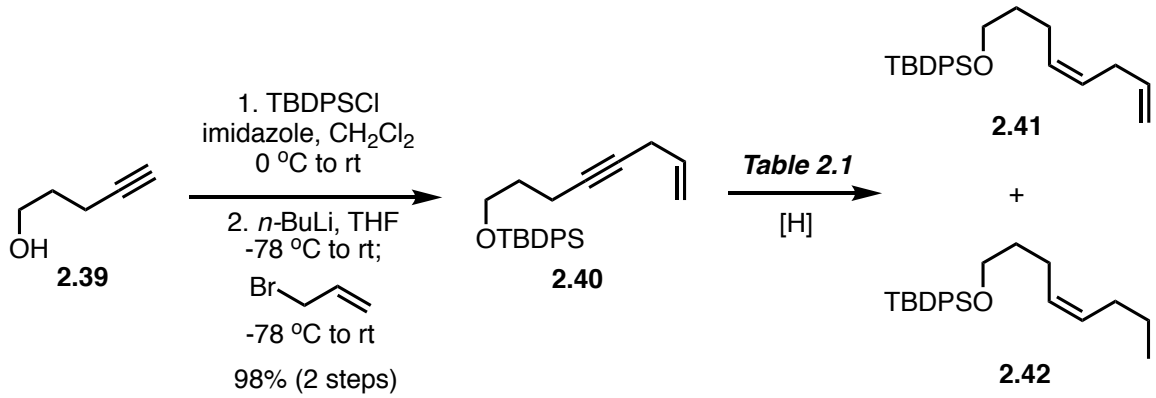

Scheme 2.6. Synthesis of diene **2.41**.

When enyne **2.40** was submit to standard Lindlar reduction conditions (H_2, Lindlar catalyst, quinoline, hexanes, rt) for 1 h, the desired diene **2.41** was generated as a 2.1:1 mixture alongside over-reduction product **2.42**. As a result, **2.41** was only isolated in an unsatisfactory 53% yield (Table 2.1, entry 1). The sensitivity of diene **2.41** to over-reduction under these reaction conditions is highlighted in entry 2, where an increase in reaction time further diminished the ratio of **2.41**:**2.42** to 1:1. 1-Alkene solvents have been shown to prevent undesired over-reduction of terminal olefins during semi-hydrogenation reactions.[8] Unfortunately, Lindlar reduction of **2.40** in 1-hexene only produced a complex mixture of products, from which diene **2.41** could not be identified (entry 3). Gratifyingly, we found that reduction of **2.40** using nickel boride/H_2 resulted in an improvement in the ratio of **2.41**:**2.42** (entry 4).[9,10] Moreover, this procedure proved to be more reproducible than its Lindlar reduction counterpart and could be run on gram-scale to consistently provide the desired diene **2.41** in an acceptable 63% isolated yield (entry 5).

Table 2.1. Stereoselective Semi-Hydrogenation of Enyne **2.40**.

Entry	Conditions[a]	Time (h)	Ratio of 2.41:2.42[b]	Isolated Yield of 2.41 (%)
1	H_2, Lindlar catalyst,[c] quinoline, hexanes	1	2.1:1	53
2	H_2, Lindlar catalyst,[c] quinoline, hexanes	4	1:1	n.d.
3	H_2, Lindlar catalyst,[c] quinoline, 1-hexene	8	n.d.[d]	n.d.
4[e]	H_2, $Ni(OAc)_2 \bullet 4H_2O$, $NaBH_4$, $(NH_2CH_2)_2$, MeOH	1	2.9:1	70
5[f]	**H_2, $Ni(OAc)_2 \bullet 4H_2O$, $NaBH_4$, $(NH_2CH_2)_2$, MeOH**	**0.5**	**2.3:1**	**63**

[a]All reactions were conducted at room temperature under 1 atm. of H_2. [b]Determined by integration of the crude ^1H NMR spectrum. [c]Palladium on calcium carbonate, poisoned with lead (5% Pd content). [d]Complex mixture. [e]0.07 mmol scale. [f]4 mmol scale.

Having established a reliable route to diene **2.41**, silyl deprotection smoothly delivered alcohol **2.43** (Scheme 2.7). Disappointingly, several conditions failed to convert dienol **2.43** to mono-epoxide **2.46**. Moreover, the corresponding aldehyde **2.44** also proved to be an incompetent substrate for oxidation to epoxy aldehyde **2.48**. Alternatively, chemoselective *m*-CPBA oxidation of the internal olefin in the TBDPS-protected diene **2.41** effectively generated epoxide **2.45** in 83% yield. Protecting group removal and oxidation to aldehyde **2.48** proceeded in 83% yield over two steps. Of note, epoxide **2.46** was found to spontaneously cyclize to tetrahydrofuran **2.47** upon exposure to acid (even in trace amounts) and thus, extreme care had to be taken during its purification and handling. Finally, model oxime **2.36** was prepared as a *ca*. 1:1 mixture of *E*/*Z* isomers *via* condensation of aldehyde **2.48** with hydroxylamine.

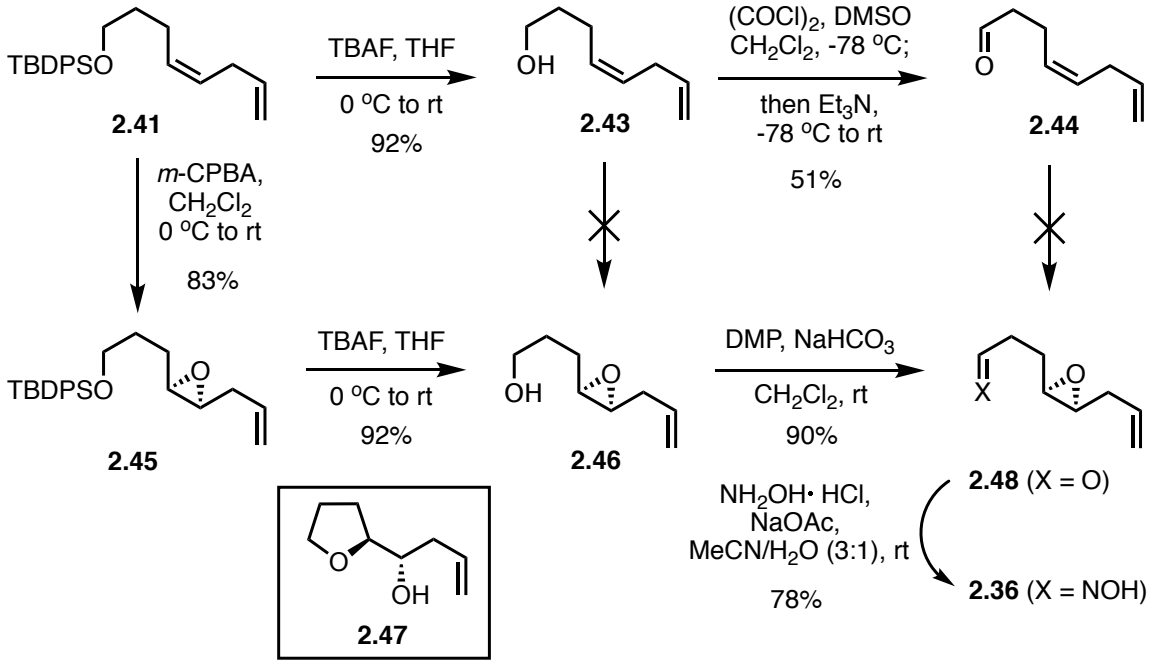

Scheme 2.7. Synthesis of model cascade precursor **2.36**.

2.3.2 Optimization of Model Cascade Reaction Sequence

With oxime **2.36** in hand, the epoxide-opening/nitrone cycloaddition cascade reaction sequence to access the bridged tricycle **2.38** was investigated (Scheme 2.8). Following the report by Grigg and coworkers, we initially heated **2.36** in xylenes at 140 °C and were pleased to find that the desired product **2.38** was in fact generated. However, the yield of the overall process suffered due to the sluggish nature of the initial epoxide-

opening step, as indicated by the persistence of **2.36** in the reaction mixture. As a result, extended reaction times were required to drive the reaction to completion and led to significant decomposition. This observation led us to screen various additives in the reaction to promote the initital epoxide-opening step. Accordingly, we found that when LiCl was employed as a mild Lewis acid additive in the reaction, oxazine **2.49** was produced as the major product in 53% yield. Notably, nitrone **2.37** was also isolated as a minor product (21% yield) along with 21% recovered starting material. This result suggests that LiCl only serves to activate the epoxide towards nucleophilic opening by both oxime isomers and does not facilitate a kinetically competitive oxime *E*/*Z* isomerization. In contrast, employing K_2CO_3 as an additive exclusively generated nitrile **2.50** in 65% yield, presumably *via* initial *O*-alkylation to give oxazine **2.49** followed by subsequent base-mediated Kemp elimination.[11] Evidence to support this proposal was gained by subjecting **2.49** to the same reaction conditions, which resulted in clean conversion to nitrile **2.50** in 84% yield. Ultimately, we found that the use of protic acids, such as *para*-toluenesulfonic acid (*p*-TSA), promoted rapid *N*-alkylation at room temperature to generate nitrone **2.37** in 81% yield. In addition to serving as an epoxide activator, the protic acid also appeared to facilitate oxime *E*/*Z* isomerization to access the required *E* isomer for cyclization to nitrone **2.37**. Gratifyingly, heating **2.37** in xylenes effected the [3+2] cycloaddition to produce **2.38** in 78% yield as a 7:1 mixture alongside the regioisomeric cycloadduct **2.51**. Furthermore, we were pleased to find that the use of catalytic protic acid at elevated temperatures (5 mol % PPTS, xylenes, 140 ^{o}C) generated **2.38** in 48% yield in a single pot process from oxime **2.36**, thereby establishing the feasibility of this cascade approach to access a simplified bridged virosaine core.

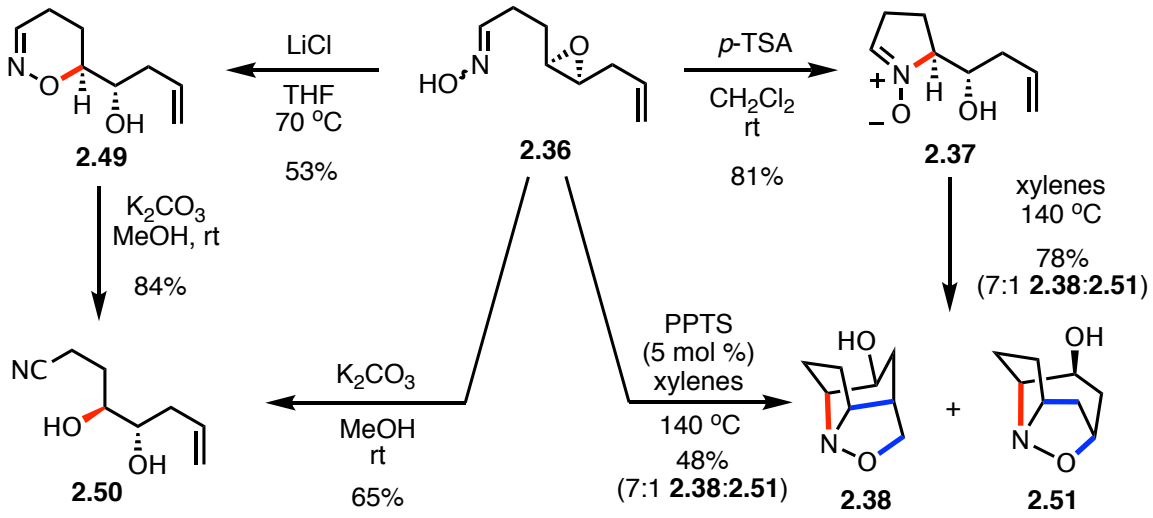

Scheme 2.8. Cascade reaction sequence of model oxime **2.36** to access the truncated virosaine core **2.38**.

2.4 Attempted Diels-Alder Reactions of 2-Bromoacrolein and 2-Substituted Furans

With the feasibility of the bio-inspired cascade reaction sequence established, we turned our attention to the Diels-Alder reaction required to construct oxabicyclo[2.2.1]heptene **2.8**.[12] The enantioselective Diels-Alder reaction of furan (**2.10**, R = H) with 2-bromoacrolein (**2.9**) was previously reported by Corey and appeared well suited to our needs.[13] However, to the best of our knowledge, this reaction had not been applied to 2-substituted furans (**2.10**, R ≠ H). Initially, we attempted the cycloaddition of ethyl 2-(furan-2-yl)acetate (**2.10**, R = CH_2CO_2Et) with 2-bromoacrolein (**2.9**) by allowing them to react in the presence of oxazaborolidinone catalyst **2.52** (Scheme 2.9). However, under these conditions, the only products generated in the reaction were furans **2.53** and **2.54**, resulting from a Friedel-Crafts conjugate addition. Disappointingly, modifying the reaction conditions (reaction time, temperature, quenching method, *etc.*) did not alter the course of the reaction and either generated **2.53** and **2.54**, in varying amounts, or resulted in polymerization of **2.9**. Moreover, several other oxazaborolidine catalysts (**2.55a-c**) and/or substituted furans (**2.10**, R = OMe, Me, TMS) yielded similarly disappointing results.[14]

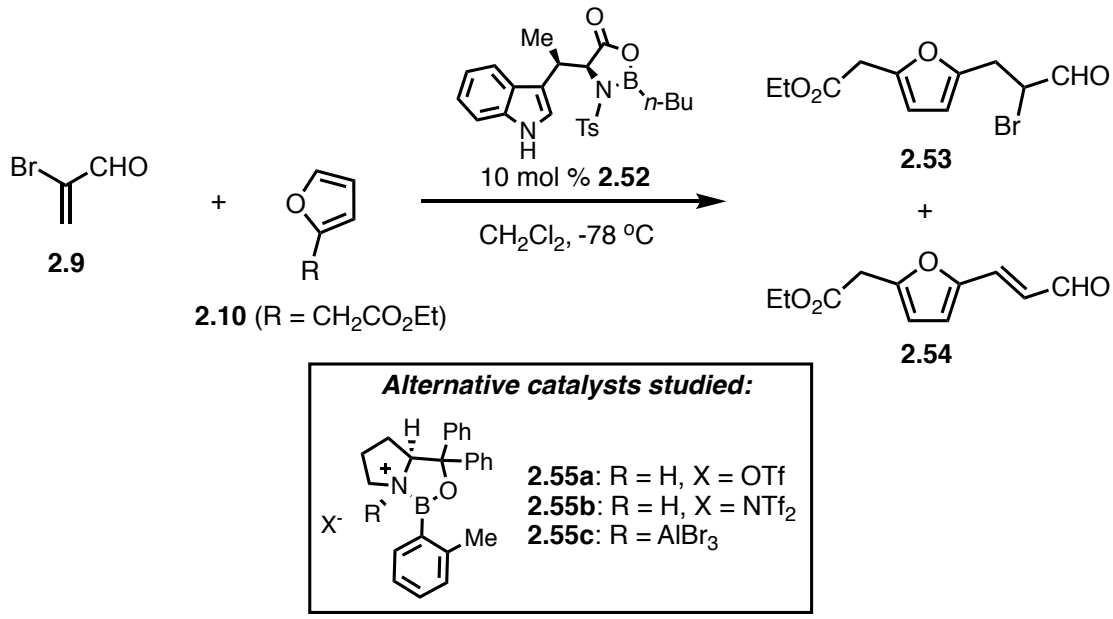

Scheme 2.9. Reaction of 2-bromoacrolein (**2.9**) with ethyl 2-(furan-2-yl)acetate (**2.10**, R = CH_2CO_2Et).

2.5 Alternative Diels-Alder Strategies

2.5.1 Intramolecular Diels-Alder Approach

The limitation of the furan Diels-Alder reaction presented a significant problem as our proposed route relied on the [4+2] cycloaddition to install requisite functionality at C14 in pentacycle **2.2** to ultimately generate the butenolide in **1.24** (*vide supra*). Further complicating the situation, we quickly realized that an intramolecular Diels-Alder approach would likely not serve as a suitable alternative. In particular, we were unsuccessful in converting furan **2.56** to the corresponding oxabicycle **2.58** (X = H,H; Scheme 2.10). Several factors may have worked against us in this regard, including the fact that the allyl moiety in **2.56** is not a great electrophile for a normal electron-demand Diels-Alder cycloaddition. Moreover, the required conformation **2.56b** for intramolecular cycloaddition to occur is presumably disfavored in comparison to other conformers of this species (e.g. **2.56a**). As a result, there are likely significant energetic and entropic barriers that must be overcome in order for this reaction to be successful. While we did not investigate this approach further, one potential strategy that could have been used to address these inadequacies might have been to modify the substrate to incorporate a more

reactive dienophile. For example, anhydride **2.57** would be more likely to undergo intramolecular cycloaddition than **2.56**. However, this species might have also suffered from undesirable conformational preferences that would have restricted its application in this setting.

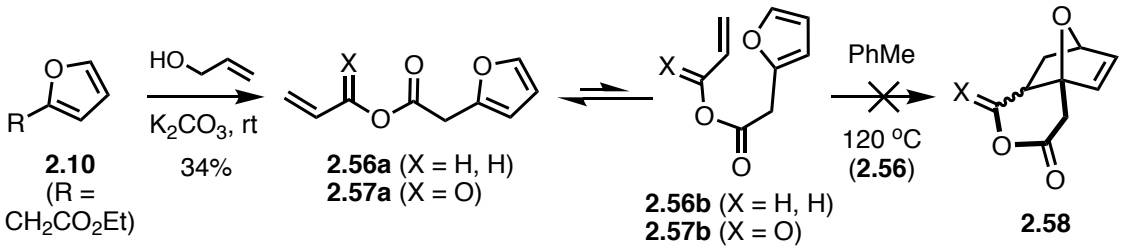

Scheme 2.10. Attempted intramolecular Diels-Alder reaction of furan **2.56**.

2.5.2 Acyclic Diene Diels-Alder Approach

In an attempt to overcome the limitations of both the intermolecular 2-substituted furan and intramolecular furan cycloaddition strategies, we devised an alternative route to access virosaine A (**1.24**) *via* Diels-Alder reaction between **2.9** and *trans,trans*-1,4-diacetoxybutadiene (**2.62**)[15] (Scheme 2.11). The success of this strategy would hinge on our ability to elaborate cyclohexene **2.61** to epoxy oxime **2.60** *via* differentiation of the two acetoxy groups as well as diastereoselective nucleophilic addition/epoxide formation. Furthermore, we anticipated that our proposed cascade reaction sequence could be employed on **2.60** to generate tetracycle **2.59**, which might serve as an immediate precursor to **1.24** *via* an intramolecular Horner-Wadsworth-Emmons reaction or an aldol condensation.

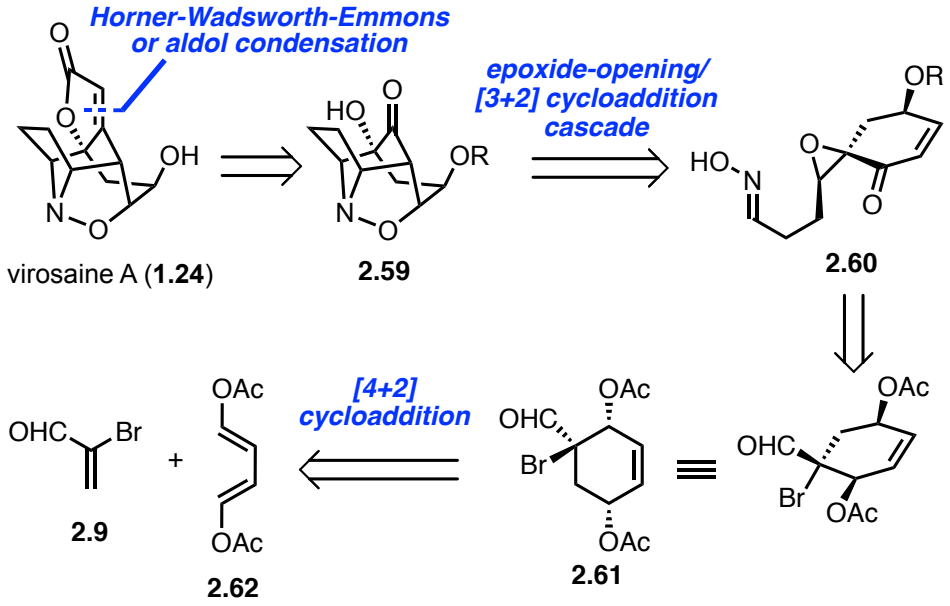

Scheme 2.11. Acyclic diene Diels-Alder strategy to access virosaine A.

2-Bromoacrolein (**2.9**) and *trans,trans*-1,4-diacetoxybutadiene (**2.62**) were found to react in the presence of oxazaborolidine **2.55b** to provide cycloadduct **2.61** in a reasonable 70% yield, with 90:10 *endo*:*exo* selectivity (Scheme 2.12).[14b] However, the product was only generated in a disappointing 12% *ee*. Attempts to enhance the enantioselectivity of the process by maintaining a lower reaction temperature were thwarted by a drastic decrease in reactivity. Nonetheless, we attempted to elaborate **2.61** to a suitable cascade precursor by reacting it with a wide range of nucleophiles, including Grignard, organolithium, organozinc, organocuprate, and higher order organometallic reagents. However, all of these attempts failed to deliver the corresponding bromohydrin **2.63** and instead resulted in complex mixtures or significant decomposition. Moreover, several undesired products were generated in many of these reactions. For example, when ethylmagnesium bromide was added to **2.61**, reduction products **2.65** and **2.66** were observed as the major components of the reaction mixture. Moreover, epoxide **2.68** was generated in several reactions and was the major product isolated when **2.61** was allowed to react with organolithium **2.67**. This result led us to believe that the acetate protecting groups in **2.61** might be impeding nucleophilic addition to the aldehyde. Consequently, we attempted to deprotect the two allylic alcohols but unfortunately only observed

decomposition under both basic and acidic conditions. Given these results, a modified route would need to be employed to generate the cascade precursor from cyclohexene **2.61**. One potential strategy that could be used to this effect is shown in Scheme 2.13. Global carbonyl reduction of **2.61** would generate triol **2.69**, at which point selective benzylidene formation might be possible followed by silyl protection of the remaining 2° alcohol to provide **2.70**. Regioselective benzylidene ring-opening and oxidation of the resulting alcohol might generate aldehyde **2.71**, which possesses orthogonally-protected alcohols that should not interfere with nucleophilic addition to access bromohydrin **2.72**. While feasible, this alternate route would require multiple undesired functional group manipulations and protection/deprotection steps that would make the synthesis highly inefficient. As such, we ultimately decided to abandon this approach.

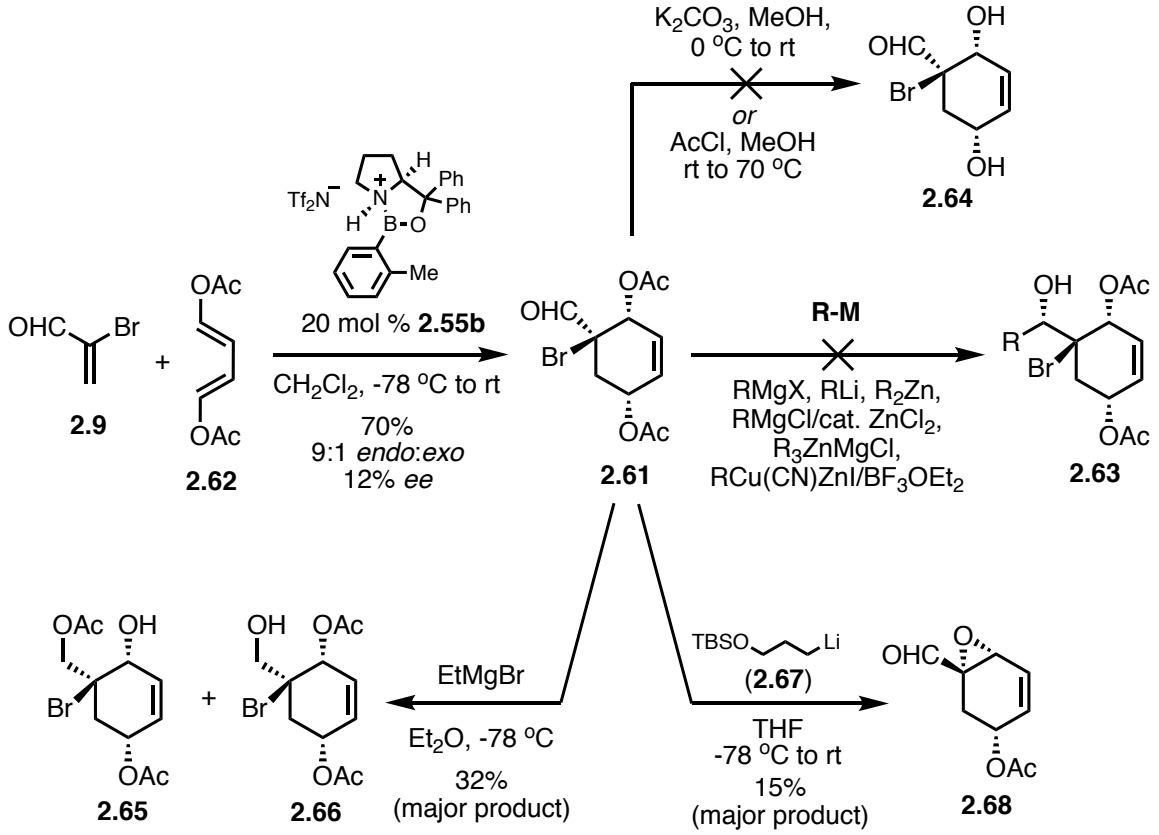

Scheme 2.12. Synthesis and attempted manipulations of cyclohexene **2.61**.

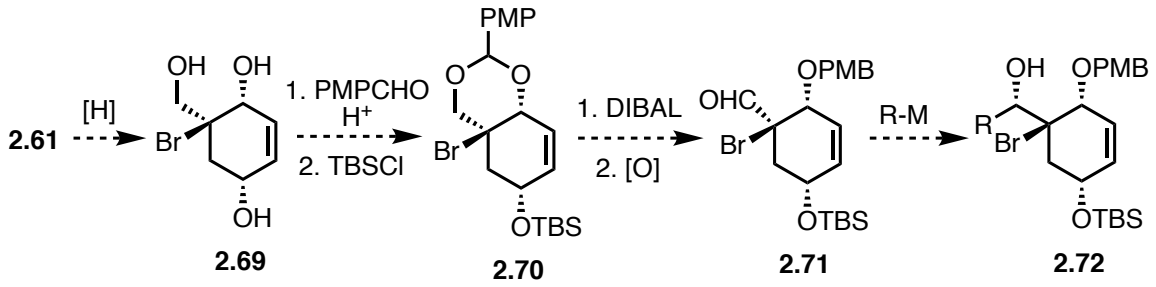

Scheme 2.13. Feasible synthetic route that could be used to access bromohydrin **2.72**.

2.6 Enantioselective Synthesis of the Virosaine Core

Faced with the unexpected obstacles delineated above, we considered the use of known oxabicycle **2.74**, resulting from cycloaddition with furan rather than its substituted congeners, within our proposed route to access pentacycle **2.73** (Scheme 2.14).[13] However, this subtle change had a significant consequence in that **2.73** would lack the C14 functionality necessary to install the butenolide ring in **1.24**. Nonetheless, we postulated that it might be possible to implement a selective late-stage functionalization at C14 of **2.73** to construct the butanolide in **2.1**. While late-stage C-H functionalization strategies have proven enabling in total synthesis, their successful implementation can be challenging within complex molecular frameworks.[16,17] In this particular case, the presence of the isoxazolidine and 12 distinct C-H bonds make selective functionalization of **2.73** an ambitious task. Nevertheless, we were greatly motivated to pursue this strategy as it would not only enable our proposed cascade reaction sequence but also, together, these key transformations would allow us to prepare **1.24** in a highly efficient manner.

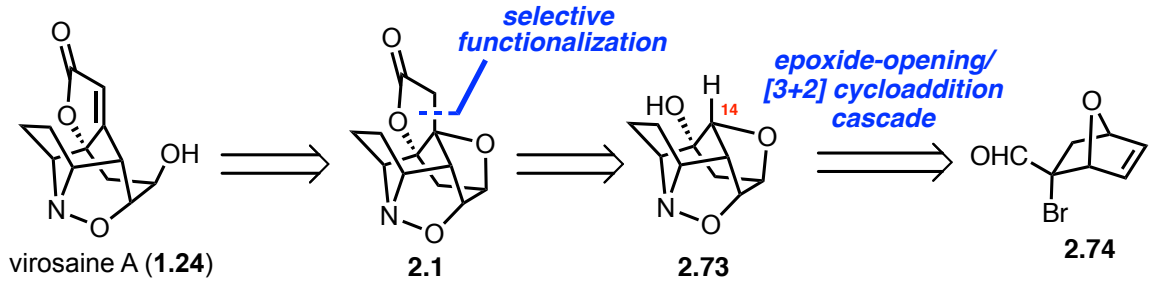

Scheme 2.14. Late-stage C14 functionalization strategy to access virosaine A *via* oxabicycle **2.74**.

2.6.1 Attempted Protecting Group Free Approach

We prepared Corey's oxabicycle **2.74** by combining 2-bromoacrolein (**2.9**) with furan (**2.75**) in the presence of oxazaborolidinone **2.52** at –78 °C in CH_2Cl_2 (Scheme 2.15). However, in our hands, isolation of **2.74** was prohibitively difficult due to its propensity to undergo rapid cycloreversion back to **2.9** and **2.75**. As a result, we were never able to isolate a pure sample of **2.74**. Similar observations with this oxabicycle were noted by Carreira and coworkers, who opted to trap the aldehyde *in situ* by addition of either an enolate, silyl ketene acetal, or $NaBH_4$.[18] Accordingly, we engaged in a similar approach to trap **2.74** *in situ* with a Grignard or equivalent nucleophile to access a bromohydrin product that was expected to be more stable. Initially, we found that allyl and 3-butenylmagnesium bromide (**2.76** and **2.77**) could be added to the unstable aldehyde to provide bromohydrins **2.78** and **2.79**, respectively. With bromohydrin products **2.78**/**2.79** in hand, we decided to probe the possibility of using a protecting group-free approach to access cascade precursor **2.6** (R = H). Specifically, we hoped to selectively transform the terminal olefin of either **2.78** or **2.79** into the requisite oxime of **2.6**. Epoxides **2.80** and **2.81** were smoothly generated from **2.78** and **2.79**, respectively. Unfortunately, several attempts to selectively manipulate the terminal olefins in **2.80**/**2.81** failed to deliver **2.83** and led either to complex mixtures or decomposition, in almost every case. The sole exception occurred upon submission of diene **2.81** to Lemieux-Johnson oxidation conditions. In this case, the only product isolated after reductive workup was diol **2.82**, resulting from exclusive reaction of the internal olefin of the bridged bicycle.

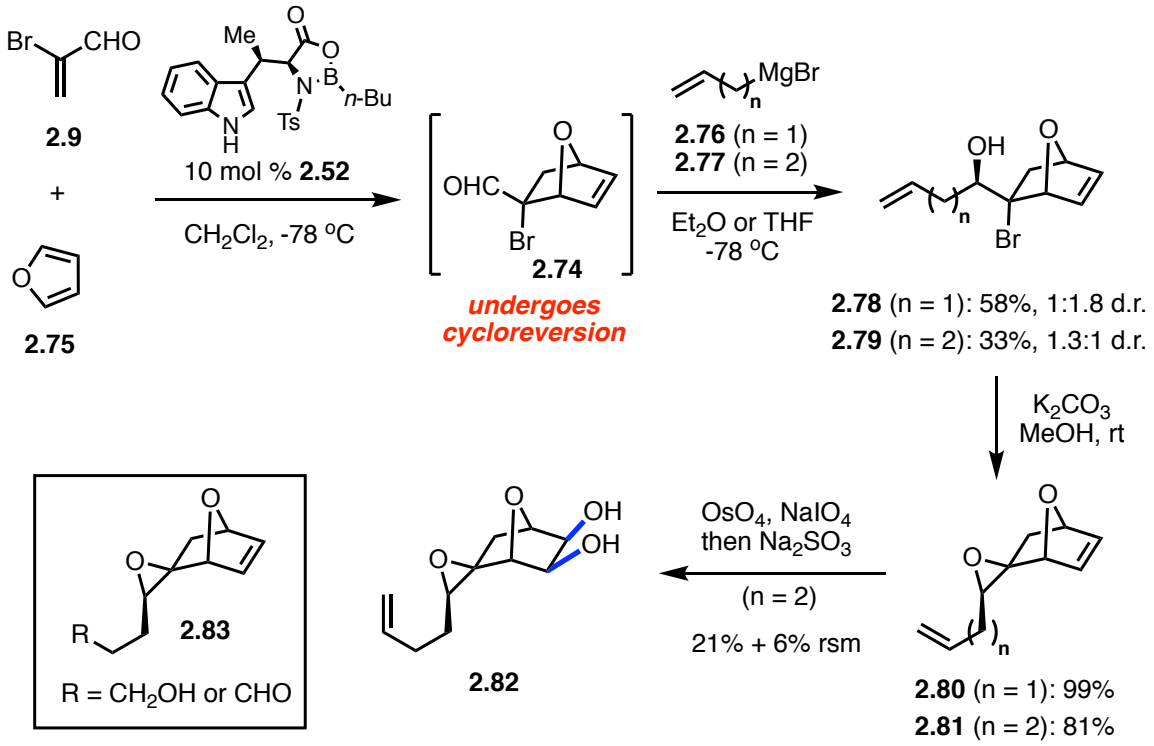

Scheme 2.15. Synthesis and manipulation of bromohydrins **2.78** and **2.79**.

2.6.2 First-Generation Synthesis of the Cascade Precursor

Given our inability to selectively manipulate the terminal olefins of **2.80**/**2.81** in the presence of their strained internal olefins, we examined other nucleophiles to trap aldehyde **2.74**. Specifically, we focused on using nucleophiles that possessed a functional group at their terminus that could be more easily converted into the requisite oxime. We were pleased to find that the silyloxy-substituted organolithium **2.84** also served as a competent nucleophile to trap the unstable aldehyde **2.74** and produced the corresponding bromohydrin product **2.85** in a modest 29% yield (Scheme 2.16). However, the diastereoselectivity of the process was found to be very poor, yielding a 1.3:1 mixture, in favor of the desired diastereomer. Although the diastereomers were disappointingly found to be inseparable by flash chromatography, we decided to proceed ahead using the mixture in hopes that their separation would be permitted at a later stage. Treatment of bromohydrin **2.85** with K_2CO_3 in MeOH smoothly generated epoxide **2.86** in excellent yield. TBAF-mediated silyl deprotection of **2.86** and subsequent Dess-Martin oxidation provided aldehyde **2.87** in modest yield over two steps. Finally, treatment of aldehyde

2.87 with hydroxylamine hydrochloride and sodium acetate generated oxime **2.88** as a mixture of *E*/*Z* isomers in 94% yield. Unfortunately, neither oxime **2.88** nor any of the intermediates prepared in this sequence could be separated from their undesired epoxide epimers. Consequently, the cascade precursor **2.88** could only be isolated as a 1.2:1 mixture of epoxide diastereomers.

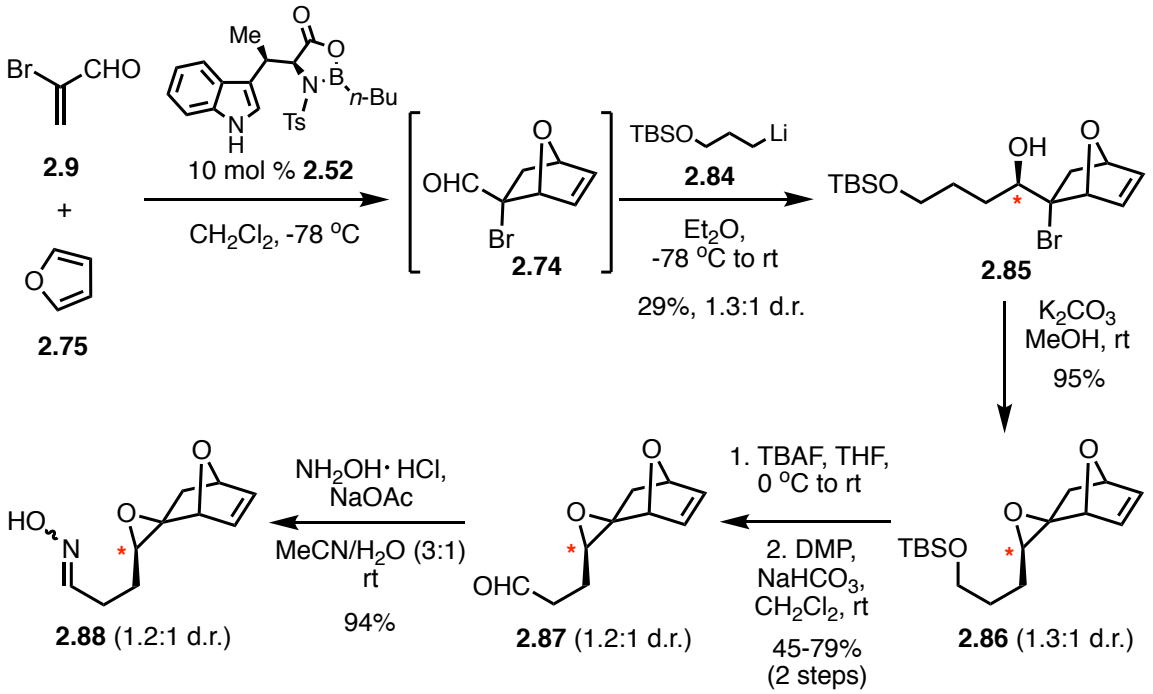

Scheme 2.16. First-generation synthesis of the cascade precursor.

Utilizing organolithium **2.84** as a nucleophilic trap for the unstable aldehyde **2.74** enabled the synthesis of cascade precursor **2.88** in a total of 5 steps from 2-bromoacrolein (**2.9**) and furan (**2.75**). However, this route suffered several drawbacks. In particular, the yield and diastereoselectivity of the nucleophilic addition of **2.84** onto **2.74** was disappointingly low and we were unable to remove the undesired diastereomer at any stage of the synthesis. Consequently, the yield of **2.88** over this 5-step sequence was only 7-11%, which we deemed unacceptable in consideration of our goal to achieve an efficient synthesis of **1.24**.

2.6.3 Second-Generation Synthesis of the Cascade Precursor

Given the poor yield and selectivity observed in the nucleophilic addition step in our first-generation synthesis of **2.88**, we examined several other conditions and nucleophiles in hopes of obtaining greater levels of diastereoselectivity (Table 2.2). Assessment of several different conformational models of aldehyde **2.74** suggested that achieving high diastereoselectivity in this transformation could be challenging and that formation of the desired diastereomer **2.89** might even be disfavored (Figure 2.2).[19] Specifically, analysis using a Felkin-Anh model, where Br sits 90 ^{o} from the carbonyl group, indicated that the desired product **2.89** would be accessible *via* nucleophilic addition to the carbonyl Re face of conformer **2.74a** (Figure 2.2 A). Yet, it was not clear whether this addition would be favored over the alternative and undesired Si face addition onto conformer **2.74b**. A comparison of **2.74a** vs. **2.74b** using a ball and stick molecular model did not provide conclusive evidence to support one pathway over the other. However, based on a comparison of the A-values for ethyl (1.75 kcal/mol) and *i*-propyl (2.15 kcal/mol) substituents, one might assume that the CH_2 unit in **2.74** would be smaller than the alternative methine bridgehead position and, consequently, that Si face addition would predominate. Moreover, we reached a similar conclusion when we assessed this nucleophilic addition using either a Cram-chelate (Figure 2.2 B) or a Cornforth model (Figure 2.2 C). While this analysis suggested that the undesired diastereomer might be generated as the major product, we were encouraged by previous results obtained by Carreira et al. for related nucleophilic additions to aldehyde **2.74**. Specifically, they showed that modest diastereoselectivity could be achieved for the addition of lithium enolates and silyl ketene acetals to access bromohydrin **2.89** (R = CH_2CO_2Et) as the major diastereomer, in up to 5:1 d.r.[18a] Thus, we were hopeful that a thorough screening of reaction parameters/nucleophiles would enable us to identify conditions that also provided **2.89** as the major product, in this case.

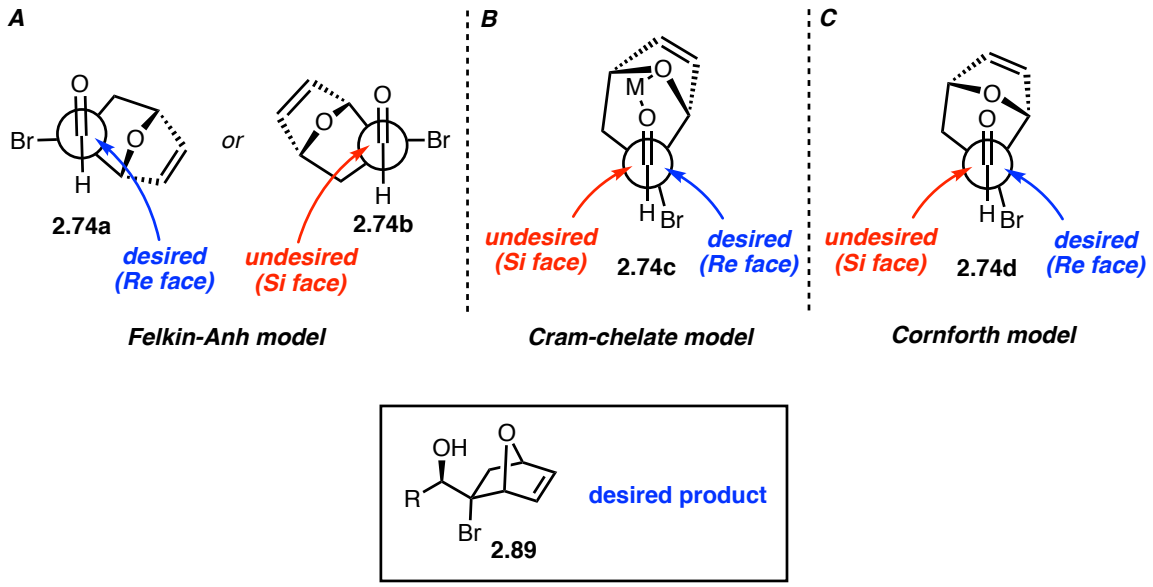

Figure 2.2. Conformational models for the nucleophilic addition onto aldehyde **2.74**.

Given the influence that solvents have on the aggregation states of alkyllithium reagents and how this can impact their reactivity, we probed the effect of substituting THF for the less-polar solvent, hexanes (Table 2.2, entry 4).[20] However, the effect that this solvent switch had on the diastereoselectivity of *n*-BuLi (**2.90**) addition was negligible and the corresponding product was only generated in 1.4:1 d.r. Moreover, polar additives (e.g. HMPA) also failed to alter the diastereoselectivity (not shown). Several other organometallic species were screened as nucleophiles in the reaction but generally led to disappointing results. Diethyl zinc (**2.91**) and trichloro(methyl)titanium (**2.93**) both failed to produce even trace amounts of the desired bromohydrin product **2.89** (entries 5 and 7). Instead, **2.91** caused decomposition of aldehyde **2.74**, while **2.93** led to the exclusive formation of furan **2.101** (Scheme 2.17). The latter result is likely due to the strong Lewis acidity of **2.93**, which might cause degradation of oxabicycle **2.74**. This could either occur *via* acid-catalyzed fragmentation to **2.100** followed by aromatization (path a) or *via* retro-[4+2] cycloaddition/Friedel-Crafts alkylation (path b). In contrast, the less acidic triisopropoxytitanium species **2.94** did afford the bromohydrin product, albeit with concomitant silyl deprotection and very poor diastereoselectivity (entry 8).

Table 2.2. Selected conditions and nucleophiles screened to trap oxabicycle **2.74**.

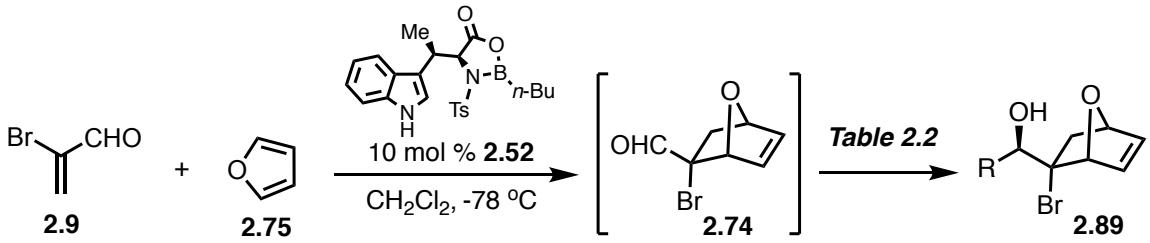

Entry	Nucleophile	Solvent	Temp (°C)	Yield (%)[a]	d.r.[b]
1	MgBr (**2.76**)	Et_2O	-78	58	1:1.8
2	MgBr (**2.77**)	THF	-78	33	1.3:1
3	TBSO Li (**2.84**)	Et_2O	-78 → 22	29	1.3:1
4	*n*-BuLi (**2.90**)	hexanes	-78 → 22	28	1.4:1
5	Et_2Zn (**2.91**)	CH_2Cl_2	-78 → 22	0	-
6	TMS (**2.92**)	CH_2Cl_2	-78 → 22	0[c]	-
7	$MeTiCl_3$ (**2.93**)	Et_2O	-40	0[c]	-
8	TBSO $Ti(O\textit{i}\text{-}Pr)_3$ (**2.94**)	Et_2O	-78 → 22	13	1:3.1
9	$(TBSO)_2CuLi$ (**2.95**)	Et_2O	-78	< 5	1.3:1
10	O O MgBr (**2.96**)	THF	-78 → 22	15	1:2.7
11	O O Li (**2.97**)	**Et_2O**	**-78**	**62**	**2.7:1**
12	O O Li (**2.97**)	THF	-78	0	-
13	O O $CeCl_3$ (**2.98**)	THF	-78 → 22	trace	n.d.

[a]Isolated yields of **2.89**. [b]Determined by integration of the ^1H NMR spectra after purification. [c]Furan **2.101** generated at the major product.

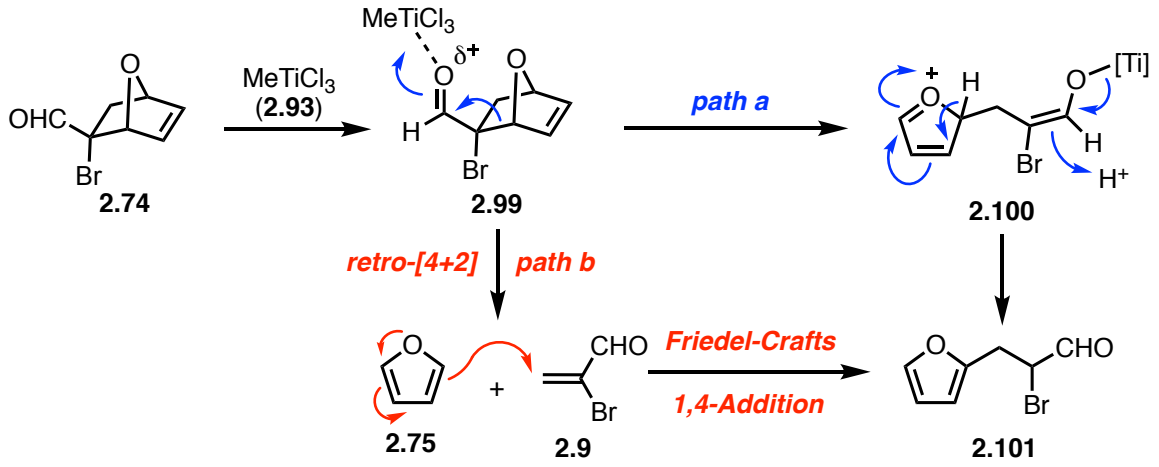

Scheme 2.17. Proposed mechanism for the formation of furan **2.101**.

Still and coworkers have shown that organocuprates can be highly stereoselective nucleophiles for the addition to α–monosubstituted aldehydes bearing β-alkoxy substitutents.[21] Disappointingly, however, we found that lithium dialkylcuprate **2.95** only gave the desired product in <5% yield and 1.3:1 d.r. when allowed to react with aldehyde **2.74** (entry 9). Notably, other soft nucleophiles, including allyltrimethylsilane (**2.92**), exclusively produced furan **2.101** when allowed to react with **2.74** (entry 6). Further screening revealed that *in situ* addition of dioxolane-protected Grignard reagent **2.96** to aldehyde **2.74** generated the corresponding bromohydrin product with a modest level of diastereoselectivity. Unfortunately, upon analyzing the mixture, we realized that the desired diastereomer was generated as the minor product in a 1:2.7 ratio. Intriguingly, when we simply changed the nature of this nucleophile to the corresponding organolithium (e.g. **2.97**), we observed a complete reversal in diastereoselectivity. Specifically, *in situ* addition of **2.97** to aldehyde **2.74** produced the bromohydrin product in 2.7:1 d.r., favoring the desired diastereomer (entry 11). While this was an encouraging improvement over previous results, we were unfortunately unable to further enhance the d.r. by changing various parameters, such as the solvent employed (entry 12), the nature of metal (entry 13), or the inclusion of additives (e.g. HMPA, TMEDA, sparteine, etc.).

Interestingly, in studying this reaction, we found that the yield and *ee* of the product was highly dependent on the method used to generate the oxazaborolidinone Diels-Alder catalyst **2.52**. Specifically, we were unable to consistently reproduce Corey's

original procedure for the preparation of **2.52**, which involves dehydrative coupling of *n*-butylboronic acid with *N*-tosyl *β*-methyl tryptophan.[13] In contrast, we found that the best yield and *ee* values were obtained when **2.52** was prepared from the *N*-tosyl *β*-methyl tryptophan ligand and neat *n*-butyldichloroborane.[18c] Notably, a toluene solution of *n*-butyldichloroborane could also be used to generate **2.52**.[18a,b] However, these solutions always contained appreciable amounts of *n*-butoxydichloroborane (^{11}B δ = +31.2), an oxidized byproduct generated during the preparation of *n*-butyldichloroborane.[22,23] Moreover, we were unable to separate these two dichloroborane species from one another *via* distillation, as they both co-distilled with toluene. This limitation proved to be problematic because the presence of *n*-butoxydichloroborane led to both lower yields and *ee* values in the Diels-Alder reaction. Consequently, we opted to use neat *n*-butyldichloroborane for the preparation of **2.52**. Ultimately, under our optimized nucleophilic addition conditions, bromohydrin **2.102** was produced in 62% yield, 2.7:1 d.r. and 83% *ee* (Scheme 2.18).[23]

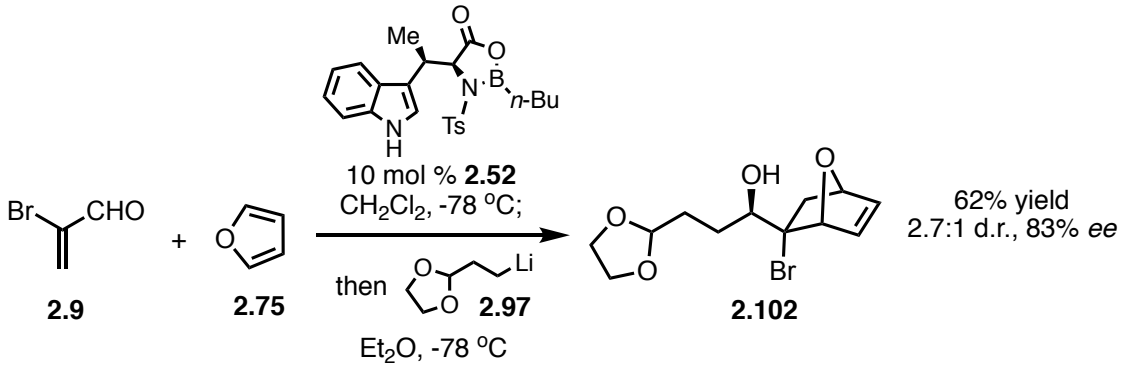

Scheme 2.18. Optimized conditions for the one-pot synthesis of **2.102**.

While we were satisfied with the yield of bromohydrin **2.102** at this point, we were still disappointed with the diastereo- and enantioselectivity of the addition reaction. Moreover, **2.102** could not be chromatographically separated from the unwanted diastereomer, *epi*-**2.102**, further complicating matters. Consequently, we decided to oxidize the diastereomeric bromohydrin mixture to ketone **2.103** and then screen several reducing agents in hopes of improving the d.r. of **2.102** (Table 2.3). However, to our disappointment, the reduction of ketone **2.103** generally proceeded with equally poor levels of diastereoselectivity. $NaBH_4$, $LiBH_4$, and DIBAL all showed a complete lack of

ketone facial preference and produced **2.102** and *epi*-**2.102** as an equimolar mixture (entries 1-3). Moreover, K-Selectride led to decomposition of material (entry 4), while LiAlH(O*t*-Bu)$_3$ preferentially generated the undesired diastereomer *epi*-**2.102** (entry 5). The only reducing agent found to preferentially generate **2.102** was $LiAlH_4$, which only led to a modest 1.3:1 d.r. (entry 6). While it is conceivable that chiral reducing agents might have helped overcome the apparent lack of ketone facial bias in this reduction reaction,[24] we ultimately discovered a simple solution to enhance the d.r. of **2.102** by recrystallization. Specifically, recrystallization of a 2.7:1 mixture of **2.102** and *epi*-**2.102** from EtOAc led to significant enrichment of **2.102**, producing the desired diastereomer in >20:1 d.r. (Figure 2.3). Moreover, we were extremely pleased to discover that, in addition to diastereomeric enrichment, recrystallization amplified the *ee* of **2.102** from 83% to >99%. As result, the Diels-Alder/nucleophilic addition/recrystallization sequence provided access to **2.102** with complete control over both the absolute and relative stereochemistries. Overall, this procedure served to install 10 of the 12 carbon atoms and 3 of the 6 stereocenters of virosaine A (**1.24**).

Table 2.3. Stereoselective reduction of ketone **2.103**.

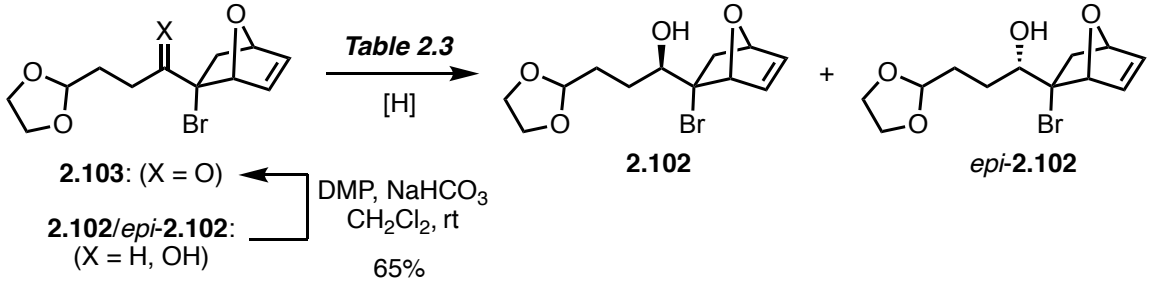

Entry	Reducing Agent	Yield (%)[a]	d.r.[b]
1	$NaBH_4$	98	1:1
2	$LiBH_4$	86	1:1
3	DIBAL	81	1:1
4	K-Selectride	0[c]	-
5	LiAlH(*Ot*-Bu)$_3$	99	1:1.8
6	$LiAlH_4$	86	1.3:1

[a]Combined isolated yield of **2.102**/*epi*-**2.102**. [b]Ratio of **2.102**:*epi*-**2.102** determined *via* integration of the ^{1}H NMR spectra after purification. [c]Decomposition of material.

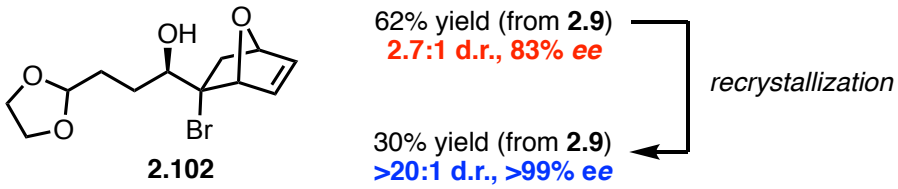

Figure 2.3. Diastero- and enantiomeric enrichment of **2.102** *via* recrystallization.

Having established an efficient procedure for the preparation of **2.102**, we focused on its elaboration to the key cascade precursor (Scheme 2.19). Initially, we found that bromohydrin **2.102** could be cleanly converted to the corresponding epoxide **2.104** by treatment with K_2CO_3 in MeOH. The stereochemical assignment of **2.102** was unambiguously confirmed by an observed nuclear Overhauser effect (nOe) between the epoxide proton and the axial proton of the bridged bicycle in **2.104**. Unfortunately, attempted acid-mediated dioxolane removal failed to reveal the latent aldehyde **2.87** and led to decomposition of material and/or complex mixtures in every case. Alternatively, we found that the dioxolane protecting group could be removed directly from bromohydrin **2.102** under mildly acidic conditions to provide the corresponding lactol **2.105** in near quantitative yield. However, all attempts at base-mediated conversion of **2.105** to aldehyde **2.87** were met with failure, indicating that access to cascade precursor **2.88** would require an alternate route. We proceeded to convert lactol **2.105** to oxime **2.106**, which we hoped would serve as a precursor to **2.88**. Interestingly, we found that condensation of lactol **2.105** with hydroxylamine led to oxime **2.106** as well as the tautomeric cyclic aminal **2.107** in a 9.9:1 ratio. Disappointingly, however, we were unable to convert either **2.106** or **2.107** to the cascade precursor **2.88** under several different base-mediated conditions.

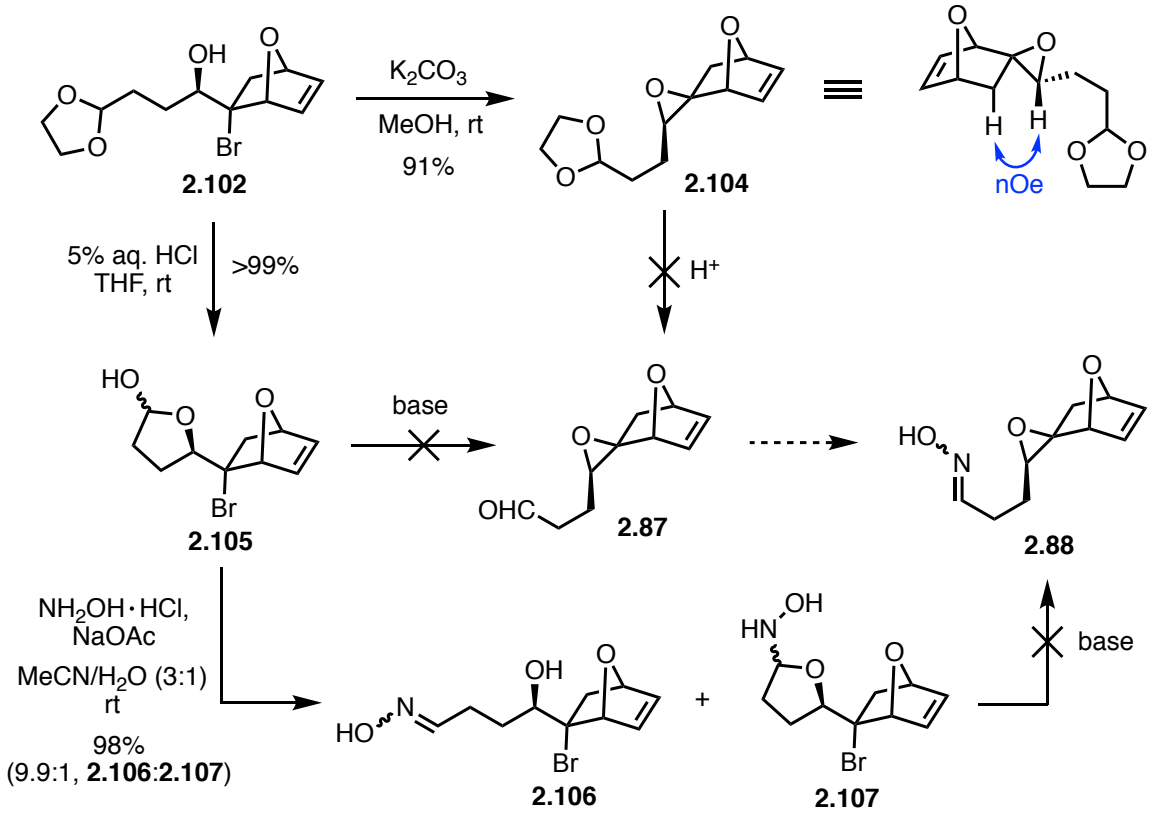

Scheme 2.19. Initial attempts to convert bromohydrin **2.102** into cascade precursor **2.88**.

As an interesting aside, over the course of these studies, we found that lactol **2.105** underwent facile dehydration to produce dimeric ether **2.108** when held under reduced pressure (< 0.1 mm Hg) for extended periods of time (Scheme 2.20). Thankfully, lactol **2.105** could be recovered quantitatively by heating **2.108** in 2.5% aq. HCl/THF. Nevertheless, care was always taken to limit the drying period for lactol **2.105** in order to prevent this undesired dimerization from occurring.

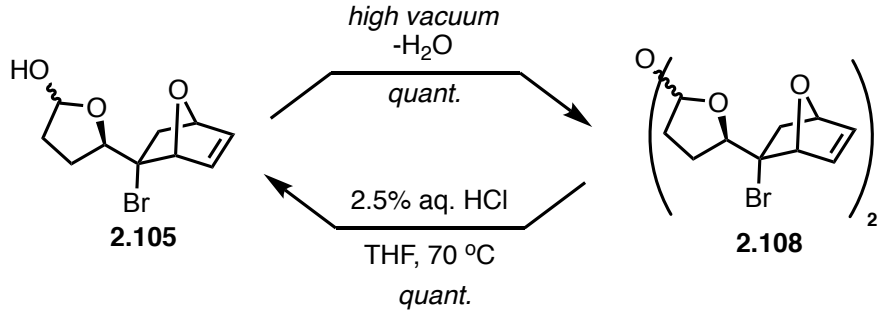

Scheme 2.20. Dehydrative dimerization of lactol **2.105**.

Given the inability to use either epoxide **2.104** or oxime **2.106** to access the requisite cascade precursor, we were pleased to find that lactol **2.105** could be converted to *O*-silylated oxime **2.109** upon treatment with $TBSONH_2$ in the presence of molecular sieves (Scheme 2.21). Moreover, **2.109** did not undergo cyclization to its aminal tautomer like its unprotected analogue **2.106** (*vide supra*). Treatment of bromohydrin **2.109** with K_2CO_3/MeOH only gave the undesired silyl-deprotected oxime **2.106**. In contrast, reaction of **2.109** with NaH provided epoxide **2.110**, a protected analogue of our cascade precursor, in 99% yield. The preparation of **2.110** concluded an optimized synthesis of the requisite cascade precursor in a total of only 4 steps (27% overall yield) from 2-bromoacrolein (**2.9**) and furan (**2.75**). Importantly, **2.110** could be prepared in >99% *ee* and as a single diastereomer.

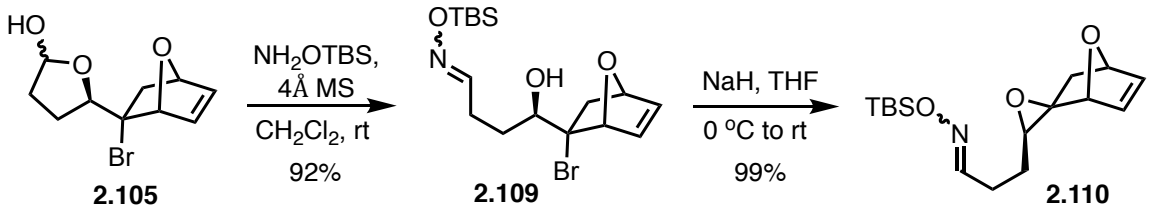

Scheme 2.21. Completion of the second-generation synthesis of the cascade precursor.

2.7 Cascade Reaction Sequence Optimization to Construct the Virosaine Core

The development of an efficient process to access epoxide **2.110** set the stage for the study of the key cascade reaction sequence to prepare the pentacyclic virosaine core **2.73** (Table 2.4). Initial cascade studies were conducted on the free oxime **2.88** and, gratifyingly, submission to the reaction conditions developed during the initial model study afforded **2.73** as the sole product in a promising 26% yield (entry 1).[25] Encouraged by this result, we examined direct cascade reactions using silyl oxime **2.110**. The amount of PPTS was increased to 1 equivalent in order to facilitate silyl group cleavage and more polar solvents were examined due to the low solubility of PPTS in xylenes. We found that both THF and MeCN improved the yield significantly (entries 3 and 4), while MeOH did not lead to any significant increase (entry 5). Additionally, we found that using microwave heating (at elevated temperature) in place of conventional heating led to a significant decrease in reaction time (entry 2 vs. 3). Among the additives assessed, both BF_3•OEt_2 and HF were found to be detrimental to reaction, producing only trace amounts

of **2.73**, at best (entries 6 and 7). Moreover, a combination of acetic acid and TBAF in THF (rt → 90 °C) only produced the desilylated oxime **2.88** in 32% yield (entry 8).

Table 2.4. Cascade reaction sequence optimization.

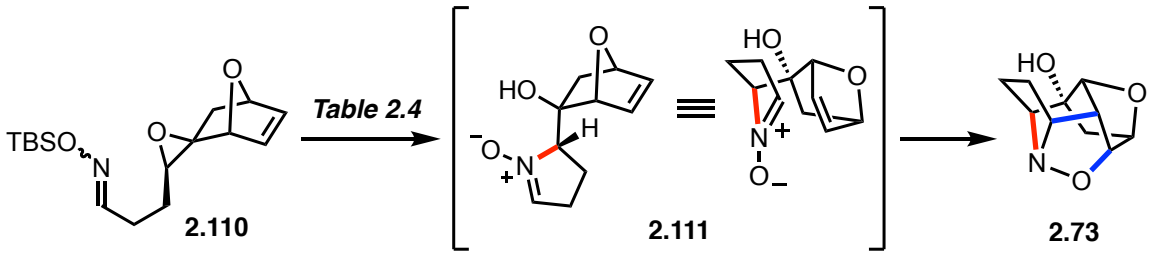

Entry	Solvent	Acid (equiv.)	Temp (°C)	Time	Yield (%)[a]
1[b]	xylenes	PPTS (0.2)	140	8 h	26
2	THF	PPTS (1)	70	12 h	40
3[c]	THF	PPTS (1)	100	1 h	45
4[c]	MeCN	PPTS (1)	120	1 h	50
5[c]	MeOH	PPTS (1)	120	1 h	28
6	CH_2Cl_2	BF_3•OEt_2 (2)	0 → 45	17 h	0
7	MeCN	HF in H_2O (5)	22 → 70	15 h	trace
8	THF	AcOH/TBAF (9/1.5)	22 → 90	40 h	0[d]
9[c]	MeCN	AcOH (5)	120	1 h	<10[e]
10[c]	AcOH	-	120	1 h	78
11[c]	**AcOH**	**-**	**120**	**30 min**	**92**
12[f]	AcOH	-	120	40 min	82

[a]Isolated yields of **2.73**. [b]Oxime **2.88** used as starting material. [c]Microwave heating. [d]Isolated 32% of **2.88**. [e]Recovered 89% starting material. [f]5.2 mmol scale.

Importantly, further screening revealed that while acetic acid was not an efficient promoter when employed as an additive in acetonitrile (entry 9), the reaction conducted in acetic acid as solvent afforded **2.73** in 78% yield (entry 10). Gratifyingly, we found that by simply reducing the reaction time to 30 minutes, **2.73** could be isolated in a remarkable 92% yield (entry 11). Moreover, the reaction could also be conducted on gram scale (5.2 mmol) using conventional heating, to produce the virosaine core in only a slightly diminished 82% yield (entry 12). Overall, this novel cascade process allowed us to access the complex core of virosaine A (**1.24**) in only 5 steps from commercially available materials.

2.8 Conclusion

A short and robust enantioselective synthesis of the virosaine core was developed, which proceeded in 5 steps and 25% overall yield from 2-bromoacrolein (**2.9**) and furan (**2.75**) (Scheme 2.22). The route featured a sequential oxazaborolidinone-catalyzed Diels-Alder cycloaddition/nucleophilic organolithium addition to furnish a functionalized intermediate (**2.102**) that contained all but two of the carbon atoms found in virosaine A (**1.24**). Moreover, a novel epoxide-opening/[3+2] nitrone cycloaddition cascade reaction was developed to access the caged pentacycle **2.73** in 92% yield from spirocyclic epoxide **2.110**. With the core of virosaine A (**1.24**) in hand, the remaining hurdle in completing its total synthesis was selective C14-H functionalization. Studies dedicated to accomplishing this goal are the focus of Chapter 3.

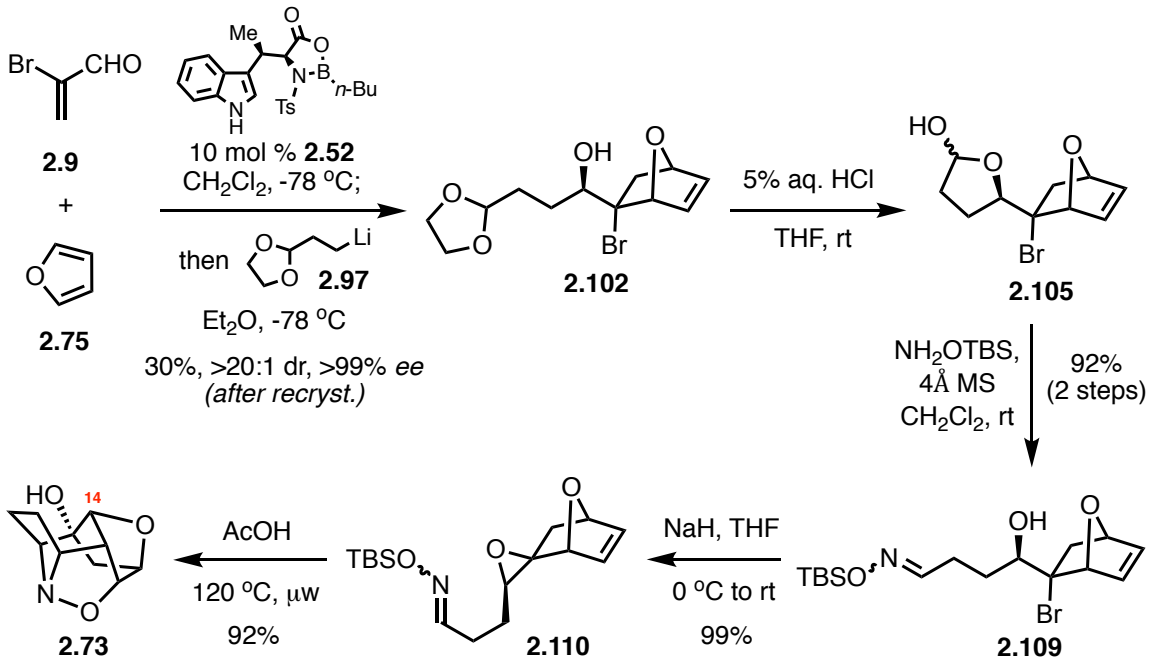

Scheme 2.22. Optimized overall route to access the virosaine core.

References

(1) Zhao, B.-X.; Wang, Y.; Zhang, D.-M.; Huang, X.-J.; Bai, L.-L.; Yan, Y.; Chen, J.-M.; Lu, T.-B.; Wang, Y.-T.; Zhang, Q.-W.; Ye, W.-C. *Org. Lett.* **2012**, *14*, 3096.

(2) For publications and highlights describing parts of this work, see: (a) Hughes, J. M. E.; Gleason, J. L. *Angew. Chem. Int. Ed.* **2017**, *56*, 10830. (b) Hughes, J. M. E.; Gleason, J. L. *Tetrahedron* **2018**, *74*, 759. (c) Carreira, E. M.; Hauser, N. *Synfacts*, **2017**, *13*, 1007. (d) Ellis, B. D.; Vanderwal, C. D. *Angew. Chem. Int. Ed.* **2017**, *56*, 13940.

(3) For recent total syntheses employing biomimetic [3+2] nitrone cycloadditions, see: (a) Miyatake-Ondozabal, H.; Bannwart, L. M.; Gademann, K. *Chem. Commun.* **2013**, *49*, 1921. (b) Wei, H.; Qiao, C.; Liu, G.; Yang, Z.; Li, C.-C. *Angew. Chem. Int. Ed.* **2013**, *52*, 620. (c) Ma, N.; Yao, Y.; Zhao, B.-X.; Wang, Y.; Ye, W.-C.; Jiang, S. *Chem. Commun.* **2014**, *50*, 9284. (d) Hong, A. Y.; Vanderwal, C. D. *J. Am. Chem. Soc.* **2015**, *137*, 7306. (e) Hong, A. Y.; Vanderwal, C. D. *Tetrahedron* **2016**, *73*, 4160.

(4) For select total syntheses employing related biomimetic 1,3-dipolar cycloadditions, see: Gerard, B.; Jones, II, G.; Porco, Jr., J. A.; *J. Am. Chem. Soc.* **2004**, *126*, 13620. (b) Snider, B. B.; Grabowski, J. F. *Tetrahedron Lett.* **2005**, *46*, 823. (c) Roethle, P. A.; Hernandez, P. T.; Trauner, D. *Org. Lett*. **2006**, *8*, 5901. (d) Tang, B.; Bray, C. D.; Pattenden, G. *Tetrahedron Lett.* **2006**, *47*, 6401. (e) Nakamura, S.; Sugano, Y.; Kikuchi, F.; Hashimoto, S. *Angew. Chem. Int. Ed.* **2006**, *45*, 6532. (f) Snider, B. B.; Wu, X.; Nakamura, S.; Hashimoto, S. *Org. Lett.* **2007**, *9*, 873. (g) Sugano, Y.; Kikuchi, F.; Toita, A.; Nakamura, S.; Hashimoto, S. *Chem. Eur. J.* **2012**, *18*, 9682. (h) Stichnoth, D.; Kçlle, P.; Kimbrough, T. J.; Riedle, E.; de Vivie-Riedle, R.; Trauner, D. *Nat. Commun.* **2014**, *5*, 5597. (i) Strych, S.; Journot, G.; Pemberton, R. P.; Wang, S. C.; Tantillo, D. J.; Trauner, D. *Angew. Chem. Int. Ed.* **2015**, *54*, 5079. (j) Ellerbrock, P.; Armanino, N.; Ilg, M. K.; Webster, R.; Trauner, D. *Nat. Chem.* **2015**, *7*, 879.

(5) For a review on furan Diels-Alder reactions, see: Kappe, C. O.; Murphree, S. S.; Padwa, A. *Tetrahedron* **1997**, *53*, 14179.

(6) For select examples of nitrone formation/[3+2] nitrone cycloaddition cascade

reactions, see: (a) Ochiai, M.; Obayashi, M.; Morita, K. *Tetrahedron* **1967**, *23*, 2641. (b) Grigg, R.; Jordan, M.; Tangthongkum, A.; Einstein, F. W. B.; Jones, T. *J. Chem. Soc., Perkin Trans 1* **1984**, 47. (c) Armstrong, P.; Grigg, R.; Warnock, W. J. *J. Chem. Soc., Chem. Commun.* **1987**, 1325. (d) Armstrong, P.; Grigg, R.; Surendrakumar, S.; Warnock, W. J. *J. Chem. Soc., Chem. Commun.* **1987**, 1327. (e) Donegan, G.; Grigg, R.; Heaney, F. *Tetrahedron Lett.* **1989**, *30*, 609. (f) Grigg, R.; Markandu, J. *Tetrahedron Lett.* **1989**, *30*, 5489. (g) Grigg, R.; Markandu, J.; Surendrakumar, S. *Tetrahedron Lett.* **1990**, *31*, 1191. (h) Grigg, R.; Markandu, J. *Tetrahedron Lett.* **1991**, *32*, 279. (i) Grigg, R.; Heaney, F.; Surendrakumar, S.; Warnock, W. J. *Tetrahedron* **1991**, *47*, 4477. (j) Armstrong, P.; Grigg, R.; Heaney, F.; Surendrakumar, S.; Warnock, W. J. *Tetrahedron* **1991**, *47*, 4495. (k) Grigg, R.; Markandu, J.; Perrior, T.; Surendrakumar, S.; Warnock, W. J. *Tetrahedron* **1992**, *48*, 6929. (l) Grigg, R.; Markandu, J.; Surendrakumar, S.; Thornton-Pett, M.; Warnock, W. J. *Tetrahedron* **1992**, *48*, 10399. (m) Grigg, R.; Hadjisoteriou, M.; Kennewell, P.; Markandu, J.; Thornton-Pett, M. *J. Chem. Soc., Chem Commun.* **1992**, 1388. (n) Frederickson, M.; Grigg, R.; Markandu, J.; Redpath, J. *J. Chem. Soc., Chem. Commun.* **1994**, 2225. (o) Markandu, J.; Dondas, H. A.; Frederickson, M.; Grigg, R. *Tetrahedron* **1997**, *53*, 13165. (p) Dondas, H. A.; Frederickson, M.; Grigg, R.; Markandu, J.; Thornton-Pett, M. *Tetrahedron* **1997**, *53*, 14339. (q) Davison, E. C.; Fox, M. E.; Holmes, A. B.; Roughley, S. D.; Smith, C. J.; Williams, G. M.; Davies, J. E.; Raithby, P. R.; Adams, J. P.; Forbes, I. T.; Press, N. J.; Thompson, M. J. *J. Chem. Soc., Perkin Trans. 1* **2002**, 1494.

(7) For select examples of nitrone formation/[3+2] cycloaddition cascade reactions in total synthesis, see: (a) Stockman, R. A.; Sinclair, A.; Arini, L. G.; Szeto, P.; Hughes, D. L. *J. Org. Chem.* **2004**, *69*, 1598. (b) Karatholuvhu, M. S.; Sinclair, A.; Newton, A. F.; Alcaraz, M.-L.; Stockman, R. A.; Fuchs, P. L. *J. Am. Chem. Soc.* **2006**, *128*, 12656. (c) Wilson, M. S.; Padwa, A. *J. Org. Chem.* **2008**, *73*, 9601. (d) Burrell, A. J. M.; Coldham, I.; Oram, N. *Org. Lett.* **2009**, *11*, 1515. (e) Stearman, C. J.; Wilson, M.; Padwa, A. *J. Org. Chem.* **2009**, *74*, 3491. (f) Flick, A. C.; Caballero,

M. J. A.; Padwa, A. *Tetrahedron* **2010**, *66*, 3643. (g) Flick, A. C.; Caballero, M. J. A.; Lee, H. I.; Padwa, A. *J. Org. Chem.* **2010**, *75*, 1992.

(8) Ho, T.-L.; Liu, S.-H. *Synth. Commun.* **1987**, *17*, 969.

(9) (a) Brown, H. C.; Brown, C. A. *J. Am. Chem. Soc.* **1963**; *85*, 1005. (b) Brown, C. A.; Ahuja, V. K. *J. Org. Chem.* **1973**, *38*, 2226. (c) Brown, C. A.; Ahuja, V. K. *J. Chem. Soc., Chem. Commun.* **1973**, 553.

(10) For a review on the synthetic utility of nickel boride, see: Khurana, J. M.; Gogia, A. *Org. Prep. Proc. Int.* **1997**, *29*, 1.

(11) Casey, M. L.; Kemp, D. S.; Paul, K. G.; Cox, D. D. *J. Org. Chem.* **1973**, *38*, 2294.

(12) Schindler, C. S.; Carreira, E. M. *Chem. Soc. Rev.* **2009**, *38*, 3222.

(13) Corey, E. J.; Loh, T. P. *Tetrahedron Lett.* **1993**, *34*, 3979.

(14) (a) Corey, E. J.; Shibata, T.; Lee, T. W. *J. Am. Chem. Soc.* **2002**, *124*, 3808. (b) Ryu, D. H.; Corey, E. J. *J. Am. Chem. Soc.* **2003**, *125*, 6388. (c) Liu, D. Canales, E. Corey, E. J. *J. Am. Chem. Soc.* **2007**, *129*, 1498.

(15) Carlson, R. M.; Hill, R. K. *Org. Synth., Coll. Vol. 6*, **1988**, 196; *Vol. 50,* **1970**, 24.

(16) For select reviews on C-H functionalization, see: (a) Godulal, K.; Sames, D. *Science* **2006**, *312*, 67. (b) Davies, H. M. L.; Manning, J. R. *Nature* **2008**, *451*, 417. (c) Gutekunst, W. R.; Baran, P. S. *Chem. Soc. Rev.* **2011**, *40*, 1976. (d) McMurray, L.; O'Hara, F.; Gaunt, M. J. *Chem. Soc. Rev.* **2011**, *40*, 1885. (e) Yamaguchi, J.; Yamaguchi, A. D.; Itami, K. *Angew. Chem. Int. Ed.* **2012**, *51*, 8960. (f) Chen, D. Y.-K.; Youn, S. W. *Chem. Eur. J.* **2012**, *18*, 9452. (g) Egger, J. Carreira, E. M. *Nat. Prod. Rep.* **2014**, *31*, 449. (h) Qiu, Y.; Gao, S. *Nat. Prod. Rep.* **2016**, *33*, 562. (i) Davies, H. M. L.; Morton, D. *J. Org. Chem.* **2016**, *81*, 343.

(17) For recent total syntheses involving late-stage C(sp^3)-H functionalizations, see: (a) Hinman, A.; Du Bois, J. *J. Am. Chem. Soc.* **2003**, *125*, 11510. (b) Bisai, A.; West, S. P.; Sarpong, R. *J. Am. Chem. Soc.* **2008**, *130*, 7222. (c) Chen, K. Baran, P. S. *Nature* **2009**, *459*, 824. (d) Stang, E. M.; White, M. C. *Nat. Chem.* **2009**, *1*, 547. (e) Yun, S. Y.; Zheng, J.-C.; Lee, D. *J. Am. Chem. Soc.* **2009**, *131*, 8413. (f) Huters, A. D.; Quasdorf, K. W.; Styduhar, E. D.; Garg, N. K. *J. Am. Chem. Soc.* **2011**, *133*, 15797. (g) Kawamura, S.; Chu, H.; Felding, J. Baran, P. S. *Nature* **2016**, *532*, 90.

(h) McCallum, M. E.; Rasik, C. M.; Wood, J. L.; Brown, M. K. *J. Am. Chem. Soc.* **2016**, *138*, 16616. (i) Hung, K.; Condakes, M. L.; Morikawa, T.; Maimone, T. J. *J. Am. Chem. Soc.* **2016**, *138*, 16616. (j) Liu, C.; Chen, R.; Shen, Y.; Liang, Z.; Hua, Y.; Zhang, Y. *Angew. Chem. Int. Ed.* **2017**; *56*, 8187.

(18) (a) Schindler, C. S.; Stephenson, C. R. J.; Carreira, E. M. *Angew. Chem. Int. Ed.* **2008**, *47*, 8852. (b) Diethelm, S.; Schindler, C. S.; Carreira, E. M. *Org. Lett.* **2010**, *12*, 3950. (c) Zipfel, H. F. Carreira, E. M. *Org. Lett.* **2014**, *16*, 2854.

(19) Reetz, M. T. *Angew. Chem. Int. Ed.* **1984**, *23*, 556.

(20) Tai, O.; Hopson, R.; Williard, P. G. *Org. Lett.* **2017**, *19*, 3966, and references therein.

(21) Still, W. C.; Schneider, J. A. *Tetrahedron Lett.* **1980**, *21*, 1035.

(22) Gerrard, W.; Mooney, E. F.; Peterson, W. G. *J. Inorg. Nucl. Chem.* **1967**, *29*, 943.

(23) See Chapter 5.2 for preparation details.

(24) Corey, E. J.; Helal, C. J. *Angew. Chem. Int. Ed.* **1998**, *37*, 1986.

(25) The significant loss in mass balance during this reaction was attributed to decomposition of material under the reaction conditions.

CHAPTER 3

C-H Functionalization of the Virosaine Core and The Total Synthesis of (−)-Virosaine A

3.1 Introduction

In Chapter 2, we established a viable route to access the core of virosaine A (**1.24**) that proceeded in only five steps from readily and commercially available materials. An efficient one-pot furan Diels-Alder cycloaddition/organolithium addition sequence was utilized to construct a bromohydrin intermediate that was subsequently elaborated to key spirocyclic epoxide **2.110** in an additional three steps (Scheme 3.1). A bio-inspired cascade reaction sequence involving sequential epoxide opening and [3+2] nitrone cycloaddition was then developed to construct the caged virosaine core **2.73**. However, a limitation in the initial Diels-Alder reaction that precluded the use of 2-substituted furans meant that pentacycle **2.73** lacked a functional handle at C14 that could be used to install the butenolide ring in **1.24**. As a result, a selective C-H functionalization at C14 was required in order to transform **2.73** into the natural product. Chapter 3 describes the gradual evolution of our approach to selectively functionalize the virosaine core as well as the successful end game used to complete the total synthesis of virosaine A (**1.24**).

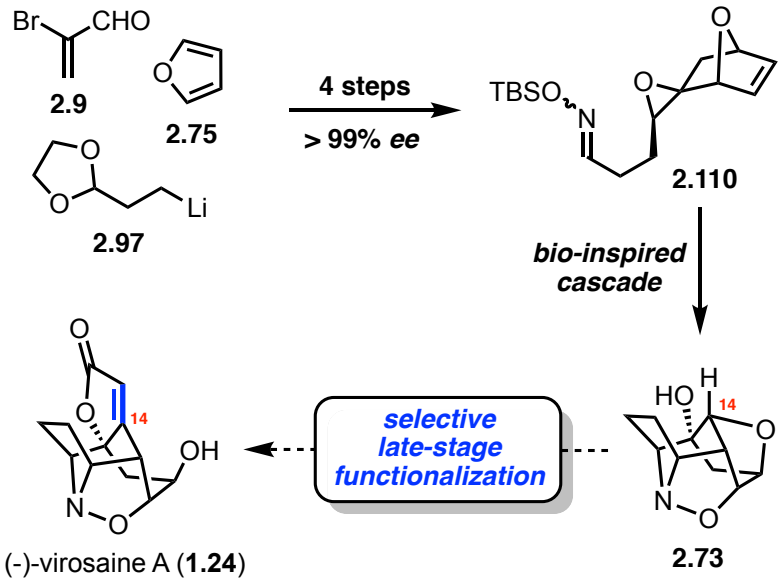

Scheme 3.1. The requirement to effect a selective late-stage C14 functionalization.

3.2 Carbene C-H Insertion Strategies to Functionalize C14 of the Virosaine Core

Over the past two decades, late-stage C-H functionalization has become a popular and powerful strategy for the synthesis of complex molecules.[1,2] Metal-catalyzed carbene insertions of α-diazocarbonyls, in particular, have been widely used to enable the

syntheses of pharmaceutical agents and natural products alike.[3] Importantly, high levels of regio-, diastereo-, and/or enantioselectivity can be achieved in these reactions by tuning the substrate and/or catalyst structures. The mechanism by which these processes occur involves the reaction of a metal-stabilized carbene (metal carbenoid) with a suitable substrate *via* a concerted three-centered transition state (Scheme 3.2).[3] This produces a C-H insertion product with complete retention of configuration at the carbon of the reacting C-H bond. Notably, the C-H insertion event is asynchronous in nature and results in the development of a partial positive charge at the carbon of the reacting C-H bond, a characteristic that can significantly impact the selectivity of the reaction. In intramolecular carbene C-H insertions, the formation of 5-membered rings is generally observed because of entropic factors. However, this preference can sometimes be overridden by electronic influences. For instance, insertion preferentially occurs at sites where electron-donating groups can stabilize the partial positive charge that is generated in the transition state. For example, alkoxy and amine substituents tend to direct insertion to their adjacent C-H bonds due to their ability to engage in effective n(O) $\rightarrow$ σ^*(C-H) electron delocalization. Moreover, inductive electronic effects are also typically observed and the reactivity of competing C-H bonds follows the trend: methine (most reactive) > methylene >> methyl (least reactive). In contrast, electron-withdrawing groups (e.g. esters or acetoxy groups) deactivate proximal C-H bonds towards C-H insertion. While important, electronics factors can sometimes be outweighed by steric and/or conformational constraints in the reacting substrate. Thus, there is always a balance between the electronic, steric, and conformational properties of a given substrate that dictate which C-H bond will react preferentially.

In addition to the properties of the reacting C-H bond, the nature of the metal carbenoid plays a vital role in influencing selectivity in these reactions.[3] In general, the more electrophilic the metal carbenoid is, the more reactive it will be towards C-H insertion. However, if it is too electrophilic, poor levels of regio- and/or stereocontrol are oftentimes observed. Advantageously, the electronic properties of this reactive species can be tuned by modifying the nature of the groups adjacent to the carbene carbon (R_4 and R_5), the metal (M), and the ligands (L) on the metal. For instance, electron-withdrawing groups (acceptor groups) adjacent to the carbene carbon are destabilizing

and make the carbenoid more electrophilic. Examples of acceptor groups include both ketones and esters. In contrast, electron-donating groups (donor groups) stabilize the carbenoid, which has the effect of making it less reactive but more selective. Examples of donor groups include both aryl and vinyl substituents. While the type of carbene precursor is important, the metal-ligand combination also has a substantial influence on the reactivity and selectivity in C-H insertion reactions.[4] The two most common types of metal catalysts that are used to mediate carbenoid C-H insertions are copper and dirhodium complexes. The former are typically much more electrophilic and are therefore less selective than dirhodium catalysts. Moreover, a wide variety of chiral dirhodium catalysts have been developed to promote a host of highly selective reactions, including both intra- and intermolecular C-H insertions. Among the dirhodium complexes that have been developed as catalysts for carbene C-H insertions, dirhodium (II) tetracarboxylates and dirhodium (II) tetracarboxamidates have been the most widely studied. By simply modifying the structures of the carboxylate or carboxamidate ligands, the electronic and steric properties of these catalysts can be tuned to influence C-H insertion selectivity. In general, carboxamidate ligands tend to be less electrophilic than their carboxylate counterparts. As a result, carbenoids generated with dirhodium (II) tetracarboxamidates tend to be less reactive but more selective than those generated using dirhodium (II) tetracarboxylates. With an understanding of how each of these factors affects reactivity and selectivity, one can make systematic changes to the diazo substrate and/or catalyst structure in an attempt to bias carbene insertion into the particular C-H bond of interest.

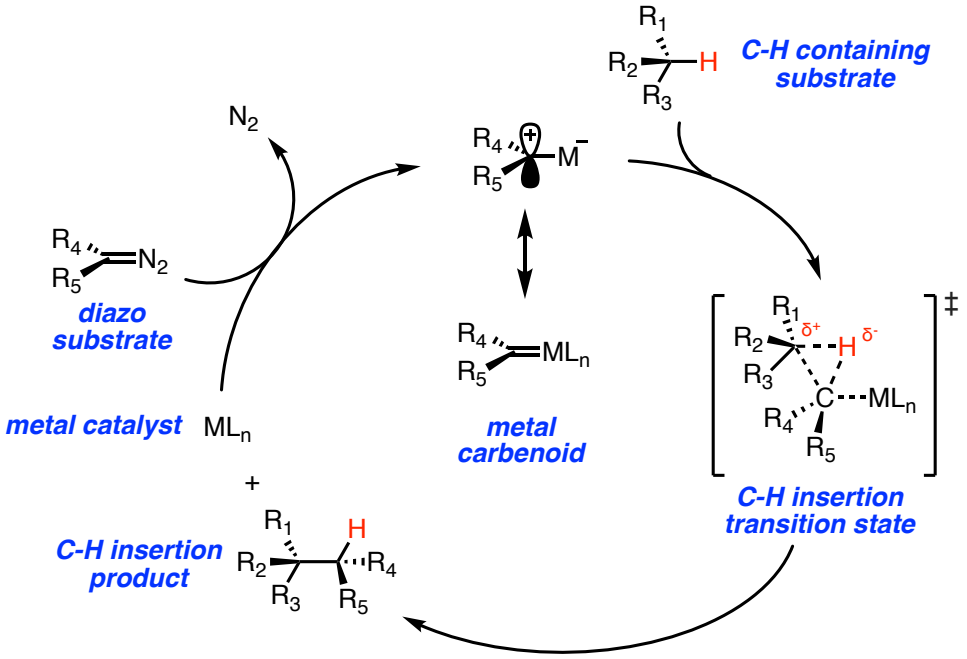

Scheme 3.2. General metal-catalyzed carbene C-H insertion mechanism.

Carbene C-H insertions can greatly simplify retrosynthetic analyses because they allow unactivated C-H bonds to be viewed as functional handles for the construction of new C-C bonds. As a result, the strategic implementation of a carbene C-H insertion into the synthesis of a complex molecule can lead to remarkable levels of synthetic efficiency. For example, Hashimoto and Doyle demonstrated that enantioselective carbene C-H insertions could be used to rapidly prepare the two pharmaceutical drugs (−)-rolipram (**3.3**) and (−)-baclofen (**3.6**), respectively (Scheme 3.3).[5] Moreover, Zhang et al. recently reported an elegant synthesis of the natural product aplydactone (**3.9**), where a late-stage carbene C-H insertion was used to construct an all-carbon quaternary stereocenter in the penultimate step.[2j]

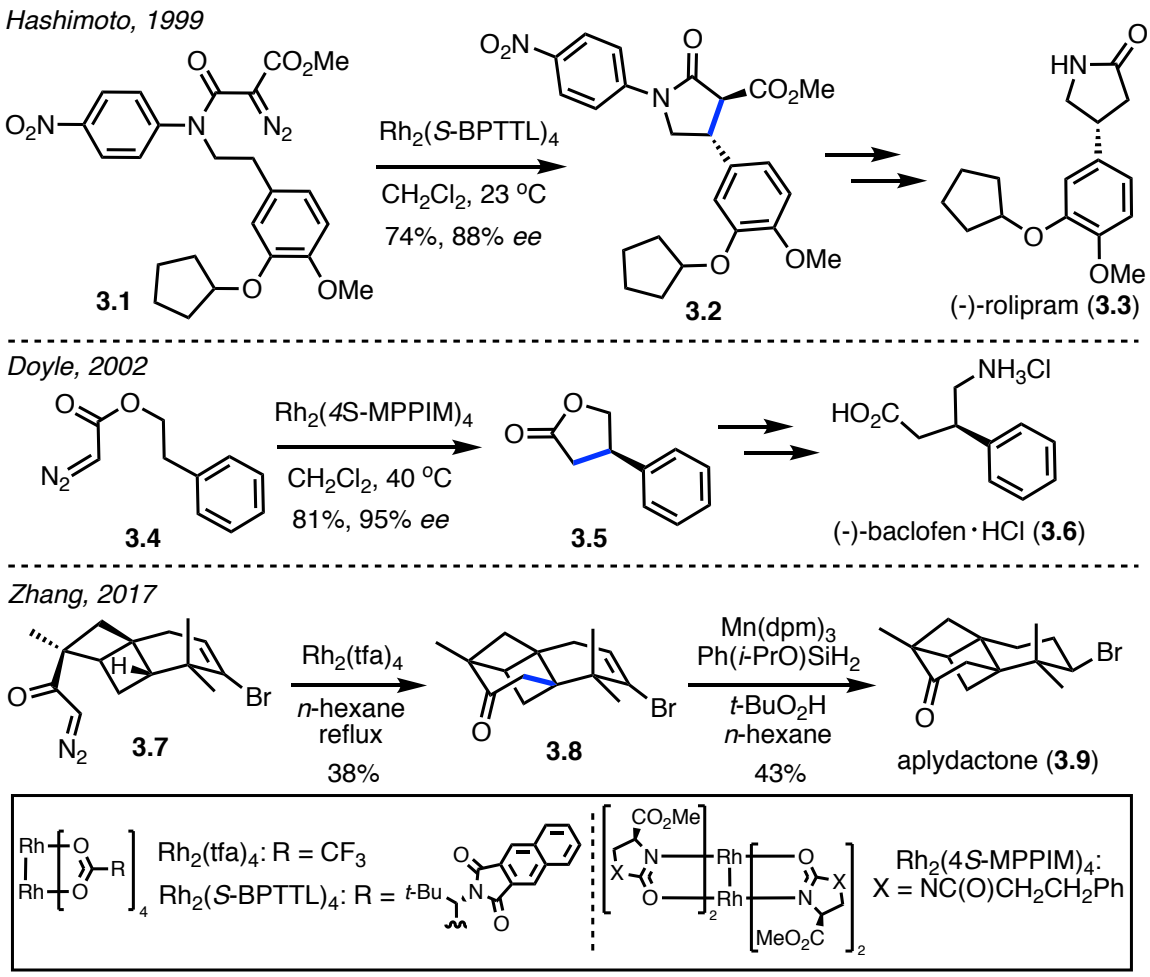

Scheme 3.3. Examples of strategic carbene C-H insertions in synthesis.

When considering potential avenues to selectively functionalize **2.73**, we initially elected to pursue a carbene C-H insertion strategy because it offered the most direct route to virosaine A (**1.24**) *via* butanolide **2.1**. Visual assessment of **2.73** suggested that a direct selective functionalization would likely be a challenging task due to potential difficulties associated with controlling regioselectivity in the presence of 12 distinct C-H bonds and chemoselectivity in the presence of the basic isoxazolidine. However, the presence of the C10 hydroxy as a tethering point opened up the possibility to carry out an intramolecular carbene C-H insertion (e.g. **3.10** → **2.1**), effectively limiting the potential sites of reactivity to the C2 methine, the C9 methylene and the (desired) C14 methine (Figure 3.1).

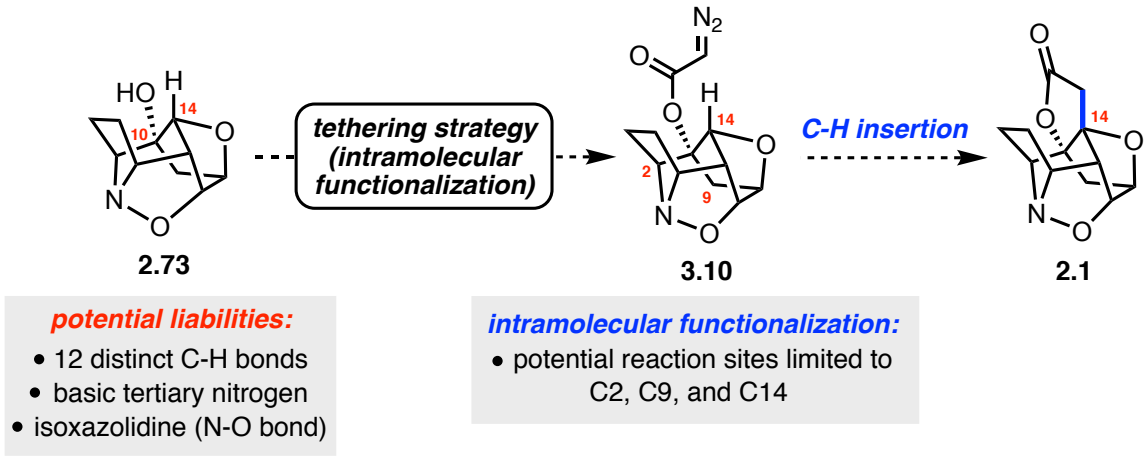

Figure 3.1. Tethering strategy for intramolecular functionalization of the virosaine core *via* carbene C-H insertion.

Of note, there are only a handful of successful examples of carbene insertions into bridgehead C-H bonds reported in the literature (Scheme 3.4).[2e,6] Osawa and Sonawane published the earliest examples of such to access cyclopentanone products **3.12** and **3.14**/**3.16**, respectively.[6a,b] However, the α-diazoketone substrates used in these reactions were relatively simple, being comprised of conformationally rigid hydrocarbon skeletons that lacked other functional groups. Since then, several examples of bridgehead C-H insertions using alkylidene carbenes and (α-silyl-)α-diazoacetates have been demonstrated on more complex oxygen-containing substrates.[2e,6c-e] In several of these cases, good yields and selectivities were observed for the insertion process (i.e. **3.17** → **3.18**, **3.22** → **3.23**, and **3.24** → **3.25**).[2e,6c,d] However, in other cases, mixtures of products were obtained due to undesired regio- and chemoselectivity preferences of the substrates in question. For example, May et al. found that α-diazoacetates **3.26a**/**b** produced lactone products **3.27a**/**b** in very low yields as a result of preferred insertion into the C2-R_1 bond (R_1 = H or D).[6e] Only by blocking the C2 position with a fluorine atom (i.e. **3.26c**) could they overcome this innate bias and access the desired C1 insertion product **3.27c** in good yield. May's work highlights the potential regioselectivity issues that can arise when trying to effect a carbene C-H insertion at the bridgehead position of a complex molecule.

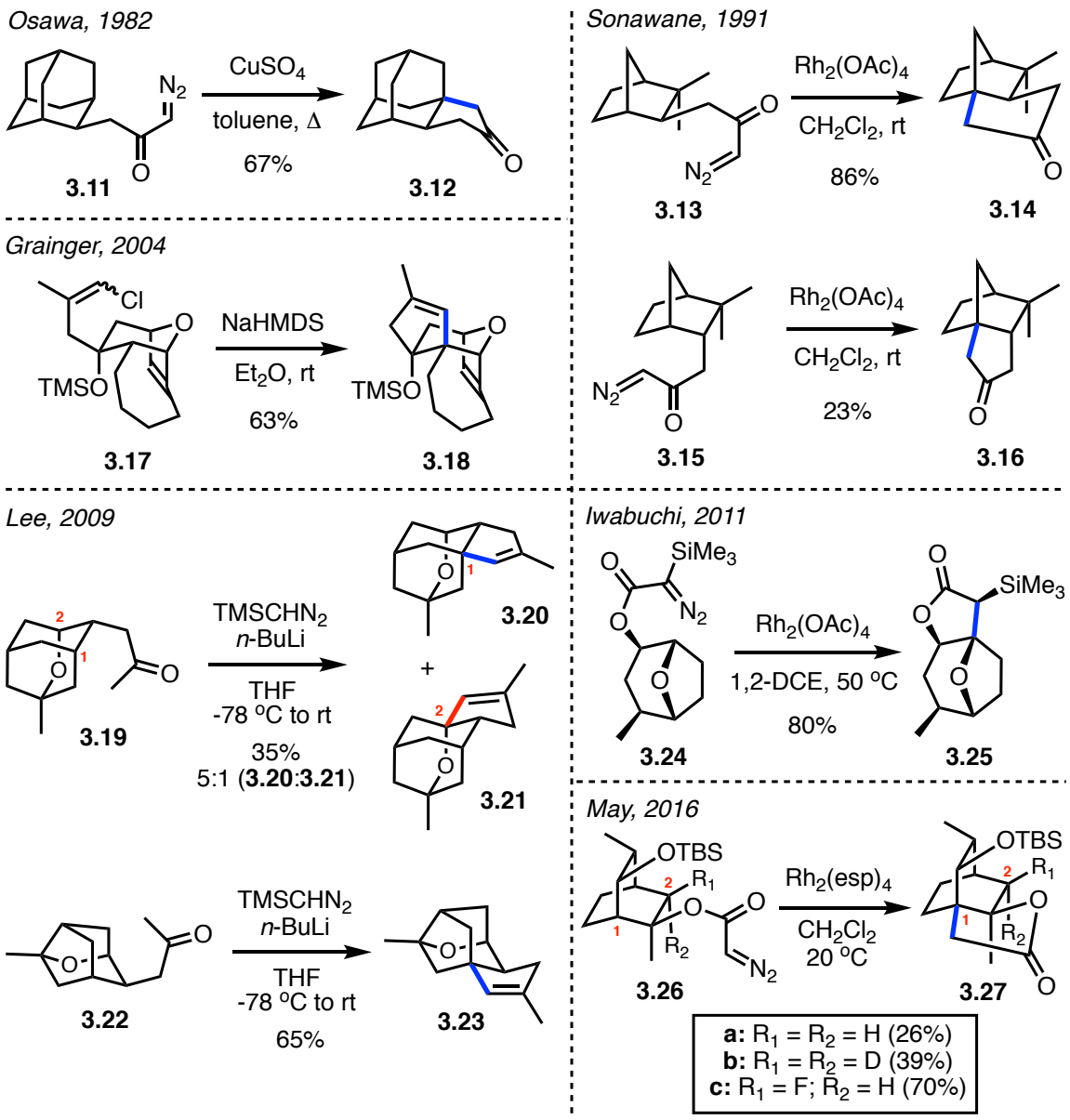

Scheme 3.4. Examples of carbene insertions into bridgehead C-H bonds.

Lee and coworkers gained additional insight into the reactivity patterns of carbenes in bridged systems.[2e] Specifically, they showed that bridgehead positions vicinal to an oxygen atom are inductively deactivated towards carbene C-H insertions. This was elegantly demonstrated in the reaction of ketone **3.19** with $TMSCHN_2$/*n*-BuLi, where competing intramolecular alkylidene carbene insertions occurred to provide tricycles **3.20** and **3.21** in a 5:1 ratio (35% combined yield). They hypothesized this product distribution to be a consequence of geometrical constraints that prevented efficient n(O) → σ*(C2-H)

electron delocalization. As a result, the bridging oxygen atom could not stabilize the buildup of positive charge at C2 in the transition state and therefore only had an inductively deactivating effect. Considering that C14 in **3.10** is also vicinal to a bridging oxygen atom, Lee's findings were disconcerting. Nonetheless, we were encouraged by Iwabuchi's successful execution of an ethereal bridgehead C-H insertion to access silyllactone **3.25** in high yield.[6d] This result, which appears to challenge the trend observed by Lee et al., suggested to us that site selectivity might be considerably substrate-dependent.

Given the limited set of examples of bridgehead carbene C-H insertions, we were cognizant of the potential difficulties that might accompany this strategy. In particular, the presence of the bridging oxygen atom adjacent to C14 suggested that selective functionalization of this position over the other potential sites (C2 or C14) might be challenging, especially given the precedent set by Lee and coworkers (*vide supra*).[2e] Moreover, there are no examples in the literature of a bridgehead carbene C-H insertion being conducted on a molecule that contains a Lewis basic nitrogen and we had concerns about the possibility of the isoxazolidine nitrogen suppressing catalyst activity *via* coordination to the Lewis acidic metal center. However, despite these concerns, we felt that the potential directness of this route merited investigation. Furthermore, the successful implementation of this C-H functionalization would validate our bio-inspired cascade reaction as a meaningful and efficient strategy to prepare virosaine A (**1.24**). From a more general perspective, this transformation would further enforce the usefulness of using C-H functionalization strategies to streamline the syntheses of complex molecules.

Since many of the reaction parameters that impact carbene C-H insertion selectivity (i.e. carbenoid electronic properties, metal-ligand combinations, etc.) can readily be tuned, we were cautiously optimistic that a thorough screening of conditions would allow access the desired insertion product **2.1**. Accordingly, diazoacetate **3.10** was prepared from **2.73** in a high-yielding one-pot procedure involving sequential diketene addition, diazo transfer, and deacetylation (Scheme 3.5). With **3.10** in hand, we surveyed several common dimeric rhodium catalysts in hopes of accessing lactone **2.1**. However, we were disappointed to find that complex, inseparable mixtures of products were

generated in every case. Moreover, ^{1}H NMR analysis of the crude reaction mixtures showed no indication of lactone **2.1** or any other C-H insertion products. Notably, the undesired *Z* and *E* alkene dimers **3.28** were observed in several reactions, even when **3.10** was added slowly *via* syringe pump addition. The dimeric products were readily identified by their characteristic olefinic singlets in the crude ^{1}H NMR spectra, which were centered at δ = 6.19 ppm (*Z*) and δ = 6.80 ppm (*E*).[7]

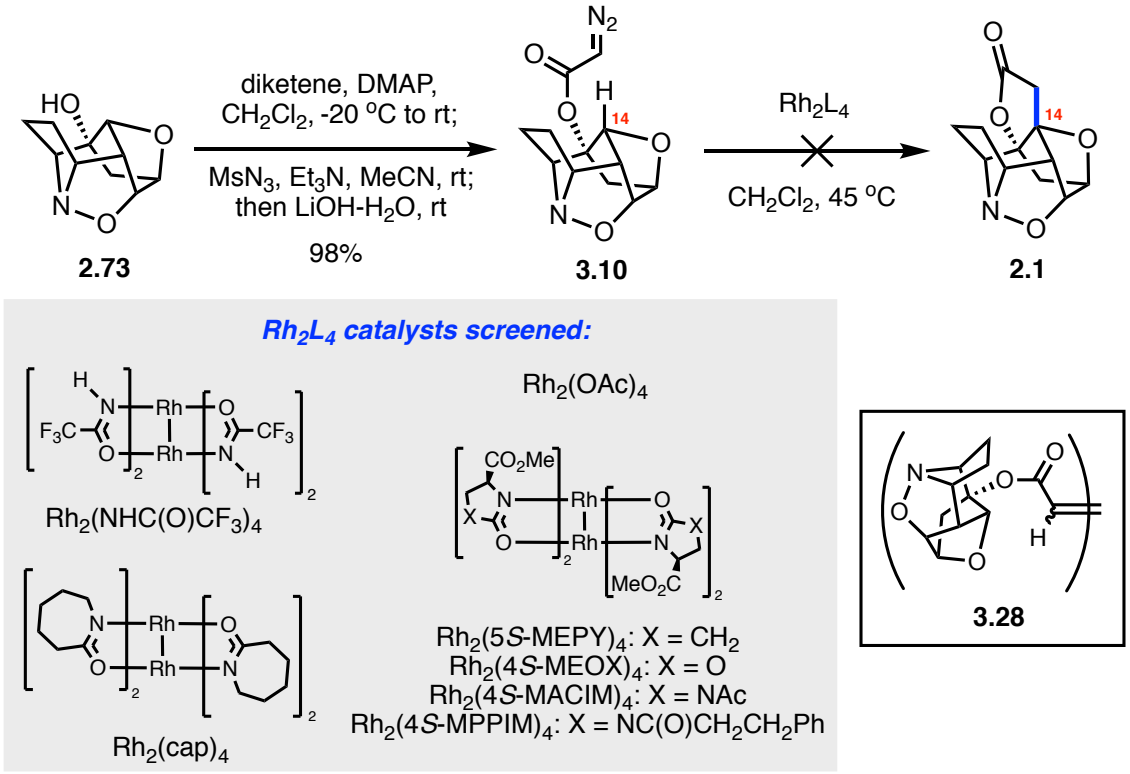

Scheme 3.5. Attempted C-H insertion of α-diazoacetate **3.10**.

Given the undesired reactivity of **3.10**, we turned our attention to the corresponding trimethylsilyl diazoacetate **3.29**, prepared by treating **3.10** with TMSOTf (Scheme 3.6). Silyl diazoacetates have been shown to attenuate C-H insertion reactivity and thus, we were hopeful that **3.29** might permit access to silyllactone **3.31** (R = TMS).[6d] Indeed, we were pleased to find that refluxing **3.29** with 3 mol % $Rh_2(OAc)_4$ in 1,2-dichloroethane (1,2-DCE) afforded a cleaner reaction profile than that of the parent diazoacetate **3.10**. The attenuated reactivity of **3.29** prevented undesired dimer formation and enabled a simple experimental protocol that avoided the use of syringe pump addition. Moreover, upon purification of the reaction mixture, we isolated a C-H insertion

product in 9% yield. Unfortunately, structural analysis revealed this product to be silyllactone **3.32**, resulting from C-H insertion into the C9 methylene (Table 3.1, entry 2). While the formation of **3.32** was undesired, we were encouraged by the tempered reactivity demonstrated by **3.29**. Thus, we decided to continue screening different metal catalysts in hopes of influencing the selectivity of the reaction to access the desired product **3.31**. However, additional reactions of **3.29** revealed a tendency for it to undergo protodesilylation. As a result, we prepared the more stable triethylsilyl diazoacetate **3.30** from **3.10** and Et_3SiOTf (Scheme 3.6) and then screened it against several metal catalysts (Table 3.1, entries 3-11).

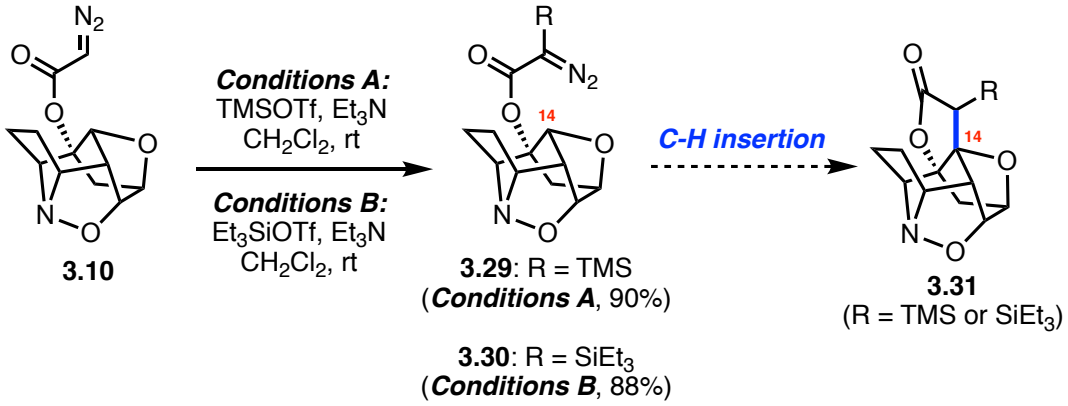

Scheme 3.6. Preparation of silyl diazoacetates **3.29** and **3.30**.

Unlike **3.29**, a mixture of **3.30** and $Rh_2(OAc)_4$ did not react at 85 °C (entry 3). However, changing the reaction solvent to toluene and heating at 120 °C delivered an analogous C9 insertion product, silyllactone **3.33**, in 9% isolated yield (entry 4). Dirhodium (II) tetracarboxamidate catalysts are less electrophilic than their dirhodium (II) tetracarboxylate counterparts and typically produce carbenoids that selectively react with tertiary C-H bonds over secondary C-H bonds.[3,4] Thus, we began screening catalysts of this type in hopes of overriding the C9 selectivity observed with $Rh_2(OAc)_4$. To our disappointment, neither $Rh_2(cap)_4$ nor $Rh_2(5S\text{-MEPY})_4$ were effective in altering the selectivity of the C-H insertion. Interestingly, however, they both delivered lactone **3.34**, resulting from C9-H insertion as well as protodesilylation (entries 5 and 6). Heating **3.30** with $Rh_2(4S\text{-MACIM})_4$ either at 110 °C in trifluorotoluene or at 120 °C in toluene did not produce any products, a potential consequence of this catalyst's insolubility in these two

solvents (entries 8 and 9). Furthermore, while $Rh_2(4S\text{-MACIM})_4$ was soluble in 1,2-dichloroethane, no reaction of **3.30** occurred in this solvent at 85 °C (entry 9). Finally, while $Rh_2(4S\text{-MPPIM})_4$ proved to be an inadequate catalyst (entry 10), we found that heating **3.30** with 5 mol % $Rh_2(NHC(O)CF_3)_4$ provided silyllactone **3.33** in a much improved 47% yield (entry 11).[8]

Table 3.1. C-H insertions of silyl diazoacetates **3.29** and **3.30**.[a]

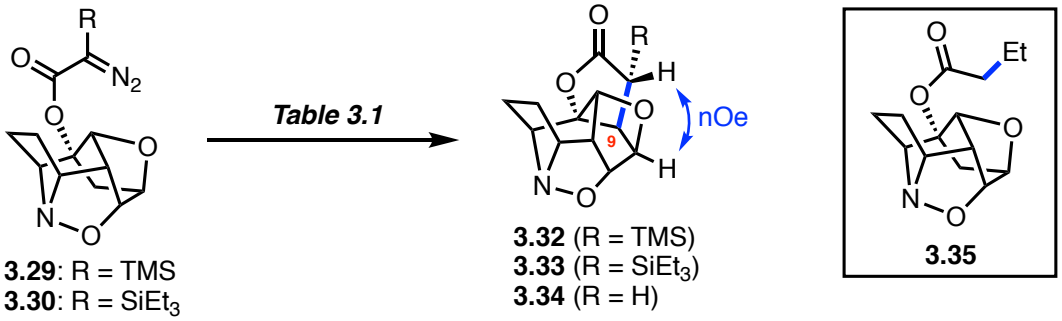

3.29: R = TMS
3.30: R = $SiEt_3$

3.32 (R = TMS)
3.33 (R = $SiEt_3$)
3.34 (R = H)

3.35

Entry	R	Catalyst (mol %)	Solvent	Temp (°C)	Yield of 3.32 or 3.33 (%)[b]
1	TMS	$Rh_2(OAc)_4$ (3)	CH_2Cl_2	45	0[c]
2	TMS	$Rh_2(OAc)_4$ (5)	1,2-DCE	85	9
3	$SiEt_3$	$Rh_2(OAc)_4$ (10)	1,2-DCE	85	0[c]
4	$SiEt_3$	$Rh_2(OAc)_4$ (10)	toluene	120	9
5	$SiEt_3$	$Rh_2(cap)_4$ (10)	toluene	120	<5[d]
6	$SiEt_3$	$Rh_2(5S\text{-MEPY})_4$ (10)	toluene	120	10[d]
7	$SiEt_3$	$Rh_2(4S\text{-MACIM})_4$ (10)	1,2-DCE	85	0[c]
8	$SiEt_3$	$Rh_2(4S\text{-MACIM})_4$ (10)	$PhCF_3$	110	0[c]
9	$SiEt_3$	$Rh_2(4S\text{-MACIM})_4$ (10)	toluene	120	0[c]
10	$SiEt_3$	$Rh_2(4S\text{-MPPIM})_4$ (10)	toluene	120	0[e]
11	$SiEt_3$	$Rh_2(NHC(O)CF_3)_4$ (5)	toluene	120	47

[a]All reactions were conducted by quickly adding **3.29** or **3.30** to a suspension of the catalyst to give a final reaction concentration of [**3.29** or **3.30**] = 0.01 M. [b]Isolated yields of **3.32** or **3.33**. [c]No reaction. [d]Lactone **3.34** generated. [e]Complex mixture containing unreacted **3.30**.

Interestingly, in addition to the lactone product **3.33**, butyrate **3.35** was consistently generated from **3.30** in minor amounts, presumably *via* silyl carbene rearrangement.[9] A plausible mechanism for the formation of **3.35** is shown in Scheme 3.7 and involves rearrangement of ylide **3.37** to generate acyl silene **3.38**. Protodesilylation of **3.38**, either on silica gel or by adventitious water, would then produce of **3.35**.

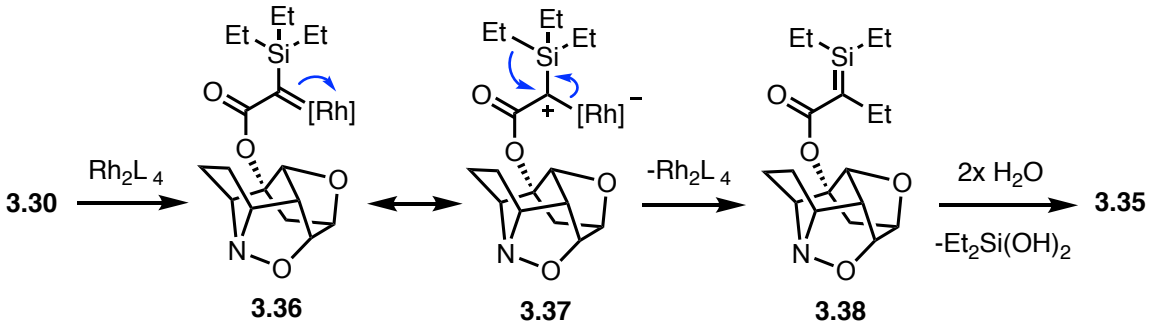

Scheme 3.7. Plausible mechanism for the formation of butyrate **3.35**.

To study the consequence of modifying the substrate electronics on the carbene insertion process, diazomalonate **3.40** was prepared from **2.73** *via* acylation with methyl malonyl chloride followed by diazo transfer on the intermediate malonate **3.39** (Scheme 3.8). Intriguingly, when diazomalonate **3.40** was treated with catalytic amounts of either $Rh_2(OAc)_4$ or $Rh_2(NHC(O)CF_3)_4$, the major product was cyclic ether **3.43**. The mechanism for the formation of **3.43** likely involves trapping of the highly electrophilic rhodium carbenoid **3.41** by an oxygen lone pair to generate oxonium ylide **3.42**. An elimination/protonation process would then deliver the observed product **3.43**.

Donor/acceptor carbenoids have been shown to undergo highly regio- and stereoselective C-H insertion reactions.[3] Consequently, we chose to prepare silyl-substituted vinyl diazoacetate **3.45** and study its potential for the intramolecular C-H insertion reaction (Scheme 3.9). A one-pot procedure involving diketene addition to alcohol **2.73** and subsequent diazo transfer with MsN_3 afforded diazo ketoester **3.44** in 97% yield. Treatment of **3.44** with TBSOTf/Et_3N then generated **3.45** in near quantitative yield. However, we were disappointed to find that reactions of **3.45** with several dimeric rhodium catalysts failed to deliver the desired C-H insertion product **3.46** and instead only generated complex mixtures.

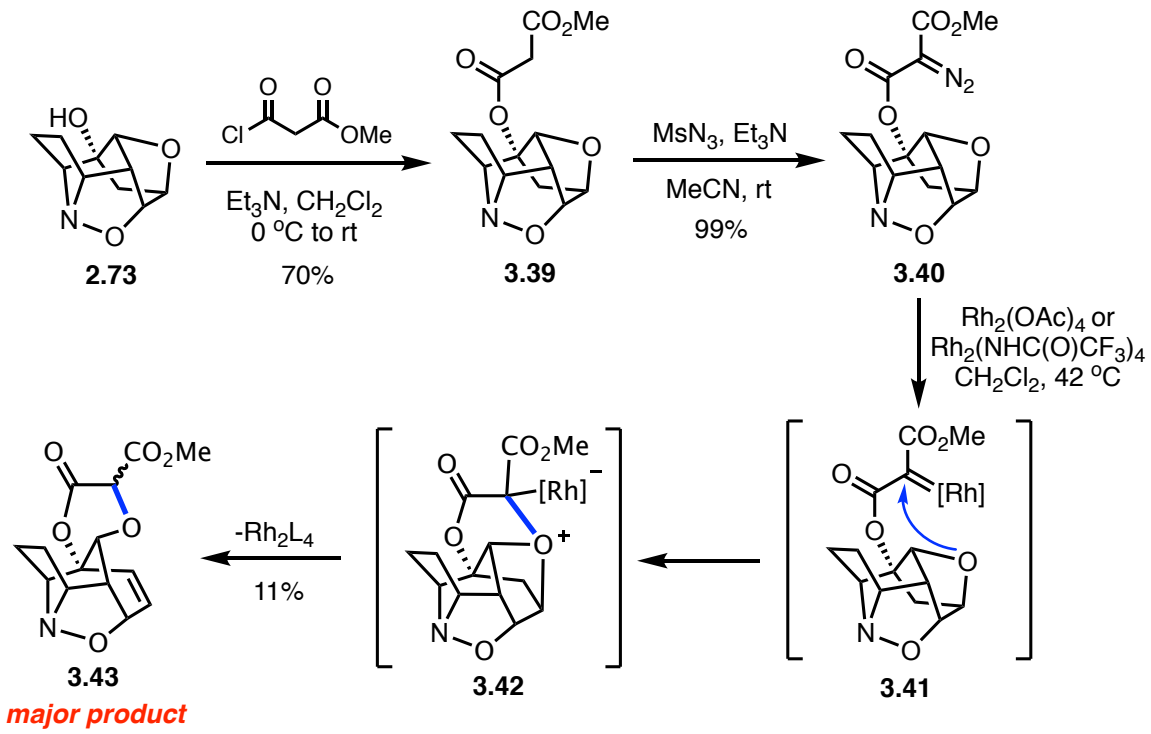

Scheme 3.8. Reactions of diazomalonate **3.40** to form cyclic ether **3.43**.

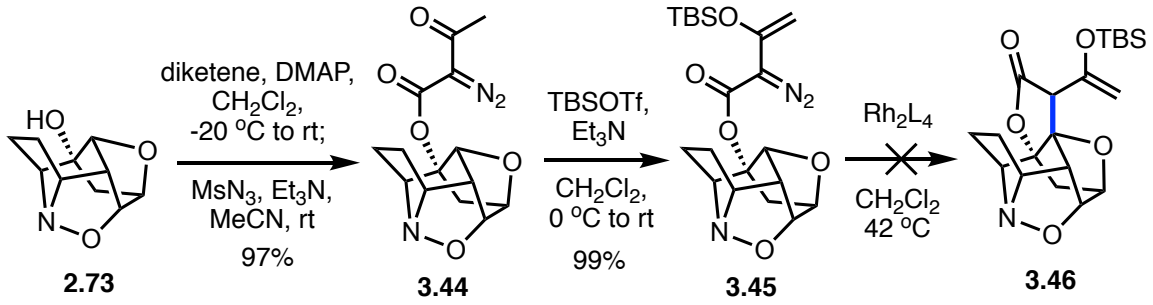

Scheme 3.9. Attempted C-H insertion of silyl-substituted vinyl diazoacetate **3.45**.

We considered whether the undesired reactivity observed in the attempted metal-catalyzed carbene insertions might be due to the sterics associated with the large rhodium carbenoid. This prompted us to explore the possibility of using a free carbene to insert into the C14-H bond. Accordingly, solutions of diazoacetates **3.10** and **3.30** in CCl_4 were exposed to ultraviolet light (254 nm) (Scheme 3.10). However, under these conditions, the only products generated in the reaction were perchlorinated esters **3.47** and **3.48**, resulting from exclusive reaction with the solvent itself. Changing the reaction medium to

the less reactive $PhCF_3$ did not prove beneficial and, in the case of both diazoacetate substrates, complex mixtures of products were generated. In the case of silyl diazoacetate **3.30**, several products could be identified in the crude reaction mixture. These included three previously known compounds (alcohol **2.73**, silyllactone **3.33**, and butyrate **3.35**) as well as an oxygen trapping/elimination product **3.49** (tentative assignment). These results indicated that a free carbene was far from selective and was unlikely to deliver the desired C-H insertion product in high yield, if at all.

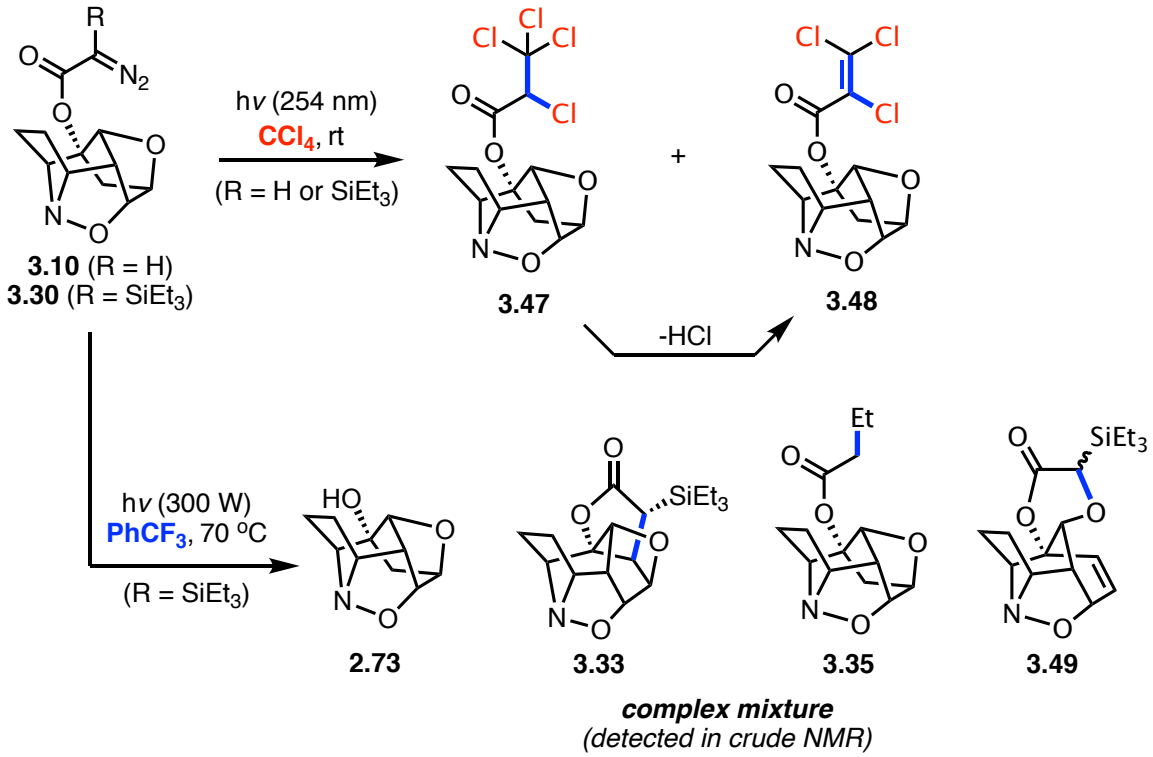

Scheme 3.10. Photolytic carbene generation from diazoacetates **3.10** and **3.30**.

As a final attempt at using a carbene C-H insertion to functionalize C14, we attempted an intermolecular carbene insertion. Specifically, we exposed the TMS-protected virosaine core **3.50** to ethyl diazoacetate in the presence of catalytic $Rh_2(OAc)_4$ (Scheme 3.11). However, the only product generated in the reaction was aminal **3.53** resulting from a formal N-O carbene insertion. Perhaps unsurprisingly, the formation of **3.53** likely occurs *via* trapping of rhodium carbenoid **3.51** by the isoxazolidine nitrogen of **3.50**. This would lead to aza ylide **3.52**, which can undergo subsequent Stevens

rearrangement.[10] While this result was clearly undesired, to the best of our knowledge, this is the first example of a carbene insertion into the N-O bond of an isoxazolidine.[11,12] In addition, this transformation clearly highlights the difficulties of employing an intermolecular functionalization strategy in the presence of the reactive isoxazolidine unit.

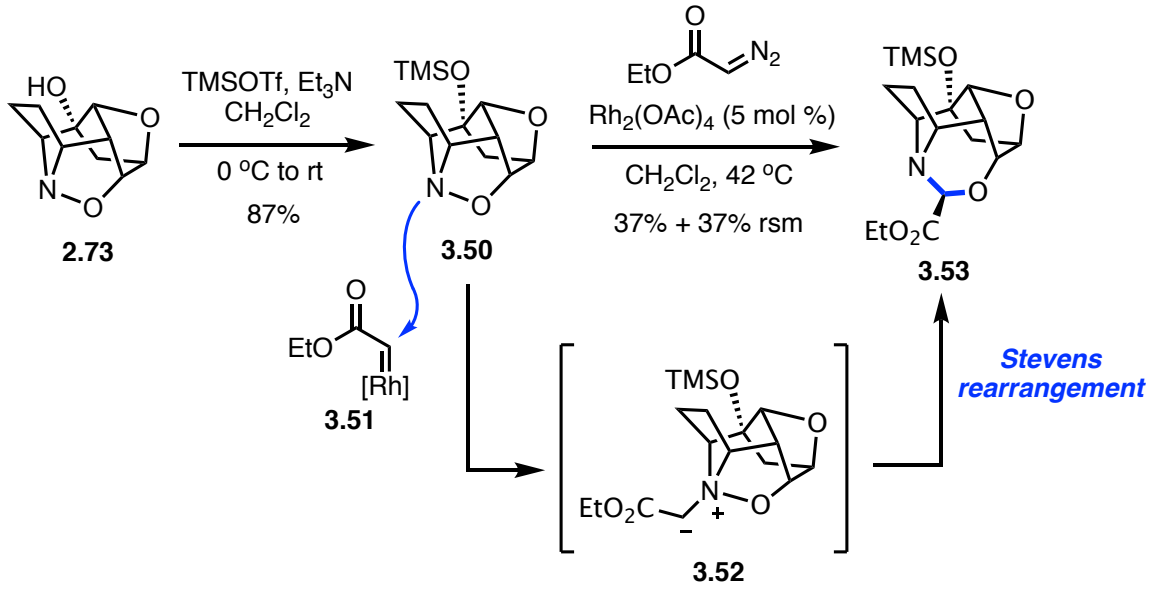

Scheme 3.11. Formal intermolecular carbene N-O insertion.

3.3 Nitrene C-H Insertion Strategy to Functionalize C14 of the Virosaine Core

The inability of carbenes/carbenoids to insert into the bridgehead position can potentially be attributed to several factors, such as the steric environment around C14 and/or the silyl rhodium carbenoid as well as the presence of other reactive functional groups in the system. As an alternative to this approach, we considered the corresponding nitrene C-H insertion reactions, which have seen considerable development throughout the past two decades and have enjoyed widespread utility in the synthesis of natural products.[13,14] Furthermore, there are several reports of the use of intramolecular nitrene C-H insertions to functionalize bridgehead positions in complex molecular settings.[2a,f,14e-g] For example, Du Bois et al. prepared the highly functionalized pentacycle **3.55** *via* intramolecular nitrene insertion of carbamate **3.54** in their synthesis of tetrodotoxin (Scheme 3.12).[2a] Moreover, Garg and coworkers utilized intramolecular nitrene C-H

insertions in their syntheses of several welwitindolinone alkaloids. For instance, the reaction of carbamate **3.56** to form oxazolidinone **3.57** was employed in the total synthesis of *N*-methylwelwitindolinone B isothiocyanate.[14g] Although a nitrene insertion at C14 in a carbamate such as **3.58** would not introduce the butanolide directly, hydrolysis of the resulting oxazolidinone **3.59** would reveal a ketone (i.e. **3.60**) which might be amenable to further manipulation to ultimately produce **1.24** (Scheme 3.13).

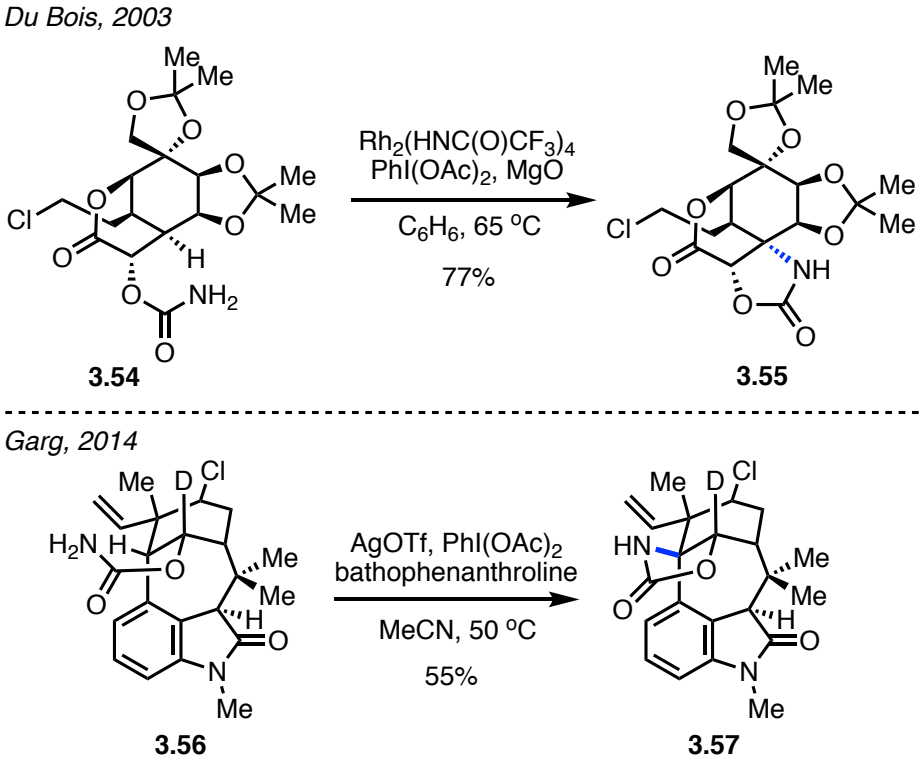

Scheme 3.12. Examples of nitrene insertions into bridgehead C-H bonds.

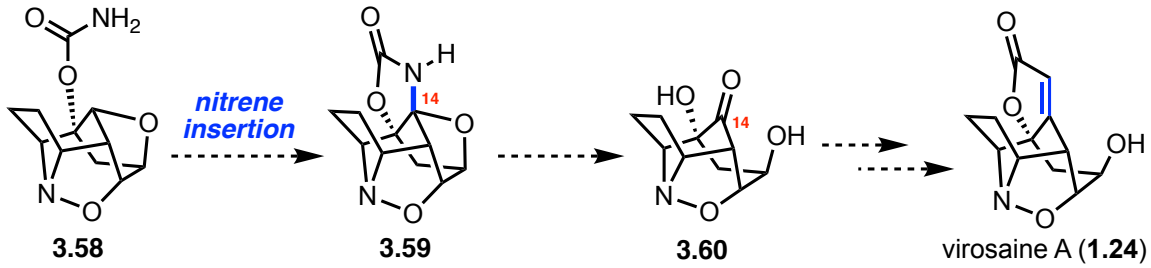

Scheme 3.13. Proposed nitrene C-H insertion route to functionalize C14 and access virosaine A.

Carbamate **3.58** was prepared in near quantitative yield from alcohol **2.73** through sequential reaction with $Cl_3CC(O)NCO$ and $NaHCO_3$/MeOH (Scheme 3.14). With **3.58** in hand, we screened various nitrene generating conditions and quickly identified He's conditions [$PhI(OAc)_2$, AgOTf, bathophenanthroline, MeCN, 82 °C, sealed tube] as optimal, providing a single reaction product in 80% yield.[2f,14e-g,15] However, structural elucidation revealed that, in contrast to the carbene insertion reaction of silyldiazoacetates **3.29**/**3.30** (*vide supra*), nitrene insertion of **3.58** had occurred at C2 to provide oxazolidinone **3.61**. Employing rhodium carboxylate catalysts in combination with $PhI(OAc)_2$ also facilitated insertion to yield **3.61**, albeit in lower yields.[16] Interestingly, we found that the same reaction conducted in CH_2Cl_2, instead of MeCN, provided a completely different product. Extensive 2D NMR analysis revealed this new product to be diacetoxy ketone **3.62**, whose formation is the result of both C2 oxidation and C10-C14 bond cleavage.

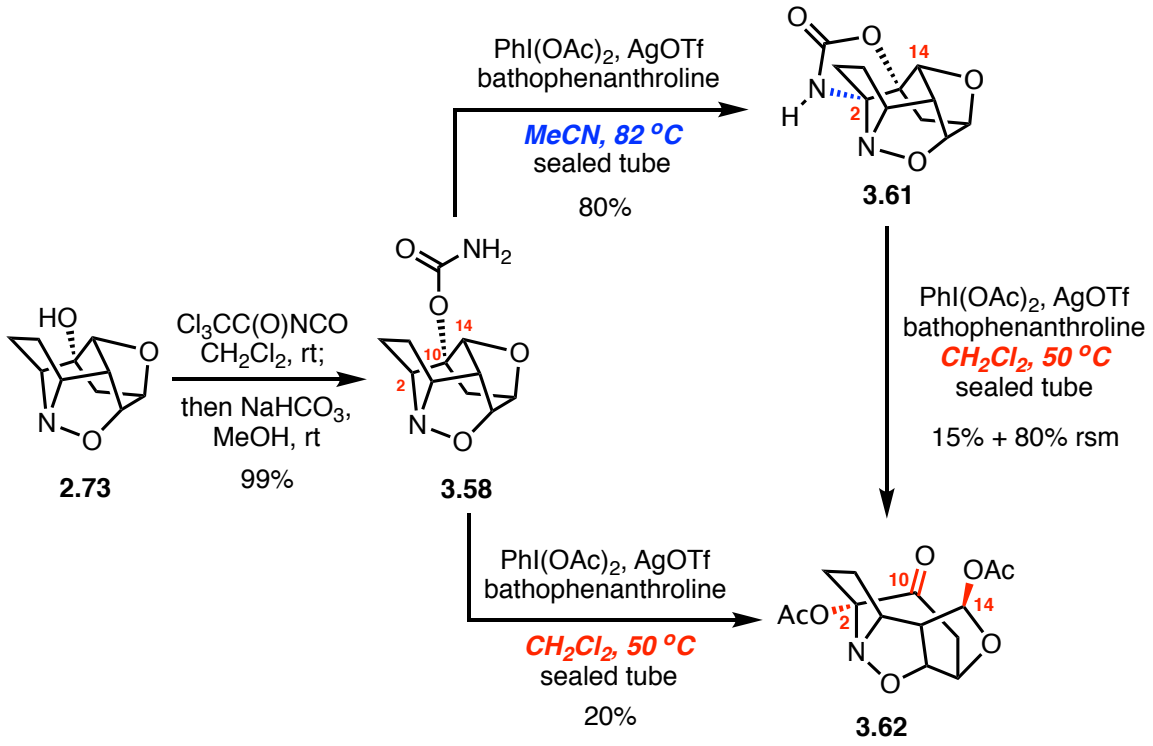

Scheme 3.14. Oxidative transformations of carbamate **3.58**.

Our preliminary mechanistic hypothesis for the formation of **3.62** is that it is generated *via* oxidation of oxazolidinone **3.61** according to one of the two routes depicted in Scheme 3.15. Under the slightly more acidic conditions (CH_2Cl_2 vs. MeCN), C2-aminal exchange might take place to generate **3.63** (path a). Subsequent oxidation of **3.63** with $PhI(OAc)_2$ might generate oxonium **3.65** *via* Grob-like C10-C14 bond cleavage of **3.64**. Finally, oxonium trapping with acetate would generate **3.62**. Alternatively, oxazolidinone **3.61** might undergo direct oxidative Grob-like fragmentation to generate oxonium **3.67** (path b). Acetate trapping of **3.67** and aminal exchange of **3.68** would then produce **3.62**.

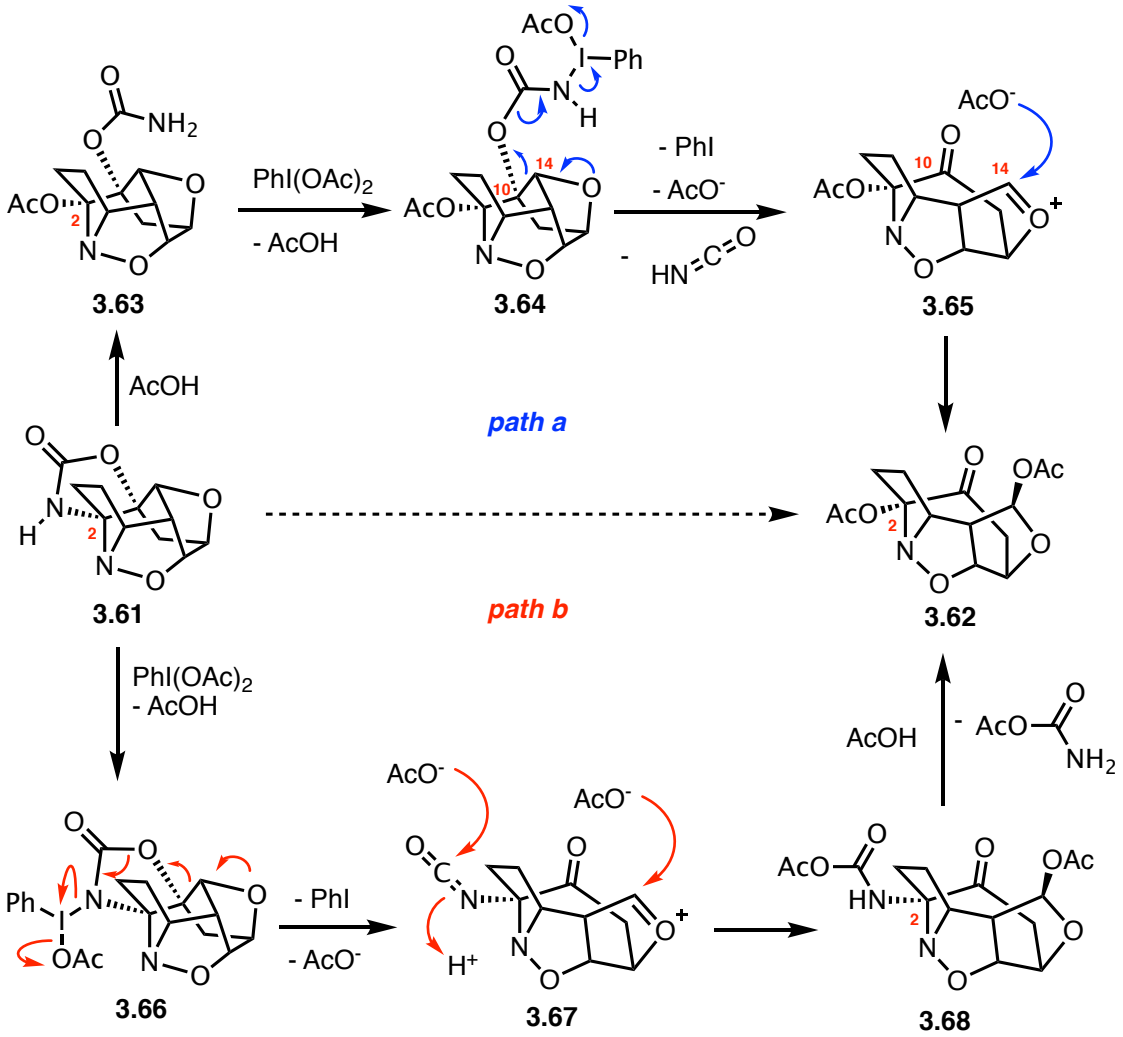

Scheme 3.15. Plausible mechanisms for the formation of diacetoxy ketone **3.62**.

While the proposed intermediates shown in Scheme 3.15 have not been observed experimentally, evidence to support these proposals was gained by converting **3.61** to **3.62** upon submission to same reaction conditions (Scheme 3.14). Moreover, the feasibility of the C2 aminal exchange step was established based on the following observations: (a) when oxazolidinone **3.61** was heated in the presence of acetic acid, C2-opening occurred to give ketone **3.69** in 79% yield and (b) diacetoxy ketone **3.62** underwent rapid C2 aminal exchange with methanol in the presence of trace acid (from a $CDCl_3$ bottle) to form **3.70** in quantitative yield (Scheme 3.16).

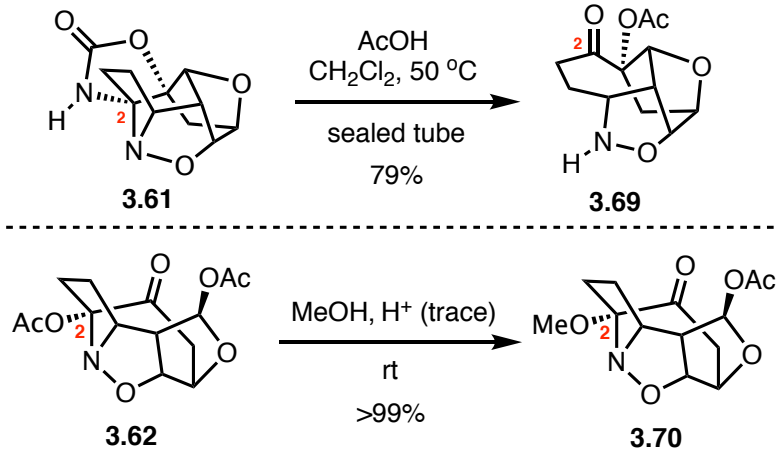

Scheme 3.16. Experimental evidence to support C2-aminal exchange.

We were pleased that nitrene insertion of carbamate **3.58** had occurred at a bridgehead position rather than the C9 methylene and wondered whether we could direct this reaction to the C14 bridgehead position by electronically deactivating C2. Several groups have independently demonstrated that C-H bonds proximal to basic aliphatic amines can be electronically deactivated through protonation or Lewis acid coordination.[17,18] Indeed, we found that protonation or Lewis-Acid coordination of carbamate **3.58** cleanly generated the corresponding ammonium ion **3.71** and that treating the latter with LiOH regenerated the former in quantitative yield (Scheme 3.17). Unfortunately, however, submission of **3.71** to He's nitrene insertion conditions led only to decomposition of material, which impeded the use of this approach.

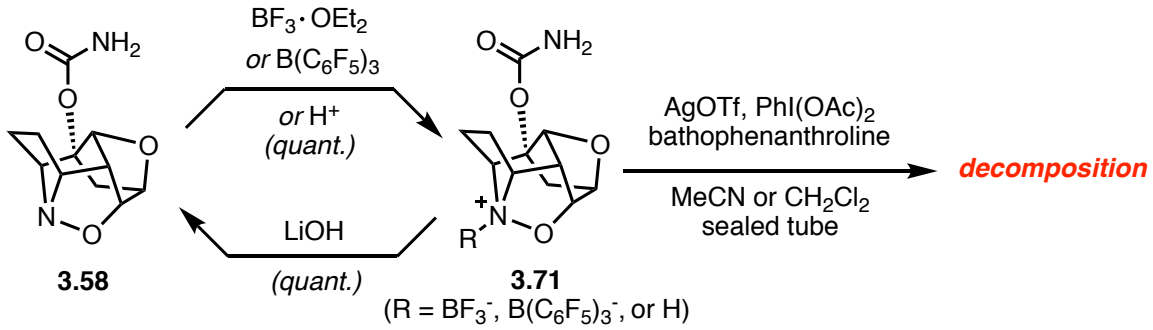

Scheme 3.17. Attempted nitrene C-H insertion of adduct **3.71**.

Sulfamate esters can also serve as useful substrates for nitrene C-H insertions and display complementary regioselectivity to their carbamate counterparts in intramolecular reactions.[15a,16b,19] Accordingly, sulfamate ester **3.72** was prepared from alcohol **2.73** and an acetonitrile solution of sulfamoyl chloride (Scheme 3.18). With **3.72** in hand, we screened several reaction conditions, including Du Bois' Rh-catalyzed conditions,[16] He's Ag-catalyzed conditions,[15] and White's Mn-catalyzed conditions[19b] in hopes of accessing oxathiazinane **3.73**. However, sulfamate ester **3.72** generally remained unreactive under the majority of these conditions. The sole exception occurred upon submitting a dichloromethane solution of **3.72** to He's conditions. In this instance, diacetoxy ketone **3.62** was generated as the major product, analogous to the reaction of carbamate **3.58** (*vide supra*).

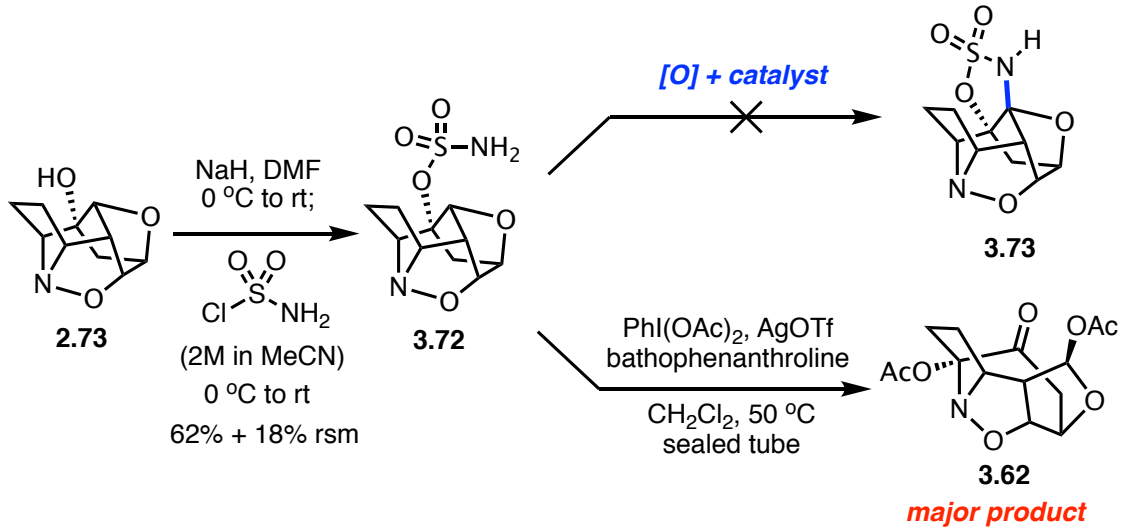

Scheme 3.18. Attempted nitrene C14-H insertion of sulfamate ester **3.72**.

3.4 Sequential C10-C14 Oxidative Cleavage/Reductive Pinacol Coupling Strategy

While the Ag-mediated oxidative transformations of carbamate **3.58** and sulfamate ester **3.72** failed to deliver the desired C14-H insertion products **3.59** and **3.73**, the formation of diacetoxy ketone **3.62** was intriguing. Although not part of the initial strategy, the C14 position was modified during the bond cleavage event to the aldehyde oxidation state. This led us to consider whether it would be possible to achieve this same bond cleavage while avoiding C2 oxidation to produce ketone **3.74** (Scheme 3.19). Further, **3.74** might be oxidized to lactone **3.75** and a subsequent lactone-ketone pinacol coupling could re-unite C10 and C14 to produce the dihydroxylated virosaine core **3.76**.[20]

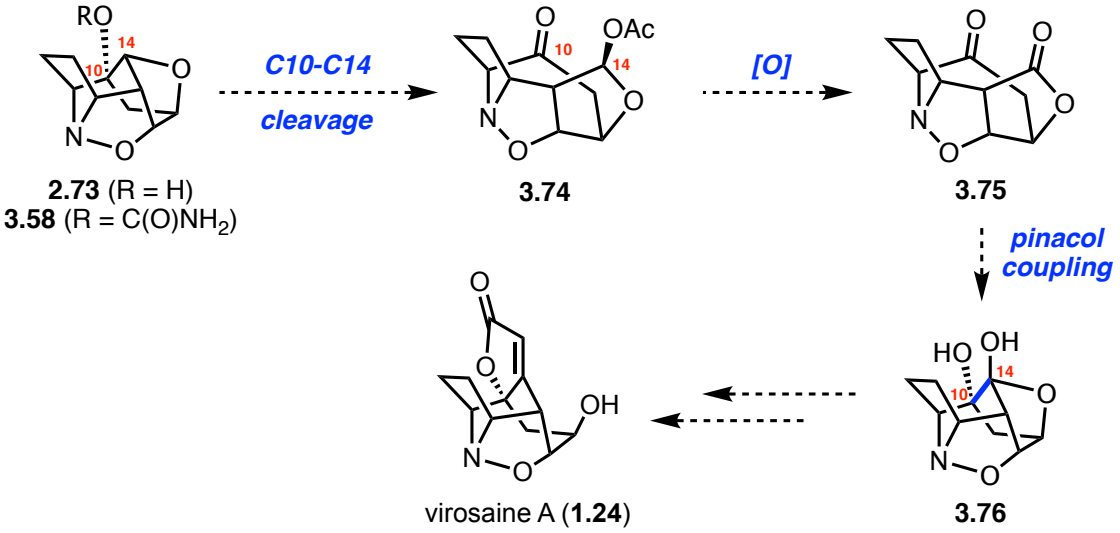

Scheme 3.19. Sequential C10-C14 oxidative cleavage/reductive pinacol coupling strategy to functionalize C14.

A series of oxidants were screened with both alcohol **2.73** and carbamate **3.58** but all failed to induce selective cleavage of the C10-C14 bond (Scheme 3.20). In contrast, we found that treating alcohol **2.73** with He's nitrene insertion conditions, as above, resulted in complementary selectivity to that observed for carbamate **3.58**. Specifically, the reaction produced tetracycles **3.77** and **3.78**, each resulting from exclusive C2-C10 bond cleavage followed by further oxidation to the *N*-alkoxylactam.[21] A potential mechanism for the formation of these two compounds is shown in Scheme 3.21. Reaction of alcohol **2.73** with $PhI(OAc)_2$ might generate **3.79**, which could undergo C2-C10

fragmentation to generate iminium **3.81**. Alternatively, this C2-C10 bond cleavage might occur from **3.80** *via* activatation of the isoxazolidine nitrogen with $PhI(OAc)_2$. Acetate interception of iminium **3.81** would generate aminal **3.82**, which might then undergo a second oxidation to yield **3.77** *via* hydrolysis of carboximidate **3.84**. α-Iodo *N*-alkoxylactam **3.78** is presumably generated upon further oxidation of **3.77**. Specifically, $PhI(OAc)_2$ could react with **3.77** to generate **3.85** which might undergo a subsequent intramolecular S_NAr reaction to give iodo enol ether **3.87**. Finally, enol ether hydrolysis of **3.87** would deliver **3.78**.[22]

Notably, alcohol **2.73** only reacts with $PhI(OAc)_2$ in the presence of AgOTf and bathophenanthroline. However, at this time, the specific role of the AgOTf/bathophenanthroline complex is not fully understood and so this mechanism cannot be considered complete. It is possible that high-valent silver species, which have been postulated in related oxidative transformations, might somehow be involved.[15,23] As with the nitrene chemistry above, attempts to deactivate C2 *via* protonation or BF_3-coordination of the isoxazolidine nitrogen failed to alter the course of the reaction.[17,18]

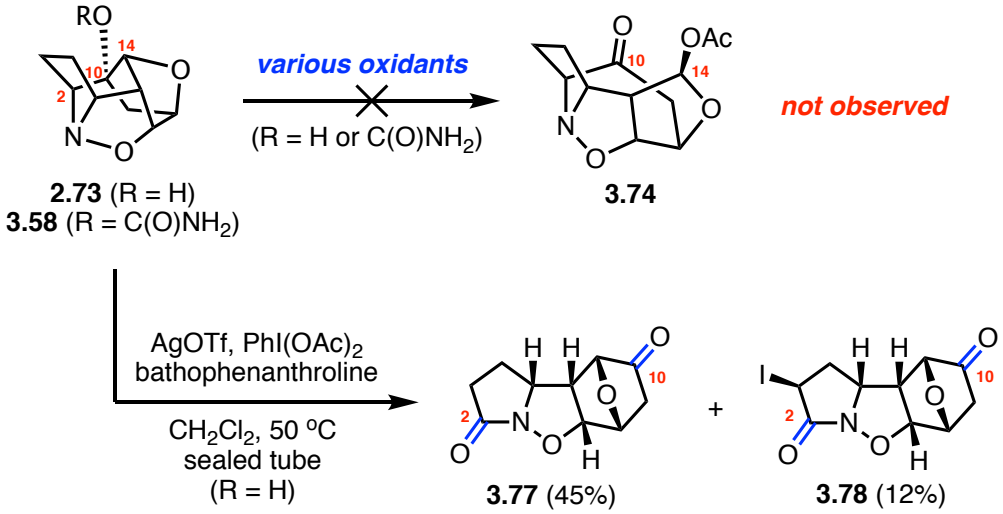

Scheme 3.20. Oxidative C2-C10 bond cleavage of alcohol **2.73**.

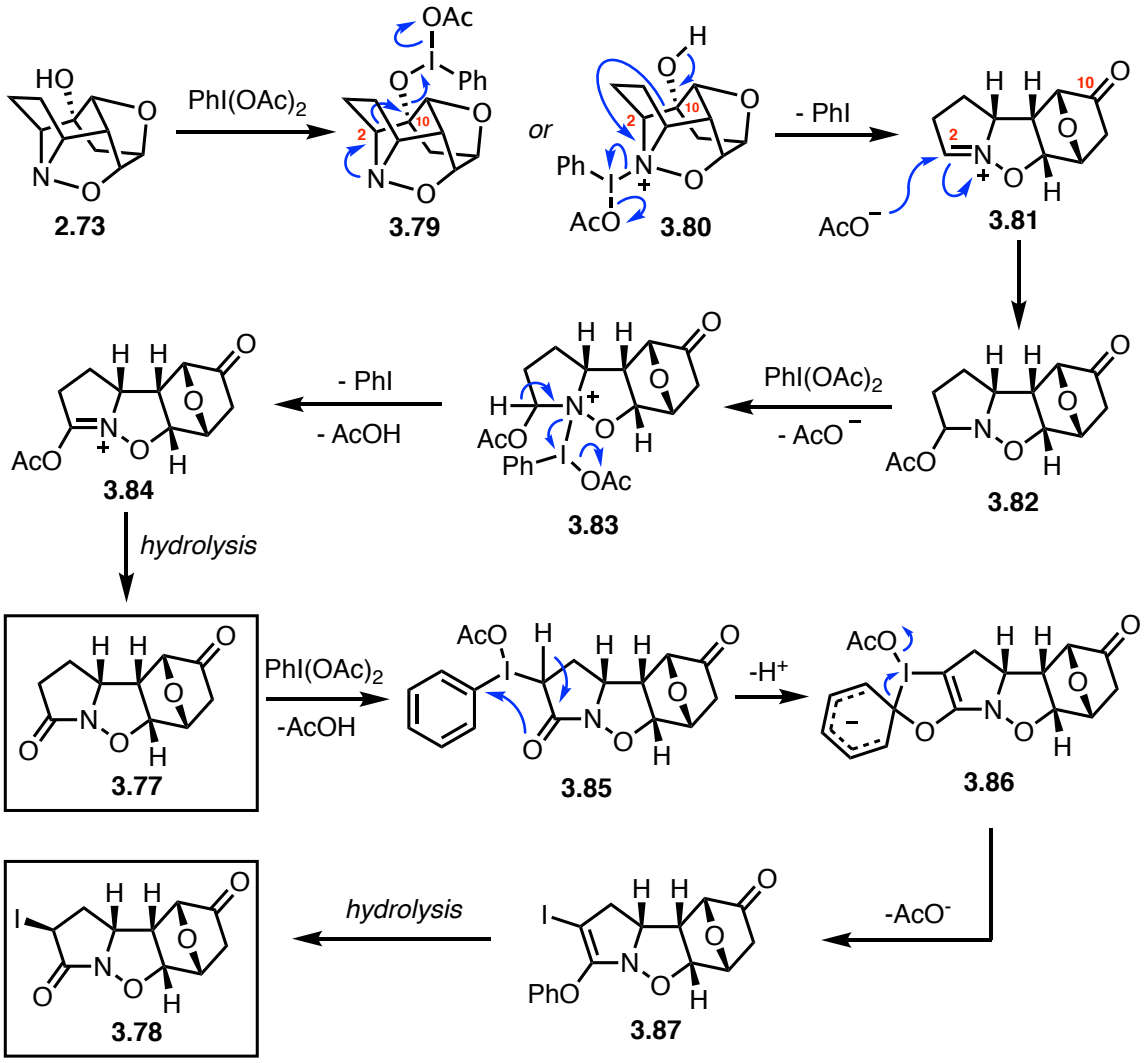

Scheme 3.21. Plausible mechanism for the formation of *N*-alkoxylactams **3.77** and **3.78**.

The complementary selectivity observed in the oxidative cleavage reactions of carbamate **3.58** and alcohol **2.73** is quite remarkable and lends itself to an interesting mechanistic question. Specifically, assuming that oxazolidinone **3.61** is an intermediate in the oxidation of **3.58** to generate diacetoxy ketone **3.62**, why does C10-C14 bond cleavage occur instead of C2-C10 bond cleavage? This question is particularly intriguing since C10-C14 bond cleavage in **3.61** would generate an oxonium intermediate (i.e. **3.88**), which would presumably be less stable than the alternate iminium intermediate **3.89** that would arise from C2-C10 bond cleavage (Scheme 3.22). One potential explanation for this selectivity can be drawn from analyzing the energy-minimized

structure of **3.61** and comparing the C14-C10-O11-C12 and C2-C10-O11-C12 dihedral angles (Figure 3.2).[24] The dihedral angle of the former was calculated to be 157 °, indicating that C14 and C12 are arranged in a near-antiperiplanar conformation, which is ideal for a concerted Grob-like fragmentation.[25] In contrast, the C2-C10-O11-C12 dihedral angle was calculated to be 35 °. This analysis suggests that a Grob-like fragmentation might be responsible for selective C10-C14 bond cleavage of oxazolidinone **3.61** to produce diacetoxy ketone **3.62** (see Scheme 3.15, path b). The analogous process to cleave the C2-C10 bond of **3.61** is not possible due to conformational restrictions that prevent necessary orbital overlap.

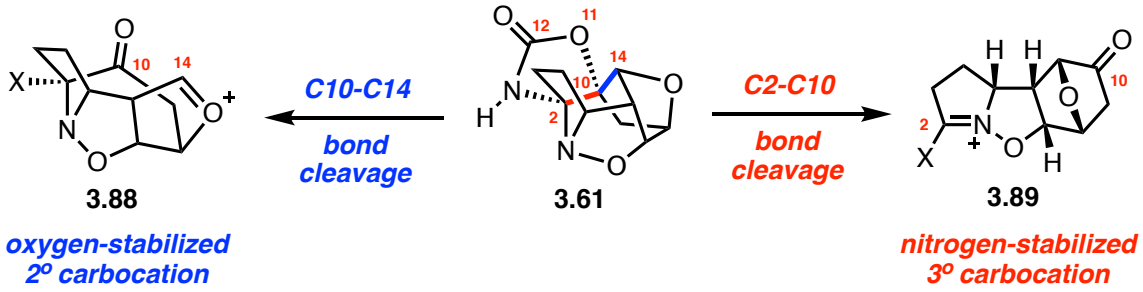

Scheme 3.22. Putative intermediates resulting from C10-C14 or C2-C10 bond cleavage of oxazolidinone **3.61**.

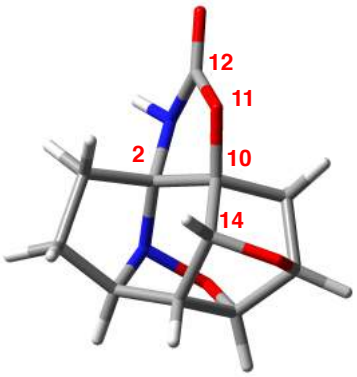

3.61
"top-down perspective"

C14-C10-O11-C12: Dihedral angle = 157 °

C2-C10-O11-C12: Dihedral angle = 35 °

Figure 3.2. The calculated C14-C10-O11-C12 and C2-C10-O11-C12 dihedral angles of the energy-minimized structure of **3.61**, determined at the B3LYP/6-311G* level of theory.

3.5 Hydrogen Atom Abstraction Strategy to Functionalize C14 of the Virosaine Core

In addition to the plethora of carbene/nitrene C-H insertion strategies present in the C-H functionalization literature, radical-based hydrogen atom abstraction methods have also enjoyed broad application in the total synthesis of complex natural products.[1,26] The flagship example of remote radical-based C-H functionalization is the Hofmann-Löffler-Freytag reaction, which was employed in Löffler and Kober's 1909 synthesis of nicotine (**3.93**) (Scheme 3.23).[27,28] In that report, irradiation of **3.90** effected homolysis of its N-Br bond to produce *N*-centered radical **3.91**. Subsequent 1,5-hydrogen atom abstraction and recombination of the resulting *C*-centered radical with a bromine atom produced **3.92**. Finally, cyclization led to the formation of **3.93**. Notably, this represents the earliest example of a direct C-H functionalization being used in total synthesis. Since then, countless other elegant examples of radical-based C-H functionalization strategies have emerged. For example, Baran et al. exploited a carbamoyl radical, generated from **3.94**, to access the remotely functionalized alkyl bromide **3.95** *en route* to several eudesmane terpenes.[2c] Furthermore, Maimone and coworkers very recently implemented a Suárez oxidation of **3.96** in order to prepare several different *Illicium* sesquiterpenes.[29]

Given the many difficulties that we had encountered in our attempts to functionalize C14 of the virosaine core using both carbene and nitrene insertion strategies, we wondered whether an alternative radical-based hydrogen atom abstraction approach would yield more favorable results. In particular, we hypothesized that an *N*-halocarbamate (e.g. **3.98**) might undergo homolytic C-N bond fission upon irradiation with ultraviolet light and that the resulting carbamoyl radical **3.99** might engage in a 1,5-hydrogen atom abstraction at C14 to generate a *C*-centered radical (Scheme 3.24). Recombination of this species with X$^{\bullet}$ might then generate the C14-functionalized product **3.100**.

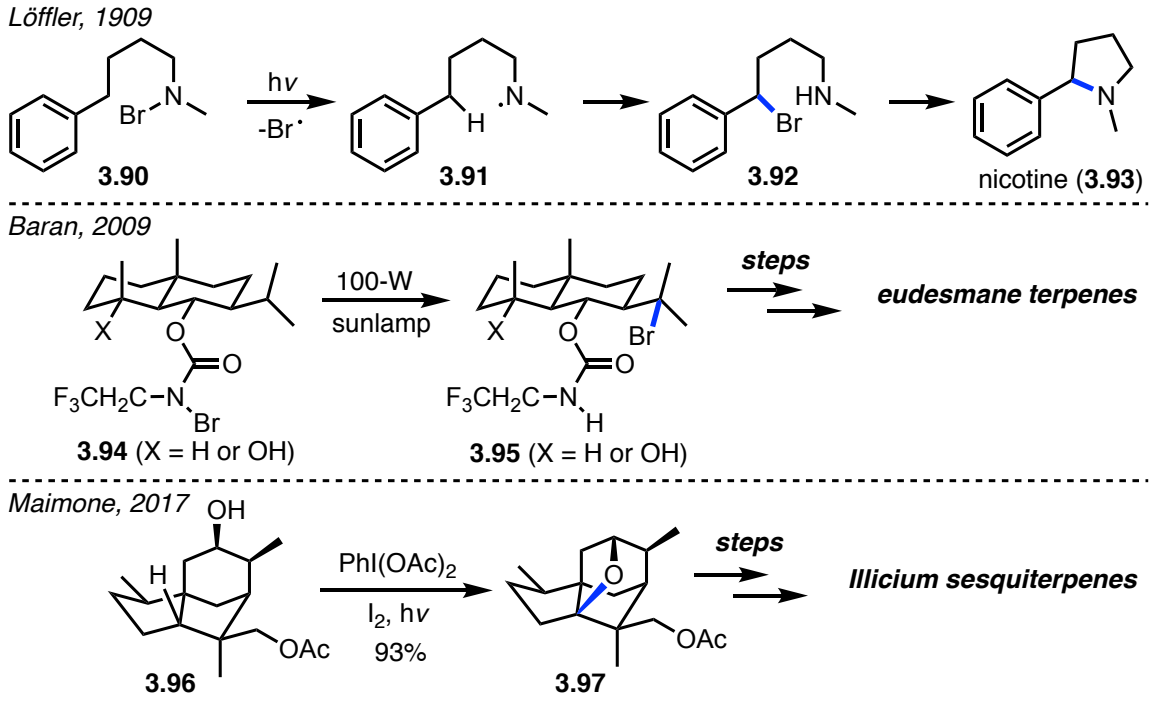

Scheme 3.23. Examples of hydrogen atom abstraction-based C-H functionalization methods in total synthesis.

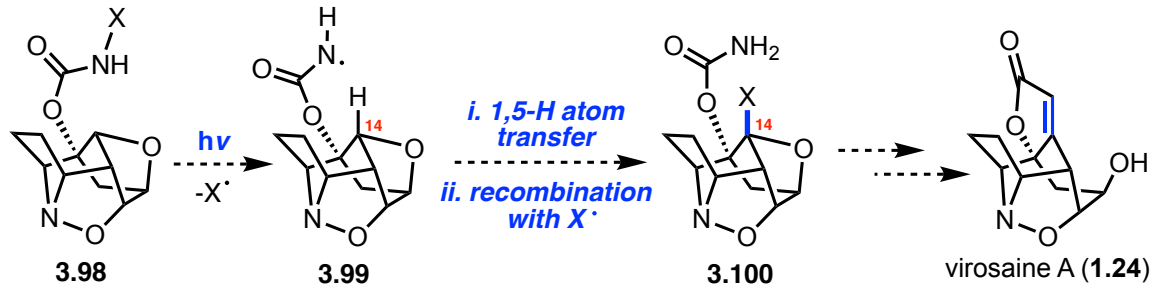

Scheme 3.24. Proposed hydrogen atom abstraction strategy to functionalize C14 of the virosaine core.

While this radical-based functionalization strategy looked good on paper, it unfortunately did not translate into experimental success when employed on our system. For instance, when carbamate **3.58** was submitted to Suárez oxidation conditions ($PhI(OAc)_2$, I_2, hν (254 nm), MeCN, rt), no products resulting from hydrogen atom abstraction were obtained and only unreacted **3.58** (42%) was recovered from the

reaction (Scheme 3.25).[30] Moreover, when we submitted a CCl_4 solution of *N*-chlorocarbamate **3.102** to ultraviolet irradiation, only **3.58** was generated in the reaction. Alternatively, the corresponding *N*-bromocarbamate **3.103** was found to be exceptionally unstable and rapidly decomposed to form **3.58** in the presence of visible light, which precluded its use in the desired radical functionalization reaction. Consistent with these disappointing results, DFT calculations also indicated that a C14 radical would be the least stable among the three positions of interest (C2, C9, and C14) on the structurally related acetate **3.104** (Figure 3.3). Consequently, we opted to abandon this radical-based functionalization strategy.

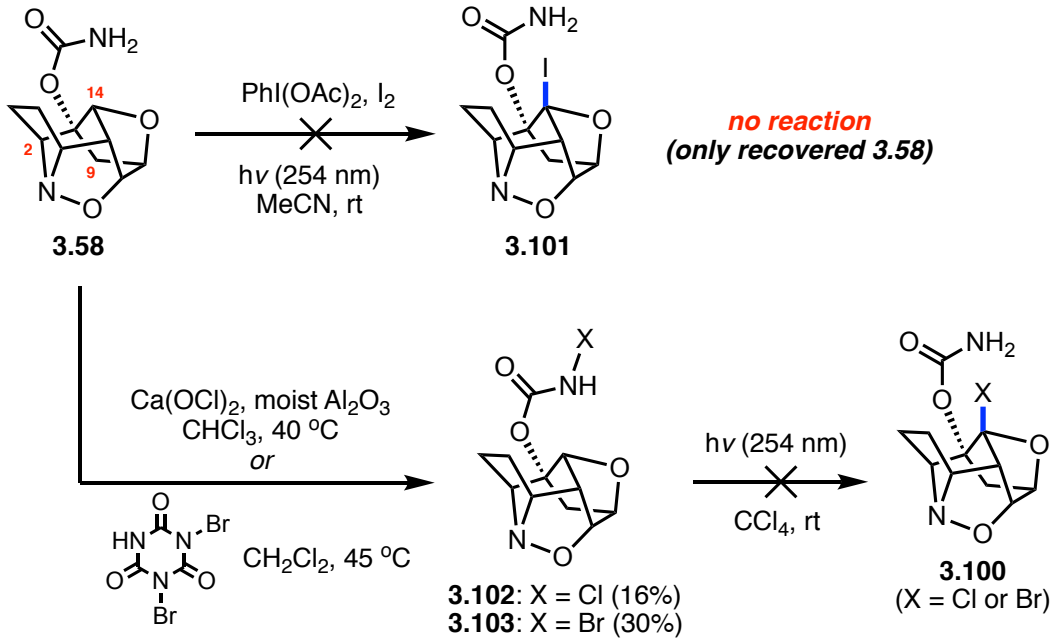

Scheme 3.25. Attempted carbamoyl radical 1,5-hydrogen atom abstraction.

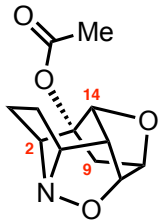

3.104

location of radical	relative enthalpies (kcal/mol)
C2	0
C9	+0.94
C14	**+7.05**

Figure 3.3. Calculated relative enthalpies of radicals at C2, C9, and C14 on the energy-minimized structure of acetate **3.104**, determined at the B3LYP/6-311G* level of theory.

3.6 Directed Lithiation Strategy to Functionalize C14 of the Virosaine Core

While we had been able to effect a bridgehead nitrene insertion on carbamate **3.58** (*vide supra*), the reaction had occurred at the undesired C2 position. The lack of reactivity at C14 suggested that a combination of unfavorable steric and stereoelectronic properties were at play. Indeed, it appeared that geometrical constraints preventing efficient n(O) → σ*(C-H) electron delocalization, as described by Lee et al. (*vide supra*), might be impeding insertion into the C14-H bond due to predominant electronic deactivation.[2e]

To gain additional insight into the electronic nature of the C14-H bond, we conducted a comparative assessment of the C2, C9, and C14 positions using methods established by others to predict site selectivity in C-H functionalizations (Figure 3.4).[2c,g,31] White and coworkers have successfully used natural population analysis (NPA) to calculate hydrogen atomic charges and predict site selectivity for C-H oxidations in several recent total syntheses.[31a-c] They showed that when there is a negligible difference in the steric environment of competing C-H sites, the lower a hydrogen's computed atomic charge is (i.e. the more electron rich the site is predicted to be), the more susceptible it is to oxidation. When we conducted a similar analysis on the energy-minimized structure of alcohol **2.73**, we found that H14 and H9 each possessed an atomic charge of +0.212, which was slightly lower than H2 (+0.218).[24] While this might suggest that oxidation (or carbene insertion) should preferentially occur at C14 over C2, this electronic difference is not large enough to be considered significant. Moreover, when steric factors are considered, C14 appears to be more sterically encumbered than both C2 and C9. This might explain why carbene/nitrene insertion occurs preferentially at C9/C2 instead of C14.

Baran and coworkers have successfully used an alternative method to predict site selectivity for various C-H functionalizations, which involved qualitative NMR analysis of the substrates in question.[2c,g,31d] Interestingly, conducting the same analysis on alcohol **2.73** revealed that both H14 and C14 were the most downfield signals in their respective NMR spectra, indicating that this position might be more electron deficient than we had initially predicted. Consistent with this notion, the NPA partial atomic charge of C14 was

calculated to be significantly more positive than both C2 and C9. In addition, natural bond orbital (NBO) analysis indicated that the C14-H14 bond has the lowest energy HOMO of all C-H bonds in **2.73**, providing further evidence to support its electron-deficient nature.

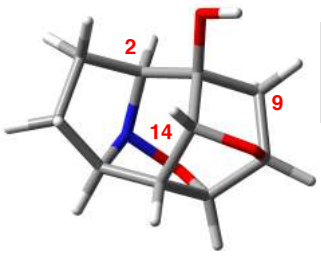

2.73
"top-down perspective"

Site	NMR δ (ppm)		NPA Partial Atomic Charge		C-H HOMO Energy (eV)
	^{1}H	^{13}C	Hydrogen	Carbon	
2	3.59	66.8	+0.218	-0.037	-13.69
9	1.73	45.5	+0.212	-0.423	-13.71
14	4.72	85.7	+0.212	+0.095	-14.48

Figure 3.4. Evaluation of the potential sites of reactivity in **2.73** by NMR chemical shift assessment and natural population analysis (NPA)/natural bond orbital (NBO) analysis of the energy-minimized structure determined at the B3LYP/6-311++G** level of theory.

The apparent electron-deficient nature of C14 suggested an alternative approach to C-H functionalization. Specifically, we postulated that it might be possible to carry out a selective directed deprotonation at C14 to produce a metalated intermediate (i.e. **3.106**) that could be functionalized through the addition of a suitable electrophile (Scheme 3.26). Directed lithiations at sp^2 centers have been widely applied for the total synthesis of natural products and other molecules of interest.[32] In contrast, directed lithiations at sp^3 centers can be more challenging and, consequently, have only seen limited application in total synthesis. Nonetheless, several elegant syntheses have emerged throughout the past two decades in which a directed C(sp^3)-H lithiation is the key step.[33] For example, in 2000, Beak and coworkers completed the total syntheses of solenopsin A (**3.110**) and dihydropinidine (**3.112**) *via* directed lithiation on the Boc-protected piperidine **3.108** (Scheme 3.27).[33a] In the event, treating **3.108** with *s*-BuLi/TMEDA produced a metalated intermediate that was quenched with either Me_2SO_4 or DMF to provide the disubstituted piperidines **3.109** and **3.111**, respectively. Notably, Sarpong and coworkers utilized a remarkable late-stage amine-directed lithiation to enable a synthesis of lyconadin A (**3.116**).[2b,33c] Specifically, they found that treating tetracycle **3.113** with 3 equiv. of *n*-

BuLi produced the chelated organolithium **3.114**. *In situ* treatment of this species with I_2 generated pentacyclc **3.115** in 80% yield *via* an iodination/annulation sequence. Recently, Aggarwal et al. developed a clever strategy to access the *Stemona* alkaloid stemaphylline (**3.121**) *via* the use of two separate diastereoselective lithiation/borylation/1,2-metallate rearrangement sequences.[33e] For instance, they demonstrated that treating aryl ester **3.117** with *s*-BuLi/(−)-sparteine produced a conformationally-stable organolithium intermediate which, upon addition of boronic ester **3.118**, produced boronate **3.119** that underwent subsequent 1,2-metallate rearrangement to provide **3.120** in an excellent 96:4 d.r. Collectively, these examples highlight the synthetic potential of directed sp^3 lithiations and demonstrate how they can be used strategically to enable the synthesis of complex molecules.

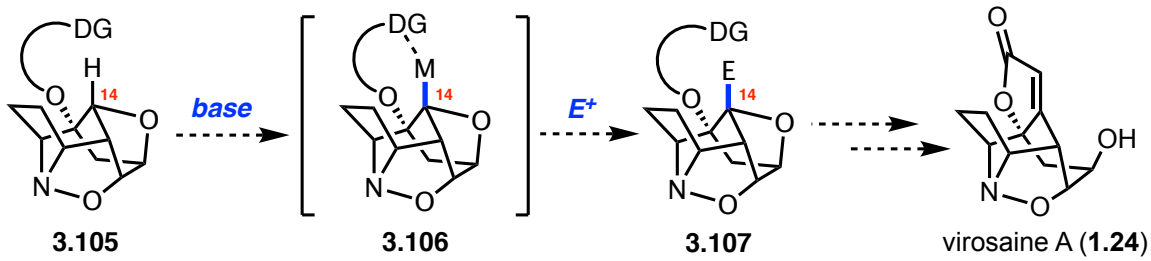

Scheme 3.26. Directed metalation strategy to functionalize C14 of the virosaine core.

In order to examine the directed lithiation strategy outlined above, both tertiary and secondary carbamates **3.122** and **3.123** were prepared from **2.73** *via* acylation with $ClC(O)NEt_2$ or sequential addition of carbonyl diimidazole and *n*-butylamine, respectively (Scheme 3.28). All attempts at directed lithiation with tertiary carbamate **3.122** returned only starting material. Gratifyingly, in contrast, we found that **3.123** could be lithiated selectively at C14 upon treatment with 2.0 equiv. of *s*-BuLi. This selectivity was confirmed by quenching the putative organolithium intermediate **3.124** with benzaldehyde, generating alcohol **3.125** in 43% yield, as the only product of the reaction. The stronger directing group ability of metalated secondary carbamates has been noted in other studies and proved to be critical for the success of this transformation.[34,35]

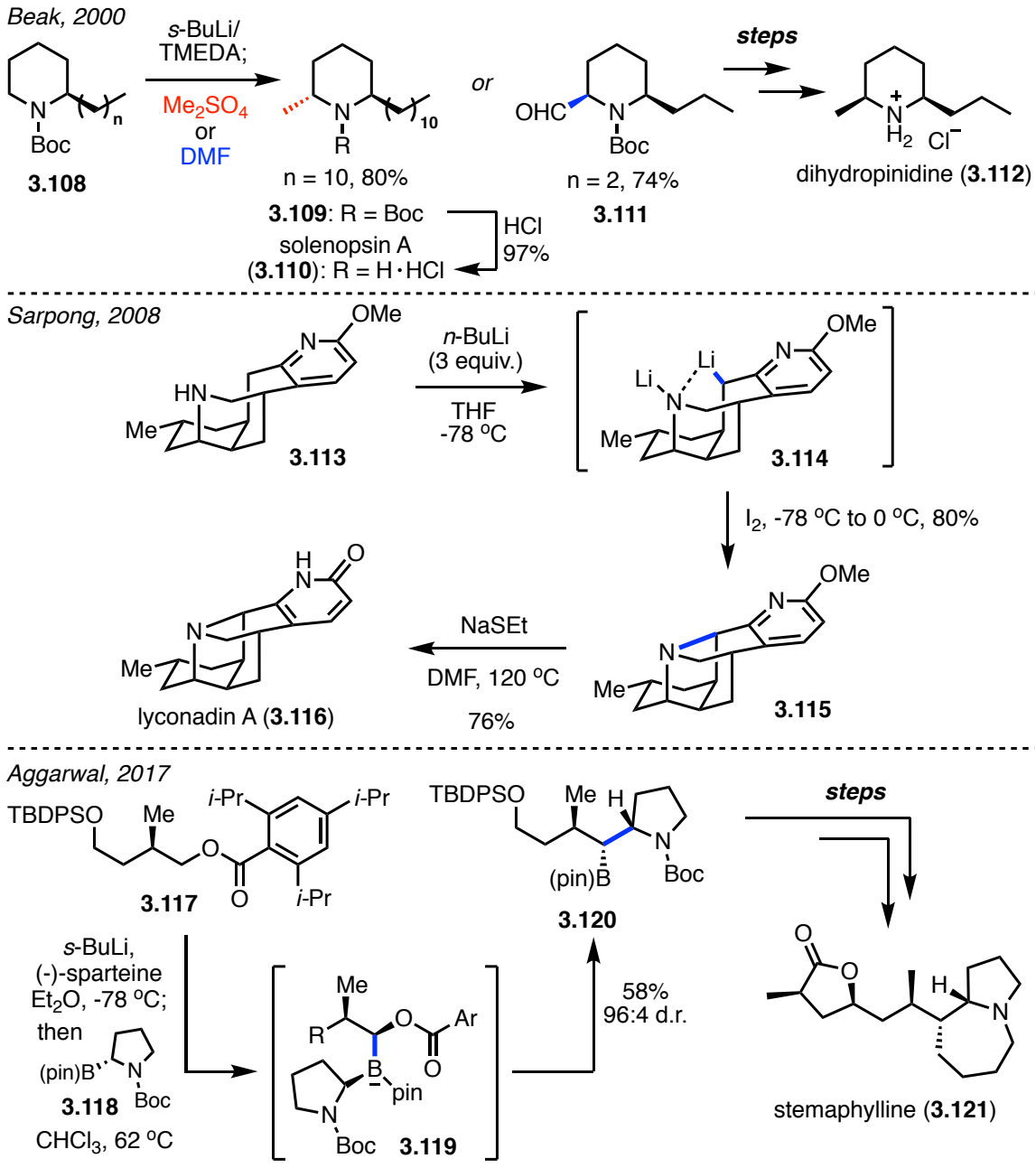

Scheme 3.27. Examples of directed C(sp^3)-H lithiations in total synthesis.

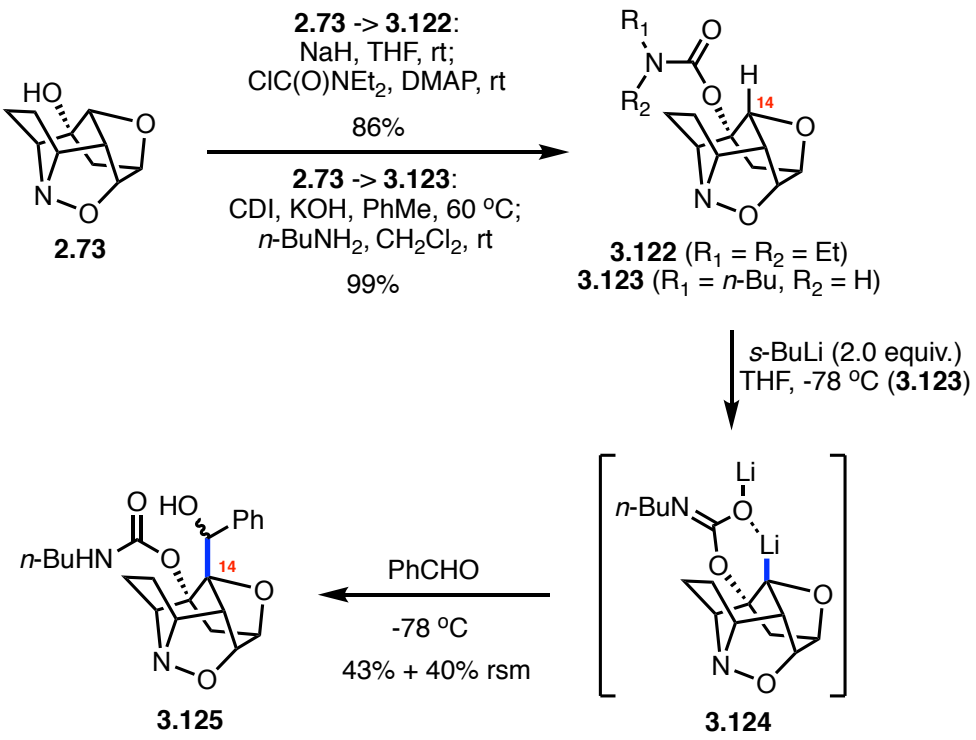

Scheme 3.28. Directed C14 lithiation/benzaldehyde addition of carbamate **3.123**.

With a method in place for selective C14 activation, we attempted to trap lithiated intermediate **3.124** with several other electrophiles (Scheme 3.29). Disappointingly, however, the desired C14-functionalized product **3.126** was never observed. In many cases, both alkyl halide and epoxide electrophiles produced alcohol **2.73** as the major product of the reaction. This is exemplified by the use of propylene oxide (**3.131**) as an electrophile, which produced **2.73** in 72% yield. Presumably, this undesired carbamate removal is the result of competing carbamate alkylation under the reaction conditions. Indeed, we found that treating a THF solution of **3.124** with a mixture of propylene oxide (**3.131**)/BF_3•OEt_2 and then quenching the reaction at -78 °C provided carbonimidic acid **3.134** in 29% yield. Subsequent cyclization of **3.134** to **3.135** might be followed by loss of **3.136** to generate alcohol **2.73**.

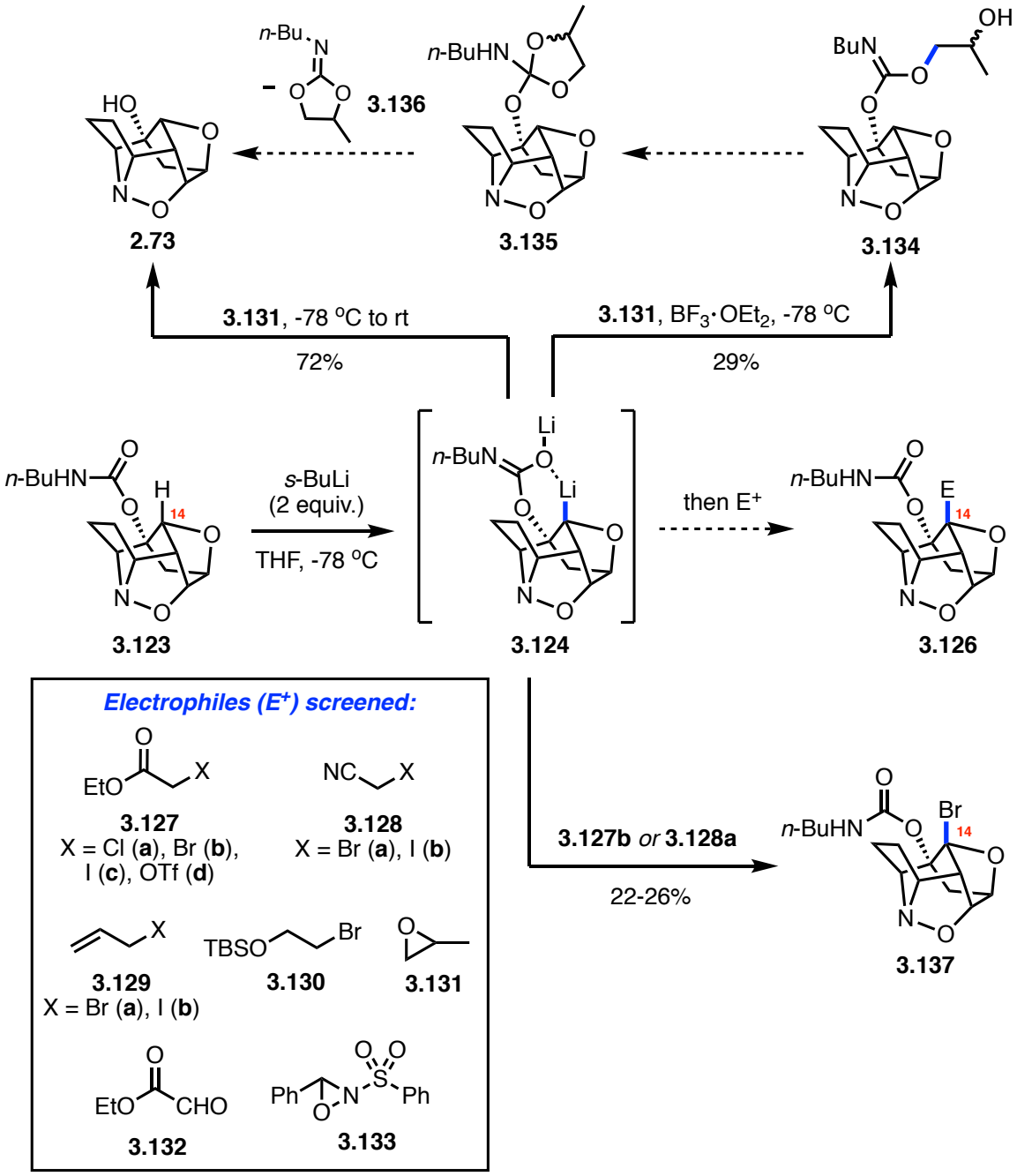

Scheme 3.29. Electrophile screening to trap organolithium **3.124**.

Similar to alkyl halide and epoxide electrophiles, both ethyl glyoxylate (**3.132**) and Davis oxaziridine (**3.133**) were found to be incompetent in the reaction, resulting in either no reaction or a complex mixture of products, respectively. Notably, in the course of our screening efforts, we found that treating organolithium **3.124** with either ethyl

bromoacetate (**3.127b**) or bromoacetonitrile (**3.128a**) produced brominated carbamate **3.137** in low yields *via* lithium-bromide exchange. While the direct installation of an acetate or acetonitrile unit could not be accomplished, bromide **3.137** was a potential candidate for elaboration. Accordingly, we surveyed alternative sources of electrophilic bromine to try and increase the yield of **3.137** (Table 3.2). 1,2-Dibromoethane was found to be a poor brominating agent in this reaction and produced bromide **3.138** in 11% yield, resulting from both bromination and carbamate removal (entry 1). In addition to **3.138**, alcohol **2.73** was generated in 30% yield in this reaction. *N*-bromosuccinimide delivered the desired product in an equally disappointing yield of <5% (entry 2). Gratifyingly, quenching organolithium **3.124** with molecular bromine delivered brominated carbamate **3.137** in a much-improved 57% yield, alongside 42% of **3.123** (entry 3). Optimization of these conditions revealed that treatment of **3.123** (0.1 M in THF) with 2.2 equiv. of *s*-BuLi for 45 minutes, prior to the addition of 5 equiv. of Br_2, delivered **3.137** in 70% yield alongside 20% recovered **3.123** (entry 4). Rapid bromination was observed at -78 ^{o}C and the reaction proceeded to completion in less than 30 minutes after Br_2 addition. Further modification of the reaction conditions failed to increase the yield of **3.137** beyond 70% but revealed several important factors that contributed to the success of the reaction. For example, increasing the amount of *s*-BuLi to 3.0 equiv. led to a significant decrease in yield (entry 5) and conducting the reaction in diethyl ether only led to recovered starting material (entry 6). Moreover, *n*-BuLi and *t*-BuLi were both less effective bases for C14 deprotonation than *s*-BuLi (entries 7 and 8). A lithiation incubation time of 45 minutes was optimal. While a shorter incubation period of 10 minutes produced **3.137** in only slightly lower yield (entry 9), stirring **3.123** with *s*-BuLi for 2 h resulted in significantly less **3.137** and an increased amount of recovered starting material (entry 10). This result suggests that, over time, the putative dilithiated intermediate **3.124** undergoes C14-protonation under the reaction conditions, potentially *via* deprotonation of the THF solvent.

Table 3.2. Optimization of the C14-bromination of carbamate **3.123**.[a]

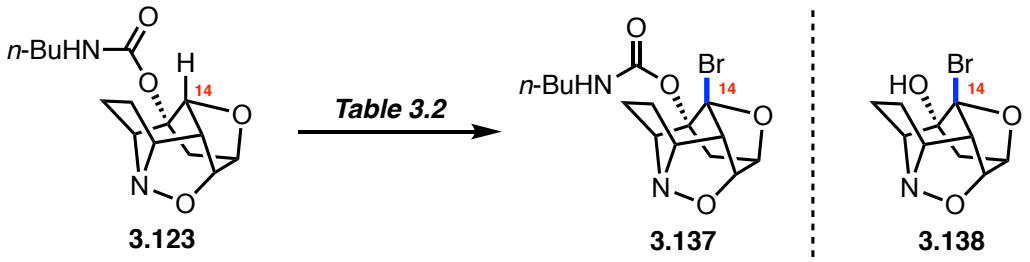

Entry	Base (equiv.)	Solvent	Lithiation Temperature (°C)	"Br^+" source[b]	3.137 (%)[c]	3.123 (%)[c]
1	*s*-BuLi (2.0)	THF	-78 (45 min)	1,2-DBE	11[d]	0
2	*s*-BuLi (2.0)	THF	-78 (45 min)	NBS	<5	45
3	*s*-BuLi (2.0)	THF	-78 (45 min)	Br_2	57	42
4	***s*-BuLi (2.2)**	**THF**	**-78 (45 min)**	**Br_2**	**70**	**20**
5	*s*-BuLi (3.0)	THF	-78 (45 min)	Br_2	55	7
6	*s*-BuLi (2.2)	Et_2O	-78 (45 min)	Br_2	0	87
7	*n*-BuLi (2.2)	THF	-78 (45 min)	Br_2	<5	95
8	*t*-BuLi (2.2)	THF	-78 (45 min)	Br_2	17	75
9	*s*-BuLi (2.2)	THF	-78 (10 min)	Br_2	58	29
10	*s*-BuLi (2.2)	THF	-78 (2 h)	Br_2	32	54

[a]All reactions were performed at [**3.123**] = 0.1 M. [b]5 equiv. of "Br^+" was added at -78 °C. [c]Isolated yields. [d]Alcohol **3.138** was generated instead of **3.137**.

3.7 Synthesis of (−)-Virosaine A

With a bromide handle in place at C14, butanolide ring construction and the completion of the total synthesis was within reach. Gratifyingly, Keck allylation of **3.137** delivered allylated carbamate **3.139** in 71% yield (Scheme 3.30).[36] Interestingly, a modest amount of debrominated carbamate **3.123** (27% yield) was also generated under these conditions. In an attempt to impede the formation of this unwanted reduction byproduct, several control experiments were run to try and identify the hydrogen atom source responsible. Benzene was immediately ruled out since the reaction of **3.137** in benzene-*d*6 led to an identical product distribution, with no deuterium incorporation at C14 in **3.123**. Moreover, the presence of molecular sieves had no effect on the reaction,

indicating that trace water was also not the cause. While carbamates have been shown to serve as hydrogen atom donors in specific radical-based transformations, they require the presence of a bond-weakening Ti(III) species in order to occur.[37] As a result, this process was unlikely to be operative in our case and was definitively rejected based on the fact that Keck allylation of alcohol **3.138** also produced both debrominated alcohol **2.73** in 33% yield along with a 62% yield of allylated product **3.140**. Based on the results of these experiments, either azobisisobutyronitrile (AIBN) or allyltributylstannane are the most probable hydrogen atom donors. Furthermore, we found that doubling the amount of allyltributylstannane in the reaction did not alter the product distribution, which suggests that it might indeed be the hydrogen atom source. While we were ultimately unable to prevent the formation of debrominated carbamate **3.123**, this compound could conveniently be recycled through the C14-bromination/allylation sequence.

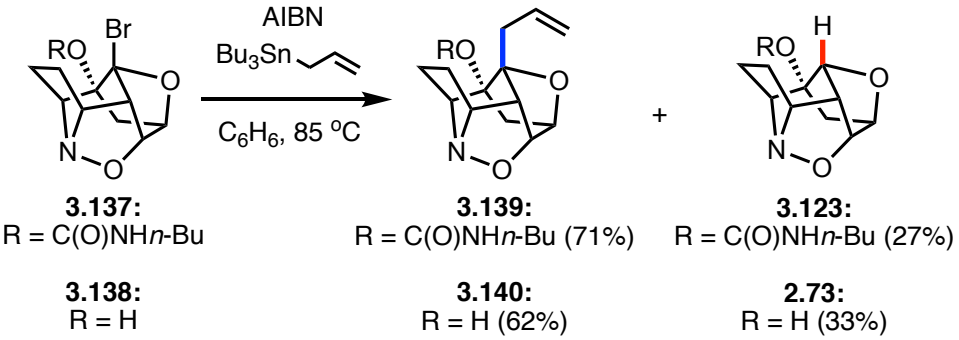

3.137: R = C(O)NH*n*-Bu

3.138: R = H

3.139: R = C(O)NH*n*-Bu (71%)

3.140: R = H (62%)

3.123: R = C(O)NH*n*-Bu (27%)

2.73: R = H (33%)

Scheme 3.30. Radical allylation reactions of alkyl bromides **3.137** and **3.138**.

With the C14-allylated product **3.139** in hand, carbamate removal could be smoothly carried out *via* $LiAlH_4$ reduction to deliver alcohol **3.140** in 94% yield (Scheme 3.31). Notably, the isoxazolidine N-O bond proved to be surprisingly stable under these reaction conditions. In order to construct the final ring of the natural product, we sequentially subjected **3.140** to ozone and dimethylsulfide to provide lactol **3.141**. Intriguingly, the crude reaction mixture also contained a minor amount of lactone **2.1**. As a result, we directly submitted the lactol/lactone mixture to Dess-Martin oxidation to exclusively provide lactone **2.1**. Serendipitously, when we first attempted to purify **2.1** by silica gel flash chromatography, we observed the formation of virosaine A (**1.24**).

However, subsequent attempts to replicate this silica gel-mediated rearrangement (**2.1→1.24**) provided inconsistent results that led us to screen other conditions for the transformation. Gratifyingly, we found that when an EtOAc solution of **2.1** was stirred with activated neutral alumina, smooth and reproducible rearrangement occurred to deliver **1.24**. Moreover, this final sequence involving ozonolysis, DMP oxidation and β-elimination could be efficiently carried out in a single pot and afforded virosaine A (**1.24**) directly from alcohol **3.140** in an excellent 77% yield.

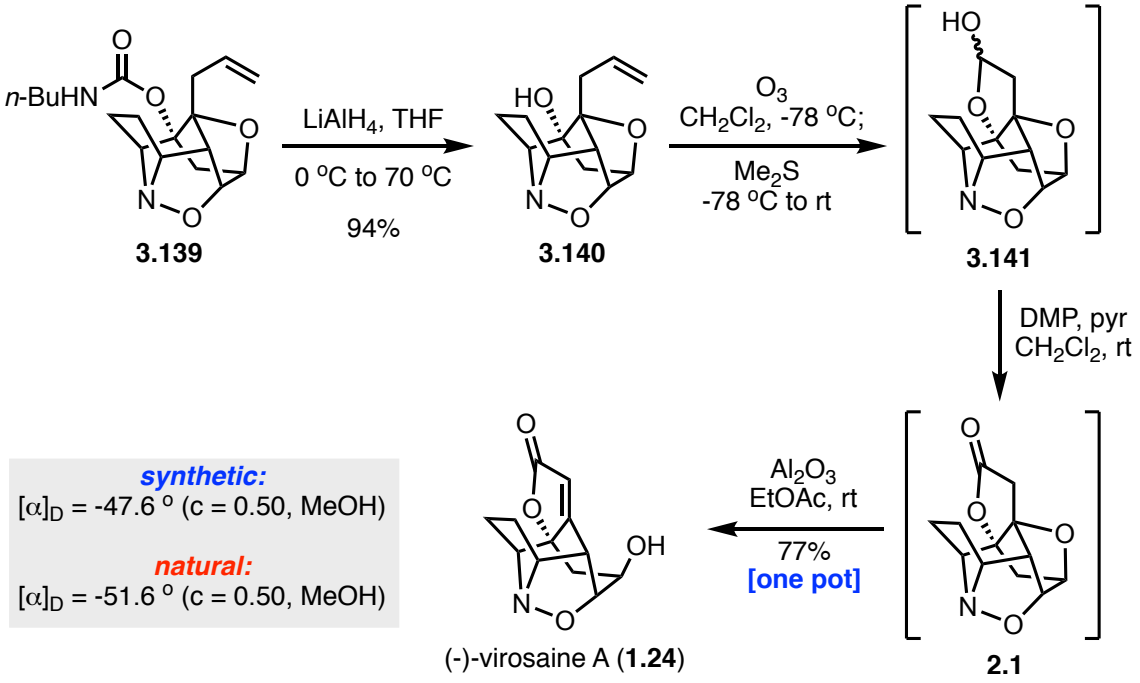

Scheme 3.31. Synthesis of (−)-virosaine A.

3.8 Conclusion

Several late-stage C-H functionalization strategies were explored in attempts to selectively functionalize C14 of the virosaine core. Ultimately, these studies provided valuable information on the differences in reactivity between several positions and reinforced the importance that method selection holds when applying a late-stage C-H functionalization strategy to the synthesis of a complex molecule. While intramolecular carbene insertion occurred preferentially at C9, its intermolecular counterpart resulted in an unprecedented isoxazolidine N-O insertion. Complementary regioselectivity was

observed for an intramolecular nitrene insertion, which exclusively produced a C2-functionalized oxazolidinone product. Several fascinating oxidative cleavages were also discovered that led to interesting mechanistic questions. Finally, a combination of NMR and computational analyses led us to a successful directed lithiation/bromination sequence to selectively functionalize C14 and complete the total synthesis of virosaine A (**1.24**). Overall, the synthesis of **1.24** was achieved in 10 steps and 9% overall yield from 2-bromoacrolein (**2.9**) and furan (**2.75**) (Scheme 3.32). This represents the shortest and most efficient synthesis of this molecule, to date.

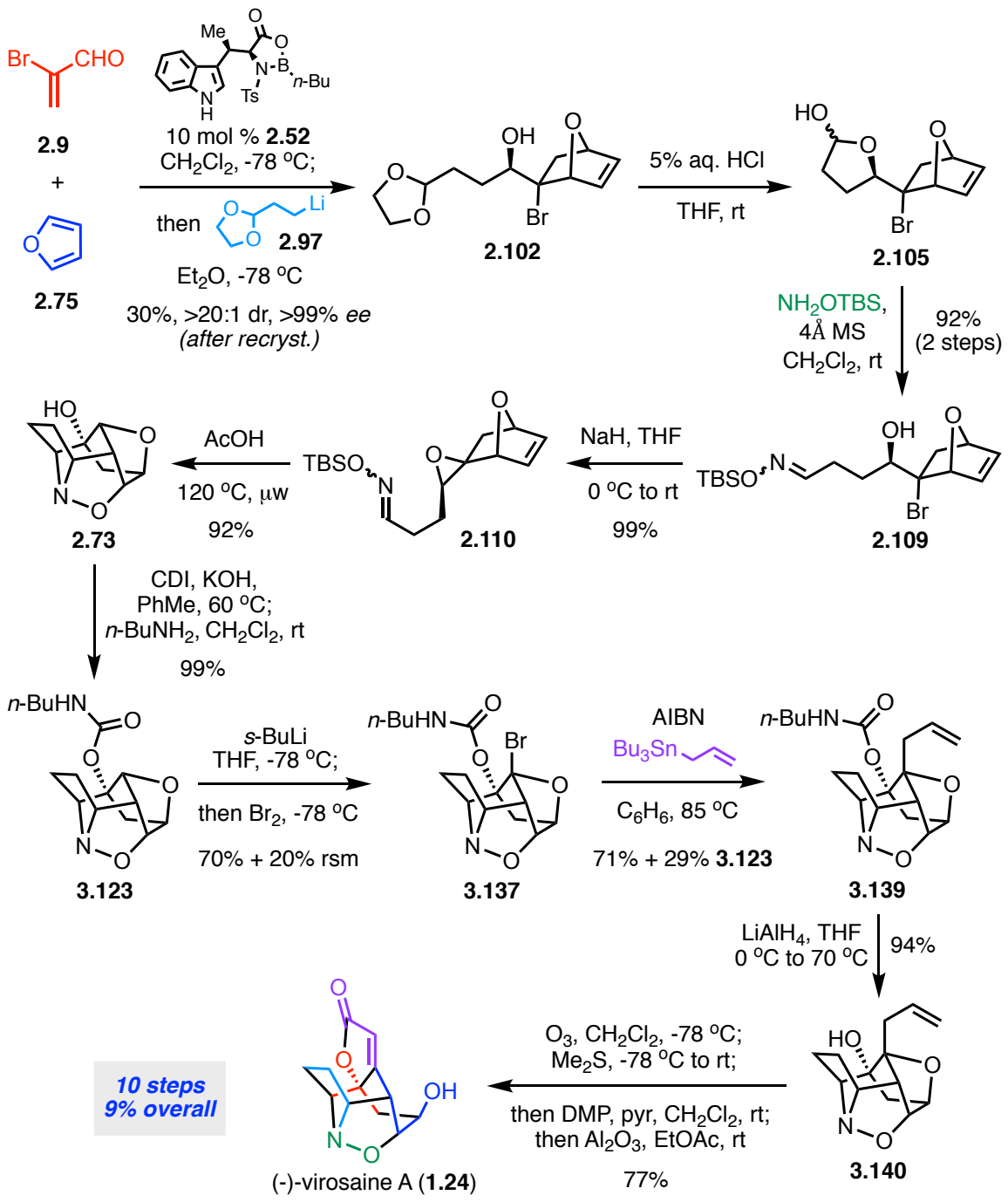

Scheme 3.32. Overall enantioselective synthesis of (−)-virosaine A.

References

(1) For select reviews on C-H functionalization, see: (a) Godulal, K.; Sames, D. *Science* **2006**, *312*, 67. (b) Davies, H. M. L.; Manning, J. R. *Nature* **2008**, *451*, 417. (c) Gutekunst, W. R.; Baran, P. S. *Chem. Soc. Rev.* **2011**, *40*, 1976. (d) McMurray, L.; O'Hara, F.; Gaunt, M. J. *Chem. Soc. Rev.* **2011**, *40*, 1885. (e) Yamaguchi, J.; Yamaguchi, A. D.; Itami, K. *Angew. Chem. Int. Ed.* **2012**, *51*, 8960. (f) Chen, D. Y.-K.; Youn, S. W. *Chem. Eur. J.* **2012**, *18*, 9452. (g) Egger, J. Carreira, E. M. *Nat. Prod. Rep.* **2014**, *31*, 449. (h) Qiu, Y.; Gao, S. *Nat. Prod. Rep.* **2016**, *33*, 562. (i) Davies, H. M. L.; Morton, D. *J. Org. Chem.* **2016**, *81*, 343.

(2) For recent total syntheses involving late-stage C(sp^3)-H functionalizations, see: (a) Hinman, A.; Du Bois, J. *J. Am. Chem. Soc.* **2003**, *125*, 11510. (b) Bisai, A.; West, S. P.; Sarpong, R. *J. Am. Chem. Soc.* **2008**, *130*, 7222. (c) Chen, K. Baran, P. S. *Nature* **2009**, *459*, 824. (d) Stang, E. M.; White, M. C. *Nat. Chem.* **2009**, *1*, 547. (e) Yun, S. Y.; Zheng, J.-C.; Lee, D. *J. Am. Chem. Soc.* **2009**, *131*, 8413. (f) Huters, A. D.; Quasdorf, K. W.; Styduhar, E. D.; Garg, N. K. *J. Am. Chem. Soc.* **2011**, *133*, 15797. (g) Kawamura, S.; Chu, H.; Felding, J. Baran, P. S. *Nature* **2016**, *532*, 90. (h) McCallum, M. E.; Rasik, C. M.; Wood, J. L.; Brown, M. K. *J. Am. Chem. Soc.* **2016**, *138*, 16616. (i) Hung, K.; Condakes, M. L.; Morikawa, T.; Maimone, T. J. *J. Am. Chem. Soc.* **2016**, *138*, 16616. (j) Liu, C.; Chen, R.; Shen, Y.; Liang, Z.; Hua, Y.; Zhang, Y. *Angew. Chem. Int. Ed.* **2017**; *56*, 8187.

(3) For select reviews on carbene C-H insertion, see: (a) Davies, H. M. L.; Beckwith, R. E. J. *Chem. Rev.* **2003**, *103*, 2861. (b) Doyle, M. P.; Duffy, R.; Ratnikov, M.; Zhou, L. *Chem. Rev.* **2010**, *110*, 704. (c) Doyle, M. P.; Ratnikov, M. Liu, Y. *Org. Biomol. Chem.* **2011**, *9*, 4007. (d) Davies, H. M. L.; Morton, D. *Chem. Soc. Rev.* **2011**, *40*, 1857. (e) Lombard, F. J.; Coster, M. J. *Org. Biomol. Chem.* **2015**, *13*, 6419. (f) Ford, A.; Miel, H.; Ring, A.; Slattery, C. N.; Maquire, A. R.; McKervey, M. A. *Chem. Rev.* **2015**, *115*, 9981.

(4) For select reviews on how the metal-ligand combination can influence C-H insertion selectivity, see: (a) Padwa, A.; Austin, D. J. *Angew. Chem. Int. Ed.* ***1994, 33, 1797.*** (b) Timmons, D. J.; Doyle, M. P. *J. Organomet. Chem.* **2001**, *617-618*,

98. (c) Merlic, C. A.; Zechman, A. L. *Synthesis*, **2003**, *8*, 1137. (d) Doyle, M. P. *J. Org. Chem.* **2006**, *71*, 9253.

(5) (a) Anada, M.; Mita, O.; Watanabe, H.; Kitagaki, S.; Hashimoto, S. *Synlett*, **1999**, *11*, 1775. (b) Doyle, M. P.; Hu, W. *Chirality*, **2002**, *14*, 169.

(6) (a) Osawa, E.; Tahara, Y.; Togashi, A.; Iizuka, T.; Tanaka, N.; Kan, T. *J. Org. Chem.* **1982**, *47*, 1923. (b) Sonawane, H. R.; Bellur, N. S.; Ahuja, J. R.; Kulkarni, D. G. *J. Org. Chem.* **1991**, *56*, 1434. (c) Grainger, R. S.; Owoare, R. B. *Org. Lett.* **2004**, *6*, 2961. (d) Kawasumi, M.; Kanoh, N.; Iwabuchi, Y. *Org. Lett.* **2011**, *13*, 3620. (e) Jansone-Popova, S.; May, J. A. *Tetrahedron* **2016**, *72*, 3734.

(7) Fan, G.-j.; Wang, Z.; Wee, A. G. H. *Chem. Commun.*, **2006**, *3732*.

(8) Employing $Cu(acac)_2$ as a catalyst failed to produce any identifiable C-H insertion products and either led to no reaction or complex mixtures.

(9) Maas, G.; In *The Chemistry of Organic Silicon Compounds*; Rappoport, Z., Apeloig, Y., Eds.; Wiley: Chichester, 1998; Vol. 2, pp. 703-778.

(10) Wang, Z.; Stevens Rearrangement. In *Comprehensive Organic Name Reactions and Reagents*; John Wiley & Sons, Inc., 2010; pp. 2668-2672, and references therein.

(11) For related carbene N-O insertions, see: (a) Manning, J. R.; Davies, H. M. L. *Tetrahedron* **2008**, *64*, 6901. (b) Xu, X.; Ratnikov, M. O.; Zavalij, P. Y.; Doyle, M. P. *Org. Lett.* **2011**, *13*, 6122.

(12) For a related reaction between α-haloketones and isoxazolin-5-ones, see: Beccalli, E. M.; Marchesini, A.; Pilati, T. *Tetrahedron*, **1988**, *44*, 6225.

(13) For select reviews on nitrene C-H insertions, see: (a) Li, Z.; He, C. *Eur. J. Org. Chem.* **2006**, 4313. (b) Zalatan, D. N.; Du Bois, J. *Top. Curr. Chem.* **2010**, *292*, 347. (c) Collet, F.; Lecot, C.; Dauben, P. *Chem. Soc. Rev.* **2011**, *40*, 1926. (d) Roizen, J. L.; Harvey, M. E.; Du Bois, J. *Acc. Chem. Res.* **2012**, *335*, 807.

(14) For select examples of intramolecular nitrene C-H insertions in total synthesis, see Ref. 2a,f and : (a) Ciufolini, M. A.; Byrne, N. E. *J. Am. Chem. Soc.* **1991**, *113*, 8016. (b) Wehn, P. M.; Du Bois, J. *J. Am. Chem. Soc.* **2002**, *124*, 12950. (c) Fleming, J. J.; Du Bois, J. *J. Am. Chem. Soc.* **2006**, *128*, 3926. (d) Tanino, T.;

Ichikawa, S.; Shiro, M.; Matsuda, A. *J. Org. Chem.* **2010**, *75*, 1366. (e) Quasdorf, K. W.; Huters, A. D.; Lodewyk, M. W.; Tantillo, D. J.; Garg, N. K. *J. Am. Chem. Soc.* **2012**, *134*, 1396. (f) Styduhar, E. D.; Huters, A. D.; Weires, N. A.; Garg, N. K. *Angew. Chem. Int. Ed.* **2013**, *52*, 12422. (g) Weires, N. A.; Styduhar, E. D.; Baker, E. L.; Garg, N. K. *J. Am. Chem. Soc.* **2014**, *136*, 14710.

(15) (a) Cui, Y.; He, C. *Angew. Chem. Int. Ed.* **2004**, *43*, 4210. (b) Li, Z.; Capretto, D. A.; Rahaman, R.; He, C. *Angew. Chem. Int. Ed.* **2007**, *46*, 5184.

(16) (a) Espino, C. G.; Du Bois, J. *Angew. Chem. Int. Ed.* **2001**, *40*, 598. (b) Espino, C. G.; Wehn, P. M.; Chow, J.; Du Bois, J. *J. Am. Chem. Soc.* **2001**, *123*, 6935. (c) Espino, C. G.; Fiori, K. W.; Kim, M.; Du Bois, J. *J. Am. Chem. Soc.* **2004**, *126*, 15378.

(17) (a) Lee, M.; Sanford, M. S. *J. Am. Chem. Soc.* **2015**, *137*, 12796. (b) Howell, J. M.; Feng, K.; Clark, J. R.; Trzepkowski, L. J.; White, M. C. *J. Am. Chem. Soc.* **2015**, *137*, 14590. (c) Mbofana, C. T.; Chong, E.; Lawniczak, J.; Sanford, M. S. *Org. Lett.* **2016**, *18*, 4258. (d) Lee, M.; Sanford, M. S. *Org. Lett.* **2017**, *19*, 572. (e) Mack, J. B. C.; Gipson, J. D.; Du Bois, J.; Sigman, M. S. *J. Am. Chem. Soc.* **2017**, *139*, 9503.

(18) For remote oxidation in pyridine-containing systems, see Ref. 17b,e and: Adams, A. M.; Du Bois, J.; Malik, H. A. *Org. Lett.* **2015**, *17*, 6066.

(19) (a) Paradine, S. M.; White, M. C. *J. Am. Chem. Soc.* **2012**, *134*, 2036. (b) Paradine, S. M.; Griffin, J. R.; Zhao, J.; Petronico, A. L.; Miller, S. M.; White, M. C. *Nature Chem.* **2015**, *7*, 987.

(20) For the recent use of a lactone-ketone pinacol coupling in a total synthesis, see: Cai, L.; Zhang, K.; Kwon, O. *J. Am. Chem. Soc.* **2016**, *138*, 3298.

(21) For an example of a similar oxidative C-C bond fragmentation, see: Hamlin, A. M.; Lapointe, D.; Owens, K.; Sarpong, R. *J. Org. Chem.* **2014**, *79*, 6783.

(22) Chen, Y.; Ju, T.; Wang, J.; Yu, W.; Du, Y.; Zhao, K. *Synlett* **2010**, *2*, 231.

(23) Cui, Y.; He, C. *J. Am. Chem. Soc.* **2003**, *125*, 16202.

(24) See Chapter 5.3 for details.

(25) Prantz, K.; Mulzer, J. *Chem. Rev.* **2010**, *110*, 3741.

(26) For reviews on remote intramolecular radical-based functionalizations, see: (a) Majetich, G.; Wheless, K. *Tetrahedron* **1995**, *51*, 7095. (b) Chiba, S.; Chen, H. *Org. Biomol. Chem.* **2014**, *12*, 4051.

(27) (a) Hofmann, A. W. *Ber.* **1883**, *16*, 558. (b) Löffler, K.; Freytag, C. A. *Ber.* **1909**, *42*, 3427.

(28) Löffler, K.; Kober, S. *Ber.* **1909**, *42*, 3431.

(29) Condakes, M. L.; Hung, K.; Harwood, S. J.; Maimone, T. J. *J. Am. Chem. Soc.* **2017**, *139*, 17783.

(30) Martin, A.; Pérez-Martín, I.; Suárez, E. *Org. Lett.* **2005**, *7*, 2027.

(31) (a) Chen, M. S.; White, M. C. *Science* **2007**, *318*, 783. (b) Bigi, M. A.; Liu, P.; Zou, L.; Houk, K. N.; White, M. C. *Synlett* **2012**, *23*, 2768. (c) Gormisky, P. E.; White, M. C. *J. Am. Chem. Soc.* **2013**, *135*, 14052. (d) Michaudel, Q.; Journot, G.; Regueiro-Ren, A.; Goswami, A.; Guo, Z.; Tully, T. P.; Zou, L.; Ramabhadran, R. O.; Houk, K. N.; Baran, P. S. *Angew. Chem. Int. Ed.* **2014**, *53*, 12091.

(32) (a) Beak, P.; Snieckus, V. *Acc. Chem. Res.* **1982**, *15*, 306. (b) Snieckus, V. *Chem. Rev.* **1990**, *90*, 879.

(33) For selected examples of directed lithiation at sp^3 centers in total synthesis, see Ref. 2b and**:** (a) Wilkinson, T. J.; Stehle, N. W.; Beak, P. *Org. Lett.* **2000**, *2*, 155. (b) Johnson, T. A.; Curtis, M. D.; Beak, P. *J. Am. Chem. Soc.* **2001**, *123*, 1004. (c) West, S. P.; Bisai, A.; Lim, A. D.; Narayan, R. R.; Sarpong, R. *J. Am. Chem. Soc.* **2009**, *131*, 11187. (d) Vu, V. H.; Louafi, F.; Girard, N.; Marion, R.; Roisnel, T.; Dorcet, V.; Hurvois, J.-P. *J. Org. Chem.* **2014**, *79*, 3358. (e) Varela, A.; Garve, L. K. B.; Leonori, D.; Aggarwal, V. K. *Angew. Chem. Int. Ed.* **2017**, *56*, 2127.

(34) Beak, P.; Meyers, A. I. *Acc. Chem. Res.* **1986**, *19*, 356.

(35) For a review on the complex-induced proximity effect, see: Whisler, M. C.; MacNeil, S.; Snieckus, V.; Beak, P. *Angew. Chem. Int. Ed.* **2004**, *43*, 2206.

(36) Keck, G. E.; Yates, J. B. *J. Am. Chem. Soc.* **1982**, *104*, 5829.

(37) (a) Diethelm, S.; Schindler, C. S.; Carreira, E. M. *Org. Lett.* **2010**, *12*, 3950. (b) Diethelm, S.; Schindler, C. S.; Carreira, E. M. *Chem. Eur. J.* **2014**, *20*, 6071. (c)

Tarantino, K. T.; Miller, D. C.; Callon, T. A.; Knowles, R. R. *J. Am. Chem. Soc.* **2015**, *137*, 6440.

PART II

A Direct Approach for the Synthesis of 1,3-Disubstituted Bicyclo[1.1.1]pentan-1-amines

CHAPTER 4

Bicyclo[1.1.1]pentanes as Unique Bioisosteres and Early Development of a Method for the Synthesis of 1,3-Disubstituted Bicyclo[1.1.1]pentan-1-amines

4.1 Introduction

The previous three chapters described our efforts in achieving a concise total synthesis of virosaine A. Upon completing that project, an opportunity arose to solve an interesting and practical synthetic problem *via* a collaboration with Inception Sciences. The primary objective of this new project was to develop a more economical synthesis of an important building block that is used to prepare a lead oncology clinical drug candidate. The main challenge in achieving this goal was efficient installation of a bioisosteric 3-alkyl bicyclo[1.1.1]pentan-1-amine motif. Chapter 4 describes how bicyclo[1.1.1]pentanes have been used as bioisosteres in drug discovery and how our strategy to access Inception Sciences' building block led to the development of a novel and efficient approach for the synthesis of 3-alkyl bicyclo[1.1.1]pentan-1-amines.

4.1.1 Bicyclo[1.1.1]pentane as a Unique Bioisostere

Modern day pharmaceutical drug discovery is often an extremely laborious process that relies on the input of millions of dollars and years of collective research. When successful, these efforts result in the development of a clinically useful drug that can have a major impact in treating/curing a disease or alleviating symptoms of a physiological disorder. One of the most important stages in developing an efficacious drug candidate is lead compound optimization. During this stage, discovery chemists are faced with the challenge of performing a balancing act where they must synthesize a molecule that not only possesses favorable pharmacological efficacy, but also overcomes pharmaceutical liabilities related to bioavailability, metabolism, and excretion.[1] One commonly employed approach to optimizing the properties of potential drug candidates is the incorporation of "bioisosteres" into their structures.[1,2,3] Bioisosteres, as initially defined by Friedman, are isosteric compounds that elicit a similar biological effect.[4] More recently, Burger broadened the definition, stating that "bioisosteres are compounds or groups that possess near-equal molecular shapes and volumes, approximately the same distribution of electrons, and which exhibit similar physical properties such as hydrophobicity… [and which should] affect the same biochemically associated systems as agonists or antagonists and thereby produce biological properties that are related to each other."[5] Interest in the use of bioisosteres in medicinal chemistry has grown

immensely over the past few decades due to a combination of factors. In particular, they have become widely recognized as having the potential to impart favorable physicochemical properties to prospective clinical drug candidates. Moreover, they enable chemists to create novel chemical space, a particularly important point given the extremely competitive intellectual property landscape of drug discovery. However, while interest in using bioisosteres in medicinal chemistry has grown, methods for their installation are, in many cases, limited or underdeveloped. As a result, lengthy synthetic sequences are often required for their installation, which can have a bottleneck effect in drug discovery efforts. Therefore, there is an imperative need to develop practical new methods to efficiently incorporate useful bioisosteres into pharmaceutically relevant molecules.

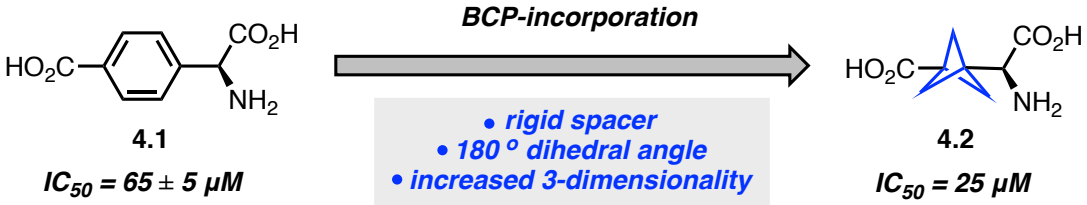

Figure 4.1. Comparison of the mGluR1a activity of **4.1** and **4.2** in baby hamster kidney (BHK) cells.

The bicyclo[1.1.1]pentane (BCP) motif has emerged as a unique bioisostere for several functional groups including *para*-substituted phenyl rings,[6] *t*-butyl groups,[7] and internal alkynes.[8] Pellicciari et al. disclosed the first example of using 1,3-disubstituted BCP as a phenyl mimic to deliver a more potent and selective antagonist against metabolic glutamate receptor 1 (mGluR1) in baby hamster kidney (BHK) cells (Figure 4.1).[6a,9] Their findings indicated that the phenyl ring in **4.1** was not necessary for its mGluR1 antagonism but instead functioned only as a spacer between the pharmacophoric groups. In this sense, the BCP motif is an excellent substitute because it acts as a rigid spacer and maintains the 180 º dihedral angle of a *para*-substituted phenyl ring. Notably, the distances between key atoms in *para*-substituted phenyl rings and 1,3-disubstituted BCP ring systems are comparable to one another (Figure 4.2).[6d] Furthermore, an important aspect of BCP incorporation into a potential drug candidate is that it increases

the molecule's 3-dimensionality, a characteristic that can be correlated to clinical trial success.[10]

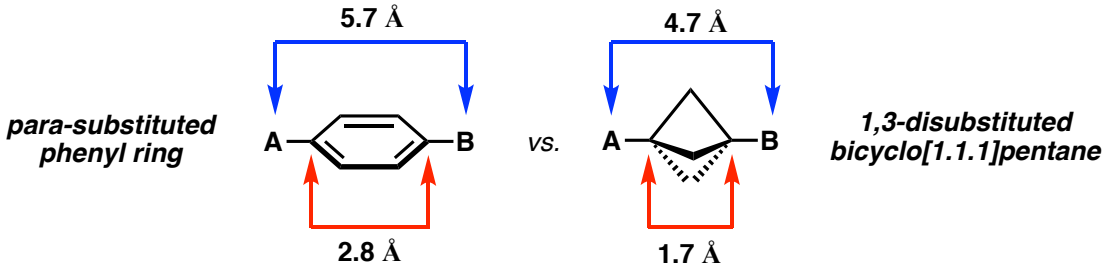

Figure 4.2. Comparison of the distances between key carbon atoms in *para*-substituted phenyl rings and 1,3-disubstituted bicyclo[1.1.1]pentanes.

In a subsequent study published by scientists at Pfizer, replacement of the *para*-substituted fluorophenyl ring in γ-secretase inhibitor BMS-708, 163 (**4.3**) with a BCP moiety produced analogue **4.4**, which exhibited significant improvements in passive permeability, aqueous solubility, and metabolic stability.[6d] These altered properties led to improved oral absorption of **4.4** in mice, relative to **4.3**. In addition, **4.4** was shown to possess γ-secretase inhibitory activity at lower concentrations than the parent compound **4.3**. A recent report has also demonstrated that replacing phenyl groups with BCPs can lower the propensity of a molecule to undergo nonspecific binding.[6h] Notably, in addition to influencing a molecule's steric and 3-dimensional properties, the replacement of a phenyl ring with a BCP motif also leads to electronic changes. Specifically, the BCP moiety lacks the conjugated π system present in a phenyl ring and, as a result, the former cannot engage in potentially useful (or detrimental) π-π or π-cation interactions.

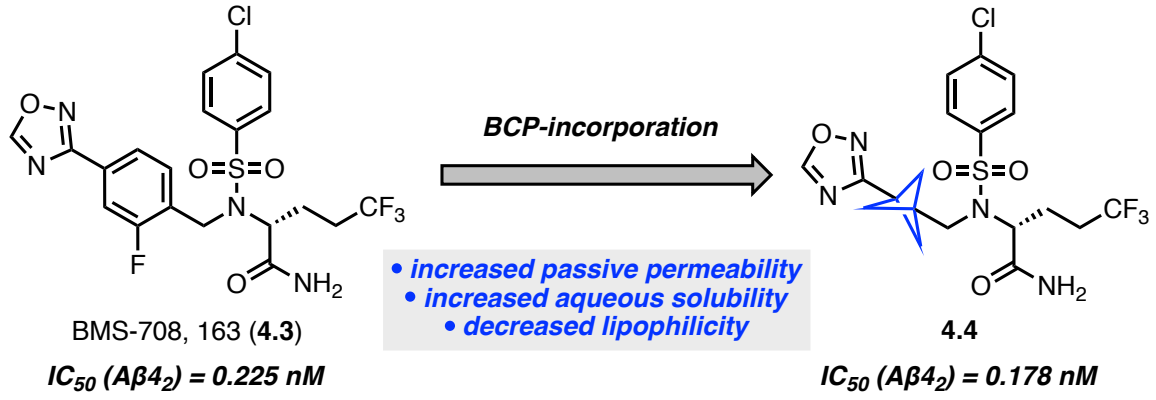

Figure 4.3. Comparison of the γ-secretase inhibitory activities of **4.3** and **4.4**.

While a large amount of research on BCP bioisosteres has focused on the effects of replacing phenyl groups, these motifs have also been studied as *t*-butyl surrogates. Carreira et al. recently conducted a systematic evaluation of several *t*-butyl bioisosteres, including BCP, in bosentan (**4.5a**) and vercimon (**4.6a**) scaffolds and found that BCP incorporation modified several physicochemical properties (Figure 4.4).[7] For example, analogues **4.5b** and **4.6b** both demonstrated greater lipophilicity and reduced sulfonamide N-H acidity than **4.5a** and **4.6a**, respectively. Moreover, **4.5b** was found to be a more active antagonist than **4.5a** against human endothelin receptor subtypes A and B (ET_A and ET_B) expressed by Chinese hamster ovary cells. Notably, several companies have incorporated *N*-substituted-BCP motifs into potential drug candidates as replacements for *N*-*t*-butyl groups (Figure 4.5).[11]

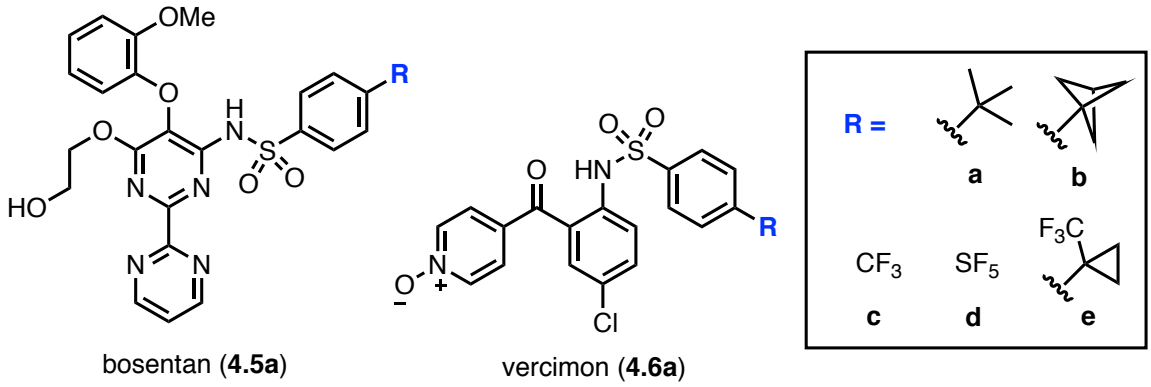

Figure 4.4. Carreira's evaluation of *t*-butyl bioisosteres in bosentan and vercimon.

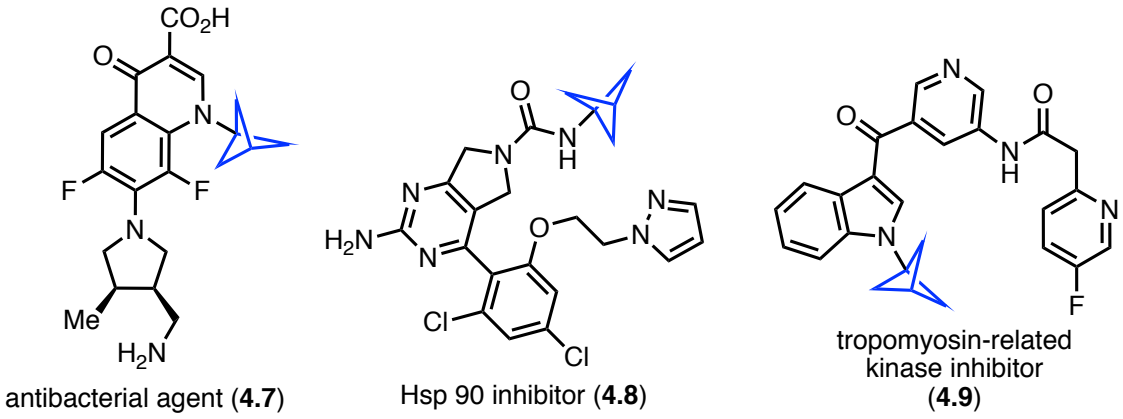

Figure 4.5. Examples of *N*-BCP containing potential drug candidates.

Knochel and coworkers recently proposed that the BCP motif can also be used as a bioisostere for internal alkynes.[8] Specifically, they developed an efficient method to prepare bis-arylated BCPs **4.12** and **4.13**, which constitute analogues of the pharmaceuticals tazarotene (**4.10**) and 2-methyl-6-(phenylethynyl)pyridine (MPEP; **4.11**), respectively (Figure 4.6). Comparison of the physicochemical properties of **4.10** vs. **4.12** and **4.11** vs. **4.13** revealed that BCP incorporation increased the basicity of the pyridine nitrogen in both analogues. Moreover, the melting point of **4.12** was found to be 64 ^{o}C higher than **4.10**, indicating better crystal packing of the former. Slight increases in non-specific binding were also observed for both BCP-based analogues when compared to **4.10** and **4.11**. This work provides a foundation for the use of BCP bioisosteres to modulate the properties of alkyne-containing drug candidates.

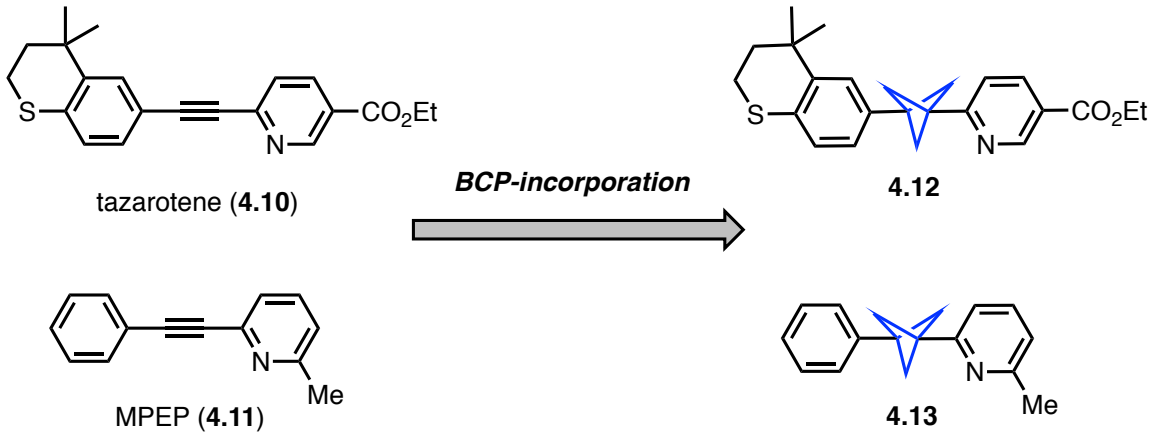

Figure 4.6. Knochel's use of BCP as an internal alkyne bioisostere.

4.1.2 Synthesis of Bridgehead Substituted Bicyclo[1.1.1]pentanes

The pharmaceutical benefits of BCP incorporation have been demonstrated within several different contexts and will undoubtedly serve as inspiration to chemists tasked with optimizing the properties of lead compounds in the future. However, the methods currently available to efficiently install BCP motifs into complex molecular scaffolds are limited and, consequently, lengthy and low-yielding synthetic sequences are often required for their installation. The vast majority of routes to bridgehead-substituted BCPs make use of [1.1.1]propellane (**4.15**), a highly strained species that was first prepared by Wiberg and Walker in 1982 (Scheme 4.1).[12,13] The most commonly employed method to

prepare **4.15** was developed by Szeimies et al. and involves the treatment of 1,1-dibromo-2,2-bis(chloromethyl)cyclopropane (**4.14**) with 2 equiv. of an organolithium base.[14]

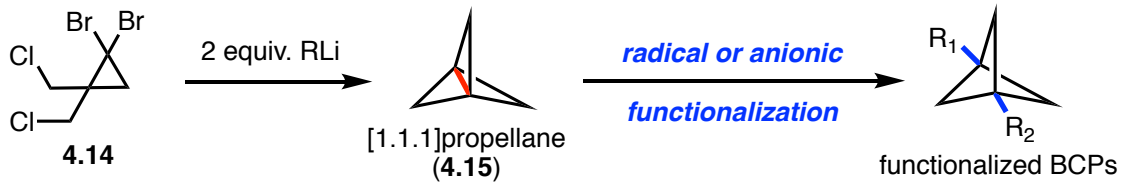

Scheme 4.1. [1.1.1]Propellane as a precursor to bridgehead-substituted BCPs.

The central σ-bond in **4.15** (highlighted in red) is reactive and can be cleaved by radical or anionic reagents in order to functionalize the bridgehead position(s). For example, Wiberg and coworkers demonstrated that a variety of 1,3-disubstituted BCPs (**4.16**) could be accessed in up to 98% yield *via* radical addition to **4.15** in the presence of light (Scheme 4.2).[15] Notably, Kaszynski and Michl showed that radical addition of biacetyl to **4.15** produces the diketo BCP **4.17** in 58% yield (Scheme 4.3).[16] A subsequent 4-step reaction sequence involving hypobromite oxidation, esterification, and selective mono-hydrolysis provided access to the nonsymmetrical 1,3-disubstituted BCP **4.19**. Monoester **4.19** has subsequently become one of the most widely utilized building blocks for the synthesis of nonsymmetrical BCP-containing molecules.[6a-f,17]

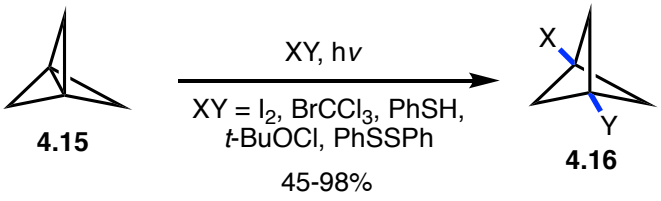

Scheme 4.2. Wiberg's synthesis of 1,3-difunctionalized BCPs *via* radical addition to [1.1.1]propellane.

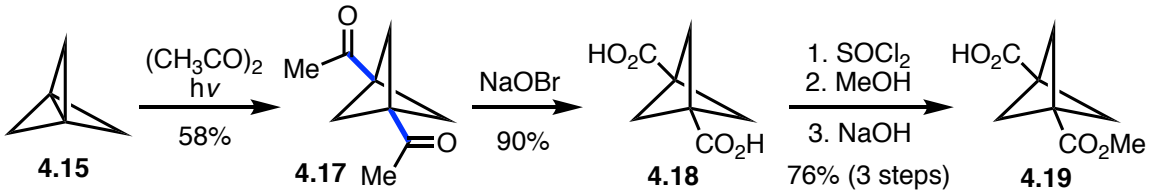

Scheme 4.3. Michl's synthesis of 3-methoxycarbonylbicyclo[1.1.1]pentane-1-carboxylic acid (**4.19**).

de Meijere and coworkers demonstrated that alkyl iodides can be added to **4.15** to generate the corresponding 3-alkyl-1-iodo BCPs **4.20** in generally excellent yields (Scheme 4.4).[18] Notably, aryl and vinyl iodides were extremely poor substrates in the reaction, providing the corresponding products in very low yields, if at all. The authors proposed that the reaction proceeds according to a radical mechanism, which likely explains the poor reactivity demonstrated by aryl and vinyl substrates. They were able to elaborate the iodide products **4.20** by performing a lithium-iodide exchange followed either by the addition an electrophile to access 1,3-difunctionalized BCPs **4.21** or by transmetalation with $ZnCl_2$ and subsequent Negishi cross-coupling to access arylated BCPs **4.22**.

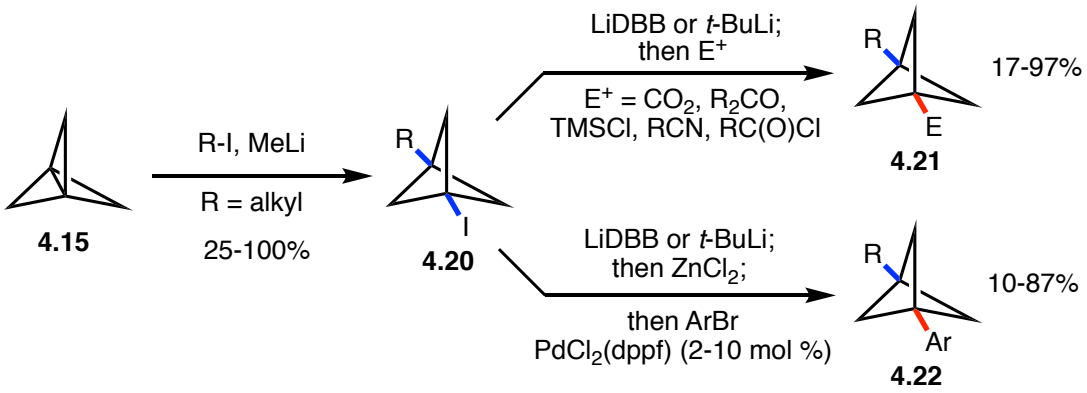

Scheme 4.4. de Meijere's radical addition of alkyl iodides to [1.1.1]propellane and subsequent functionalizations.

In order to overcome the limitation posed by aryl iodide substrates in the radical addition reaction shown in Scheme 4.4, de Meijere et al. developed a complementary method for the addition of aryl Grignards to **4.15** (Scheme 4.5).[18] Subsequent quenching of the resulting metalated BCP intermediates **4.23** with electrophiles generated the corresponding arylated mono- and di-functionalized BCPs **4.24** in up to 99% yield in one pot. Moreover, they demonstrated that a one-pot aryl Grignard addition/Kumada cross-coupling reaction could be conducted to access a range of diarylated BCP products **4.25** in moderate to excellent yields. Szeimies extended the scope of the one-pot Grignard addition/Kumada cross-coupling reaction to also include the use of alkyl Grignard nucleophiles (Scheme 4.6).[19]

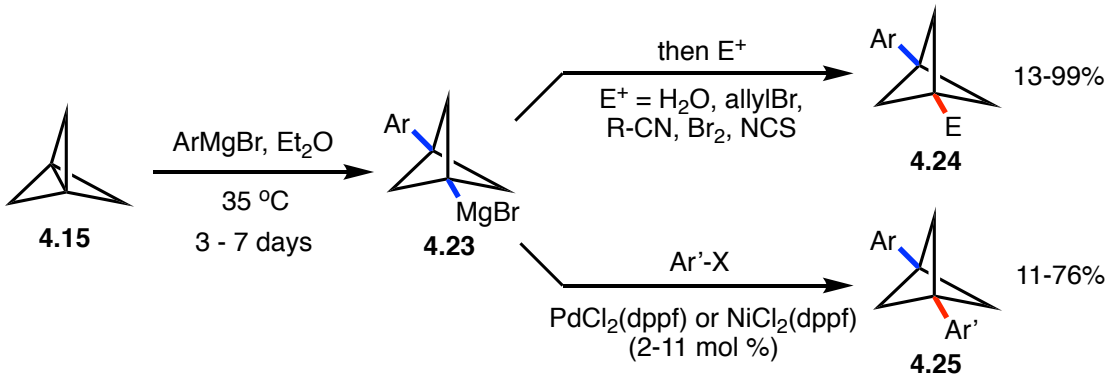

Scheme 4.5. de Meijere's aryl Grignard addition to [1.1.1]propellane and subsequent *in situ* electrophile addition or Kumada cross-coupling.

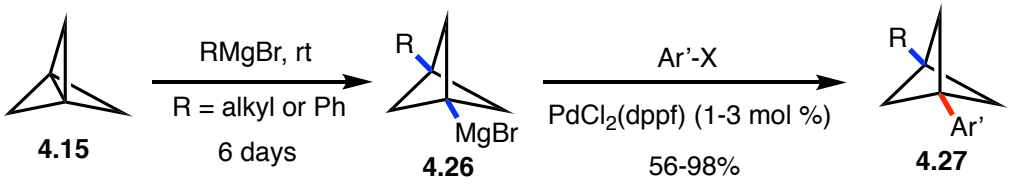

Scheme 4.6. Szeimies one-pot Grignard addition/Kumada cross-coupling reaction of [1.1.1]propellane.

While de Meijere and Szeimies' one-pot aryl Grignard addition/Kumada cross-coupling methods enabled access to several useful bisarylated BCPs, there were several notable drawbacks. For example, aryl Grignard addition to **4.15** was exceedingly slow, only reaching completion after 3-7 days. Moreover, the subsequent Kumada cross-coupling reactions required a large excess (up to 4 equiv.) of the metalated BCP intermediates (**4.23** or **4.26**) relative to the Ar'-X coupling partners. Knochel and coworkers recently addressed these limitations in an extension of these works.[8] Specifically, they demonstrated that by simply raising the Grignard addition reaction temperature to 100 °C, the reaction proceeded to completion in 3 h or less (Scheme 4.7). Subsequent *in situ* addition of ethyl chloroformate to the metalated intermediate **4.23** produced arylated BCP esters **4.28** in good to excellent yields. Importantly, they also found that transmetalation of **4.23** with $ZnCl_2$ followed by treatment with Ar'X/$PdCl_2$(dppf) enabled access to a diverse set of bisarylated BCP products **4.25** *via* Negishi cross-coupling.

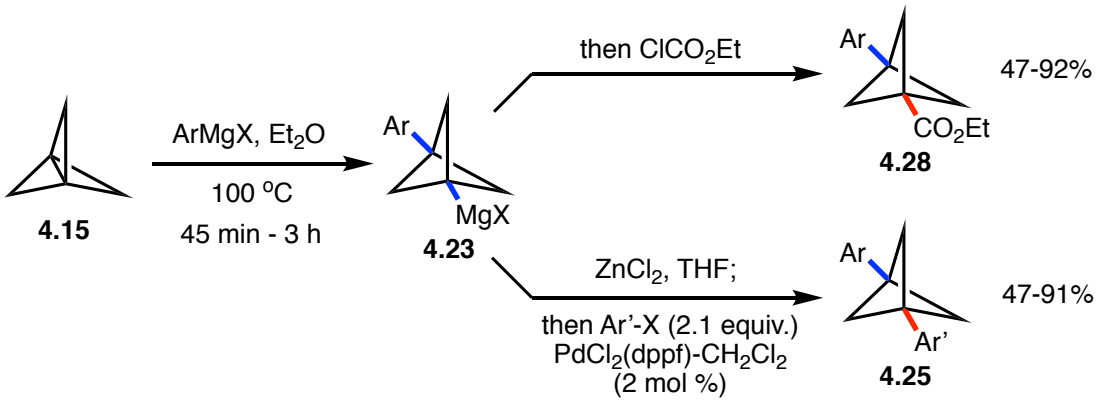

Scheme 4.7. Knochel's one-pot aryl Grignard addition/ethyl chloroformate addition and aryl Grignard addition/Negishi cross-coupling reactions of [1.1.1]propellane.

A substantial contribution to the area of [1.1.1]propellane functionalization was made by Baran and coworkers in 2016.[20] In collaboration with Pfizer, they developed the first direct amination of **4.15** using "turbo amide" nucleophiles (Scheme 4.8). Using this new method, they were able to access 30 different aminated BCPs **4.29** in moderate to excellent yields. Several functional groups were tolerated on the amide nucleophiles, including various aryl and heteroaryl rings, acetals, ketals, benzyl ethers and basic amines, thus offering rapid access to an extensive array of useful products. They further demonstrated that this method could be used for late-stage incorporation of the BCP motif onto 6 different commercialized pharmaceutical drugs. Finally, they also developed a one-pot reaction sequence to access the dibenzylated amino BCP **4.30** on >100 g scale without isolation of the volatile [1.1.1]propellane (**4.15**) intermediate (Scheme 4.9). This process-friendly sequence enabled the rapid and large-scale synthesis of amino BCP **4.31**, an important building block for the synthesis of various drug candidates such as those displayed in Figure 4.5 (*vide supra*).

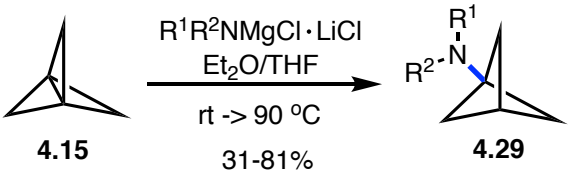

Scheme 4.8. Baran's "turbo amide" addition to [1.1.1]propellane.

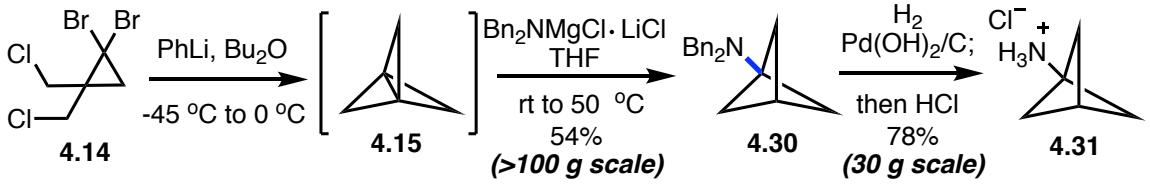

Scheme 4.9. Process-friendly synthesis of bicyclo[1.1.1]pentan-1-amine **4.31**.

Recently, Kanazawa et al. published an elegent method for the direct carboamination of **4.15** to access 1,3-disubstituted BCP hydrazine dicarboxylates **4.34** (Scheme 4.10).[21] By reacting **4.15** with di-*tert*-butyl azodicarboxylate (**4.32**) and hydrazine-based radical precursors **4.33** in the presence of iron(II) phthalocyanine [Fe(Pc)] and *tert*-butylhydroperoxide (TBHP), they prepared a set of useful difunctionalized products in 38-72% yield. In the majority of cases, incorporation of (hetero)aryl R groups were demonstrated, with two exceptions that involved incorporation of either a methyl ester or a trifluoroethyl motif. Notably, this is the only radical-based method to functionalize **4.15** with two different substituents that originate from separate precursors. Moreover, this method enabled rapid access to certain 1,3-disubstituted bicyclo[1.1.1]pentan-1-amines **4.35** *via* acidic Boc-deprotection and PtO_2-catalyzed hydrazine reduction. These structural units might serve as useful bioisosteres in drug discovery efforts. Ester-substituted amino BCP **4.35** (R = CO_2Me), in particular, has been incorporated into various peptides but previously could only be produced *via* lengthy reaction sequences (4-7 steps from **4.15**).[6f,17,22]

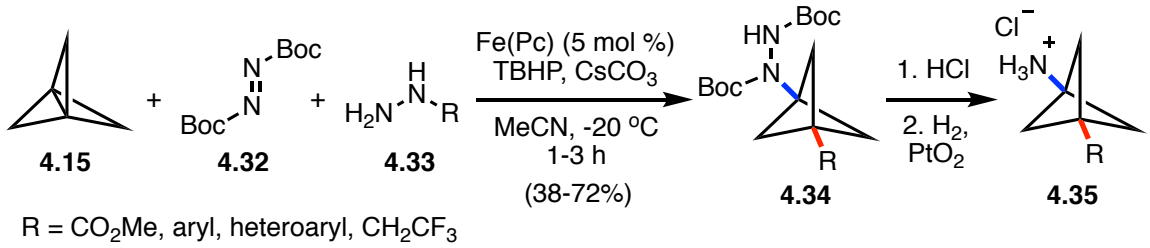

Scheme 4.10 Kanazawa and Uchiyama's radical multicomponent carboamination of [1.1.1]propellane.

4.2 The Development of a Direct Approach for the Synthesis of 1,3-Disubstituted Bicyclo[1.1.1]pentan-1-amines

The rapid pace at which new patents and publications are emerging on the use of BCP-containing molecules highlights the growing interest in this intriguing bioisostere within the drug discovery community. As new methods are developed for the efficient preparation of BCP-based building blocks, this interest and utilization will only continue to grow. Notably, Baran's method for the direct amination of [1.1.1]propellane (**4.15**) represents an important advance in accessing bicyclo[1.1.1]pentan-1-amines (i.e. **4.29**). Furthermore, Kanazawa and Uchiyama's method to access 1,3-disubstituted bicyclopentyl hydrazines offers a new avenue for the preparation of 1,3-disubstituted bicyclo[1.1.1]pentan-1-amines **4.35** that proceeds in only 3 steps from **4.15**. However, despite these significant advances, there is still a notable absence of methods available to directly prepare 1,3-disubstituted bicyclo[1.1.1]pentan-1-amines (i.e. **4.36**) directly (in 1 step) from **4.15** (Scheme 4.11). The development of an efficient method to do so would make these building blocks more readily accessible and, as a result, would favorably impact how chemists are able to assemble molecules during drug discovery campaigns.

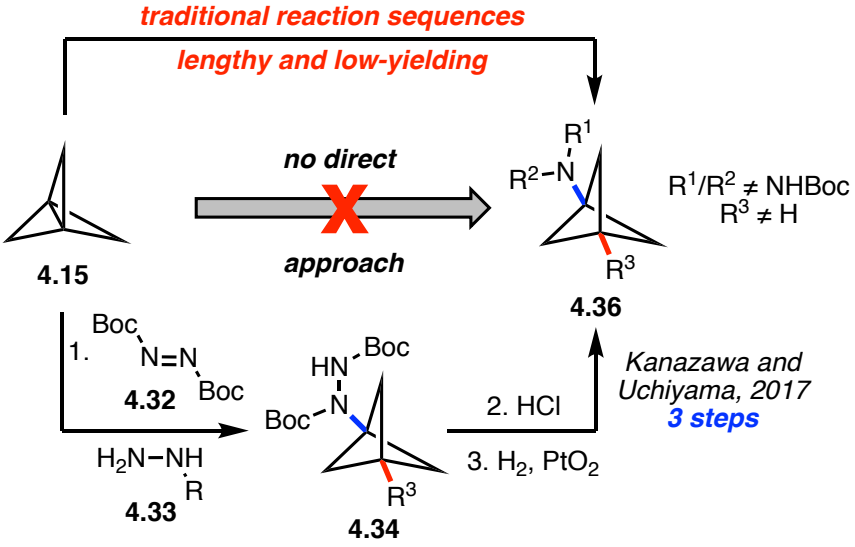

Scheme 4.11. Current limitation for the synthesis of 1,3-disubstituted bicyclo[1.1.1]pentan-1-amines.

4.2.1 Inception Sciences' Key Building Block

Recently, our group engaged in a collaboration with Inception Sciences to develop a novel and direct approach for the synthesis of 1,3-disubstituted bicyclo[1.1.1]pentan-1-amines (i.e. **4.36**).[23,24] In addition to the reasons outlined above, this specific objective was inspired by an ongoing oncology program at Inception Sciences, where they had identified a lead clinical candidate that was prepared from key building block **4.37** (Figure 4.7). At the time that this collaboration was initiated, this lead compound was being evaluated in pre-clinical toxicology studies and, pending a successful outcome, there would be an immediate need to prepare **4.37** on kilogram scale.

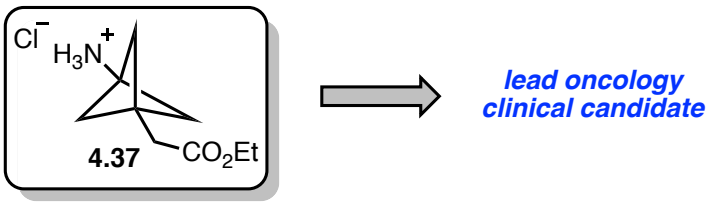

Figure 4.7. Inception Sciences' 1,3-disubstituted bicyclo[1.1.1]pentan-1-amine building block.

The route that Inception Sciences had outsourced for the synthesis of **4.37** is shown in Scheme 4.12. Like many of the other syntheses of nonsymmetrical BCP-containing molecules, it relied on the use of monoester **4.19** (*vide supra*). However, instead of preparing **4.19** according to Michl's original route,[16] they utilized a shorter sequence that was developed by Szeimies et al.[17] Accordingly, [1.1.1]propellane (**4.15**) was prepared from cyclopropane **4.14** and then functionalized *via* sequential addition of phenylmagnesium bromide and methyl chloroformate to provide **4.38** in 32% yield. Subsequent oxidation with $RuCl_3/NaIO_4$ provided acid **4.19** in 49% yield. A Curtius rearrangement was employed to convert the acid to a Boc-protected amine and then $LiBH_4$ reduction generated alcohol **4.39** in 62% yield over two steps. A nucleophilic displacement sequence, involving mesylation of alcohol **4.39** followed by treatment with KCN, delivered nitrile **4.40** in excellent yield. Finally, Boc-deprotection and nitrile hydrolysis afforded the key BCP building block **4.37** in a total of 8 steps and 8% overall yield. While serviceable, Inception Sciences' original route to **4.37** suffered from a lengthy step count and low overall yield. As a result, the quote provided by their CRO for

the production of 1 kg of material was $221,000 USD. Thus, we were tasked with the immediate goal of developing a more concise and economical synthesis of **4.37**.

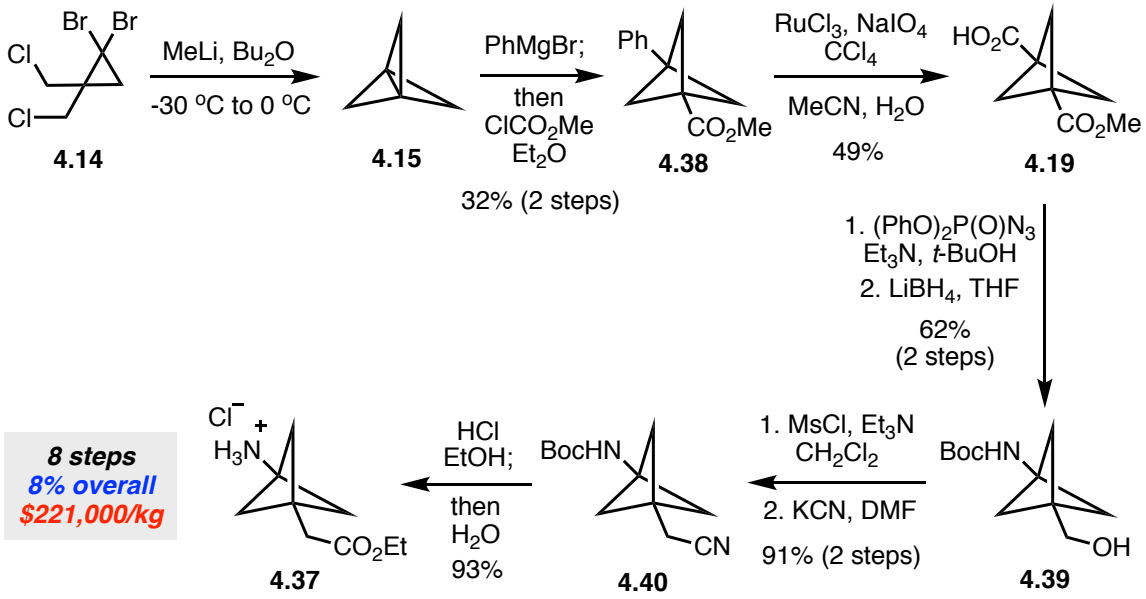

Scheme 4.12. Inception Sciences' route to key building block **4.37**.

4.2.2 Synthesis of 3-Allyl-*N*,*N*-dibenzylbicyclo[1.1.1]pentan-1-amine

Our proposed strategy to access **4.37** in a more concise manner was inspired by Baran's recent method for the direct amination of [1.1.1]propellane and is shown in Scheme 4.13.[20] Specifically, we hypothesized that metalated intermediate **4.41** might be trapped by an electrophile to provide a 1,3-disubstituted amino BCP (i.e. **4.42**), instead of undergoing protonation to provide **4.30** (*vide supra*). However, in order for this strategy to be successful, metalated species **4.41** would have to be sufficiently stable under the amination reaction conditions to allow for a subsequent electrophilic functionalization.

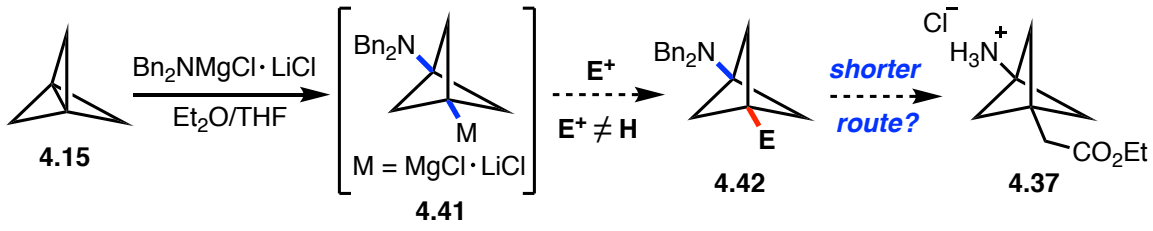

Scheme 4.13. Proposed strategy to access 1,3-disubstituted bicyclo[1.1.1]pentan-1-amines directly from [1.1.1]propellane.

To assess the feasibility of our hypothesis, we designed a deuterium-quenching experiment in order to probe the stability of metalated intermediate **4.41** under Baran's amination conditions (Scheme 4.14). Following the known procedure, [1.1.1]propellane (**4.15**) was prepared from cyclopropane **4.14** and isolated as a solution in diethyl ether in *ca.* 53% yield. Submission of **4.15** to Baran's standard amination conditions (Bn_2NMgCl•LiCl, 90 °C, sealed tube, 16 h) followed by a D_2O quench produced aminated BCP **4.43** in 68% yield with only 28% deuterium incorporation. However, we were encouraged to find that when the amination reaction was instead conducted at 50 °C, **4.43** could be isolated in 87% yield with almost complete deuterium incorporation (98% D). This experiment provided conclusive evidence that metalated species **4.41** was sufficiently stable at 50 °C and suggested that, in theory, it should be possible to intercept it with an electrophile other than H/D^+. Importantly, we found that the amination reaction was highly sensitive to even trace amounts of moisture and that high levels of deuterium incorporation were only achieved when this reaction was conducted in a Schlenk flask under an inert Ar atmosphere.

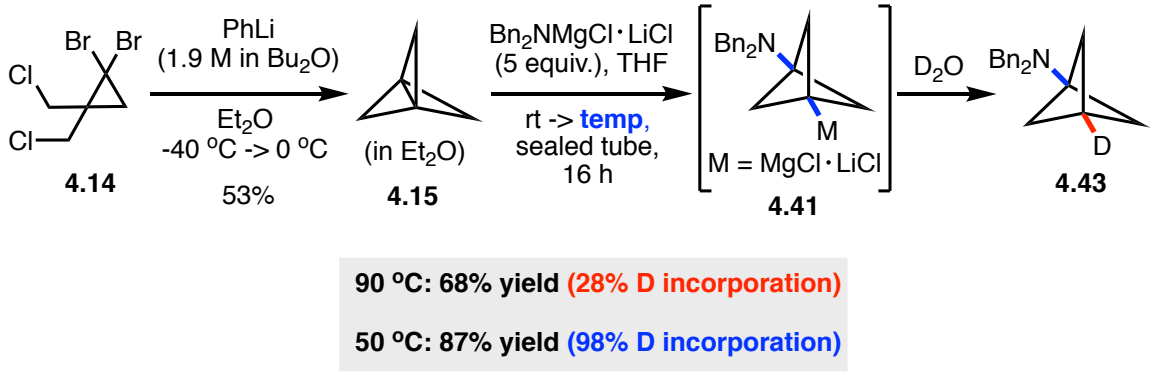

Scheme 4.14. Deuterium-quenching experiments to trap metalated intermediate **4.41**.

Having identified amination conditions that produced the persisting metalated intermediate **4.41**, we focused our efforts on trying to trap this species with a carbon-based electrophile. Disappointingly, all attempts to add ethyl haloacetates (i.e **4.44**) to **4.41** failed to deliver the desired product **4.46** (Scheme 4.15). Instead, we observed the formation of tertiary amine **4.48** (R = CO_2Et) among a complex mixture of unidentified products. Furthermore, attempts to trap **4.41** with iodoacetonitrile (**4.45**) were equally

ineffective and amine **4.48** (R = CN) was the only product that could be identified in the reaction mixture.

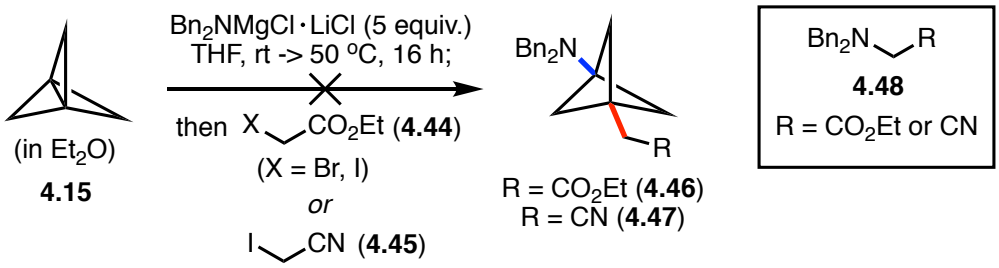

Scheme 4.15. Failed attempts to access acetate- or acetonitrile-trapped 1-amino BCPs.

Gratifyingly, further experimentation revealed that when metalated intermediate **4.41** was stirred with allyl iodide (10 equiv.) at 50 °C for 5.5 h, 3-allyl-*N*,*N*-dibenzylbicyclo[1.1.1]pentan-1-amine (**4.49**) was produced in 64% yield alongside 31% of the protonated species **4.30** (Table 4.1, entry 1). Notably, this represents the first example of a 3-alkyl bicyclo[1.1.1]pentan-1-amine substrate being prepared from **4.15** in a single step. The isolated yield of **4.49** was further improved to 89% (<6% of **4.30**) simply by extending the allylation reaction time to 24 h (entry 3). The marked reactivity of metalated intermediate **4.41** in this reaction is a testament to the unique properties of turbo Grignard reagents when compared to their standard Grignard counterparts.[25] Interestingly, a significant rate-enhancement was observed when CuI was employed as an additive in the allylation reaction. For example, when metalated intermediate **4.41** was added to a suspension of CuI (1 equiv.) in allyl iodide (10 equiv.), the alkylation was complete in less than 5.5 h and **4.49** was isolated as the sole product in 70% yield (compare entries 1 and 4).

Considering the possibility that this reaction might be run on kilogram scale, the large excesses of Bn_2NMgCl•LiCl and allyl iodide being employed were less than ideal. Moreover, the excess Bn_2NMgCl•LiCl in the reaction generated allyl dibenzylamine (**4.50**) as a side product, which was difficult to separate from **4.49** when produced in such large quantities. Cognizant of these issues, we were pleased to find that the amounts of Bn_2NMgCl•LiCl and allyl iodide could be reduced to 2.5 and 7.5 equiv., respectively, to produce **4.49** in a respectable 60% yield (entry 5). In addition, we found that CuI could be employed in catalytic amounts (10 mol %) to produce **4.49** in 72% yield (entry 6).

Table 4.1. Optimization of the one-pot reaction sequence to prepare 3-allyl-*N*,*N*-dibenzylbicyclo[1.1.1]pentan-1-amine.

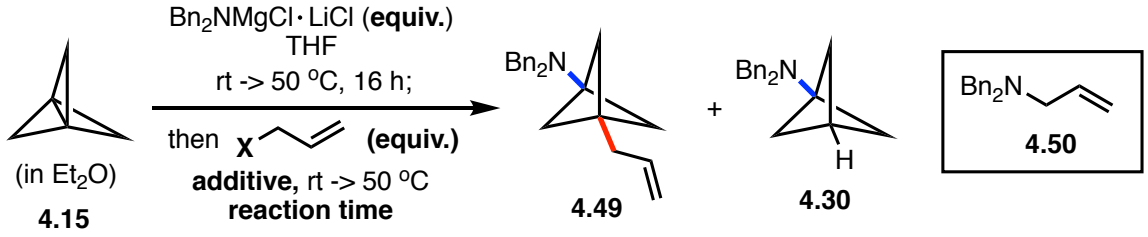

Entry	$Bn_2NMgCl \bullet LiCl$ Equivalents	Allyl halide (equiv.)	Additive (mol %)	Allylation Time (h)	4.49 (%)[a]	4.30 (%)[a]
1	5.0	I (10)	-	5.5	64	31
2	5.0	I (10)	-	10	69	24
3	5.0	I (10)	-	24	89	<6%
4	5.0	I (10)	CuI (100)	5.5	70	-
5	2.5	I (7.5)	CuI (100)	8	60	-
6	2.5	I (7.5)	CuI (10)	24	72	<5%
7	5.0	Br (10)	-	24	60	15
8	2.5	Br (10)	CuI (100)	24	complex mixture	
9	2.5	Br (10)	TBAI (20)	24	48	44
10	2.5	Br (10)	NaI (20)[b]	24	59	26
11	**2.5**	**Br (10)**	**CuBr (10)**	**24**	**68**	**11**

[a]Isolated yields. [b]DMF employed as a co-solvent.

Allyl bromide (*ca.* $150/kg) is a significantly less expensive reagent than allyl iodide (*ca.* $187/100 g), which makes its use more desirable on scale.[26] We found that the former could be employed in the allylation reaction to yield **4.49** in 60% yield alongside 15% of **4.30** (entry 7). Interestingly, the presence of stoichiometric CuI was found to be detrimental to the reaction when allyl bromide was employed as the electrophile and led to a complex mixture of products (entry 8). Further screening revealed that while TBAI and NaI both failed to improve the yield of **4.49** (entries 9 and 10), employing 10 mol % of CuBr in the allylation led to the production of **4.49** in a satisfactory 68% yield (entry 11). At this time, the specific role of the Cu(I) additive is not fully understood. However,

it might facilitate the *in situ* formation of a higher order organocuprate species that is more reactive in the allylation step.[27]

While the synthesis of **4.49** from [1.1.1]propellane (**4.15**) was an important achievement, we wondered whether the former could be prepared directly from 1,1-dibromo-2,2-bis(chloromethyl)cyclopropane (**4.14**) in one-pot. The development of such a procedure would be highly beneficial from a process chemistry standpoint because it would enable the large-scale synthesis of **4.49** without the need to isolate the highly volatile [1.1.1]propellane (**4.15**). With this consideration in mind, we were pleased to find that **4.49** could indeed be prepared in 33% yield on gram scale (4 mmol), directly from **4.14**, according to the process shown in Scheme 4.16. Although this procedure has not yet been optimized, it enabled the synthesis of **4.49** in a comparable yield to that of the two-step process above. This one-pot protocol could serve as a foundation for the development of an efficient process-scale synthesis of **4.49**.

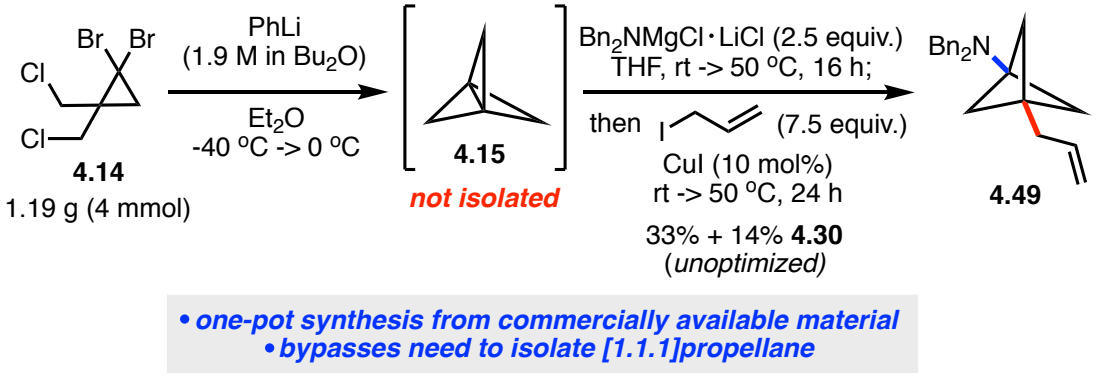

Scheme 4.16. One-pot synthesis of 3-allyl-*N*,*N*-dibenzylbicyclo[1.1.1]pentan-1-amine from commercially available 1,1-dibromo-2,2-bis(chloromethyl)cyclopropane.

4.2.3 Synthesis of Inception Sciences' Building Block

With optimized conditions in hand to prepare **4.49**, we turned our attention to the synthesis of Inception Sciences' building block **4.37** (Scheme 4.17). Sharpless dihydroxylation of **4.49** smoothly generated diol **4.51** in excellent yield. A subsequent $NaIO_4$-mediated diol cleavage produced an aldehyde that was immediately subjected to Oxone oxidation to yield acid **4.52** in 55% yield over two steps. Advantageously, we found that acid **4.52** could also be accessed from **4.49** in one step and in 62% yield *via*

Borhan oxidation (OsO_4, Oxone, TFA, DMF, rt).[28] Finally, Fischer esterification of **4.52** and subsequent benzyl hydrogenolysis of **4.53** delivered key building block **4.37** in 90% yield over two steps.

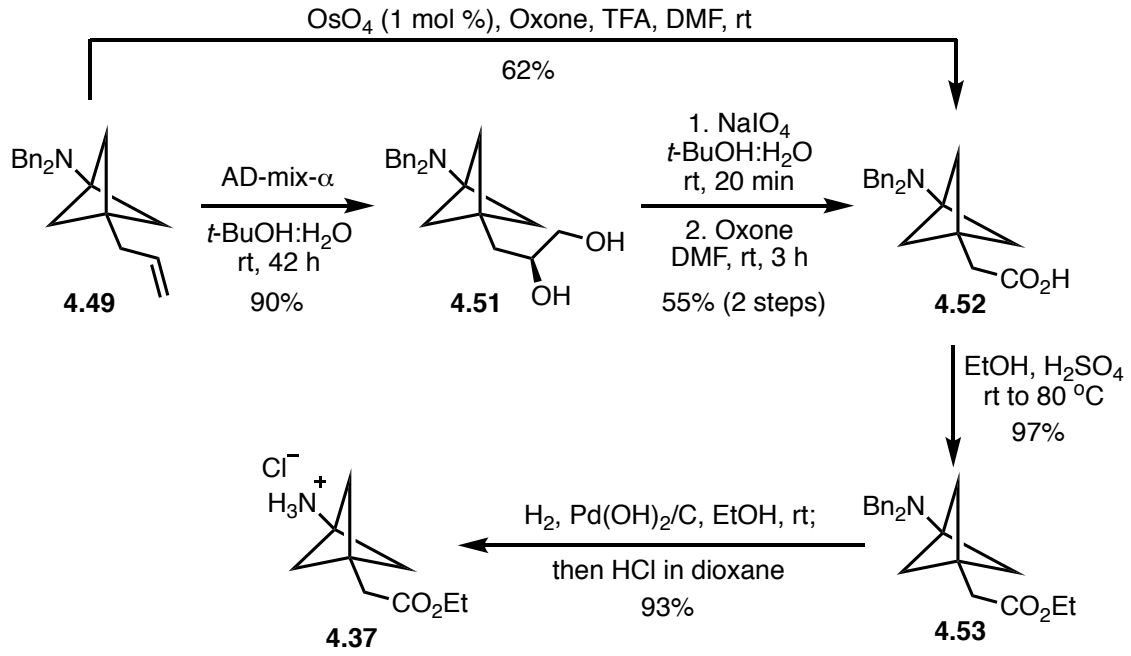

Scheme 4.17. Elaboration of **4.49** to Inception Sciences' key building block.

Our optimized synthesis of **4.37**, which is shown in Scheme 4.18, requires a total of only 5 steps and delivers the final product in 20% overall yield. The successful development of a difunctionalization reaction to produce **4.49** directly from **4.15** allowed us to avoid using several undesired functional group manipulations present in the original route. Importantly, the CRO quote to deliver 1 kg of **4.37** using this new route ($47,000 USD) was significantly lower than that of the previous ($221,000 USD). This difference represents a cost savings of $174,000/kg and highlights the beneficial impact of our novel difunctionalization reaction on the synthetic efficiency of the route.

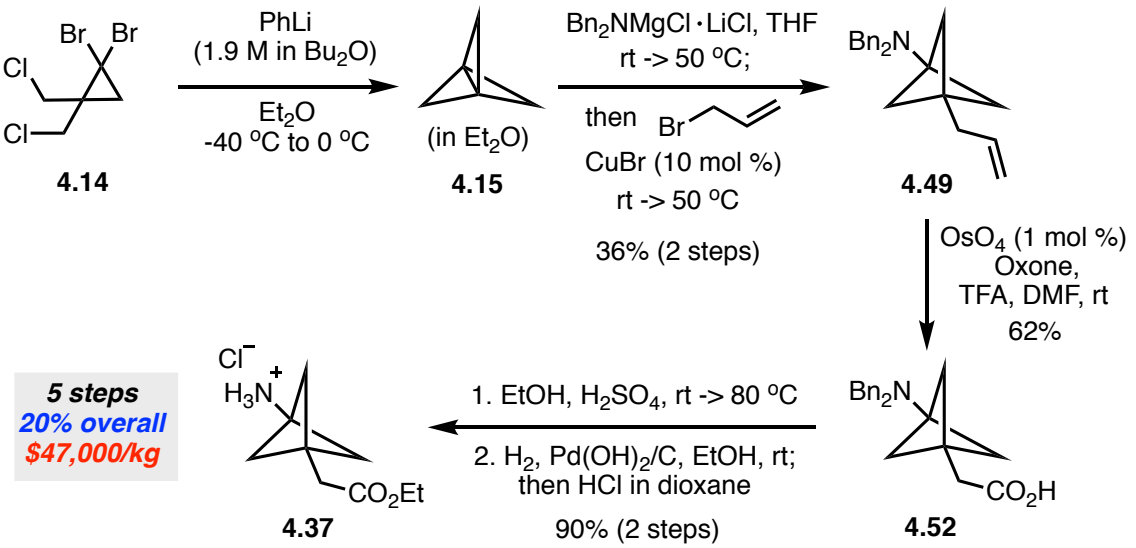

Scheme 4.18. Summary of the optimized route to Inception Sciences' key building block.

4.3 A General Method for the Synthesis of 3-Alkyl Bicyclo[1.1.1]pentan-1-amines

Having succeeded in delivering an improved synthesis of Inception Sciences' building block, we wondered whether the scope of the pivotal difunctionalization reaction could be extended to include other electrophiles. In order to assess whether a general method for the synthesis of disubstituted bicyclo[1.1.1]pentan-1-amines was feasible, we surveyed a varied set of alkyl iodides and other electrophiles in the reaction (Scheme 4.19). Accordingly, we were pleased to find that benzyl iodide could also be employed to deliver the 1,3-difunctionalized BCP **4.54** in 67% isolated yield. Importantly, in addition to allyl and benzyl electrophiles, we found that unactivated alkyl iodides are equally competent in the reaction. For example, reacting metalated intermediate **4.41** with 1-iodopropane produced **4.55** in 67% yield. Moreover, branched alkyl substituents can also be directly incorporated onto the BCP scaffold using this methodology, as evidenced by the reaction with 2-iodopropane, which afforded **4.56** in a respectable 58% yield. We also found that a dioxolane-substituted alkyl iodide could be employed to deliver **4.57**, which contains a protected aldehyde that could be used for further elaboration. While the majority of alkyl iodide electrophiles screened so far have yielded positive results, we were unable to add *t*-butyl iodoacetate (**4.58**) to metalated intermediate **4.41** using this methodology. In addition, when ethyl chloroformate (**4.59**) was employed as an electrophile, a complex mixture of products was produced.[29] Lastly, initial attempts to

access boron-substituted bicyclo[1.1.1]pentan-1-amines by adding trimethyl borate (**4.60**) to **4.41** were unsuccessful.[29] Nonetheless, the successful incorporation of a diverse set of alkyl groups provides both proof-of-concept and a foundation for the development of a general method for the direct synthesis of 3-alkyl bicyclo[1.1.1]pentan-1-amines from readily available [1.1.1]propellane (**4.15**). Further development of this method is currently underway and we are enthusiastic about its potential impact on the field of drug discovery.

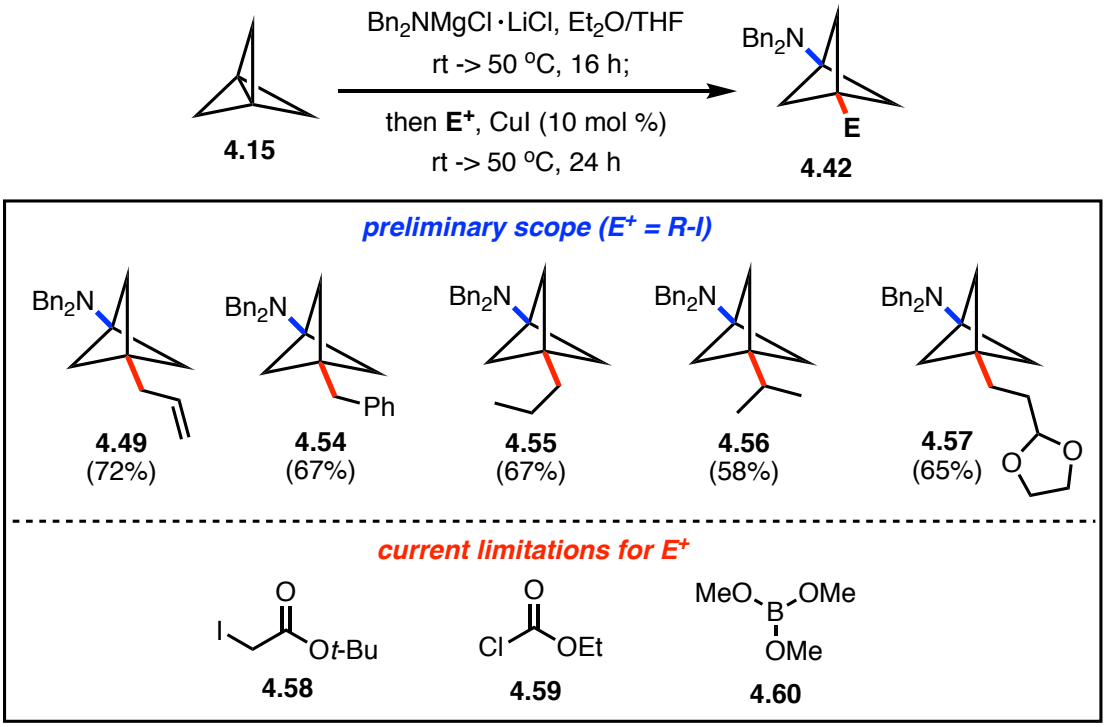

Scheme 4.19. Preliminary scope and limitations for the direct conversion of [1.1.1]propellane into 1,3-disbstituted bicyclo[1.1.1]pentan-1-amines.

4.4 Conclusion

In conclusion, a novel difunctionalization reaction of [1.1.1]propellane was developed based on a one-pot amination/allylation strategy. This transformation allowed access to 3-allyl-*N*,*N*-dibenzylbicyclo[1.1.1]pentan-1-amine in a single step and enabled an efficient synthesis of a key pharmaceutical building block that is used to prepare a lead oncology clinical candidate. Moreover, the scope of the reaction was extended to include the use of other alkyl iodide electrophiles and enabled direct access to a diverse set of 3-

alkyl bicyclo[1.1.1]pentan-1-amines. These examples serve as a proof-of-concept for the development of a general method to access 3-alkyl bicyclo[1.1.1]pentan-1-amines directly from [1.1.1]propellane.

References

(1) Patani, G. A.; LaVoie, E. J. *Chem. Rev.* **1996**, *96*, 3147, and references therein.

(2) Meanwell, N. A. *J. Med. Chem.* **2011**, *54*, 2529, and references therein.

(3) Brown, N.; Mannhold, R. *Bioisosteres in Medicinal Chemistry*; Wiley-VCH: Weinheim, 2012.

(4) Friedman, H. L. *NASNRS* **1951**, *206*, 295.

(5) Burger, A. *Prog. Drug Res.* **1991**, *37*, 287.

(6) (a) Pellicciari, R.; Raimondo, M.; Marinozzi, M.; Natalini, B.; Costantino, G.; Thomsen, C. *J. Med. Chem.* **1996**, *39*, 2874. (b) Costantino, G.; Maltoni, K.; Marinozzi, M.; Camaioni, E.; Prezeau, L.; Pin, J.-P.; Pellicciari, R. *Bioorg. Med Chem.* **2001**, *9*, 221. (c) Filosa, R.; Fulco, M. C.; Marinozzi, M.; Giacchè, N.; Macchiarulo, A.; Peduto, A.; Massa, A.; de Caprariis, P.; Thomsen, C.; Christoffersen, C. T.; Pellicciari, R. *Bioorg. Med. Chem.* **2009**, *17*, 242. (d) Stepan, A. F.; Subramanyam, C.; Efremov, I. V.; Dutra, J. K.; O'Sullivan, T. J.; DiRico, K. J.; McDonald, W. S.; Won, A.; Dorff, P. H.; Nolan, C. E.; Becker, S. L.; Pustilnik, L. R.; Riddell, D. R.; Kauffman, G. W.; Kormos, B. L.; Zhang, L.; Lu, Y.; Capetta, S. H.; Green, M. E.; Karki, K.; Sibley, E.; Atchison, K. P.; Hallgren, A. J.; Oborski, C. E.; Robshaw, A. E.; Sneed, B. *J. Med. Chem.* **2012**, *55*, 3414. (e) Nicolaou, K. C.; Vourloumis, D.; Totokotsopoulos, S.; Papakyriakou, A.; Karsunky, H.; Fernando, H.; Gavrilyuk, J.; Webb, D.; Stepan, A. F. *ChemMedChem*, **2016**, *11*, 31. (f) Nicolaou, K. C.; Yin, J.; Mandal, D.; Erande, R. D.; Klahn, P.; Jin, M.; Aujay, M.; Sandoval, J.; Gavrilyuk, J.; Vourloumis, D. *J. Am. Chem. Soc.* **2016**, *138*, 1698. (g) Measom, N. D.; Down, K. D.; Hirst, D. J.; Jamieson, C.; Manas, E. S.; Patel, V. K.; Somers, D. O. *ACS Med. Chem. Lett.* **2017**, *8*, 43. (h) Auberson, Y. P.; Brocklehurst, C.; Furegati, M.; Fessard, T. C.; Koch, G.; Decker, A.; La Vecchia, L.; Briard, E. *ChemMedChem*, **2017**, *12*, 590.

(7) Westphal, M. V.; Wolfstädter, B. T.; Plancher, J.-M.; Gatfield, J.; Carreira, E. M. *ChemMedChem*, **2015**, *10*, 461.

(8) Makarov, I. S.; Brocklehurst, C. E.; Karaghiosoff, K.; Koch, G.; Knochel, P. *Angew. Chem. Int. Ed.* **2017**, *56*, 12774.

(9) Thomsen, C.; Boel, E.; Suzdak, P. D. *Eur. J. Pharmacol. Molecular Pharm. Sect.* **1994**, *267*, 77.

(10) Lovering, F.; Bikker, J.; Humblet, C. *J. Med. Chem.* **2009**, *52*, 6752.

(11) For select examples, see: (a) Barbachyn, M. R.; Hutchison, D. K.; Toops, D. S.; Reid, R. J.; Zurenko, G. E.; Yagi, B. H.; Schaadt, R. D.; Allison, J. W. *Bioorg. Med. Chem. Lett.* **1993**, *3*, 671. (b) Gammill, R. B.; Bisaha, S. N.; Timko, J. M.; Judge, T. M.; Barbachyn, M. R.; Kim, K. S. U.S. Patent Appl. US5262417A, 1993. (c) Bennett, M. J.; Zehnder, L. R.; Ninkovic, S.; Kung, P.; Meng, J. J.; Huang, B. U.S. Patent Appl. US2010093696A1, 2010. (d) Andrews, M. D.; Bagal, S. K.; Gibson, K. R.; Omoto, K.; Ryckmans, T.; Skerratt, S. E.; Stupple, P. A. US Patent Appl. US20140364415A1, 2014.

(12) Wiberg, K. B.; Walker, F. H. *J. Am. Chem. Soc.* **1982**, *104*, 5239.

(13) (a) Wiberg, K. B. *Chem. Rev.* **2000**, *89*, 975. (b) Della, E. W.; Lochert, I. J. *Org. Prep. Proc. Int.* **1996**, *28*, 411. (c) Levin, M. D.; Kaszynski, P.; Michl, J. *Chem. Rev.* **2000**, *100*, 169. (d) Dilmaç, A. M.; Spuling, E.; de Meijere, A.; Bräse, S. *Angew. Chem. Int. Ed.* **2017**, *56*, 5684.

(14) (a) Semmler, K.; Szeimies, G.; Belzner, J. *J. Am. Chem. Soc.* **1985**, *107*, 6410. (b) Belzner, J.; Bunz, U.; Semmler, K.; Szeimies, G.; Opitz, K.; Schlüter, A.-D. *Chem. Ber.* **1989**, *122*, 397. (c) Mondanaro, K. R.; Dailey, W. P. *Org. Synth., Coll. Vol. 10*, **2004**, 658; *Vol. 75*, **1998**, 98.

(15) (a) Wiberg, K. B.; Waddell, S. T.; Laidig, K. *Tetrahedron Lett.* **1986**, *27*, 1553. (b) Wiberg, K. B.; Waddell, S. T. *J. Am. Chem. Soc.* **1990**, *112*, 2194.

(16) Kaszynski, P.; Michl, J. *J. Org. Chem.* **1988**, *53*, 4593.

(17) Pätzel, M.; Sanktjohanser, M.; Doss, A.; Henklein, P.; Szeimies, G. *Eur. J. Org. Chem.* **2004**, 493.

(18) Messner, M.; Kozhushkov, S. I.; de Meijere, A. *Eur. J. Org. Chem.* **2000**, 1137.

(19) Rehm, J. D. D.; Ziemer, B.; Szeimies, G. *Eur. J. Org. Chem.* **1999**, 2079.

(20) (a) Gianatassio, R.; Lopchuk, J. M.; Wang, J.; Pan, C.-M.; Malins, L. R.; Prieto, L.; Brandt, T. A.; Collins, M. R.; Gallego, G. M.; Sach, N. W.; Spangler, J. E.; Zhu, H.; Zhu, J.; Baran, P. S. *Science* **2016**, *351*, 6270. (b) Lopchuk, J. M.; Fjelbye, K.;

Kawamata, Y.; Malins, L. R.; Pan, C.-M.; Gianatassio, R.; Wang, J.; Prieto, L.; Bradow, J.; Brandt, T. A.; Collins, M. R.; Elleraas, J.; Ewanicki, J.; Farrell, W.; Fadeyi, O. O.; Gallego, G. M.; Mousseau, J. J.; Oliver, R.; Sach, N. W.; Smith, J. K.; Spangler, J. E.; Zhu, H.; Zhu, J.; Baran, P. S. *J. Am. Chem. Soc.* **2017**, *139*, 3209.

(21) Kanazawa, J.; Maeda, K.; Uchiyama, M. *J. Am. Chem. Soc.* **2017**, *139*, 17791.

(22) Nicolaou, K. C.; Vourloumis, D.; Yin, J.; Erande, R.; Mandal, D.; Klahn, P. U.S. Patent Appl. US2016/019604, 2016.

(23) This project was funded by an Engage grant provided by the Natural Sciences and Engineering Research Council of Canada (NSERC).

(24) For an account of academia-industry collaborative partnerships, see Michaudel, Q.; Ishihara, Y.; Baran, P. S. *Acc. Chem. Res.* **2015**, *48*, 712.

(25) (a) Krasovskiy, A.; Knochel, P. *Angew. Chem. Int. Ed.* **2004**, *43*, 3333. (b) Bao, R. L.-Y.; Zhao, R.; Shi, L. *Chem Commun.* **2015**, *51*, 6884.

(26) Prices in CAD, according to the Sigma Aldrich website (November 13, 2017).

(27) (a) Lipshutz, B. H.; Wilhelm, R. S.; Kozlowski, J. A. *Tetrahedron* **1984**, *40*, 5005. (b) Weiberth, F. J.; Hall, S. S. *J. Org. Chem.* **1987**, *52*, 3901.

(28) Travis, B. R.; Narayan, R. S.; Borhan, B. *J. Am. Chem. Soc.* **2002**, *124*, 3824.

(29) CuI was not employed as an additive in this reaction.

CONTRIBUTIONS TO KNOWLEDGE

1. The first example of an epoxide-opening/[3+2] nitrone cycloaddition cascade reaction sequence to access a bridged polycyclic ring system was demonstrated on acyclic model system **2.36** in order to access the truncated virosaine core **2.38**.

2. A one-pot enantioselective furan Diels-Alder cycloaddition/organolithium addition was developed to prepare bromohydrin **2.102**, which contains all but two of the carbon atoms found in virosaine A. The virosaine core **2.73** was subsequently prepared in an additional 4 steps *via* an efficient bio-inspired epoxide-opening/nitrone cycloaddition cascade.

3. Selective C14 functionalization of the virosaine core was attempted using several carbene/nitrene C-H insertions, hydrogen atom abstractions, and oxidative fragmentations. While these studies were unsuccessful in functionalizing C14, they uncovered valuable information about the differences in reactivity of several positions on this polycyclic ring system.

   Selective C14 functionalization of the virosaine core was achieved using a directed lithiation/bromination strategy, which was guided by a combination of NMR and computational analyses. Subsequent radical allylation at C14 of **3.137** installed the final carbon atoms present in the virosaine skeleton. A final one-pot oxidation/β-elimination sequence completed the total synthesis of (-)-virosaine A in a total of 10 steps and 9% overall yield.

4. A novel one-pot amination/alkylation protocol was developed to prepare 3-allyl bicyclo[1.1.1]pentan-1-amine **4.49** directly from [1.1.1]propellane. This enabled an efficient synthesis of the pharmaceutically important building block **4.37**. The scope of the amination/alkylation reaction was expanded to include several different alkyl iodide electrophiles, which facilitated the preparation of a diverse set of 3-alkyl bicyclo[1.1.1]pentan-1-amines.

Experimental Procedures
and
Compound Characterization

CHAPTER 5

Experimental Procedures

5.1 General Experimental

All reactions were performed under an inert argon atmosphere in oven or flame-dried round bottom flasks fitted with rubber septa and using magnetic stirring, unless otherwise stated. Liquids and solutions were transferred via syringe or stainless steel cannula under inert conditions. Thin-layer chromatography (TLC) was carried out on glass plates, coated with 250 μm of 230-400 mesh silica gel that had been saturated with F-254 indicator. TLC plates were visualized using ultraviolet light and/or by exposure to an acidic solution of cerium (IV) ammonium molybdate followed by heating, a basic solution of potassium permanganate followed by heating or an acidic solution of *p*-anisaldehyde followed by heating. Flash column chromatography was carried out on 230-400 mesh silica gel (Silicycle) using reagent grade solvents. Room temperature (rt) indicates a temperature of 22 ^{o}C. All commercial reagents were used without further purification with the following exceptions: tetrahydrofuran (THF) and diethyl ether (Et-$_2$O) were distilled from sodium/benzophenone ketyl radical under a nitrogen atmosphere. Dichloromethane, toluene, and triethylamine were distilled from calcium hydride under a dry air atmosphere. Acetonitrile (MeCN), methanol (MeOH) and pyridine were degassed and passed through activated alumina columns. Benzene and 1,2-dichloroethane (1,2-DCE) were distilled from calcium hydride under an argon atmosphere and stored over 4Å molecular sieves under argon. Furan was distilled from calcium hydride under an argon atmosphere immediately prior to use. Azobisisobutyronitrile (AIBN) was recrystallized from MeOH and stored in the dark at -20 ^{o}C. Diketene was distilled under reduced pressure and stored at -20 ^{o}C. Dibenzylamine was distilled from CaH_2 under reduced pressure and stored over 4Å molecular sieves under argon. All alkyl halide reagents were passed through a short plug of activated basic Al_2O_3 immediately prior to use. Melting points were obtained in open capillaries on a Gallenkamp apparatus and are uncorrected. Infrared (IR) spectra were obtained using a Perkin-Elmer Spectrum One FT-IR spectrophotometer. NMR spectra were recorded on 300, 400, 500 MHz Varian or 400, 500 MHz Bruker spectrometers. Chemical shifts (δ) were internally referenced to the residual proton resonance $CDCl_3$ (δ 7.26 ppm), CD_3OD (δ 3.31 ppm), $(CD_3)_2SO$ (δ 2.50 ppm). The following abbreviations were used to explain NMR peak multiplicities: s = singlet, d = doublet, t = triplet, q = quartet, sext = sextet, m = multiplet. Coupling

constants (*J*) are reported in Hertz (Hz). Microwave reactions were conducted in a Biotage Initiator microwave. Photochemical reactions were conucted in a Luzchem LZC-4V photoreactor. High-resolution mass spectrometry (HRMS) was conducted by Dr. Alexander Wahba or Dr. Nadim Saadé in the Mass Spectrometry Facility in the Department of Chemistry, McGill University. Optical rotations were recorded on a Jasco DIP-140 Digital Polarimeter at 22 ^{o}C. Chiral HPLC was performed using AGILENT Infinity 1260. Details of chromatographic conditions are indicated under each compound analyzed.

General Note: For Part I (A Total Synthesis of (-)-Virosaine A), all exploratory chemistry was carried out using racemic material, which was obtained using *rac*-(2*S*,3*R*)-3-(1*H*-indol-3-yl)-2-((4-methylphenyl)sulfonamido)butanoic acid for the preparation of the Diels-Alder catalyst **2.52**.[1] Once the final route to virosaine A had been optimized, enantiopure (2*S*,3*R*)-3-(1*H*-indol-3-yl)-2-((4-methylphenyl)-sulfonamido)- butanoic acid was employed instead.[2] Only the compounds necessary to produce (-)-virosaine A were prepared in enantiopure form.

5.2 Experimental Procedures for Chapter 2

neat *n*-butyldichloroborane[3]

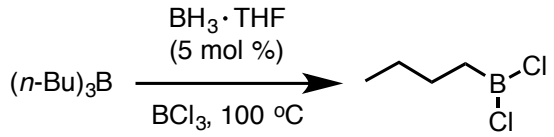

A 100 mL Schlenk flask was flame-dried under high vacuum and then cooled to rt under a stream of Ar. The flask was charged with neat tributylborane[4] (11.8 mL, 48.4 mmol, 1.0 equiv.) and then BH_3-THF complex (1.0 M in THF, 2.4 mL, 2.4 mmol, 0.05 equiv.) was added dropwise. The resulting solution was stirred at room temperature for 30 min and then the THF was removed *in vacuo* (< 0.1 mm Hg) for 10 min. The flask was flushed with Ar and then was topped with a dry ice condenser. The reaction setup was evacuated and back-filled with Ar (x3). The mixture was heat to 100 ^{o}C (bath temp.) and the condenser was filled with dry ice/acetone. BCl_3 gas (~11 mL, 125 mmol, 2.6 equiv.) was then condensed slowly into the reaction mixture. After the addition was complete the reaction mixture was stirred at 100 ^{o}C for 2 h (maintaining the condenser temp. at ~ -78 ^{o}C). 1-Hexene (6.0 mL, 48.3 mmol, 1.0 equiv.) was added and the reaction was stirred at the same temperature for an addition 30 min. The solution was cooled to rt and the condenser was replaced with a 6" vigreux column topped with a short-path fractional distillation apparatus. Unreacted BCl_3 was removed from the reaction flask at 375 mm Hg and collected in a cold trap (cooled with liquid N_2). Fractional distillation was then carried out at 120 mm Hg and *n*-butyldichloroborane was collected at 45-51 ^{o}C as a colorless, highly pyrophoric liquid (yield not determined).

Neat *n*-butyldichloroborane was stored in a Schlenk flask at -20 ^{o}C and retained its purity for several weeks. If necessary, it could be repurified by vacuum distillation.

The density of *n*-butyldichloroborane was approximated by NMR analysis using 1,2-dichloroethane (1,2-DCE) as an internal standard (IS) as follows:

An oven-dried NMR tube was capped with a septum and allowed to cool to rt under a stream of Ar. *n*-Butyldichloroborane (200 μL), 1,2-DCE (100 μL, 1.27 mmol) and dry

$CDCl_3$ (0.5 mL) were sequentially added and then the NMR tube was shaken briefly to efficiently mix the components. The *n*-butyldichloroborane:1,2-DCE ratio was determined to be 1.05:1 based on the integrations of the 1,2-DCE singlet centered at 3.71 ppm and the *n*-butyldichloroborane triplet centered at 0.92 ppm in the ^{1}H NMR spectrum. Based on this ratio, the amount of *n*-butyldichloroborane was determined to be 1.33 mmol (0.185 g). Therefore, the **density of *n*-butyldichloroborane** was calculated to be **0.93 g/mL**

^{1}H NMR (400 MHz, $CDCl_3$) δ 1.63 – 1.49 (m, 4H), 1.41 – 1.30 (m, 2H), 0.92 (t, *J* = 7.3 Hz, 3H).

^{13}C NMR (101 MHz, $CDCl_3$) δ 29.3, 27.1, 24.7, 13.7.

^{11}B NMR (128 MHz, $CDCl_3$) δ 63.3.

***n*-butyldichloroborane (as a solution in PhMe)**[5]

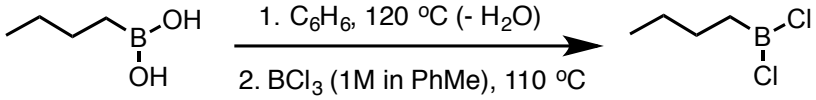

Note: We found that neat *n*-butyldichloroborane (prepared according to the previous procedure) provided optimal yield and *ee* for the Diels-Alder reaction of furan with 2-bromoacrolein. However, a PhMe solution of *n*-butyldichloroborane (prepared according to the following procedure) could also be used but provided the product in lower yield and *ee*:

A 100 mL flask was charged with an oven-dried stir bar and *n*-butylboronic acid[6] (2.09 g, 20.5 mmol, 1.0 equiv.). The flask was equipped with a 25 mL pressure-equalizing addition funnel (containing a cotton plug topped with a small layer of sand and CaH_2 (~10 g), and functioning as a Soxhlet extractor) fitted on top with a reflux condenser that was sealed with a septum and attached to a Schlenk manifold. The entire system was evacuated and back-filled with Ar (x3) and then benzene (50 mL) was added through the top of the reflux condenser and allowed to pass through the layer of CaH_2/sand. The

system was briefly evacuated and back-filled with Ar again (x3) and then the solution was heat to rapid reflux at 120 ^{o}C (bath temp.) for 17 h.

Note: It is very important to maintain rapid reflux so that the solvent/water vapors move up the arm of the addition funnel and then condense over onto the CaH_2 at a constant rate of at least ~1 drop/s. We found that large chunks of CaH_2 work best for this setup, as powdered CaH_2 prevents efficient passage of the solvent back into the reaction flask.

The reaction setup was then cooled to rt and the addition funnel was *quickly* replaced by a dry reflux condenser. The benzene was immediately removed under reduced pressure and the resulting clear boroxine oil was kept under high vacuum (< 0.1 mm Hg) for 8 h. An Ar atmosphere was then established and the oil was heat to 110 ^{o}C (bath temp.). BCl_3 (1 M in PhMe, 13.0 mL, 13.0 mmol, 0.63 equiv.) was then added and the resulting mixture was heat at 110 ^{o}C for 16 h. The reaction mixture was cooled to rt and the reflux condenser was quickly replaced by a short path distillation apparatus. Fractional distillation was carried out at 120 mm Hg and *n*-$BuBCl_2$ (0.95 M in PhMe) was collected at 53-55 ^{o}C as a colorless pyrophoric solution.

PhMe solutions of *n*-butyldichloroborane were stored under Ar at -20 ^{o}C and maintained their purity for approx. 1 month.

The concentration of the solution was determined by NMR analysis using 1,2-dichloroethane (1,2-DCE) as an internal standard (IS) as follows:

An oven-dried NMR tube was capped with a septum and allowed to cool to rt under a stream of Ar. The *n*-$BuBCl_2$ solution (100 μL), 1,2-DCE (10 μL, 0.127 mmol) and dry $CDCl_3$ (1 mL) were sequentially added and then the NMR tube was shaken briefly to efficiently mix the components. The concentration of the *n*-$BuBCl_2$ solution was approximated based on the integrations of the 1,2-DCE singlet centered at 3.70 ppm and the *n*-$BuBCl_2$ triplet centered at 0.92 ppm in the ^{1}H NMR spectrum.

***O*-(*tert*-butyldimethylsilyl)hydroxylamine**

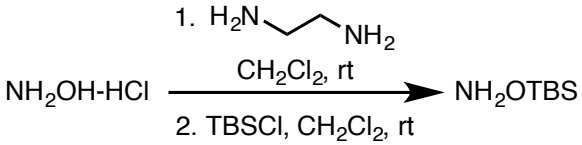

To hydroxylamine hydrochloride (2.78 g, 40.0 mmol, 1.0 equiv.) stirring in CH_2Cl_2 (16 mL) was added ethylenediamine (2.67 mL, 40.0 mmol, 1.0 equiv.) and the resulting solution was stirred at rt for 24 h. A solution of TBSCl (6.03 g, 40.0 mmol, 1.0 equiv.) in CH_2Cl_2 (4 mL) was then added via cannula and the reaction mixture was stirred for an additional 48 h. The mixture was vacuum filtered to remove the solids, which were washed with CH_2Cl_2 (3 x 20 mL). The solvent was removed *in vacuo* and then the product was purified by distillation (87-90 ^oC at 40 mm Hg) to give the title compound (4.36 g, 29.6 mmol, 74%) as a white waxy solid.

IR (neat) ν = 3357, 3318, 3250, 2955, 2930, 2886, 2857, 1583, 1473, 1463, 1390, 1362, 1319, 1254, 1186, 1007, 904, 830, 812, 780, 738, 693 cm^{-1}.

^{1}H NMR (400 MHz, $CDCl_3$) δ 5.07 (s, 2H), 0.92 (s, 9H), 0.12 (s, 6H).

^{13}C NMR (101 MHz, $CDCl_3$) δ 26.3, 18.1, -5.8.

HRMS (ESI) m/z calcd for $C_6H_{18}NOSi$: 148.1152 [$(M+H)^+$], measured: 148.1152.

***tert*-butyl(pent-4-yn-1-yloxy)diphenylsilane (S1)**

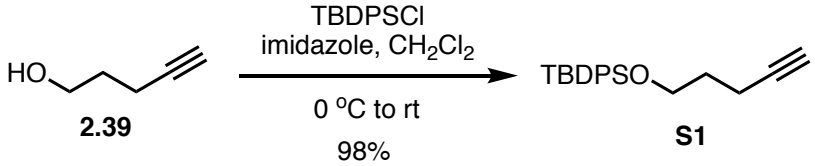

To a solution of pent-4-yn-1-ol (**2.39**) (1.02 g, 12.13 mmol, 1.0 equiv.) and imidazole (2.14 g, 31.43 mmol, 2.6 equiv.) stirring in CH_2Cl_2 (15 mL) at 0 ^oC was added *tert*-butyl(chloro)diphenylsilane (4.31 mL, 16.57 mmol, 1.4 equiv.). The reaction mixture was stirred at 0 ^oC for 15 min and then at rt for 5 h. The reaction was diluted with CH_2Cl_2 and then was quenched by the addition of saturated aq. NH_4Cl. The two layers were separated

and the aqueous layer was extracted with CH_2Cl_2 (x3). The combined organic layers were dried (Na_2SO_4) and concentrated *in* vacuo. Purification by flash chromatography (petroleum ether → 2% Et_2O:petroleum ether) gave the title compound **S1** (3.83 g, 11.88 mmol, 98 %) as a clear oil. All spectral data matched that previously reported.[7]

***tert*-butyl(oct-7-en-4-yn-1-yloxy)diphenylsilane (2.40)**

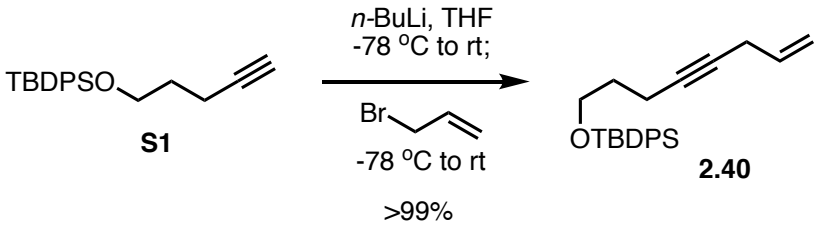

To a solution of **S1** (1.67 g, 5.18 mmol, 1.0 equiv.) stirring in THF (16 mL) at -78 °C was added *n*-BuLi (2.24 M, 2.8 mL, 6.27 mmol, 1.2 equiv.) dropwise. The solution was stirred at this temperature for 20 min and then at 0 °C for 20 min. The solution was then cooled back to -78 °C, where allyl bromide (1.4 mL, 16.18 mmol, 3.1 equiv.) was added dropwise. The reaction mixture was allowed to slowly warm to rt and was stirred for a total of 42 h. The reaction was quenched by the addition of saturated aq. NH_4Cl and then the THF was removed *in vacuo*. The resulting solution was diluted with CH_2Cl_2 and H_2O and the two layers were separated. The aqueous layer was extracted with CH_2Cl_2 (x3) and then the combined organic layers were dried over $MgSO_4$ and concentrated *in vacuo* to provide the crude title compound **2.40** (1.87 g, 5.16 mmol, >99%) as a yellow oil. The product was used in the next step without any further purification.

IR (neat) ν = 3071, 2931, 2858, 1642, 1590, 1472, 1428, 1390, 1361, 1329, 1285, 1189, 1106, 1070, 1030, 976, 915, 822, 777, 740, 700, 687 cm^{-1}.

^{1}H NMR (400 MHz, $CDCl_3$) δ 7.75 – 7.67 (m, 4H), 7.48 – 7.35 (m, 6H), 5.83 (ddt, *J* = 16.9, 10.3, 5.3 Hz, 1H), 5.32 (dq, *J* = 17.0, 1.9 Hz, 1H), 5.10 (dq, *J* = 9.9, 1.7 Hz, 1H), 3.78 (t, *J* = 6.0 Hz, 2H), 2.99 – 2.90 (m, 2H), 2.38 (tt, *J* = 7.1, 2.4 Hz, 2H), 1.85 – 1.73 (m, 2H), 1.08 (s, 9H).

^{13}C NMR (75 MHz, $CDCl_3$) δ 135.5, 133.8, 133.2, 129.5, 127.6, 115.6, 82.2, 76.7, 62.4, 31.9, 26.8, 23.1, 19.2, 15.3.

HRMS (ESI) m/z calcd for $C_{24}H_{30}NaOSi$: 385.1958 [$(M+Na)^+$], measured: 385.1960.

(*Z*)-*tert*-butyl(octa-4,7-dien-1-yloxy)diphenylsilane (2.41)

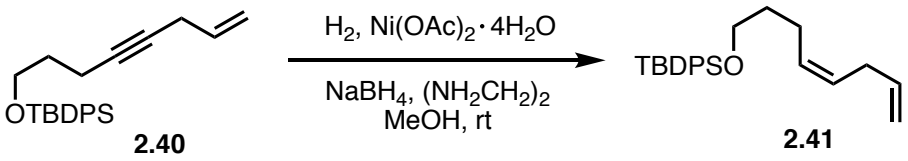

2.40 **2.41**

63%

To a solution of $Ni(OAc)_2$•$4H_2O$ (1.66 g, 6.67 mmol, 1.7 equiv.) stirring in MeOH (130 mL) was added $NaBH_4$ (298 mg, 7.88 mmol, 2.0 equiv.) portionwise. The reaction flask was purged with H_2 gas and ethylene diamine (0.67 mL, 10.00 mmol, 2.5 equiv.) was added. The resulting solution was stirred for 10 min, at which time **2.40** (1.43 g, 3.94 mmol, 1.0 equiv.) in MeOH (16 mL) was added via cannula. The reaction mixture was stirred under an atmosphere of H_2 for 30 min. Et_2O (53 mL) was added and the solution was filtered first through a bed of Celite followed by a plug of silica. The filtrate was concentrated *in vacuo* and then purified by flash chromatography (hexanes → 1% Et_2O:hexanes) to yield the title compound **2.41** (905 mg, 2.48 mmol, 63%) as a colorless oil.

IR (neat) ν = 3072, 3012, 2931, 2858, 1638, 1590, 1472, 1428, 1389, 1361, 1188, 1106, 1029, 998, 938, 910, 823, 736, 700 cm^{-1}.

^{1}H NMR (400 MHz, $CDCl_3$) δ 7.71 – 7.63 (m, 4H), 7.45 – 7.33 (m, 6H), 5.79 (ddt, *J* = 17.1, 10.1, 6.2 Hz, 1H), 5.49 – 5.32 (m, 2H), 5.02 (dq, *J* = 17.1, 1.8 Hz, 1H), 4.96 (dq, *J* = 10.1, 1.6 Hz, 1H), 3.67 (t, *J* = 6.3 Hz, 2H), 2.83 – 2.75 (m, 2H), 2.14 (q, *J* = 6.9 Hz, 2H), 1.67 – 1.55 (m, 2H), 1.05 (s, 9H).

^{13}C NMR (75 MHz, $CDCl_3$) δ 137.1, 135.6, 134.1, 130.5, 129.6, 127.6, 127.1, 114.6, 63.4, 32.6, 31.5, 26.9, 23.5, 19.3.

HRMS (ESI) m/z calcd for $C_{24}H_{32}NaOSi$: 387.2115 [$(M+Na)^+$], measured: 387.2128.

Note: Over-reduction to alkene **2.42** was a recurring problem in this reaction and despite significant experimental effort to prevent its formation, it was always generated as a minor byproduct.

(*Z*)-*tert*-butyl(oct-4-en-1-yloxy)diphenylsilane (2.42)

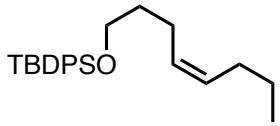

2.42

IR (neat) ν = 3071, 3050, 3001, 2957, 2930, 2858, 1590, 1472, 1428, 1389, 1361, 1307, 1188, 1105, 1007, 998, 972, 938, 860, 822, 737, 699, 612, 503, 487, 426 cm^{-1}.

^{1}H NMR (400 MHz, $CDCl_3$) δ 7.88 – 7.78 (m, 4H), 7.58 – 7.44 (m, 6H), 5.58 – 5.44 (m, 2H), 3.84 (t, *J* = 6.3 Hz, 2H), 2.29 (dtd, *J* = 7.4, 5.8, 2.7 Hz, 2H), 2.20 – 2.12 (m, 2H), 1.81 – 1.71 (m, 2H), 1.50 (dt, *J* = 14.7, 7.4 Hz, 2H), 1.23 (s, 9H), 1.04 (t, *J* = 7.4 Hz, 3H).

^{13}C NMR (101 MHz, $CDCl_3$) δ 135.6, 134.1, 130.1, 129.5, 129.4, 127.6, 63.4, 32.7, 29.3, 26.9, 23.6, 22.9, 19.2, 13.8.

HRMS (APCI) m/z calcd for $C_{24}H_{35}OSi$: 367.2452 [$(M+H)^+$], measured: 367.2447.

(*Z*)-octa-4,7-dien-1-ol (2.43)

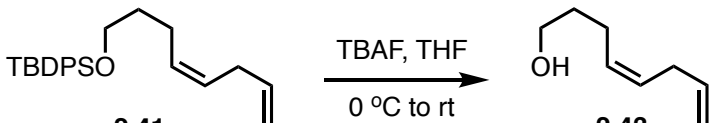

2.41 **2.43**

To a solution of **2.41** (146 mg, 0.40 mmol, 1.0 equiv.) in THF (2.2 mL) stirring at 0 °C was added TBAF (1M in THF, 0.6 mmol, 1.5 equiv.). The reaction mixture was stirred at 0 °C for 15 min and then at rt for 3 h. The reaction was quenched with saturated aq. NH_4Cl and a minimum amount of H_2O was added to dissolve the salts that were generated. The THF was removed on the rotary evaporator and then the aqueous layer

was extracted with CH_2Cl_2 (x3). The combined organic layers were washed with brine, dried (Na_2SO_4), and concentrated *in vacuo*. Purification by flash chromatography (column packed with petroleum ether; product eluted with 6:1 petroleum ether:Et_2O → 3:1 petroleum ether:Et_2O) yielded the title compound **2.43** (46.2 mg, 0.37 mmol, 92%) as a colorless oil.

IR (neat) ν = 3333, 3080, 3009, 2932, 2867, 1638, 1433, 1412, 1377, 1275, 1171, 1057, 993, 964, 909, 717, 636, 535 cm^{-1}.

^{1}H NMR (300 MHz, $CDCl_3$) δ 5.82 (ddt, *J* = 17.1, 10.1, 6.2 Hz, 1H), 5.55 – 5.37 (m, 2H), 5.10 – 4.92 (m, 2H), 3.65 (t, *J* = 6.5 Hz, 2H), 2.81 (tt, *J* = 5.9, 1.7 Hz, 2H), 2.21 – 2.08 (m, 2H), 1.70 – 1.58 (m, 2H).

^{13}C NMR (101 MHz, $CDCl_3$) δ 136.9, 130.2, 127.4, 114.6, 62.3, 32.4, 31.4, 23.4.

HRMS (APCI) m/z calcd for $C_8H_{15}O$: 127.1117 [$(M+H)^+$], measured: 127.1118.

(*Z*)-octa-4,7-dienal (2.44)

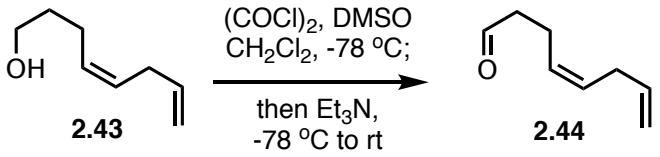

51%

A solution of oxalyl chloride (24 μL, 0.28 mmol, 2.0 equiv.) in CH_2Cl_2 (1 mL) was added slowly dropwise to a solution of DMSO (0.04 mL, 0.56 mmol, 4.0 equiv.) in CH_2Cl_2 (0.25 mL) at -78 °C. The resulting solution was stirred at this temperature for 10 min, at which time a solution of **2.43** (18 mg, 0.14 mmol, 1.0 equiv.) in CH_2Cl_2 (0.75 mL) was added. This solution was stirred for 15 min at -78 °C and then Et_3N (0.08 mL, 0.57 mmol, 4.1 equiv.) was added. The reaction mixture was stirred at -78 °C for 40 min and then at 0 °C for 40 min before warming to rt. The solution was diluted with H_2O and the two layers were separated. The aqueous layer was extracted with EtOAc (x3) and then the combined organic layers were sequentially washed with H_2O and brine, dried (Na_2SO_4) and

concentrated *in vacuo*. Purification by flash chromatography (column packed with petroleum ether; product eluted with 30:1 petroleum ether:Et_2O) provided the title compound **2.44** (8.9 mg, 0.072 mmol, 51%) as a colorless oil.

IR (neat) ν = 3079, 3012, 2957, 2925, 2721, 1820, 1724, 1638, 1411, 1365, 1185, 1042, 996, 910, 856, 720, 639, 569, 525, 448, 421, 410 cm^{-1}.

^{1}H NMR (500 MHz, $CDCl_3$) δ 9.77 (t, *J* = 1.6 Hz, 1H), 5.80 (ddt, *J* = 16.4, 10.1, 6.2 Hz, 1H), 5.52 – 5.39 (m, 2H), 5.07 – 4.95 (m, 2H), 2.82 (tt, *J* = 6.5, 1.6 Hz, 2H), 2.54 – 2.46 (m, 2H), 2.43 – 2.34 (m, 2H).

^{13}C NMR (126 MHz, $CDCl_3$) δ 202.0, 136.5, 128.4, 128.3, 114.9, 43.7, 31.4, 20.0.

HRMS (APCI) m/z calcd for $C_8H_{13}O$: 125.0961 [$(M+H)^+$], measured: 125.0961.

***rac*-(3-((2*R*,3*S*)-3-allyloxiran-2-yl)propoxy)(*tert*-butyl)diphenylsilane (2.45)**

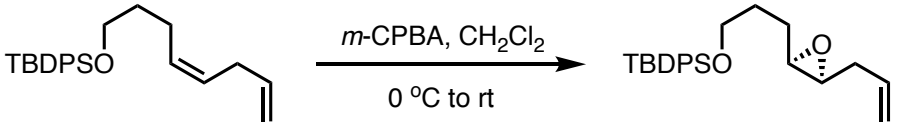

2.41 **2.45**

To a solution of **2.41** (379 mg, 1.03 mmol, 1.0 equiv.) in CH_2Cl_2 (10 mL) was added *m*-CPBA (80%, 266 mg, 1.23 mmol, 1.2 equiv.). The reaction mixture was stirred at 0 °C for 30 min and then at rt for 2 h. It was then cooled again to 0 °C, quenched with saturated aq. Na_2SO_3 (5 mL), and stirred for an additional 30 min at rt. The solution was diluted with CH_2Cl_2 and H_2O and then saturated aq. Na_2CO_3 (10 mL) was added. The mixture was stirred vigorously until two clear layers were obtained. The two layers were separated and the aqueous layer was extracted with CH_2Cl_2 (x3). The combined organic layers were washed with saturated aq. Na_2CO_3 and brine, dried (Na_2SO_4) and concentrated *in vacuo*. Purification by flash chromatography (10% Et_2O:hexanes) yielded the title compound **2.45** (325 mg, 0.85 mmol, 83%) as a colorless oil.

IR (neat) ν = 3071, 2960, 2931, 2897, 2858, 1642, 1590, 1472, 1461, 1428, 1389, 1361, 1264, 1190, 1106, 1092, 1029, 997, 916, 823, 740, 700, 687 cm^{-1}.

^{1}H NMR (400 MHz, $CDCl_3$) δ 7.70 – 7.63 (m, 4H), 7.47 – 7.34 (m, 6H), 5.86 (ddt, *J* = 16.9, 10.3, 6.5 Hz, 1H), 5.16 (dq, *J* = 17.2, 1.7 Hz, 1H), 5.11 (dq, *J* = 10.3, 1.4 Hz, 1H), 3.79 – 3.63 (m, 2H), 3.04 – 2.92 (m, 2H), 2.40 – 2.29 (m, 1H), 2.27 – 2.17 (m, 1H), 1.83 – 1.59 (m, 4H), 1.05 (s, 9H).

^{13}C NMR (75 MHz, $CDCl_3$) δ 135.6, 135.6, 133.9, 133.8, 133.7, 129.6, 127.6, 117.1, 63.4, 56.8, 56.0, 32.3, 29.5, 26.9, 24.4, 19.2.

HRMS (ESI) m/z calcd for $C_{24}H_{32}NaO_2Si$: 403.2064 [$(M+Na)^+$], measured: 403.2076.

***rac*-3-((2*R*,3*S*)-3-allyloxiran-2-yl)propan-1-ol (2.46)**

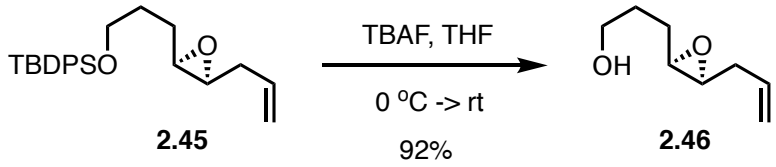

To a solution of **2.45** (407 mg, 1.07 mmol, 1.0 equiv.) stirring in THF (10 mL) at 0 °C was added TBAF (1M in THF, 1.5 mL, 1.50 mmol, 1.4 equiv.). The reaction mixture was stirred at 0 °C for 20 min and then at rt for 4 h. The reaction mixture was concentrated *in vacuo* (100 mbar, rt) and was then quickly passed through a short plug of silica (eluting with 2:1 Et_2O:petroleum ether) to yield the title compound **2.46** (140 mg, 0.98 mmol, 92%) as a colorless oil.

IR (neat) ν = 3393, 3075, 2956, 2933, 2873, 1642, 1449, 1429, 1387, 1265, 1229, 1187, 1142, 1114, 1061, 1031, 997, 969, 918, 866, 824, 783, 743, 706 cm^{-1}.

^{1}H NMR (400 MHz, $CDCl_3$) δ 5.93 – 5.80 (m, 1H), 5.17 (dqd, *J* = 17.2, 1.7, 0.6 Hz, 1H), 5.14 – 5.09 (m, 1H), 3.77 – 3.67 (m, 2H), 3.08 – 2.96 (m, 2H), 2.43 – 2.32 (m, 1H), 2.31 – 2.18 (m, 1H), 1.83 – 1.47 (m, 5H).

^{13}C NMR (75 MHz, $CDCl_3$) δ 133.5, 117.2, 62.2, 56.9, 56.2, 32.2, 29.6, 24.3.

HRMS (ESI) m/z calcd for $C_8H_{14}NaO_2$: 165.0886 [$(M+Na)^+$], measured: 165.0887.

Note: Tetrahydrofuran **2.47** was always a small inseparable contaminant of the desired product **2.46**. Epoxide **2.46** spontaneously cyclized to form **2.47** if exposed to acid (even in trace amounts) or if slow flash chromatography was conducted.

***rac*-(*S*)-1-((*S*)-tetrahydrofuran-2-yl)but-3-en-1-ol (2.47)**

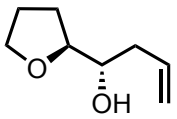

2.47

IR (neat) ν = 3438, 3074, 2973, 2955, 2930, 2870, 1641, 1462, 1429, 1399, 1292, 1217, 1185, 1111, 1056, 999, 911, 868, 821, 742, 704, 623, 607 cm^{-1}.

^{1}H NMR (400 MHz, $CDCl_3$) δ 5.90 (ddt, *J* = 17.2, 9.9, 7.1 Hz, 1H), 5.18 – 5.06 (m, 2H), 3.88 – 3.68 (m, 3H), 3.55 – 3.45 (m, 1H), 2.37 – 2.19 (m, 3H), 2.01 – 1.83 (m, 3H), 1.71 – 1.60 (m, 1H).

^{13}C NMR (101 MHz, $CDCl_3$) δ 134.7, 117.3, 81.7, 73.3, 68.2, 38.4, 27.9, 26.3.

HRMS (ESI) m/z calcd for $C_8H_{14}NaO_2$: 165.0886 [$(M+Na)^+$], measured: 165.0887.

***rac*-3-((2*R*,3*S*)-3-allyloxiran-2-yl)propanal (2.48)**

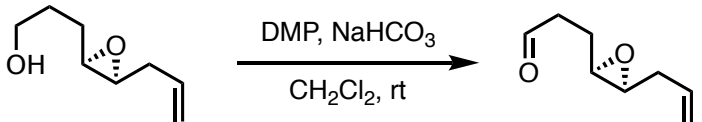

2.46 90% **2.48**

To a solution of **2.46** (138 mg, 0.97 mmol, 1.0 equiv.) stirring in CH_2Cl_2 (9.7 mL) was added $NaHCO_3$ (277 mg, 3.30 mmol, 3.4 equiv.) followed by DMP (699 mg, 1.65 mmol, 1.7 equiv.).[8] The reaction mixture was stirred at rt for 2 h before quenching with saturated aq. $NaHCO_3$ (5 mL) and saturated aq. $Na_2S_2O_3$ (5 mL). The mixture was stirred

vigorously at rt for 1.5 h and then the two layers were separated. The aqueous layer was extracted with CH_2Cl_2 (x2) and then the combined organic layers were washed with brine, dried (Na_2SO_4), and concentrated *in vacuo*. The crude mixture was passed through a plug of silica (eluting with 2:1 petroleum ether:Et_2O) to provide the title compound **2.48** (124 mg, 0.87 mmol, 90%) as a colorless oil.

IR (neat) ν = 3080, 2978, 2928, 2828, 2725, 1712, 1641, 1452, 1413, 1388, 1355, 1267, 1196, 1140, 1108, 1058, 996, 917, 859, 823, 763, 633, 542, 466, 439 cm^{-1}.

^{1}H NMR (400 MHz, $CDCl_3$) δ 9.83 (t, *J* = 1.2 Hz, 1H), 5.86 (ddt, *J* = 16.9, 10.3, 6.5 Hz, 1H), 5.21 – 5.09 (m, 2H), 3.08 – 2.95 (m, 2H), 2.77 – 2.55 (m, 2H), 2.37 (dtt, *J* = 15.7, 6.5, 1.5 Hz, 1H), 2.24 (dtt, *J* = 15.4, 6.4, 1.4 Hz, 1H), 2.01 – 1.87 (m, 1H), 1.84 – 1.68 (m, 1H).

^{13}C NMR (75 MHz, $CDCl_3$) δ 201.2, 133.2, 117.3, 56.3, 55.9, 40.8, 32.1, 20.4.

HRMS (ESI) m/z calcd for $C_8H_{13}O_2$: 141.0910 [$(M+H)^+$], measured: 141.0911.

***rac*-3-((2*R*,3*S*)-3-allyloxiran-2-yl)propanal oxime (2.36)**

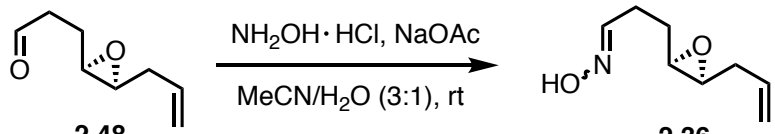

2.48 **2.36**

To a solution of **2.48** (120 mg, 0.86 mmol, 1.0 equiv.) stirring in 2:1 MeCN:H_2O (4.3 mL) was added NaOAc (139 mg, 1.69 mmol, 2.0 equiv.) followed by NH_2OH□HCl (117 mg, 1.68 mmol, 2.0 equiv.). The resulting reaction mixture was stirred at rt for 3.5 h and then the MeCN was removed *in vacuo*. The resulting mixture was diluted with H_2O and CH_2Cl_2 and then the two layers were separated. The aqueous layer was saturated with NaCl and extracted with CH_2Cl_2 (x3). The combined organic layers were dried (Na_2SO_4) and concentrated *in vacuo*. Purification by flash chromatography (3:1 petroleum ether:Et_2O → 3:2 petroleum ether:Et_2O) provided the title compound **2.36** (103 mg, 0.66 mmol, 78%) as a ~1:1 mixture of *E* and *Z* isomers as a colorless oil.

IR (neat) ν = 3330, 3081, 2977, 2916, 1642, 1432, 1387, 1341, 1285, 994, 916, 828, 791, 746, 629, 553, 473, 410 cm^{-1}.

^{1}H NMR (400 MHz, $CDCl_3$) δ 9.36 (s, 1H), 8.92 (s, 1H), 7.45 (t, *J* = 5.8 Hz, 1H), 6.78 (t, *J* = 5.5 Hz, 1H), 5.90 – 5.75 (m, 1H), 5.21 – 5.04 (m, 2H), 3.07 – 2.90 (m, 2H), 2.62 – 2.46 (m, 1H), 2.46 – 2.27 (m, 2H), 2.27 – 2.15 (m, 1H), 1.83 – 1.63 (m, 2H).

^{13}C NMR (101 MHz, $CDCl_3$) δ 150.9, 150.6, 133.2, 117.2, 56.3, 56.1, 56.0, 55.9, 32.1, 26.7, 24.8, 24.3, 22.2.

HRMS (ESI) m/z calcd for $C_8H_{13}NNaO_2$: 178.0838 [$(M+Na)^+$], measured: 178.0835.

***rac*-(*S*)-1-((*S*)-5,6-dihydro-4*H*-1,2-oxazin-6-yl)but-3-en-1-ol (2.49)**

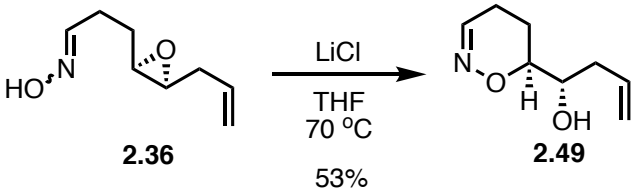

2.36 **2.49**

To **2.36** (19 mg, 0.12 mmol, 1.0 equiv.) stirring in THF (1.2 mL) was added LiCl (5 mg, 0.12 mg, 1.0 equiv.). The reaction mixture was stirred at rt for 1 h and then at 70 °C (bath temp.) for 16 h. The mixture was cooled to rt and then concentrated *in vacuo.* Purification by flash chromatography (5:1 Et_2O:petroleum ether) yielded the title compound **2.49** (10 mg, 0.064 mmol, 53%) as a white wax-like solid.

Unreacted **2.36** (4 mg, 0.026 mmol, 21%)) and nitrone **2.37** (4 mg, 0.026 mmol, 21%) were also isolated from the reaction mixture.

IR (neat) ν = 3389, 3076, 2923, 2873, 1724, 1642, 1623, 1430, 1291, 1231, 1056, 1015, 915, 892, 870, 848, 796, 754 cm^{-1}.

^{1}H NMR (400 MHz, CD_3OD) δ 7.25 (t, *J* = 3.0 Hz, 1H), 5.90 (ddt, *J* = 17.2, 10.2, 7.0 Hz, 1H), 5.13 (dq, *J* = 17.1, 1.6 Hz, 1H), 5.06 (ddt, *J* = 10.3, 2.3, 1.2 Hz, 1H), 3.69 (dt, *J*

= 8.8, 4.1 Hz, 1H), 3.63 (dt, *J* = 8.7, 4.6 Hz, 1H), 2.49 – 2.19 (m, 4H), 1.92 – 1.73 (m, 2H).

^{13}C NMR (101 MHz, CD_3OD) δ 151.0, 136.2, 117.5, 78.8, 73.2, 38.3, 22.8, 20.9.

HRMS (ESI) m/z calcd for $C_8H_{13}NNaO_2$: 178.0839 [$(M+Na)^+$], measured: 178.0838.

***rac*-(4*S*,5*S*)-4,5-dihydroxyoct-7-enenitrile (2.50)**

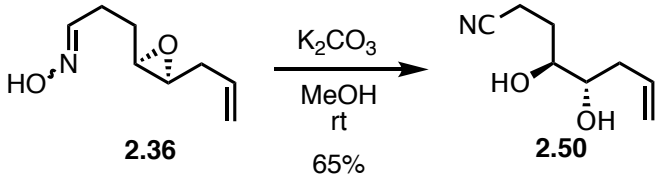

2.36 **2.50**

To **2.36** (12.4 mg, 0.080 mmol, 1.0 equiv.) stirring in MeOH (1 mL) was added K_2CO_3 (11 mg, 0.080 mmol, 1.0 equiv.). The reaction mixture was stirred at rt for 1 h and then was concentrated *in vacuo*. Purification by flash chromatography (5:1 Et_2O:petroleum ether) yielded the title compound **2.50** (8 mg, 0.052 mmol, 65 %) as a clear oil.

IR (neat) ν = 3422, 3078, 2925, 2852, 2247, 1716, 1642, 1426, 1267, 1062, 997, 918, 868, 799, 740, 703 cm^{-1}.

^{1}H NMR (400 MHz, CD_3OD) δ 5.89 (ddt, *J* = 17.2, 10.2, 7.0 Hz, 1H), 5.12 (dq, *J* = 17.2, 1.7 Hz, 1H), 5.06 (ddt, *J* = 10.2, 2.2, 1.2 Hz, 1H), 3.53 (dt, *J* = 8.9, 3.9 Hz, 1H), 3.47 (ddd, *J* = 8.4, 4.9, 3.6 Hz, 1H), 2.64 – 2.47 (m, 2H), 2.38 – 2.29 (m, 1H), 2.29 – 2.18 (m, 1H), 1.88 – 1.72 (m, 2H).

^{13}C NMR (126 MHz, CD_3OD) δ 136.5, 121.2, 117.3, 74.6, 72.8, 38.7, 30.1, 14.3.

HRMS (ESI) m/z calcd for $C_8H_{14}NO_2$: 156.1019 [$(M+H)^+$], measured: 156.1025.

***rac*-(*S*)-2-((*S*)-1-hydroxybut-3-en-1-yl)-3,4-dihydro-2*H*-pyrrole 1-oxide (2.37)**

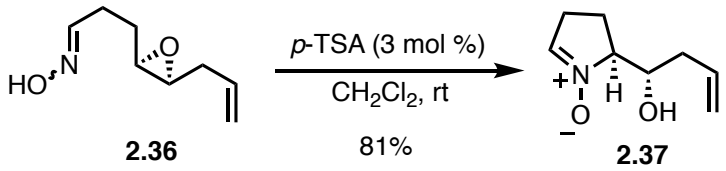

2.36 **2.37**

To **2.36** (26 mg, 0.17 mmol, 1.0 equiv.) stirring in CH_2Cl_2 (1 mL) was added *para*-toluenesulfonic acid (1 mg, 5.26 μmol, 0.03 equiv.) and the reaction mixture was stirred at rt for 2.5 h. The mixture was concentrated *in vacuo* and purified by flash chromatography (5:1 EtOAc:MeOH) to yield the title compound **2.37** (21 mg, 0.14 mmol, 81%) as a white wax-like solid.

IR (neat) ν = 3298, 3079, 2926, 2873, 1725, 1641, 1597, 1437, 1352, 1286, 1229, 1193, 1123, 1076, 1012, 916, 817, 683 cm^{-1}.

^{1}H NMR (400 MHz, $CDCl_3$) δ 6.95 (q, *J* = 2.4 Hz, 1H), 6.54 (s, 1H), 5.99 (dddd, *J* = 17.7, 9.7, 7.9, 6.0 Hz, 1H), 5.18 – 5.07 (m, 2H), 4.02 – 3.83 (m, 2H), 2.74 – 2.55 (m, 2H), 2.46 – 2.27 (m, 2H), 2.19 (ddd, *J* = 14.4, 7.9, 6.3 Hz, 1H), 1.85 (dq, *J* = 13.1, 9.0 Hz, 1H).

^{13}C NMR (101 MHz, $CDCl_3$) δ 135.9, 133.5, 117.8, 73.9, 73.3, 37.7, 26.4, 22.6.

HRMS (ESI) m/z calcd for $C_8H_{14}NO_2$: 156.1019 [$(M+H)^+$], measured: 156.1019.

***rac*-(3*S*,3a*R*,6*S*,7*S*,8*S*)-hexahydro-6,3-ethanopyrrolo[1,2-*b*]isoxazol-8-ol (2.38)**

[3+2] Cycloaddition of 2.37:

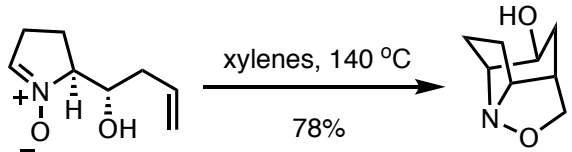

2.37 **2.38**

A solution of **2.37** (11.5 mg, 0.074 mmol, 1.0 equiv.) in xylenes (2 mL) was heat to 140 °C (bath temp.) and stirred for 5.5 h. After cooling to rt, the reaction mixture was

concentrated *in vacuo* and purified by flash chromatography (25:1 EtOAc:MeOH) to yield the title compound **2.38** (9 mg, 0.058 mmol, 78%) as a white solid.

One-pot synthesis of 2.38 from oxime 2.36:

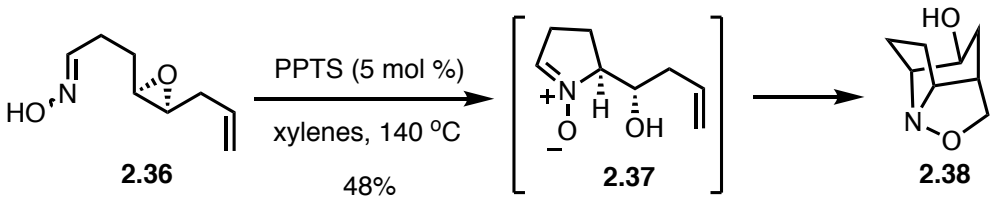

2.36 **2.37** **2.38**

To a solution of **2.36** (11.5 mg, 0.074 mmol, 1.0 equiv.) stirring in xylenes (1.5 mL) at rt was added pyridinium *para*-toluenesulfonate (1 mg, 0.040 mmol, 0.05 equiv.). The reaction mixture was then heat to 140 °C (bath temp.) and stirred for 6.5 h. After cooling to rt, the mixture was concentrated *in vacuo* and purified by flash chromatography (25:1 EtOAc:MeOH) to yield the title compound **2.38** (5.5 mg, 0.035 mmol, 48%) as a white solid.

mp = 106-110 °C

IR (neat) ν = 3302, 2937, 2874, 1648, 1474, 1451, 1339, 1304, 1253, 1221, 1149, 1129, 1076, 1042, 990, 972, 935, 903, 880, 858, 826, 780, 759, 713 cm^{-1}.

^{1}H NMR (500 MHz, $CDCl_3$) δ 4.24 (ddd, *J* = 10.6, 6.5, 4.3 Hz, 1H), 3.95 – 3.87 (m, 2H), 3.51 (dd, *J* = 7.4, 3.6 Hz, 1H), 3.46 – 3.42 (m, 1H), 2.47 – 2.40 (m, 1H), 2.21 – 1.94 (m, 2H), 1.94 – 1.83 (m, 2H), 1.86 – 1.72 (m, 2H), 1.53 (ddq, *J* = 14.3, 10.4, 1.7 Hz, 1H).

^{13}C NMR (126 MHz, $CDCl_3$) δ 75.6, 66.0, 64.9, 64.0, 42.0, 31.7, 20.2, 19.8.

HRMS (ESI) m/z calcd for $C_8H_{14}NO_2$: 156.1019 [$(M+H)^+$], measured: 156.1025.

Attempted Diels-Alder reaction of 2-bromoacrolein (2.9) and ethyl 2-(furan-2-yl)acetate (2.10, R = CH_2CO_2Et):

Several different catalysts and conditions were screened for the reaction of **2.9** with **2.10**. Only one set of conditions is reported, which generated both furan products **2.53** and **2.54** in the highest isolated yield:

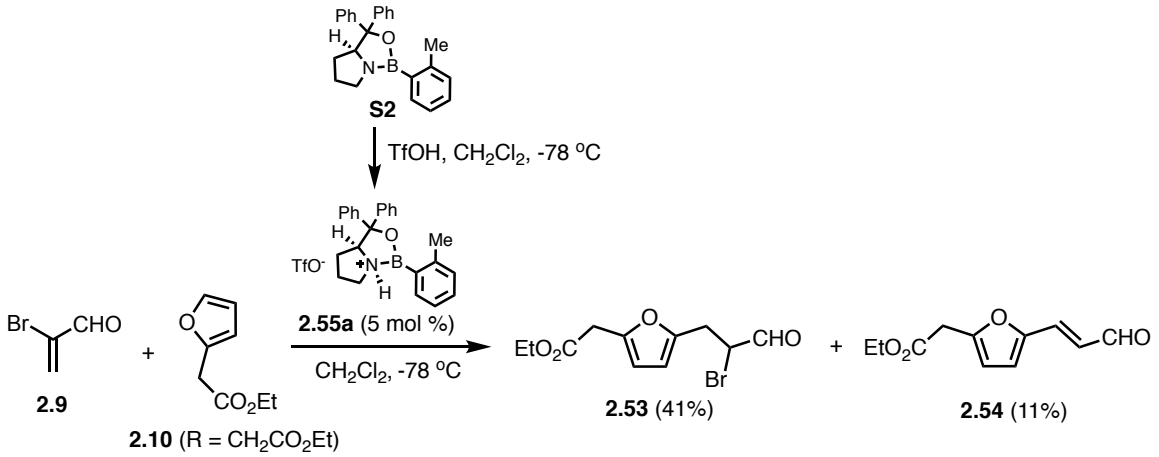

To a solution of oxazaborolidine **S2**[9] (51.2 mg, 0.145 mmol, 0.07 equiv.) stirring in CH_2Cl_2 (10 mL) at -78 °C was added triflic acid (0.20 M in CH_2Cl_2, 605 µL, 0.121 mmol, 0.06 equiv.) and the resulting solution was stirred at this temp. for 45 min to provide the active catalyst **2.55a**. 2-Bromoacrolein (**2.9**)[10] (161 µL, 2.00 mmol, 1.0 equiv.) was added followed by a solution of ethyl 2-(furan-2-yl)acetate[11] (1.54 g, 10.00 mmol, 5.0 equiv.) in CH_2Cl_2 (1.5 mL) and the reaction mixture was stirred at -78 °C for 1.5 h before quenching with Et_3N (200 µL). The mixture was warmed to rt, concentrated *in vacuo*, and then purified by flash chromatography (5:1 pet. ether:Et_2O for **2.53** and 2:1 pet. ether:Et_2O for **2.54**) to give **2.53** (235 mg, 0.813 mmol, 41%) as a colorless oil and **2.54** (44 mg, 0.211 mmol, 11%) as a yellow oil.

***rac*-ethyl 2-(5-(2-bromo-3-oxopropyl)furan-2-yl)acetate (2.53)**

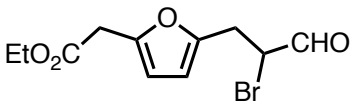

2.53

IR (neat) ν = 3109, 2983, 2936, 2854, 2727, 1730, 1615, 1563, 1465, 1447, 1419, 1370, 1337, 1266, 1226, 1182, 1143, 1096, 1064, 1029, 1017, 975, 911, 856, 790 730, 690 cm^{-1}.

^{1}H NMR (400 MHz, $CDCl_3$) δ 9.47 (d, *J* = 2.5 Hz, 1H), 6.13 (d, *J* = 3.2 Hz, 1H), 6.11 (d, *J* = 3.2 Hz, 1H), 4.49 (td, *J* = 7.1, 2.5 Hz, 1H), 4.17 (q, *J* = 7.1 Hz, 2H), 3.61 (s, 2H), 3.46 (dd, *J* = 15.7, 7.0 Hz, 1H), 3.20 (dd, *J* = 15.8, 7.2 Hz, 1H), 1.26 (t, *J* = 7.1 Hz, 3H).

^{13}C NMR (126 MHz, $CDCl_3$) δ 191.4, 169.1, 149.3, 147.4, 109.1, 108.8, 61.1, 51.2, 34.1, 30.7, 14.1.

HRMS (ESI) m/z calcd for $C_{11}H_{14}BrO_4$: 289.0076 [$(M+H)^+$], measured: 289.0087.

ethyl (*E*)-2-(5-(3-oxoprop-1-en-1-yl)furan-2-yl)acetate (2.54)

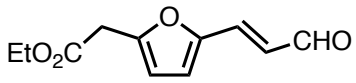

2.54

IR (neat) ν = 2983, 2934, 2819, 2728, 1735, 1671, 1628, 1575, 1513, 1465, 1447, 1395, 1369, 1335, 1263, 1225, 1179, 1149, 1113, 1021, 965, 869, 795, 682 cm^{-1}.

^{1}H NMR (400 MHz, $CDCl_3$) δ 9.59 (d, *J* = 7.9 Hz, 1H), 7.15 (d, *J* = 15.6 Hz, 1H), 6.72 (d, *J* = 3.4 Hz, 1H), 6.53 (dd, *J* = 15.6, 7.9 Hz, 1H), 6.40 (d, *J* = 3.4 Hz, 1H), 4.20 (q, *J* = 7.1 Hz, 2H), 3.73 (s, 2H), 1.28 (t, *J* = 7.1 Hz, 3H).

^{13}C NMR (126 MHz, $CDCl_3$) δ 192.8, 168.4, 152.0, 150.1, 137.6, 125.5, 117.9, 111.5, 61.5, 34.4, 14.1.

HRMS (ESI) m/z calcd for $C_{11}H_{12}NaO_4$: 231.0628 [$(M+Na)^+$], measured: 231.0628.

allyl 2-(furan-2-yl)acetate (2.56a)

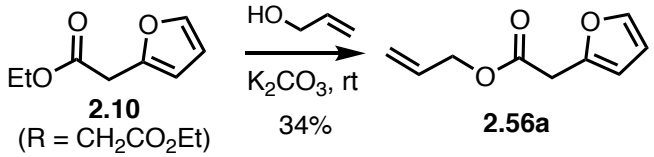

2.10
(R = CH_2CO_2Et)

2.56a

To a solution of **2.10** (298 mg, 1.93 mmol, 1.0 equiv.) stirring in allyl alcohol (36 mL, 529 mmol, 274 equiv.) was added K_2CO_3 (800 mg, 5.79 mmol, 3.0 equiv.). The reaction mixture was stirred at rt for 18 h before being quenched by sequential addition of

saturated aq. NH_4Cl (10 mL) and then 10% aq. HCl until gas evolution ceased. The majority of the unreacted allyl alcohol was removed on the rotary evaporator and then the aqueous layer was extracted with CH_2Cl_2 (x2). The combined organic layers were washed with brine, dried (Na_2SO_4), and then concentrated *in vacuo*. Purification by flash chromatography (hexanes → 20:1 hexanes:Et_2O) yielded the title compound **2.56a** (110 mg, 0.66 mmol, 34%) as a colorless oil.

IR (neat) ν = 3151, 3123, 3089, 2944, 2885, 1739, 1649, 1602, 1506, 1450, 1414, 1364, 1334, 1273, 1224, 1151, 1074, 1012, 988, 936, 885, 810, 733, 690 cm^{-1}.

^{1}H NMR (400 MHz, $CDCl_3$) δ 7.36 (dd, *J* = 1.9, 0.8 Hz, 1H), 6.33 (dd, *J* = 3.3, 1.9 Hz, 1H), 6.23 (dd, *J* = 3.2, 0.9 Hz, 1H), 5.91 (ddt, *J* = 17.2, 10.4, 5.6 Hz, 1H), 5.29 (dq, *J* = 17.2, 1.6 Hz, 1H), 5.23 (dq, *J* = 10.5, 1.3 Hz, 1H), 4.62 (dt, *J* = 5.7, 1.4 Hz, 2H), 3.71 (s, 2H).

^{13}C NMR (101 MHz, $CDCl_3$) δ 168.9, 147.5, 142.0, 131.7, 118.3, 110.4, 108.0, 65.6, 33.9.

HRMS (ESI) m/z calcd for $C_9H_{10}NaO_3$: 189.0522 [$(M+Na)^+$], measured: 231.0523.

(1*R*,4*R*,5*R*)-5-bromo-5-formylcyclohex-2-ene-1,4-diyl diacetate (2.61)

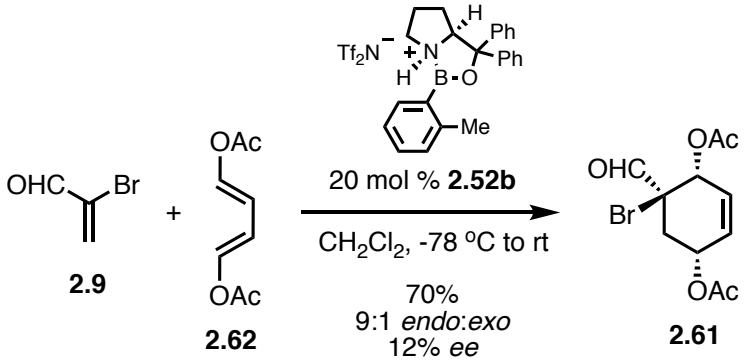

To a solution of oxazaborolidine **S2**[9] (113.4 mg, 0.321 mmol, 0.24 equiv.) stirring in CH_2Cl_2 (1 mL) at -25 °C was added Tf_2NH (0.2 M in CH_2Cl_2, 1.33 mL, 0.266 mmol, 0.2 equiv.) and the resulting solution was stirred at this temperature for 15 min before being

cooled to -78 ^{o}C.[12] 2-Bromoacrolein (**2.9**)[10] (107 μL, 1.33 mmol, 1.0 equiv.) was added followed by *trans,trans*-1,4-diacetoxybutadiene (**2.62**)[13] (1.13 g, 6.64 mmol, 5.0 equiv.) in CH_2Cl_2 (4.32 mL) dropwise via cannula. The reaction mixture was stirred at -78 ^{o}C for 2 h and then was slowly allowed to warm to rt and was stirred for an additional 3 days. The reaction was quenched by the addition of Et_3N (50 μL) and then was concentrated *in vacuo*. Purification by flash chromatography (20% EtOAc:hexanes) yielded the title compound **2.61** (284 mg, 0.931 mmol, 70%) as an orange oil (90:10 *endo*:*exo*).

Alternatively, **2.61** can be prepared in racemic form by allowing 2-bromoacrolein (**2.9**) (2.5 equiv.) and *trans,trans*-1,4-diacetoxybutadiene (**2.62**) (1 equiv.) to react in the presence of ethyl aluminum dichloride (1 equiv.) in CH_2Cl_2 at -78 to -20 ^{o}C.

IR (neat) ν = 2972, 2937, 2842, 2734, 1729, 1435, 1370, 1212, 1147, 1098, 1030, 1011, 959, 935, 898, 736 cm^{-1}.

^{1}H NMR (500 MHz, $CDCl_3$) δ 9.23 (s, 1H), 6.01 – 5.96 (m, 1H), 5.89 (ddd, *J* = 10.1, 4.7, 1.9 Hz, 1H), 5.57 (dt, *J* = 4.8, 1.3 Hz, 1H), 5.53 – 5.47 (m, 1H), 2.54 (ddt, *J* = 14.3, 6.0, 1.4 Hz, 1H), 2.16 (dd, *J* = 14.3, 9.1 Hz, 1H), 2.03 (s, 3H), 1.97 (s, 3H).

^{13}C NMR (75 MHz, $CDCl_3$) δ 188.6, 170.2, 169.4, 133.0, 123.4, 68.1, 68.0, 63.6, 30.5, 21.0, 20.7.

HRMS (ESI) m/z calcd for $C_{11}H_{13}BrNaO_5$: 326.9839 [$(M+Na)^+$], measured: 326.9835.

HPLC: Enantiomeric excess (*ee*) of the *endo* product **2.62** was determined using a Diacel CHIRALPAK AD (0.46 cm x 25 cm) column:

Eluent: HPLC grade hexane:isopropanol (99:1)
Flow rate: 1.0 mL/min.
Detection wavelength: 220 nm.
Retention time = 8.8 min (minor) and 10.1 min (major)

(1*S*,3*R*,6*R*)-1-formyl-7-oxabicyclo[4.1.0]hept-4-en-3-yl acetate (2.68)

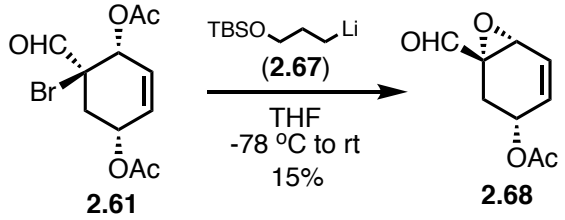

To a solution of *tert*-butyl(3-iodopropoxy)dimethylsilane[14] (74 mg, 0.25 mmol, 1.1 equiv.) in THF (0.9 mL) at -78 °C was added *t*-BuLi[15] (1.71 M in pentane, 0.36 mL, 0.62 mmol, 2.9 equiv.). The resulting solution was stirred at -78 °C for 15 min and then a solution of **2.61** (66 mg, 0.216 mmol, 1.0 equiv.) in THF (0.8 mL) was added *via* cannula. The reaction mixture was stirred at -78 °C for 3.5 h and then at rt for 45 min. The reaction was quenched with saturated aq. NH_4Cl, diluted with EtOAc and H_2O and then the two layers were separated. The aqueous layer was extracted with EtOAc (x2) and then the combined organic layers were washed with brine, dried ($MgSO_4$), and concentrated *in vacuo*. Purification by flash chromatography (20% EtOAc:hexanes) yielded the title compound **2.68** (6 mg, 0.033 mmol, 15%) as a colorless oil.

IR (neat) ν = 2956, 2932, 2859, 1726, 1435, 1415, 1371, 1240, 1223, 1171, 1033, 1003, 855, 779, 761, 705, 671 cm^{-1}.

^{1}H NMR (400 MHz, $CDCl_3$) δ 9.03 (s, 1H), 6.36 (dd, *J* = 9.9, 4.0 Hz, 1H), 6.22 (dd, *J* = 9.7, 6.0 Hz, 1H), 5.41 (td, *J* = 5.9, 2.2 Hz, 1H), 3.66 – 3.59 (m, 1H), 2.46 (dd, *J* = 16.7, 5.8 Hz, 1H), 2.37 (dd, *J* = 16.8, 2.2 Hz, 1H), 2.05 (s, 3H).

^{13}C NMR (101 MHz, $CDCl_3$) δ 197.5, 170.5, 131.7, 127.3, 64.2, 63.9, 49.4, 24.6, 21.2.

HRMS (ESI) m/z calcd for $C_9H_{10}NaO_4$: 205.0471 [$(M+Na)^+$], measured: 205.0468.

((1*S*,2*R*,5*R*)-5-acetoxy-1-bromo-2-hydroxycyclohex-3-en-1-yl)methyl acetate (2.65)

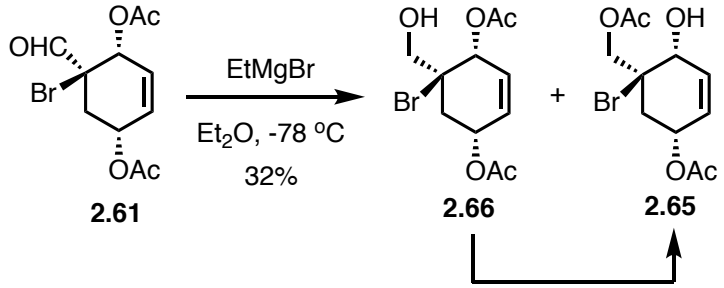

To a solution of **2.61** (25 mg, 0.082 mmol, 1.0 equiv.) stirring in Et_2O (0.41 mL) at -78 °C was added EtMgBr (3.0 M in Et_2O, 30 μL, 0.090 mmol, 1.1 equiv.) dropwise. The reaction mixture was stirred at -78 °C for 30 min and then was quenched with saturated aq. NH_4Cl, diluted with Et_2O, and warmed to rt. The salts were dissolved by adding a minimum amount of H_2O and then the two layers were separated. The aqueous layer was saturated with NaCl and then extracted with Et_2O (x2). The combined organic layers were dried ($MgSO_4$), concentrated *in vacuo* and purified by flash chromatography (40% EtOAc:hexanes) to yield the title compounds **2.65** and **2.66** (8 mg, 0.026 mmol, 32%) as colorless oil.

Note: Upon isolation, spontaneous intramolecular transacetylation of **2.66** took place to afford **2.65** as the sole product.

IR (neat) ν = 3125, 3060, 3028, 2988, 2917, 2877, 2806, 1724, 1703, 1604, 1514, 1494, 1454, 1384, 1370, 1337, 1320, 1273, 1223, 1193, 1111, 1091, 1070, 1028, 1014, 971, 933, 904, 864, 811, 746, 698 cm^{-1}.

^{1}H NMR (500 MHz, $CDCl_3$) δ 5.97 (dd, *J* = 10.1, 4.2 Hz, 1H), 5.88 (dd, *J* = 9.9, 1.6 Hz, 1H), 5.52 – 5.46 (m, 1H), 4.59 (d, *J* = 12.1 Hz, 1H), 4.42 (d, *J* = 3.1 Hz, 1H), 4.36 (d, *J* = 12.1 Hz, 1H), 2.72 (s, 1H), 2.38 (dd, *J* = 13.9, 6.0 Hz, 1H), 2.24 (dd, *J* = 14.0, 7.5 Hz, 1H), 2.16 (s, 3H), 2.06 (s, 3H).

^{13}C NMR (126 MHz, $CDCl_3$) δ 171.0, 170.3, 129.0, 129.0, 69.7, 68.4, 68.1, 65.8, 34.0, 21.1, 20.8.

HRMS (ESI) m/z calcd for $C_{11}H_{15}BrNaO_5$: 328.9995 [$(M+Na)^+$], measured: 328.9992.

***rac*-1-((1*R*,2*S*,4*R*)-2-bromo-7-oxabicyclo[2.2.1]hept-5-en-2-yl)but-3-en-1-ol (2.78)**

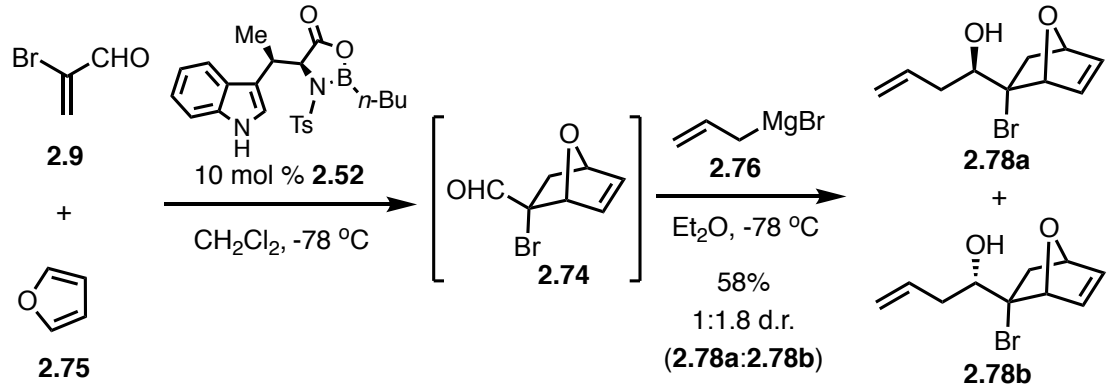

To a suspension of *rac*-(2*S*,3*R*)-3-(1*H*-indol-3-yl)-2-((4-methylphenyl)sulfonamido) butanoic acid[1] (400 mg, 1.07 mmol, 0.107 equiv.) stirring in CH_2Cl_2 (4 mL) was added *n*-butyldichloroborane (0.95 M in PhMe, 1.05 mL, 1.00 mmol, 0.10 equiv.). The resulting solution was stirred at rt for 1 hr, at which point all volatiles were removed *in vacuo* (< 0.1 mm Hg) for 1 h to provide catalyst **2.52**.

The freshly prepared catalyst **2.52** was dissolved in CH_2Cl_2 (8 mL) and the solution was cooled to -78 °C. Freshly distilled furan (**2.75**) (12.6 mL, 173 mmol, 17.4 equiv.) was added and the resulting solution was stirred for 10 min at this temperature. 2-Bromoacrolein (**2.9**)[10] (0.80 mL, 9.96 mmol, 1.0 equiv.) was added dropwise and the reaction mixture was stirred at -78 °C for 4.5 h. Allylmagnesium bromide (**2.76**) (1.0 M in Et_2O, 20.0 mL, 20.00 mmol, 20.0 equiv.) was added dropwise and the reaction mixture was stirred at -78 °C for 15 min before carefully quenching with saturated aq. NH_4Cl. The mixture was warmed to rt and diluted with Et_2O and 1 M aq. HCl. The two layers were separated and the aqueous layer was extracted with Et_2O (x3). The combined organic layers were washed with 1 M aq. HCl and brine, dried ($MgSO_4$) and concentrated *in vacuo*. Purification by flash chromatography (15% Et_2O:pentane) yielded the title

compound (1.42 g, 5.79 mmol, 58%) as a mixture of diastereomers **2.78a** and **2.78b** (d.r. = 1:1.8 dr) as a colorless oil.

IR (neat) ν = 3453, 3077, 3007, 2976, 2956, 2913, 2877, 1737, 1724, 1641, 1575, 1447, 1433, 1415, 1383, 1346, 1318, 1266, 1215, 1172, 1118, 1071, 994, 959, 916, 887, 864, 835, 816, 795, 733, 707 cm^{-1}.

^{1}H NMR (400 MHz, $CDCl_3$) δ 6.55 – 6.43 (m, 2H (major + minor)), 6.00 – 5.84 (m, 1H (major + minor)), 5.27 – 5.12 (m, 3H (major + minor)), 5.07 – 5.00 (m, 1H (major + minor)), 4.97 (d, *J* = 1.7 Hz, 1H (major)), 3.68 (ddd, *J* = 9.2, 6.2, 2.6 Hz, 1H (major)), 3.45 (ddd, *J* = 10.3, 8.8, 2.5 Hz, 1H (minor)), 2.62 (dt, *J* = 14.7, 3.6 Hz, 1H (major)), 2.52 (dd, *J* = 13.0, 4.8 Hz, 1H (major)), 2.50 – 2.42 (m, 1H (minor)), 2.39 (d, *J* = 6.1 Hz, 1H (major)), 2.37 – 2.26 (m, 1H (major + minor)), 2.07 (dd, *J* = 12.7, 4.7 Hz, 1H (minor)), 1.96 (d, *J* = 8.6 Hz, 1H (minor)), 1.74 – 1.67 (m, 1H (major + minor)).

^{13}C NMR (126 MHz, $CDCl_3$) δ 135.8, 135.7, 135.1, 134.8, 134.5, 134.5, 117.3, 117.2, 82.1, 81.4, 79.2, 79.1, 76.4, 75.4, 72.1, 70.2, 39.2, 39.2, 39.1, 38.8.

HRMS (ESI) m/z calcd for $C_{10}H_{14}BrO_2$: 245.0172 [$(M+H)^+$], measured: 245.0179.

***rac*-1-((1*R*,2*S*,4*R*)-2-bromo-7-oxabicyclo[2.2.1]hept-5-en-2-yl)pent-4-en-1-ol (2.79)**

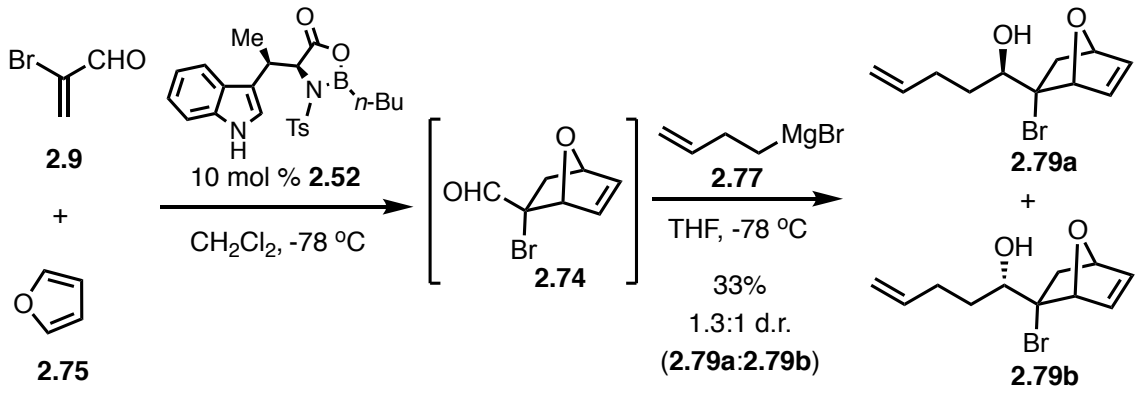

To a suspension of *rac*-(2*S*,3*R*)-3-(1*H*-indol-3-yl)-2-((4-methylphenyl)sulfonamido) butanoic acid[1] (200 mg, 0.54 mmol, 0.108 equiv.) stirring in CH_2Cl_2 (2 mL) was added *n*-butyldichloroborane (0.95 M in PhMe, 0.53 mL, 0.50 mmol, 0.10 equiv.). The resulting solution was stirred at rt for 1 hr, at which point all volatiles were removed *in vacuo* (< 0.1 mm Hg) for 1 h to provide catalyst **2.52**.

The freshly prepared catalyst **2.52** was dissolved in CH_2Cl_2 (4 mL) and the solution was cooled to – 78 ^oC. Freshly distilled furan (**2.75**) (6.4 mL, 88.0 mmol, 17.7 equiv.) was added and the resulting solution was stirred for 10 min at this temperature. 2-Bromoacrolein[10] (**2.9**) (0.40 mL, 4.98 mmol, 1.0 equiv.) was added dropwise and the reaction mixture was stirred at – 78 ^oC for 4.5 h.

A separate 3-necked round bottom flask (fitted with a reflux condenser, an addition funnel, and a glass stopper) was charged Mg powder. The Mg was flame-dried under high vacuum and then allowed to cool under a stream of Ar. THF (3 mL) was added and 1,2-dibromoethane (0.3 mL, 3.47 mmol, 0.7 equiv.) was added dropwise to the suspension without stirring until gas evolution was observed. The mixture was then stirred vigorously until the exotherm subsided. A solution of 4-bromo-1-butene (2.52 mL, 24.8 mmol, 5.0 equiv.) in THF (13 mL) was then added dropwise from the addition funnel to the suspension of Mg at a rate sufficient to maintain a gentle reflux. Once the addition was complete, the resulting solution was stirred at rt for an additional 2.5 h. The Grignard solution was then added dropwise, via cannula, to the aldehyde solution (kept at -78 ^oC). The reaction mixture was stirred at -78 ^oC for 12 h before being carefully quenched with saturated aq. NH_4Cl. The mixture was warmed to rt and diluted with Et_2O and 1 M aq. HCl. The two layers were separated and the aqueous layer was extracted with Et_2O (x3). The combined organic layers were washed with 1 M aq. HCl and brine, dried ($MgSO_4$), and concentrated *in vacuo*. Purification by flash chromatography (10% EtOAc:hexanes) yielded the title compound (425 mg, 1.64 mmol, 33%) as a mixture of diastereomers **2.79a** and **2.79b** (d.r. = 1.3:1) as a colorless oil.

IR (neat) ν = 3447, 3077, 3008, 2976, 2948, 2929, 2853, 1640, 1575, 1445, 1415, 1384, 1319, 1267, 1214, 1173, 1118, 1081, 1010, 997, 977, 949, 913, 878, 856, 836, 794, 732, 705 cm^{-1}.

^{1}H NMR (500 MHz, $CDCl_3$) δ 6.52 – 6.42 (m, 2H (major + minor)), 5.90 – 5.78 (m, 1H (major + minor)), 5.21 (d, *J* = 1.6 Hz, 1H (major)), 5.12 – 4.97 (m, 3H (major + minor)), 4.93 (d, *J* = 1.7 Hz, 1H (minor)), 3.61 – 3.54 (m, 1H (minor)), 3.34 (t, *J* = 9.0 Hz, 1H (major)), 2.47 (dd, *J* = 13.0, 4.8 Hz, 1H (minor)), 2.42 – 2.28 (m, 2H (major + minor)), 2.24 – 2.12 (m, 2H (major + minor)), 2.10 – 2.01 (m, 1H (minor)), 2.01 (dd, *J* = 12.8, 4.8 Hz, 1H (major)) 1.95 – 1.83 (m, 1H (major + minor)), 1.76 – 1.56 (m, 3H (major + minor)).

^{13}C NMR (126 MHz, $CDCl_3$) δ 138.1, 138.0, 136.2, 136.1, 135.6, 135.3, 115.4, 115.2, 82.8, 81.9, 79.6, 79.5, 77.1, 76.1, 73.9, 71.1, 39.2, 39.1, 34.4, 34.0, 30.3, 30.2.

HRMS (ESI) m/z calcd for $C_{11}H_{16}BrO_2$: 259.0328 [$(M+H)^+$], measured: 259.0324.

***rac*-(1*R*,2*R*,3'*R*,4*R*)-3'-allyl-7-oxaspiro[bicyclo[2.2.1]heptane-2,2'-oxiran]-5-ene (2.80)**

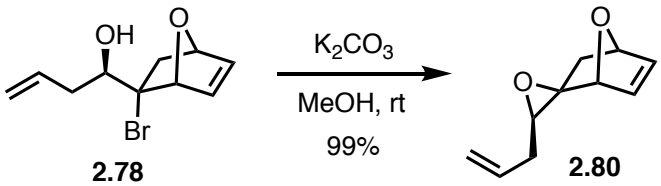

2.78 **2.80**

To a solution of **2.78** (103 mg, 0.42 mmol, 1.0 equiv.) in MeOH (2 mL) at rt was added K_2CO_3 (290 mg, 2.10 mmol, 5.0 equiv.). The reaction mixture was stirred at rt for 3 days and then was diluted with H_2O and EtOAc. The two layers were separated and the aqueous layer was extracted with EtOAc (x3). The combined organic layers were washed with brine, dried ($MgSO_4$), and then concentrated *in vacuo* to provide the title compound **2.80** (68 mg, 0.41 mmol, 99%) as a slightly yellow oil.

IR (neat) ν = 3080, 3007, 2980, 2947, 1740, 1642, 1572, 1475, 1437, 1338, 1311, 1266,

1216, 1171, 1139, 1098, 1056, 1008, 903, 876, 862, 846, 798, 750, 704 cm^{-1}.

^{1}H NMR (400 MHz, cdcl$_3$) δ 6.55 (dd, *J* = 5.9, 1.6 Hz, 1H), 6.39 (dd, *J* = 5.9, 1.8 Hz, 1H), 5.84 (ddt, *J* = 16.9, 10.3, 6.5 Hz, 1H), 5.20 – 5.06 (m, 3H), 4.60 – 4.55 (m, 1H), 3.14 (t, *J* = 6.2 Hz, 1H), 2.43 – 2.31 (m, 1H), 2.28 – 2.19 (m, 1H), 1.94 (dd, *J* = 12.1, 4.5 Hz, 1H), 1.69 (d, *J* = 12.1 Hz, 1H).

^{13}C NMR (126 MHz, CDCl$_3$) δ 139.6, 132.9, 132.6, 117.5, 80.7, 78.3, 69.3, 58.5, 34.6, 32.8.

HRMS (ESI) m/z calcd for $C_{10}H_{12}NaO_2$: 187.0730 [$(M+Na)^+$], measured: 187.0730.

***rac*-(1*R*,2*R*,3'*R*,4*R*)-3'-(but-3-en-1-yl)-7-oxaspiro[bicyclo[2.2.1]heptane-2,2'-oxiran]-5-ene (2.81)**

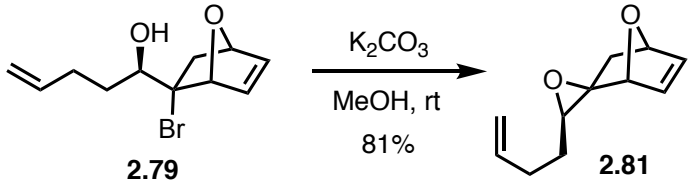

2.79 **2.81**

To a solution of **2.79** (83 mg, 0.32 mmol, 1.0 equiv.) in MeOH (1.6 mL) at rt was added K_2CO_3 (221 mg, 1.60 mmol, 5.0 equiv.). The reaction mixture was stirred at rt for 2 days and then was diluted with H_2O and EtOAc. The two layers were separated and the aqueous layer was extracted with EtOAc (x3). The combined organic layers were washed with brine, dried ($MgSO_4$), and then concentrated *in vacuo* to provide the title compound **2.81** (46 mg, 0.26 mmol, 81%) as a slightly yellow oil.

IR (neat) ν = 3077, 3006, 2977, 2945, 2925, 2853, 1738, 1641, 1439, 1365, 1310, 1217, 1167, 1091, 1068, 1023, 1009, 960, 906, 862, 849, 796, 742, 707, 707, 609, 528 cm^{-1}.

^{1}H NMR (500 MHz, CDCl$_3$) δ 6.54 (dd, *J* = 5.9, 1.7 Hz, 1H), 6.39 (dd, *J* = 5.9, 1.8 Hz, 1H), 5.82 (ddt, *J* = 16.9, 10.2, 6.6 Hz, 1H), 5.11 – 4.96 (m, 3H), 4.52 (dd, *J* = 1.8, 0.9 Hz, 1H), 3.05 (dd, *J* = 7.8, 4.4 Hz, 1H), 2.32 – 2.13 (m, 2H), 1.90 (dd, *J* = 12.1, 4.5 Hz, 1H), 1.69 – 1.59 (m, 2H), 1.52 (dddd, *J* = 14.0, 8.7, 7.8, 6.3 Hz, 1H).

^{13}C NMR (126 MHz, $CDCl_3$) δ 139.8, 137.2, 132.5, 115.5, 80.8, 78.4, 69.4, 59.2, 32.8, 30.6, 29.7.

HRMS (ESI) m/z calcd for $C_{11}H_{14}NaO_2$: 201.0886 [$(M+Na)^+$], measured: 201.0887.

***rac*-(1*R*,2*R*,3'*R*,4*R*,5*S*,6*R*)-3'-(but-3-en-1-yl)-7-oxaspiro[bicyclo[2.2.1]heptane-2,2'-oxirane]-5,6-diol (2.82)**

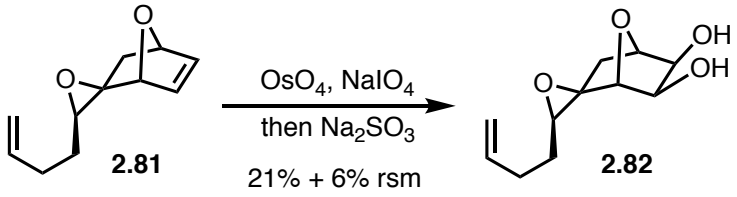

To a solution of **2.81** (16 mg, 0.090 mmol, 1.0 equiv.) stirring in 2:1 H_2O:THF (0.9 mL) at rt was added NaOAc (44 mg, 0.54 mmol, 6.0 equiv.) followed by OsO_4 (0.04 M in C_6H_6, 0.45 mL, 0.018 mmol, 0.2 equiv.). The resulting solution was stirred for 10 min, at which time $NaIO_4$ (58 mg, 0.27 mmol, 3.0 equiv.) was added. The reaction mixture was stirred at rt for 20 h and then another aliquot of OsO_4 (0.04 M in C_6H_6, 0.45 mL, 0.018 mmol, 0.2 equiv.) was added. The solution was stirred for an additional 2 h and a second portion of $NaIO_4$ (38 mg, 0.18 mmol, 2.0 equiv.) was added. The reaction mixture was stirred for 20 min and then was quenched with $NaHCO_3$ and diluted with CH_2Cl_2. The two layers were separated and the aqueous layer was extracted with CH_2Cl_2 (x3). The combined organic layers were dried (Na_2SO_4) and concentrated *in vacuo*. The crude residue was taken onto silica gel and unreacted **2.81** (1 mg, 0.0056 mmol, 6%) was recovered by flash chromatography (20% Et_2O:petroleum ether). The crude osmate ester was recovered from the silica gel by stirring in EtOAc, filtering off the silica, and concentration of the filtrate *in vacuo*. The crude green osmate ester (*ca.* 10 mg) was taken into THF (5 mL) and aq. Na_2SO_3 (5 mL) was added. The mixture was stirred vigorously for 24 h, H_2O was added and the solution was extracted with EtOAc (x3). The combined organic layers were dried ($MgSO_4$) and concentrated *in vacuo* to give the title compound **2.82** (4 mg, 0.019 mmol, 21%) as a colorless wax.

IR (neat) ν = 3392, 3075, 2924, 2852, 1727, 1641, 1440, 1261, 1187, 1156, 1067, 1036, 995, 960, 918, 898, 839, 804, 737 cm^{-1}.

^{1}H NMR (400 MHz, $CDCl_3$) δ 5.84 (ddt, *J* = 16.9, 10.2, 6.7 Hz, 1H), 5.14 – 5.00 (m, 2H), 4.52 (dd, *J* = 6.1, 1.6 Hz, 1H), 4.07 (s, 1H), 4.00 (s, 2H), 3.14 (dd, *J* = 8.5, 3.6 Hz, 1H), 2.86 (s, 1H), 2.78 (s, 1H), 2.40 – 2.18 (m, 2H), 1.92 (dd, *J* = 13.8, 6.2 Hz, 1H), 1.89 – 1.78 (m, 1H), 1.72 (d, *J* = 13.8 Hz, 1H), 1.56 – 1.44 (m, 1H).

^{13}C NMR (126 MHz, $CDCl_3$) δ 136.9, 115.8, 84.6, 82.1, 74.0, 71.2, 66.6, 59.0, 34.0, 30.8, 29.7.

HRMS (ESI) m/z calcd for $C_{11}H_{16}NaO_4$: 235.0941 [$(M+Na)^+$], measured: 235.0934.

***rac*-(*R*)-1-((1*R*,2*S*,4*R*)-2-bromo-7-oxabicyclo[2.2.1]hept-5-en-2-yl)-4-((*tert*-butyldimethylsilyl)oxy)butan-1-ol (2.85)**

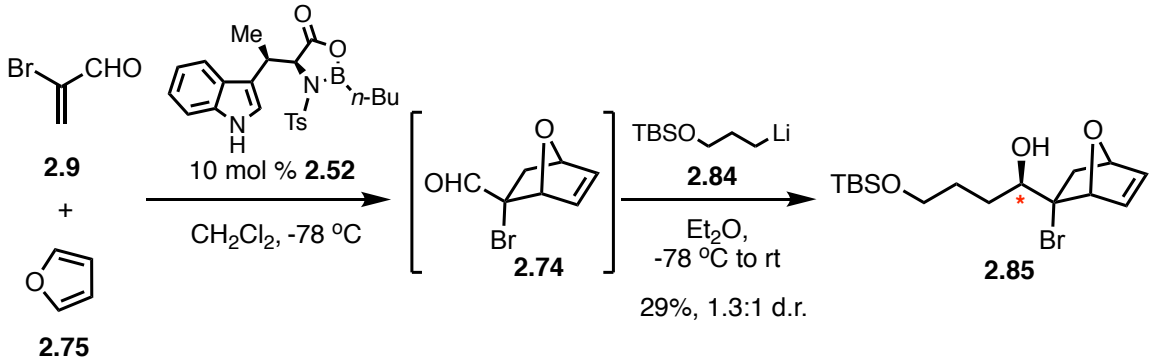

To a suspension of *rac*-(2*S*,3*R*)-3-(1*H*-indol-3-yl)-2-((4-methylphenyl)sulfonamido) butanoic acid[1] (298 mg, 0.80 mmol, 0.107 equiv.) stirring in CH_2Cl_2 (3 mL) was added *n*-butyldichloroborane (0.95 M in PhMe, 0.79 mL, 0.75 mmol, 0.10 equiv.). The resulting solution was stirred at rt for 1 hr, at which point all volatiles were removed *in vacuo* (< 0.1 mm Hg) for 1 h to provide catalyst **2.52**.

The freshly prepared catalyst **2.52** was dissolved in CH_2Cl_2 (6 mL) was added and the solution was cooled to – 78 °C. Freshly distilled furan (**2.75**) (9.7 mL, 133 mmol, 17.7 equiv.) was added and the resulting solution was stirred for 10 min at this temperature. 2-

Bromoacrolein[10] (**2.9**) (602 μL, 7.50 mmol, 1.0 equiv.) was added dropwise and the reaction mixture was stirred at – 78 °C for 4.5 h.

In a separate flask, a solution of *tert*-butyl(3-iodopropoxy)dimethylsilane[14] (5.64 g, 18.8 mmol, 2.5 equiv.) in Et_2O (93 mL) was cooled to -78 °C and *t*-BuLi[15] (1.41 M in pentane, 27.4 mL, 38.6 mmol, 5.2 equiv.) was added dropwise. The solution was stirred at -78 °C for 15 min and then at rt for 1 h before being cooled again to -78 °C. The aldehyde solution (-78 °C) was then added quickly via cannula to the cooled organolithium solution and the reaction mixture was allowed to slowly warm to rt and was stirred for a total of 18 h. The reaction was quenched by the addition of saturated aq. NH_4Cl, was diluted with H_2O and Et_2O and then the two layers were separated. The aqueous layer was extracted with Et_2O (x2) and then the combined organic layers were dried ($MgSO_4$) and concentrated *in vacuo*. Purification by flash chromatography (10% EtOAc:hexanes) gave the title compound **2.85** (563 mg, 1.49 mmol, 29 %) in 1.3:1 d.r. as a slightly yellow oil.

IR (neat) ν = 3452, 2954, 2933, 2889, 2857, 1738, 1472, 1463, 1445, 1383, 1362, 1320, 1255, 1215, 1093, 1007, 954, 835, 776, 706 cm^{-1}.

^{1}H NMR (400 MHz, $CDCl_3$) δ 6.54 – 6.41 (m, 2H), 5.26 (dd, *J* = 1.7, 0.8 Hz, 1H (major)), 5.04 – 5.01 (m, 1H (minor)), 5.01 – 4.98 (m, 1H (major)), 4.92 (dd, *J* = 1.8, 0.7 Hz, 1H (minor)), 3.75 – 3.64 (m, 2H), 3.54 (ddd, *J* = 9.8, 6.3, 2.0 Hz, 1H (minor)), 3.35 (ddd, *J* = 9.9, 7.9, 1.7 Hz, 1H (major)), 2.98 (d, *J* = 6.3 Hz, 1H (minor)), 2.84 (d, *J* = 8.0 Hz, 1H (major)), 2.51 (dd, *J* = 13.0, 4.8 Hz, 1H (minor)), 2.06 – 1.99 (m, 1H (major)), 1.99 – 1.89 (m, 1H (minor)), 1.86 – 1.52 (m, 4H (major + minor)), 0.90 (s, 9H), 0.07 (s, 6H).

^{13}C NMR (75 MHz, $CDCl_3$) δ 136.2, 136.0, 135.5, 135.0, 82.6, 81.9, 79.6, 79.5, 77.3, 76.2, 73.3, 71.3, 63.1, 63.0, 39.7, 39.2, 31.9, 31.7, 29.3, 29.3, 25.9, 25.9, 18.3, 18.3, -5.3, -5.4.

HRMS (ESI) m/z calcd for $C_{16}H_{29}BrNaO_3Si$: 399.0962 [$(M+Na)^+$], measured: 399.0955.

***rac*-(3-((1*R*,2*R*,3'*R*,4*R*)-7-oxaspiro[bicyclo[2.2.1]heptane-2,2'-oxiran]-5-en-3'-yl)propoxy)(*tert*-butyl)dimethylsilane (2.86)**

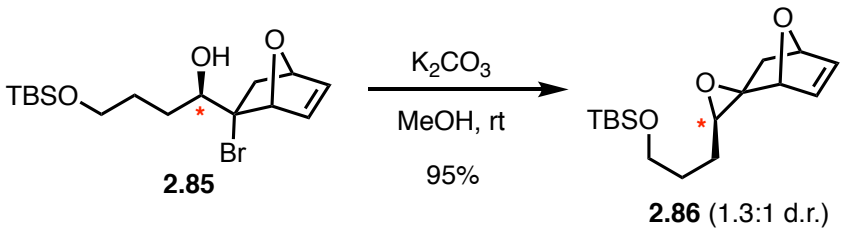

To a solution of **2.85** (257 mg, 0.68 mmol, 1.0 equiv.) in MeOH (6.8 mL) at rt was added K_2CO_3 (941 mg, 6.81 mmol, 10.0 equiv.). The reaction mixture was stirred at rt for 42 h and then was diluted with H_2O and EtOAc. The MeOH was removed on the rotary evaporator and then the aqueous layer was extracted with EtOAc (x3). The combined organic layers were washed with brine, dried ($MgSO_4$), and concentrated *in vacuo* to provide the title compound **2.86** (191 mg, 0.64 mmol, 95%) in 1.3:1 d.r. as an orange oil. The product was used in the next step without any further purification.

IR (neat) ν = 2952, 2929, 2889, 2857, 1737, 1719, 1472, 1463, 1439, 1388, 1361, 1311, 1254, 1168, 1094, 1023, 1008, 965, 906, 835, 797, 775, 705, 662 cm^{-1}.

^{1}H NMR (400 MHz, $CDCl_3$) δ 6.50 (dd, *J* = 5.9, 1.5 Hz, 2H), 6.37 (dd, *J* = 5.7, 1.8 Hz, 1H (major)), 6.33 (dd, *J* = 5.9, 1.8 Hz, 1H (minor)), 5.04 (tt, *J* = 4.8, 1.2 Hz, 1H), 4.48 (s, 1H (major)), 4.34 (s, 1H (minor)), 3.70 – 3.46 (m, 2H), 3.02 (dd, *J* = 7.3, 4.5 Hz, 1H (major)), 2.93 (t, *J* = 5.8 Hz, 1H (minor)), 1.88 – 1.38 (m, 6H), 0.85 (s, 9H (major)), 0.83 (s, 9H (minor)), 0.00 (s, 6H (major)), -0.02 (s, 6H (major)).

^{13}C NMR (75 MHz, $CDCl_3$) δ 139.5, 133.0, 132.4, 82.6, 80.7, 78.3, 78.0, 69.4, 69.3, 62.3, 62.2, 59.4, 57.4, 32.7, 29.7, 29.4, 29.1, 27.3, 26.7, 25.8, 25.8, 18.1, 18.1, -5.5, -5.5.

HRMS (ESI) m/z calcd for $C_{16}H_{28}NaO_3Si$: 319.1700 [$(M+Na)^+$], measured: 319.1701.

***rac*-3-((1*R*,2*R*,3'*R*,4*R*)-7-oxaspiro[bicyclo[2.2.1]heptane-2,2'-oxiran]-5-en-3'-yl)propanal (2.87)**

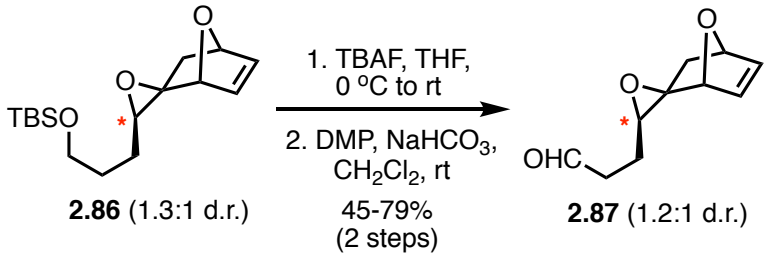

To a solution of **2.86** (498 mg, 1.68 mmol, 1.0 equiv.) in THF (16.8 mL) stirring at 0 °C was added TBAF (1M in THF, 2.6 mL, 2.60 mmol, 1.5 equiv.). The reaction mixture was stirred at 0 °C for 15 min and then at rt for 1.5 h. H_2O was added and the THF was removed on the rotary evaporator. The aqueous layer was extracted with EtOAc (x4) and then the combined organic layers were dried ($MgSO_4$) and concentrated *in vacuo*. The resulting crude oil (*ca.* 610 mg) was dissolved in CH_2Cl_2 (16.8 mL) and then $NaHCO_3$ (850 mg, 10.12 mmol, 6.0 equiv.) and DMP[8] (850 mg, 10.12 mmol, 6.0 equiv.) were added sequentially. The reaction mixture was stirred at rt for 1.5 h before being quenched by the addition of saturated aq. $NaHCO_3$ (25 mL) and saturated aq. $Na_2S_2O_3$ (25 mL). The resulting solution was stirred vigorously for 2.5 h and then the two layers were separated. The aqueous layer was extracted with CH_2Cl_2 (x3) and then the combined organic layers were washed with saturated aq. $NaHCO_3$, dried (Na_2SO_4), and concentrated *in vacuo*. Purification by flash chromatography (20% pentane:Et_2O) yielded the title compound **2.87** (202 mg, 1.12 mmol, 67%) in 1.2:1 d.r. as a yellow oil.

Note: the yield for this reaction typically varied from 45-79%.

IR (neat) ν = 3008, 2947, 2837, 2730, 1719, 1478, 1438, 1411, 1390, 1334, 1311, 1295, 1271, 1240, 1218, 1190, 1168, 1139, 1103, 1076, 1021, 1006, 960, 904, 862, 847, 799, 749, 709, 676, 609, 566, 526 cm^{-1}.

^{1}H NMR (400 MHz, $CDCl_3$) δ 9.84 (d, *J* = 1.0 Hz, 1H (major)), 9.80 (t, *J* = 1.1 Hz, 1H

(minor)), 6.57 (m, 1H), 6.42 (dd, *J* = 5.9, 1.8 Hz, 1H (major)), 6.38 (dd, *J* = 5.8, 1.8 Hz, 1H (minor)), 5.15 – 5.06 (m, 1H), 4.55 (dd, *J* = 1.8, 0.9 Hz, 1H (major)), 4.39 (dd, *J* = 1.8, 0.9 Hz, 1H (minor)), 3.09 (dd, *J* = 8.9, 3.6 Hz, 1H (major)), 3.02 (dd, *J* = 7.6, 4.6 Hz, 1H (minor)), 2.77 – 2.67 (m, 1H), 2.63 (ddt, *J* = 8.3, 7.2, 1.3 Hz, 1H), 2.08 – 1.90 (m, 1H), 1.94 – 1.82 (m, 1H), 1.71 – 1.54 (m, 2H).

^{13}C NMR (75 MHz, $CDCl_3$) δ 200.7, 200.7, 139.9, 139.7, 132.9, 132.2, 82.5, 80.6, 78.4, 78.1, 69.9, 69.8, 58.4, 56.5, 40.5, 40.3, 32.7, 29.8, 23.5, 22.7.

HRMS (ESI) m/z calcd for $C_{10}H_{12}NaO_3$: 203.0679 [$(M+Na)^+$], measured: 203.0676.

***rac*-3-((1*R*,2*R*,3'*R*,4*R*)-7-oxaspiro[bicyclo[2.2.1]hept[5]ene-2,2'-oxiran]-3'-yl)propanal oxime (2.88)**

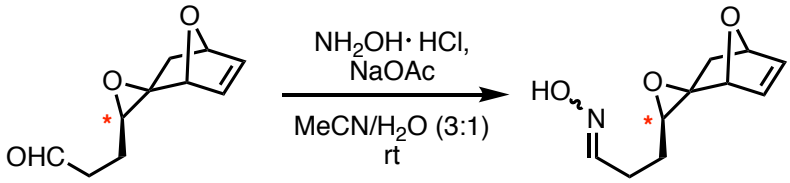

2.87 (1.2:1 d.r.) **2.88** (1.2:1 d.r.)

To **2.87** (225 mg, 1.25 mmol, 1.0 equiv.) stirring in 2:1 MeCN:H_2O (12.5 mL) was added NaOAc (174 mg, 2.50 mmol, 2.0 equiv.) followed by hydroxylamine hydrochloride (205 mg, 2.50 mmol, 2.0 equiv.). The reaction mixture was stirred at rt for 2 h and then the MeCN was removed *in vacuo*. The resulting residue was diluted with CH_2Cl_2 and brine and the two layers were separated. The aqueous layer was extracted with CH_2Cl_2 (x3) and then the combined organic layers were dried (Na_2SO_4) and concentrated *in vacuo* to give the title compound **2.88** (229 mg, 1.17 mmol, 94%) in 1.2:1 d.r. and as a 1.2:1 mixture of oxime isomers (for each diastereomer) as a yellow oil.

Note: The product decomposes on silica gel.

IR (neat) ν = 3379, 3085, 2949, 1721, 2437, 1333, 1311, 1270, 1217, 1170, 1122, 1096, 1020, 1008, 957, 904, 862, 847, 798, 732, 702, 681, 622, 608, 567, 524, 511 cm^{-1}.

^{1}H NMR (300 MHz, $CDCl_3$) δ 8.95 (s, 1H), 7.41 (t, *J* = 5.7 Hz, 1H (major diast./major isomer)), 7.35 (t, *J* = 5.9 Hz, 1H (minor diast./major isomer)), 6.75 (t, *J* = 5.5 Hz, 1H (major diast./minor isomer)), 6.68 (t, *J* = 5.6 Hz, 1H (minor diast./minor isomer)), 6.54 – 6.46 (m, 1H), 6.40 – 6.28 (m, 1H), 5.10 – 4.97 (m, 1H), 4.53 – 4.45 (m, 1H (major diast.)), 4.34 (s, 1H (minor diast.)), 3.08 – 2.99 (m, 1H (major diast.)), 2.96 (td, *J* = 6.1, 2.4 Hz, 1H (minor diast.)), 2.60 – 2.15 (m, 2H), 1.91 – 1.48 (m, 4H).

^{13}C NMR (75 MHz, $CDCl_3$) δ 150.3, 150.1, 150.1, 139.7, 139.7, 139.6, 139.5, 132.8, 132.8, 132.1, 82.4, 80.5, 78.3, 78.0, 78.0, 69.6, 69.5, 69.4, 58.9, 58.6, 56.9, 56.7, 32.5, 29.7, 29.6, 27.7, 27.2, 27.1, 26.6, 26.4, 26.1, 22.1, 21.7.

HRMS (ESI) m/z calcd for $C_{10}H_{13}NNaO_3$: 218.0788 [$(M+Na)^+$], measured: 218.0787.

Nucleophilic Addition Products from Table 2.2:

***rac*-(*R*)-1-((1*R*,2*S*,4*R*)-2-bromo-7-oxabicyclo[2.2.1]hept-5-en-2-yl)pentan-1-ol (S3) (Table 2.2, entry 4)**

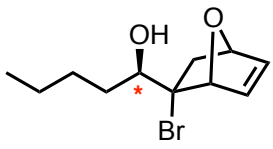

S3 (1.4:1 d.r.)

IR (neat) ν = 3452, 3008, 2955, 2933, 2860, 1709, 1615, 1575, 1466, 1457, 1445, 1380, 1319, 1244, 1213, 1173, 1129, 1084, 1071, 1010, 992, 943, 910, 879, 853, 795, 731, 704 cm^{-1}.

^{1}H NMR (400 MHz, $cdcl_3$) δ 6.53 – 6.42 (m, 2H), 5.22 (t, *J* = 1.2 Hz, 1H (major)), 5.05 – 5.02 (m, 1H (minor)), 5.02 – 4.99 (m, 1H (major)), 4.94 (dd, *J* = 1.8, 0.7 Hz, 1H (minor)), 3.54 (d, *J* = 9.3 Hz, 1H (minor)), 3.31 (t, *J* = 8.7 Hz, 1H (major)), 2.49 (dd, *J* = 13.0, 4.7 Hz, 1H (minor)), 2.21 (s, 1H (minor)), 2.03 (dd, *J* = 12.8, 4.7 Hz, 1H (major)), 1.85 – 1.23 (m, 7H), 0.96 – 0.89 (m, 3H).

^{13}C NMR (75 MHz, $CDCl_3$) δ 135.9, 135.9, 135.3, 134.9, 82.4, 81.7, 79.4, 79.3, 77.4, 76.3, 73.7, 71.4, 39.3, 38.9, 34.5, 34.3, 28.2, 28.1, 22.4, 22.4, 13.9.

HRMS (ESI) m/z calcd for $C_{11}H_{17}BrNaO_2$: 283.0304 [$(M+Na)^+$], measured: 283.0301.

***rac*-2-bromo-3-(furan-2-yl)propanal (2.101) (Table 2.2, entries 6 and 7)**

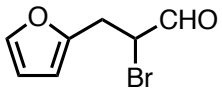

2.101

Rac-2-bromo-3-(furan-2-yl)propanal (**2.101**) was formed as the major product in these two reactions but was found to be very unstable. As a result, it was reduced ($NaBH_4$, 5:1 THF:H_2O, 0 ^oC) to *rac*-2-bromo-3-(furan-2-yl)propan-1-ol (**S4**) for characterization:

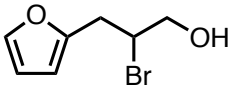

S4

IR (neat) ν = 3500-3100, 3155, 3121, 2928, 2875, 1599, 1506, 730 cm^{-1}.

^{1}H NMR ($CDCl_3$, 500 MHz) δ 7.37 (m, 1H), 6.34 (m, 1H), 6.19 (m, 1H), 4.39 (m, 1H), 3.86 (dd, *J* = 12.5, 4.0 Hz, 1H), 3.78 (dd, *J* = 12.5, 6.0 Hz, 1H), 3.30 (dd, *J* = 15.5, 7.0 Hz, 1H), 3.26 (dd, *J* = 15.5, 7.0 Hz, 1H)

^{13}C NMR ($CDCl_3$, 125 MHz) δ 151.4, 141.9, 110.4, 107.8, 66.2, 55.0, 33.8.

HRMS (APCI) m/z calcd for $C_7H_{10}BrO_2$: 204.9859 [$(M+H)^+$], measured: 204.9858.

***rac*-(*S*)-1-((1*R*,2*S*,4*R*)-2-bromo-7-oxabicyclo[2.2.1]hept-5-en-2-yl)butane-1,4-diol (S5) (Table 2.2, entry 8)**

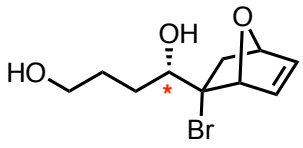

S5 (1.3:1 d.r.)

IR (neat) ν = 3380, 3008, 2950, 2874, 1575, 1446, 1403, 1320, 1269, 1214, 1176, 1121, 1090, 1053, 1010, 985, 946, 888, 860, 833, 794, 732, 705 cm^{-1}.

^{1}H NMR (400 MHz, $CDCl_3$) δ 6.55 – 6.44 (m, 2H), 5.24 (s, 1H (minor)), 5.05 (dd, *J* = 4.6, 1.6 Hz, 1H (major)), 5.03 – 5.00 (m, 1H (minor)), 4.97 – 4.94 (m, 1H (major)), 3.78

– 3.68 (m, 2H), 3.65 (dd, *J* = 10.1, 1.9 Hz, 1H (major)), 3.39 (m, 1H (minor)), 2.50 (dd, *J* = 13.0, 4.8 Hz, 1H (major)), 2.02 (dd, *J* = 12.8, 4.7 Hz, 1H (minor)), 1.91 – 1.53 (m, 5H).

^{13}C NMR (75 MHz, $CDCl_3$) δ 136.1, 136.0, 135.5, 135.2, 82.8, 81.9, 79.6, 79.5, 77.6, 76.5, 73.2, 70.6, 62.6, 60.4, 39.2, 31.8, 31.6, 29.3, 21.0, 14.1.

HRMS (ESI) m/z calcd for $C_{10}H_{15}BrNaO_3$: 285.0097 [$(M+Na)^+$], measured: 285.0096.

(*R*)-1-((1*R*,2*S*,4*R*)-2-bromo-7-oxabicyclo[2.2.1]hept-5-en-2-yl)-3-(1,3-dioxolan-2-yl)propan-1-ol (2.102)

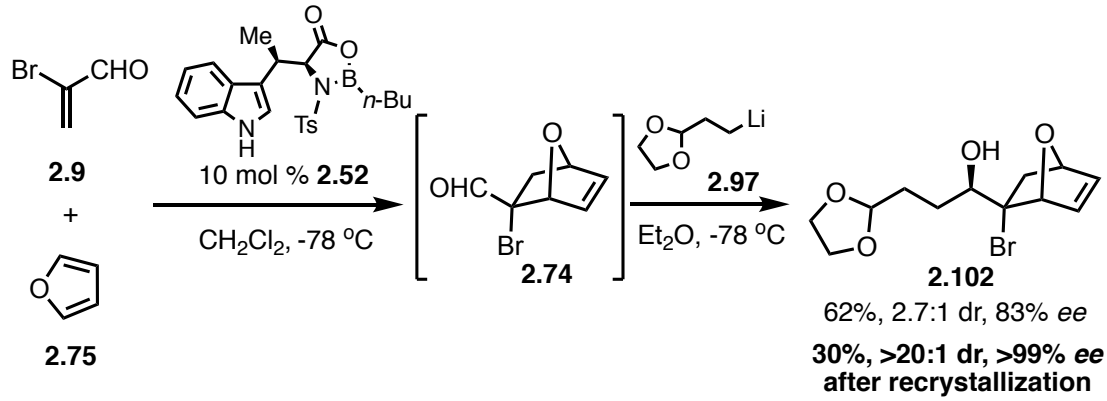

To a suspension of (2*S*,3*R*)-3-(1*H*-indol-3-yl)-2-((4-methylphenyl)sulfonamido)butanoic acid[1,2] (398 mg, 1.07 mmol, 1.07 equiv.) stirring in CH_2Cl_2 (3 mL) was added neat *n*-butyldichloroborane (150 μL, 1.00 mmol, 1 equiv.). The resulting solution was stirred at rt for 1 hr, at which point all volatiles were removed *in vacuo* (< 0.1 mm Hg) for 1 h to provide the catalyst **2.52** as a white solid which was used immediately after its preparation.

Oxazaborolidinone **2.52** (1.00 mmol, 0.1 equiv.) was dissolved in CH_2Cl_2 (8 mL) and then cooled to -78 °C. Freshly distilled furan (**2.75**) (12.4 mL, 170 mmol, 17.0 equiv.) was added and the resulting solution was stirred for 10 min at this temperature. 2-Bromoacrolein (**2.9**)[10] (805 μL, 10.0 mmol, 1.0 equiv.) was then added dropwise and the reaction mixture was stirred at -78 °C for 5 h.

In a separate flask, a solution of 2-(2-iodoethyl)-1,3-dioxolane[16] (11.48 g, 50.3 mmol, 5.0 equiv.) in Et_2O (250 mL) was cooled to -78 °C and freshly titrated *t*-BuLi[15] (1.7 M in

pentane, 62 mL, 105.4 mmol, 10.5 equiv.) was added dropwise. The resulting solution was stirred at -78 ^{o}C for 15 min and then at rt for 1 h. This solution was cooled back down to -78 ^{o}C and then the aldehyde solution (also at -78 ^{o}C) was added quickly to it via cannula. The reaction mixture was stirred at -78 ^{o}C for 18 h and then warmed to rt, where it was quenched by the addition of saturated aq. NH_4Cl. The mixture was vacuum filtered through a pad of Celite (washing with EtOAc) and the two resulting filtrate layers were separated. The aqueous layer was extracted with EtOAc (x2) and then the combined organic layers were washed with brine, dried over $MgSO_4$ and concentrated *in vacuo*. Purification by flash chromatography (pack with CH_2Cl_2; elute with 25% → 40% EtOAc:hexanes) provided the title compound **2.102** (1.89 g, 6.19 mmol, 62%) in 2.7:1 d.r. and 83% *ee* (major diastereomer) as a yellow amorphous solid. The product was dissolved in a minimum amount of boiling EtOAc and then allowed to slowly cool to rt, where it was left undisturbed for 2 days. Filtration yielded a first crop of crystals (791 mg, >20:1 d.r., >99% *ee*). The mother liquor was concentrated, triturated with EtOAc:hexanes (1:1) and then recrystallized in the same way to yield a second crop of crystals (125 mg, >20:1 d.r., >99% *ee*).

The combined yield of the title compound **2.102** (>20:1 d.r., >99% *ee*) was 916 mg (3.0 mmol, 30%).

$[\alpha]_D$ = +42.0 ^{o} (c = 0.30, $CHCl_3$)

mp = 88-92 ^{o}C

IR (neat) ν = 3459, 2992, 2950, 2873, 1725, 1458, 1441, 1341, 1319, 1215, 1186, 1101, 1080, 1042, 982, 940, 881, 861, 794, 733, 706 cm^{-1}.

^{1}H NMR (500 MHz, $CDCl_3$) δ 6.48 (dd, *J* = 5.8, 1.7 Hz, 1H), 6.45 (dd, *J* = 5.8, 1.7 Hz, 1H), 5.24 (dd, *J* = 1.8, 0.8 Hz, 1H), 5.00 (ddd, *J* = 4.7, 1.8, 0.8 Hz, 1H), 4.93 (t, *J* = 4.4 Hz, 1H), 4.06 – 3.92 (m, 2H), 3.93 – 3.81 (m, 2H), 3.37 (ddd, *J* = 10.4, 9.1, 2.0 Hz, 1H),

2.45 (d, J = 9.1 Hz, 1H), 2.04 (dd, J = 12.7, 4.8 Hz, 1H), 1.97 (dddd, J = 13.9, 8.0, 5.9, 4.4 Hz, 1H), 1.91 – 1.77 (m, 2H), 1.70 (d, J = 12.7 Hz, 1H), 1.71 – 1.62 (m, 1H).

^{13}C NMR (126 MHz, $CDCl_3$) δ 136.1, 135.2, 104.1, 82.0, 79.5, 76.4, 73.4, 65.0, 64.9, 39.1, 30.3, 28.9.

HRMS (ESI) m/z calcd for $C_{12}H_{17}BrNaO_4$: 327.0202 [$(M+Na)^+$], measured: 327.0208.

HPLC: Enantiomeric excess (*ee*) of the major diastereomer **39** was determined using a Diacel CHIRALPAK AD (0.46 cm x 25 cm) column:

Eluent: HPLC grade hexane:isopropanol (80:20)
Flow rate: 1.0 mL/min.
Detection wavelength: 214 nm.
Retention time = 12.6 min (minor) and 16.1 min (major).

Racemate:

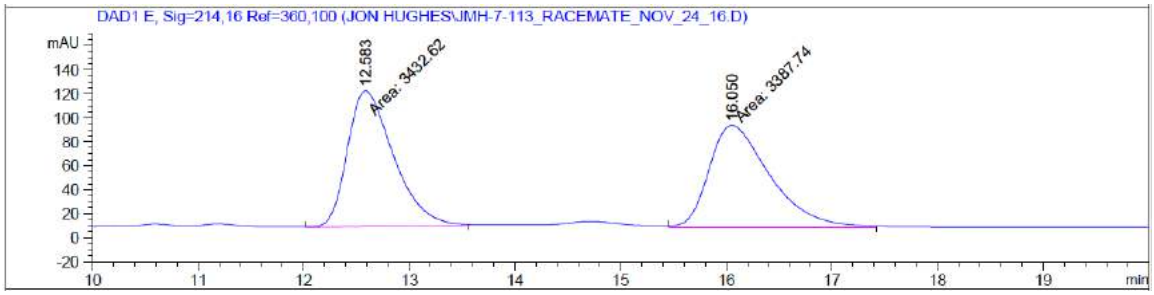

Peak #	RetTime [min]	Type	Width [min]	Area [mAU*s]	Height [mAU]	Area %
1	12.583	MM	0.5058	3432.62207	113.09915	50.3290
2	16.050	MM	0.6656	3387.73804	84.82941	49.6710
Totals :				6820.36011	197.92857	

Before recrystallization (83% *ee*):

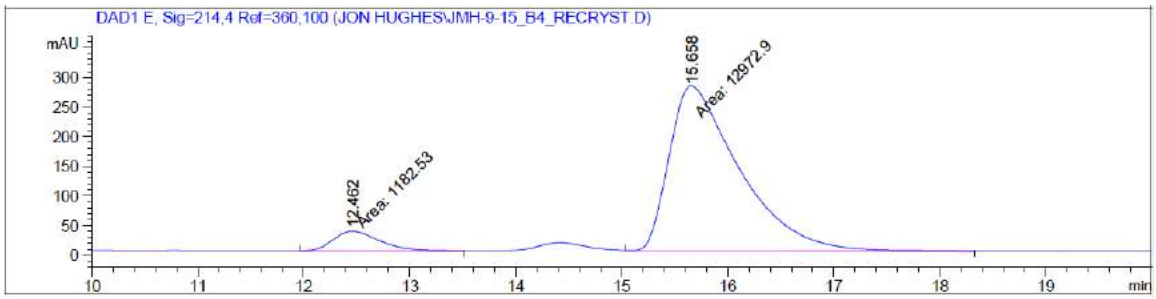

Peak #	RetTime [min]	Type	Width [min]	Area [mAU*s]	Height [mAU]	Area %
1	12.462	MM	0.5635	1182.53491	34.97629	8.3539
2	15.658	MM	0.7759	1.29729e4	278.64767	91.6461
Totals :				1.41555e4	313.62396	

After recrystallization (>99% *ee*):

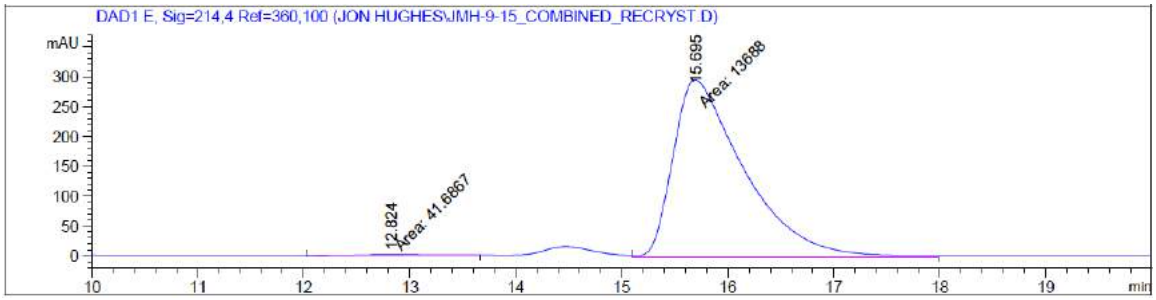

Peak #	RetTime [min]	Type	Width [min]	Area [mAU*s]	Height [mAU]	Area %
1	12.824	MM	0.5007	41.68671	1.38768	0.3036
2	15.695	MM	0.7705	1.36880e4	296.09927	99.6964
Totals :				1.37297e4	297.48695	

(*S*)-1-((1*R*,2*S*,4*R*)-2-bromo-7-oxabicyclo[2.2.1]hept-5-en-2-yl)-3-(1,3-dioxolan-2-yl)propan-1-ol (*epi*-2.102)

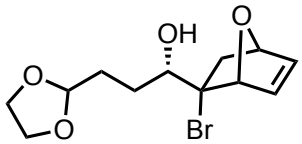

epi-**2.102**

A pure sample of the undesired bromohydrin diastereomer *epi*-**2.102** was obtained by concentrating the mother liquor from the first trituration and carrying out a second

trituration with EtOAc:hexanes (1:1) to provide **2.102** as white needles.

mp = 108-110 °C

IR (neat) ν = 3448, 3087, 3004, 2961, 2886, 2770, 1631, 1574, 1475, 1449, 1404, 1362, 1319, 1247, 1215, 1172, 1142, 1091, 1063, 1025, 1012, 984, 967, 940, 888, 860, 835, 796, 734, 709 cm^{-1}.

^{1}H NMR (500 MHz, $CDCl_3$) δ 6.50 (dd, *J* = 5.8, 1.7 Hz, 1H), 6.47 (dd, *J* = 5.7, 1.7 Hz, 1H), 5.03 (dd, *J* = 4.8, 1.7 Hz, 1H), 4.96 – 4.92 (m, 2H), 4.05 – 3.95 (m, 2H), 3.92 – 3.82 (m, 2H), 3.59 (ddd, *J* = 10.1, 6.9, 1.9 Hz, 1H), 2.66 (d, *J* = 7.0 Hz, 1H), 2.51 (dd, *J* = 13.0, 4.8 Hz, 1H), 2.06 – 1.93 (m, 2H), 1.90 – 1.80 (m, 1H), 1.74 – 1.63 (m, 2H).

^{13}C NMR (126 MHz, $CDCl_3$) δ 136.2, 135.6, 104.2, 82.7, 79.7, 77.4, 71.1, 65.0, 64.9, 39.5, 30.2, 28.8.

HRMS (ESI) m/z calcd for $C_{12}H_{17}BrNaO_4$: 327.0202 [$(M+Na)^+$], measured: 327.0208.

***rac*-1-((1*R*,2*R*,4*R*)-2-bromo-7-oxabicyclo[2.2.1]hept-5-en-2-yl)-3-(1,3-dioxolan-2-yl)propan-1-one (2.103)**

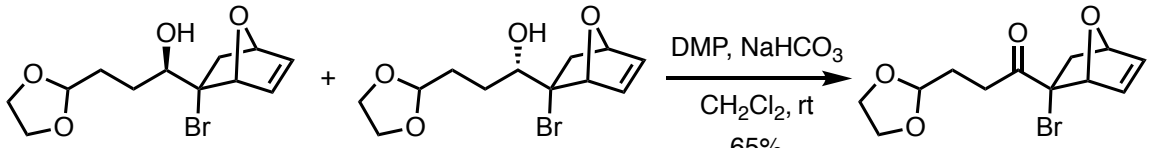

2.102 *epi*-**2.102** **2.103**

To a solution of **2.102**/*epi*-**2.102** (108 mg, 0.354 mmol, 1.0 equiv.) in CH_2Cl_2 (3.5 mL) was sequentially added $NaHCO_3$ (119 mg, 1.42 mmol, 4.0 equiv.) and DMP[8] (300 mg, 0.707 mmol, 2.0 equiv.) and the reaction mixture was stirred at rt for 2 h. The reaction was quenched by the addition of saturated aq. $NaHCO_3$ and saturated aq. $Na_2S_2O_3$ and the resulting mixture was stirred vigorously until all solids had gone into solution. The two layers were separated and the aqueous layer was extracted with CH_2Cl_2 (x3). The combined organic layers were washed with saturated $NaHCO_3$, dried ($MgSO_4$) and then concentrated *in vacuo*. Purification by flash chromatography (hexanes to 15%

EtOAc:hexanes) gave the title compound **2.103** (70 mg, 0.23 mmol, 65%) as a colorless oil.

IR (neat) ν = 2961, 2885, 1713, 1441, 1412, 1367, 1318, 1263, 1215, 1172, 1132, 1067, 1029, 1013, 941, 899, 864, 795, 703 cm^{-1}.

^{1}H NMR (400 MHz, $CDCl_3$) δ 6.56 (dd, *J* = 5.8, 1.8 Hz, 1H), 6.48 (dd, *J* = 5.8, 1.8 Hz, 1H), 5.39 (dd, *J* = 1.7, 0.8 Hz, 1H), 5.06 – 4.99 (m, 1H), 4.92 (t, *J* = 4.4 Hz, 1H), 4.03 – 3.90 (m, 2H), 3.90 – 3.78 (m, 2H), 3.03 – 2.87 (m, 2H), 2.81 (dd, *J* = 12.9, 4.8 Hz, 1H), 2.10 – 1.99 (m, 2H), 1.67 (d, *J* = 12.9 Hz, 1H).

^{13}C NMR (75 MHz, $CDCl_3$) δ 201.5, 137.5, 134.5, 103.1, 81.5, 79.3, 65.0, 64.9, 62.1, 38.3, 31.9, 28.4.

HRMS (ESI) m/z calcd for $C_{12}H_{15}BrNaO_4$: 325.0046 [$(M+Na)^+$], measured: 325.0051.

***rac*-(1*R*,2*R*,3'*R*,4*R*)-3'-(2-(1,3-dioxolan-2-yl)ethyl)-7-oxaspiro[bicyclo[2.2.1]heptane-2,2'-oxiran]-5-ene (2.104)**

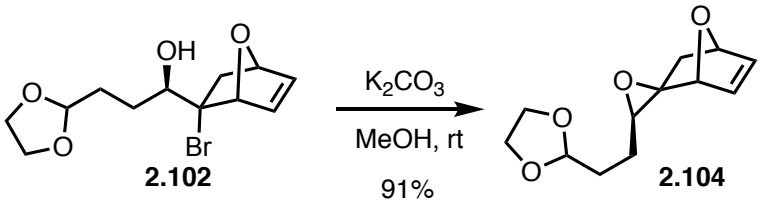

To **2.102** (12 mg, 0.039 mmol, 1.0 equiv.) stirring in MeOH (1 mL) at rt was added K_2CO_3 (27 mg, 0.195 mmol, 5.0 equiv.). The reaction mixture was stirred at rt for 72 h and then was diluted with H_2O and EtOAc. The two layers were separated and the aqueous layer was extracted with EtOAc. The combined organic layers were washed with brine, dried over $MgSO_4$ and concentrated *in vacuo*. Purification by flash chromatography (10% Et_2O:CH_2Cl_2) provided the title compound **2.104** (8 mg, 0.036 mmol, 91%) as a colorless oil.

IR (neat) ν = 2949, 2886, 1732, 1633, 1477, 1440, 1411, 1363, 1351, 1330, 1311, 1221, 1195, 1141, 1108, 1023, 1007, 958, 943, 906, 863, 850, 798, 744, 710, 609 cm^{-1}.

^{1}H NMR (500 MHz, $CDCl_3$) δ 6.55 (dd, *J* = 5.9, 1.6 Hz, 1H), 6.42 (dd, *J* = 5.9, 1.8 Hz, 1H), 5.09 (dt, *J* = 4.7, 1.2 Hz, 1H), 4.92 (t, *J* = 4.5 Hz, 1H), 4.56 (dd, *J* = 1.9, 0.9 Hz, 1H), 4.02 – 3.93 (m, 2H), 3.91 – 3.82 (m, 2H), 3.09 (dd, *J* = 7.6, 4.8 Hz, 1H), 1.96 – 1.87 (m, 2H), 1.77 (dddd, *J* = 13.8, 10.0, 5.6, 4.8 Hz, 1H), 1.73 – 1.64 (m, 2H), 1.63 – 1.54 (m, 1H).

^{13}C NMR (126 MHz, $CDCl_3$) δ 139.8, 132.6, 103.7, 80.9, 78.5, 69.6, 65.0, 59.4, 32.8, 30.6, 24.7.

HRMS (ESI) m/z calcd for $C_{12}H_{16}NaO_4$: 247.0941 $[(M+Na)^+]$, measured: 247.0937.

(5*R*)-5-((1*R*,2*S*,4*R*)-2-bromo-7-oxabicyclo[2.2.1]hept-5-en-2-yl)tetrahydrofuran-2-ol (2.105)

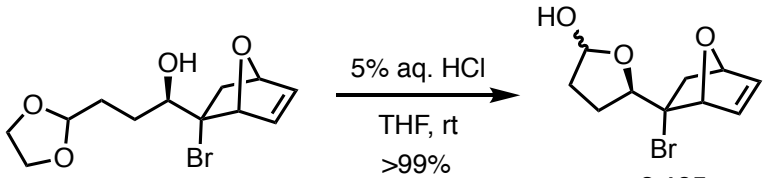

2.102 **2.105**

To **2.102** (2.03 g, 6.65 mmol, 1.0 equiv.) stirring in THF (34 mL) was added 5% aq. HCl (34 mL) and the reaction mixture was stirred at rt for 13.5 h. The reaction mixture was diluted with H_2O and the THF was removed *in vacuo*. The aqueous layer was extracted with EtOAc (x3) and the combined organic layers were washed with brine, dried ($MgSO_4$) and then concentrated *in vacuo* to give the crude lactol product **2.105** (1.74 g, 6.65 mmol, >99%) as a 1.7:1 mixture of hemiacetal epimers. The crude product was used in the next step without any further purification.

For characterization purposes, purification was carried out by flash chromatography (20% → 30% EtOAc:hexanes) to provide **2.105** as a colorless oil.

$[\alpha]_D$ = +1.4 ^{o} (c = 0.70, $CHCl_3$)

IR (neat) ν = 3424, 2984, 2951, 2869, 1723, 1459, 1443, 1346, 1319, 1290, 1214, 1184, 1085, 1052, 1024, 979, 938, 881, 869, 848, 794, 733, 706 cm^{-1}.

^{1}H NMR (400 MHz, $CDCl_3$) δ 6.49 – 6.42 (m, 2H), 5.67 (dd, *J* = 4.5, 1.6 Hz, 1H (major)), 5.51 – 5.46 (m, 1H (minor)), 5.13 (s, 1H), 4.99 (td, *J* = 4.8, 1.4 Hz, 1H), 4.22 (dd, *J* = 7.6, 5.6 Hz, 1H (major)), 4.01 (dd, *J* = 9.7, 5.5 Hz, 1H (minor)), 3.03 (s, 1H (major)), 2.91 (s, 1H (minor)), 2.26 – 1.80 (m, 5H), 1.74 (d, *J* = 12.7 Hz, 1H (minor)), 1.71 (d, *J* = 12.6 Hz, 1H (major)).

^{13}C NMR (75 MHz, $CDCl_3$) δ 136.0, 135.9, 135.4, 135.3, 99.4, 98.9, 85.6, 82.8, 82.6, 82.5, 79.4, 69.5, 69.0, 39.3, 38.9, 34.3, 32.6, 26.8, 26.5.

HRMS (ESI) m/z calcd for $C_{10}H_{13}BrNaO_3$: 282.9940 [$(M+Na)^+$], measured: 282.9933.

Note: The lactol **2.105** underwent dehydration to generate a mixture of diastereomeric dimers **2.108** when held under reduced pressure (< 0.1 mm Hg). Over time, these products converged to one major C2-symmetric dimeric product, which exhibited the following spectroscopic properties:

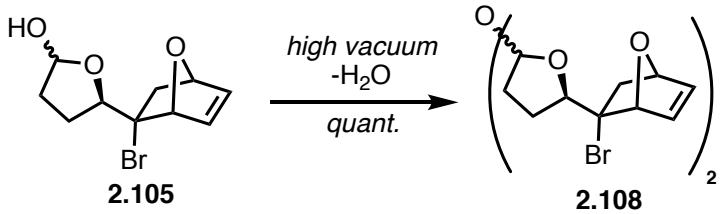

2.105 **2.108**

IR (neat) ν = 2988, 2952, 2865, 1742, 1573, 1458, 1441, 1319, 1292, 1214, 1180, 1089, 1043, 1023, 982, 956, 939, 981, 852, 841, 794, 733, 704 cm^{-1}.

^{1}H NMR (400 MHz, $CDCl_3$) δ 6.50 – 6.41 (m, 4H), 5.64 – 5.57 (m, 2H), 5.18 (d, *J* = 1.5 Hz, 2H), 4.99 (dd, *J* = 4.7, 1.5 Hz, 2H), 4.07 (dd, *J* = 7.7, 5.5 Hz, 2H), 2.20 – 1.67 (m, 12H).

^{13}C NMR (75 MHz, $CDCl_3$) δ 136.1, 135.2, 100.5, 82.6, 82.6, 79.3, 69.4, 39.4, 31.7, 26.7.

HRMS (ESI) m/z calcd for $C_{20}H_{24}Br_2NaO_5$: 524.9883 [$(M+Na)^+$], measured: 524.9886.

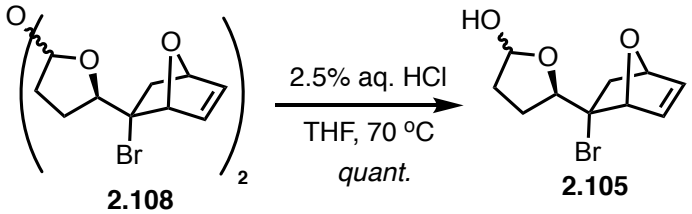

Lactol **2.105** could be recovered from **2.108** in quantitative yield using the following procedure:

To a solution of **2.108** (730 mg, 1.39 mmol, 1 equiv.) in THF (13 mL) was added 2.5% aq. HCl (10 mL). The reaction mixture was stirred at 70 °C for 4 h and then was cooled to rt and quenched with solid $NaHCO_3$ until gas evolution ceased. The mixture was diluted with EtOAc and the two layers were separated. The aqueous layer was extracted with EtOAc (x2) and then the combined organic layers were washed with brine, dried ($MgSO_4$), concentrated *in vacuo* to provide lactol **2.105** (363 mg, 1.39 mmol, 100%) as a colorless oil.

***rac*-(*R*)-4-((1*R*,2*S*,4*R*)-2-bromo-7-oxabicyclo[2.2.1]hept-5-en-2-yl)-4-hydroxybutanal oxime (2.106)**

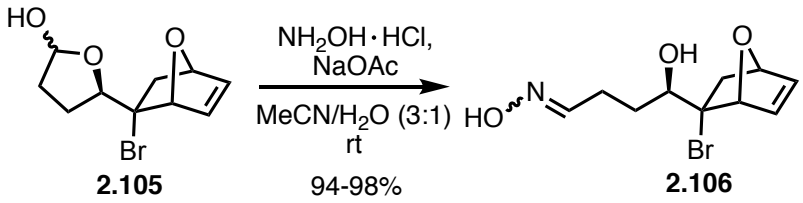

To **2.105** (28 mg, 0.107 mmol, 1.0 equiv.) stirring in 2:1 MeCN:H_2O (1 mL) was sequentially added NaOAc (18 mg, 0.219 mmol, 2.0 equiv.) and hydroxylamine hydrochloride (15 mg, 0.216 mmol, 2.0 equiv.). The reaction mixture was stirred at rt for 30 min and then was concentrated *in vacuo*. The resulting residue was diluted with CH_2Cl_2 and brine, the two layers were separated, and then the aqueous layer was extracted

with CH_2Cl_2 (x3). The combined organic layers were dried (Na_2SO_4), concentrated *in vacuo* and then purified by flash chromatography (20% EtOAc:hexanes) to give **2.106** (26.3 mg, 0.095 mmol, 89%) as a 1:1 mixture of *E*/*Z* oxime isomers.

IR (neat) ν = 3366, 3091, 3008, 2952, 2927, 2869, 1711, 1649, 1574, 1445, 1387, 1321, 1290, 1215, 1185, 1118, 1089, 1012, 979, 941, 877, 860, 837, 795, 732, 708 cm^{-1}.

^{1}H NMR (500 MHz, $CDCl_3$) δ 7.51 (t, *J* = 4.9 Hz, 1H (isomer A)), 6.87 (s, 1H (isomer B)), 6.51 – 6.41 (m, 2H), 5.24 – 5.19 (m, 1H), 5.05 – 4.99 (m, 1H), 3.38 (ddd, *J* = 12.3, 10.0, 2.0 Hz, 1H), 2.67 – 2.33 (m, 3H), 2.08 – 2.00 (m, 1H), 1.92 – 1.82 (m, 1H), 1.80 – 1.68 (m, 2H).

^{13}C NMR (126 MHz, $CDCl_3$) δ 151.6, 136.0, 135.3, 81.9, 81.9, 79.6, 79.5, 76.1, 75.9, 73.3, 72.9, 39.2, 39.1, 31.5, 31.3, 26.4.

HRMS (ESI) m/z calcd for $C_{10}H_{14}BrNNaO_3$: 298.0049 [$(M+Na)^+$], measured: 298.0045.

Note: ~9% of aminal **2.107** (tentative assignment) was detected in the crude ^{1}H NMR spectrum of the above reaction, as a 1:1 mixture of aminal epimers. This species was found to decompose upon attempted silica gel purification but its structure was inferred based on the following ^{1}H NMR signals:

***rac-N*-((5*R*)-5-((1*R*,2*S*,4*R*)-2-bromo-7-oxabicyclo[2.2.1]hept-5-en-2-yl)tetrahydro-furan-2-yl)hydroxylamine (2.107)**

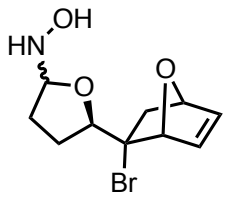

2.107

^{1}H NMR (400 MHz, $CDCl_3$) δ 6.53 – 6.36 (m, 2H), 5.60 (d, *J* = 4.6 Hz, 1H (epimer A)), 5.47 (t, *J* = 4.0 Hz, 1H (epimer B)), 5.22 (s, 1H (epimer A)), 5.17 (s, 1H (epimer B)),

5.00 – 4.93 (m, 1H), 4.15 (dd, *J* = 7.6, 5.7 Hz, 1H (epimer A)), 4.06 (dd, *J* = 7.8, 5.4 Hz, 1H (epimer B)), 2.21 – 1.65 (m, 6H).

(*R*)-4-((1*R*,2*S*,4*R*)-2-bromo-7-oxabicyclo[2.2.1]hept-5-en-2-yl)-4-hydroxybutanal *O*-(*tert*-butyldimethylsilyl) oxime (2.109)

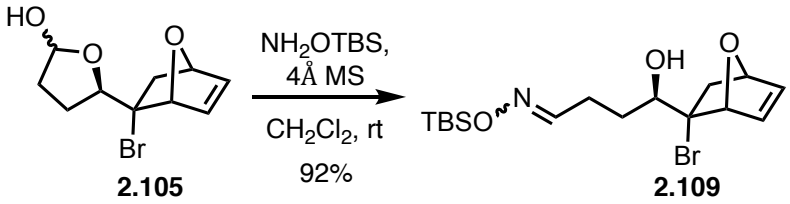

To the crude lactol **2.105** (1.74 g, 6.65 mmol, 1.0 equiv.) and 4Å MS (2.00 g) stirring in CH_2Cl_2 (66 mL) was added $TBSONH_2$ (1.96 g, 13.31 mmol, 2.0 equiv.) and the reaction mixture was stirred at rt for 14 h. The mixture was diluted EtOAc and then vacuum filtered to remove the solids. Concentration *in vacuo* and purification by flash chromatography (10% EtOAc:hexanes) gave the title compound **2.109** (2.40 g, 6.15 mmol, 92% over 2 steps) as a 1.3:1 mixture of oxime isomers as a colorless oil.

$[\alpha]_D$ = +15.2 ^{o} (c = 0.50, $CHCl_3$)

IR (neat) ν = 3426, 2954, 2929, 2889, 2857, 1729, 1472, 1463, 1445, 1390, 1362, 1320, 1251, 1214, 1186, 1120, 1088, 1013, 929, 877, 836, 784, 731, 706, 678 cm^{-1}.

^{1}H NMR (400 MHz, $CDCl_3$) δ 7.59 (t, *J* = 5.1 Hz, 1H (major)), 6.95 (dd, *J* = 6.3, 5.2 Hz, 1H (minor)), 6.51 – 6.42 (m, 2H), 5.24 – 5.19 (m, 1H), 5.02-4.98 (m, 1H), 3.42 (dd, *J* = 10.1, 1.9 Hz, 1H (major)), 3.33 (dd, *J* = 10.0, 2.3 Hz, 1H (minor)), 2.67 (dtd, *J* = 14.6, 8.2, 6.3 Hz, 1H (minor)), 2.54 – 2.36 (m, 2H (major + minor)), 2.10 – 1.67 (m, 5H), 0.94 (s, 9H (minor)), 0.93 (s, 9H (major)), 0.18 (s, 6H (minor)), 0.16 (s, 6H (major)).

^{13}C NMR (75 MHz, $CDCl_3$) δ 155.2, 154.8, 136.1, 135.3, 135.2, 82.0, 81.9, 79.5, 79.5, 77.2, 75.9, 75.9, 73.6, 72.8, 39.2, 39.0, 31.3, 31.2, 26.4, 26.1, 26.0, 22.4, 18.1, -5.3, -5.3.

HRMS (ESI) m/z calcd for $C_{16}H_{28}BrNNaO_3Si$: 412.0914 [$(M+Na)^+$], measured: 412.0910.

3-((1*R*,2*R*,3'*R*,4*R*)-7-oxaspiro[bicyclo[2.2.1]hept[5]ene-2,2'-oxiran]-3'-yl)propanal *O*-(*tert*-butyldimethylsilyl) oxime (2.110)

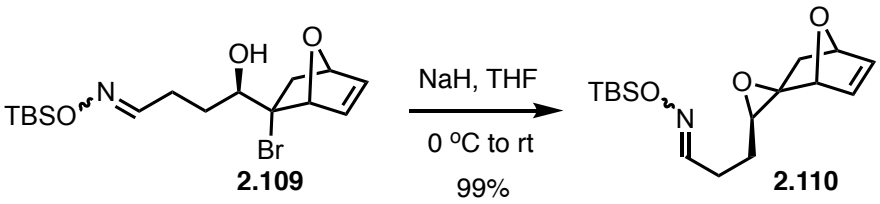

Sodium hydride (60% in mineral oil, 180 mg, 4.50 mmol, 1.06 equiv.) was washed with dry pentane under a stream of Ar (x3) and then dried under high vacuum. THF (15 mL) was added and the suspension was cooled to 0 °C. To the stirring suspension was added **2.109** (1.66 g, 4.25 mmol, 1.0 equiv.) in THF (27 mL) *via* cannula. The reaction mixture was stirred at rt for 19.5 h before being quenched with saturated aq. NH_4Cl and diluted with EtOAc. A minimum amount of H_2O was added to dissolve the salts present and the THF was removed on the rotary evaporator. The aqueous layer was extracted with EtOAc (x3) and the combined organic layers were washed with brine, dried ($MgSO_4$) and concentrated *in vacuo*. Purification by flash chromatography (20% EtOAc:hexanes) gave the title compound **2.110** (1.30 g, 4.20 mmol, 99%) as a 2:1 mixture of oxime isomers as a colorless oil.

$[\alpha]_D$ = +131.3 ° (c = 0.60, $CHCl_3$)

IR (neat) ν = 2952, 2930, 2857, 1473, 1463, 1440, 1390, 1362, 1334, 1311, 1250, 1166, 1023, 1011, 985, 905, 838, 783, 706, 677 cm^{-1}.

^{1}H NMR (400 MHz, $CDCl_3$) δ 7.55 (t, *J* = 5.5 Hz, 1H (major)), 6.93 (t, *J* = 5.4 Hz, 1H (minor)), 6.56 (dd, *J* = 5.9, 1.6 Hz, 1H), 6.44 – 6.38 (m, 1H), 5.10 (d, *J* = 4.4 Hz, 1H), 4.54 (s, 1H), 3.10 (dd, *J* = 7.7, 4.5 Hz, 1H (major)), 3.06 (dd, *J* = 7.5, 4.9 Hz, 1H (minor)), 2.63 – 2.31 (m, 2H), 1.93 (dd, *J* = 12.1, 4.5 Hz, 1H), 1.86 – 1.56 (m, 3H), 0.93 (s, 9H (two peaks (s), minor + major)), 0.17 (s, 6H (minor)), 0.15 (s, 6H (major)).

^{13}C NMR (75 MHz, $CDCl_3$) δ 154.2, 153.7, 140.0, 139.9, 132.4, 132.4, 80.8, 78.4, 69.6, 69.5, 59.0, 58.8, 32.8, 32.7, 27.3, 27.0, 26.7, 26.1, 26.0, 22.6, 18.2, 18.1, -5.3, -5.3.
HRMS (ESI) m/z calcd for $C_{16}H_{27}NNaO_3Si$: 332.1652 [$(M+Na)^+$], measured: 332.1657.

(1*R*,3a*R*,5*S*,6*S*,8a*R*,8b*R*,9*R*)-octahydro-1,6,3-(epiethane[1,1,2]triyl)furo[3,4-*d*]pyrrolo[1,2-*b*]isoxazol-9-ol (2.73)

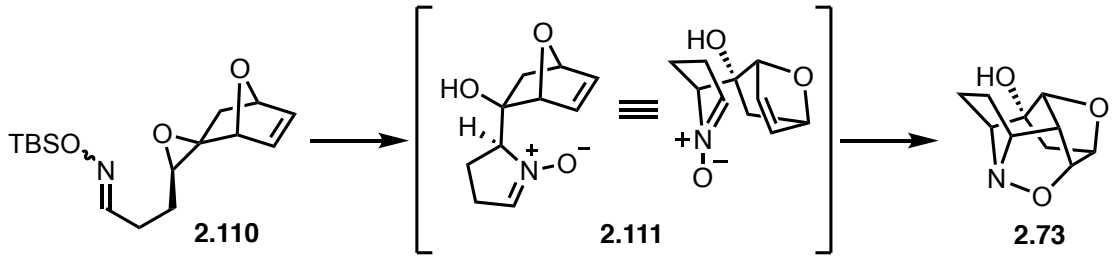

Procedure A (Table 2.4, Entry 11):

A 20 mL microwave reaction vessel was charged with a stir bar, **2.110** (79 mg, 0.255 mmol, 1.0 equiv.) and AcOH (10 mL). The reaction mixture was then heat to 120 ^oC under microwave irradiation for 30 min. After cooling to rt, the AcOH was removed *in vacuo* and the resulting crude product was purified by flash chromatography (column packed with CH_2Cl_2; elution with EtOAc → 5% MeOH:EtOAc) to provide the title compound **2.73** (45.8 mg, 0.235 mmol, 92%) as a white crystalline solid.

Procedure B (Table 2.4, Entry 12):

A 500 mL round bottom flask was charged with a stir bar, **2.110** (1.61 g, 5.20 mmol, 1.0 equiv.) and AcOH (200 mL). It was topped with a reflux condenser, sealed with a septum and flushed with Ar. The reaction mixture was then heat to 120 ^oC (bath temp.) for 40 min. After cooling to rt, the AcOH was removed *in vacuo* and the resulting crude product was purified by flash chromatography (column packed with CH_2Cl_2; elution with EtOAc → 5% MeOH:EtOAc) to provide the title compound **2.73** (833 mg, 4.27 mmol, 82%) as a white crystalline solid.

$[\alpha]_D$ = -13.8 ^{o} (c = 0.80, $CHCl_3$)

mp = 129-131 ^{o}C

IR (neat) ν = 3408, 2952, 2923, 2852, 1467, 1448, 1378, 1313, 1289, 1258, 1211, 1168, 1116, 1099, 1078, 1042, 1015, 1005, 994, 978, 962, 935, 910, 884, 836, 789, 735 cm^{-1}.

^{1}H NMR (400 MHz, $CDCl_3$) δ 4.74 – 4.70 (m, 1H), 4.67 (td, *J* = 4.3, 1.5 Hz, 1H), 4.06 (d, *J* = 4.5 Hz, 1H), 3.59 (d, *J* = 5.4 Hz, 1H), 3.56 – 3.50 (m, 1H), 2.91 – 2.82 (m, 1H), 2.70 (d, *J* = 11.4 Hz, 1H), 2.30 – 2.11 (m, 2H), 2.06 – 1.88 (m, 2H), 1.79-1.71 (m, 2H).

^{13}C NMR (126 MHz, $CDCl_3$) δ 85.7, 82.0, 81.0, 78.9, 66.8, 63.1, 56.5, 45.5, 22.2, 19.0.

HRMS (ESI) m/z calcd for $C_{10}H_{13}NNaO_3$: 218.0788 [$(M+Na)^+$], measured: 218.0787.

5.3 Experimental Procedures for Chapter 3

rac-(1*R*,3a*R*,5*S*,6*S*,8a*R*,8b*R*,9*R*)-octahydro-1,6,3-(epiethane[1,1,2]triyl)furo[3,4-*d*]pyrrolo[1,2-*b*]isoxazol-9-yl 2-diazoacetate (3.10)

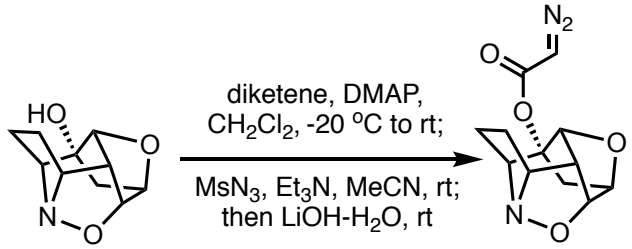

2.73 **3.10**

To a solution of **2.73** (105 mg, 0.538 mmol, 1.0 equiv.) and DMAP (3.3 mg, 0.027 mmol, 0.05 equiv.) stirring in CH_2Cl_2 (10.8 mL) at -20 °C was added diketene (83 μL, 1.076 mmol, 2.0 equiv.). The reaction mixture was warmed to rt and stirred for 30 min. MeOH (1 mL) was added and then the solution was concentrated *in vacuo*. The resulting yellow oil was dissolved in MeCN (3.8 mL) and then sequentially treated with Et_3N (157 μL, 1.13 mmol, 2.1 equiv.) and a solution of methanesulfonyl azide[17] (136 mg, 1.12 mmol, 2.1 equiv.) in MeCN (7 mL). The solution was stirred at rt for 16 h. Next, H_2O (3 mL) was added followed by $LiOH•H_2O$ (135 mg, 3.22 mmol, 6.0 equiv.) and the reaction mixture was stirred for an additional 2 h at rt. The mixture was then diluted with H_2O and CH_2Cl_2 and the two layers were separated. The aqueous layer was extracted with CH_2Cl_2 (x2) and then the combined organic layers were washed with brine, dried over Na_2SO_4 and concentrated *in vacuo*. Purification by flash chromatography (50 → 75% EtOAc:hexanes) yielded the title compound **3.10** (139 mg, 0.528 mmol, 98%) as a yellow oil.

IR (neat) ν = 3095, 2960, 2925, 2110, 1742, 1688, 1469, 1447, 1433, 1372, 1346, 1292, 1254, 1223, 1186, 1157, 1099, 1069, 1049, 1018, 998, 984, 965, 947, 887, 871, 838, 796, 740 cm^{-1}.

^{1}H NMR (400 MHz, $CDCl_3$) δ 4.80 – 4.71 (m, 2H), 4.71 (td, *J* = 4.4, 1.7 Hz, 1H), 4.43 (d, *J* = 5.2 Hz, 1H), 4.21 (d, *J* = 4.5 Hz, 1H), 3.55 (dd, *J* = 7.2, 4.3 Hz, 1H), 3.02 (d, *J* = 12.3 Hz, 1H), 2.93 (dt, *J* = 6.5, 4.5 Hz, 1H), 2.11 – 1.84 (m, 4H), 1.82 – 1.69 (m, 1H).

^{13}C NMR (126 MHz, $CDCl_3$) δ 165.1, 86.7, 85.9, 81.1, 80.2, 63.5, 62.7, 57.0, 46.8, 43.6, 22.1, 19.0.

HRMS (ESI) m/z calcd for $C_{12}H_{13}N_3NaO_4$: 286.0798 [$(M+Na)^+$], measured: 286.0800.

***rac*-(1*R*,5*S*,6*S*,8a*R*,8b*R*,9*R*)-octahydro-1,6,3-(epiethane[1,1,2]triyl)furo[3,4-*d*]pyrrolo[1,2-*b*]isoxazol-9-yl 2-diazo-2-(trimethylsilyl)acetate (3.29)**

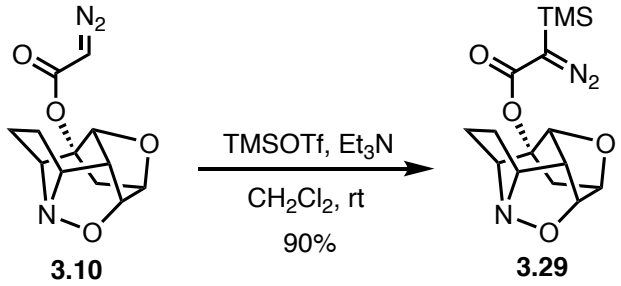

3.10 **3.29**

To **3.10** (99 mg, 0.186 mmol, 1.0 equiv.) stirring in CH_2Cl_2 (8 mL) at rt was added Et_3N (130 μL, 0.933 mmol, 5.0 equiv.) followed by TMSOTf (135 μL, 0.747 mmol, 4.0 mmol). The resulting solution was stirred at rt for 45 min and then was quenched with H_2O. The two layers were separated and the organic layer was washed with H_2O (x2), brine and then dried over Na_2SO_4. Purification by flash chromatography (50% EtOAc:hexanes) provided the title compound **3.29** (56.2 mg, 0.168 mmol, 90%) as a yellow amorphous solid.

IR (neat) ν = 2958, 2090, 1682, 1469, 1269, 1208, 1186, 1174, 1160, 1099, 1081, 1018, 997, 977, 951, 996, 929, 887, 837, 805, 764, 737, 700 cm^{-1}.

^{1}H NMR (400 MHz, $CDCl_3$) δ 4.75 (t, *J* = 5.5 Hz, 1H), 4.67 (td, *J* = 4.4, 1.6 Hz, 1H), 4.39 (d, *J* = 5.3 Hz, 1H), 4.18 (d, *J* = 4.6 Hz, 1H), 3.52 (dd, *J* = 7.1, 4.3 Hz, 1H), 2.98 (d, *J* = 12.2 Hz, 1H), 2.90 (dt, *J* = 6.5, 4.4 Hz, 1H), 2.05 – 1.83 (m, 4H), 1.79 – 1.69 (m, 1H), 0.24 (s, 9H).

^{13}C NMR (126 MHz, $CDCl_3$) δ 167.6, 86.5, 85.9, 81.1, 80.3, 63.6, 62.7, 57.0, 43.6, 22.1, 19.1, -1.4.

HRMS (ESI) m/z calcd for $C_{15}H_{22}N_3O_4Si$: 336.1374 [$(M+H)^+$], measured: 336.1368.

***rac*-(1*R*,3a*R*,5*S*,6*S*,8a*R*,8b*R*,9*R*)-octahydro-1,6,3-(epiethane[1,1,2]triyl)furo[3,4-*d*]pyrrolo[1,2-*b*]isoxazol-9-yl 2-diazo-2-(triethylsilyl)acetate (3.30)**

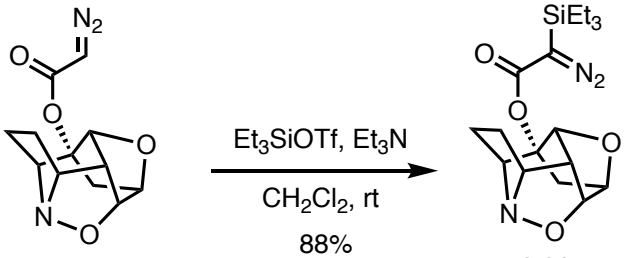

3.10 **3.30**

To **3.10** (19 mg, 0.072 mmol, 1.0 equiv.) stirring in CH_2Cl_2 (3 mL) at rt was added Et_3N (50 μL, 0.359 mmol, 5.0 equiv.) followed by Et_3SiOTf (65.3 μL, 0.289 mmol, 4.0 mmol). The resulting solution was stirred at rt for 45 min and then was quenched with H_2O. The two layers were separated and the organic layer was washed with H_2O (x2), brine and then dried over Na_2SO_4. Purification by flash chromatography (50% EtOAc:hexanes) provided the title compound **3.30** (24 mg, 0.064 mmol, 88%) as a slightly yellow oil.

IR (neat) ν = 3421, 2954, 2923, 2108, 1688, 1458, 1377, 1270, 1180, 1082, 748 cm^{-1}.

^{1}H NMR (500 MHz, $CDCl_3$) δ 4.78 – 4.75 (m, 1H), 4.69 (td, *J* = 4.3, 1.6 Hz, 1H), 4.43 (d, *J* = 5.7 Hz, 1H), 4.20 (dt, *J* = 4.6, 1.2 Hz, 1H), 3.54 (dd, *J* = 7.2, 4.3 Hz, 1H), 3.01 (d, *J* = 12.2 Hz, 1H), 2.91 (dt, *J* = 6.5, 4.5 Hz, 1H), 2.07 – 1.85 (m, 4H), 1.79 – 1.72 (m, 1H), 0.98 (t, *J* = 7.9 Hz, 9H), 0.79 – 0.70 (m, 6H).

^{13}C NMR (126 MHz, $CDCl_3$) δ 167.9, 86.4, 86.0, 81.1, 80.2, 63.6, 62.7, 57.0, 43.7, 22.1, 19.1, 7.1, 3.2.

HRMS (ESI) m/z calcd for $C_{18}H_{28}N_3O_4Si$: 378.1844 [$(M+H)^+$], measured: 378.1844.

***rac*-(3*R*,5a*R*,6*R*,7*R*,10*S*,10a*R*,11*S*)-3-(trimethylsilyl)octahydro-7,10,4,6-(epinitrilooxymethanetriyl)cyclohepta[*b*]furo[2,3-*c*]furan-2(3*H*)-one (3.32)**

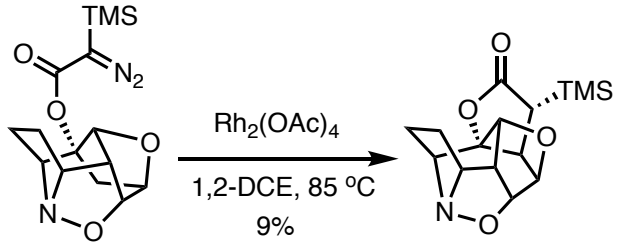

3.29 **3.32**

A 25 mL round bottom flask was charged with a stir bar and $Rh_2(OAc)_4$ (2.8 mg, 6.34 μmol, 0.05 equiv.), topped with a reflux condenser and then sealed with a rubber septum. The rhodium catalyst was dried under high vacuum at 90 °C for 1 h and then cooled to rt. The flask was flushed with Ar and PhMe (2.5 mL) was added. Next, **3.29** (42 mg, 0.125 mmol, 1.0 equiv.) was dissolved in PhMe (10 mL) and added to the catalyst solution *via* cannula. The reaction mixture was then heat to 85 °C (bath temp.) for 22 h. After cooling to rt, the reaction mixture was concentrated *in vacuo* and purified by flash chromatography (slow gradient: hexanes → 80% EtOAc:hexanes) to yield the title compound **3.32** (3.5 mg, 0.011 mmol, 9%) as a white film.

IR (neat) ν = 2956, 2925, 2875, 1766, 1454, 1410, 1377, 1225, 1198, 1150, 1096, 1068, 1011, 979, 940, 907, 840, 798, 733, 703 cm^{-1}.

^{1}H NMR (500 MHz, $CDCl_3$) δ 4.85 – 4.81 (m, 1H), 4.36 (dd, *J* = 4.3, 1.5 Hz, 1H), 4.24 (dt, *J* = 4.6, 1.3 Hz, 1H), 3.65 (d, *J* = 4.4 Hz, 1H), 3.63 – 3.59 (m, 1H), 3.20 (d, *J* = 7.0 Hz, 1H), 2.98 (q, *J* = 4.7 Hz, 1H), 2.25 (d, *J* = 7.1 Hz, 1H), 2.11 – 2.03 (m, 3H), 1.84 – 1.76 (m, 1H), 0.19 (s, 9H).

^{13}C NMR (126 MHz, $CDCl_3$) δ 176.3, 89.8, 86.5, 83.0, 81.1, 64.5, 63.2, 56.8, 48.0, 33.3, 23.2, 19.3, -3.1.

HRMS (ESI) m/z calcd for $C_{15}H_{21}NNaO_4Si$: 330.1132 [$(M+Na)^+$], measured: 330.1131.

***rac*-(3*R*,5a*R*,6*R*,7*R*,10*S*,10a*R*,11*S*,13*R*)-3-(triethylsilyl)octahydro-7,10,4,6-(epinitrilooxymethanetriyl)cyclohepta[*b*]furo[2,3-*c*]furan-2(3*H*)-one (3.33)**

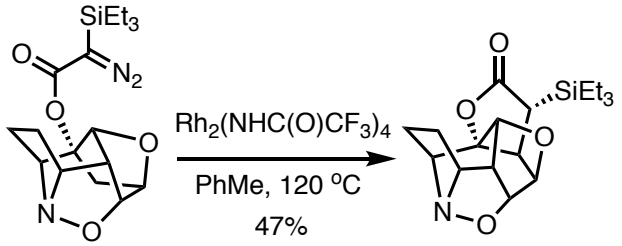

3.30 **3.33**

A 25 mL round bottom flask was charged with a stir bar and $Rh_2(NHC(O)CF_3)_4$ (4.2 mg, 6.42 μmol, 0.05 equiv.),[18] topped with a reflux condenser and then sealed with a rubber septum. The rhodium catalyst was dried under high vacuum at 90 °C for 1 h and then cooled to rt. The flask was flushed with Ar and PhMe (2.7 mL) was added. Next, **3.30** (48 mg, 0.127 mmol, 1.0 equiv.) was dissolved in PhMe (10 mL) and added to the catalyst solution *via* cannula. The reaction mixture was then heat to 120 °C (bath temp.) for 5 h. After cooling to rt, the reaction mixture was concentrated *in vacuo* and purified by flash chromatography (40 → 50% EtOAc:hexanes) to yield the title compound **3.33** (21 mg, 0.060 mmol, 47%) as a white crystalline solid.

mp = 165-167 °C

IR (neat) ν = 2956, 2927, 2877, 1765, 1457, 1415, 1377, 1228, 1198, 1152, 1096, 1071, 1014, 980, 944, 900, 841, 798, 733, 702 cm^{-1}.

^{1}H NMR (400 MHz, $CDCl_3$) δ 4.85 – 4.80 (m, 1H), 4.36 (dd, *J* = 4.4, 1.4 Hz, 1H), 4.24 (d, *J* = 4.5 Hz, 1H), 3.69 – 3.65 (m, 1H), 3.63 – 3.59 (m, 1H), 3.24 (d, *J* = 7.2 Hz, 1H), 2.98 (dt, *J* = 6.6, 4.4 Hz, 1H), 2.32 (d, *J* = 7.2 Hz, 1H), 2.15 – 2.00 (m, 3H), 1.88 – 1.72 (m, 1H), 1.00 (t, *J* = 7.9 Hz, 9H), 0.73 (m, 6H).

^{13}C NMR (126 MHz, $CDCl_3$) δ 178.3, 89.9, 86.5, 83.0, 81.2, 64.6, 63.2, 56.8, 47.9, 29.8, 23.3, 19.3, 7.3, 2.4.

HRMS (ESI) m/z calcd for $C_{18}H_{27}NNaO_4Si$: 372.1602 [$(M+Na)^+$], measured: 372.1598.

***rac*-(1*R*,5*S*,6*S*,8a*R*,8b*R*,9*R*)-octahydro-1,6,3-(epiethane[1,1,2]triyl)furo[3,4-*d*]pyrrolo [1,2-*b*]isoxazol-9-yl butyrate (3.35)**

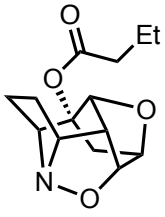

3.35

IR (neat) ν = 2963, 2876, 1732, 1467, 1432, 1349, 1307, 1291, 1260, 1181, 1158, 1101, 1072, 1047, 1017, 997, 978, 958, 940, 894, 883, 867, 835, 802, 782, 737 cm^{-1}.

^{1}H NMR (500 MHz, $CDCl_3$) δ 4.76 (t, *J* = 5.5 Hz, 1H), 4.68 (td, *J* = 4.3, 1.6 Hz, 1H), 4.39 (d, *J* = 5.8 Hz, 1H), 4.24 (d, *J* = 4.5 Hz, 1H), 3.54 (dd, *J* = 7.3, 4.4 Hz, 1H), 3.03 (d, *J* = 12.2 Hz, 1H), 2.91 (dt, *J* = 6.9, 4.5 Hz, 1H), 2.25 (t, *J* = 7.4 Hz, 2H), 2.07 – 1.82 (m, 4H), 1.81 – 1.71 (m, 1H), 1.63 (sext, *J* = 7.4 Hz, 2H), 0.94 (t, *J* = 7.4 Hz, 3H).

^{13}C NMR (126 MHz, $CDCl_3$) δ 172.1, 86.0, 85.8, 81.0, 80.3, 63.0, 62.7, 57.0, 43.6, 36.6, 22.0, 19.1, 18.4, 13.6.

HRMS (ESI) m/z calcd for $C_{14}H_{20}NO_4$: 266.1387 [$(M+H)^+$], measured: 266.1379.

***rac*-methyl ((1*R*,5*S*,6*S*,8a*R*,8b*R*,9*R*)-octahydro-1,6,3-(epiethane[1,1,2]triyl)furo[3,4-*d*]pyrrolo[1,2-*b*]isoxazol-9-yl) malonate (3.39)**

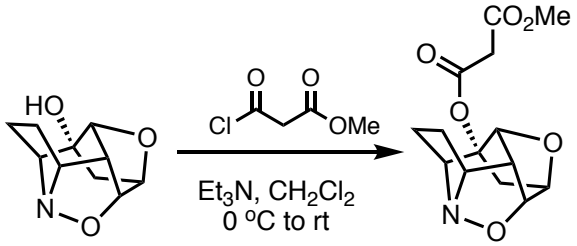

2.73 70% **3.39**

To a solution of **2.73** (31 mg, 0.16 mmol, 1.0 equiv.) stirring in CH_2Cl_2 (1.6 mL) at 0 °C was added Et_3N (92 μL, 0.66 mmol, 4.0 equiv.) followed by methyl malonyl chloride (70 μL, 0.66 mmol, 4.0 equiv.). The reaction mixture was stirred at 0 °C for 30 min and then at rt for 19.5 h. The reaction was quenched with H_2O and then the two layers were

separated. The aqueous layer was extracted with CH_2Cl_2 (x2) and then the combined organic layers were washed with brine, dried (Na_2SO_4), and concentrated *in vacuo*. Purification by flash chromatography (EtOAc) yielded the title compound **3.39** (33 mg, 0.12 mmol, 70%) as a colorless oil.

IR (neat) ν = 2957, 1750, 1734, 1437, 1411, 1342, 1272, 1213, 1149, 1099, 1071, 1049, 1018, 980, 943, 887, 870, 836, 798, 739, 706 cm^{-1}.

^{1}H NMR (500 MHz, $CDCl_3$) δ 4.77 – 4.73 (m, 1H), 4.69 (td, *J* = 4.3, 1.7 Hz, 1H), 4.38 (dd, *J* = 4.8, 1.7 Hz, 1H), 4.24 (dt, *J* = 4.7, 1.3 Hz, 1H), 3.73 (s, 3H), 3.53 (dd, *J* = 7.4, 4.3 Hz, 1H), 3.37 (d, *J* = 15.9 Hz, 1H), 3.32 (d, *J* = 15.9 Hz, 1H), 3.02 (d, *J* = 12.3 Hz, 1H), 2.91 (dt, *J* = 6.6, 4.5 Hz, 1H), 2.04 – 1.90 (m, 4H), 1.79 – 1.71 (m, 1H).

^{13}C NMR (126 MHz, $CDCl_3$) δ 166.7, 164.8, 87.3, 85.9, 81.0, 80.0, 62.9, 62.7, 57.0, 52.5, 43.3, 41.7, 22.0, 19.0.

HRMS (ESI) m/z calcd for $C_{14}H_{17}NNaO_6$: 318.0948 [$(M+Na)^+$], measured: 318.0945.

***rac*-1-methyl 3-((1*R*,5*S*,6*S*,8a*R*,8b*R*,9*R*)-octahydro-1,6,3-(epiethane[1,1,2]triyl)furo [3,4-*d*]pyrrolo[1,2-*b*]isoxazol-9-yl) 2-diazomalonate (3.40)**

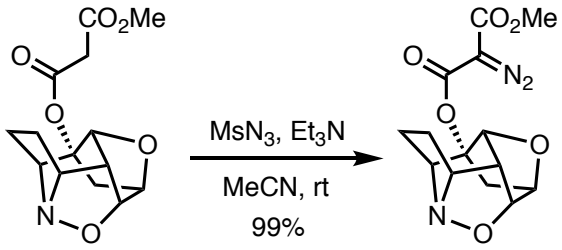

3.39 **3.40**

To a solution of **3.39** (69 mg, 0.23 mmol, 1.0 equiv.) stirring in MeCN (1.7 mL) was added Et_3N (130 μL, 0.93 mmol, 4.0 equiv.) followed by a solution of methanesulfonyl azide[17] (113 mg, 0.93 mmol, 4.0 equiv.) in MeCN (3 mL). The reaction mixture was stirred at rt for 24 h before diluting with H_2O and CH_2Cl_2. The two layers were separated and then the aqueous layer was extracted with CH_2Cl_2 (x2). The combined organic layers were washed with brine, dried (Na_2SO_4), and concentrated *in vacuo*. The crude product

was purified by passing it through a short plug of silica (EtOAc) to yield the title compound **3.40** (74 mg, 0.23 mmol, >99%) as a slightly yellow foam.

IR (neat) ν = 2957, 2139, 1755, 1732, 1693, 1437, 1330, 1273, 1176, 1160, 1100, 1095, 1018, 998, 978, 967, 946, 929, 900, 868, 847, 835, 760, 723, 698 cm^{-1}.

^{1}H NMR (400 MHz, $CDCl_3$) δ 4.76 (dd, *J* = 6.5, 4.5 Hz, 1H), 4.70 (td, *J* = 4.3, 1.6 Hz, 1H), 4.40 (d, *J* = 5.1 Hz, 1H), 4.24 (dt, *J* = 4.5, 1.3 Hz, 1H), 3.82 (s, 3H), 3.61 – 3.49 (m, 1H), 3.03 (d, *J* = 12.3 Hz, 1H), 2.98 – 2.89 (m, 1H), 2.11 – 1.69 (m, 5H).

^{13}C NMR (75 MHz, $CDCl_3$) δ 161.2, 159.1, 87.9, 85.9, 81.0, 80.0, 63.3, 62.7, 57.1, 52.6, 43.6, 22.2, 19.0.

HRMS (ESI) m/z calcd for $C_{14}H_{15}N_3NaO_6$: 344.0853 [$(M+Na)^+$], measured: 344.0851.

***rac*-methyl (4a*R*,8*S*,9*R*,9a*R*,9b*R*,12*S*)-3-oxo-2,3,9a,9b-tetrahydro-6a*H*,9*H*-4a,8,9-(epipropane[1,1,3]triyl)[1,4]dioxino[2',3':5,6]benzo[1,2-*d*]isoxazole-2-carboxylate (3.43)**

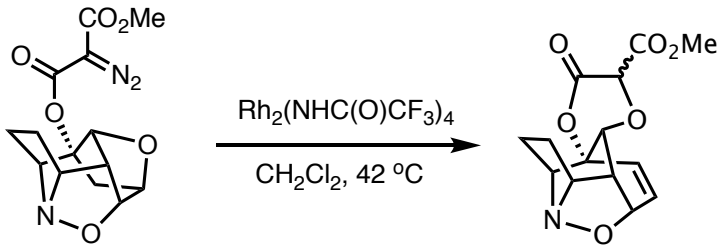

3.40 **3.43**

A 50 mL round bottom flask was charged with a stir bar and $Rh_2(NHC(O)CF_3)_4$ (4.5 mg, 0.007 mmol, 0.07 equiv.),[18] topped with a reflux condenser and then sealed with a rubber septum. The rhodium catalyst was dried under high vacuum at 90 °C for 1 h and then cooled to rt. The flask was flushed with Ar, CH_2Cl_2 (1 mL) was added, and then the resulting solution was heat to 42 °C (bath temp.). A solution of **3.40** (32 mg, 0.10 mmol, 1.0 equiv.) in CH_2Cl_2 (9 mL) was added *via* syringe pump over 5 h and then the reaction mixture was stirred at this temp. for an additional 12 h. After cooling to rt, the reaction mixture was concentrated *in vacuo* and purified by flash chromatography (50% → 100%

EtOAc:hexanes). The fractions containing the title compound **3.43** were concentrated *in vacuo* and repurified by preparative thin layer chromatography (EtOAc) to yield the title compound **3.43** (3.1 mg, 0.011 mmol, 11%) as a mixture of diastereomers (1.5:1 d.r.) as a clear oil.

Note: Ether **3.43** is the major product present in the crude NMR but was unstable and decomposed on silica gel, resulting in a low isolated yield.

$\mathbf{R}_f$ = 0.51 (EtOAc)

IR (neat) ν = 2958, 2925, 2854, 1806, 1745, 1455, 1438, 1370, 1332, 1262, 1229, 1195, 1167, 1130, 1100, 1078, 1064, 1015, 999, 958, 924, 893, 861, 836, 803, 761, 733, 702, 660 cm^{-1}.

^{1}H NMR (400 MHz, $CDCl_3$) δ 6.79 (dd, *J* = 8.9, 5.3 Hz, 1H (major + minor)), 6.14 – 6.10 (dt, *J* = 8.8, 1.9 Hz, 1H (minor)), 6.06 (dt, *J* = 8.8, 1.9 Hz, 1H (major)), 5.02 (s, 1H (major)), 4.76 (s, 1H (major)), 4.76 – 4.69 (m, 1H (major + minor)), 4.54 (s, 1H (minor)), 4.10 (s, 1H (minor)), 3.91 – 3.86 (m, 1H (major + minor), 3.85 (s, 3H (major)), 3.82 (s, 3H (minor)), 3.54 (t, *J* = 5.1 Hz, 1H (major + minor)), 3.18 – 3.11 (m, 1H (major + minor)), 2.29 – 2.13 (m, 1H (major + minor)), 1.98 – 1.67 (m, 3H (major + minor)).

^{13}C NMR (101 MHz, $CDCl_3$) δ 167.0, 164.8, 163.6, 163.0, 136.0, 136.0, 135.5, 134.3, 83.8, 83.6, 76.8, 75.2, 74.4, 73.3, 71.5, 69.2, 57.1, 53.4, 47.2, 22.3, 19.4.

HRMS (ESI) m/z calcd for $C_{14}H_{16}NO_6$: 294.0972 [$(M+H)^+$], measured: 294.0969.

***rac*-(1*R*,5*S*,6*S*,8a*R*,8b*R*,9*R*)-octahydro-1,6,3-(epiethane[1,1,2]triyl)furo[3,4-*d*]pyrrolo[1,2-*b*]isoxazol-9-yl 2-diazo-3-oxobutanoate (3.44)**

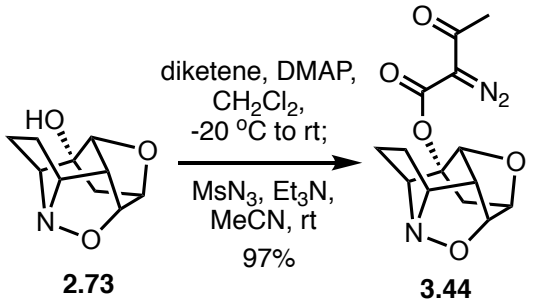

To a solution of **2.73** (53 mg, 0.271 mmol, 1.0 equiv.) and DMAP (1.7 mg, 0.014 mmol) stirring in CH_2Cl_2 (5.4 mL) at -20 °C was added diketene (42 μL, 0.544 mmol, 2.0 equiv.). The reaction mixture was stirred at rt for 1 h, at which time MeOH was added to quench the unreacted diketene. The solution was concentrated *in vacuo* and the resulting oil was dissolved in MeCN (4.4 mL). Et_3N (80 μL, 0.574 mmol, 2.1 equiv.) was added followed by a solution of methanesulfonyl azide[17] (70 mg, 0.578 mmol, 2.1 equiv.) in MeCN (1 mL) and the reaction mixture was stirred at rt for 14 h. The reaction was quenched by the addition of H_2O and then the MeCN was removed on the rotary evaporator. The aqueous layer was extracted with CH_2Cl_2 (x3) and then the combined organic layers were washed with brine, dried (Na_2SO_4) and concentrated *in vacuo*. Purification by flash chromatography (50% EtOAc:hexanes → EtOAc) yielded the title compound **3.44** (80 mg, 0.262 mmol, 97%) as a yellow foam.

IR (neat) ν = 2961, 2933, 2857, 2141, 1716, 1654, 1566, 1470, 1421, 1366, 1327, 1292, 1252, 1152, 1100, 1074, 1018, 997, 977, 967, 951, 930, 903, 889, 869, 847, 836, 745 cm^{-1}.

^{1}H NMR (400 MHz, $CDCl_3$) δ 4.80 (dd, *J* = 6.5, 4.6 Hz, 1H), 4.74 (td, *J* = 4.4, 1.6 Hz, 1H), 4.41 (d, *J* = 5.4 Hz, 1H), 4.28 – 4.21 (m, 1H), 3.58 (s, 1H), 3.06 (d, *J* = 12.3 Hz, 1H), 3.02 – 2.90 (m, 1H), 2.45 (s, 3H), 2.13 – 1.95 (m, 3H), 1.92 – 1.75 (m, 2H).

^{13}C NMR (126 MHz, $CDCl_3$) δ 189.6, 159.5, 87.8, 85.8, 81.0, 79.9, 63.3, 62.6, 57.0, 43.5, 28.1, 22.2, 18.9, 14.1.

HRMS (ESI) m/z calcd for $C_{14}H_{16}NO_5$: 306.1085 [$(M+H)^+$], measured: 306.1086.

***rac*-(1*R*,5*S*,6*S*,8a*R*,8b*R*,9*R*)-octahydro-1,6,3-(epiethane[1,1,2]triyl)furo[3,4-*d*]pyrrolo[1,2-*b*]isoxazol-9-yl 3-((*tert*-butyldimethylsilyl)oxy)-2-diazobut-3-enoate (3.45)**

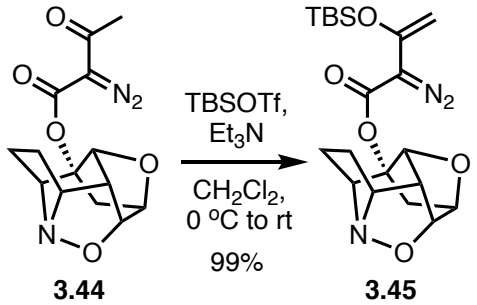

To a solution of **3.44** (19.9 mg, 0.065 mmol, 1.0 equiv.) in CH_2Cl_2 (0.6 mL), stirring at 0 ^oC, was added Et_3N (35 μL, 0.251 mmol, 3.9 equiv.). The solution was stirred for 5 min at this temperature before adding *t*-butyldimethylsilyl trifluoromethanesulfonate (43 μL, 0.187, 2.9 equiv.). The reaction mixture was allowed to slowly warm to rt and was stirred for a total of 11 h. The solution was diluted with hexanes (2 mL) and aq. $NaHCO_3$ (1 mL)/H_2O (1 mL) and then stirred vigorously for 30 min. The two layers were separated and the organic layer was sequentially washed with an aq. $NaHCO_3$ (1 mL)/H_2O (1 mL) solution and brine (2 mL), and then dried (Na_2SO_4). Concentration *in vacuo* yielded the crude title compound **3.45** (27 mg, 0.64 mmol, 99%) as a yellow amorphous solid.

Note: Silyl enol ether **3.45** was found to be very unstable and underwent rapid hydrolysis following its isolation. Consequently, it was always used immediately following its preparation and was characterized based solely on its ^1H NMR spectrum.

^1H NMR (400 MHz, $CDCl_3$) δ 4.92 (d, *J* = 2.2 Hz, 1H), 4.77 (dd, *J* = 6.6, 4.4 Hz, 1H), 4.71 (td, *J* = 4.3, 1.6 Hz, 1H), 4.41 (d, *J* = 5.3 Hz, 1H), 4.24 (d, *J* = 2.2 Hz, 1H), 4.20 (dt, *J* = 4.6, 1.3 Hz, 1H), 3.54 (dd, *J* = 6.9, 4.4 Hz, 1H), 3.04 (d, *J* = 12.3 Hz, 1H), 2.92 (dt, *J* = 6.6, 4.5 Hz, 1H), 2.13 – 1.84 (m, 4H), 1.77 (ddd, *J* = 10.4, 8.0, 5.1 Hz, 1H), 0.91 (s, 9H), 0.22 (s, 3H), 0.21 (s, 3H).

***rac*-(1*R*,5*S*,6*S*,8a*R*,8b*R*,9*R*)-octahydro-1,6,3-(epiethane[1,1,2]triyl)furo[3,4-*d*]pyrrolo[1,2-*b*]isoxazol-9-yl 2,3,3-trichloroacrylate (3.48)**

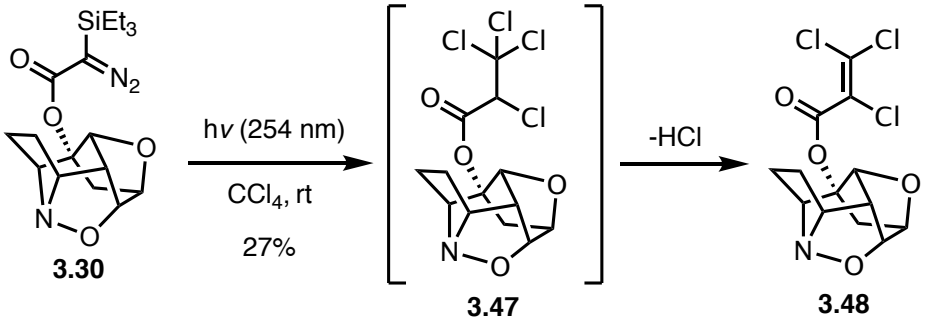

A solution of **3.30** (28.6 mg, 0.076 mmol, 1.0 equiv.) in CCl_4 (2.6 mL) was transferred to a quartz tube and stirred at rt in a Luzchem LZC-4V photoreactor at 254 nm and an intensity of 4.0 mW cm^{-2} for 6 h. After concentrating the mixture *in vacuo*, purification by flash chromatography (40 → 50% EtOAc:hexanes) yielded the title compound **3.48** (7.2 mg, 0.020 mmol, 27%) as a colorless oil.

Note: Employing diazoacetate **3.10** as the starting material in this reaction led to an inseparable mixture of **3.47** and **3.48**. Upon standing, tetrachloroester **3.47** slowly converted to enoate **3.48** *via* loss of HCl.

IR (neat) ν = 2959, 2889, 1728, 1552, 1468, 1447, 1432, 1378, 1348, 1331, 1257, 1224, 1175, 1162, 1098, 1065, 1018, 998, 977, 967, 951, 935, 919, 898, 888, 867, 855, 835, 790, 767, 736 cm^{-1}.

^{1}H NMR (400 MHz, $CDCl_3$) δ 4.80 (dd, *J* = 6.4, 4.6 Hz, 1H), 4.74 (td, *J* = 4.3, 1.7 Hz, 1H), 4.40 (d, *J* = 4.7 Hz, 1H), 4.37 – 4.33 (m, 1H), 3.64 – 3.52 (m, 1H), 3.08 (d, *J* = 12.3 Hz, 1H), 2.97 (q, *J* = 4.4 Hz, 1H), 2.11 – 1.89 (m, 4H), 1.86 – 1.75 (m, 1H).

^{13}C NMR (126 MHz, $CDCl_3$) δ 158.9, 130.2, 122.0, 89.0, 86.0, 81.0, 79.9, 62.8, 62.8, 57.1, 43.3, 22.2, 19.1.

HRMS (APCI) m/z calcd for $C_{13}H_{13}NO_4Cl_3$: 351.9905 [$(M+H)^+$], measured: 351.9903.

***rac*-(1*R*,5*S*,6*S*,8a*R*,8b*R*,9*R*)-9-((trimethylsilyl)oxy)octahydro-1,6,3-(epiethane[1,1,2] triyl)furo[3,4-*d*]pyrrolo[1,2-*b*]isoxazole (3.50)**

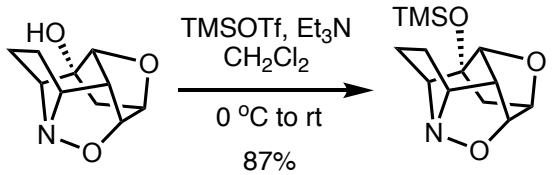

2.73 **3.50**

To a solution of **2.73** (31 mg, 0.16 mmol, 1.0 equiv.) in CH_2Cl_2 (1.6 mL) at 0 °C was added Et_3N (89 μL, 0.64 mmol, 4.0 equiv.) followed by trimethylsilyl trifluoromethanesulfonate (87 μL, 0.48 mmol, 3.0 equiv.). The reaction mixture was warmed to rt and stirred for 17 h. The reaction was quenched with H_2O, stirred for 45 min and then the two layers were separated. The organic layer was washed with H_2O and brine, dried (Na_2SO_4), and concentrated *in vacuo*. Purification by flash chromatography (75% EtOAc:hexanes) yielded the title compound **3.50** (37 mg, 0.14 mmol, 87%)

mp = 43-45 °C

IR (neat) ν = 2989, 2954, 2889, 1652, 1471, 1446, 1401, 1314, 1290, 1274, 1255, 1226, 1212, 1168, 1116, 1100, 1079, 1060, 1042, 1015, 1005, 994, 978, 962, 935, 909, 884, 836, 789, 735, 719 cm^{-1}.

^{1}H NMR (500 MHz, $CDCl_3$) δ 4.68 (ddt, *J* = 6.5, 4.6, 1.0 Hz, 1H), 4.63 (td, *J* = 4.3, 1.6 Hz, 1H), 4.01 (dt, *J* = 4.6, 1.2 Hz, 1H), 3.55 (d, *J* = 6.0 Hz, 1H), 3.49 (dd, *J* = 7.2, 4.3 Hz, 1H), 2.82 (dt, *J* = 6.6, 4.4 Hz, 1H), 2.53 (d, *J* = 11.2 Hz, 1H), 2.17 – 2.08 (m, 1H), 2.00 – 1.82 (m, 3H), 1.75 – 1.65 (m, 1H), 0.13 (s, 9H).

^{13}C NMR (126 MHz, $CDCl_3$) δ 85.9, 82.4, 81.5, 80.9, 67.8, 63.2, 56.7, 44.2, 22.5, 18.8, 2.2.

HRMS (ESI) m/z calcd for $C_{13}H_{21}NNaO_3Si$: 290.1183 [$(M+Na)^+$], measured: 290.1175.

***rac*-ethyl (1*R*,5*S*,6*S*,7*S*,9a*R*,9b*S*,10*R*)-10-((trimethylsilyl)oxy)octahydro-5*H*-1,7,3-(epiethane[1,1,2]triyl)furo[3,4-*e*]pyrrolo[1,2-*c*][1,3]oxazine-5-carboxylate (3.53)**

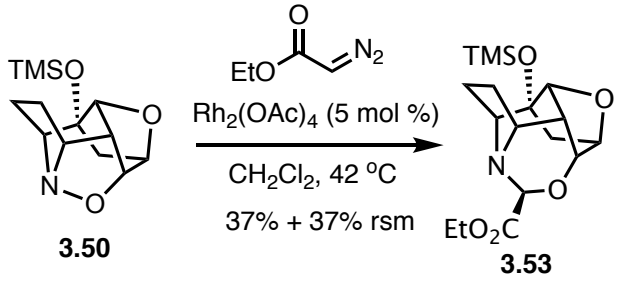

A 25 mL round bottom flask was charged with **3.50** (25 mg, 0.093 mmol, 1.0 equiv.) and $Rh_2(OAc)_4$ (2 mg, 4.3 μmol, 0.05 equiv.), topped with a reflux condenser and sealed with a rubber septum. CH_2Cl_2 (1.3 mL) was added and the resulting solution was heat to 42 °C (bath temp.). A solution of ethyl diazoacetate (11 μL, 0.105 mmol, 1.1 equiv.) in CH_2Cl_2 (8 mL) was then added *via* syringe pump over 18.5 h. The reaction mixture was stirred at this temp. for an additional 1.5 h and then was cooled to rt. After concentrating *in vacuo*, purification by flash chromatography (10 → 15% EtOAc:hexanes to elute the product **3.53**; 40% EtOAc:hexanes to elute unreacted **3.50**) yielded the title compound **3.53** (12 mg, 0.034 mmol, 37%) as a colorless oil and recovered starting material **3.50** (9.2 mg, 0.034 mmol, 37%).

IR (neat) ν = 2984, 2956, 2933, 2853, 1752, 1467, 1447, 1368, 1330, 1251, 1231, 1201, 1165, 1140, 1084, 1054, 1029, 1011, 973, 959, 931, 864, 836, 795, 757 cm^{-1}.

^{1}H NMR (500 MHz, $CDCl_3$) δ 5.48 (s, 1H), 4.54 (td, *J* = 5.1, 1.1 Hz, 1H), 4.44 (ddd, *J* = 10.7, 5.2, 1.4 Hz, 1H), 4.28 – 4.13 (m, 2H), 4.09 (d, *J* = 5.0 Hz, 1H), 3.82 (dd, *J* = 7.1, 3.7 Hz, 1H), 3.39 (d, *J* = 6.4 Hz, 1H), 2.36 (d, *J* = 13.5 Hz, 1H), 2.14 (ddd, *J* = 10.8, 5.0, 3.7 Hz, 1H), 2.05 – 1.89 (m, 3H), 1.89 – 1.79 (m, 1H), 1.55 – 1.46 (m, 1H), 1.30 (t, *J* = 7.1 Hz, 3H), 0.16 (s, 9H).

^{13}C NMR (126 MHz, $CDCl_3$) δ 169.3, 83.8, 83.2, 80.8, 80.3, 72.7, 63.8, 61.3, 47.4, 42.1, 38.5, 26.3, 24.9, 14.1, 2.3.

HRMS (ESI) m/z calcd for $C_{17}H_{27}NNaO_5Si$: 376.1551 [$(M+Na)^+$], measured: 376.1544.

***rac*-(1*R*,5*S*,6*S*,8a*R*,8b*R*,9*R*)-octahydro-1,6,3-(epiethane[1,1,2]triyl)furo[3,4-*d*]pyrrolo[1,2-*b*]isoxazol-9-yl carbamate (3.58)**

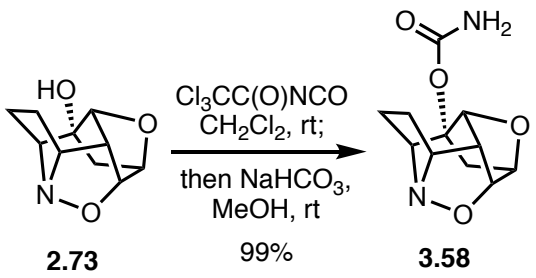

2.73 **3.58**

To a solution of **2.73** (122 mg, 0.625 mmol, 1.0 equiv.) stirring in CH_2Cl_2 (12.5 mL) at rt was added trichloroacetyl isocyanate (149 μL, 1.25 mmol, 2.0 equiv.) dropwise. The reaction mixture was stirred at rt for for 30 min and then concentrated *in vacuo*. The resulting oil was dissolved in MeOH (12.5 mL) and then $NaHCO_3$ (158 mg, 1.88 mmol, 3.0 equiv.) was added. The mixture was stirred at rt for 3.5 h before being concentrated *in vacuo*. The crude product was taken up in CH_2Cl_2:MeOH (9:1) and filtered through a pad of Celite. After concentration *in vacuo*, purification by flash chromatography (20:1 CH_2Cl_2:MeOH) provided the title compound **3.58** (148 mg, 0.621 mmol, 99%) as a white crystalline solid.

mp = 190 °C (dec.)

IR (neat) ν = 3437, 3352, 3195, 2963, 1719, 1610, 1365, 1105, 1079, 1016, 994, 947, 889, 876, 835, 786, 733 cm^{-1}.

^{1}H NMR (400 MHz, $CDCl_3$) δ 4.76 (dd, *J* = 6.5, 4.5 Hz, 1H), 4.75 – 4.59 (m, 3H), 4.46 – 4.41 (m, 1H), 4.19 (dt, *J* = 4.6, 1.3 Hz, 1H), 3.55 (dd, *J* = 7.1, 4.2 Hz, 1H), 2.97 (d, *J* = 12.3 Hz, 1H), 2.91 (dt, *J* = 6.5, 4.4 Hz, 1H), 2.11 – 1.92 (m, 4H), 1.80 – 1.71 (m, 1H).

^{13}C NMR (126 MHz, $CDCl_3$) δ 154.9, 85.9, 85.5, 81.1, 80.3, 63.4, 62.7, 56.9, 43.4, 22.0, 19.1.

HRMS (ESI) m/z calcd for $C_{11}H_{15}N_2O_4$: 239.1026 [$(M+H)^+$], measured: 239.1024.

***rac*-(3a*S*,6*R*,7*S*,12*R*,12a*R*,14*R*)-tetrahydro-4*H*,12*H*-6,9,12-(epimethanetriyl)-10,12a-methanooxazolo[4,5-*c*]pyrrolo[1,2-*b*][1,6,2]dioxazocin-2(3*H*)-one (3.61)**

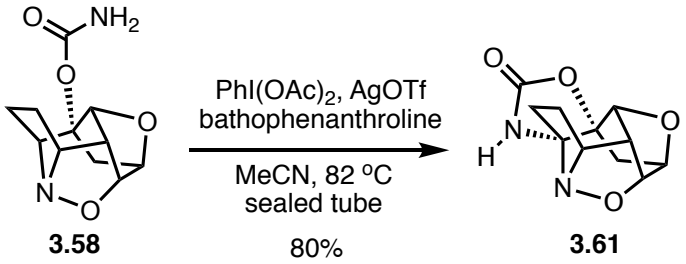

3.58 **3.61**

A 15 mL pressure reaction vessel was charged with **3.58** (35.7 mg, 0.150 mmol, 1.0 equiv.), $PhI(OAc)_2$ (195 mg, 0.605 mmol, 4.0 equiv.) and a stir bar. A 4-dram vial was charged with bathophenanthroline (49.4 mg, 0.149 mmol, 1.0 equiv.) and a stir bar. A 1-dram vial was charged with AgOTf (37.8 mg, 0.147 mmol, 1.0 equiv.). Each of these was transferred into a glove box. The AgOTf was dissolved in MeCN (2 mL) and then added to the bathophenanthroline vial. The resulting yellow suspension was stirred at rt for 20 min. Next, MeCN (3 mL) was added to the pressure vessel containing **3.58** and $PhI(OAc)_2$ and then the AgOTf/bathophenanthroline suspension was added to the same vessel. The pressure vessel was sealed, removed from the glove box and then heat to 82 ^oC (bath temp.) for 20 h. The reaction mixture was cooled to rt, filtered through a plug of silica (eluting with EtOAc), concentrated *in vacuo* and then purified by flash chromatography (EtOAc) to give the title compound **3.61** (28.3 mg, 0.120 mmol, 80%) as a white wax-like solid.

IR (neat) ν = 3513, 3298, 2963, 1761, 1637, 1257, 1228, 1167, 1106, 1076, 1034, 1011, 997, 942, 917, 898, 880, 833, 777, 762 cm^{-1}.

^{1}H NMR (500 MHz, CD_3OD) δ 4.82 – 4.79 (m, 1H), 4.78 – 4.74 (m, 2H), 3.74 – 3.70 (m, 1H), 3.32 (d, *J* = 11.4 Hz, 1H), 3.09 – 3.02 (m, 1H), 2.60 – 2.49 (m, 1H), 2.11 – 1.90 (m, 3H), 1.71 (ddd, *J* = 11.7, 4.0, 1.0 Hz, 1H).

^{13}C NMR (126 MHz, CD_3OD) δ 161.0, 92.8, 87.3, 86.6, 80.4, 76.4, 68.8, 59.8, 39.6, 30.8, 16.7.

^{1}H NMR (400 MHz, $(CD_3)_2SO$) δ 8.01 (s, 1H), 4.80 (d, *J* = 4.3 Hz, 1H), 4.75 – 4.68 (m, 2H), 3.60 – 3.56 (m, 1H), 3.09 (d, *J* = 11.5 Hz, 1H), 2.95 (dt, *J* = 8.0, 4.2 Hz, 1H), 2.43 – 2.28 (m, 1H), 1.93 – 1.78 (m, 3H), 1.51 (dd, *J* = 11.5, 3.6 Hz, 1H).

^{13}C NMR (101 MHz, $(CD_3)_2SO$) δ 158.6, 90.9, 85.5, 85.3, 78.8, 75.0, 67.1, 58.5, 39.0, 29.9, 15.8.

HRMS (ESI) m/z calcd for $C_{11}H_{12}N_2NaO_4$: 259.0689 [$(M+Na)^+$], measured: 259.0693.

***rac*-(1*R*,6*R*)-9-oxohexahydro-3,6-ethanofuro[3,4-*d*]pyrrolo[1,2-*b*]isoxazole-1,6(1*H*)-diyl diacetate (3.62)**

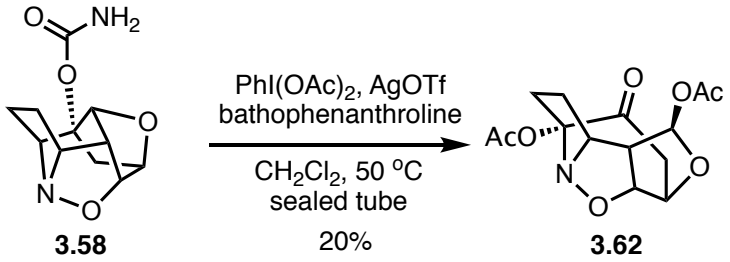

3.58 **3.62**

A 15 mL pressure reaction vessel was charged with **3.58** (29 mg, 0.122 mmol, 1.0 equiv.), $PhI(OAc)_2$ (158 mg, 0.491 mmol, 4.0 equiv.) and a stir bar. A 4-dram vial was charged with AgOTf (31 mg, 0.121 mmol, 1.0 equiv.) and a stir bar. A 1-dram vial was charged with bathophenanthroline (41 mg, 0.123 mmol, 1.0 equiv.). Each of these was transferred into a glove box. The bathophenanthroline was dissolved in CH_2Cl_2 (2 mL) and then added to the AgOTf vial. The resulting yellow suspension was stirred at rt for 20 min, over which time it became a slightly yellow homogenous solution. Next, CH_2Cl_2 (2.4 mL) was added to the pressure vessel containing **3.58** and $PhI(OAc)_2$ and then the AgOTf/bathophenanthroline solution was added to the same vessel. The pressure vessel was sealed, removed from the glove box and then heat to 50 °C (bath temp.) for 20 h. The reaction mixture was cooled to rt, filtered through a plug of silica (eluting with EtOAc), concentrated *in vacuo* and then purified by flash chromatography (column loaded with CH_2Cl_2; elution with 30% hexanes:EtOAc) to give the title compound **3.62** (7.5 mg, 0.024 mmol, 20%) as a colorless oil.

IR (neat) ν = 2927, 2853, 1739, 1714, 1437, 1369, 1233, 1171, 1128, 1109, 1076, 1017, 998, 946, 931, 898, 734 cm^{-1}.

^{1}H NMR (500 MHz, $CDCl_3$) δ 6.34 (s, 1H), 5.22 (t, *J* = 7.2 Hz, 1H), 4.63 (ddd, *J* = 6.8, 4.8, 2.0 Hz, 1H), 4.04 (dd, *J* = 9.9, 6.9 Hz, 1H), 3.29 – 3.21 (m, 2H), 3.15 (dd, *J* = 17.3, 4.9 Hz, 1H), 2.53 – 2.33 (m, 2H), 2.19 – 2.01 (m, 8H).

^{13}C NMR (126 MHz, $CDCl_3$) δ 200.6, 170.3, 169.7, 101.9, 97.7, 85.3, 77.9, 67.4, 56.9, 44.4, 34.5, 21.9, 21.1, 21.0.

HRMS (ESI) m/z calcd for $C_{14}H_{17}NNaO_7$: 334.0897 [$(M+Na)^+$], measured: 334.0895.

***rac*-(8*S*)-7-oxooctahydro-1,3-dioxa-4-aza-2,8-methanocyclopenta[*cd*]azulen-8(4*H*)-yl acetate (3.69)**

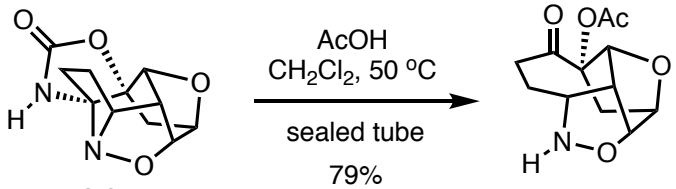

3.61 **3.69**

A 1 dram vial was charged with a stir bar, **3.61** (3.5 mg, 0.015 mmol, 1.0 equiv.), CH_2Cl_2 (1 mL), and AcOH (0.01 mL, 0.175 mmol, 11.7 equiv.). The vial was sealed and then the reaction mixture was stirred at 50 °C (bath temp.) for 7 days before being concentrated *in vacuo*. Purification by flash chromatography (EtOAc) yielded the title compound **3.69** (3 mg, 0.012 mmol, 79%) as a white film.

IR (neat) ν = 3438, 2956, 2924, 2853, 1764, 1738, 1694, 1667, 1445, 1373, 1317, 1252, 1232, 1202, 1172, 1117, 1079, 1036, 976, 936, 903, 843, 794, 777, 733, 667 cm^{-1}.

^{1}H NMR (500 MHz, $CDCl_3$) δ 4.87 (s, 1H), 4.87 – 4.78 (m, 2H), 4.71 (dd, *J* = 10.6, 4.8 Hz, 1H), 4.25 (d, *J* = 6.0 Hz, 1H), 3.56 (td, *J* = 10.2, 5.9 Hz, 1H), 3.23 (t, *J* = 13.8 Hz, 1H), 2.95 (d, *J* = 13.6 Hz, 1H), 2.66 (dd, *J* = 13.9, 7.4 Hz, 1H), 2.37 (dt, *J* = 13.7, 5.9 Hz, 1H), 2.15 (s, 3H), 1.99 (dd, *J* = 13.7, 5.9 Hz, 1H), 1.66 (t, *J* = 14.3 Hz, 1H).

^{13}C NMR (126 MHz, $CDCl_3$) δ 209.1, 171.6, 85.7, 85.2, 84.6, 78.5, 53.4, 53.0, 39.6, 33.1, 26.2, 20.3.

HRMS (ESI) m/z calcd for $C_{12}H_{15}NNaO_5$: 276.0842 [$(M+Na)^+$], measured: 276.0834.

***rac*-(1*R*,6*R*)-6-methoxy-9-oxooctahydro-3,6-ethanofuro[3,4-*d*]pyrrolo[1,2-*b*]isoxazol-1-yl acetate (3.70)**

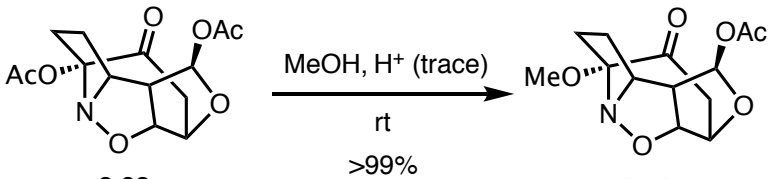

3.62 **3.70**

A drop of $CDCl_3$ was added to a solution of **3.62** (3 mg, 0.0096 mmol, 1.0 equiv.) in MeOH (1 mL) and then it was stirred at rt for 15 h. Concentration *in vacuo* provided the title compound **3.70** (2.7 mg, 0.0095 mmol, 99%) as a white film.

IR (neat) ν = 2956, 2928, 2857, 1742, 1711, 1463, 1443, 1367, 1232, 1113, 1070, 1052, 1013, 997, 952, 923, 874, 849, 734 cm^{-1}.

^{1}H NMR (400 MHz, $CDCl_3$) δ 6.32 (s, 1H), 5.23 (t, *J* = 7.3 Hz, 1H), 4.58 (dt, *J* = 7.1, 3.5 Hz, 1H), 4.10 (ddd, *J* = 10.3, 7.6, 2.6 Hz, 1H), 3.32 (s, 3H), 3.31 – 3.22 (m, 1H), 3.10 (dd, *J* = 17.2, 4.3 Hz, 1H), 2.87 (dd, *J* = 17.2, 2.6 Hz, 1H), 2.50 (dt, *J* = 13.4, 8.8 Hz, 1H), 2.28 (dq, *J* = 14.0, 8.6 Hz, 1H), 2.06 (s, 3H), 2.10 – 1.96 (m, 1H), 1.83 (ddd, *J* = 13.0, 8.5, 4.2 Hz, 1H).

^{13}C NMR (126 MHz, $CDCl_3$) δ 202.5, 169.7, 102.8, 97.4, 85.4, 76.5, 65.3, 57.1, 51.0, 44.1, 32.9, 22.6, 21.1.

HRMS (ESI) m/z calcd for $C_{13}H_{17}NNaO_6$: 306.0948 [$(M+Na)^+$], measured: 306.0937.

***rac*-(1*R*,5*S*,6*S*,8a*R*,8b*R*,9*R*)-octahydro-1,6,3-(epiethane[1,1,2]triyl)furo[3,4-*d*]pyrrolo[1,2-*b*]isoxazol-9-yl sulfamate (3.72)**

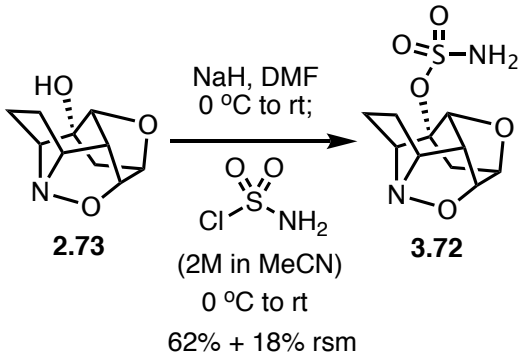

Preparation of 2 M sulfamoyl chloride solution in MeCN:

Chlorosulfonyl isocyanate (697 μL, 8.00 mmol, 1.0 equiv.) was cooled to 0 °C and formic acid (302 μL, 8.00 mmol, 1.0 equiv.) was added dropwise while stirring vigorously. Stirring was continued at 0 °C for 5 min and then MeCN (4 mL) was added. The solution was stirred at 0 °C for 1 h and then at rt for 16 h, providing a 2 M solution of sulfamoyl chloride in MeCN.

Preparation of 3.72:

In a 2-necked round bottom flask, NaH (60% in mineral oil, 16 mg, 0.400 mmol, 1.1 equiv.) was washed with dry pentane (x3) under a stream of Ar and then dried under *in vacuo* (<0.01 mm Hg). DMF (240 μL) was added, the suspension was cooled to 0 °C, and then a solution of **2.73** (70 mg, 0.359 mmol, 1.0 equiv.) in DMF (480 μL) was added *via* cannula. The mixture was warmed to rt and stirred for 1 h. After cooling again to 0 °C, sulfamoyl chloride (2 M in MeCN, 270 μL, 0.540 mmol, 1.5 equiv.) was added dropwise. The reaction mixture was warmed to rt and stirred for 16 h. The reaction was quenched with H_2O (1 mL) and diluted with CH_2Cl_2 (10 mL). The two layers were separated and the aqueous layer was extracted with CH_2Cl_2 (x5). The combined organic layers were dried ($MgSO_4$) and concentrated *in vacuo*. The crude product was triturated twice with ice-cold MeOH (1 mL) to provide **3.72** (39.5 mg, 0.152 mmol, 42%) as a white powder. The combined mother liquor was concentrated *in vacuo* and purified by flash chromatography (EtOAc → 5% MeOH:EtOAc) to yield a second batch of **3.72** (18.8 mg, 0.072 mmol, 20%) as a white powder and unreacted **2.73** (12.7 mg, 0.065 mmol, 18%).

The combined yield of **3.72** was 58.3 mg (0.224 mmol, 62%).

mp = 142 °C (dec.)

IR (neat) ν = 3291, 3254, 1960, 2924, 2853, 1708, 1664, 1571, 1468, 1365, 1317, 1294, 1230, 1185, 1131, 1110, 1095, 1060, 1045, 1017, 998, 978, 934, 910, 885, 842, 815, 781, 762, 735 cm^{-1}.

^{1}H NMR (500 MHz, MeOD) δ 4.80 – 4.73 (m, 2H), 4.38 (dt, *J* = 4.6, 1.2 Hz, 1H), 4.18 – 4.13 (m, 1H), 3.54 (td, *J* = 4.5, 2.1 Hz, 1H), 2.98 (dt, *J* = 6.4, 4.5 Hz, 1H), 2.69 (d, *J* = 12.2 Hz, 1H), 2.63 (ddd, *J* = 12.1, 4.0, 1.0 Hz, 1H), 2.37 – 2.28 (m, 1H), 2.05 – 1.88 (m, 3H).

^{13}C NMR (126 MHz, MeOD) δ 92.4, 87.3, 82.3, 81.7, 66.2, 64.5, 58.5, 42.7, 23.9, 19.4.

HRMS (ESI) m/z calcd for $C_{10}H_{14}N_2NaO_5S$: 297.0516 [$(M+Na)^+$], measured: 297.0508.

***rac*-(5a*R*,6*R*,9*R*,9a*R*,9b*R*)-hexahydro-6,9-epoxybenzo[*d*]pyrrolo[1,2-*b*]isoxazole-3,8(2*H*,5a*H*)-dione (3.77) and *rac*-(2*S*,5a*R*,6*R*,9*R*,9a*R*,9b*R*)-2-iodohexahydro-6,9-epoxybenzo[*d*]pyrrolo[1,2-*b*]isoxazole-3,8(2*H*,5a*H*)-dione (3.78)**

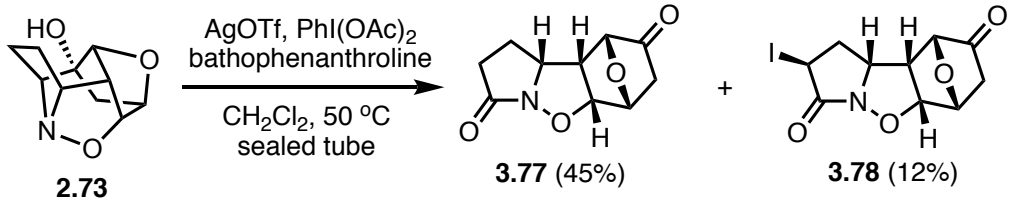

A 15 mL pressure reaction vessel was charged with **2.73** (22 mg, 0.113 mmol, 1.0 equiv.), $PhI(OAc)_2$ (147 mg, 0.456 mmol, 4.0 equiv.) and a stir bar. A 4-dram vial was charged with AgOTf (29 mg, 0.113 mmol, 1.0 equiv.) and a stir bar. A 1-dram vial was charged with bathophenanthroline (38 mg, 0.114 mmol, 1.0 equiv.). Each of these was transferred into a glove box. The bathophenanthroline was dissolved in CH_2Cl_2 (2 mL) and then added to the AgOTf vial. The resulting yellow suspension was stirred at rt for 20 min, over which time it became a slightly yellow homogenous solution. Next, CH_2Cl_2 (2

mL) was added to the pressure vessel containing **2.73** and $PhI(OAc)_2$ and then the AgOTf/bathophenanthroline solution was added to the same vessel. The pressure vessel was sealed, removed from the glove box and then heat to 50 ^oC (bath temp.) for 28 h. The reaction mixture was cooled to rt, filtered through a plug of silica (eluting with EtOAc), concentrated *in vacuo* and then purified by preparative thin layer chromatography (EtOAc) to provide **3.78** (4.6 mg, 0.013 mmol, 12%) as a yellow film and **3.77** (10.7 mg, 0.051 mmol, 45%) as a white waxy solid.

***rac*-(5a*R*,6*R*,9*R*,9a*R*,9b*R*)-hexahydro-6,9-epoxybenzo[*d*]pyrrolo[1,2-*b*]isoxazole-3,8(2*H*,5a*H*)-dione (3.77)**

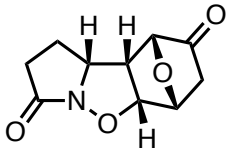

3.77

$\mathbf{R}_f$ = 0.26 (EtOAc)

IR (neat) ν = 2980, 2929, 2853, 1755, 1698, 1465, 1407, 1282, 1262, 1143, 1083, 1059, 1042, 1028, 1010, 1001, 972, 947, 910, 892, 849, 820, 776, 744, 728, 685 cm^{-1}.

^{1}H NMR (400 MHz, CD_3OD) δ 5.33 (ddd, *J* = 8.3, 5.0, 0.9 Hz, 1H), 5.05 (t, *J* = 5.5 Hz, 1H), 4.45 (dq, *J* = 6.3, 1.2 Hz, 1H), 4.33 – 4.24 (m, 1H), 3.42 (dt, *J* = 8.3, 6.4 Hz, 1H), 2.76 – 2.60 (m, 2H), 2.47 (dddt, *J* = 18.2, 6.4, 1.5, 0.9 Hz, 1H), 2.35 – 2.04 (m, 3H).

^{13}C NMR (101 MHz, CD_3OD) δ 210.8, 168.6, 90.7, 82.4, 80.0, 58.5, 55.4, 39.5, 32.9, 18.6.

HRMS (ESI) m/z calcd for $C_{10}H_{11}NNaO_4$: 232.0580 [$(M+Na)^+$], measured: 232.0579.

***rac*-(2*S*,5a*R*,6*R*,9*R*,9a*R*,9b*R*)-2-iodohexahydro-6,9-epoxybenzo[*d*]pyrrolo[1,2-*b*]isoxazole-3,8(2*H*,5a*H*)-dione (3.78)**

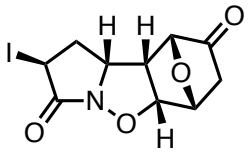

3.78

R_f = 0.62 (EtOAc)

IR (neat) ν = 2956, 2924, 2853, 1752, 1706, 1449, 1405, 1304, 1264, 1142, 1104, 1080, 1040, 1009, 975, 945, 849, 819, 730, 694 cm^{-1}.

^{1}H NMR (400 MHz, $CDCl_3$) δ 5.38 – 5.29 (m, 1H), 5.05 (t, *J* = 5.7 Hz, 1H), 4.44 – 4.28 (m, 3H), 3.43 (dt, *J* = 8.3, 6.4 Hz, 1H), 2.99 – 2.81 (m, 2H), 2.58 – 2.44 (m, 2H).

^{13}C NMR (126 MHz, $CDCl_3$) δ 208.9, 164.6, 89.0, 80.9, 78.8, 55.2, 53.0, 38.9, 31.9, 13.9.

HRMS (ESI) m/z calcd for $C_{10}H_{10}NNaO_4I$: 357.9552 [$(M+Na)^+$], measured: 357.9547.

***rac*-(1*R*,5*S*,6*S*,8a*R*,8b*R*,9*R*)-octahydro-1,6,3-(epiethane[1,1,2]triyl)furo[3,4-*d*]pyrrolo[1,2-*b*]isoxazol-9-yl chlorocarbamate (3.102)**[19]

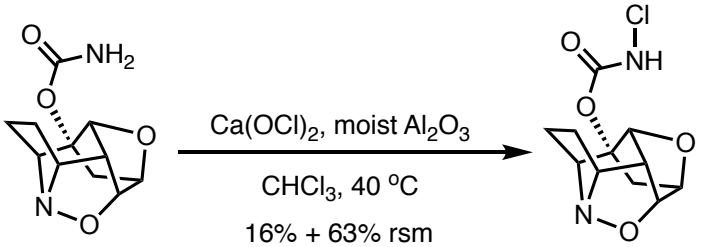

3.58 **3.102**

Finely ground calcium hypochlorite (57 mg, 0.40 mmol, 4.0 equiv.) was added to a suspension of moist Al_2O_3 (100 mg) [note: moist Al_2O_3 was prepared by adding H_2O (1 mL) to Brockman grade I 150 mesh Al_2O_3 (5g) and shaking until a free-flowing powder was obtained] in $CHCl_3$ (1 mL) and then the resulting suspension was stirred at 40 °C for 10 min. **3.58** (24 mg, 0.10 mmol, 1.0 equiv.) was added, the flask was covered in Al foil

and the reaction mixture was stirred at 40 °C for 20 h. Another portion of moist Al_2O_3 (100 mg) was added and the reaction was stirred at 40 °C for an additional 16 h. The reaction mixture was cooled to rt and then the suspension was immediately loaded onto silica gel. Purification by flash chromatography (10% hexanes:EtOAc to elute **3.102**; then 5% MeOH:EtOAc to elute unreacted **3.58**) yielded the title compound **3.102** (4.4 mg, 0.016 mmol, 16%) as a white solid and recovered **3.58** (15 mg, 0.063 mmol, 63%) as a white solid.

mp = 138 °C (dec.)

IR (neat) ν = 3210, 2960, 2925, 2853, 1741, 1722, 1469, 1449, 1435, 1348, 1334, 1314, 1292, 1249, 1222, 1175, 1102, 1078, 1019, 837, 754 cm^{-1}.

^{1}H NMR (400 MHz, $CDCl_3$) δ 5.50 (s, 1H), 4.78 (t, *J* = 5.6 Hz, 1H), 4.73 (d, *J* = 4.6 Hz, 1H), 4.40 (d, *J* = 5.2 Hz, 1H), 4.24 (d, *J* = 4.6 Hz, 1H), 3.60 – 3.52 (m, 1H), 3.01 (d, *J* = 12.2 Hz, 1H), 2.94 (q, *J* = 5.1 Hz, 1H), 2.11 – 1.86 (m, 4H), 1.82 – 1.72 (m, 1H).

^{13}C NMR (126 MHz, $CDCl_3$) δ 154.1, 88.2, 85.9, 81.0, 80.1, 63.3, 62.7, 57.0, 43.3, 22.1, 19.1.

HRMS (ESI) m/z calcd for $C_{11}H_{13}N_2NaO_4$: 295.0456 [$(M+Na)^+$], measured: 295.0444.

***rac*-(1*R*,5*S*,6*S*,8a*R*,8b*R*,9*R*)-octahydro-1,6,3-(epiethane[1,1,2]triyl)furo[3,4-*d*]pyrrolo[1,2-*b*]isoxazol-9-yl bromocarbamate (3.103)**

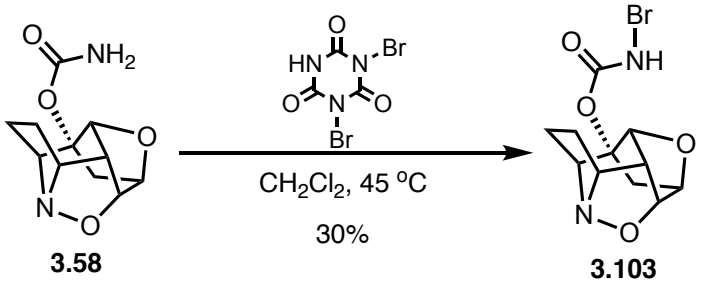

3.58 **3.103**

To a solution of **3.58** (24 mg, 0.101 mmol, 1.0 equiv.) in CH_2Cl_2 (1 mL) was added dibromoisocyanuric acid[20] (18 mg, 0.063 mmol, 0.62 equiv.). The flask was fitted with a

reflux condenser, wrapped with Al foil, and then the reaction mixture was stirred at 45 °C (bath temp.) for 24 h. The reaction mixture was cooled to rt, filtered (washing the precipitate with CH_2Cl_2), and then the filtrate was concentrated *in vacuo* to provide a mixture of **3.103** (~30%, tentative assignment) and unreacted **3.58** (~70%). *N*-Bromocarbamate **3.103** underwent rapid debromination to return **3.58** in the presence of visible light, which precluded its isolation and full characterization.

***rac*-(1*R*,5*S*,6*S*,8a*R*,8b*R*,9*R*)-octahydro-1,6,3-(epiethane[1,1,2]triyl)furo[3,4-*d*]pyrrolo [1,2-*b*]isoxazol-9-yl diethylcarbamate (3.122)**

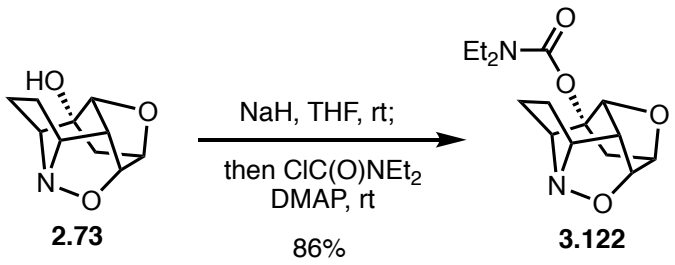

Sodium hydride (60% in mineral oil, 17 mg, 0.425 mmol, 2.2 equiv.) was washed with dry pentane under a stream of Ar (x3) and then dried under high vacuum. THF (0.5 mL) was added and then a solution of **2.73** (37 mg, 0.190 mmol, 1.0 equiv.) in THF (0.9 mL) was added to this suspension *via* cannula and stirred at rt for 30 min. In a separate flask, DMAP (3 mg, 0.025 mmol, 0.13 equiv.) was dissolved in THF (0.5 mL) and then diethylcarbamoyl chloride (72.8 μL, 0.57 mmol, 3.0 equiv.) was added. The resulting cloudy white solution was transferred to the reaction vessel *via* cannula and then the reaction mixture was stirred at rt for 22 h. The reaction was quenched with MeOH, concentrated *in vacuo*, and then purified by flash chromatography (EtOAc) to yield the title compound **3.122** (48.3 mg, 0.164 mmol, 86%) as a white wax-like solid.

IR (neat) ν = 2969, 2937, 2877, 1694, 1475, 1459, 1421, 1380, 1347, 1313, 1274, 1223, 1171, 1159, 1104, 1075, 1018, 981, 943, 928, 902, 888, 867, 843, 789, 767, 736, 726 cm^{-1}.

^{1}H NMR (500 MHz, $CDCl_3$) δ 4.76 (dd, *J* = 6.5, 4.6 Hz, 1H), 4.68 (td, *J* = 4.3, 1.6 Hz, 1H), 4.49 – 4.44 (m, 1H), 4.21 (d, *J* = 4.5 Hz, 1H), 3.54 (dd, *J* = 7.2, 4.3 Hz, 1H), 3.36 – 3.25 (m, 2H), 3.24 – 3.13 (m, 2H), 2.98 (d, *J* = 12.3 Hz, 1H), 2.91 (dt, *J* = 6.5, 4.4 Hz, 1H), 2.07 – 1.87 (m, 4H), 1.81 – 1.71 (m, 1H), 1.19 – 1.05 (m, 6H).

^{13}C NMR (126 MHz, $CDCl_3$) δ 153.9, 86.0, 85.3, 81.1, 80.6, 63.8, 62.8, 57.0, 43.7, 41.5, 22.1, 19.1, 14.3, 13.4.

HRMS (ESI) m/z calcd for $C_{15}H_{23}N_2O_4$: 295.1652 [$(M+H)^+$], measured: 295.1651.

(1*R*,3a*R*,5*S*,6*S*,8a*R*,8b*R*,9*R*)-octahydro-1,6,3-(epiethane[1,1,2]triyl)furo[3,4-*d*]pyrrolo[1,2-*b*]isoxazol-9-yl butylcarbamate (3.123)

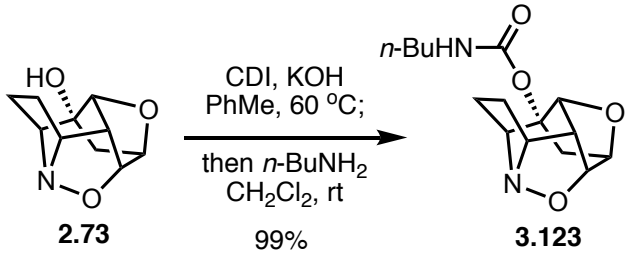

A 100 mL flask was charged with a stir bar, alcohol **2.73** (267 mg, 1.37 mmol, 1.0 equiv.), carbonyl diimidazole (444 mg, 2.74 mmol, 2.0 equiv.), KOH (7.7 mg, 0.14 mmol, 0.1 equiv.) and PhMe (27 mL). The reaction mixture was then stirred at 60 °C (bath temp.) for 19.5 h. After cooling to rt, the mixture was concentrated *in vacuo* and then dissolved in CH_2Cl_2 (14 mL). Butylamine (406 μL, 4.11 mmol, 3.0 equiv.) was added and the resulting solution was stirred at rt for 24 h. The reaction mixture was concentrated *in vacuo* and then purified by flash chromatography (column loaded with CH_2Cl_2; elution with 80% EtOAc:hexanes) to provide the title compound **3.123** (401 mg, 1.36 mmol, 99%) as a white crystalline solid.

$[\alpha]_D$ = -7.3 ° (c = 0.60, $CHCl_3$)

mp = 112-115 °C

IR (neat) ν = 3337, 3234, 2958, 2933, 2873, 1705, 1528, 1467, 1437, 1379, 1347, 1257, 1226, 1175, 1141, 1112, 1074, 1018, 997, 979, 952, 937, 888, 838, 777, 737 cm^{-1}.

^{1}H NMR (400 MHz, $CDCl_3$) δ 4.80 – 4.64 (m, 3H), 4.43 (t, *J* = 3.1 Hz, 1H), 4.15 (d, *J* = 4.5 Hz, 1H), 3.56 – 3.49 (m, 1H), 3.19 – 3.03 (m, 2H), 2.96 (d, *J* = 12.3 Hz, 1H), 2.89 (dt, *J* = 6.4, 4.5 Hz, 1H), 2.08 – 1.88 (m, 4H), 1.79 – 1.67 (m, 1H), 1.49 – 1.40 (m, 2H), 1.36 – 1.26 (m, 2H), 0.90 (t, *J* = 7.3 Hz, 3H).

^{13}C NMR (101 MHz, $CDCl_3$) δ 154.5, 86.0, 85.1, 81.1, 80.5, 63.8, 62.8, 57.0, 43.5, 40.6, 32.0, 22.1, 19.9, 19.1, 13.7.

HRMS (ESI) m/z calcd for $C_{15}H_{23}N_2O_4$: 295.1652 [$(M+H)^+$], measured: 295.1655.

***rac*-(1*S*,5*S*,6*S*,8a*R*,8b*S*,9*R*)-1-(hydroxy(phenyl)methyl)octahydro-1,6,3-(epiethane[1,1,2]triyl)furo[3,4-*d*]pyrrolo[1,2-*b*]isoxazol-9-yl butylcarbamate (3.125)**

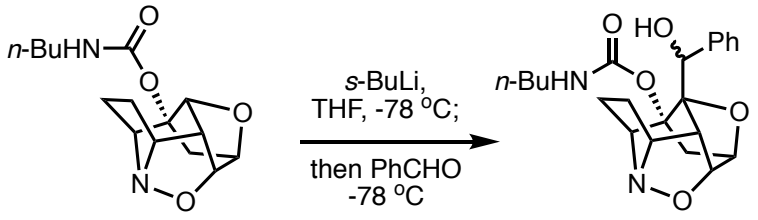

A solution of **3.123** (25 mg, 0.085 mmol, 1.0 equiv.) in THF (0.85 mL) was cooled to -78 °C and *s*-BuLi[15] (1.4 M in cyclohexane, 130 μL, 0.182 mmol, 2.1 equiv.) was added dropwise. The resulting bright yellow solution was stirred at -78 °C for 30 min and then benzaldehyde (43 μL, 0.425 mmol, 5.0 equiv.) was added. The reaction mixture was stirred at -78 °C for 30 min before being quenched with saturated aq. NH_4Cl. The mixture was warmed to rt, diluted with EtOAc, and then the two layers were separated. The aqueous layer was extracted with EtOAc (x2) and then the combined organic layers with washed with brine, dried ($MgSO_4$), and concentrated *in vacuo*. Purification by flash chromatography (60% EtOAc:hexanes to elute **3.125**; 60 → 75% EtOAc:hexanes to elute unreacted **3.123**) yielded the title compound **3.125** (14.7 mg, 0.037 mmol, 43%) as a mixture of diastereomers (d.r. = ~1:1) as an amorphous white solid and recovered **3.123**

(10 mg, 0.034 mmol, 40%). A second purification of **3.125** by preparative thin layer chromatography (75% EtOAc:hexanes, developed twice) allowed separation of the individual diastereomers for characterization.

Diastereomer A:

R_f = 0.51 (75% EtOAc:hexanes, developed twice)

mp = 215 ^{o}C (dec.)

IR (neat) ν = 3330, 2957, 2929, 2869, 1724, 1554, 1469, 1455, 1391, 1298, 1267, 1244, 1225, 1185, 1162, 1136, 1124, 1112, 1063, 1015, 998, 961, 930, 914, 906, 872, 854, 836, 789, 773, 732, 703 cm^{-1}.

^{1}H NMR (500 MHz, $CDCl_3$) δ 7.53 – 7.45 (m, 2H), 7.42 – 7.31 (m, 3H), 5.07 (s, 1H), 4.98 – 4.89 (m, 1H), 4.78 – 4.72 (m, 1H), 4.66 (t, *J* = 4.5 Hz, 1H), 4.54 – 4.49 (m, 1H), 3.39 (s, 1H), 3.30 (s, 1H), 3.21 – 3.07 (m, 3H), 2.37 – 2.19 (m, 2H), 2.18 – 2.10 (m, 1H), 2.08 – 1.87 (m, 3H), 1.52 – 1.43 (m, 2H), 1.39 – 1.29 (m, 2H), 0.93 (t, *J* = 7.3 Hz, 3H).

^{13}C NMR (126 MHz, $CDCl_3$) δ 153.4, 139.2, 128.6, 128.5, 119.0, 89.3, 88.6, 87.3, 76.9, 73.6, 64.0, 63.3, 58.4, 44.6, 40.8, 31.9, 21.4, 19.9, 18.7, 13.7.

HRMS (ESI) m/z calcd for $C_{22}H_{29}N_2O_5$: 401.2071 [$(M+H)^+$], measured: 401.2073.

Diastereomer B:

R_f = 0.36 (75% EtOAc:hexanes, developed twice)

IR (neat) ν = 3340, 2958, 2929, 2868, 1720, 1534, 1455, 1384, 1290, 1268, 1242, 1185, 1162, 1135, 1124, 1112, 1070, 1062, 1051, 995, 961, 930, 907, 872, 836, 785, 732, 706 cm^{-1}.

^{1}H NMR (400 MHz, $CDCl_3$) δ 7.58 – 7.53 (m, 2H), 7.40 – 7.29 (m, 3H), 4.99 (s, 1H), 4.91 – 4.86 (m, 1H), 4.62 (t, *J* = 4.4 Hz, 1H), 4.46 – 4.40 (m, 1H), 3.76 – 3.68 (m, 1H), 3.63 – 3.56 (m, 1H), 3.27 – 3.20 (m, 1H), 3.01 (d, *J* = 12.2 Hz, 1H), 2.99 – 2.87 (m, 2H), 2.31 – 2.15 (m, 2H), 2.15 – 1.98 (m, 3H), 1.87 (dd, *J* = 12.3, 4.4 Hz, 1H), 1.36 – 1.15 (m, 4H), 0.89 (t, *J* = 7.2 Hz, 3H).

^{13}C NMR (101 MHz, $CDCl_3$) δ 153.7, 142.8, 128.7, 128.0, 127.7, 89.7, 87.8, 85.7, 77.2, 72.8, 64.3, 63.9, 55.9, 44.3, 40.2, 31.6, 22.0, 19.7, 18.2, 13.6.

HRMS (ESI) m/z calcd for $C_{22}H_{28}N_2NaO_5$: 423.1890 [$(M+Na)^+$], measured: 423.1881.

***rac*-2-hydroxypropyl ((1*R*,5*S*,6*S*,8a*R*,8b*R*,9*R*)-octahydro-1,6,3-(epiethane[1,1,2]triyl) furo[3,4-*d*]pyrrolo[1,2-*b*]isoxazol-9-yl) (*E*)-butylcarbonimidate (3.134)**

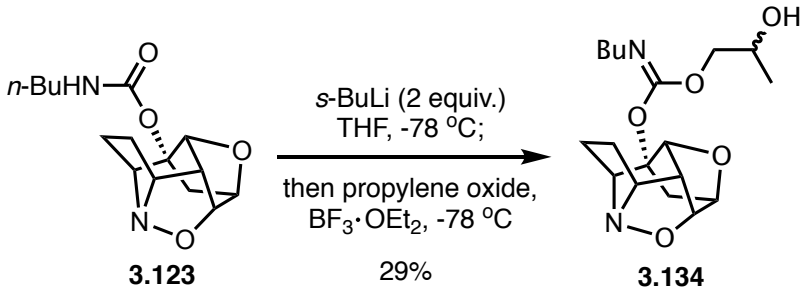

Carbamate **3.123** (10 mg, 0.034 mmol, 1.0 equiv.) was dissolved in THF (340 μL) and cooled to -78 °C. *s*-BuLi[15] (1.4 M in cyclohexane, 53 μL, 0.074 mmol, 2.2 equiv.) was then added dropwise and the resulting bright yellow solution was stirred at this temperature for 30 min. Propylene oxide (11.9 μL, 0.170 mmol, 5.0 equiv.) was added followed immediately by BF_3•OEt_2 (21.4 μL, 0.170 mmol, 5.0 equiv.) and the reaction mixture was stirred at -78 °C for 2 h. The reaction was quenched with a 1:1 MeOH:Et_3N solution (1 mL), warmed to rt and stirred for 1.5 h. The solution was concentrated *in vacuo* and then purified by flash chromatography (5% MeOH:EtOAc) to yield the title compound **3.134** (3.5 mg, 0.010 mmol, 29%) as a mixture was diastereomers and isomers as a colorless oil.

IR (neat) ν = 3441, 2960, 2932, 2873, 1695, 1471, 1418, 1376, 1347, 1312, 1289, 1225,

1155, 1104, 1079, 1018, 997, 978, 939, 911, 889, 859, 836, 770, 737 cm^{-1}.

^{1}H NMR (400 MHz, MeOD) δ 4.79 (t, *J* = 5.6 Hz, 1H), 4.73 – 4.68 (m, 1H), 4.41 – 4.36 (m, 1H), 4.36 – 4.31 (m, 1H), 4.04 – 3.90 (m, 1H), 3.57 – 3.51 (m, 1H), 3.45 – 3.06 (m, 4H), 3.04 – 2.94 (m, 1H), 2.91 – 2.84 (m, 1H), 2.09 – 1.84 (m, 5H), 1.65 – 1.48 (m, 2H), 1.40 – 1.27 (m, 2H), 1.20 – 1.10 (m, 3H), 1.02 – 0.91 (m, 3H).

^{13}C NMR (126 MHz, MeOD) δ 156.5, 156.1, 87.4, 86.9, 82.2, 81.6, 67.2, 67.1, 65.1, 65.1, 64.2, 58.1, 55.6, 55.5, 55.4, 55.3, 49.5, 49.3, 44.8, 44.8, 31.7, 31.7, 30.8, 30.8, 23.1, 23.1, 23.0, 23.0, 21.1, 21.1, 21.0, 21.0, 19.6, 18.2, 14.2, 14.2.

HRMS (ESI) m/z calcd for $C_{18}H_{28}N_2NaO_5$: 375.1890 [$(M+Na)^+$], measured: 375.1885.

(1*S*,3a*R*,5*S*,6*S*,8a*R*,8b*S*,9*R*)-1-bromooctahydro-1,6,3-(epiethane[1,1,2]triyl)furo[3,4-*d*]pyrrolo[1,2-*b*]isoxazol-9-yl butylcarbamate (3.137)

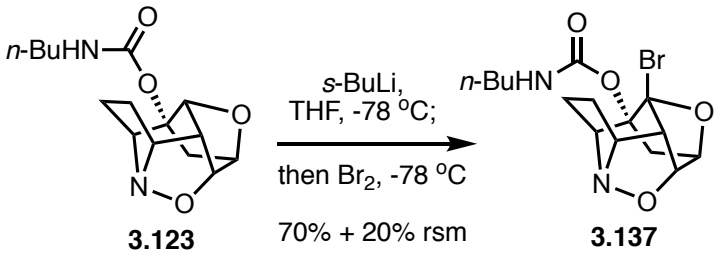

Carbamate **3.123** (59 mg, 0.20 mmol, 1.0 equiv.) was dissolved in THF (2 mL) and cooled to -78 °C. *s*-BuLi[15] (1.37 M in cyclohexane, 322 μL, 0.44 mmol, 2.2 equiv.) was then added dropwise and the resulting bright yellow solution was stirred at this temperature for 45 min. Br_2 (51 μL, 1.00 mmol, 5 equiv.) was then added and the reaction mixture was stirred at -78 °C for 30 min, at which time it was quenched with saturated aq. NH_4Cl and saturated aq. $Na_2S_2O_3$. The mixture was diluted with EtOAc and H_2O and then was warmed to rt, where it was stirred vigorously for 45 min. The two layers were separated and the aqueous layer was extracted with EtOAc (x2). The combined organic layers were washed with brine, dried over $MgSO_4$ and concentrated *in vacuo*. Purification by flash chromatography (column loaded with CH_2Cl_2; **3.137** eluted with 50% EtOAc:hexanes; then unreacted **3.123** eluted with EtOAc) yielded the title compound

3.137 (52 mg, 0.139 mmol, 70%) as a white crystalline solid and unreacted **3.123** (12 mg, 0.041 mmol, 20%) as a white crystalline solid.

$[\alpha]_D$ = +31.3 ^{o} (c = 0.60, $CHCl_3$)

mp = 120-122 ^{o}C

IR (neat) ν = 3348, 2958, 2931, 2873, 1713, 1516, 1465, 1392, 1348, 1298, 1259, 1235, 1215, 1195, 1175, 1135, 1111, 1070, 1024, 1012, 982, 958, 908, 869, 849, 837, 770, 736, 702 cm^{-1}.

^{1}H NMR (500 MHz, $CDCl_3$) δ 4.88 (t, *J* = 6.0 Hz, 1H), 4.86 – 4.80 (m, 1H), 4.65 (t, *J* = 4.7 Hz, 1H), 4.42 (d, *J* = 6.5 Hz, 1H), 3.57 (dd, *J* = 6.9, 4.2 Hz, 1H), 3.32 – 3.05 (m, 3H), 3.02 (d, *J* = 12.3 Hz, 1H), 2.43 – 2.31 (m, 1H), 2.14 (dd, *J* = 12.3, 4.5 Hz, 1H), 2.06 – 1.83 (m, 3H), 1.53 – 1.41 (m, 2H), 1.38 – 1.27 (m, 2H), 0.91 (t, *J* = 7.3 Hz, 3H).

^{13}C NMR (126 MHz, $CDCl_3$) δ 153.7, 92.2, 86.8, 83.1, 77.7, 63.6, 63.4, 63.3, 43.1, 40.6, 31.9, 21.3, 19.9, 17.2, 13.7.

HRMS (ESI) m/z calcd for $C_{15}H_{21}BrN_2NaO_4$: 395.0577 [$(M+Na)^+$], measured: 395.0583.

***rac*-(1*S*,5*S*,6*S*,8a*R*,8b*S*,9*R*)-1-bromooctahydro-1,6,3-(epiethane[1,1,2]triyl)furo[3,4-*d*]pyrrolo[1,2-*b*]isoxazol-9-ol (3.138)**

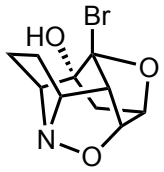

3.138

mp = 160 ^{o}C (dec.)

IR (neat) ν = 3359, 2954, 2923, 2852, 1517, 1464, 1447, 1377, 1310, 1245, 1191, 1172, 1104, 1051, 996, 981, 956, 939, 914, 894, 870, 847, 832, 803, 737 cm^{-1}.

^{1}H NMR (400 MHz, $CDCl_3$) δ 4.82 (t, *J* = 5.9 Hz, 1H), 4.64 (t, *J* = 4.7 Hz, 1H), 3.65 – 3.55 (m, 2H), 3.17 (dd, *J* = 6.9, 4.1 Hz, 1H), 2.71 (d, *J* = 11.6 Hz, 1H), 2.65 (s, 1H), 2.39 – 2.24 (m, 1H), 2.10 – 1.87 (m, 4H).

^{13}C NMR (101 MHz, $CDCl_3$) δ 96.4, 86.6, 78.3, 77.6, 66.5, 63.8, 62.3, 43.9, 21.5, 17.1.

HRMS (ESI) m/z calcd for $C_{10}H_{13}BrNO_3$: 274.0073 [$(M+H)^+$], measured: 274.0065.

(1*R*,3a*R*,5*S*,6*S*,8a*R*,8b*S*,9*R*)-1-allyloctahydro-1,6,3-(epiethane[1,1,2]triyl)furo[3,4-*d*]pyrrolo[1,2-*b*]isoxazol-9-yl butylcarbamate (3.139)

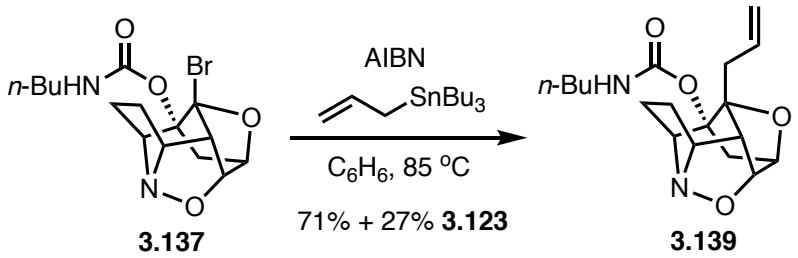

A 50 mL round bottom flask was charged with **3.137** (258 mg, 0.691 mmol, 1.0 equiv.), AIBN (56.7 mg, 0.345 mmol, 0.5 equiv.) and a stir bar. It was topped with a reflux condenser, sealed with a rubber septum and then evacuated and back-filled with Ar (x3). Benzene (13.8 mL) was added followed by allyltributylstannane (1.1 mL, 3.55 mmol, 5.1 equiv.) and then Ar was bubbled through the reaction mixture for 20 min. The reaction mixture was then stirred at 85 °C (bath temp.) for 15 h. After cooling to rt, the reaction mixture was concentrated *in vacuo* and then purified by flash chromatography (column loaded with CH_2Cl_2; **3.139** eluted with 60% EtOAc:hexanes; then **3.123** eluted with EtOAc) to yield the title compound **3.139** (163 mg, 0.487 mmol, 71%) as a colorless oil and **3.123** (54 mg, 0.183 mmol, 27%) as a white crystalline solid.

$[\alpha]_D$ = -3.1 ° (c = 0.70, $CHCl_3$)

IR (neat) ν = 3349, 3071, 2958, 2932, 2873, 1719, 1702, 1640, 1525, 1468, 1431, 1380, 1353, 1336, 1301, 1263, 1250, 1237, 1222, 1209, 1166, 1145, 1110, 1070, 1011, 985, 962, 917, 906, 871, 854, 837, 774, 734 cm^{-1}.

^{1}H NMR (500 MHz, $CDCl_3$) δ 5.93 – 5.81 (m, 1H), 5.23 – 5.12 (m, 2H), 4.83 (dd, *J* = 6.8, 4.7 Hz, 1H), 4.68 (t, *J* = 6.1 Hz, 1H), 4.51 (t, *J* = 4.4 Hz, 1H), 4.45 – 4.40 (m, 1H), 3.48 (dd, *J* = 6.8, 4.2 Hz, 1H), 3.19 – 3.07 (m, 2H), 3.04 (d, *J* = 12.3 Hz, 1H), 2.83 (dd, *J* = 15.6, 5.6 Hz, 1H), 2.77 (dd, *J* = 6.8, 4.3 Hz, 1H), 2.40 (dd, *J* = 15.5, 8.9 Hz, 1H), 2.08 – 1.88 (m, 4H), 1.86 – 1.77 (m, 1H), 1.51 – 1.41 (m, 2H), 1.37 – 1.28 (m, 2H), 0.91 (t, *J* = 7.3 Hz, 3H).

^{13}C NMR (126 MHz, $CDCl_3$) δ 154.3, 133.4, 118.5, 88.0, 86.9, 85.5, 85.0, 63.8, 63.7, 56.0, 44.2, 40.6, 34.2, 32.0, 21.5, 19.9, 18.0, 13.7.

HRMS (ESI) m/z calcd for $C_{18}H_{27}N_2O_4$: 335.1965 [$(M+H)^+$], measured: 335.1952.

(1*R*,3a*R*,5*S*,6*S*,8a*R*,8b*S*,9*R*)-1-allyloctahydro-1,6,3-(epiethane[1,1,2]triyl)furo[3,4-*d*]pyrrolo[1,2-*b*]isoxazol-9-ol (3.140)

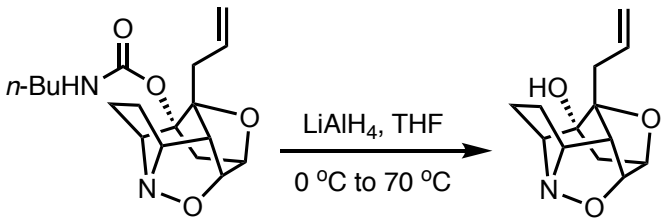

3.139 **3.140**

A solution of **3.139** (49 mg, 0.147 mmol, 1.0 equiv.) in THF (2.9 mL) was cooled to 0 °C and $LiAlH_4$ (16.8 mg, 0.443 mmol, 3.0 equiv.) was added in one portion. The flask was then quickly topped with a reflux condenser that was sealed at the top with a rubber septum. After flushing Ar through the reaction vessel for 5 min, the reaction mixture was heated to 70 °C (bath temp.) and stirred for 2 h at this temp. The mixture was then cooled to 0 °C and the reaction was carefully quenched by sequential addition of H_2O (0.2 mL), 15% aq. NaOH (0.2 mL) and then H_2O again (0.6 mL). The solution was warmed to rt and stirred vigorously for 20 min. After diluting with EtOAc, $MgSO_4$ was added and

vigorous stirring was continued for an additional 20 min. The slurry was then vacuum filtered through a pad of Celite and concentrated *in vacuo*. Purification by flash chromatography (5% MeOH:CH_2Cl_2) yielded the title compound **3.140** (32.5 mg, 0.138 mmol, 94%) as a white waxy solid.

$[\alpha]_D$ = -26.7 ^{o} (c = 0.51, $CHCl_3$)

IR (neat) ν = 3361, 3075, 2957, 2929, 2853, 1640, 1516, 1471, 1432, 1417, 1370, 1311, 1257, 1236, 1219, 1186, 1168, 1104, 1075, 1048, 1007, 985, 961, 923, 907, 888, 872, 854, 834, 718 cm^{-1}.

^{1}H NMR (400 MHz, $CDCl_3$) δ 5.97 – 5.81 (m, 1H), 5.23 – 5.12 (m, 2H), 4.83 – 4.78 (m, 1H), 4.48 (t, *J* = 4.4 Hz, 1H), 3.57 – 3.53 (m, 1H), 3.49 (dd, *J* = 6.6, 4.2 Hz, 1H), 2.81 – 2.71 (m, 3H), 2.39 (dd, *J* = 15.4, 8.6 Hz, 1H), 2.15 – 2.04 (m, 1H), 2.02 – 1.86 (m, 3H), 1.85 – 1.77 (m, 1H), 1.74 (ddd, *J* = 11.4, 4.2, 1.0 Hz, 1H).

^{13}C NMR (101 MHz, $CDCl_3$) δ 133.5, 118.5, 88.0, 86.9, 79.1, 76.7, 67.3, 64.1, 55.5, 46.4, 33.9, 21.6, 17.8.

HRMS (ESI) m/z calcd for $C_{13}H_{18}NO_3$: 236.1281 [$(M+H)^+$], measured: 236.1281.

(-)-virosaine A (1.24)

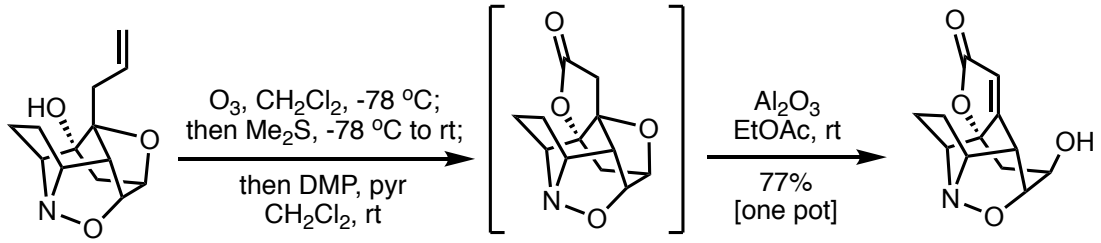

3.140 **2.1** (-)-virosaine A (**1.24**)

A solution of **3.140** (30 mg, 0.128 mmol, 1.0 equiv.) in CH_2Cl_2 (2.6 mL) was cooled to -78 ^{o}C and ozone was bubbled through it until the solution turned blue (~10 s). At this point, O_2 was bubbled through the solution until it became clear again (~10 s). Me_2S (470 μL, 6.40 mmol, 50.0 equiv.) was added and the solution was warmed to rt and stirred

overnight. All volatiles were then removed *in vacuo* (< 0.1 mm Hg) for 1 h and the crude lactol was re-dissolved in CH_2Cl_2 (2.6 mL). Pyridine (103 μL, 1.28 mmol, 10.0 equiv.) was added followed by DMP[8] (81 mg, 0.191 mmol, 1.5 equiv.) and the reaction mixture was stirred at rt for 2 h. MeOH (1 mL) was added to consume the unreacted DMP and the solution was stirred for an additional 15 min at rt. The reaction mixture was then concentrated *in vacuo* before adding EtOAc (1 mL) and activated neutral Al_2O_3 (~1 g). The resulting slurry was stirred at rt for 3 h before filtering through a plug of activated neutral Al_2O_3 (eluting with 5% MeOH:EtOAc). The filtrate was concentrated *in vacuo* and then purified by flash chromatography (2 → 5% MeOH:CH_2Cl_2) to yield (-)-virosaine A (**1.24**) (23.1 mg, 0.098 mmol, 77%) as a white crystalline solid.

$[\alpha]_D$ = -47.6 ^{o} (c = 0.50, MeOH); lit.[21] **$[\alpha]_D$** = -51.6 ^{o} (c = 0.50, MeOH)

mp = 177-178 ^{o}C; lit.[21] **mp** = 177-178 ^{o}C

IR (neat) ν = 3406, 3111, 2955, 2881, 1737, 1654, 1465, 1445, 1350, 1300, 1249, 1212, 1191, 1175, 1157, 1110, 1061, 1048, 1027, 993, 962, 937, 912, 896, 866, 855, 830, 790, 745, 730, 655 cm^{-1}.

^{1}H NMR (500 MHz, CD_3OD) δ 5.85 (s, 1H), 4.68 (ddd, *J* = 6.0, 5.0, 1.3 Hz, 1H), 4.30 (t, *J* = 5.2 Hz, 1H), 4.02 (dd, *J* = 6.8, 4.8 Hz, 1H), 3.92 – 3.88 (m, 2H), 2.93 (dd, *J* = 14.2, 5.7 Hz, 1H), 1.92 (dddd, *J* = 13.4, 11.8, 6.9, 3.1 Hz, 1H), 1.84 (dd, *J* = 14.2, 1.2 Hz, 1H), 1.71 (ddt, *J* = 14.0, 11.9, 6.0 Hz, 1H), 1.49 (ddd, *J* = 13.4, 10.7, 6.1 Hz, 1H), 1.21 (ddd, *J* = 13.9, 10.7, 3.2 Hz, 1H).

^{13}C NMR (126 MHz, CD_3OD) δ 175.5, 171.9, 110.8, 88.0, 85.4, 74.1, 70.9, 65.4, 50.3, 44.7, 22.2, 20.8.

HRMS (ESI) m/z calcd for $C_{12}H_{14}NO_4$: 236.0917 [$(M+H)^+$], measured: 236.0920.

HPLC: Enantiomeric excess (*ee*) of (-)-virosaine A (**1.24**) was determined using a Diacel CHIRALPAK AD (0.46 cm x 25 cm) column:

Eluent: HPLC grade hexane:isopropanol (75:25)

Flow rate: 1.0 mL/min.

Detection wavelength: 254 nm.

Retention time = 6.2 min (minor) and 8.0 min (major).

virosaine A (racemate):

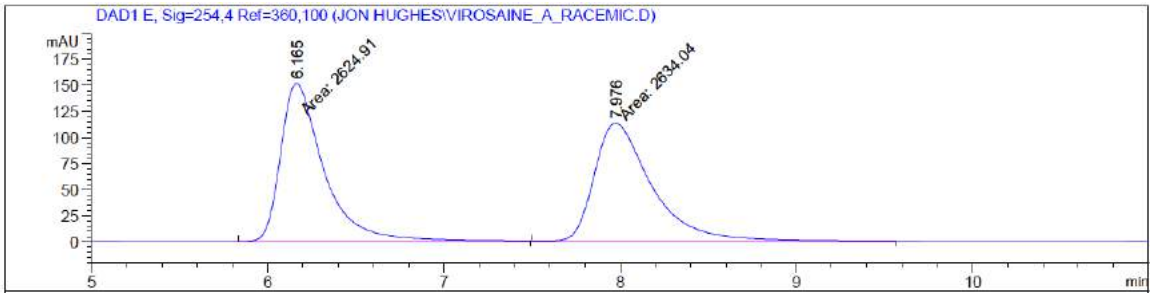

Peak #	RetTime [min]	Type	Width [min]	Area [mAU*s]	Height [mAU]	Area %
1	6.165	MM	0.2886	2624.90869	151.60689	49.9132
2	7.976	MM	0.3865	2634.04053	113.59435	50.0868
Totals :				5258.94922	265.20123	

(-)-virosaine A (>99% *ee*):

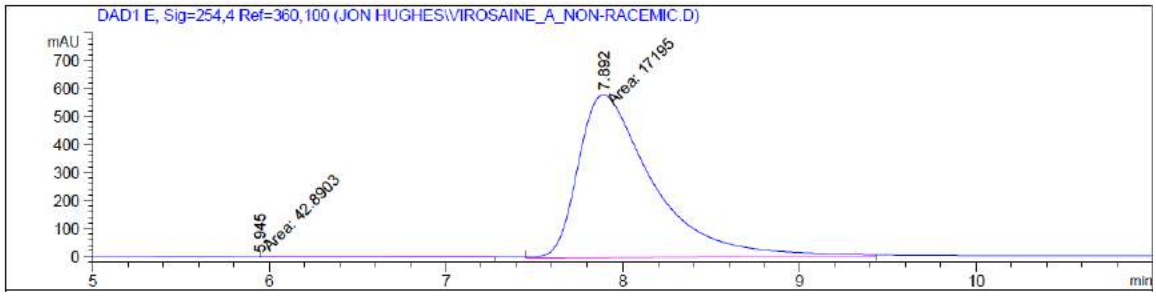

Peak #	RetTime [min]	Type	Width [min]	Area [mAU*s]	Height [mAU]	Area %
1	5.945	MM	0.6010	42.89034	8.35620e-1	0.2488
2	7.892	MM	0.4904	1.71950e4	584.40076	99.7512
Totals :				1.72379e4	585.23638	

5.3.1 Computational Details:

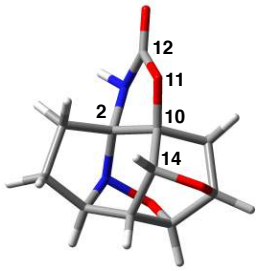

3.61

"top-down perspective"

C14-C10-O11-C12: Dihedral angle = 157 °

C2-C10-O11-C12: Dihedral angle = 35 °

Structure optimized using B3LYP/6-31G*

Charge = 0 Multiplicity = 1

O	0.93668	0.12118	-0.00317
O	2.38582	1.68489	2.79341
C	2.39401	1.84026	0.42076
N	1.98865	3.0107	2.39094
C	2.49724	0.85227	1.60855
C	0.92984	1.55585	0.0218
C	-0.01619	1.92414	1.2281
C	0.04459	0.60283	2.05201
C	2.64306	3.19992	1.07834
C	0.53822	3.1274	2.04906
C	1.25127	-0.06287	1.39185
C	0.5537	4.43448	1.24103
C	1.90306	4.39766	0.46696
H	-0.31464	4.50209	0.58735
H	0.14829	0.76482	3.1237
H	3.43661	0.30444	1.68983
H	-0.83552	-0.00753	1.85238
H	3.0648	1.60093	-0.4055
H	1.76329	4.2763	-0.60937
H	3.71155	3.37374	1.22579
H	0.53037	5.28828	1.92069
H	1.39833	-1.12158	1.59812
H	2.46767	5.31953	0.61461
H	0.58502	1.94627	-0.93259
O	-1.30181	2.2412	0.72335
N	-0.23717	3.25055	3.29184
H	0.28254	3.78636	3.95728
C	-1.51256	3.92452	3.0089
O	-2.21188	4.37076	3.95515

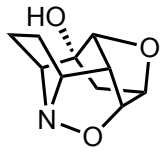

2.73

Structure optimized using B3LYP/6-31G*

Cartesian Coordinates:
Charge = 0 Multiplicity = 1

O	0.21287	2.51255	-0.02453
O	1.98426	0.12671	1.21505
O	0.16863	-1.52313	-1.30979
C	0.04696	-1.10345	1.02764
N	-1.07363	-0.85143	-1.00126
C	0.98949	-1.56289	-0.11242
C	0.56352	0.34307	1.16811
C	0.33524	1.10609	-0.19378
C	1.61841	0.69665	-0.97969
C	-1.34699	-1.23068	0.40205
C	-0.94934	0.63595	-0.92065
C	2.09887	-0.45852	-0.10274
C	-2.22953	0.97705	-0.13805
C	-2.39807	-0.20579	0.86256
H	-2.14251	1.95051	0.34769
H	1.41895	0.42764	-2.01739
H	1.38215	-2.57873	-0.0228
H	2.35246	1.50935	-0.95305
H	0.18407	-1.65452	1.9615
H	-2.23342	0.09729	1.90143
H	-0.95328	1.05953	-1.92877
H	-1.6983	-2.26663	0.43985
H	-3.08031	1.01548	-0.82408
H	3.11978	-0.80823	-0.26008
H	-3.40424	-0.63002	0.8068
H	0.23707	0.90005	2.04757
H	1.03555	2.82439	0.38614

Table S1. NPA partial atomic charges and NBO C-H HOMO energies of **2.73** calculated using B3LYP/6-311++G**.

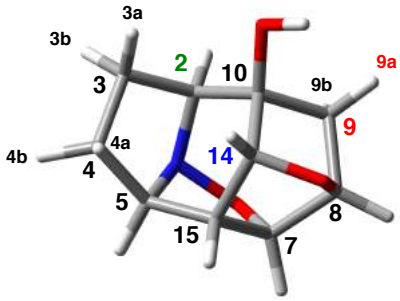

2.73

"top-down perspective"

Site	NPA partial atomic charge		C-H HOMO Energy (eV)
	Hydrogen	Carbon	
2	0.218	-0.037	-13.69
3	**3a:** +0.227 **3b:** +0.213	-0.394	C_3-H_{3a}: -13.55 C_3-H_{3b}: -13.42
4	**4a:** +0.202 **4b:** +0.213	-0.392	C_4-H_{4a}: -13.77 C_4-H_{4b}: -13.63
5	0.213	-0.032	-13.88
7	0.204	0.1	-14.31
8	0.204	0.095	-14.45
9	**9a:** +0.212 **9b:** +0.233	-0.423	C_9-H_{9a}: -13.71 C_9-H_{9b}: -13.80
14	0.212	0.095	-14.48
15	0.233	-0.27	-14.01

5.4 Experimental Procedures for Chapter 4

[1.1.1]Propellane (4.15) as a solution in Et_2O[22]

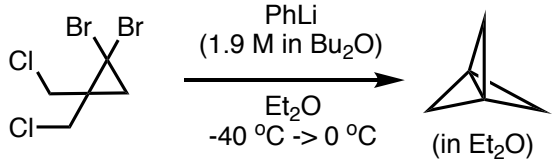

4.14 **4.15**

A flame-dried 250 mL flask, equipped with a stir bar, was charged with 1,1-dibromo-2,2-bis(chloromethyl)cyclopropane (**4.14**) (9.59 g, 32.3 mmol, 1.0 equiv.) and dry Et_2O (20 mL). The resulting solution was cooled to -40 °C, where **4.14** crashed out to give a white slurry. At this temperature, PhLi (1.9 M in Bu_2O, 34 mL, 64.6 mmol, 2.0 equiv.) was added dropwise and the resulting solution was warmed to 0 °C and, after stirring at 0 °C for 2 h, the solution was warmed to rt. The flask was then topped with a 3-way glass adaptor, which was connected at the side to a dry ice condenser and topped with a glass stopper. The dry ice condenser was fitted at the bottom with a 3-necked round bottom flask (receiving flask). The remaining two necks of the receiving flask were fitted with a glass stopper and a rubber septum (see Figure S1 below). The receiving flask was cooled to -78 °C and the condenser was charged with dry ice/acetone. A needle, connected to a Schlenk manifold, was then inserted into the septum of the receiving flask. The title compound **4.15** was then distilled under vacuum by slowly dropping the pressure inside the distillation setup to a final pressure of ~4 mm Hg (the reaction mixture was maintained at rt throughout the duration of distillation). The title compound **4.15** was collected in the receiving flask as a solution in Et_2O (~20 mL).

The concentration of the solution was determined by NMR using 1,2-dichloroethane as an internal standard (IS), as follows:

An aliquot of **4.15** in Et_2O (200 μL) was added to an NMR tube and diluted with $CDCl_3$ (~0.5 mL) and 1,2-dichloroethane (50 μL, 0.63 mmol). The ratio of **4.15** to 1,2-dichloroethane was calculated based on their ^1H NMR integrations and the concentration of **4.15** was determined to be ~0.85 M in Et_2O.

Therefore, the yield of **4.15** (0.85 M in Et_2O, 20 mL) was ~53%.

^{1}H NMR (400 MHz, $CDCl_3$) δ 1.94 (s, 6H).

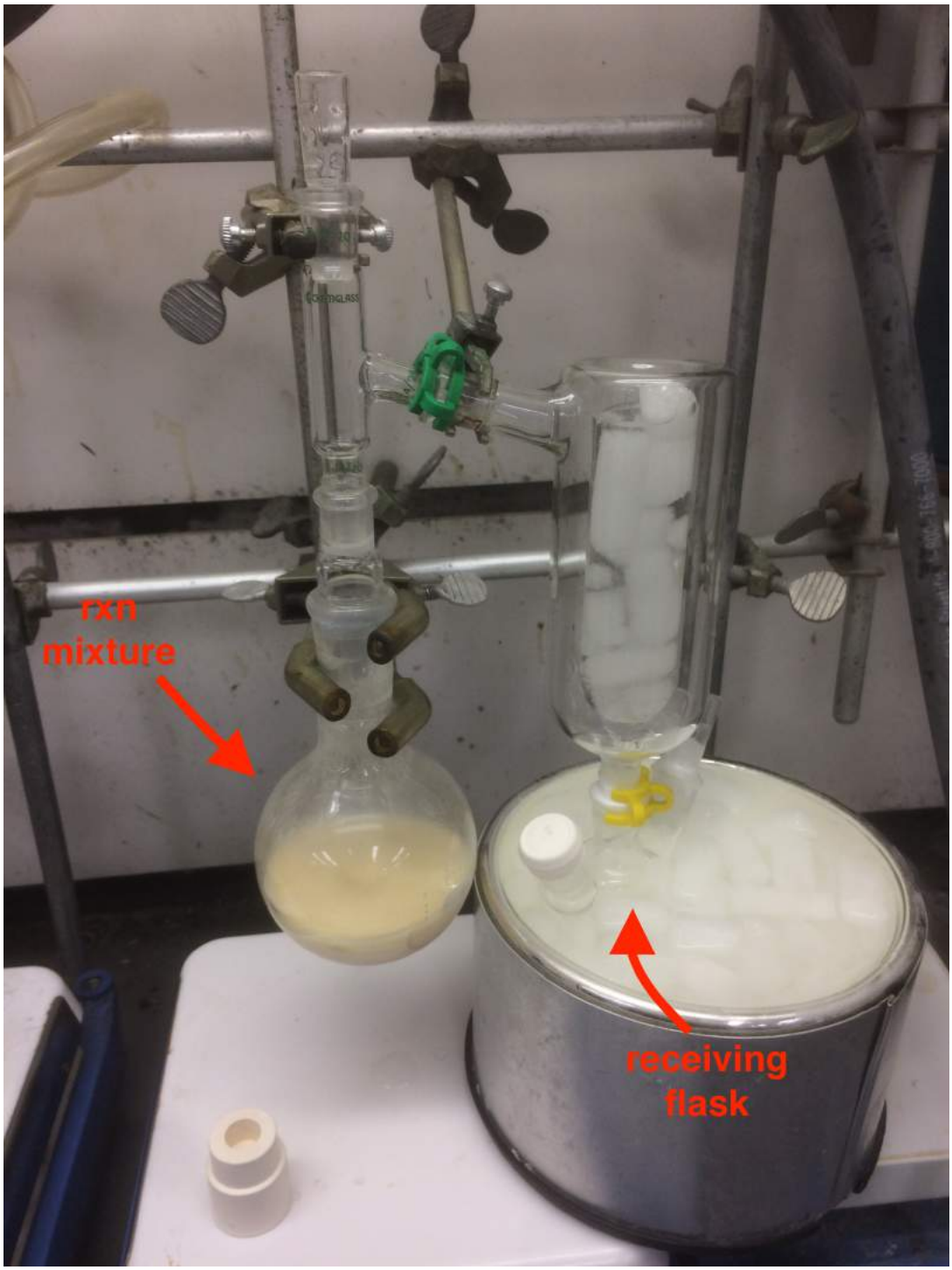

Figure S1. Distillation setup for the isolation of [1.1.1]propellane as a solution in Et_2O.

***N*,*N*-dibenzylbicyclo[1.1.1]pentan-1-amine-3-*d* (4.43)**

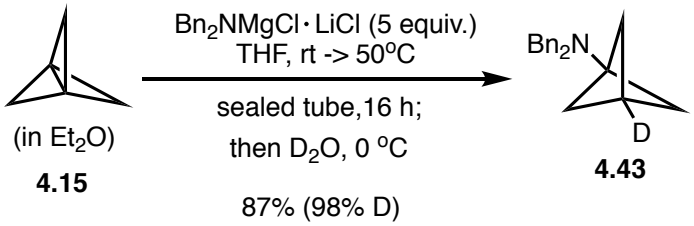

A 25 mL Schlenk flask, equipped with a stir bar, was flame-dried under high vacuum and then cooled to rt under a stream of Ar. The flask was charged with dibenzylamine (480 μL, 2.50 mmol, 5.0 equiv.) and THF (2.5 mL). *i*-PrMgCl•LiCl (1.1 M in THF, 2.28 mL, 2.51 mmol, 5.0 equiv.) was added dropwise and the resulting bright pink solution was stirred at rt for 2 h, after which time it had become a dark red. A solution of **4.15** in Et_2O (0.76 M, 658 μL, 0.50 mmol, 1.0 equiv.) was added dropwise, the Schlenk flask was sealed, and then the reaction mixture was stirred at 50 °C (bath temp.) for 16 h. The solution was cooled to 0 °C and D_2O (2 mL) was added quickly. The resulting white slurry was stirred vigorously for 10 min, at which point saturated aq. NH_4Cl (2 mL) was added. The mixture was extracted with EtOAc (x2) and then the combined organic layers were dried (Na_2SO_4) and concentrated *in vacuo*. Purification by flash chromatography (hexanes → 1% EtOAc:hexanes) yielded the title compound **4.43** (115 mg, 0.435 mmol, 87%) at a white solid.

mp = 59-61 °C

IR (neat) ν = 3086, 3063, 3027, 2964, 2908, 2870, 2803, 1867, 1806, 1746, 1603, 1504, 1494, 1453, 1379, 1325, 1273, 1225, 1187, 1140, 1116, 1102, 1073, 1028, 955, 925, 903, 844, 805, 789, 739, 696 cm^{-1}.

^{1}H NMR (500 MHz, $CDCl_3$) δ 7.39 – 7.35 (m, 4H), 7.30 – 7.23 (m, 4H), 7.22 – 7.15 (m, 2H), 3.63 (s, 4H), 1.67 (s, 6H).

^{13}C NMR (101 MHz, $CDCl_3$) δ 140.7, 128.3, 128.0, 126.5, 61.2, 54.9, 49.5, 22.5 (t, $J_{C\text{-}D}$ = 25.9 Hz).

HRMS (ESI) m/z calcd for $C_{19}H_{21}DN$: 265.1810 [$(M+H)^+$], measured: 265.1801.

3-Allyl-*N*,*N*-dibenzylbicyclo[1.1.1]pentan-1-amine (4.49)

Table 4.1, Entry 11:

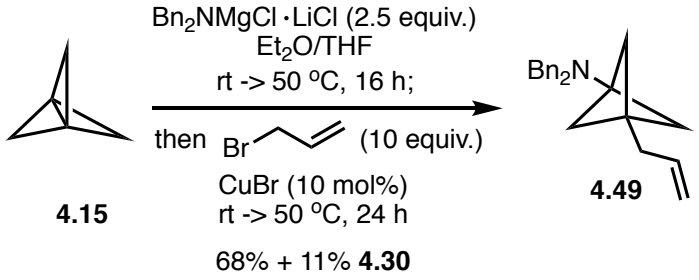

Preparation of "turbo Grignard" solution:

A 25 mL Schlenk flask, equipped with a stir bar, was flame dried under high vacuum and then cooled to rt under a stream of Ar. The flask was charged with dibenzylamine (0.5 mL, 2.6 mmol, 2.5 equiv.) and THF (2.6 mL). *i*-PrMgCl•LiCl (1.3 M in THF, 2.0 mL, 2.6 mmol, 2.5 equiv.) was then added dropwise and the resulting bright pink solution was stirred for 2 h at rt, after which time it had become a dark red. A solution of **4.15** in Et_2O (0.81 M, 1.3 mL, 1.05 mmol, 1.0 equiv.) was added dropwise and the reaction mixture was then heat to 50 °C (bath temp.) and stirred at this temperature for 16 h, before cooling again to rt.

Allylation:

A separate 50 mL Schlenk flask, equipped with a stir bar, was flame-dried under high vacuum and then cooled to rt under a stream of Ar. The flask was charged with CuBr (98%, 16 mg, 0.11 mmol, 0.1 equiv.) and it was then flame-dried under high vacuum for ~ 30 s and then allowed to cool to rt under a stream of Ar. Allyl bromide (0.91 mL, 10.5 mmol, 10.0 equiv.) was added to the CuBr and then the "turbo Grignard" solution (from above) was added to the CuBr/allyl bromide suspension *via* cannula (under vacuum). The flask was sealed and then heat again to 50 °C for 24 h. The reaction mixture was cooled to rt and quenched by the addition of saturated aq. NH_4Cl. The mixture was diluted with H_2O and EtOAc and then was stirred vigorously for 3 h. The two layers were separated and then the aqueous layer was extracted with EtOAc (x2). The combined organic layers

were washed with brine, dried over Na_2SO_4, filtered and concentrated *in vacuo*. Purification by flash chromatography (column packed with hexanes; crude product applied by 'pre-loading' onto silica gel (dry load) and then the product was eluted with 20% CH_2Cl_2:hexanes) provided the title compound **4.49** (68%) + **4.30**[23] (11%) as an inseparable mixture (250 mg total) as a slightly yellow oil.

One-Pot Synthesis of 4.49 from 4.14:

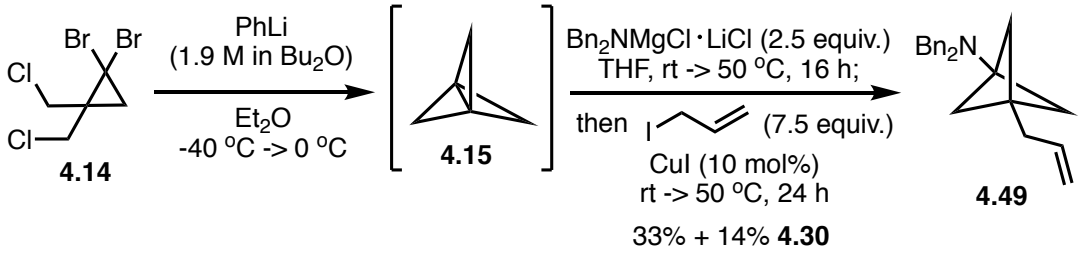

Preparation of "turbo amide" solution:

Dibenzylamine (1.95 mL, 10.1 mmol, 2.5 equiv.) was dissolved in THF (10 mL) and then *i*-PrMgCl•LiCl (1.3 M in THF, 7.8 mL, 10.1 mmol, 2.5 equiv.) was added dropwise. The resulting bright pink solution was stirred at rt for 2 h, after which time it had become a dark red.

Preparation of "turbo Grignard":

A separate flame-dried 100 mL Schlenk flask, equipped with a stir bar, was charged with **4.14** (1.19 g, 4.0 mmol, 1.0 equiv.) and then evacuated and back-filled with Ar (x3). Et_2O (5 mL) was added and the solution was cooled to -40 °C (where a suspension was formed). PhLi (1.9 M in Bu_2O, 4.3 mL, 8.2 mmol, 2.04 equiv.) was added dropwise and the resulting mixture was warmed to 0 °C and stirred for 2 h. The mixture was then warmed to rt and the "turbo amide" solution was added to it *via* cannula (under vacuum). The Schlenk flask was sealed and then the reaction mixture was stirred at 50 °C (bath temp.) for 16 h, at which time it was cooled to rt.

Allylation:

A separate flame-dried 250 mL Schlenk flask, equipped with a stir bar, was charged with CuI (98%, 78 mg, 0.40 mmol, 0.1 equiv.). The CuI was flame-dried under high vacuum

(< 0.01 mm Hg) for ~ 30 seconds and then was allowed to cool to rt under a stream of Ar. Allyl iodide (2.74 mL, 30.0 mmol, 7.5 equiv.) was added and then the "turbo amide" solution was added *via* cannula (under vacumm). The Schlenk flask was sealed and the reaction mixture was stirred at 50 ^{o}C for 24 h. The mixture was cooled to rt and the reaction was quenched with saturated aq. NH_4Cl. The mixture was diluted with EtOAc and H_2O and then stirred vigorously for 2 h. The two layers were separated and the aqueous layer was extracted with EtOAc (x2). The combined organic layers were washed with brine, dried (Na_2SO_4), and concentrated *in vacuo*. Purification by flash chromatography (column packed with hexanes, product eluted with 20% CH_2Cl_2:hexanes) to yield the title compound **4.49** (33%) + **4.30**[23] (14%) as an inseparable mixture (571 mg total) as a yellow oil.

IR (neat) ν = 3063, 3027, 2964, 2906, 2867, 2820, 2800, 1641, 1603, 1510,1494, 1454, 1379, 1363, 1335, 1261, 1226, 1114, 1072, 1028, 991, 941, 912, 740, 697 cm^{-1}.

^{1}H NMR (500 MHz, $CDCl_3$) δ 7.39 – 7.34 (m, 4H), 7.29 – 7.23 (m, 4H), 7.22 – 7.15 (m, 2H), 5.65 (ddt, *J* = 17.3, 10.2, 7.2 Hz, 1H), 4.98 – 4.89 (m, 2H), 3.61 (s, 4H), 2.19 (dt, *J* = 7.2, 1.2 Hz, 2H), 1.51 (s, 6H).

^{13}C NMR (101 MHz, $CDCl_3$) δ 140.7, 135.7, 128.3, 127.9, 126.5, 115.6, 58.0, 55.1, 49.5, 35.4, 34.5.

HRMS (APCI) m/z calcd for $C_{22}H_{26}N$: 304.2060 [$(M+H)^+$], measured: 304.2055.

(*S*)-3-(3-(dibenzylamino)bicyclo[1.1.1]pentan-1-yl)propane-1,2-diol (4.51)

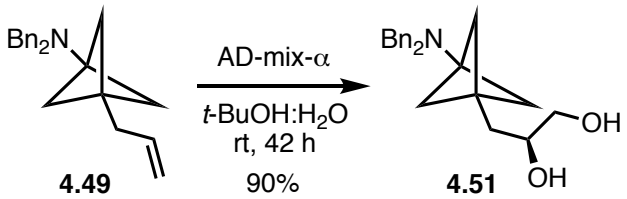

A 25 mL flask was charged with **4.49** (63 mg, 0.21 mmol, 1.0 equiv.), *t*-BuOH (1.4 mL) and H_2O (1.4 mL). While stirring vigorously, AD-mix-α (400 mg) was added in one

portion. The resulting yellow solution was stirred at rt for 42 h before being quenched with solid Na_2SO_3 (420 mg). The mixture was stirred for an additional 1 h and then extracted with EtOAc (x4). The combined organic layers were dried (Na_2SO_4), concentrated *in vacuo*, and purified by flash chromatography (1:1 hexanes:EtOAc) to yield the title compound **4.51** (64 mg, 0.19 mmol, 90%) as a white solid.

mp = 91-93 ^oC

IR (neat) ν = 3365, 3087, 3063, 3027, 2962, 2905, 2867, 1602, 1586, 1494, 1454, 1381, 1363, 1331, 1263, 1226, 1175, 1074, 1043, 1028, 940, 900, 890, 858, 741, 697 cm^{-1}.

^{1}H NMR (400 MHz, $CDCl_3$) δ 7.39 – 7.33 (m, 4H), 7.29 – 7.23 (m, 4H), 7.21 – 7.15 (m, 2H), 3.67 (tdd, *J* = 7.6, 5.0, 3.0 Hz, 1H), 3.61 (s, 4H), 3.57 (dd, *J* = 11.1, 3.1 Hz, 1H), 3.36 (dd, *J* = 11.0, 7.5 Hz, 1H), 1.90 (s, 2H), 1.63 – 1.52 (m, 8H).

^{13}C NMR (101 MHz, $CDCl_3$) δ 140.6, 128.3, 128.0, 126.6, 71.3, 66.9, 57.9, 55.1, 50.6, 34.0, 33.1.

HRMS (ESI) m/z calcd for $C_{22}H_{28}NO_2$: 338.2115 [$(M+H)^+$], measured: 338.2122.

2-(3-(Dibenzylamino)bicyclo[1.1.1]pentan-1-yl)acetic acid (4.52)

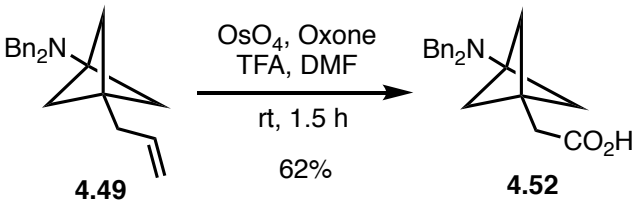

4.49 **4.52**

To a solution of **4.49** (62 mg, 0.20 mmol, 1.0 equiv.) stirring in DMF (1 mL) at rt was added trifluoroacetic acid (80 μL, 1.0 mmol, 5.0 mmol). The solution was stirred at rt for 5 min. Oxone (492 mg, 0.80 mmol, 4.0 equiv.) was added followed by OsO_4 (2.5% in *t*-BuOH, 20 μL, 2.0 μmol, 0.01 equiv.) and the reaction mixture was stirred at rt for 1.5 h. The reaction was quenched by the addition of solid Na_2SO_3 (380 mg), diluted with EtOAc and then stirred vigorously at rt for 4 h. A pH 7.5 phosphate buffer solution (1 M,

~10 mL) was added and the pH of the aq. layer was confirmed to be neutral with litmus paper. The two layers were separated and the aq. layer was extracted with EtOAc (x2). The combined organic layers were dried over Na_2SO_4, filtered and then concentrated *in vacuo*. Purification by flash chromatography (column packed with CH_2Cl_2; product eluted with 40% EtOAc:hexanes) yielded the title compound **4.52** (39.8 mg, 62%) as a white solid.

Note: This oxidation can also be carried out in the absence of trifluoroacetic acid, to provide the compound **4.52** with only a slightly lower yield of 59%.

Oxidation of an inseparable mixture of 4.49 + 4.30:

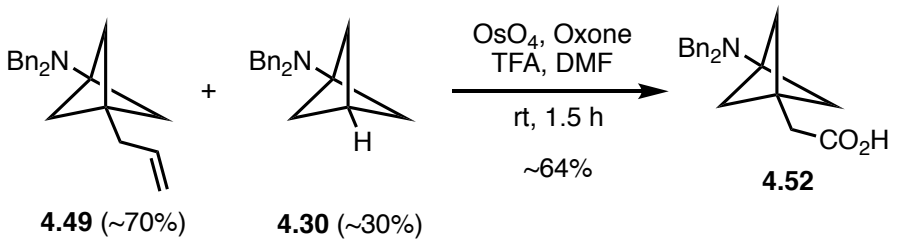

Note: Although **4.49** and **4.30** are inseparable by column chromatography, the mixture can be submitted to the OsO_4/Oxone-mediated oxidation reaction to provide acid **4.52** in comparable yields to those obtained when using pure **4.49**. *When submitting a mixture of* **4.49**/**4.30** *to this reaction, the quantity of the reagents employed should be adjusted such that the stoichiometry is based on the amount of* **4.49** *in the mixture only.*

A mixture of **4.49** (~70%) and **4.30** (~30%) (567 mg total, ~1.31 mmol of **4.49**) was dissolved in DMF (6.6 mL). Trifluoroacetic acid (0.5 mL, 6.53 mmol, 5.0 equiv.) was added and the solution was stirred for 5 min. Oxone (3.22 g, 5.24 mmol, 4.0 equiv.) was added followed by OsO_4 (2.5% in *t*-BuOH, 130 μL, 0.013 mmol, 0.01 equiv.) and the reaction mixture was stirred at rt for 1.5 h. The reaction was quenched by the addition of solid Na_2SO_3 (3.4 g), diluted with EtOAc and then stirred vigorously at rt for 2 h. A pH 7.5 phosphate buffer solution (1 M, ~50 mL) was added and the pH of the aq. layer was confirmed to be neutral with litmus paper. The two layers were separated and the aq. layer was extracted with EtOAc (x2). The combined organic layers were dried over

Na_2SO_4, filtered and then concentrated *in vacuo*. Purification by flash chromatography (column packed with CH_2Cl_2; product eluted with 40% EtOAc:hexanes) yielded the title compound **4.52** (268 mg, ~64% based on **4.49** in the starting mixture) as a white solid.

mp = 123 °C (dec.)

IR (neat) ν = 3300-2500 (br), 3057, 3022, 2969, 2909, 2805, 1708, 1601, 1512, 1494, 1454, 1382, 1364, 1330, 1300, 1258, 1225, 1138, 1110, 1071, 1028, 1002, 970, 941, 904, 743, 670 cm^{-1}.

^{1}H NMR (400 MHz, $CDCl_3$) δ 10.00 (s, 1H), 7.40 (d, *J* = 7.4 Hz, 4H), 7.30 (t, *J* = 7.5 Hz, 4H), 7.23 (t, *J* = 7.2 Hz, 2H), 3.66 (s, 4H), 2.55 (s, 2H), 1.72 (s, 6H).

^{13}C NMR (101 MHz, $CDCl_3$) δ 177.8, 140.5, 128.4, 128.1, 126.7, 57.8, 55.2, 50.7, 36.0, 31.6.

HRMS (ESI) m/z calcd for $C_{21}H_{24}NO_2$: 322.1802 [$(M+H)^+$], measured: 322.1803.

Ethyl 2-(3-(dibenzylamino)bicyclo[1.1.1]pentan-1-yl)acetate (4.53)

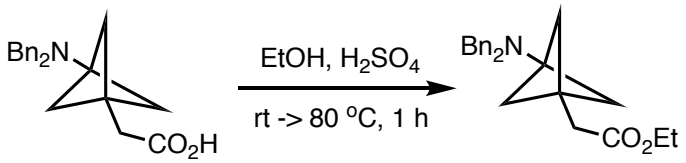

4.52 **4.53**

To a solution of **4.52** (20 mg, 0.062 mmol, 1.0 equiv.) stirring in EtOH (6 mL) was added 1 drop of concentrated H_2SO_4. The reaction flask was topped with a reflux condenser and then heat to 80 °C (bath temp.) for 1 h. The reaction mixture was cooled to 0 °C and quenched with saturated aq. $NaHCO_3$ (~2 mL). A minimum amount of H_2O was added to dissolve the formed salts and then the EtOH was removed *in vacuo* on a rotary evaporator. The aqueous layer was then extracted with EtOAc (x3). The combined organic layers were washed with brine, dried over Na_2SO_4, filtered, and concentrated *in*

vacuo to provide the title compound **4.53** (21 mg, 97%) as a clear oil, which was used in the next step without any further purification.

Note: Alternatively, the title compound **4.53** can be prepared by conducting the same reaction at rt, with an extended reaction time of 5 h to give a crude yield of 95%.

IR (neat) ν = 3063, 3028, 2972, 2908, 2871, 2810, 1734,1668, 1603, 1581, 1515, 1494, 1454, 1367, 1302, 1259, 1226, 1192, 1139, 1096, 1073, 1046, 1028, 1003, 972, 941, 906, 827, 741, 697, 671 cm^{-1}.

^{1}H NMR (400 MHz, $CDCl_3$) δ 7.40 – 7.34 (m, 4H), 7.30 – 7.23 (m, 4H), 7.22 – 7.16 (m, 2H), 4.09 (q, *J* = 7.2 Hz, 2H), 3.63 (s, 4H), 2.47 (s, 2H), 1.66 (s, 6H), 1.23 (t, *J* = 7.1 Hz, 3H).

^{13}C NMR (101 MHz, $CDCl_3$) δ 171.6, 140.5, 128.4, 128.0, 126.6, 60.2, 57.8, 55.2, 50.6, 36.3, 31.9, 14.3.

HRMS (ESI) m/z calcd for $C_{23}H_{28}NO_2$: 350.2115 [$(M+H)^+$], measured: 350.2108.

3-(2-Ethoxy-2-oxoethyl)bicyclo[1.1.1]pentan-1-aminium chloride (4.37)

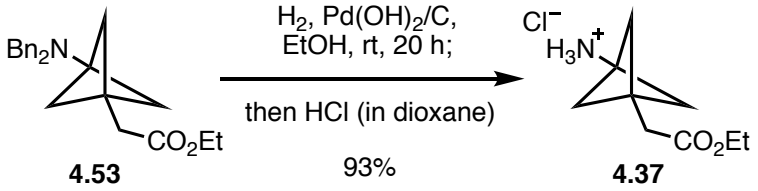

4.53 **4.37**

To a solution of **4.53** (41 mg, 0.12 mmol, 1.0 equiv.) in EtOH (1.2 mL) was added $Pd(OH)_2/C$ (20% Pd, 8.2 mg, 20 wt. %). The flask was briefly evacuated and then back-filled with H_2 (x3). H_2 was then bubbled through the reaction mixture for ~30 s and then the reaction was stirred under 1 atm (balloon) of H_2 for 20 h. The reaction mixture was vacuum filtered through a pad of Celite, washing several times with EtOH, and then the filtrate was treated with HCl (4.0 M in dioxane) and concentrated *in vacuo*. EtOAc was

added to the resulting residue and it was concentrated *in vacuo* to provide the title compound **4.37** (23 mg, 93%) as an off-white amorphous solid.

IR (neat) ν = 3393, 2983, 2921, 2849, 2820, 2735, 2573, 2494, 1732, 1596, 1449, 1375, 1311, 1249, 1195, 1133, 1105, 1076, 1033, 923, 911, 867, 800 cm^{-1}.

^{1}H NMR (500 MHz, $(CD_3)_2SO$) δ 8.77 (s, 3H), 4.05 (q, *J* = 7.1 Hz, 2H), 2.61 (s, 2H), 1.94 (s, 6H), 1.17 (t, *J* = 7.1 Hz, 3H).

^{13}C NMR (126 MHz, $(CD_3)_2SO$) δ 170.9, 60.5, 52.5, 44.0, 34.9, 33.4, 14.7.

HRMS (ESI) m/z calcd for $C_9H_{16}NO_2$: 170.1176 $[(M+H)^+]$, measured: 170.1176.

General Procedure for the Synthesis of 3-Alkyl Bicyclo[1.1.1]pentan-1-amines:

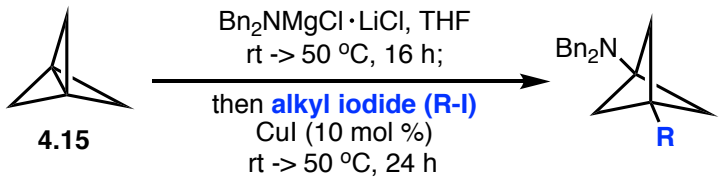

Procedure A (for liquid alkyl iodides with known density):

Preparation of "turbo Grignard" solution:

A 25 mL Schlenk flask, equipped with a stir bar, was flame dried under high vacuum and then cooled to rt under a stream of Ar. The flask was charged with dibenzylamine (240 μL, 1.25 mmol, 2.5 equiv.) and dry THF (1.2 mL). *i*-PrMgCl-LiCl (1.3 M in THF, 1.0 mL, 1.30 mmol, 2.6 equiv.) was then added dropwise and the resulting bright pink solution was stirred for 2 h at rt, after which time it had become a dark red. A solution of **4.15** in Et_2O (0.85 M, 590 μL, 0.50 mmol, 1.0 equiv.) was added dropwise and the reaction mixture was then heat to 50 °C (bath temp.) and stirred at this temperature for 16 h, before cooling again to rt.

A separate 50 mL Schlenk flask, equipped with a stir bar, was flame-dried under high vacuum and then cooled to rt under a stream of Ar. The flask was charged with CuI

(98%, 10 mg, 0.051 mmol, 0.1 equiv.) and it was then flame-dried under high vacuum for ~ 30 seconds and then allowed to cool to rt under a stream of Ar. The alkyl iodide (7.5 equiv.) was added *via* syringe to the CuI and then the "turbo Grignard" solution (from above) was added to the CuI/alkyl iodide suspension *via* cannula (under vacuum). The flask was sealed and the reaction mixture was heat to 50 ^{o}C for 24 h. The reaction was then cooled to rt and quenched by the addition of saturated aq. NH_4Cl. The mixture was diluted with H_2O and EtOAc and then was stirred vigorously for 3 h. The two layers were separated and then the aqueous layer was extracted with EtOAc (x2). The combined organic layers were washed with brine, dried (Na_2SO_4), and concentrated *in vacuo*. The product was purified by flash chromatography (column packed with hexanes; crude product applied by 'pre-loading' onto silica gel (dry load) and then the product was eluted using the indicated solvent system).

Procedure B (for solid alkyl iodides or liquid alkyl iodides with no known density):

Preparation of "turbo Grignard" solution:

A 25 mL Schlenk flask, equipped with a stir bar, was flame dried under high vacuum and then cooled to rt under a stream of Ar. The flask was charged with dibenzylamine (240 μL, 1.25 mmol, 2.5 equiv.) and dry THF (1.2 mL). *i*-PrMgCl-LiCl (1.3 M in THF, 1.0 mL, 1.30 mmol, 2.6 equiv.) was then added dropwise and the resulting bright pink solution was stirred for 2 h at rt, after which time it had become a dark red. A solution of **4.15** in Et_2O (0.85 M, 590 μL, 0.50 mmol, 1.0 equiv.) was added dropwise and the reaction mixture was then heat to 50 ^{o}C (bath temp.) and stirred at this temperature for 16 h, before cooling again to rt.

A separate 50 mL Schlenk flask, equipped with a stir bar, was flame-dried under high vacuum and then cooled to rt under a stream of Ar. The flask was charged with CuI (98%, 10 mg, 0.051 mmol, 0.1 equiv.) and it was then flame-dried under high vacuum for ~ 30 seconds and then allowed to cool to rt under a stream of Ar. The alkyl iodide (7.5 equiv.) was added as a solution in THF (1 mL) to the CuI and then the "turbo Grignard" solution (from above) was added to the CuI/alkyl iodide suspension *via* cannula (under vacuum). The flask was sealed and the reaction mixture was heat to 50 ^{o}C for 24 h. The

reaction was then cooled to rt and quenched by the addition of saturated aq. NH_4Cl. The mixture was diluted with H_2O and EtOAc and then was stirred vigorously for 3 h. The two layers were separated and then the aqueous layer was extracted with EtOAc (x2). The combined organic layers were washed with brine, dried (Na_2SO_4), and concentrated *in vacuo*. The product was purified by flash chromatography (column packed with hexanes; crude product applied by 'pre-loading' onto silica gel (dry load) and then the product was eluted using the indicated solvent system).

3-Allyl-*N*,*N*-dibenzylbicyclo[1.1.1]pentan-1-amine (4.49)

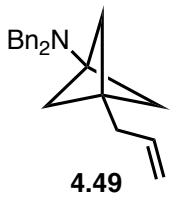

4.49

Prepared according to: Procedure A

Alkyl halide: allyl iodide

Purified by eluting with: 20% CH_2Cl_2:hexanes

Yield = 109 mg (72%)

Physical state: slightly yellow oil

*See page 257 for spectral data

***N*,*N*,3-tribenzylbicyclo[1.1.1]pentan-1-amine (4.54)**

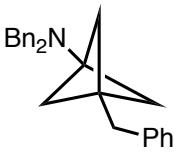

4.54

Prepared according to: Procedure B

Alkyl halide: benzyl iodide

Purified by eluting with: 20% → 40% CH_2Cl_2:hexanes

Yield = 116 mg (67%)

Physical state: white solid

mp = 92-94 ^{o}C

IR (neat) ν = 3085, 3062, 3026, 2964, 2905, 2867, 2803, 2869, 1807, 1730, 1603, 1584, 1512, 1494, 1453, 1380, 1363, 1333, 1297, 1262, 1225, 1174, 1113, 1073, 1028, 999, 971, 940, 904, 843, 740, 697, 658 cm^{-1}.

^{1}H NMR (400 MHz, $CDCl_3$) δ 7.33 (m, 4H), 7.27 – 7.21 (m, 6H), 7.20 – 7.14 (m, 3H), 7.06 – 7.02 (m, 2H), 3.58 (s, 4H), 2.74 (s, 2H), 1.48 (s, 6H).

^{13}C NMR (126 MHz, $CDCl_3$) δ 140.7, 139.9, 128.9, 128.3, 128.1, 128.0, 126.5, 125.7, 58.2, 55.1, 49.6, 37.8, 36.0.

HRMS (ESI) m/z calcd for $C_{26}H_{28}N$: 354.2216 [$(M+H)^{+}$], measured: 354.2228.

***N*,*N*-dibenzyl-3-propylbicyclo[1.1.1]pentan-1-amine (4.55)**

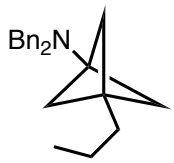

4.55

Prepared according to: Procedure A

Alkyl halide: 1-iodopropane

Purified by eluting with: 20% CH_2Cl_2:hexanes

Yield = 102 mg (67%)

Physical state: slightly yellow wax-like solid

IR (neat) ν = 3086, 3063, 3027, 2958, 2905, 2867, 2840, 1706, 1671, 1603, 1585, 1513, 1494, 1454, 1379, 1363, 1332, 1260, 1225, 1179, 1114, 1104, 1071, 1028, 985, 941, 915, 902, 827, 805, 739, 696 cm^{-1}.

^{1}H NMR (400 MHz, $CDCl_3$) δ 7.40 – 7.33 (m, 4H), 7.30 – 7.21 (m, 4H), 7.21 – 7.14 (m, 2H), 3.60 (s, 4H), 1.48 (s, 6H), 1.42 – 1.33 (m, 2H), 1.26 – 1.12 (m, 2H), 0.84 (t, *J* = 7.3 Hz, 3H).

^{13}C NMR (101 MHz, $CDCl_3$) δ 140.9, 128.4, 127.9, 126.5, 57.3, 55.1, 49.6, 35.5, 32.8, 20.3, 14.3.

HRMS (ESI) m/z calcd for $C_{22}H_{28}N$: 306.2216 [$(M+H)^+$], measured: 306.2214.

***N*,*N*-dibenzyl-3-isopropylbicyclo[1.1.1]pentan-1-amine (4.56)**

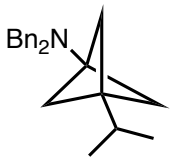

4.56

Prepared according to: Procedure A
Alkyl halide: 2-iodopropane
Purified by eluting with: 20% CH_2Cl_2:hexanes
Yield = 88 mg (58%)
Physical state: white solid

mp = 49-51 ^oC

IR (neat) ν = 3086, 3063, 3027, 2958, 2905, 2867, 2801, 1604, 1512, 1494, 1454, 1380, 1363, 1326, 1295, 1263, 1225, 1181, 1155, 1112, 1073, 1028, 987, 940, 902, 834, 803, 777, 738, 697 cm^{-1}.

^{1}H NMR (400 MHz, $CDCl_3$) δ 7.38 (d, *J* = 7.5 Hz, 4H), 7.27 (t, *J* = 7.5 Hz, 4H), 7.19 (t, *J* = 7.3 Hz, 2H), 3.62 (s, 4H), 1.72 – 1.62 (m, 1H), 1.44 (s, 6H), 0.77 (d, *J* = 6.7 Hz, 6H).

^{13}C NMR (101 MHz, $CDCl_3$) δ 140.9, 128.3, 127.9, 126.5, 56.7, 55.1, 47.0, 40.2, 27.6, 19.2.

HRMS (ESI) m/z calcd for $C_{22}H_{28}N$: 306.2216 [$(M+H)^+$], measured: 306.2227.

3-(2-(1,3-dioxolan-2-yl)ethyl)-*N*,*N*-dibenzylbicyclo[1.1.1]pentan-1-amine (4.57)

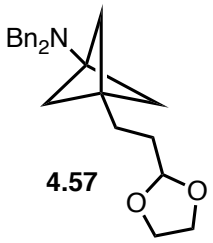

4.57

Prepared according to: Procedure B

Alkyl halide: 2-(2-iodoethyl)-1,3-dioxolane[16]

Purified by eluting with: CH_2Cl_2 → 0.5% Et_2O:CH_2Cl_2

Yield = 118 mg (65%)

Physical state: white solid

mp = 75-77 ^oC

IR (neat) ν = 3062, 3027, 2961, 2904, 2866, 1603, 1514, 1494, 1452, 1407, 1382, 1362, 1332, 1266, 1225, 1123, 1064, 1028, 969, 942, 895, 834, 781, 740, 698 cm^{-1}.

^{1}H NMR (400 MHz, $CDCl_3$) δ 7.39 – 7.33 (m, 4H), 7.29 – 7.23 (m, 3H), 7.21 – 7.15 (m, 2H), 4.83 – 4.78 (m, 1H), 3.98 – 3.87 (m, 2H), 3.87 – 3.77 (m, 2H), 3.61 (s, 4H), 1.57 – 1.53 (m, 4H), 1.50 (s, 6H).

^{13}C NMR (101 MHz, $CDCl_3$) δ 140.7, 128.4, 128.0, 126.5, 104.4, 64.9, 57.3, 55.1, 49.4, 35.1, 31.5, 24.8.

HRMS (ESI) m/z calcd for $C_{24}H_{30}NO_2$: 364.2271 [$(M+H)^+$], measured: 364.2288.

References

(1) Racemic 3-(1H-indol-3-yl)-2-((4-methylphenyl)sulfonamido)butanoic acid was synthesized according to: (a) Sawai, Y.; Mizuno, M.; Ito, T.; Kawakami, J.-I.; Yamano, M. *Tetrahedron* **2009**, *65*, 7122. (b) Zipfel, H. F.; Carreira, E. M. *Org. Lett.* **2014**, *16*, 2854.

(2) Resolution to the 2*S*,3*R* enantiomer was achieved by recrystallization of the diastereomeric 1:1 salts with (-)-norephedrine, according to: Corey, E. J.; Loh, T.-P.; Roper, T. D.; Azimioara, M. D.; Noe, M. C. *J. Am. Chem. Soc.* **1992**, *114*, 8290.

(3) Brown, H. C.; Levy, A. B. *J. Organomet. Chem.* **1972**, *44*, 233.

(4) Brown, H. C.; Racherla, U. S. *J. Org. Chem.* **1986**, *51*, 427.

(5) Modified from Schindler, C. S.; Stephenson, C. R. J.; Carreira, E. M. *Angew. Chem. Int. Ed.* **2008**, *47*, 8852.

(6) Charette, A. B.; Lebel, H. *Org. Synth., Coll. Vol. 10*. **2004**, 613.

(7) Armbrust, K. W.; Beaver, M. G.; Jamison, T. F. *J. Am. Chem. Soc.* **2015**, *137*, 6941.

(8) Boeckman, Jr., R. K.; Shao, P.; Mullins, J. J. *Org. Synth., Coll. Vol. 10,* **2004**, 696; *Vol. 77*, **2000**, 141.

(9) Corey, E. J.; Shibata, T.; Lee, T. W. *J. Am. Chem. Soc.* **2002**, *124*, 3808.

(10) 2-Bromoacrolein is commercially available and can also be easily prepared: Nicolaou, K. C.; Brenzovich, W. E.; Bulger, P. G.; Francis, T. M. *Org. Biomol. Chem.* **2006**, *4*, 2119. We found that best results were obtained when using freshly prepared 2-bromoacrolein. However, it can be stored under argon in the dark at -20 ^{o}C for several weeks and then redistilled prior to use without significant decreases in its quality.

(11) (a) Baciocchi, E.; Muraglia, E.; Sleiter, G. *J. Org. Chem.* **1992**, *57*, 6817. (b) Baciocchi, E.; Muraglia, E. *Tetrahedron Lett.* **1993**, *34*, 5015. (c) Loiseau, F.; Simone, J.-M.; Carcache, D.; Bobal, P.; Neier, R. *Monatshefte für Chem.* **2007**, *138*, 121.

(12) Ryu, D. H.; Corey, E. J. *J. Am. Chem. Soc.* **2003**, *125*, 6388

(13) Carlson, R. M.; Hill, R. K. *Org. Synth., Coll. Vol. 6*, **1988**, 196; *Vol. 50,* **1970**, 24

(14) Jakobsche, C. E.; Peris, G.; Miller, S. J. *Angew. Chem. Int. Ed.* **2008**, *47*, 6707.

(15) Titrated following the procedure in: Watson, S. C.; Eastham, J. F. *J. Organomet. Chem.* **1967**, *9*, 165.

(16) Zhao, Y.; Chen, G. *Org. Lett.* **2011**, *13*, 4850.

(17) Danheiser, R. L.; Miller, R. F.; Brisbois, R. G.; Park, S. Z. *J. Org. Chem.* **1990**, *55*, 1959.

(18) Guthikonda, K.; Du Bois, J. *J. Am. Chem. Soc.* **2002**, *124*, 13672.

(19) Prepared according to: Larinov, O. V.; Kozhushkov, S. I.; de Meijere, A. *Synthesis* **2003**, *12*, 1916.

(20) Demko, Z. P.; Bartsch, M.; Sharpless, K. B. *Org. Lett.* **2000**, *2*, 2221.

(21) Zhao, B.-X.; Wang, Y.; Zhang, D.-M.; Huang, X.-J.; Bai, L.-L.; Yan, Y.; Chen, J.-M.; Lu, T.-B.; Wang, Y.-T.; Zhang, Q.-W.; Ye, W.-C. *Org. Lett.* **2012**, *14*, 3096.

(22) Gianatassio, R.; Lopchuk, J. M.; Wang, J.; Pan, C.-M.; Malins, L. R.; Prieto, L.; Brandt, T. A.; Collins, M. R.; Gallego, G. M.; Sach, N. W.; Spangler, J. E.; Zhu, H.; Zhu, J.; Baran, P. S. *Science*, **2016**, *351*, 241.

(23) See Ref. 22 for full characterization.

CHAPTER 6

Selected NMR Spectra

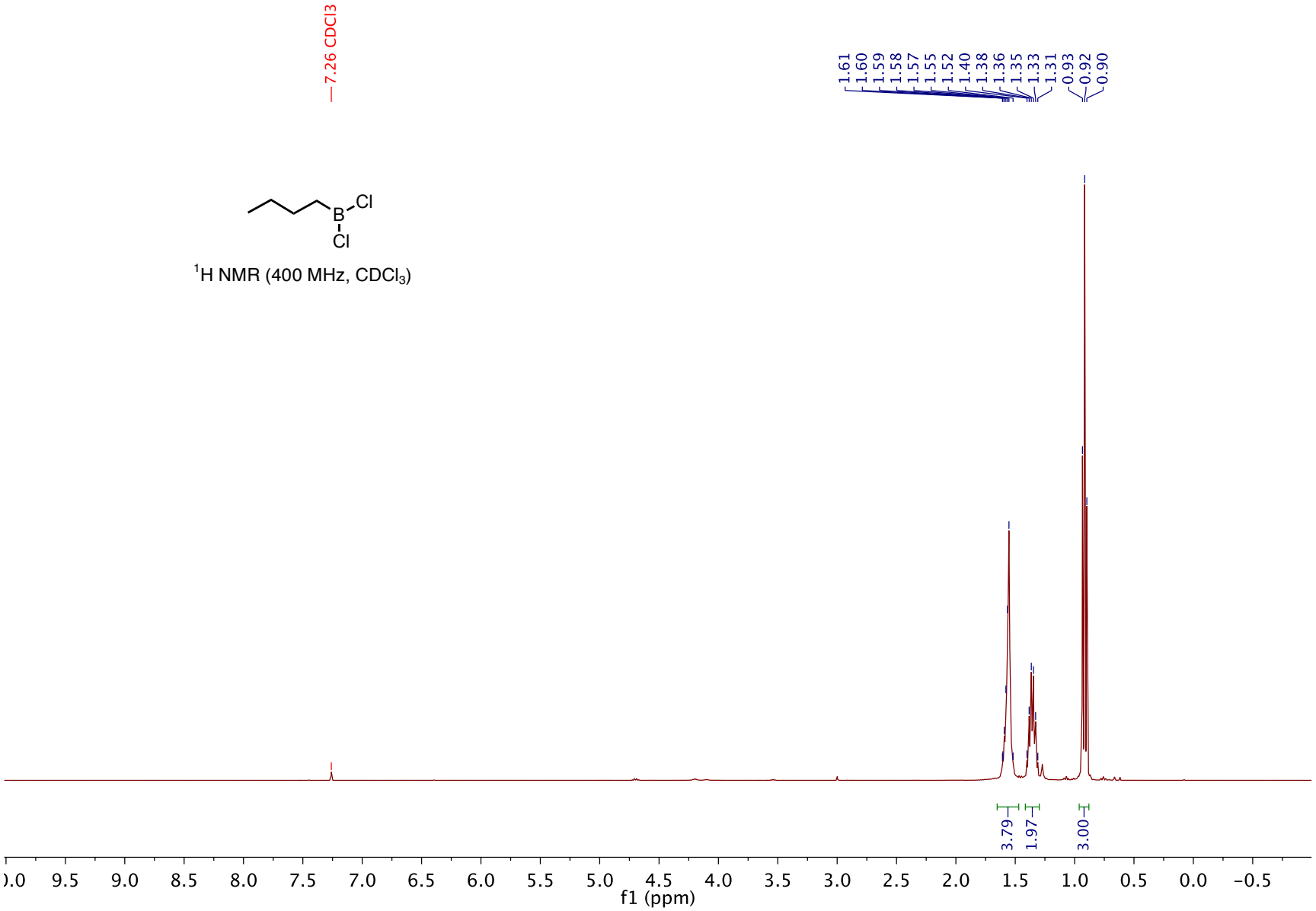

^{1}H NMR (400 MHz, $CDCl_3$)

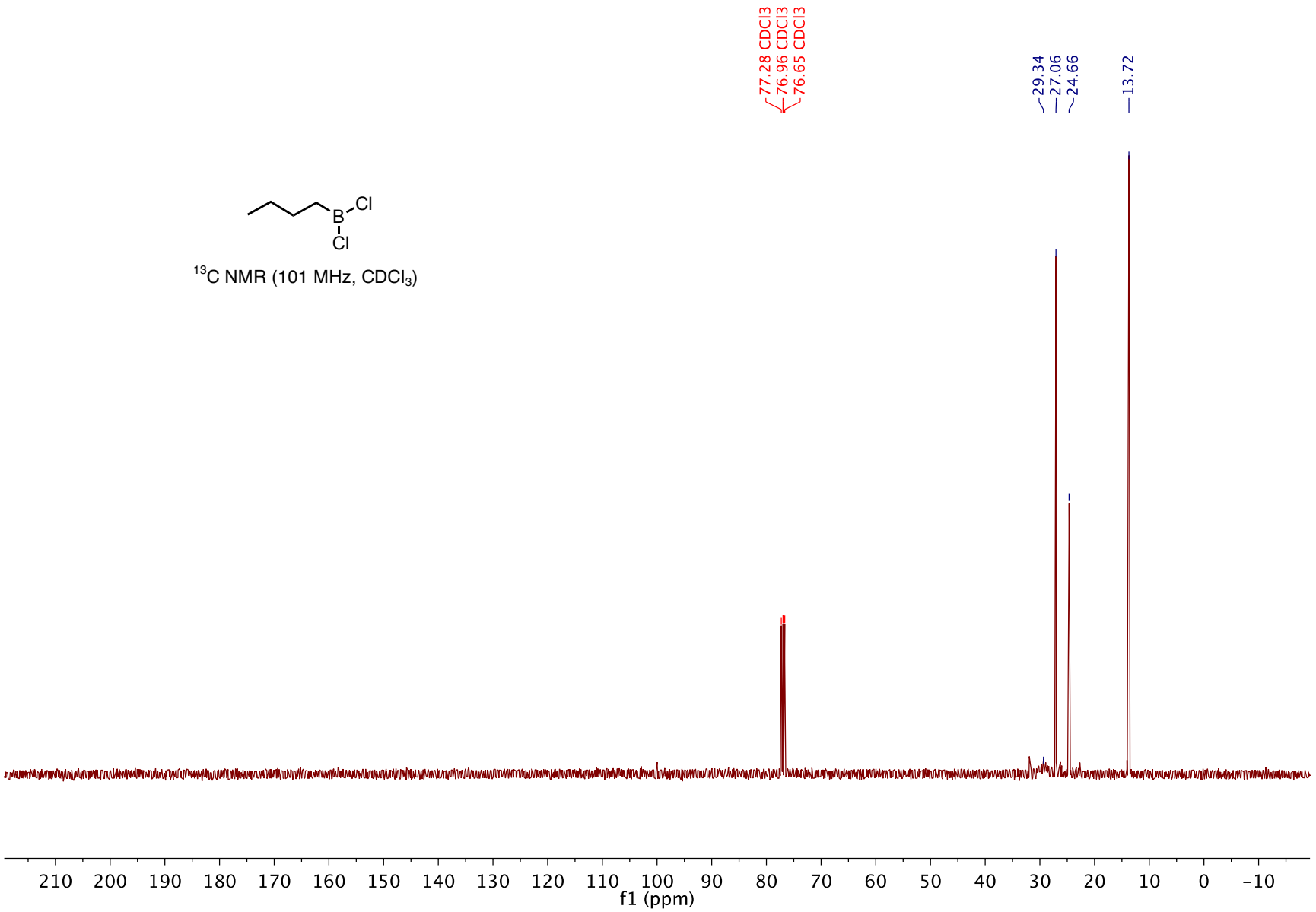

^{13}C NMR (101 MHz, $CDCl_3$)

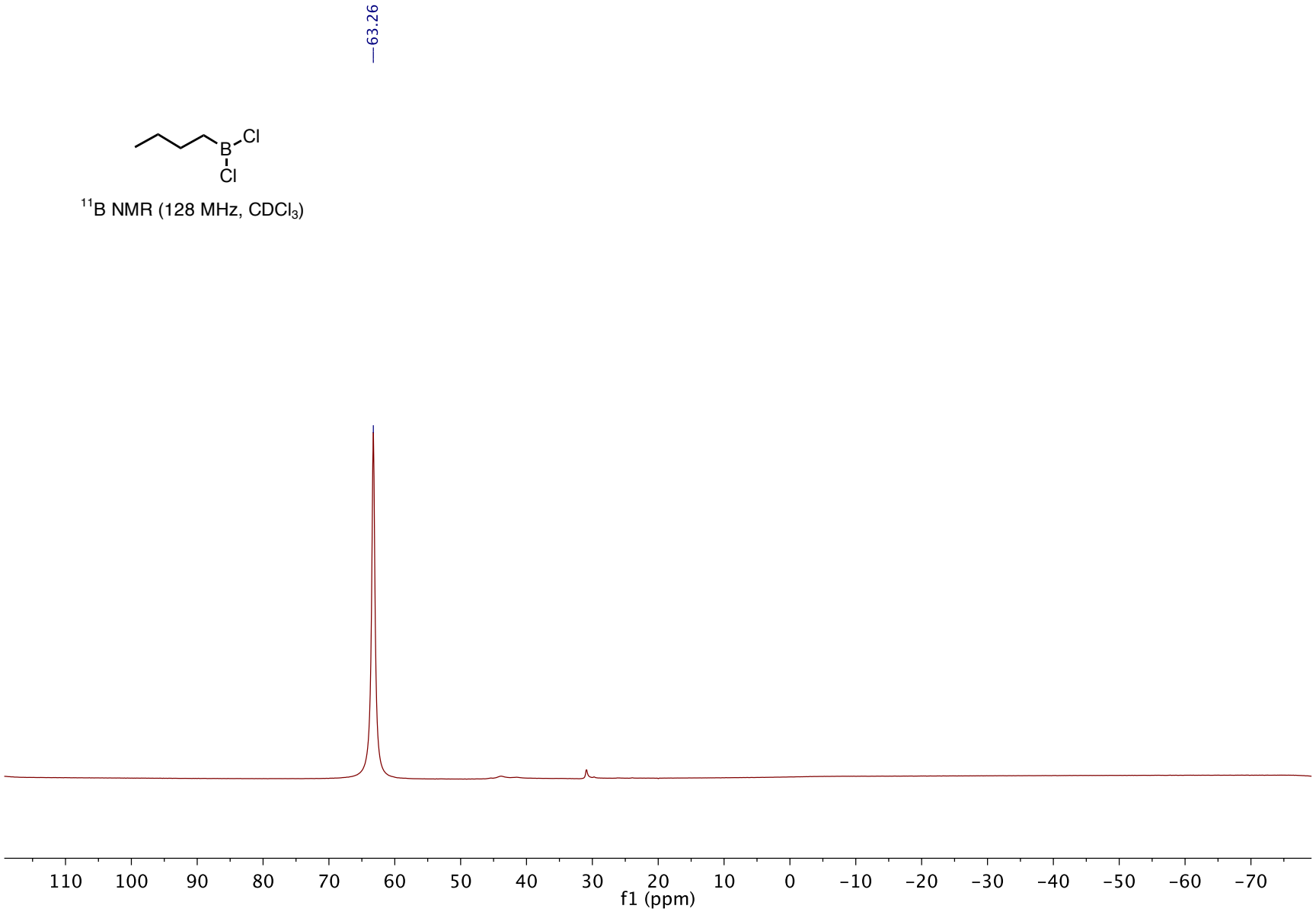

^{11}B NMR (128 MHz, $CDCl_3$)

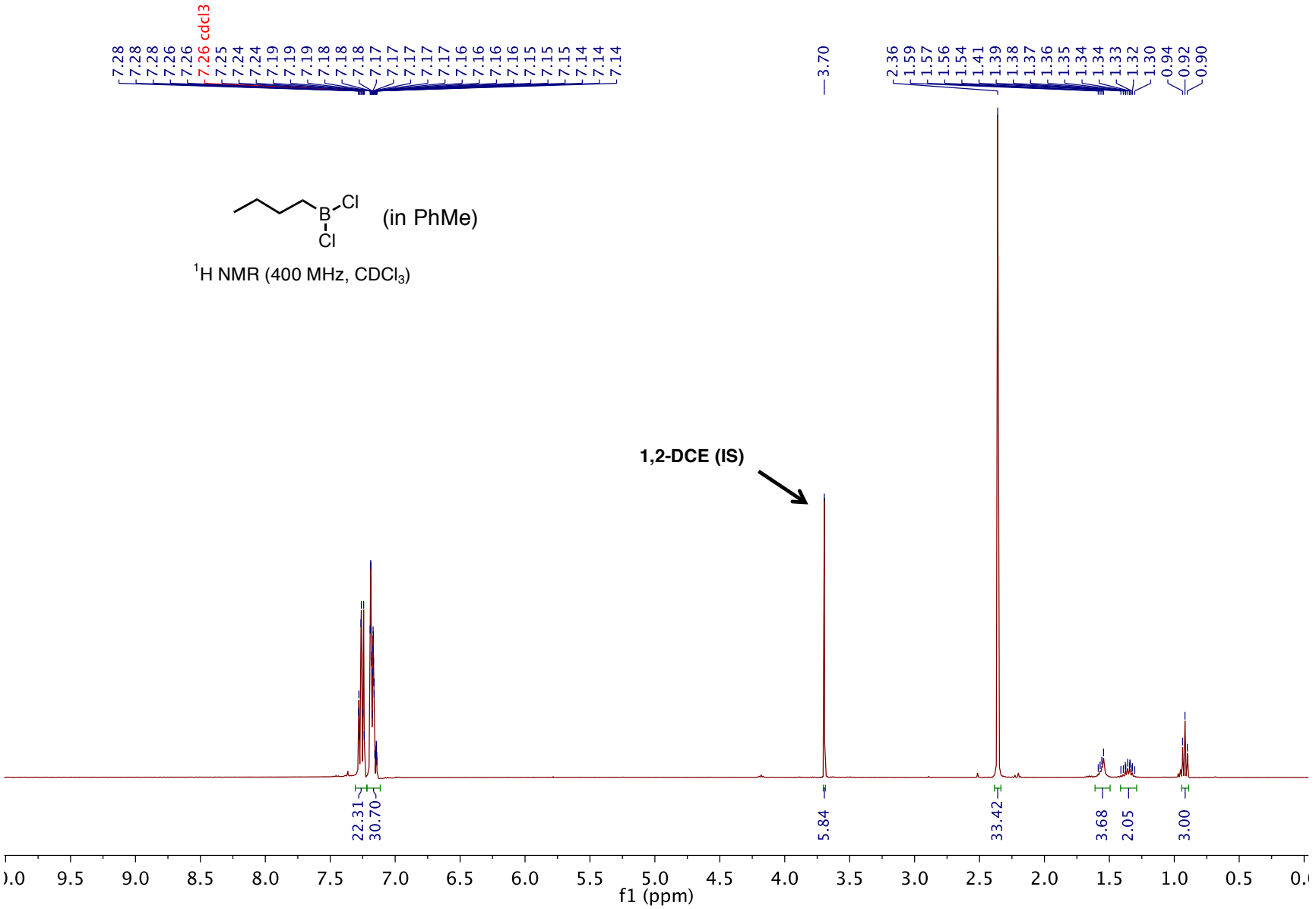
7.28
7.28
7.28
7.26
7.26
7.26 cdcl3
7.25
7.24
7.24
7.19
7.19
7.18
7.18
7.18
7.17
7.17
7.17
7.17
7.16
7.16
7.16
7.15
7.15
7.15
7.14
7.14
7.14
3.70
2.36
1.59
1.57
1.56
1.54
1.41
1.39
1.38
1.37
1.36
1.35
1.34
1.34
1.33
1.32
1.30
0.94
0.92
0.90
Cl
B
Cl
(in PhMe)
1H NMR (400 MHz, CDCl3)
1,2-DCE (IS)
22.31
30.70
5.84
33.42
3.68
2.05
3.00
9.5
9.0
8.5
8.0
7.5
7.0
6.5
6.0
5.5
5.0
4.5
4.0
3.5
3.0
2.5
2.0
1.5
1.0
0.5
f1 (ppm)

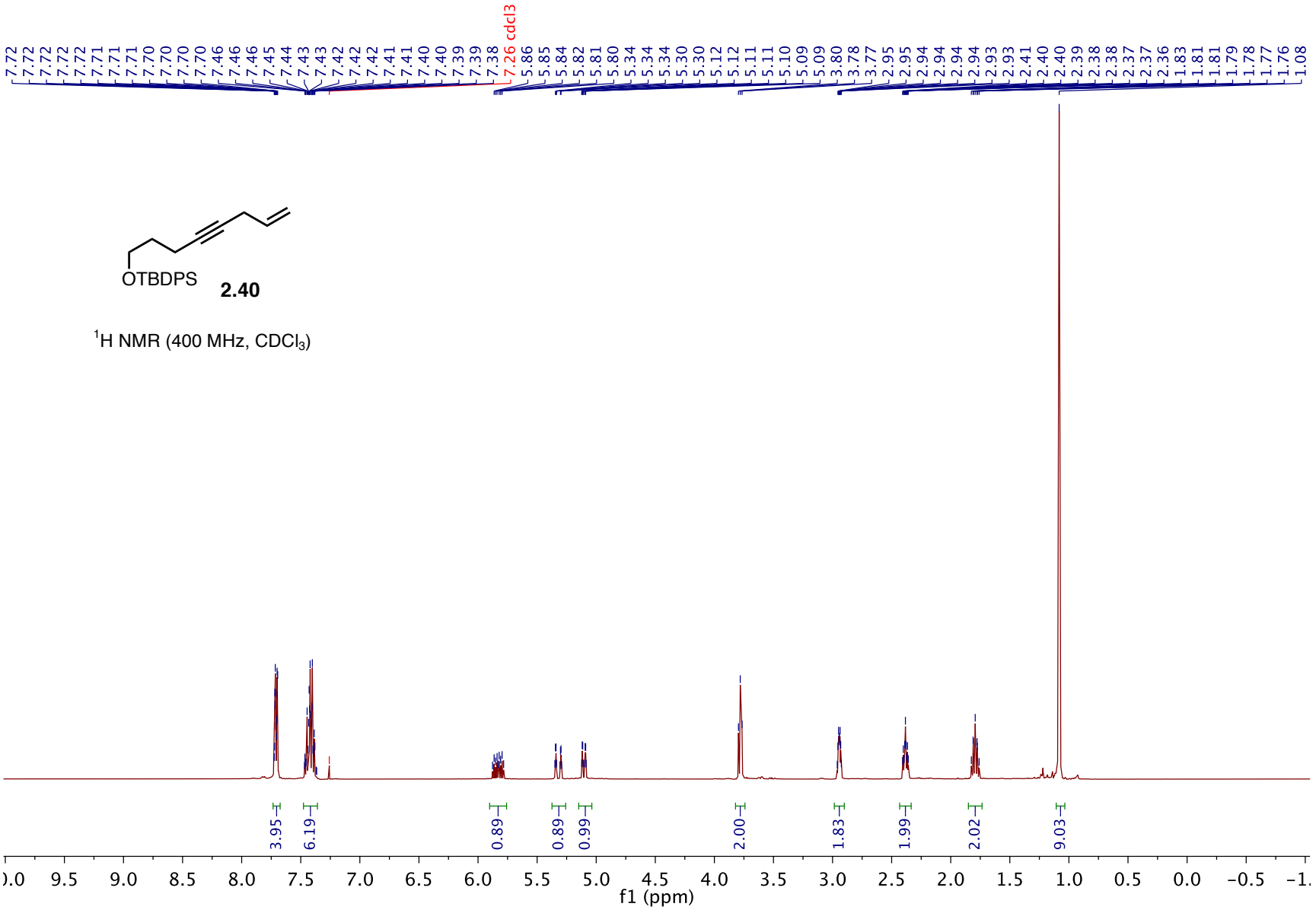
7.72 7.72 7.72 7.72 7.72 7.71 7.71 7.71 7.70 7.70 7.70 7.70 7.46 7.46 7.46 7.45 7.44 7.43 7.43 7.42 7.42 7.42 7.41 7.41 7.40 7.40 7.39 7.38 7.26 cdcl3 5.86 5.85 5.84 5.82 5.81 5.80 5.34 5.34 5.30 5.30 5.12 5.11 5.11 5.10 5.09 5.09 3.80 3.78 3.77 2.95 2.95 2.94 2.94 2.94 2.94 2.93 2.41 2.40 2.40 2.39 2.38 2.38 2.37 2.37 2.36 1.83 1.81 1.81 1.79 1.78 1.77 1.76 1.08
OTBDPS
2.40
1H NMR (400 MHz, CDCl3)
3.95
6.19
0.89
0.89
0.99
2.00
1.83
1.99
2.02
9.03
f1 (ppm)

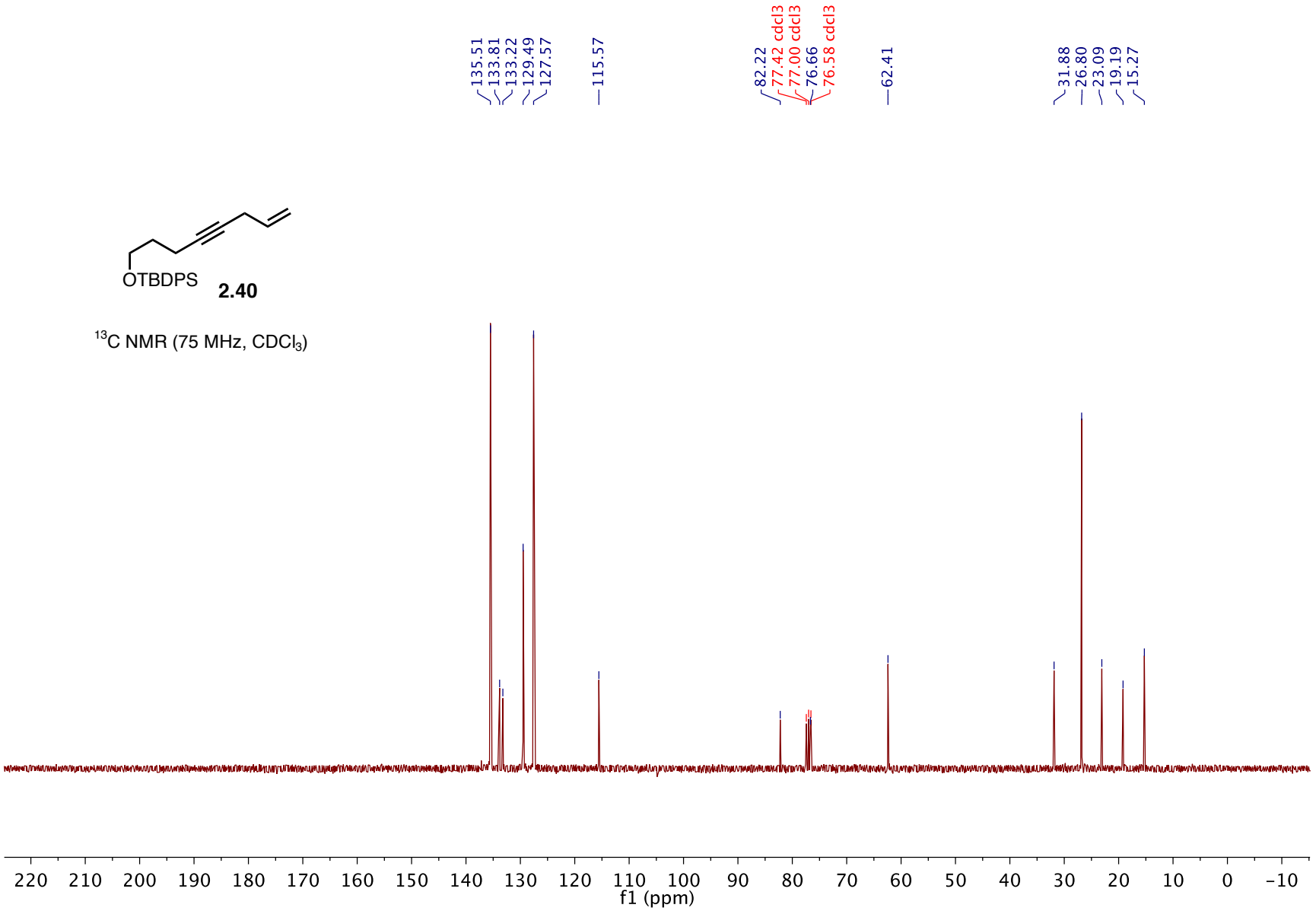
135.51
133.81
133.22
129.49
127.57
115.57
82.22
77.42 cdcl3
77.00 cdcl3
76.66
76.58 cdcl3
62.41
31.88
26.80
23.09
19.19
15.27
OTBDPS
2.40
^{13}C NMR (75 MHz, $CDCl_3$)
220 210 200 190 180 170 160 150 140 130 120 110 100 90 80 70 60 50 40 30 20 10 0 −10
f1 (ppm)

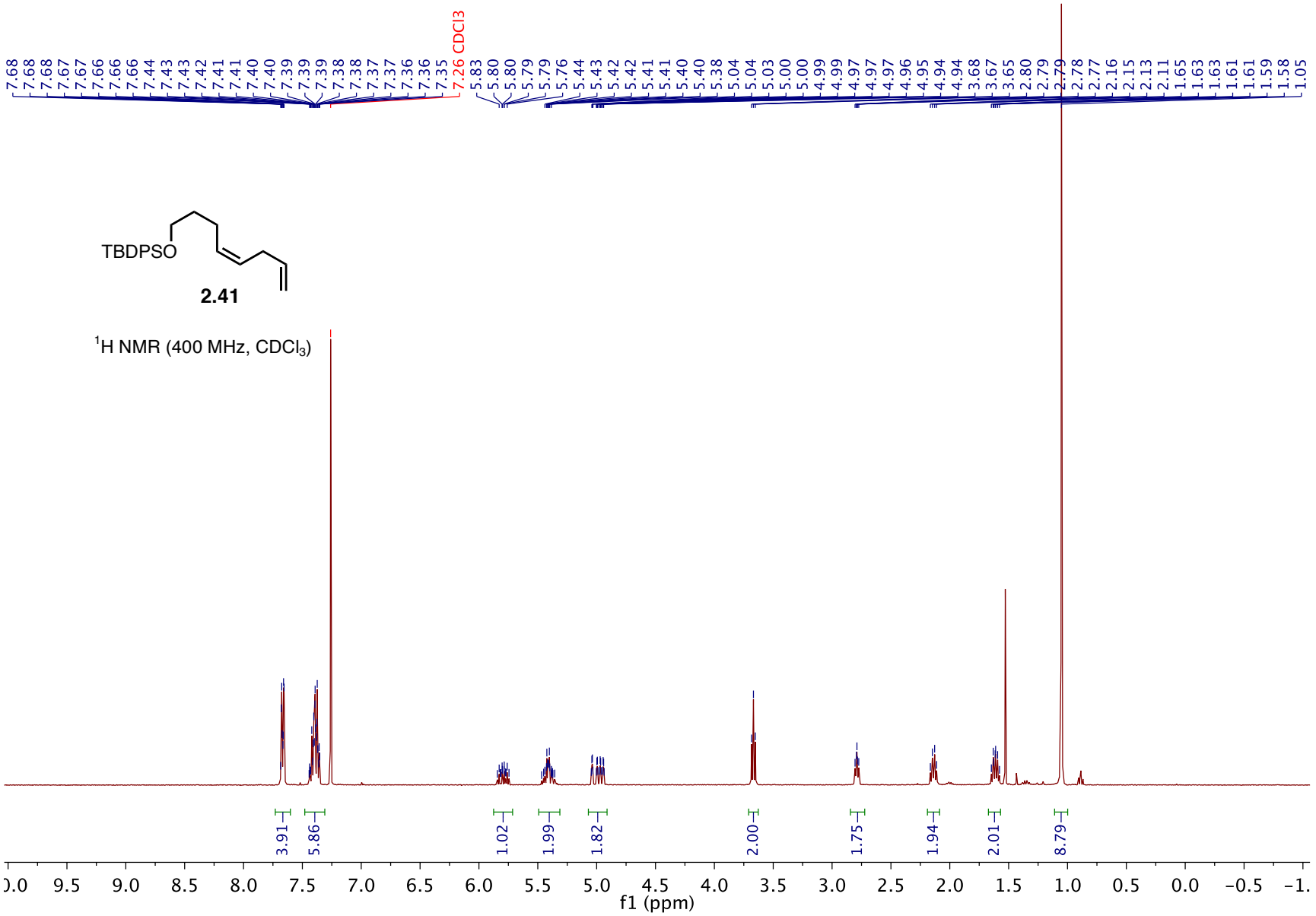
7.68 7.68 7.68 7.67 7.67 7.66 7.66 7.66 7.44 7.43 7.43 7.42 7.41 7.41 7.40 7.40 7.39 7.39 7.39 7.38 7.38 7.37 7.37 7.36 7.36 7.35 7.26 CDCl3
5.83 5.80 5.80 5.79 5.79 5.76 5.44 5.43 5.42 5.42 5.41 5.41 5.40 5.40 5.38 5.04 5.03 5.00 5.00 4.99 4.99 4.97 4.97 4.97 4.96 4.95 4.94 4.94 3.68 3.67 3.65 2.80 2.79 2.79 2.78 2.77 2.16 2.15 2.13 2.11 1.65 1.63 1.63 1.61 1.61 1.59 1.58 1.05
TBDPSO
2.41
^{1}H NMR (400 MHz, $CDCl_3$)
3.91 5.86 1.02 1.99 1.82 2.00 1.75 1.94 2.01 8.79
f1 (ppm)

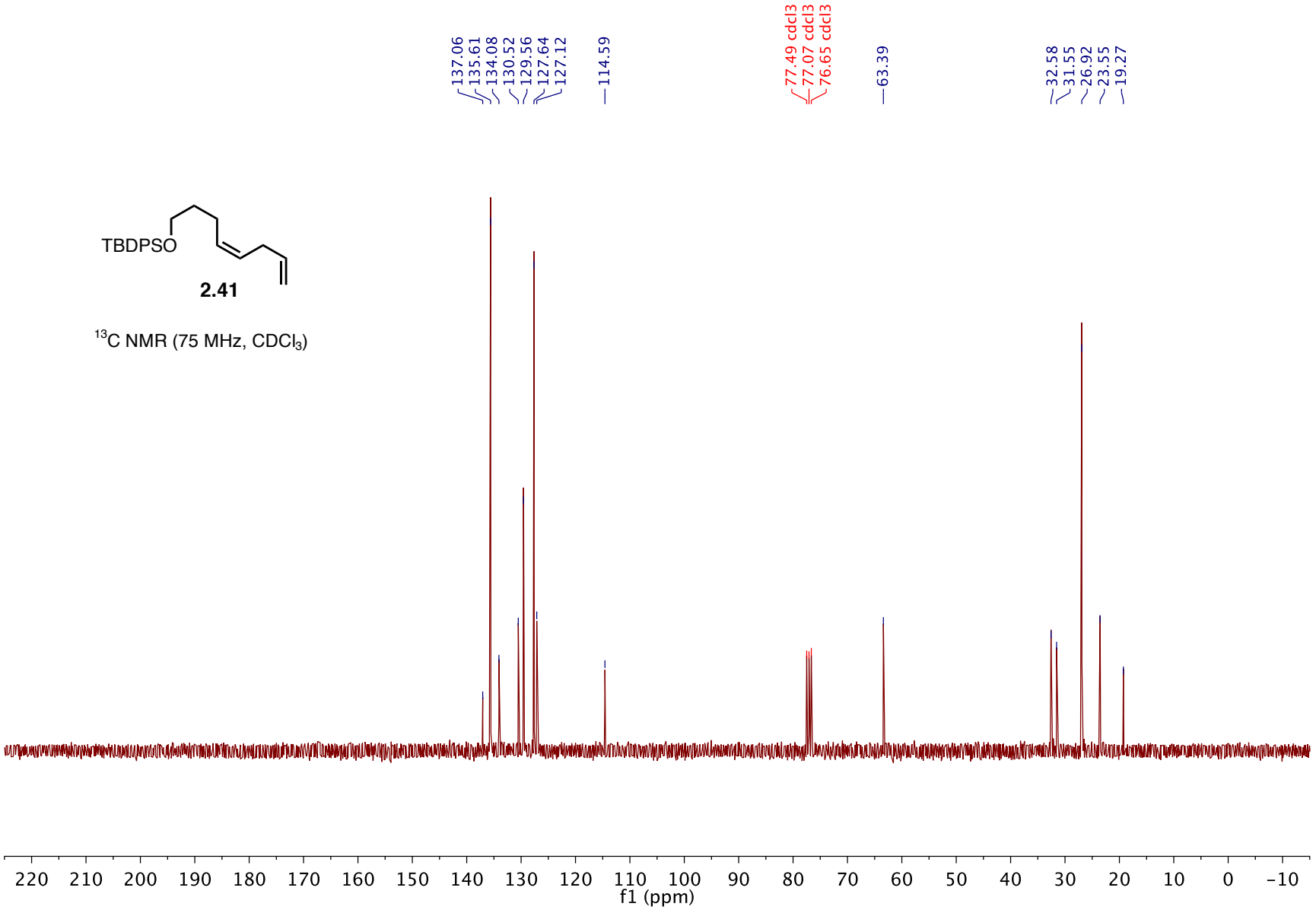
137.06
135.61
134.08
130.52
129.56
127.64
127.12
114.59
77.49 cdcl3
77.07 cdcl3
76.65 cdcl3
63.39
32.58
31.55
26.92
23.55
19.27
TBDPSO
2.41
^{13}C NMR (75 MHz, $CDCl_3$)
220 210 200 190 180 170 160 150 140 130 120 110 100 90 80 70 60 50 40 30 20 10 0 -10
f1 (ppm)

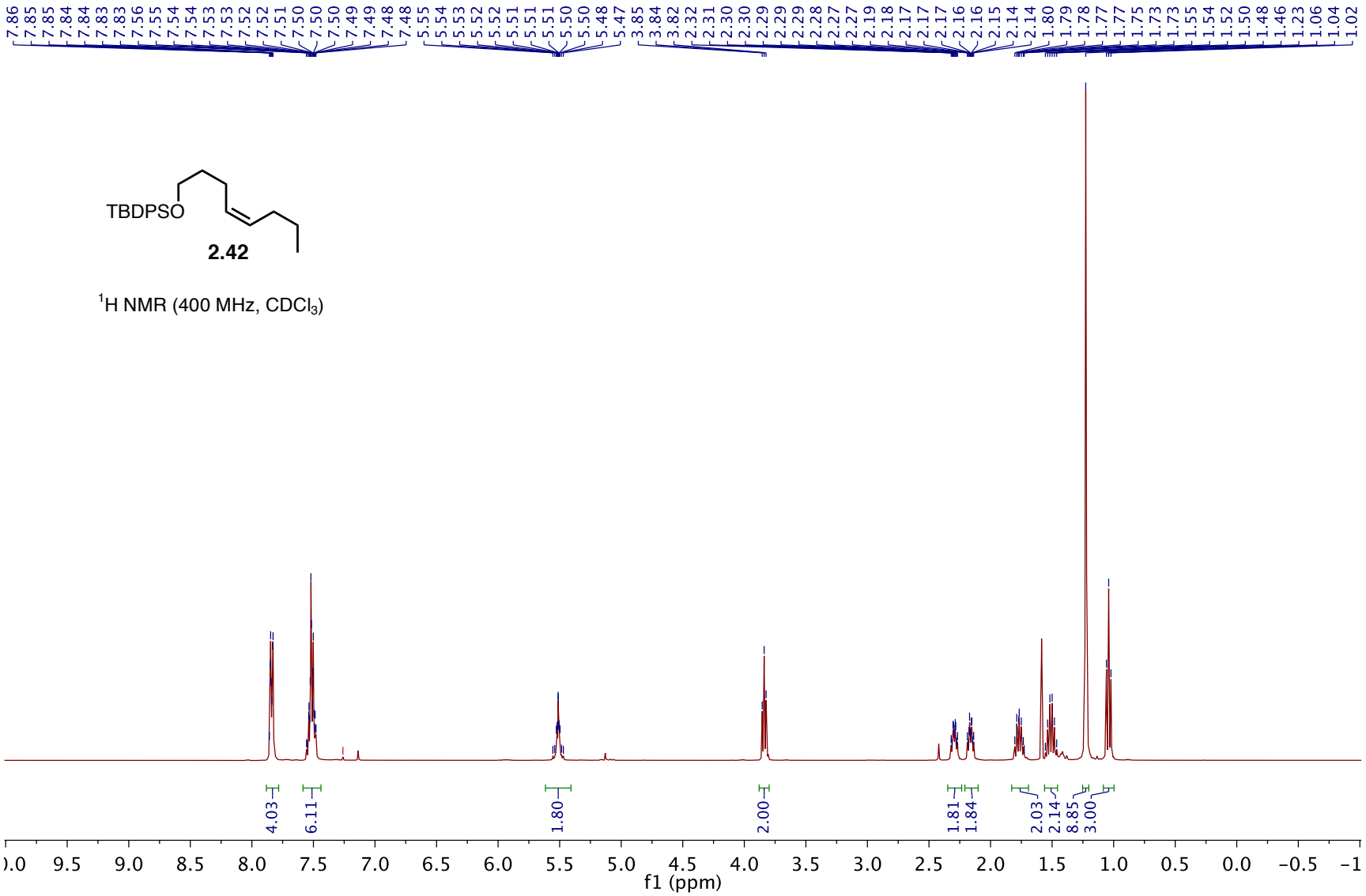
TBDPSO
2.42
1H NMR (400 MHz, CDCl3)
f1 (ppm)

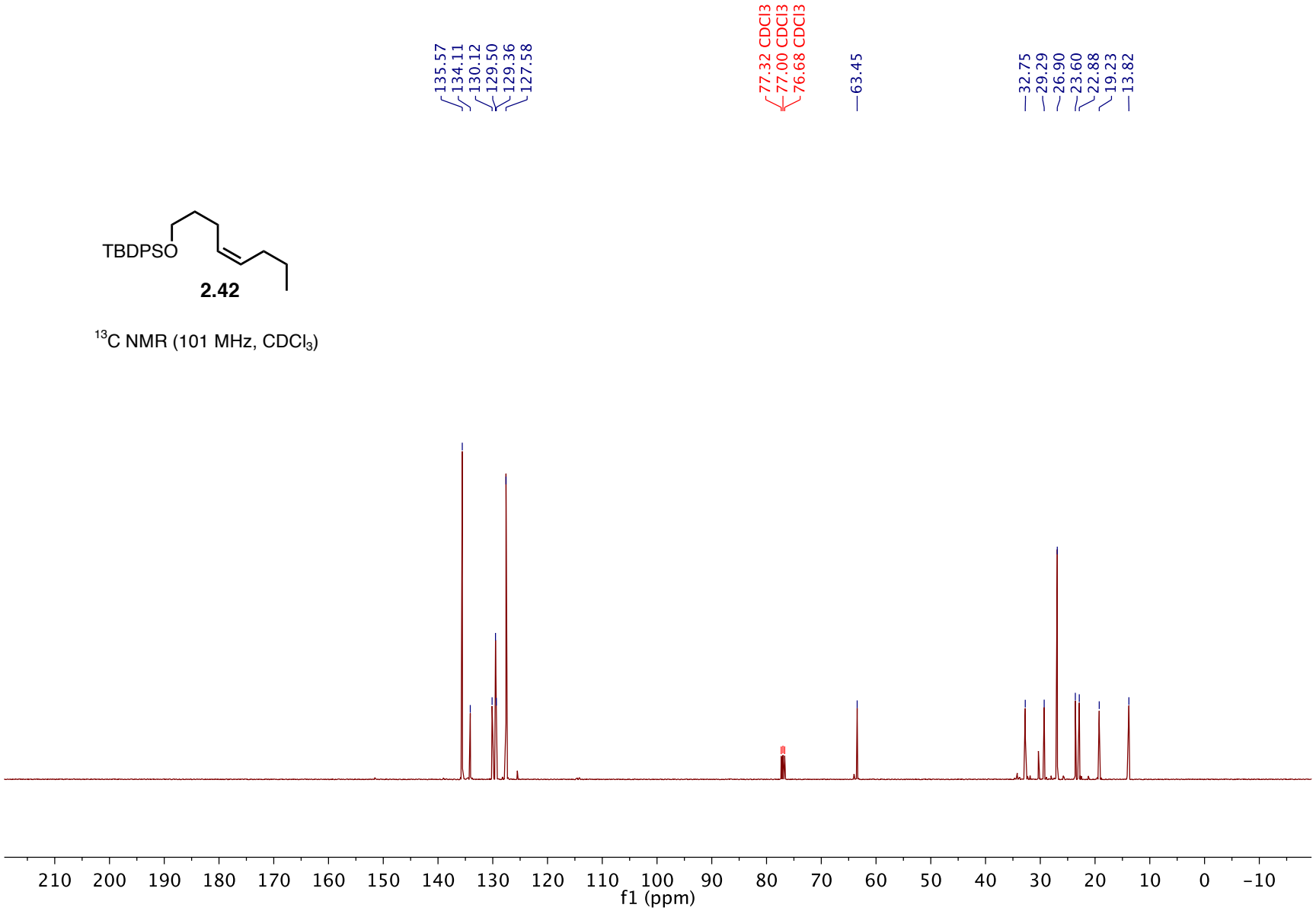
135.57
134.11
130.12
129.50
129.36
127.58
77.32 CDCl3
77.00 CDCl3
76.68 CDCl3
63.45
32.75
29.29
26.90
23.60
22.88
19.23
13.82
TBDPSO
2.42
^{13}C NMR (101 MHz, $CDCl_3$)
210 200 190 180 170 160 150 140 130 120 110 100 90 80 70 60 50 40 30 20 10 0 -10
f1 (ppm)

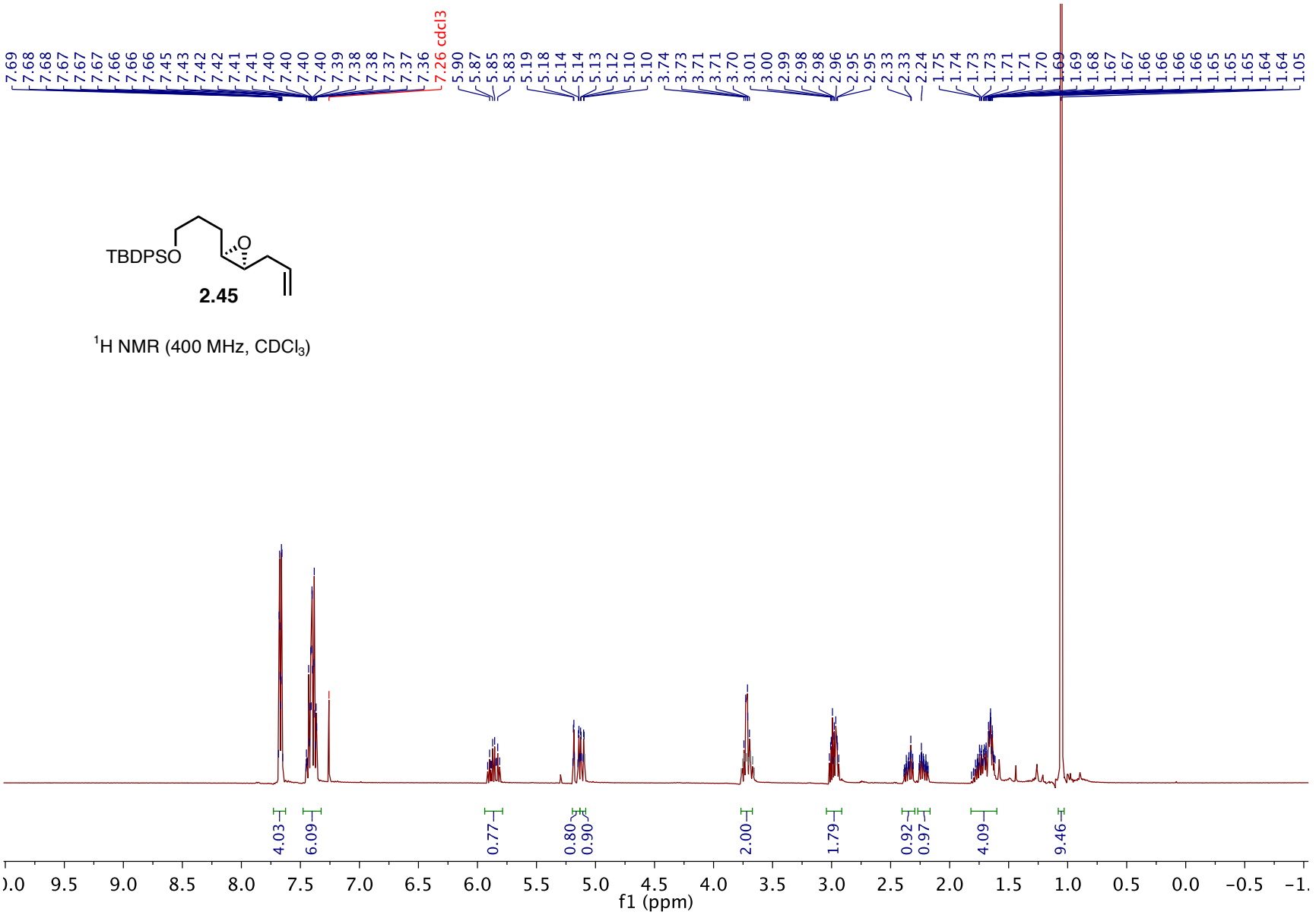
TBDPSO
O
2.45
1H NMR (400 MHz, CDCl3)
7.26 cdcl3
4.03
6.09
0.77
0.80
0.90
2.00
1.79
0.92
0.97
4.09
9.46
f1 (ppm)

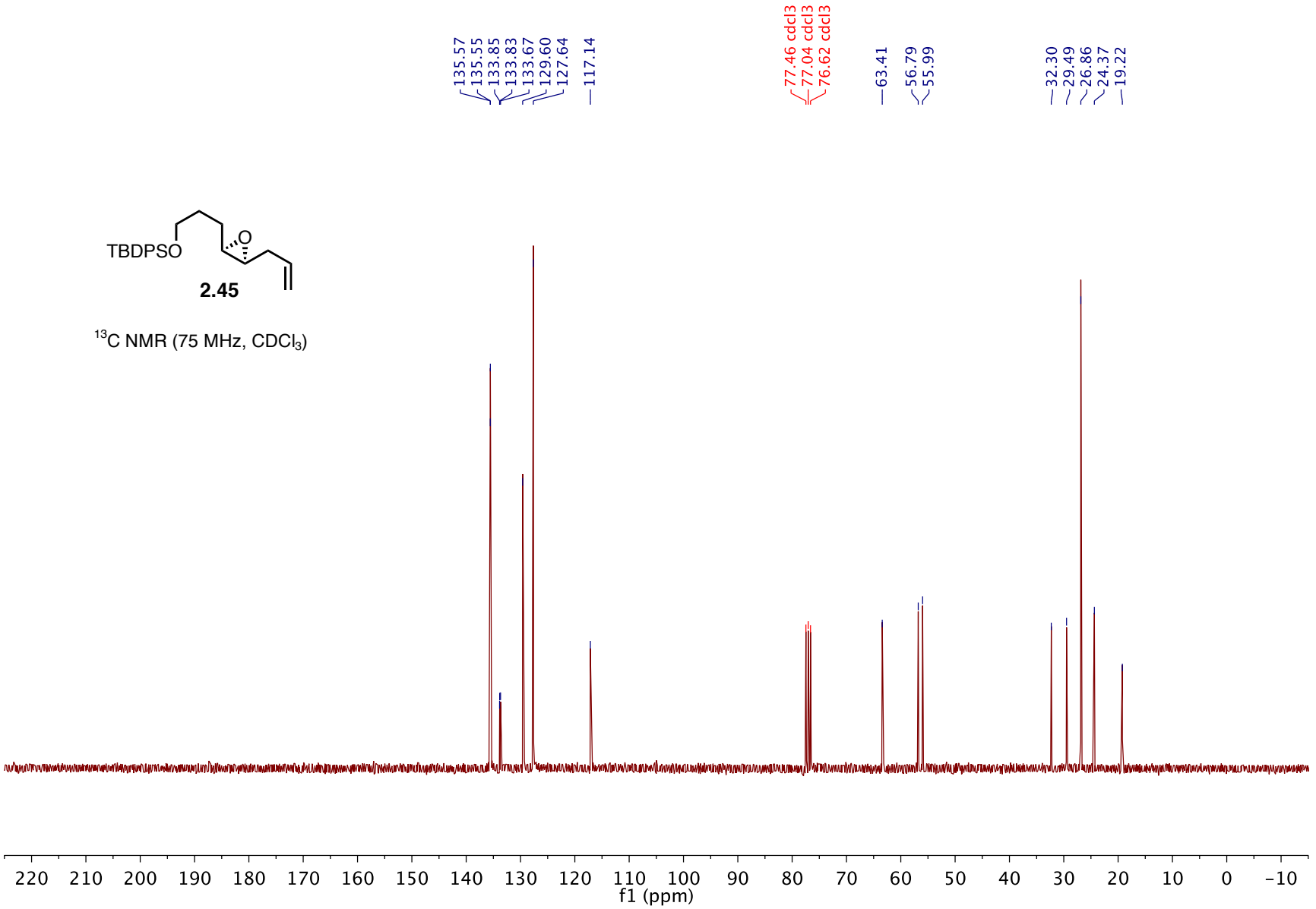
135.57
135.55
133.85
133.83
133.67
129.60
127.64
117.14
77.46 cdcl3
77.04 cdcl3
76.62 cdcl3
63.41
56.79
55.99
32.30
29.49
26.86
24.37
19.22
TBDPSO
O
2.45
^{13}C NMR (75 MHz, $CDCl_3$)
220 210 200 190 180 170 160 150 140 130 120 110 100 90 80 70 60 50 40 30 20 10 0 -10
f1 (ppm)

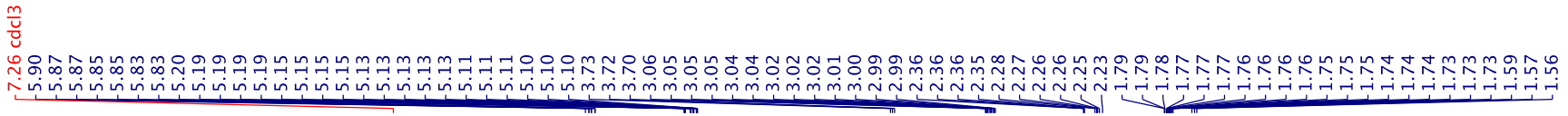

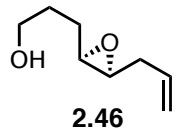

2.46

^{1}H NMR (400 MHz, $CDCl_3$)

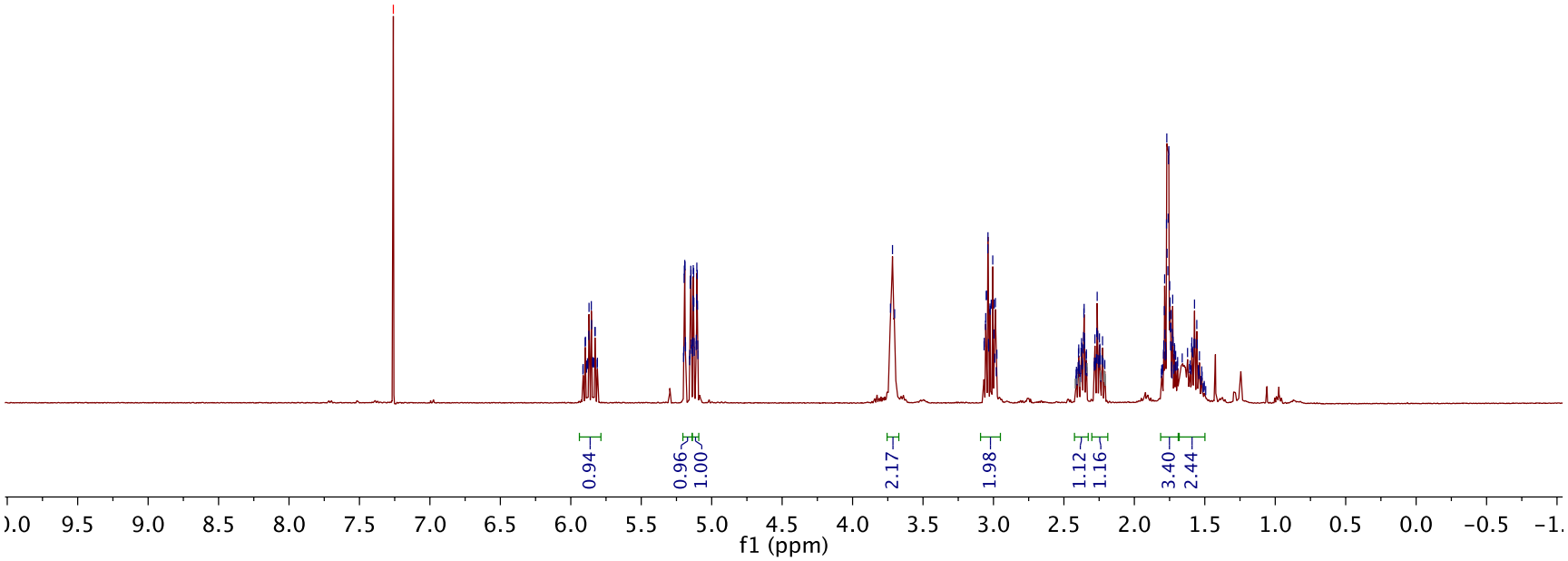

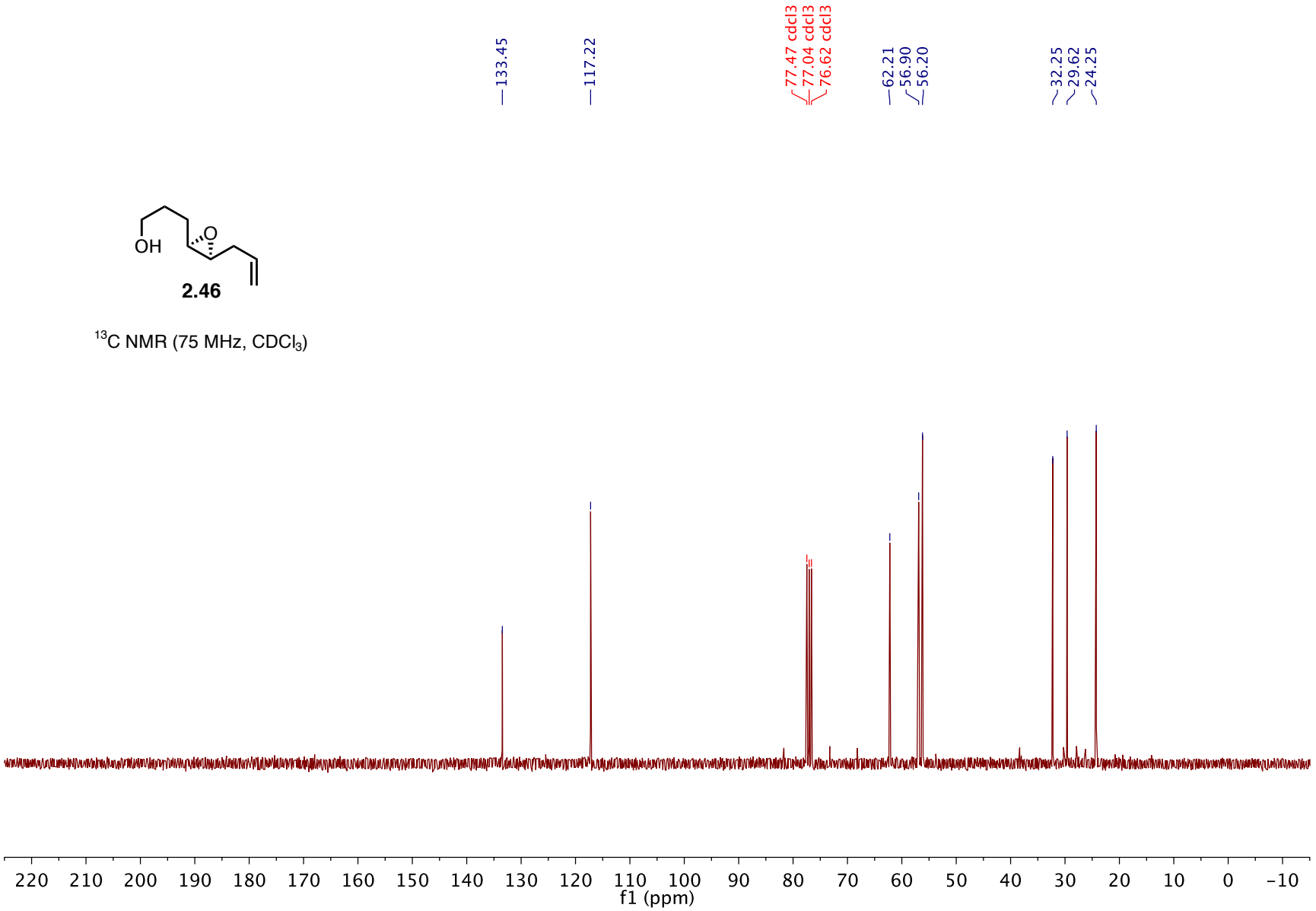
133.45
117.22
77.47 cdcl3
77.04 cdcl3
76.62 cdcl3
62.21
56.90
56.20
32.25
29.62
24.25
OH
O
2.46
^{13}C NMR (75 MHz, $CDCl_3$)
220 210 200 190 180 170 160 150 140 130 120 110 100 90 80 70 60 50 40 30 20 10 0 -10
f1 (ppm)

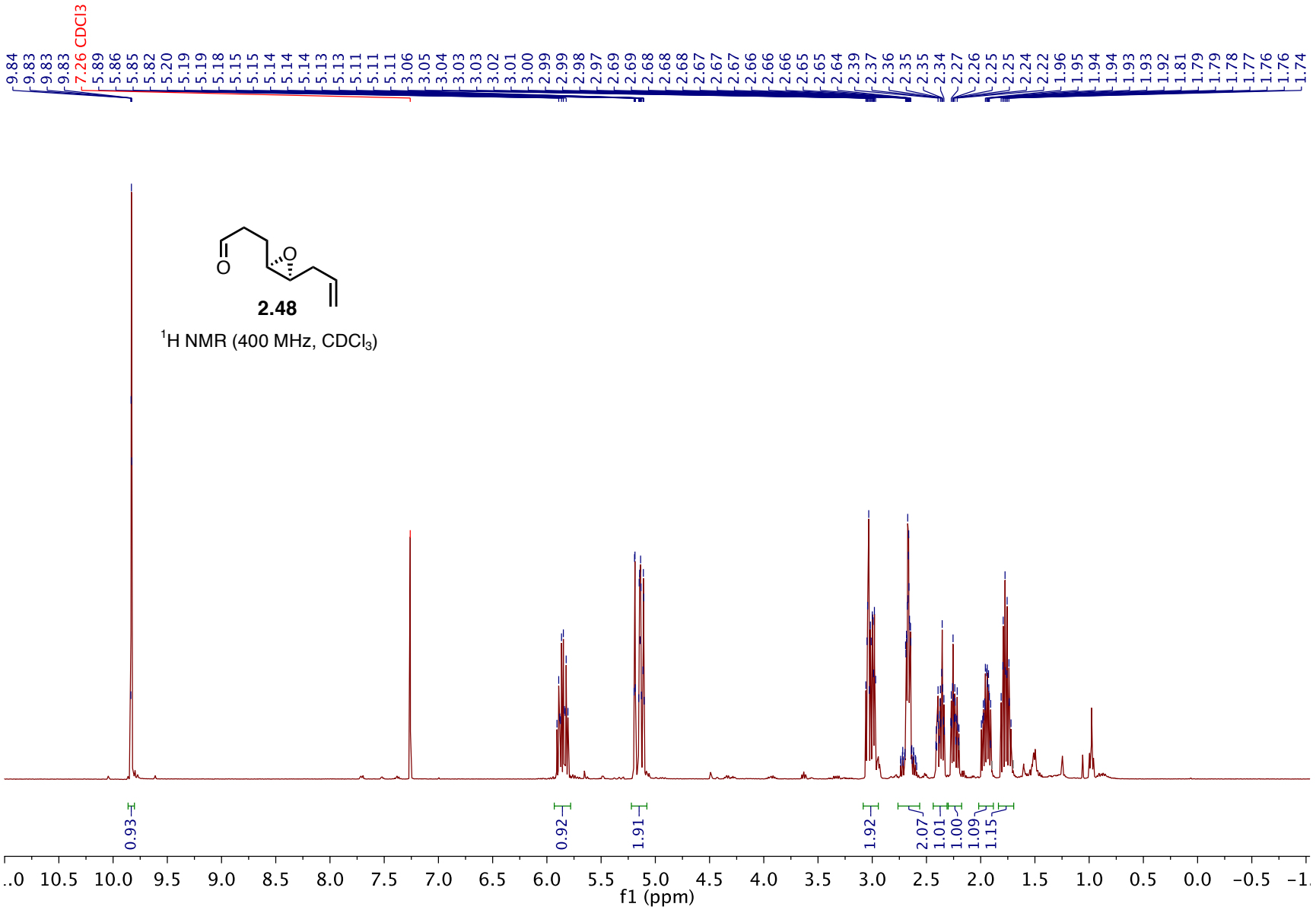
9.84 9.83 9.83 9.83 7.26 CDCl3 5.89 5.86 5.85 5.82 5.20 5.19 5.19 5.18 5.15 5.15 5.14 5.14 5.14 5.13 5.13 5.11 5.11 5.11 3.06 3.05 3.04 3.03 3.03 3.02 3.01 3.00 2.99 2.99 2.98 2.97 2.69 2.69 2.68 2.68 2.68 2.67 2.67 2.67 2.66 2.66 2.66 2.65 2.65 2.64 2.39 2.37 2.36 2.35 2.34 2.27 2.26 2.25 2.25 2.24 2.22 1.96 1.95 1.94 1.94 1.93 1.93 1.92 1.81 1.79 1.79 1.78 1.77 1.76 1.76 1.74
O
O
2.48
1H NMR (400 MHz, CDCl3)
0.93
0.92
1.91
1.92
2.07
1.01
1.00
1.09
1.15
..0 10.5 10.0 9.5 9.0 8.5 8.0 7.5 7.0 6.5 6.0 5.5 5.0 4.5 4.0 3.5 3.0 2.5 2.0 1.5 1.0 0.5 0.0 -0.5 -1.
f1 (ppm)

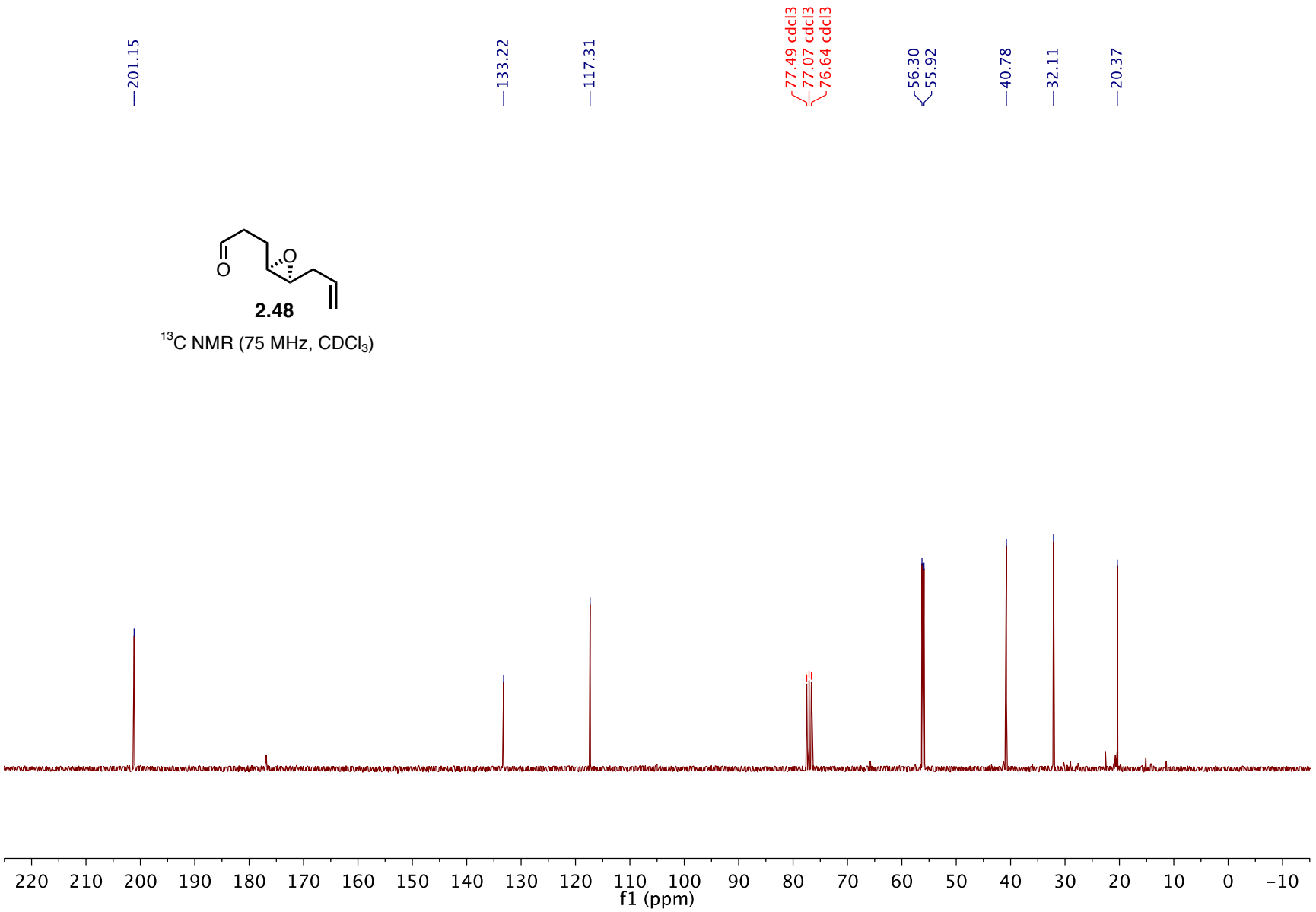

2.48

^{13}C NMR (75 MHz, $CDCl_3$)

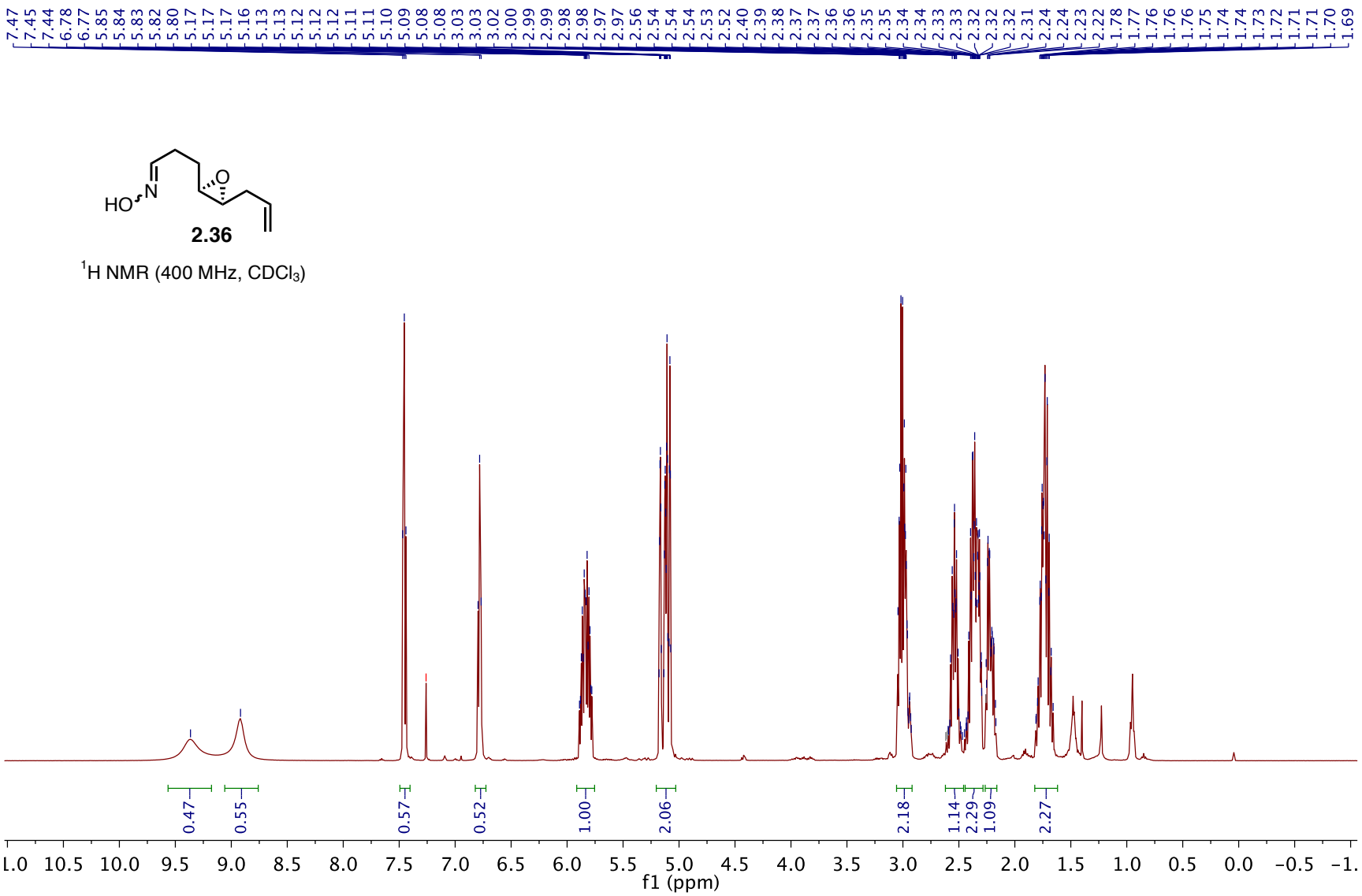
7.47 7.45 7.44 6.78 6.77 5.85 5.84 5.83 5.82 5.80 5.17 5.17 5.16 5.13 5.13 5.12 5.12 5.12 5.11 5.11 5.10 5.09 5.08 5.08 3.03 3.03 3.02 3.00 2.99 2.99 2.98 2.98 2.97 2.97 2.56 2.54 2.54 2.53 2.52 2.40 2.39 2.38 2.37 2.37 2.36 2.36 2.35 2.35 2.34 2.34 2.33 2.32 2.32 2.32 2.31 2.24 2.24 2.23 2.22 1.78 1.77 1.76 1.76 1.76 1.75 1.74 1.74 1.73 1.72 1.71 1.71 1.70 1.69
HO
N
O
2.36
^{1}H NMR (400 MHz, $CDCl_3$)
0.47
0.55
0.57
0.52
1.00
2.06
2.18
1.14
2.29
1.09
2.27
f1 (ppm)

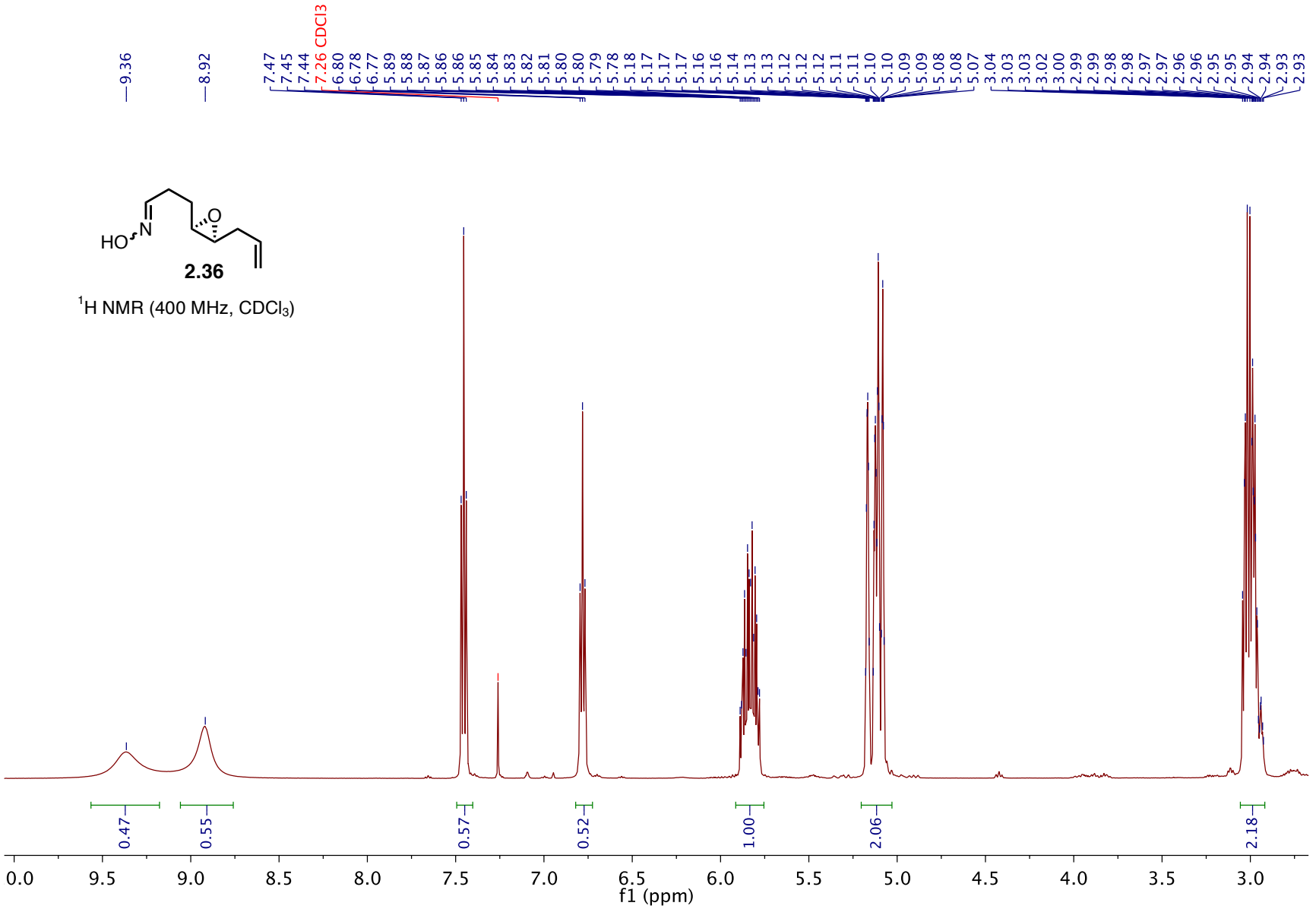
9.36
8.92
7.47
7.45
7.44
7.26 CDCl3
6.80
6.78
6.77
5.89
5.88
5.87
5.86
5.86
5.85
5.84
5.83
5.82
5.81
5.80
5.80
5.79
5.78
5.18
5.17
5.17
5.16
5.16
5.14
5.13
5.13
5.12
5.12
5.12
5.11
5.11
5.10
5.10
5.09
5.09
5.08
5.08
5.07
3.04
3.03
3.03
3.02
3.00
2.99
2.99
2.98
2.98
2.97
2.97
2.96
2.96
2.95
2.95
2.94
2.94
2.93
2.93
HO
N
O
2.36
1H NMR (400 MHz, CDCl3)
0.47
0.55
0.57
0.52
1.00
2.06
2.18
0.0
9.5
9.0
8.5
8.0
7.5
7.0
6.5
6.0
5.5
5.0
4.5
4.0
3.5
3.0
f1 (ppm)

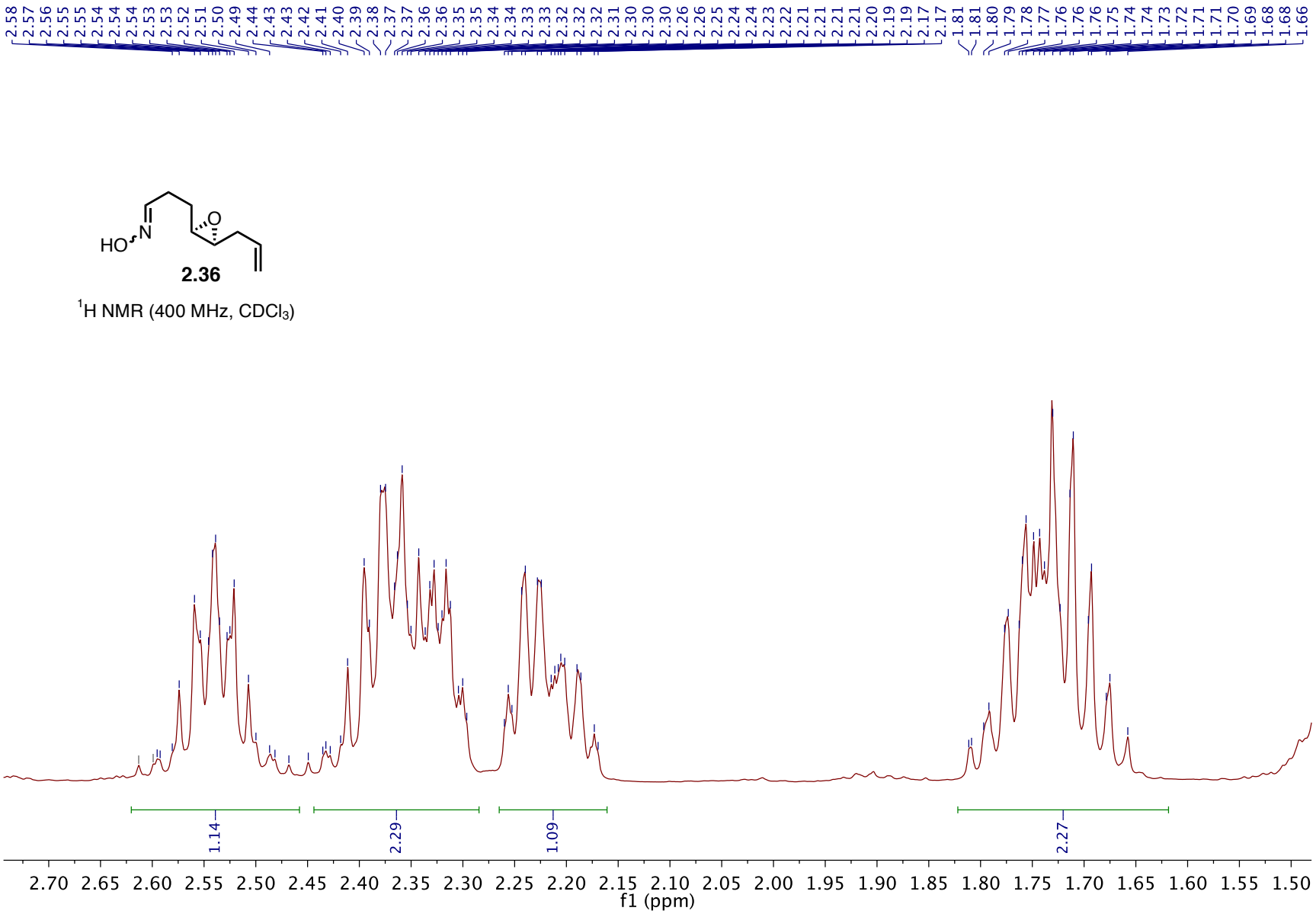
2.58 2.57 2.56 2.55 2.55 2.54 2.54 2.54 2.53 2.53 2.52 2.51 2.50 2.49 2.44 2.43 2.43 2.42 2.41 2.40 2.39 2.38 2.37 2.37 2.36 2.36 2.35 2.35 2.34 2.34 2.33 2.33 2.32 2.32 2.32 2.31 2.30 2.30 2.30 2.26 2.26 2.25 2.24 2.24 2.23 2.22 2.21 2.21 2.21 2.21 2.20 2.19 2.19 2.17 2.17 1.81 1.81 1.80 1.79 1.78 1.77 1.76 1.76 1.76 1.75 1.74 1.74 1.73 1.72 1.71 1.71 1.70 1.69 1.68 1.68 1.66
HO
N
O
2.36
1H NMR (400 MHz, CDCl3)
1.14
2.29
1.09
2.27
2.70 2.65 2.60 2.55 2.50 2.45 2.40 2.35 2.30 2.25 2.20 2.15 2.10 2.05 2.00 1.95 1.90 1.85 1.80 1.75 1.70 1.65 1.60 1.55 1.50
f1 (ppm)

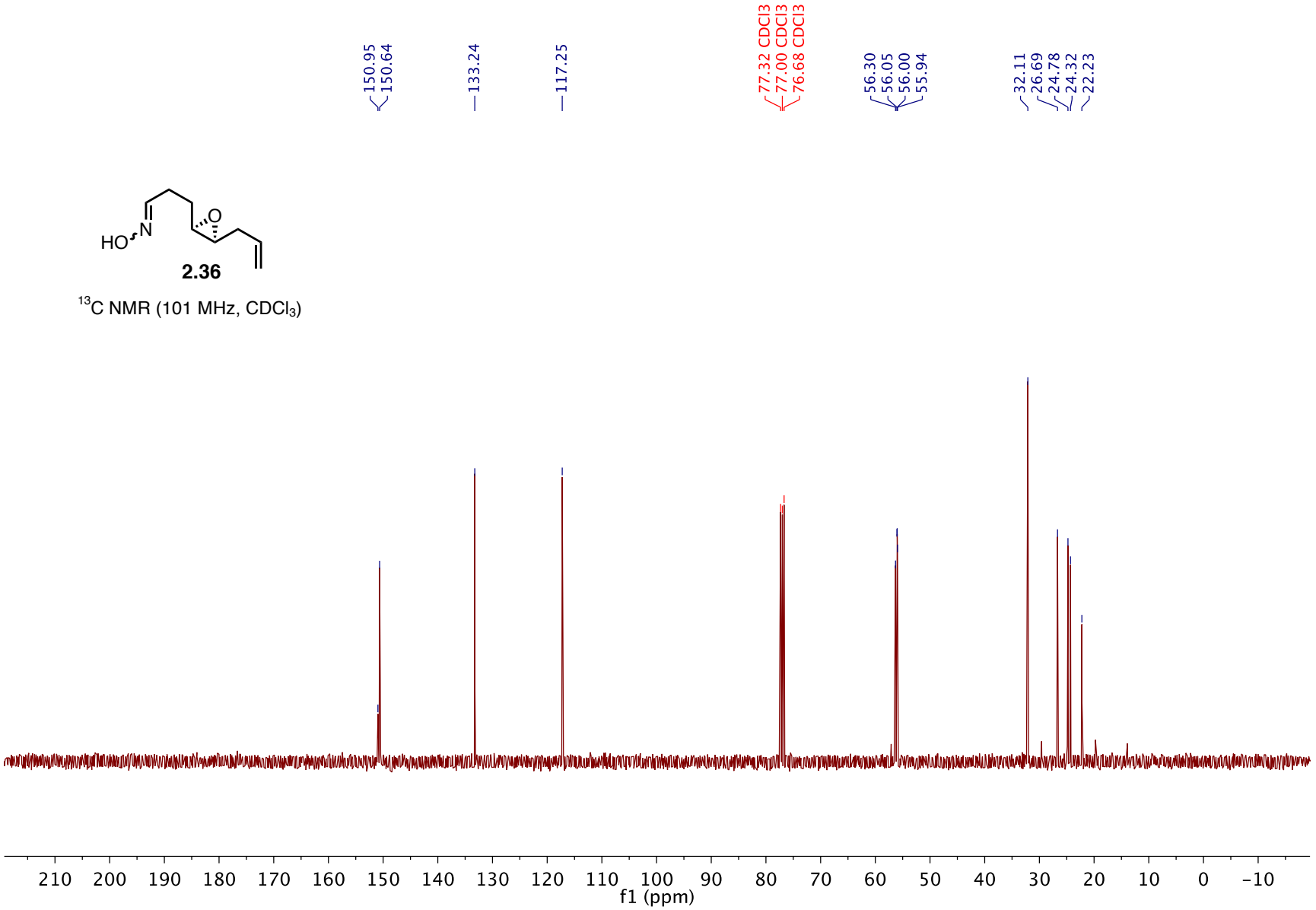
150.95
150.64
133.24
117.25
77.32 CDCl3
77.00 CDCl3
76.68 CDCl3
56.30
56.05
56.00
55.94
32.11
26.69
24.78
24.32
22.23
HO
N
O
2.36
13C NMR (101 MHz, CDCl3)
210 200 190 180 170 160 150 140 130 120 110 100 90 80 70 60 50 40 30 20 10 0 -10
f1 (ppm)

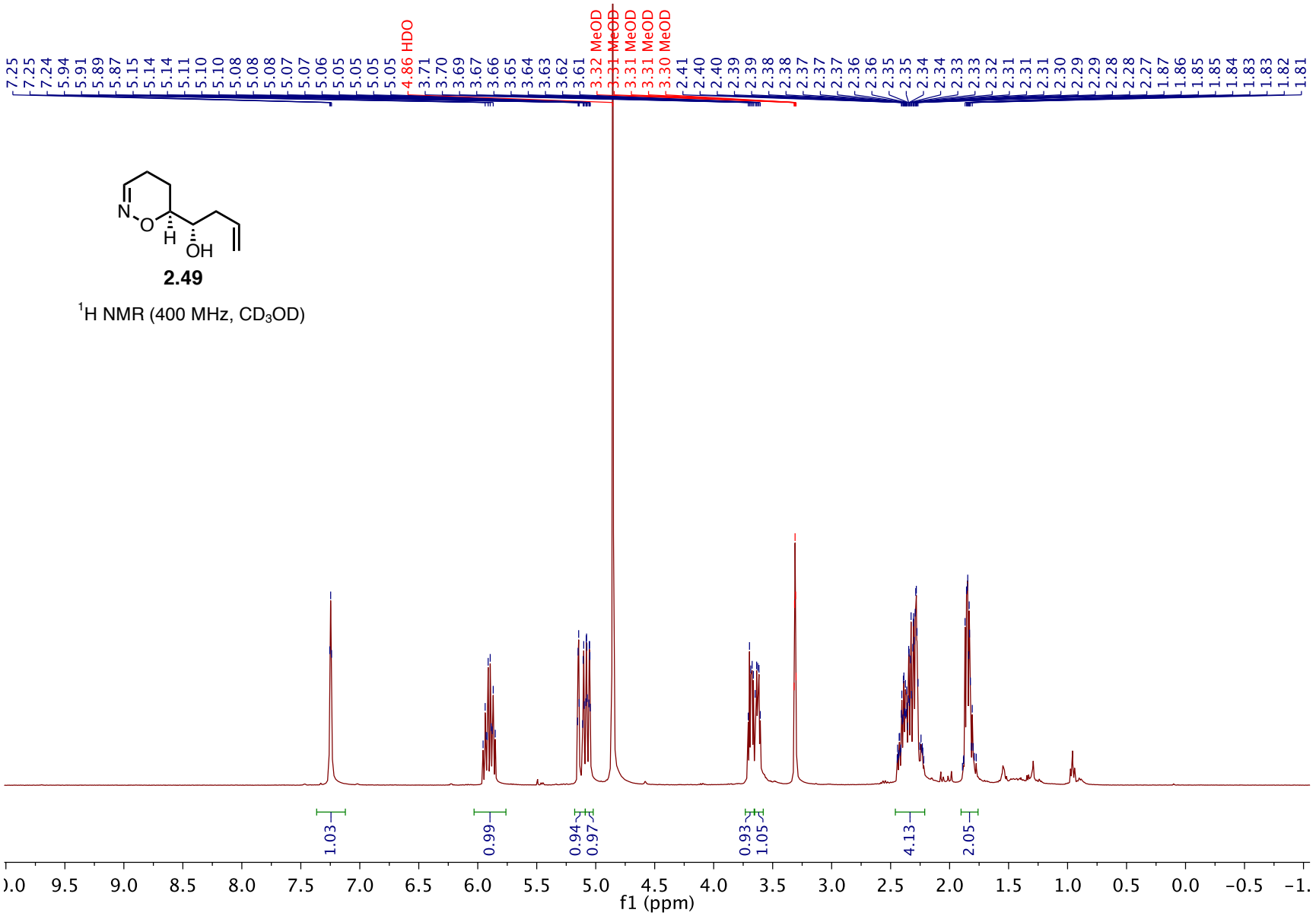

2.49

^{1}H NMR (400 MHz, CD_3OD)

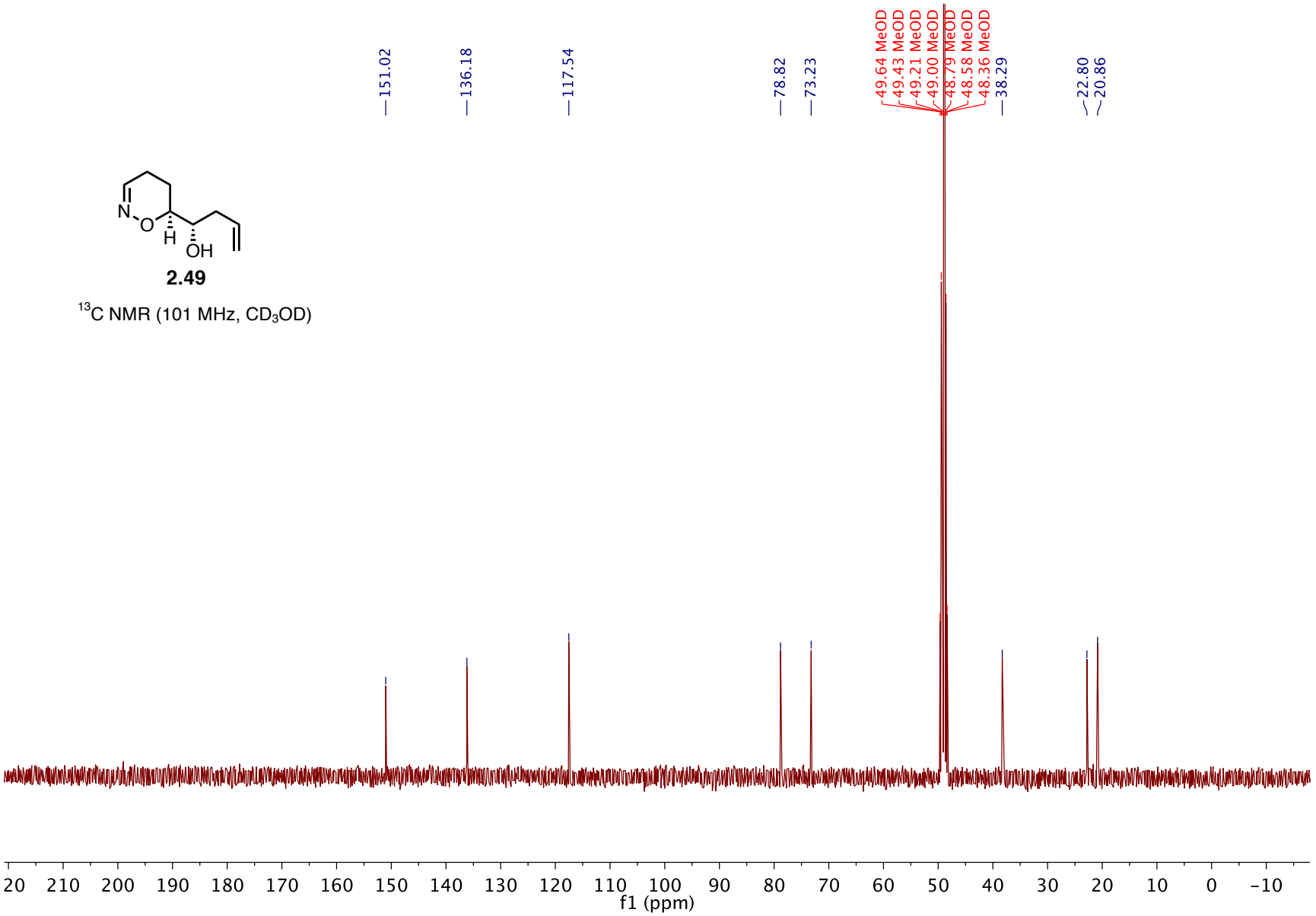
151.02
136.18
117.54
78.82
73.23
49.64 MeOD
49.43 MeOD
49.21 MeOD
49.00 MeOD
48.79 MeOD
48.58 MeOD
48.36 MeOD
38.29
22.80
20.86
N
O
H
OH
2.49
13C NMR (101 MHz, CD3OD)
f1 (ppm)

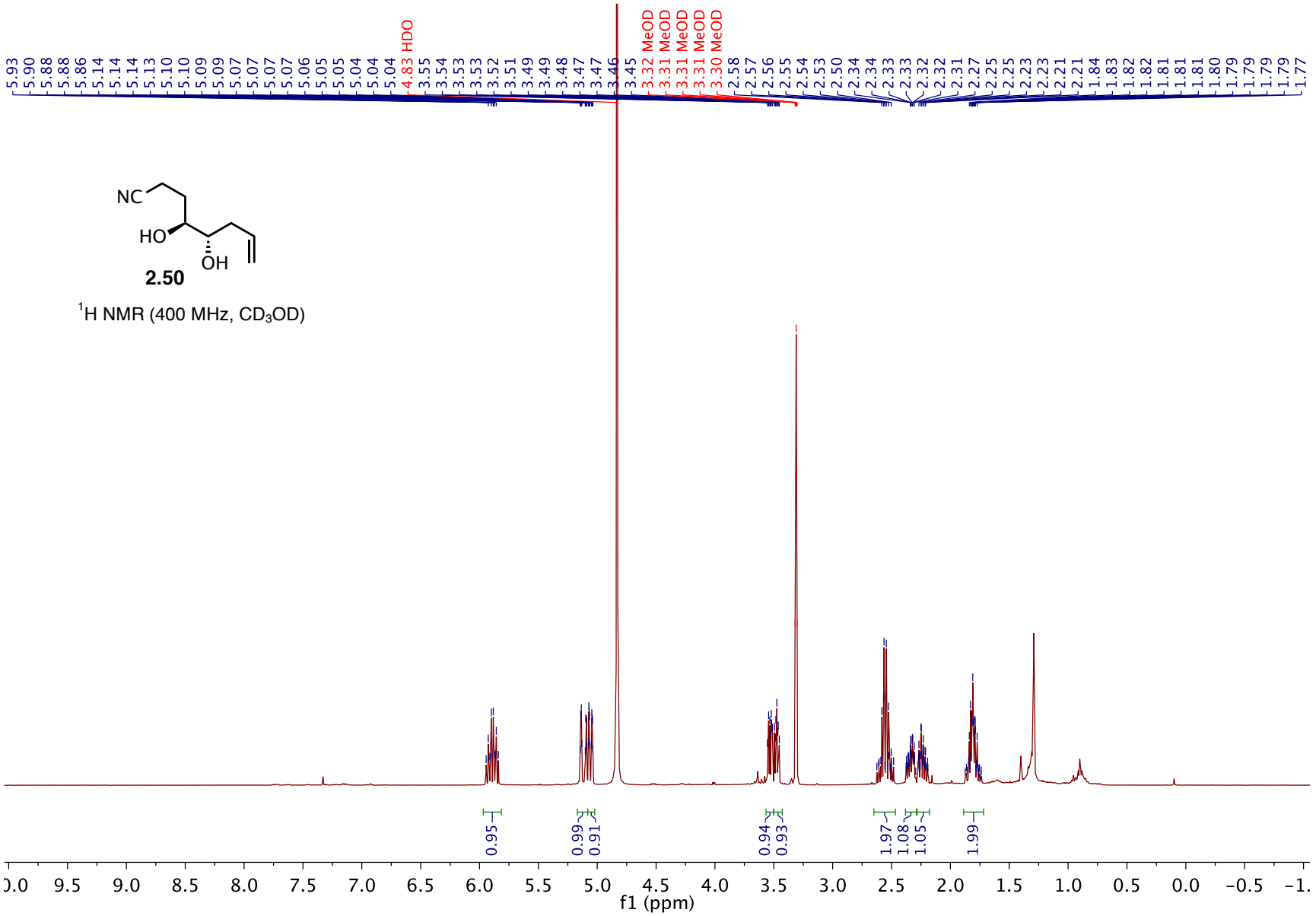
NC
HO
OH
2.50
1H NMR (400 MHz, CD3OD)
HDO
MeOD
f1 (ppm)

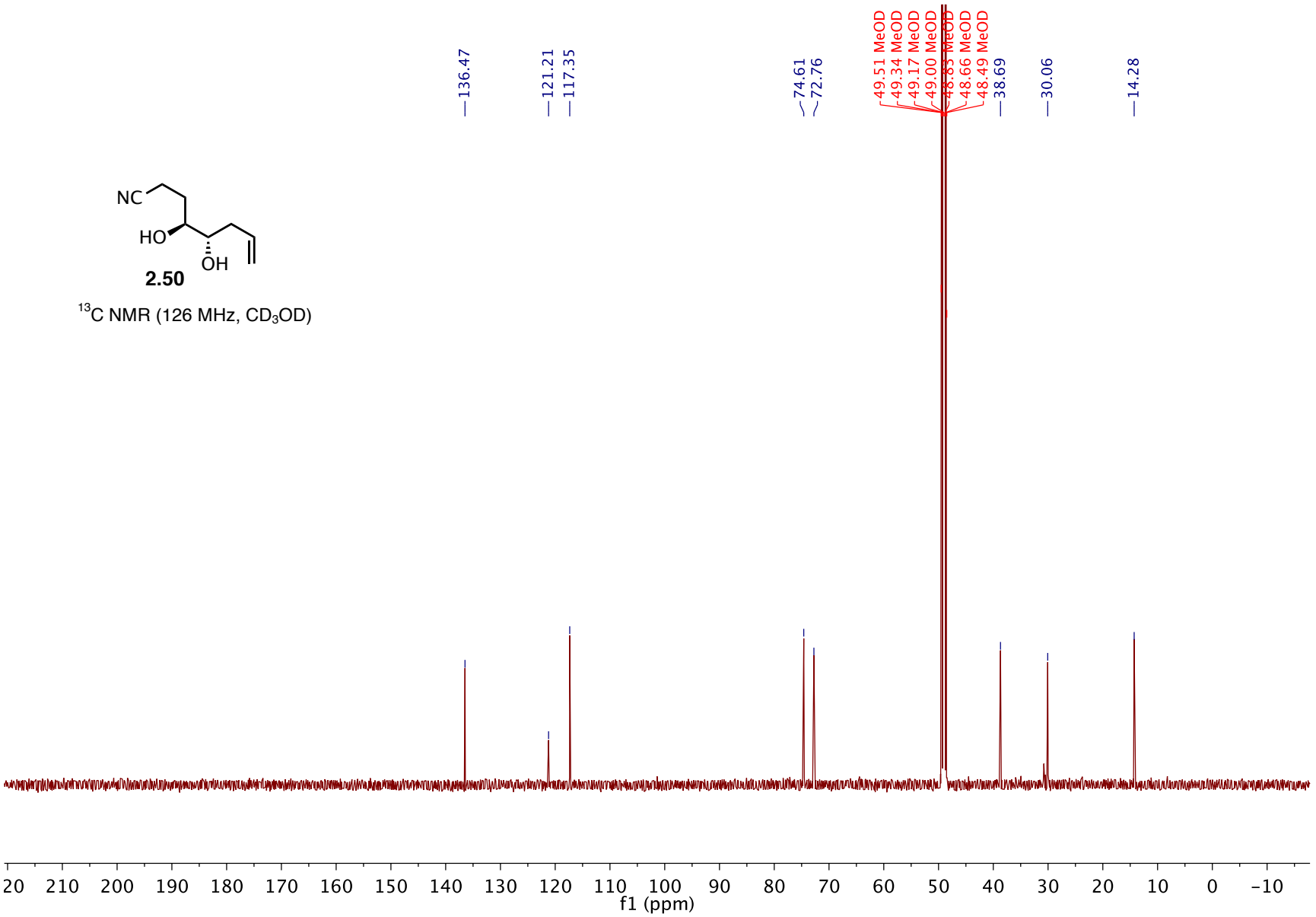
NC
HO
OH
2.50
^{13}C NMR (126 MHz, CD$_3$OD)
136.47
121.21
117.35
74.61
72.76
49.51 MeOD
49.34 MeOD
49.17 MeOD
49.00 MeOD
48.83 MeOD
48.66 MeOD
48.49 MeOD
38.69
30.06
14.28
f1 (ppm)

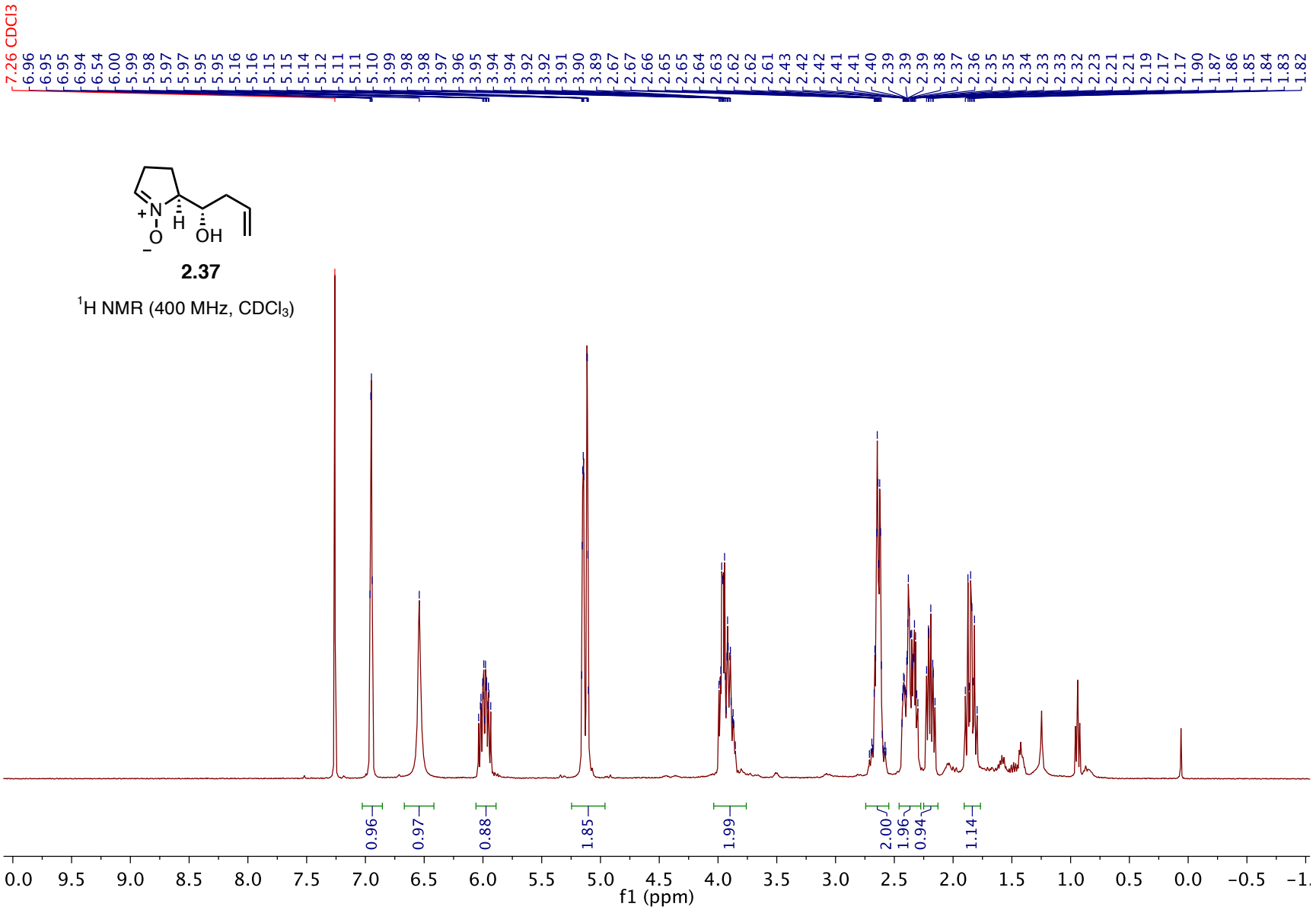
7.26 CDCl3
6.96 6.95 6.95 6.94 6.54 6.00 5.99 5.98 5.97 5.97 5.95 5.95 5.16 5.16 5.15 5.15 5.14 5.12 5.11 5.11 5.10 3.99 3.98 3.98 3.97 3.96 3.95 3.94 3.94 3.92 3.92 3.91 3.90 3.89 2.67 2.67 2.66 2.65 2.65 2.64 2.63 2.62 2.62 2.61 2.43 2.42 2.42 2.41 2.41 2.40 2.39 2.39 2.38 2.37 2.36 2.35 2.35 2.34 2.33 2.33 2.32 2.23 2.21 2.21 2.19 2.17 2.17 1.90 1.87 1.86 1.85 1.84 1.83 1.82
N
O
H
OH
2.37
1H NMR (400 MHz, CDCl3)
0.96
0.97
0.88
1.85
1.99
2.00
1.96
0.94
1.14
0.0 9.5 9.0 8.5 8.0 7.5 7.0 6.5 6.0 5.5 5.0 4.5 4.0 3.5 3.0 2.5 2.0 1.5 1.0 0.5 0.0 −0.5 −1.
f1 (ppm)

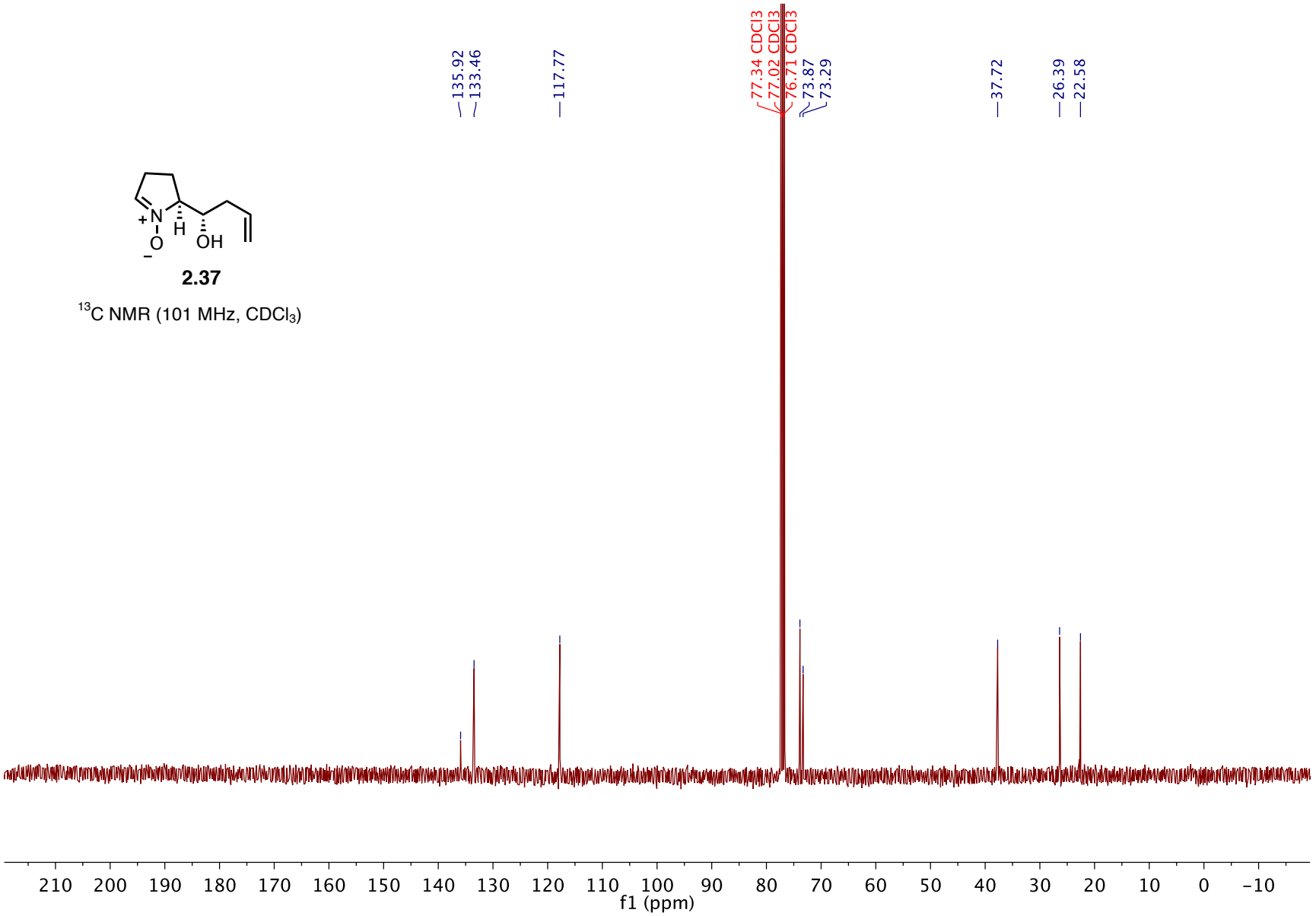

2.37

^{13}C NMR (101 MHz, $CDCl_3$)

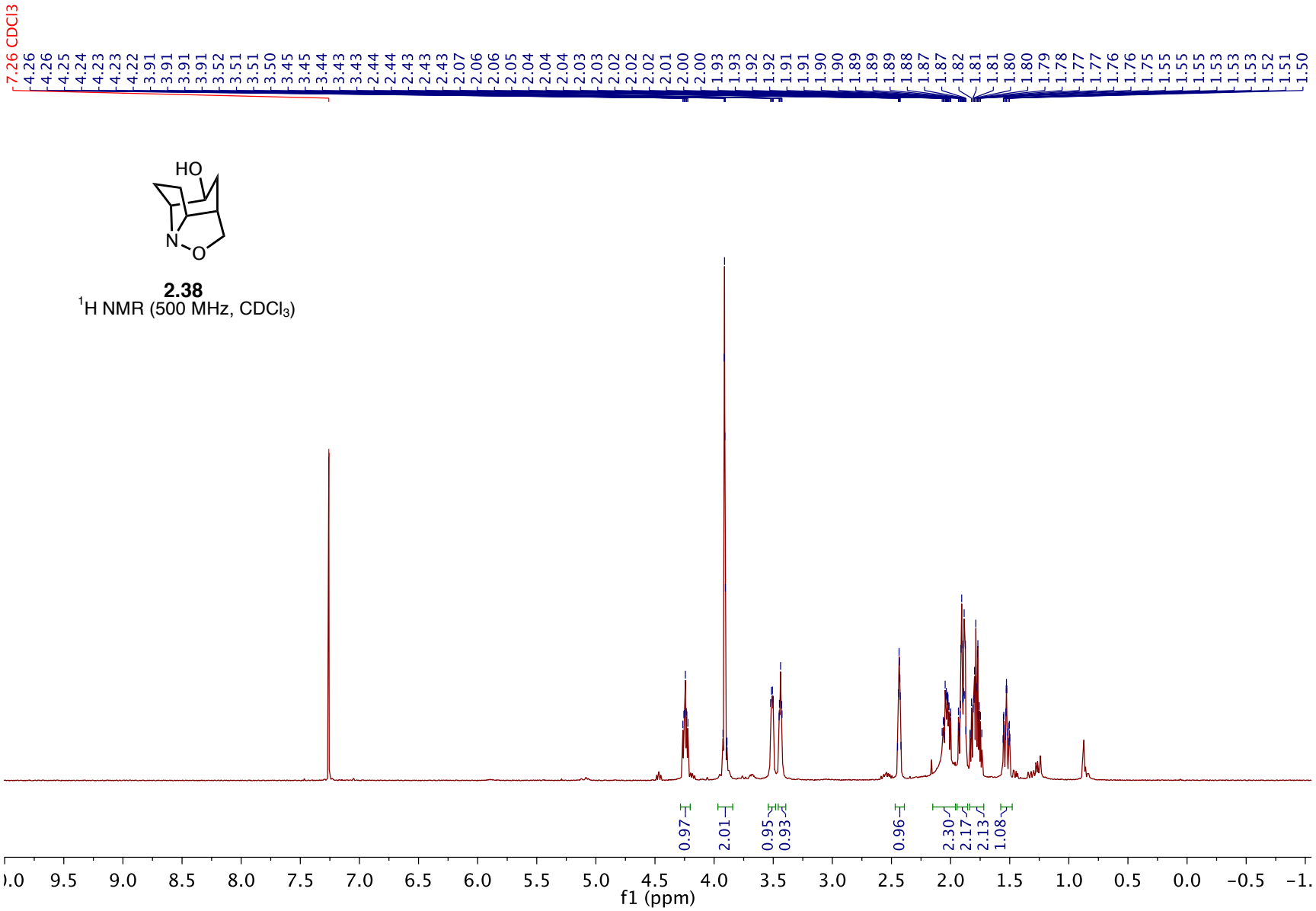

2.38

^{1}H NMR (500 MHz, $CDCl_3$)

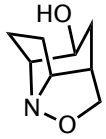

2.38

^{13}C NMR (126 MHz, $CDCl_3$)

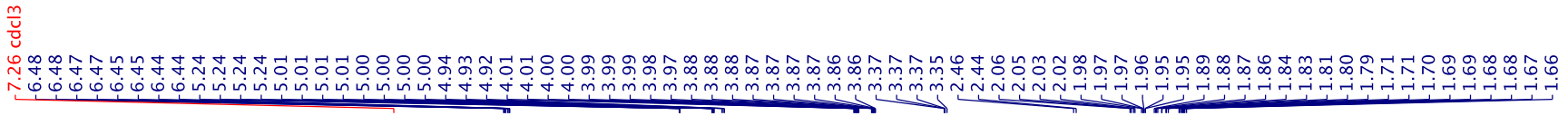

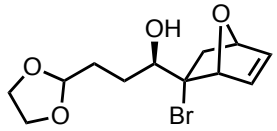

2.102

^{1}H NMR (500 MHz, $CDCl_3$)

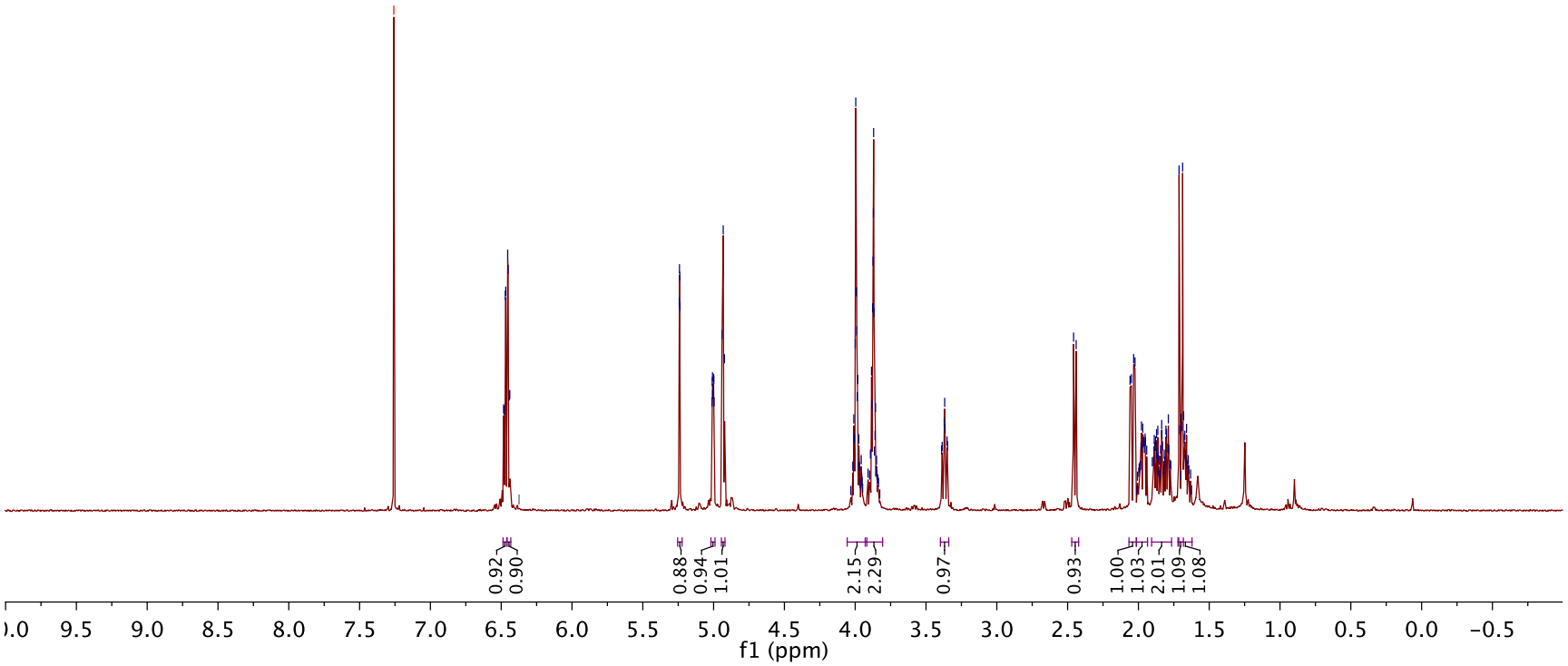

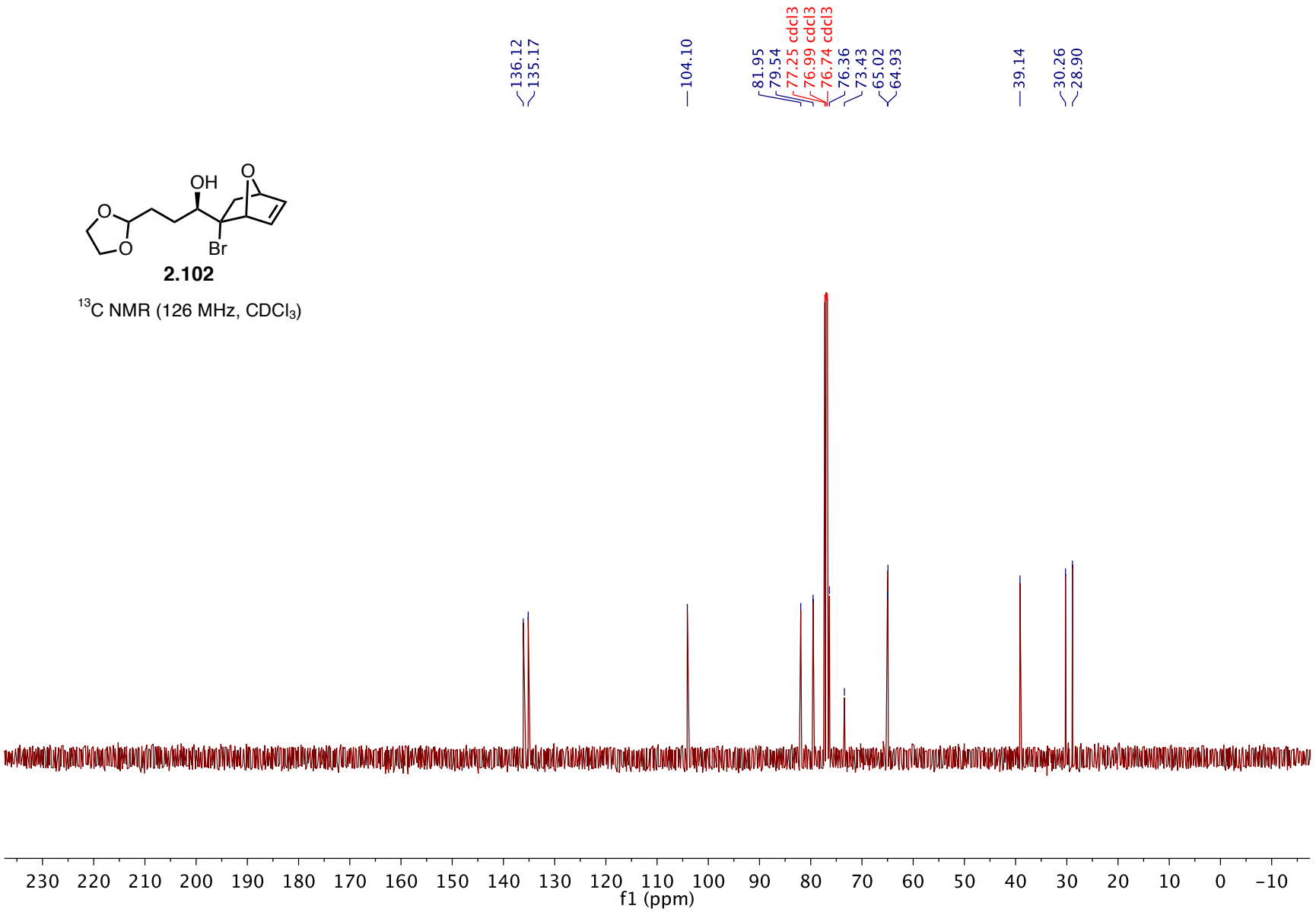
136.12
135.17
104.10
81.95
79.54
77.25 cdcl3
76.99 cdcl3
76.74 cdcl3
76.36
73.43
65.02
64.93
39.14
30.26
28.90
OH
O
O
O
Br
2.102
13C NMR (126 MHz, CDCl3)
230 220 210 200 190 180 170 160 150 140 130 120 110 100 90 80 70 60 50 40 30 20 10 0 -10
f1 (ppm)

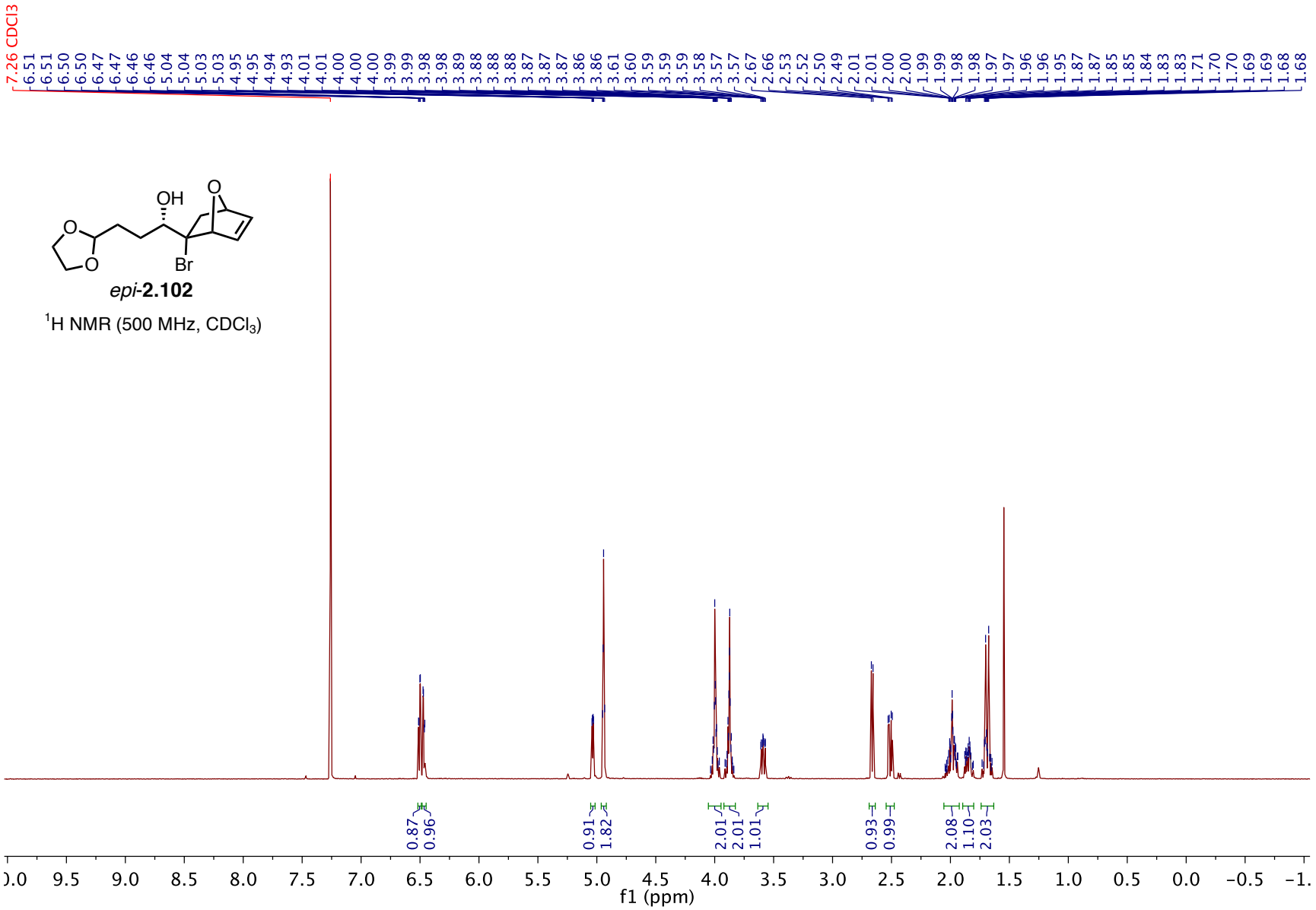
7.26 CDCl3
6.51 6.51 6.50 6.50 6.47 6.46 6.46 5.04 5.04 5.03 5.03 4.95 4.95 4.94 4.93 4.01 4.01 4.00 4.00 4.00 3.99 3.99 3.98 3.98 3.89 3.88 3.88 3.88 3.87 3.87 3.87 3.86 3.86 3.61 3.60 3.59 3.59 3.59 3.58 3.57 3.57 2.67 2.66 2.53 2.52 2.50 2.49 2.01 2.01 2.00 2.00 1.99 1.99 1.98 1.98 1.97 1.97 1.96 1.96 1.95 1.87 1.87 1.85 1.85 1.84 1.83 1.83 1.71 1.70 1.70 1.69 1.69 1.68 1.68
OH
O
O
O
Br
epi-2.102
1H NMR (500 MHz, CDCl3)
0.87
0.96
0.91
1.82
2.01
2.01
1.01
0.93
0.99
2.08
1.10
2.03
9.5 9.0 8.5 8.0 7.5 7.0 6.5 6.0 5.5 5.0 4.5 4.0 3.5 3.0 2.5 2.0 1.5 1.0 0.5 0.0 -0.5
f1 (ppm)

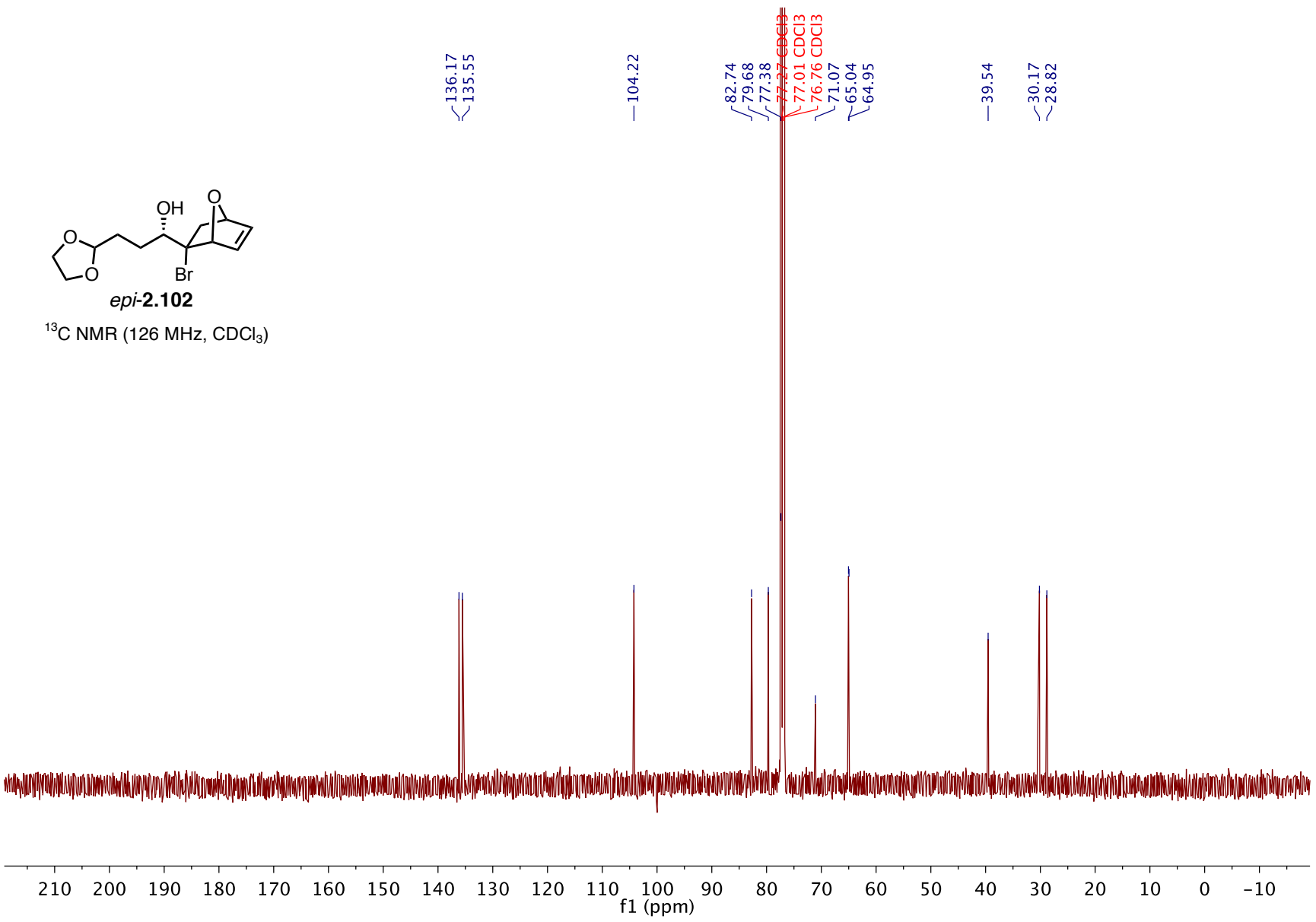

epi-**2.102**

^{13}C NMR (126 MHz, $CDCl_3$)

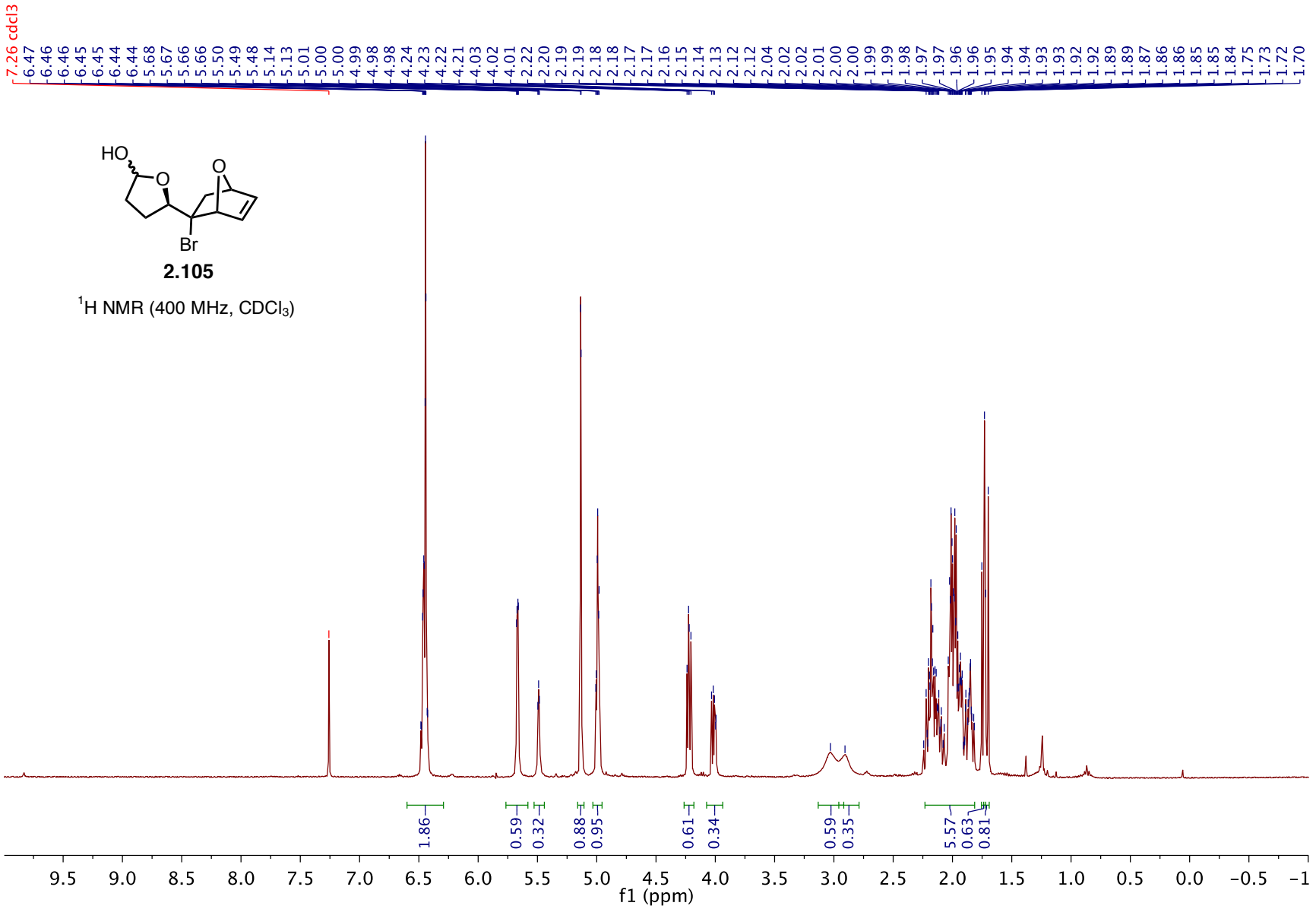
7.26 cdcl3
6.47 6.46 6.46 6.45 6.45 6.44 6.44 5.68 5.67 5.66 5.66 5.50 5.49 5.48 5.14 5.13 5.01 5.00 5.00 4.99 4.98 4.98 4.24 4.23 4.22 4.21 4.03 4.02 4.01 2.22 2.20 2.19 2.19 2.18 2.18 2.17 2.17 2.16 2.15 2.14 2.13 2.12 2.12 2.04 2.02 2.02 2.01 2.00 2.00 1.99 1.99 1.98 1.97 1.97 1.96 1.96 1.95 1.94 1.94 1.93 1.93 1.92 1.92 1.89 1.89 1.87 1.86 1.86 1.85 1.85 1.84 1.75 1.73 1.72 1.70
HO
O
O
Br
2.105
^{1}H NMR (400 MHz, $CDCl_3$)
1.86
0.59
0.32
0.88
0.95
0.61
0.34
0.59
0.35
5.57
0.63
0.81
9.5 9.0 8.5 8.0 7.5 7.0 6.5 6.0 5.5 5.0 4.5 4.0 3.5 3.0 2.5 2.0 1.5 1.0 0.5 0.0 -0.5 -1
f1 (ppm)

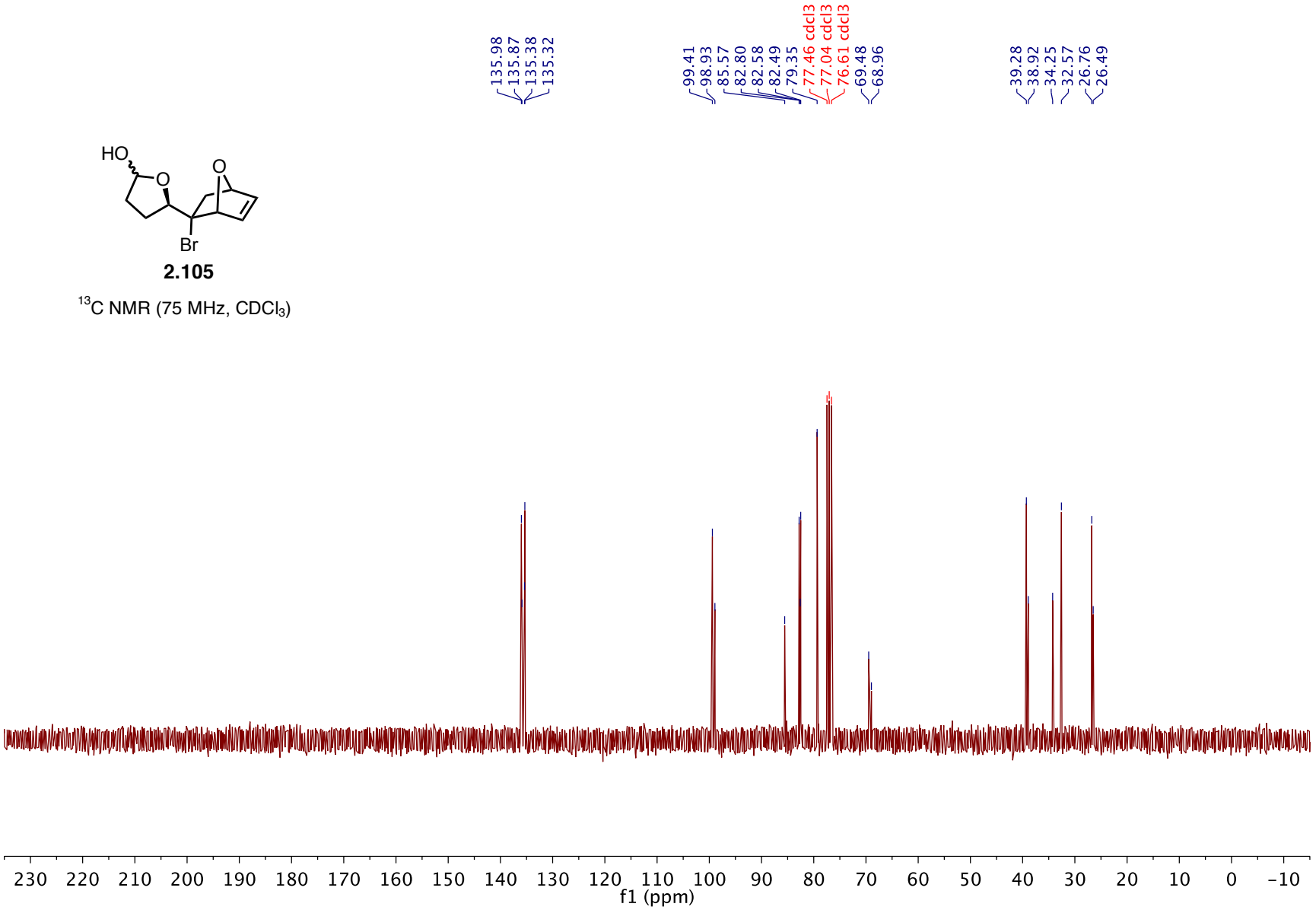

2.105

^{13}C NMR (75 MHz, $CDCl_3$)

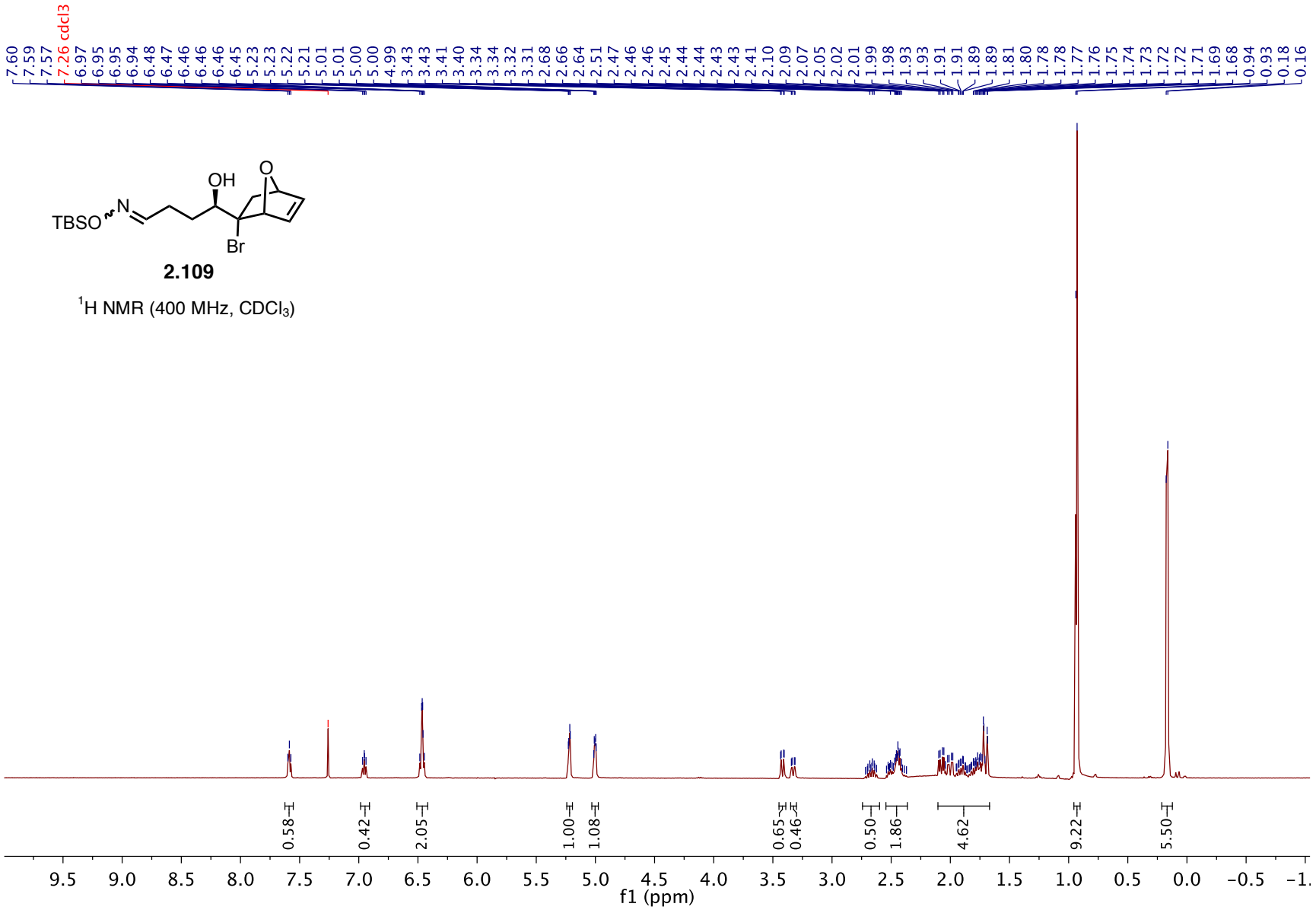

2.109

^{1}H NMR (400 MHz, $CDCl_3$)

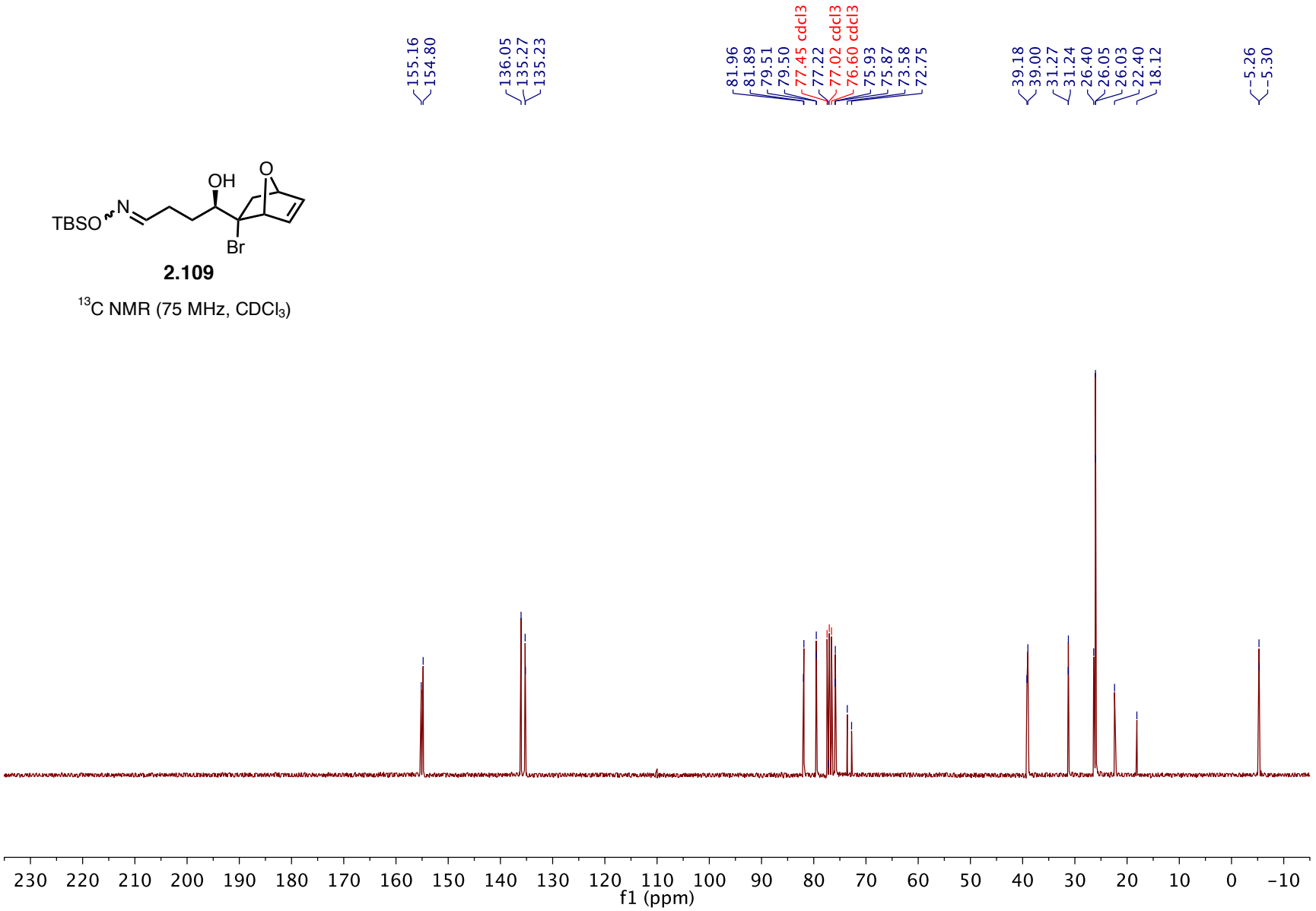

2.109

^{13}C NMR (75 MHz, $CDCl_3$)

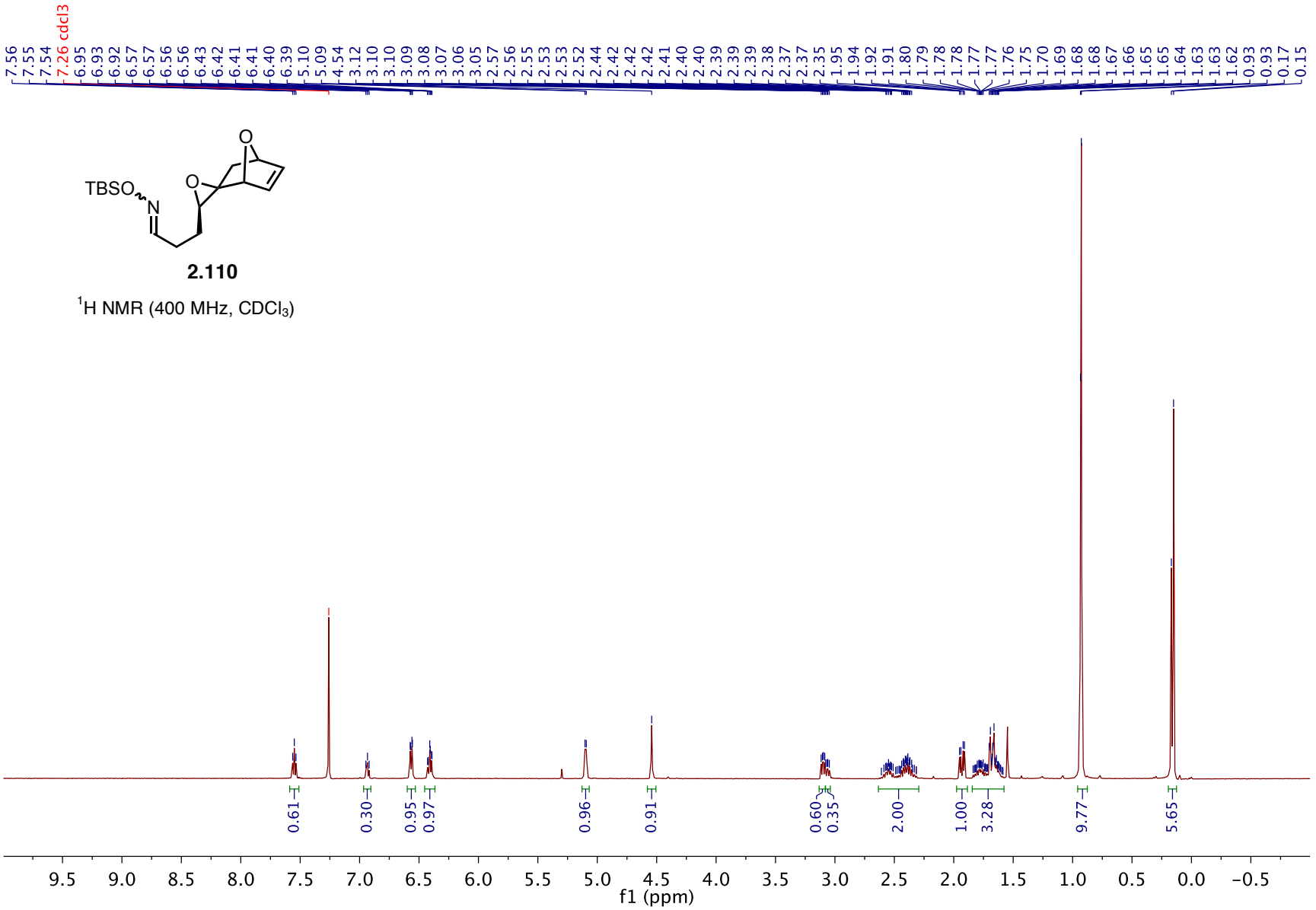

2.110

^{1}H NMR (400 MHz, $CDCl_3$)

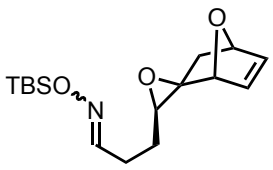

2.110

^{13}C NMR (75 MHz, $CDCl_3$)

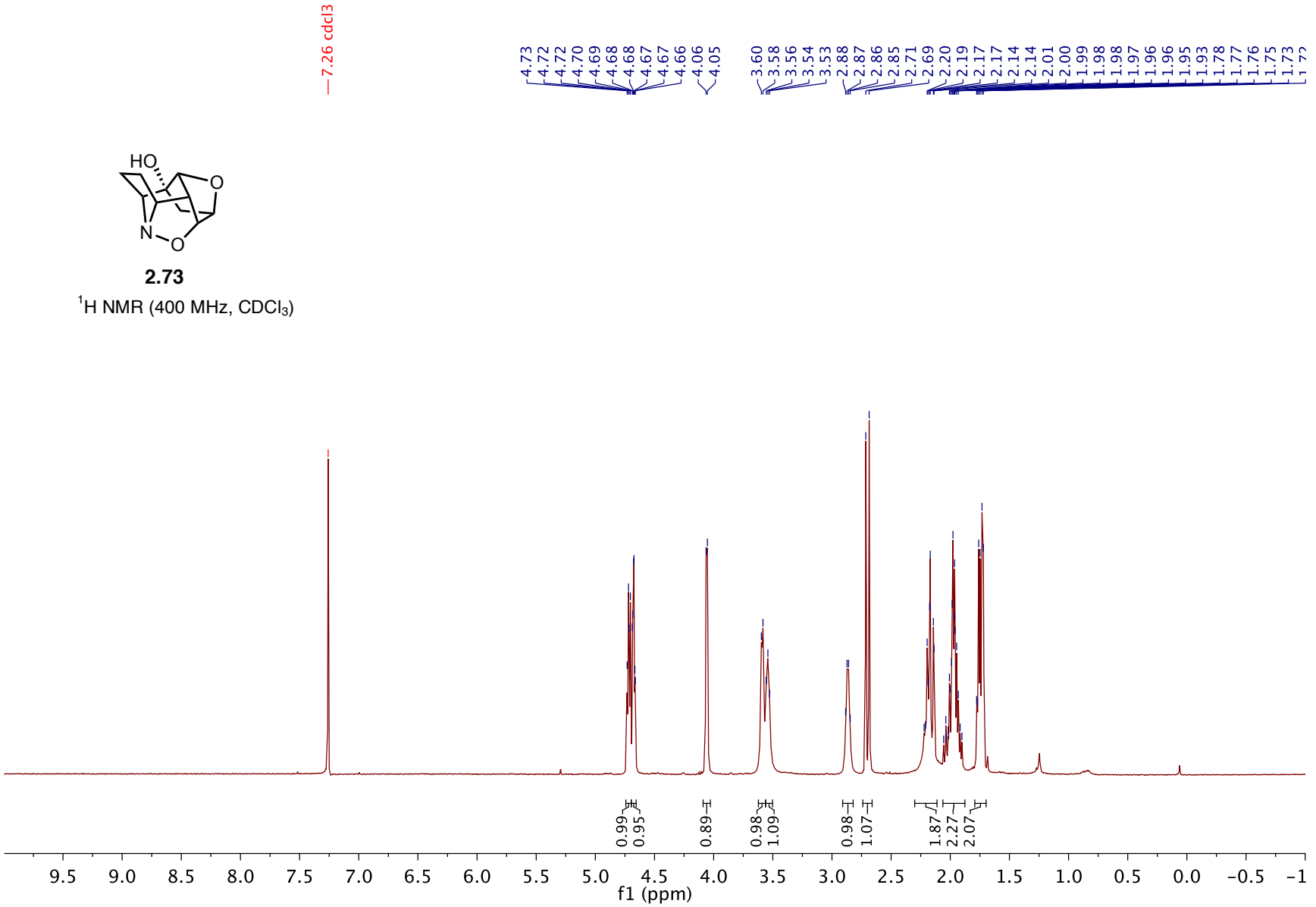

2.73

^{1}H NMR (400 MHz, $CDCl_3$)

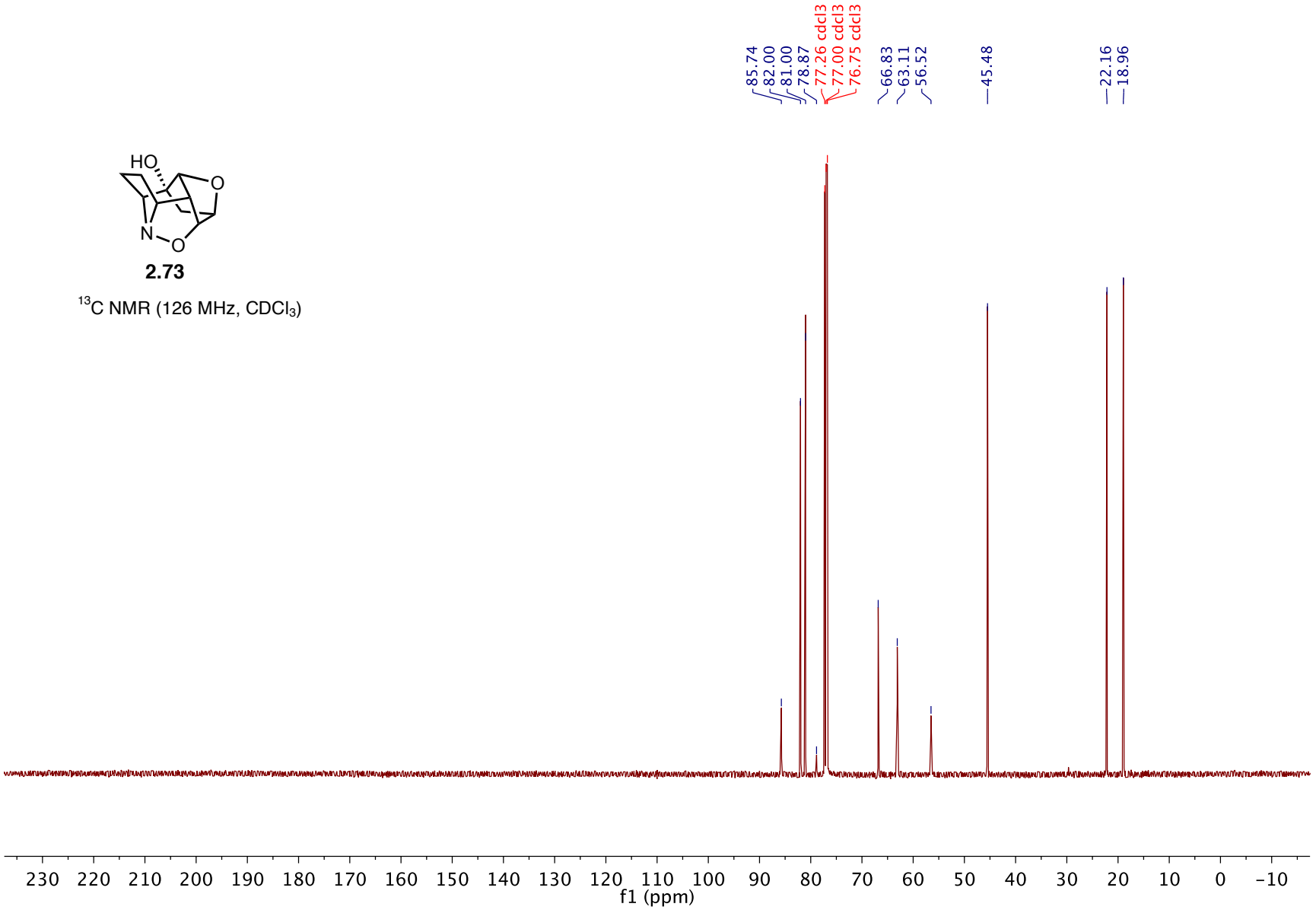
HO
O
N
O
2.73
^{13}C NMR (126 MHz, $CDCl_3$)
85.74
82.00
81.00
78.87
77.26 cdcl3
77.00 cdcl3
76.75 cdcl3
66.83
63.11
56.52
45.48
22.16
18.96
230 220 210 200 190 180 170 160 150 140 130 120 110 100 90 80 70 60 50 40 30 20 10 0 -10
f1 (ppm)

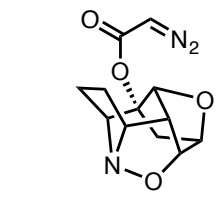

3.10

^{1}H NMR (400 MHz, $CDCl_3$)

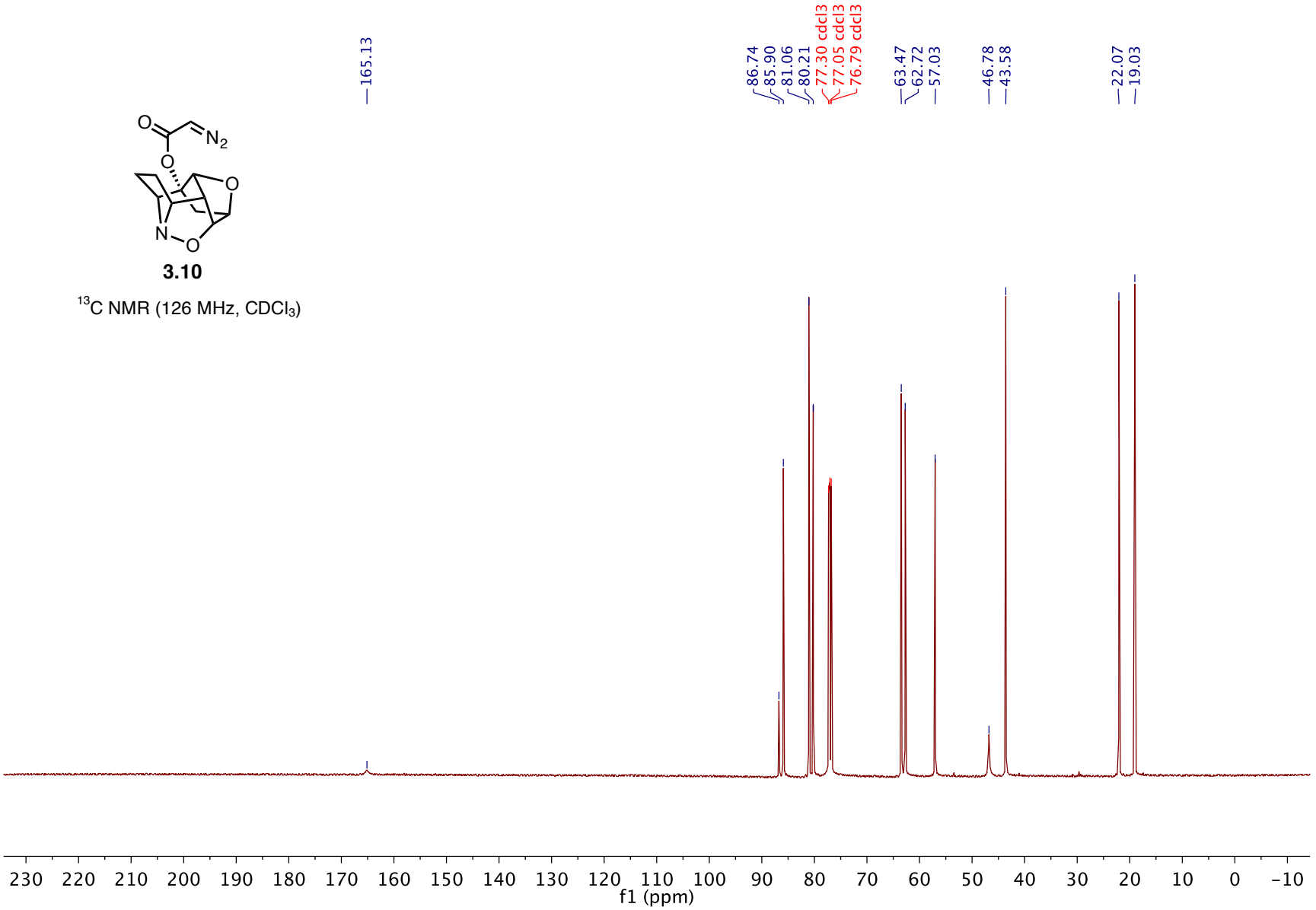
O
N2
O
O
N
O
3.10
13C NMR (126 MHz, CDCl3)
165.13
86.74
85.90
81.06
80.21
77.30 cdcl3
77.05 cdcl3
76.79 cdcl3
63.47
62.72
57.03
46.78
43.58
22.07
19.03
230 220 210 200 190 180 170 160 150 140 130 120 110 100 90 80 70 60 50 40 30 20 10 0 -10
f1 (ppm)

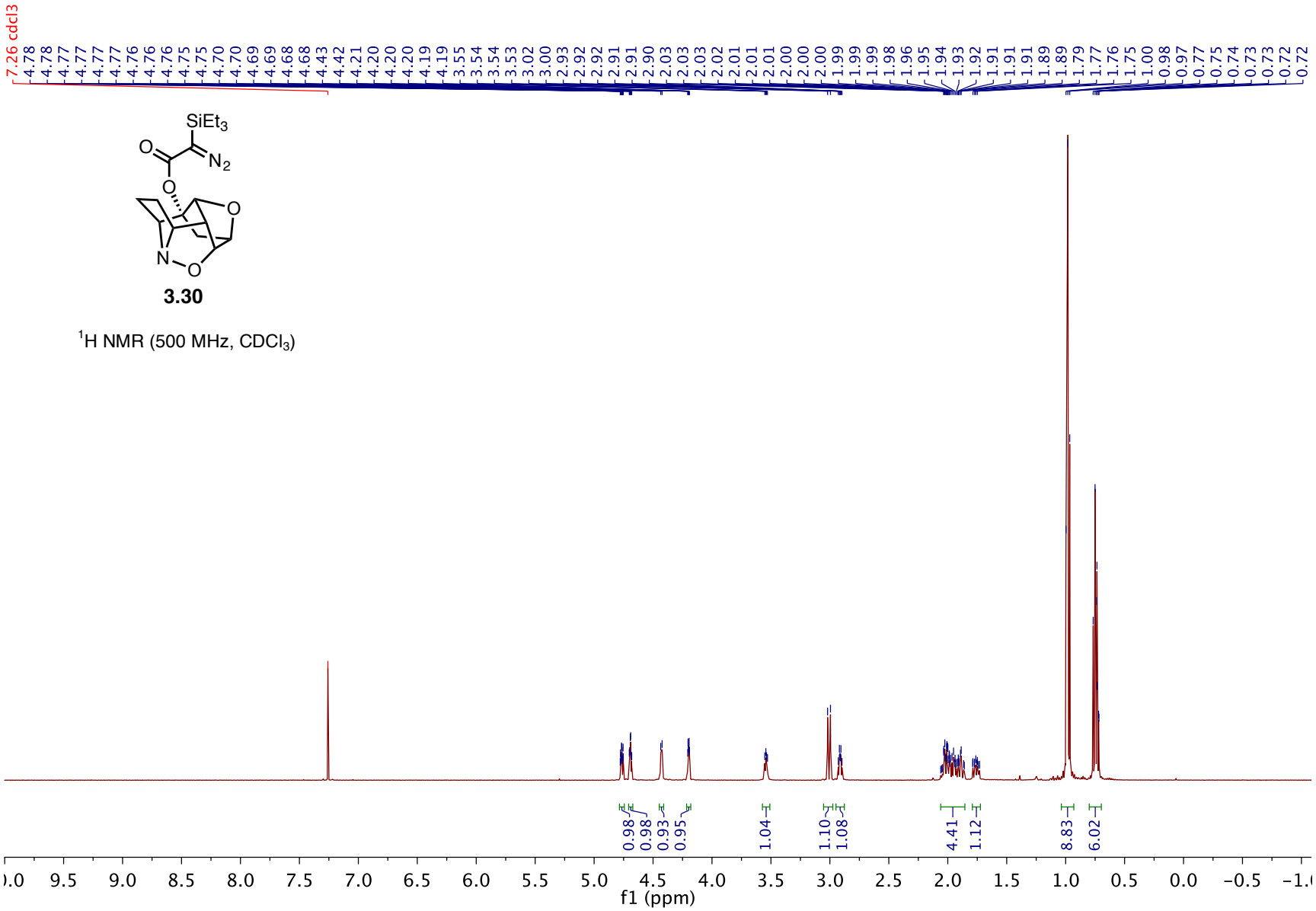
7.26 cdcl3
SiEt3
O
N2
O
O
N
O
3.30
1H NMR (500 MHz, CDCl3)
0.98
0.98
0.93
0.95
1.04
1.10
1.08
4.41
1.12
8.83
6.02
f1 (ppm)

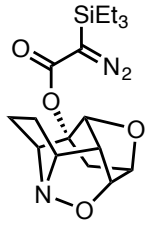

3.30

^{13}C NMR (126 MHz, $CDCl_3$)

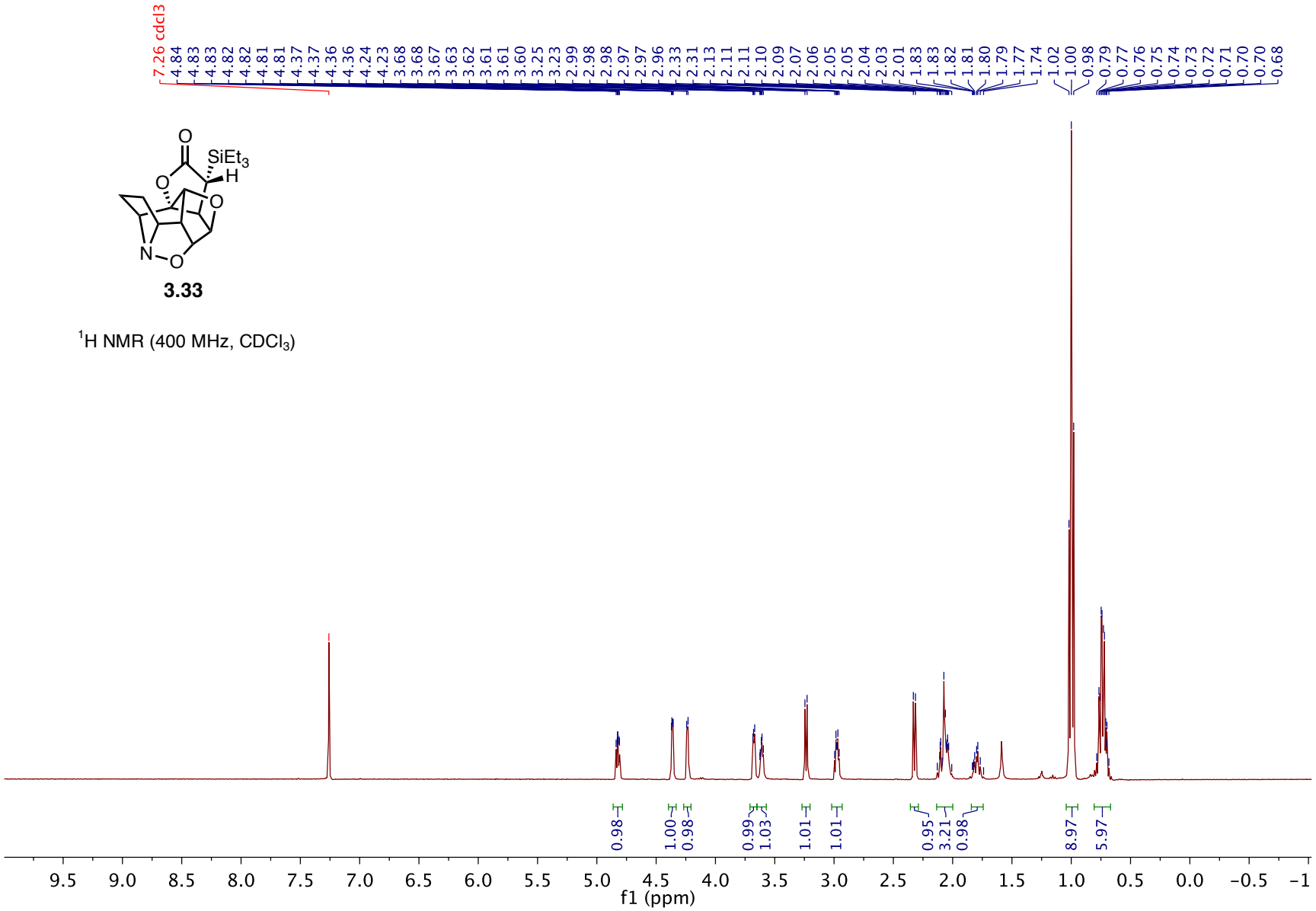

3.33

^{1}H NMR (400 MHz, $CDCl_3$)

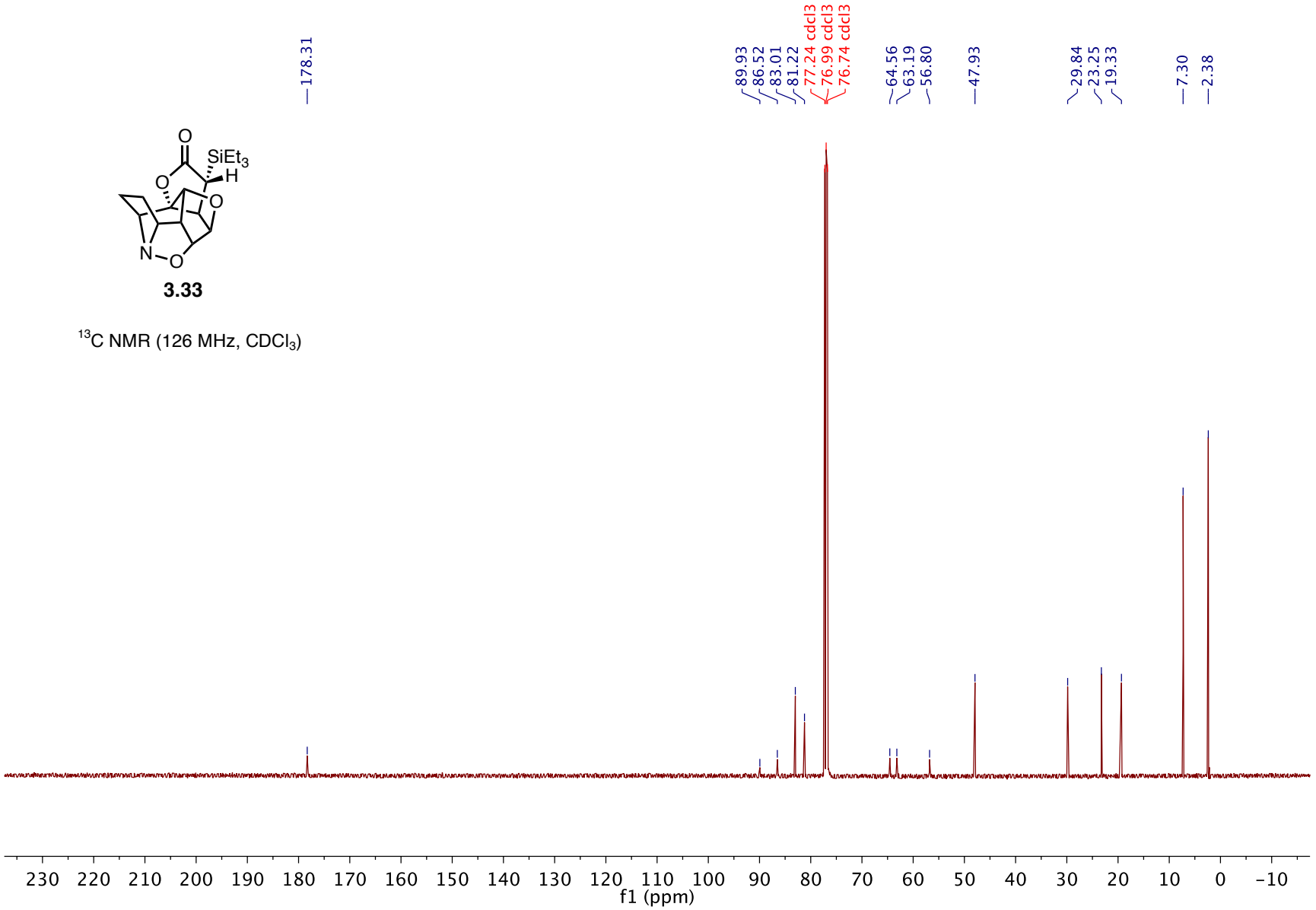

3.33

^{13}C NMR (126 MHz, $CDCl_3$)

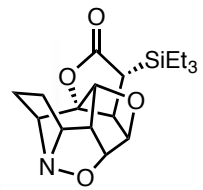

3.33

COSY ($CDCl_3$)

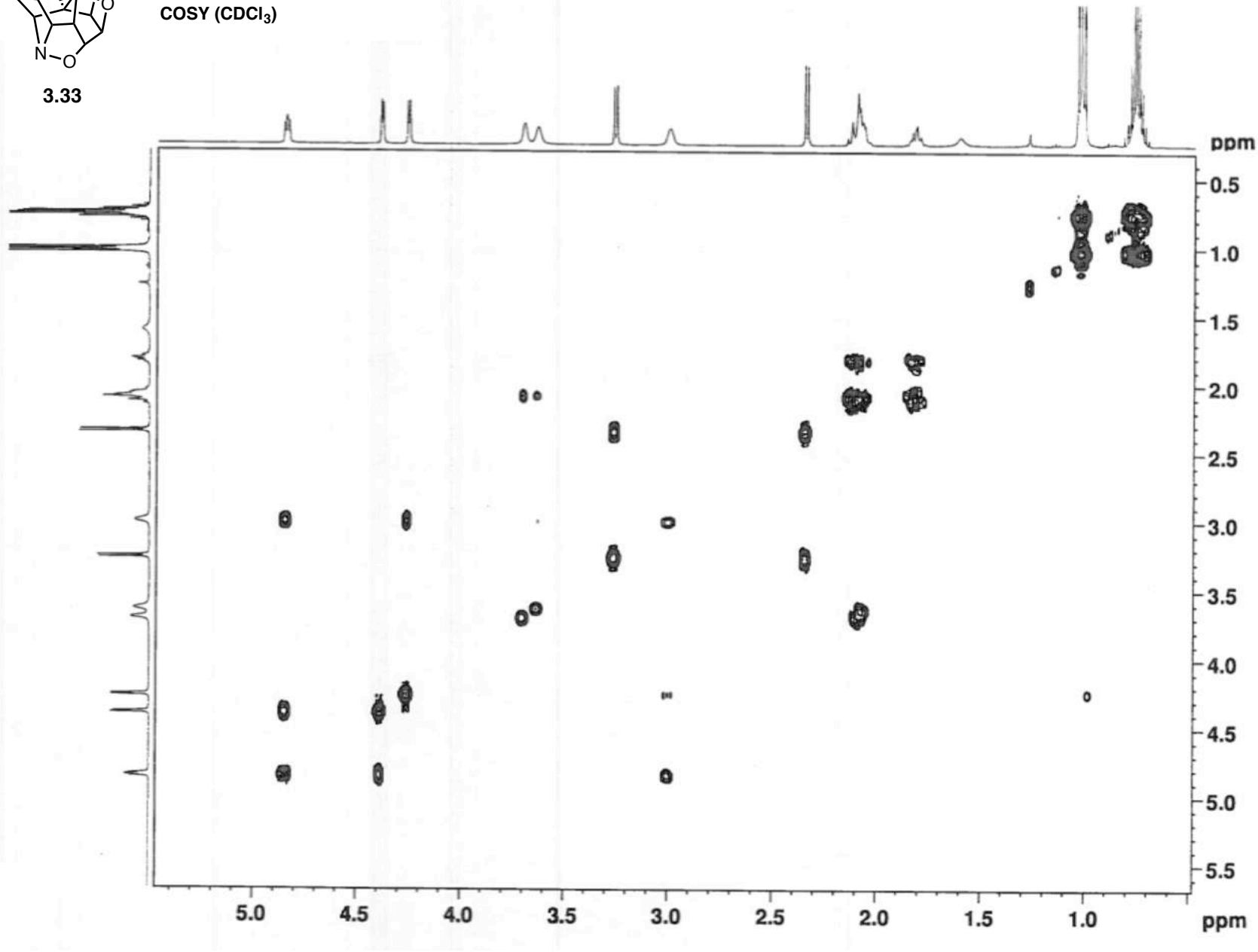

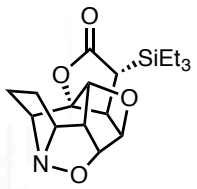

HSQC ($CDCl_3$)

3.33

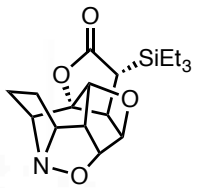

3.33

HMBC ($CDCl_3$)

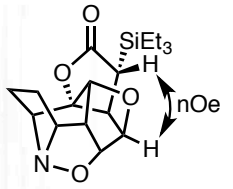

3.33

NOESY ($CDCl_3$)

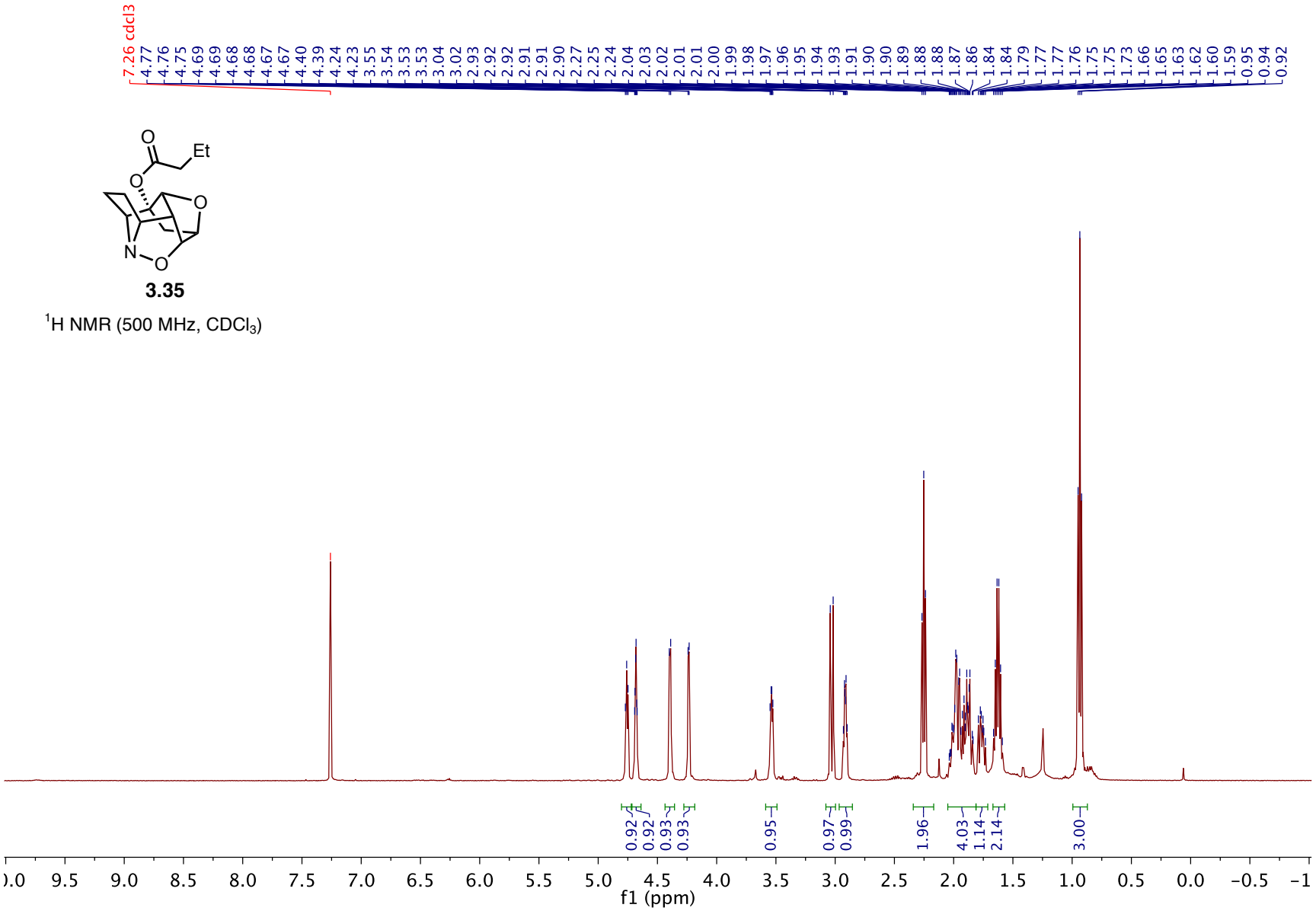

3.35

^{1}H NMR (500 MHz, $CDCl_3$)

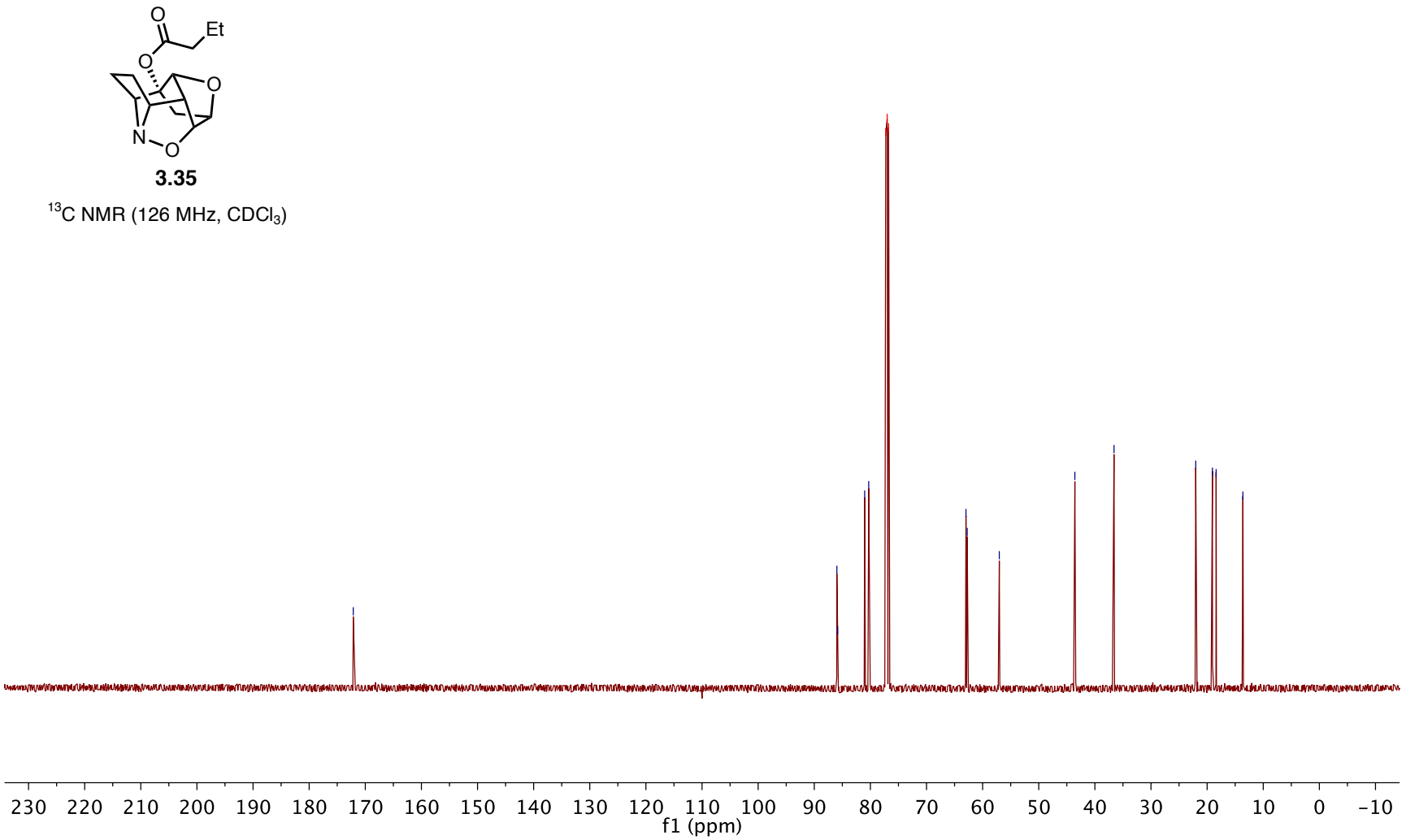

3.35

^{13}C NMR (126 MHz, $CDCl_3$)

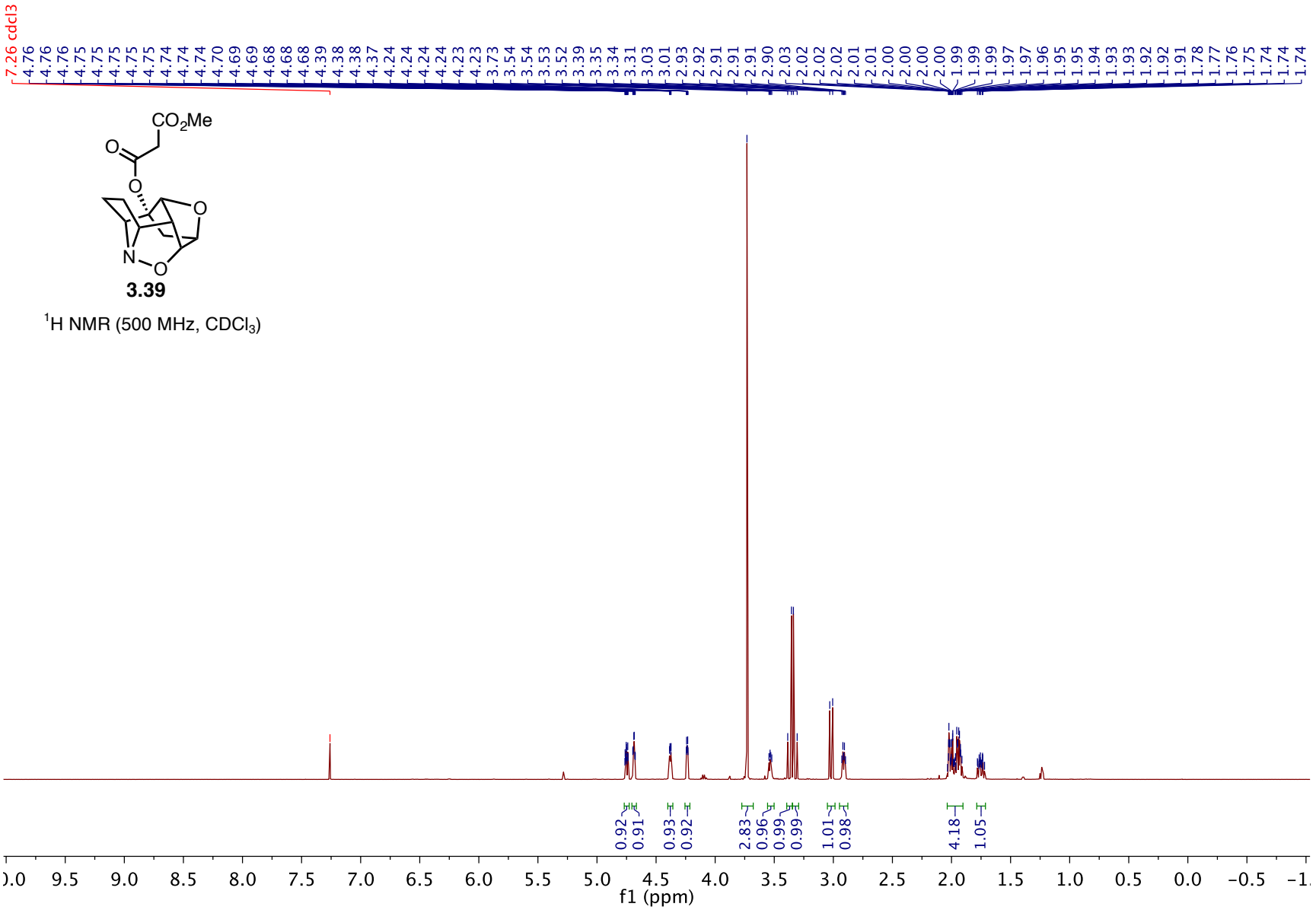
7.26 cdcl3
CO2Me
O
O
O
N
O
3.39
1H NMR (500 MHz, CDCl3)
0.92
0.91
0.93
0.92
2.83
0.96
0.99
0.99
1.01
0.98
4.18
1.05
f1 (ppm)

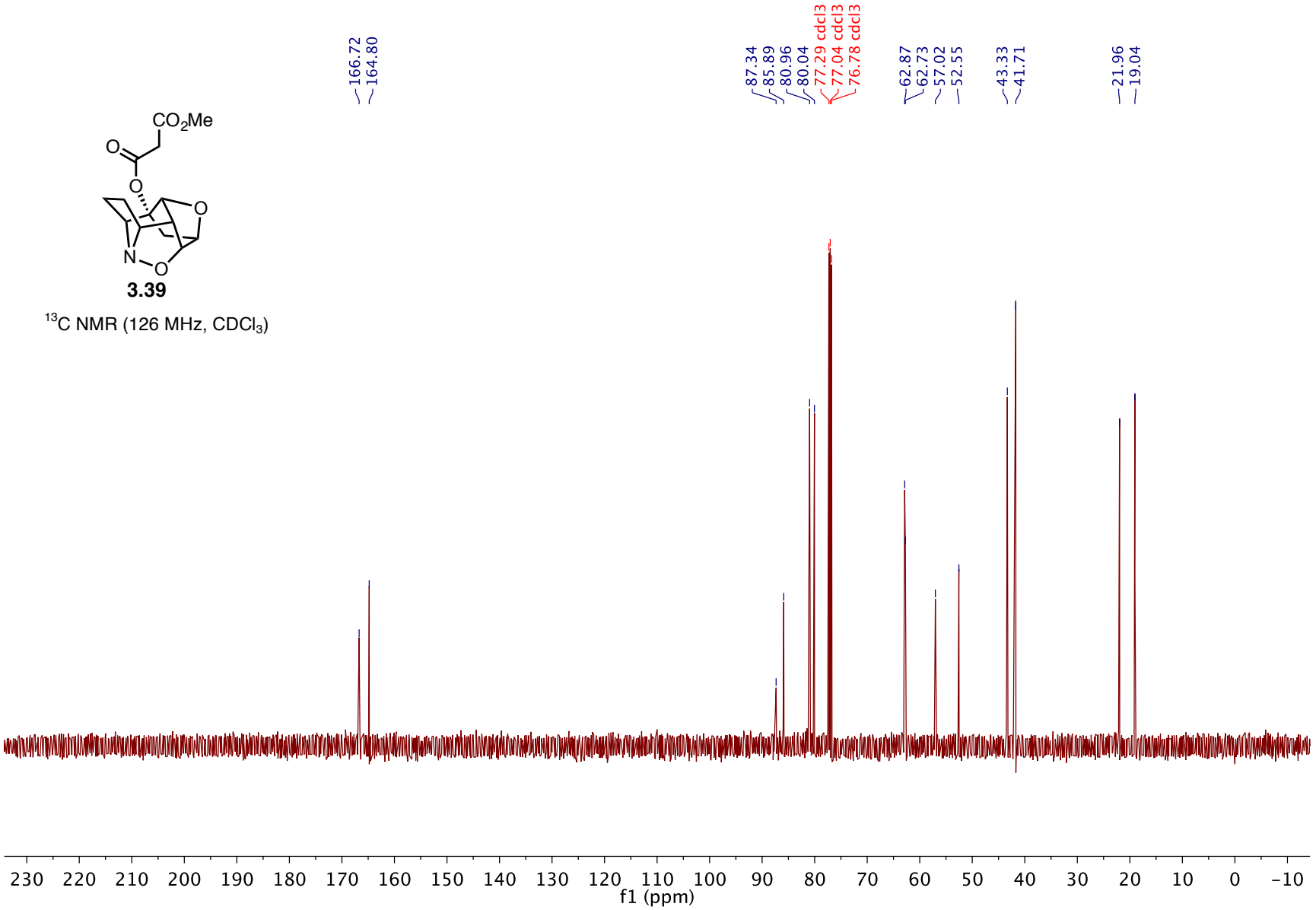
CO2Me
O
O
O
N
O
3.39
13C NMR (126 MHz, CDCl3)
166.72
164.80
87.34
85.89
80.96
80.04
77.29 cdcl3
77.04 cdcl3
76.78 cdcl3
62.87
62.73
57.02
52.55
43.33
41.71
21.96
19.04
230 220 210 200 190 180 170 160 150 140 130 120 110 100 90 80 70 60 50 40 30 20 10 0 -10
f1 (ppm)

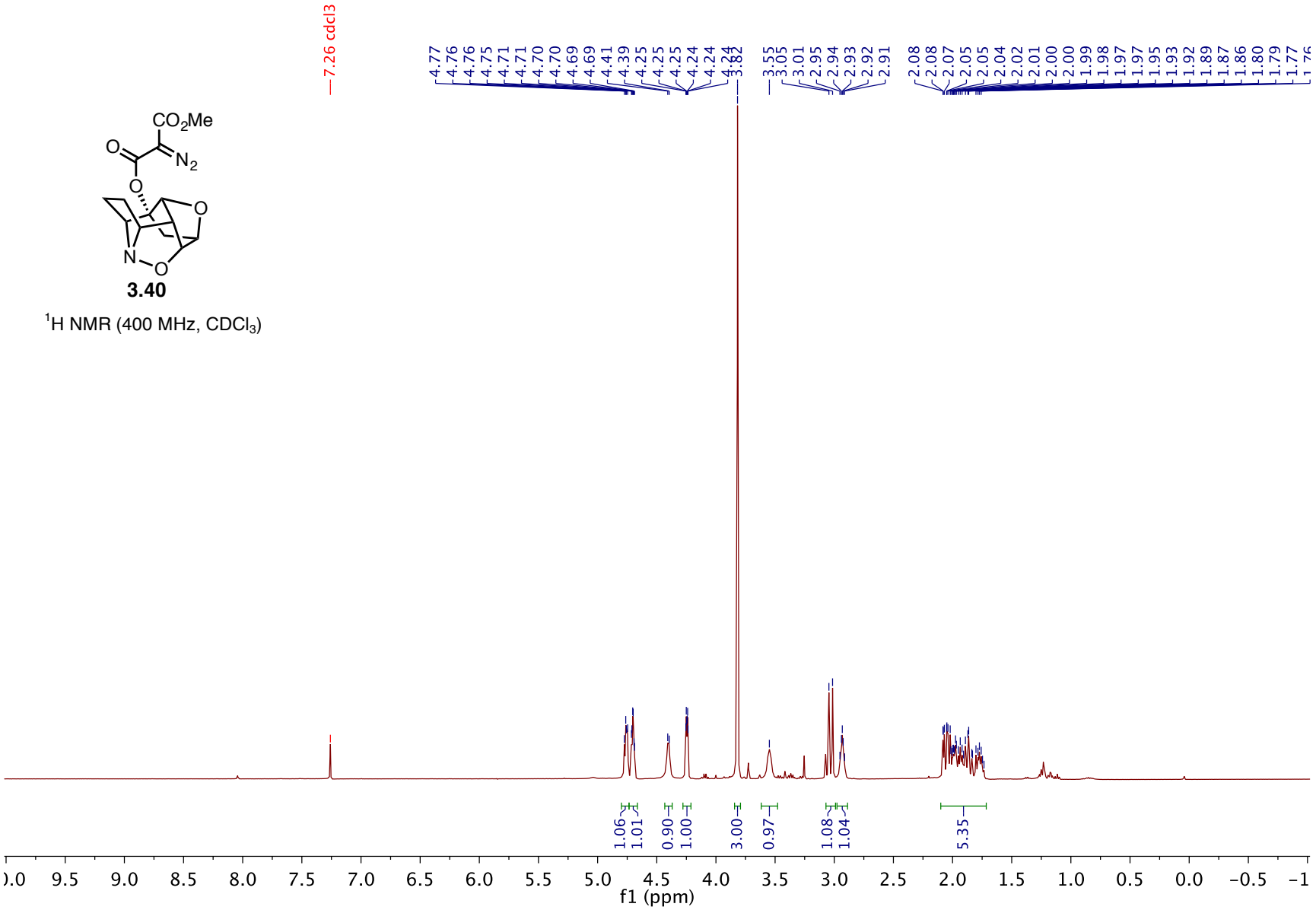

CO_2Me

N_2

3.40

^{1}H NMR (400 MHz, $CDCl_3$)

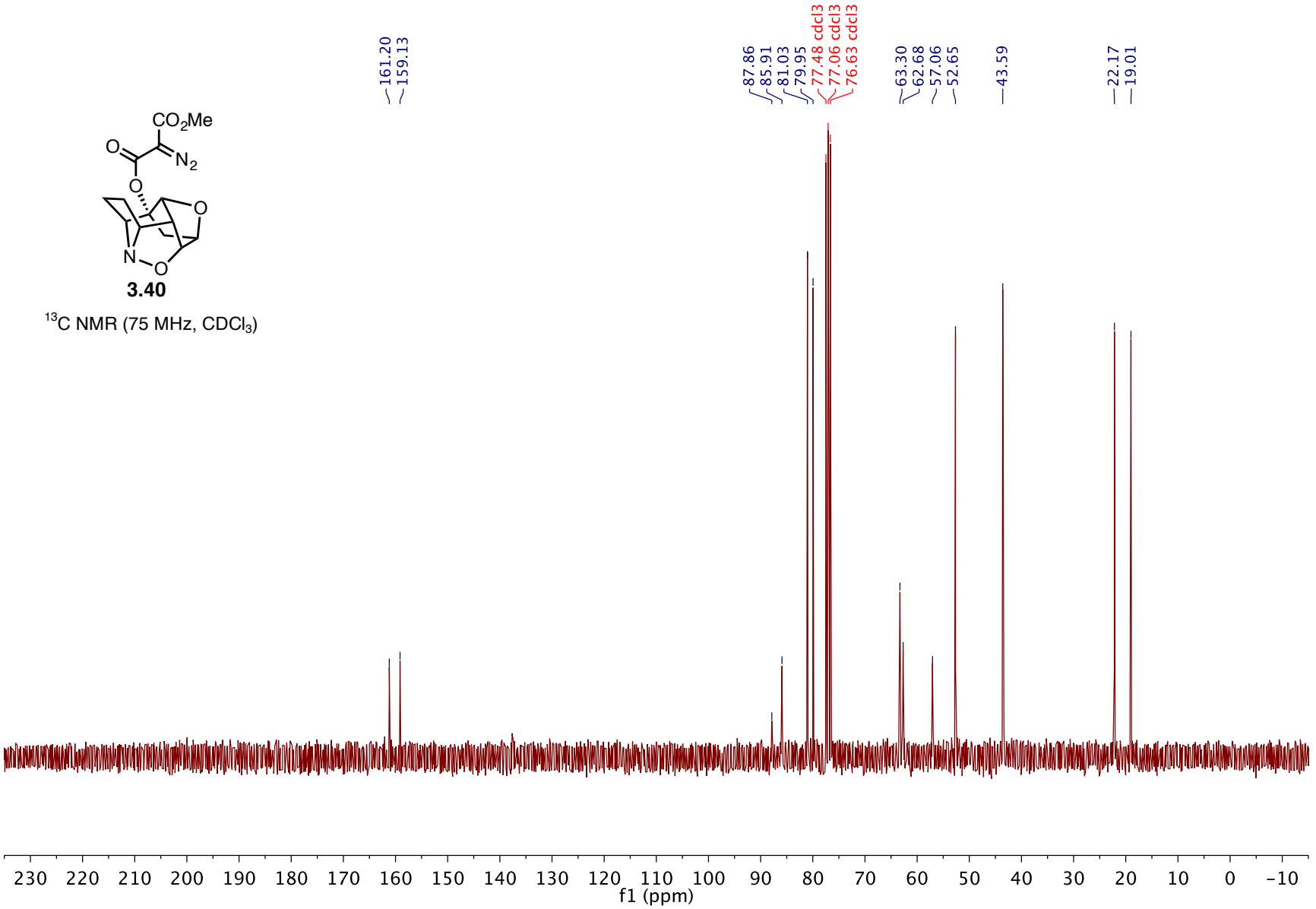
CO2Me
O
N2
O
O
N
O
3.40
13C NMR (75 MHz, CDCl3)
161.20
159.13
87.86
85.91
81.03
79.95
77.48 cdcl3
77.06 cdcl3
76.63 cdcl3
63.30
62.68
57.06
52.65
43.59
22.17
19.01
230 220 210 200 190 180 170 160 150 140 130 120 110 100 90 80 70 60 50 40 30 20 10 0 -10
f1 (ppm)

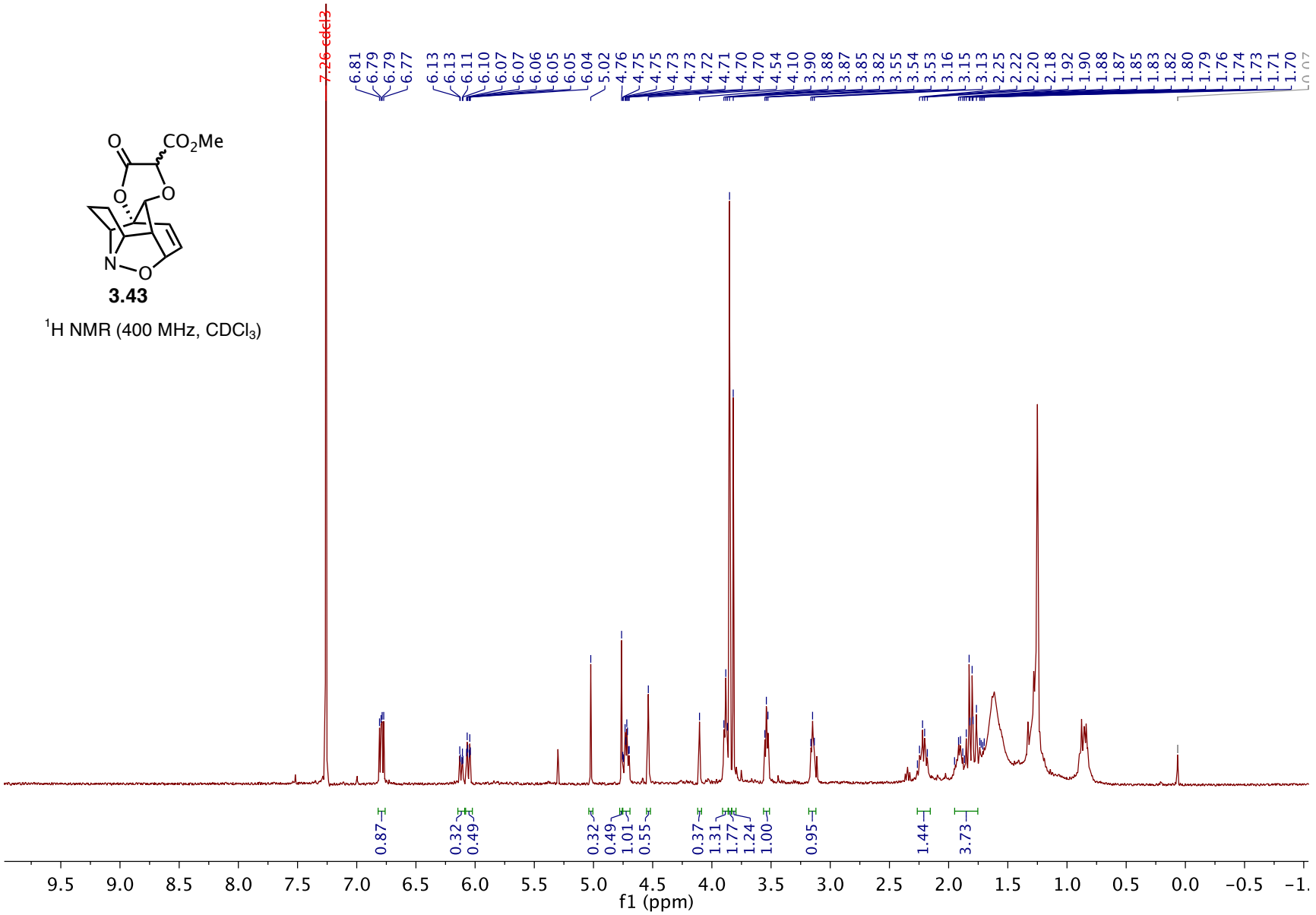
O
CO2Me
O
O
N
O
3.43
1H NMR (400 MHz, CDCl3)
7.26 cdcl3
6.81
6.79
6.79
6.77
6.13
6.13
6.11
6.10
6.07
6.07
6.06
6.05
6.05
6.04
5.02
4.76
4.75
4.75
4.73
4.73
4.72
4.71
4.70
4.70
4.54
4.10
3.90
3.88
3.87
3.85
3.82
3.55
3.54
3.53
3.16
3.15
3.13
2.25
2.22
2.20
2.18
1.92
1.90
1.88
1.87
1.85
1.83
1.82
1.80
1.79
1.76
1.74
1.73
1.71
1.70
0.87
0.32
0.49
0.32
0.49
1.01
0.55
0.37
1.31
1.77
1.24
1.00
0.95
1.44
3.73
9.5
9.0
8.5
8.0
7.5
7.0
6.5
6.0
5.5
5.0
4.5
4.0
3.5
3.0
2.5
2.0
1.5
1.0
0.5
0.0
−0.5
f1 (ppm)

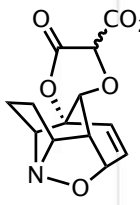

3.43

COSY ($CDCl_3$)

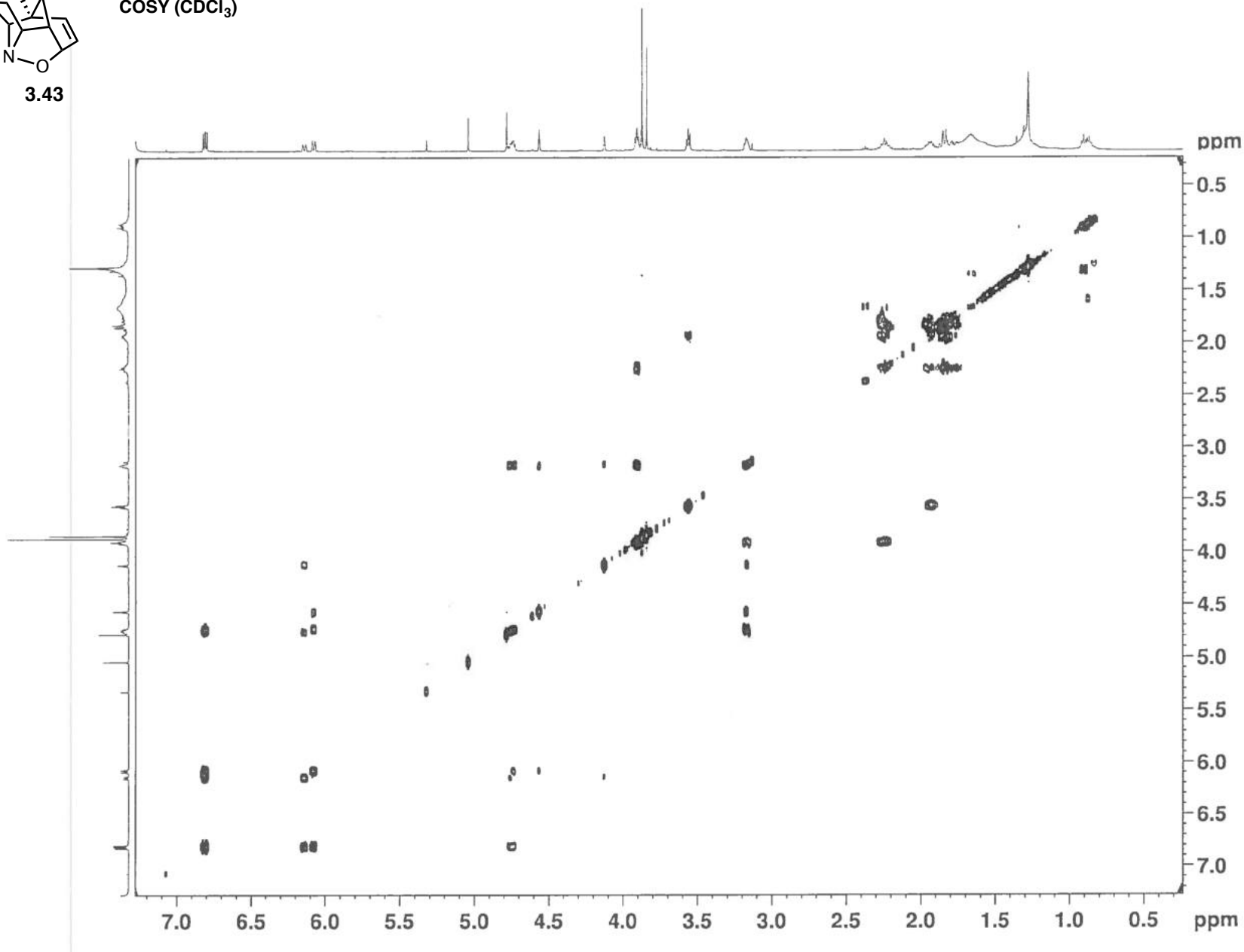

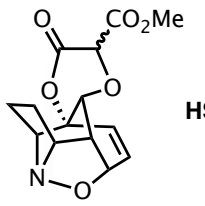

3.43

HSQC ($CDCl_3$)

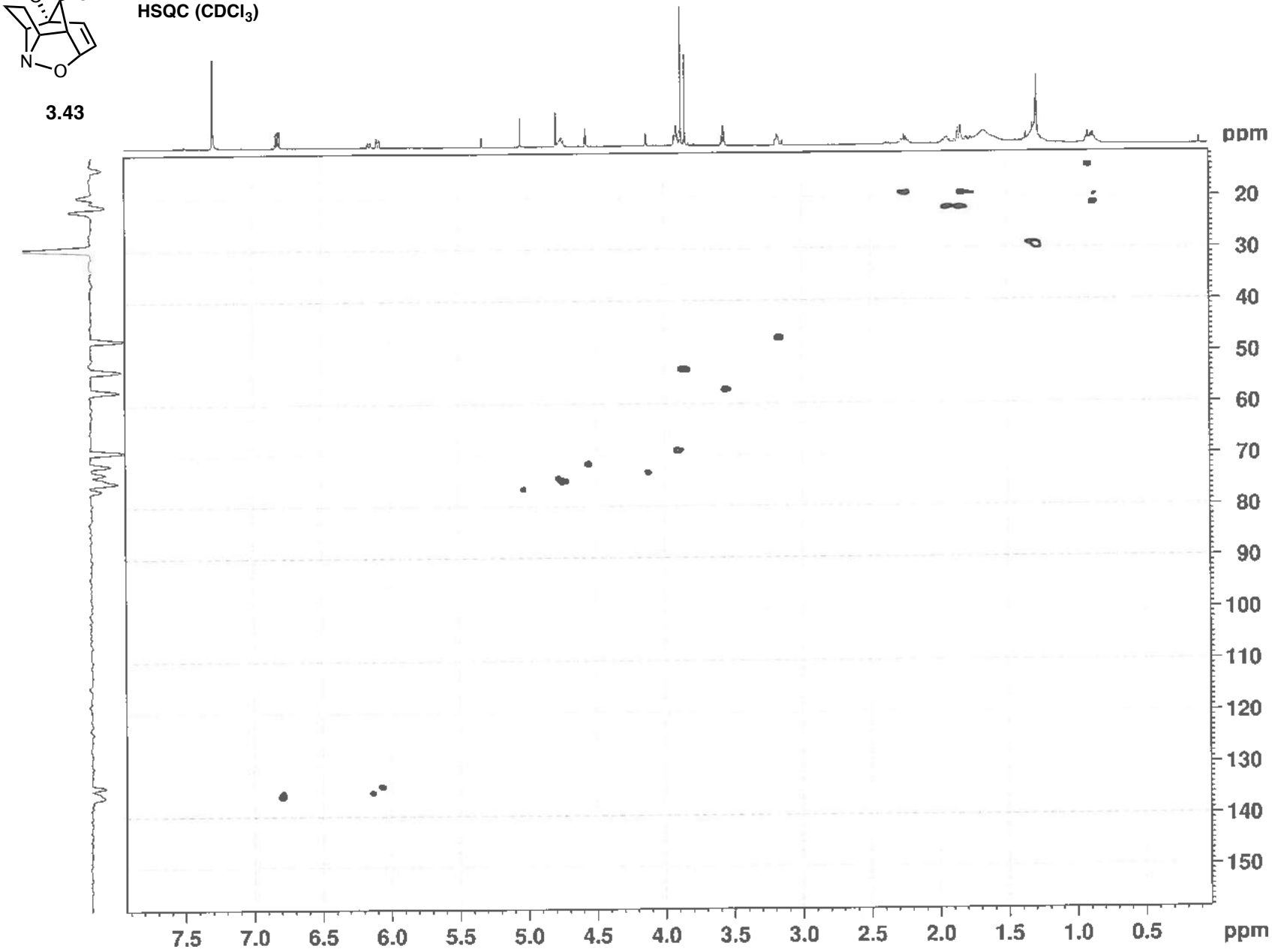

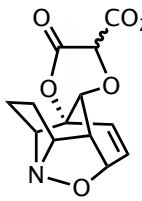

3.43

HMBC ($CDCl_3$)

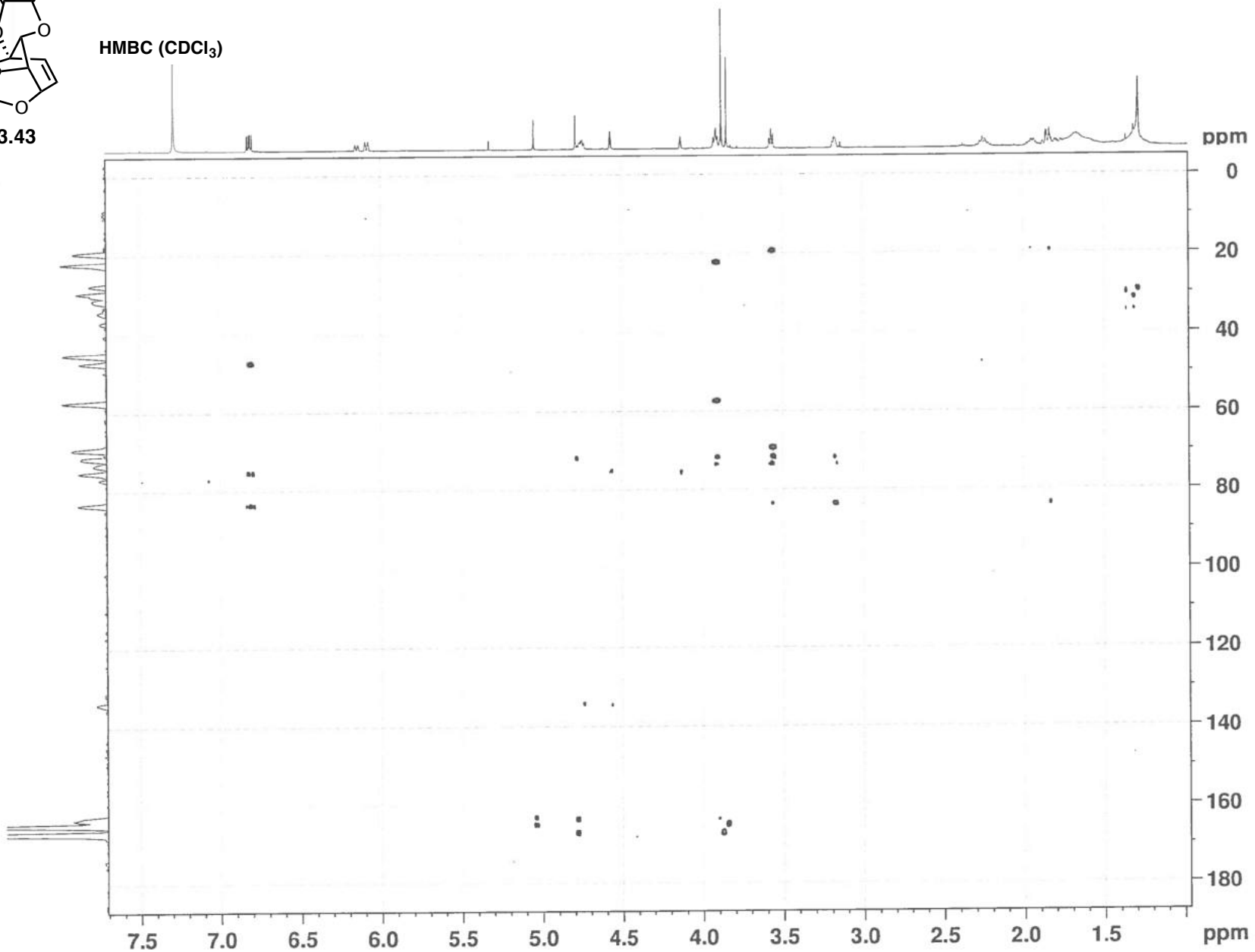

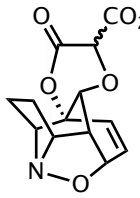

3.43

NOESY ($CDCl_3$)

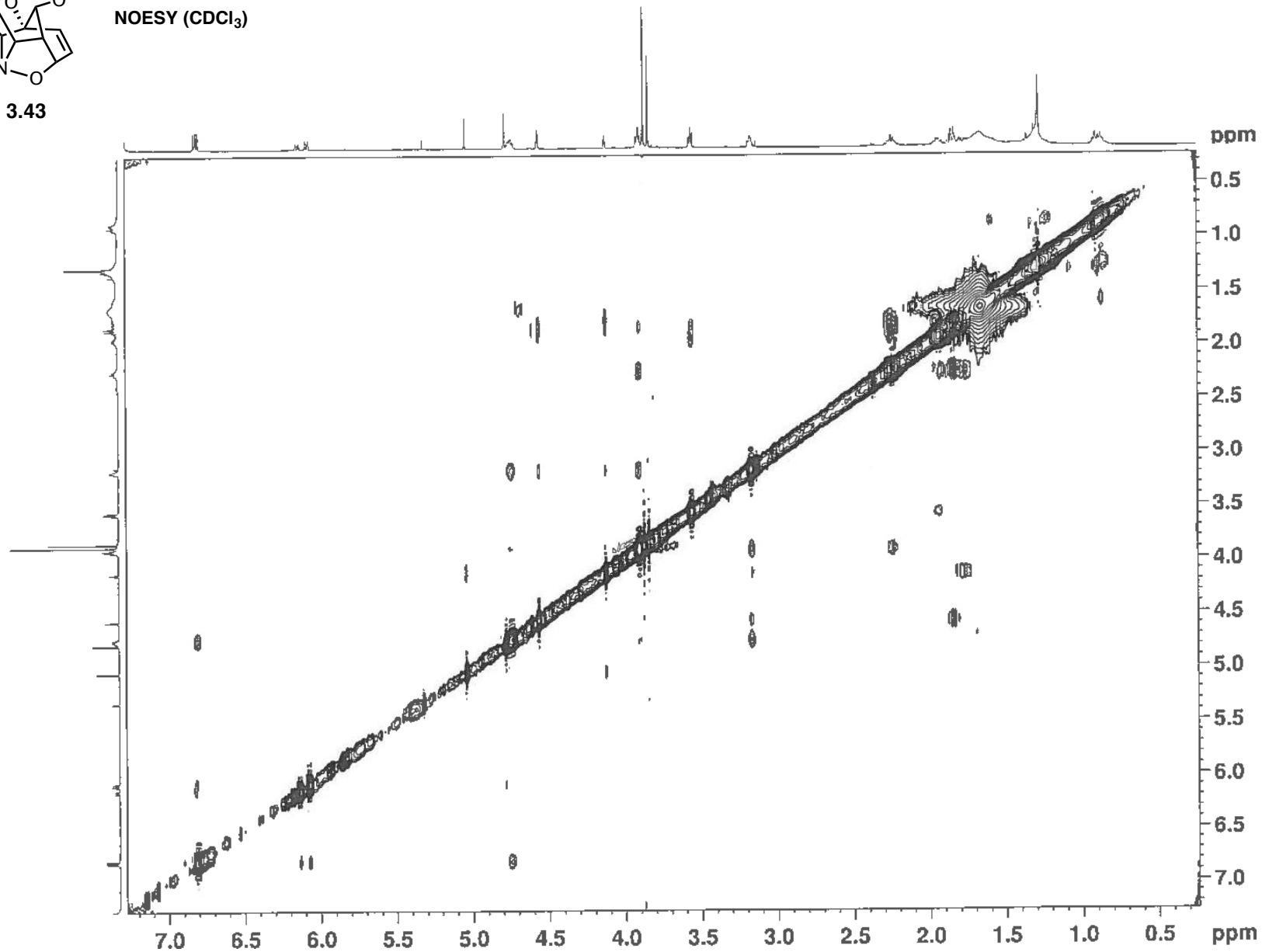

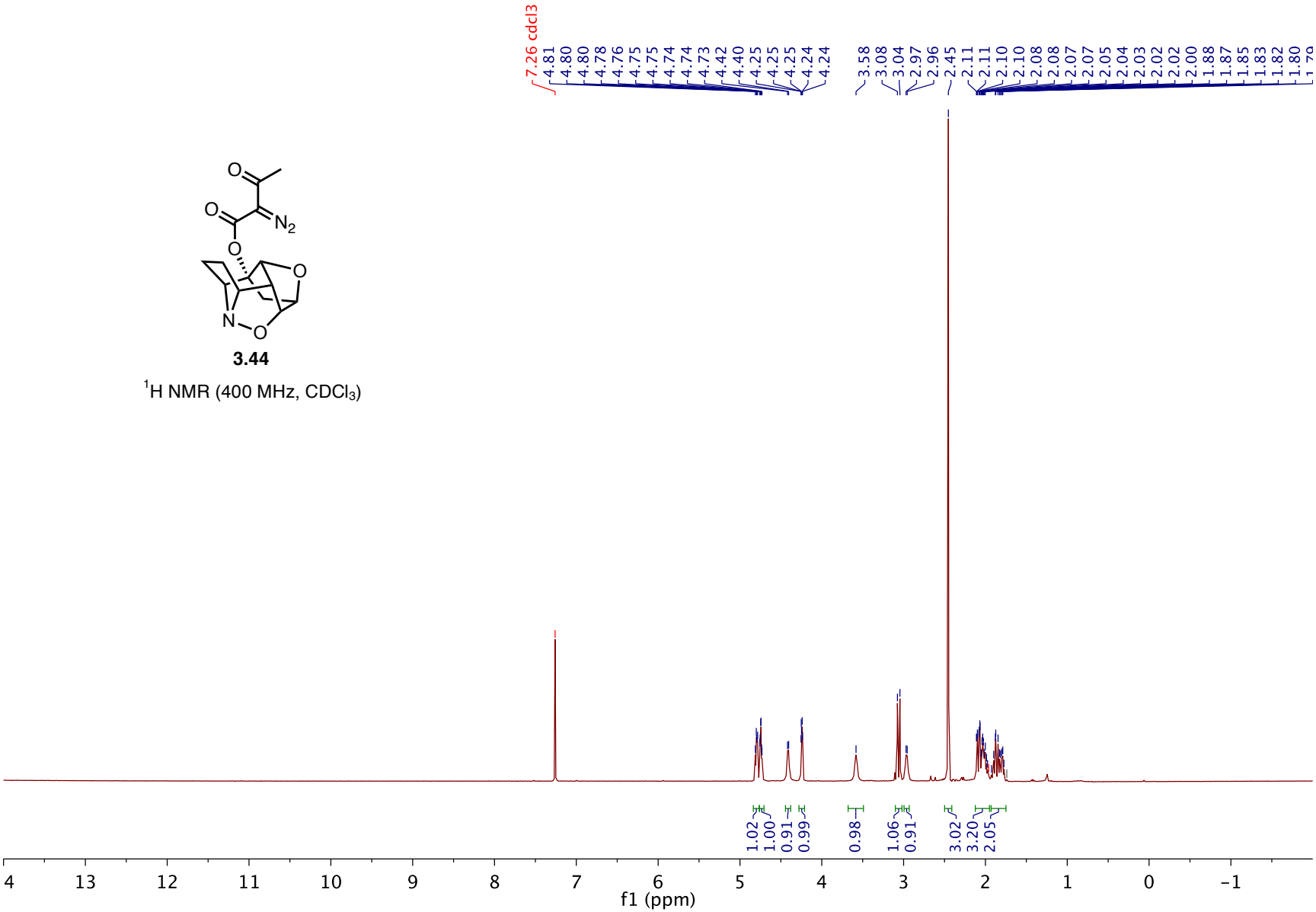

3.44

^{1}H NMR (400 MHz, $CDCl_3$)

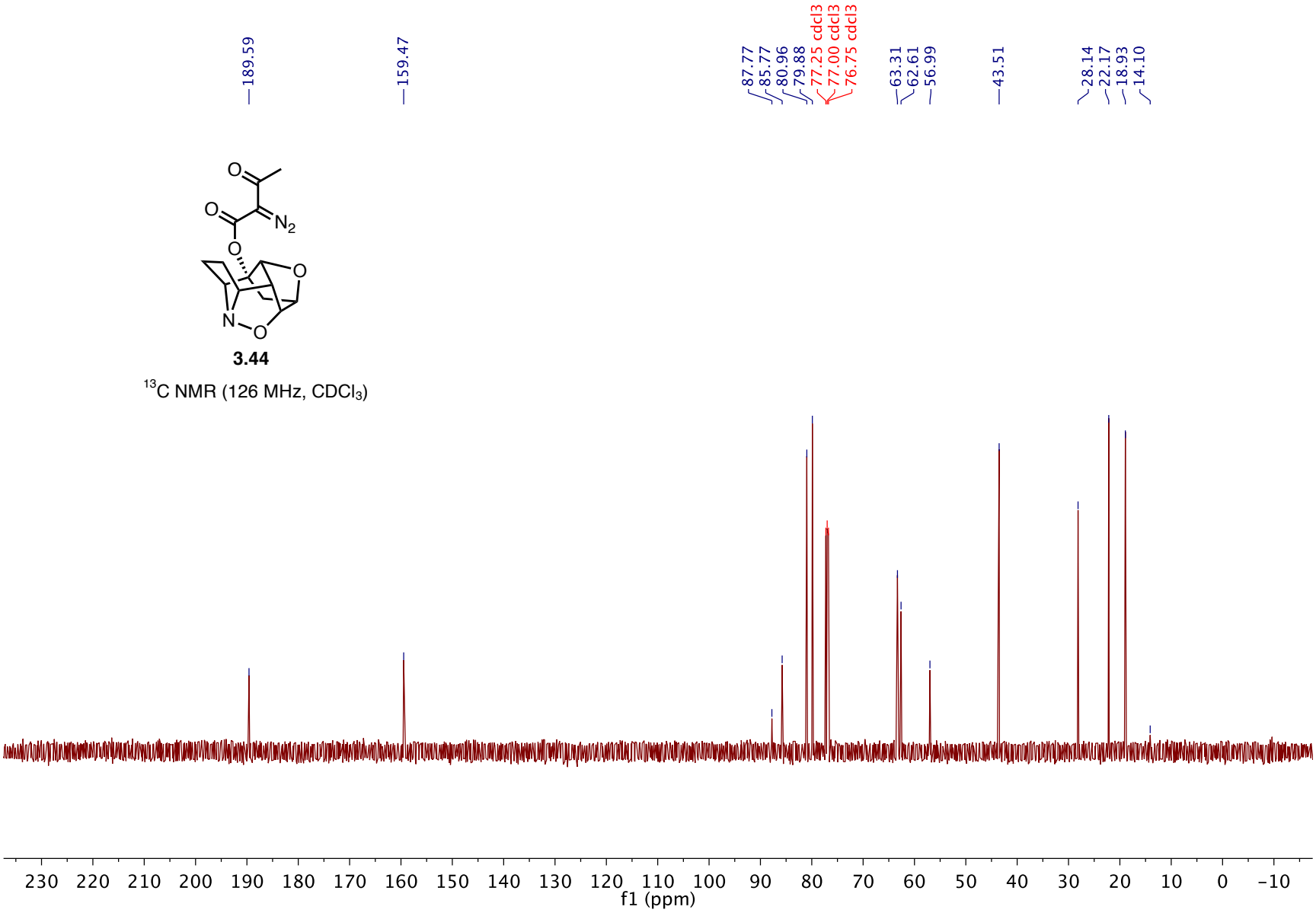
189.59
159.47
87.77
85.77
80.96
79.88
77.25 cdcl3
77.00 cdcl3
76.75 cdcl3
63.31
62.61
56.99
43.51
28.14
22.17
18.93
14.10
O
O
N2
O
O
N
O
3.44
13C NMR (126 MHz, CDCl3)
230 220 210 200 190 180 170 160 150 140 130 120 110 100 90 80 70 60 50 40 30 20 10 0 -10
f1 (ppm)

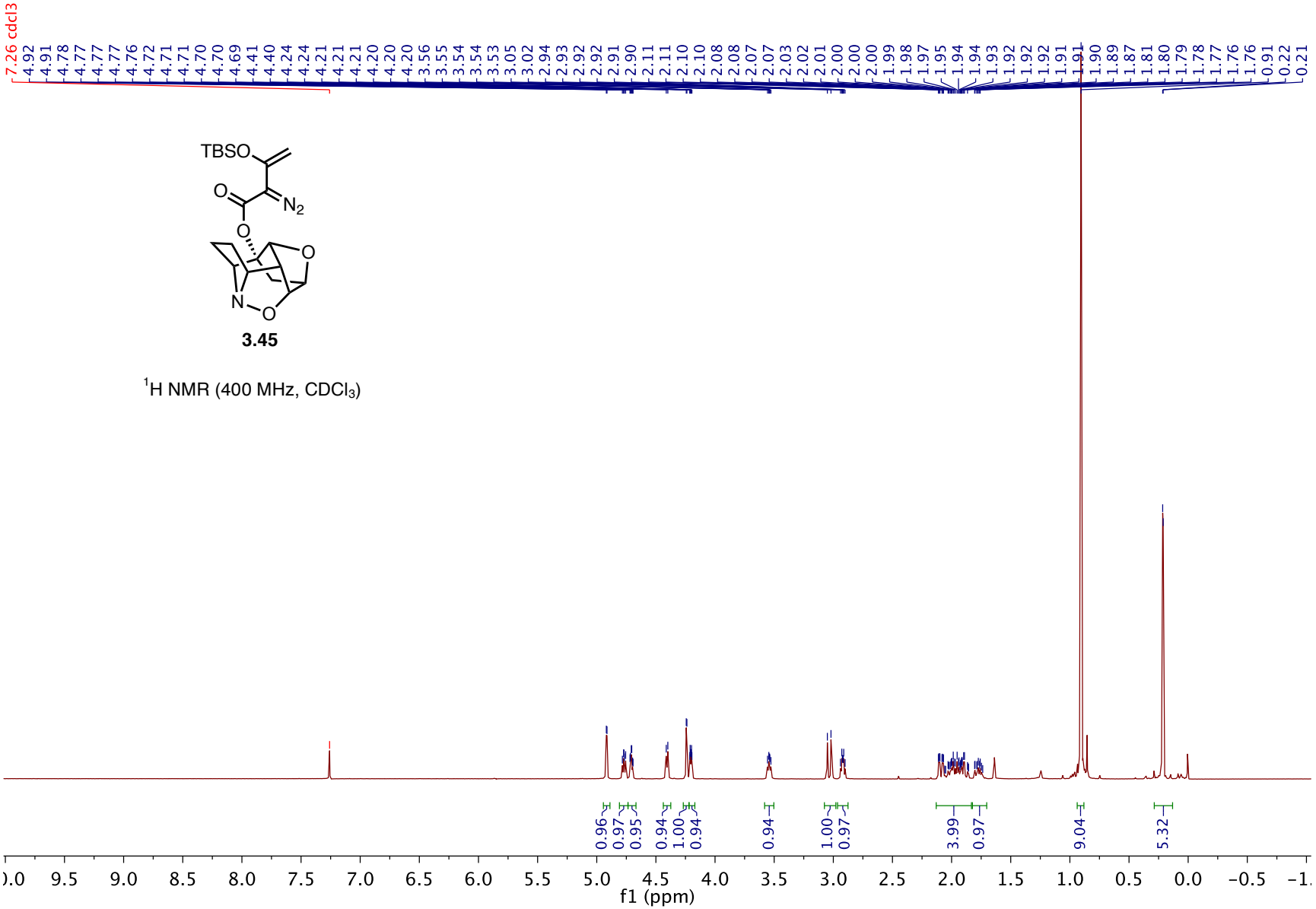
7.26 cdcl3
TBSO
O
N2
O
O
N
O
3.45
1H NMR (400 MHz, CDCl3)
0.96
0.97
0.95
0.94
1.00
0.94
0.94
1.00
0.97
3.99
0.97
9.04
5.32
f1 (ppm)

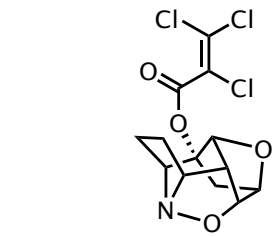

3.48

^{1}H NMR (400 MHz, $CDCl_3$)

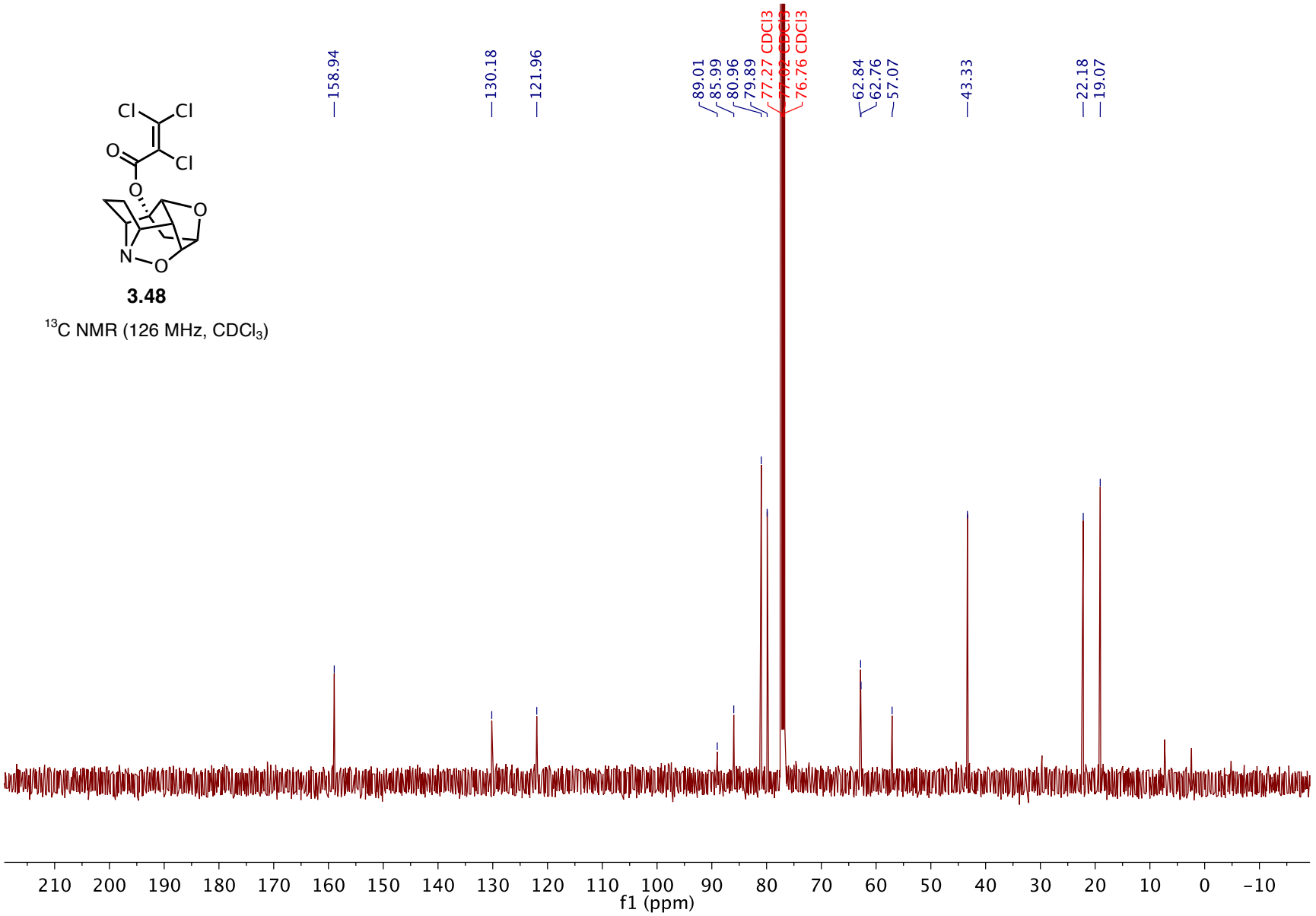
158.94
130.18
121.96
89.01
85.99
80.96
79.89
77.27 CDCl3
77.02 CDCl3
76.76 CDCl3
62.84
62.76
57.07
43.33
22.18
19.07
Cl
Cl
Cl
O
O
O
O
N
O
3.48
13C NMR (126 MHz, CDCl3)
210 200 190 180 170 160 150 140 130 120 110 100 90 80 70 60 50 40 30 20 10 0 −10
f1 (ppm)

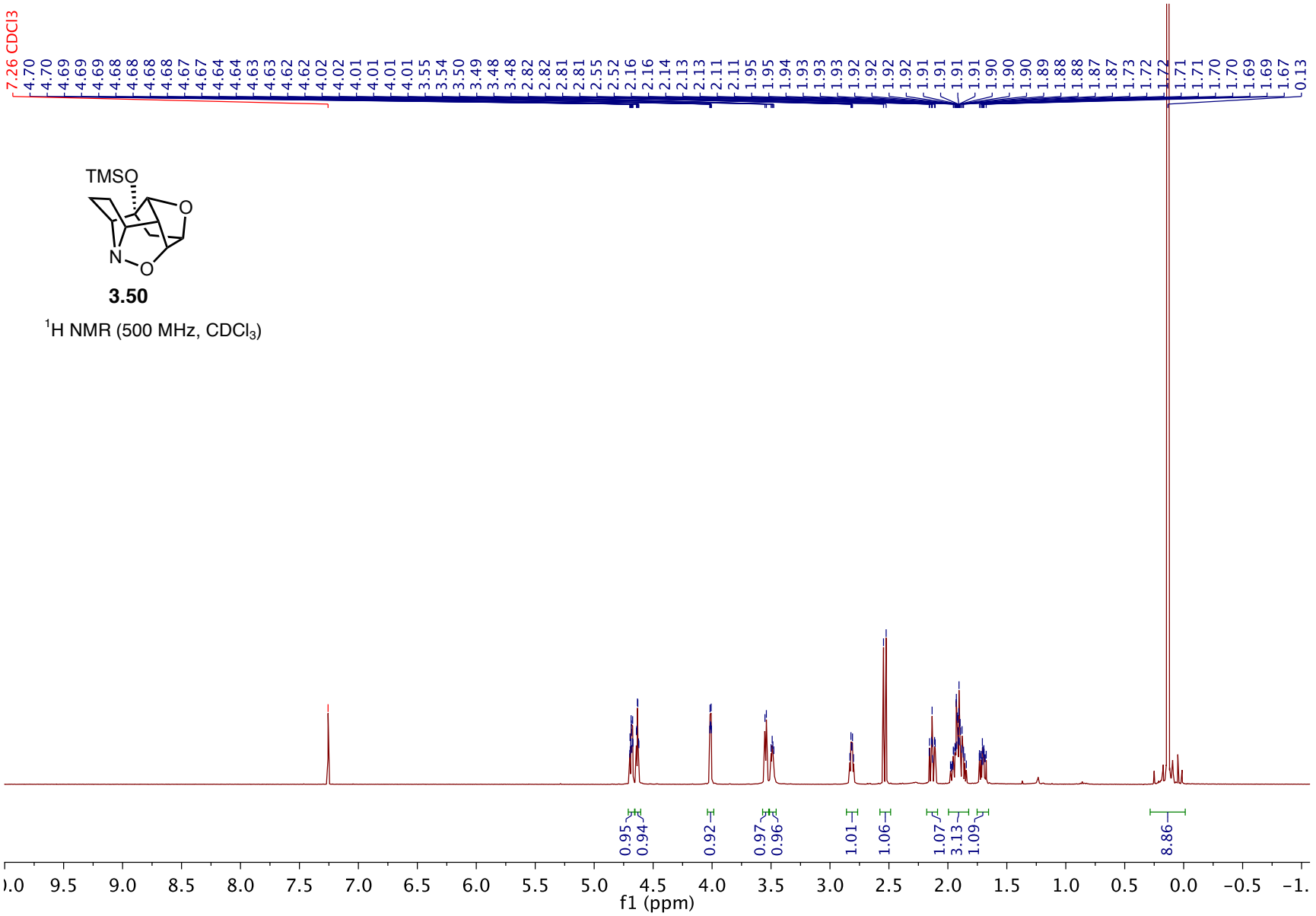

3.50

^{1}H NMR (500 MHz, $CDCl_3$)

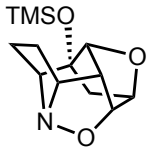

3.50

^{13}C NMR (126 MHz, $CDCl_3$)

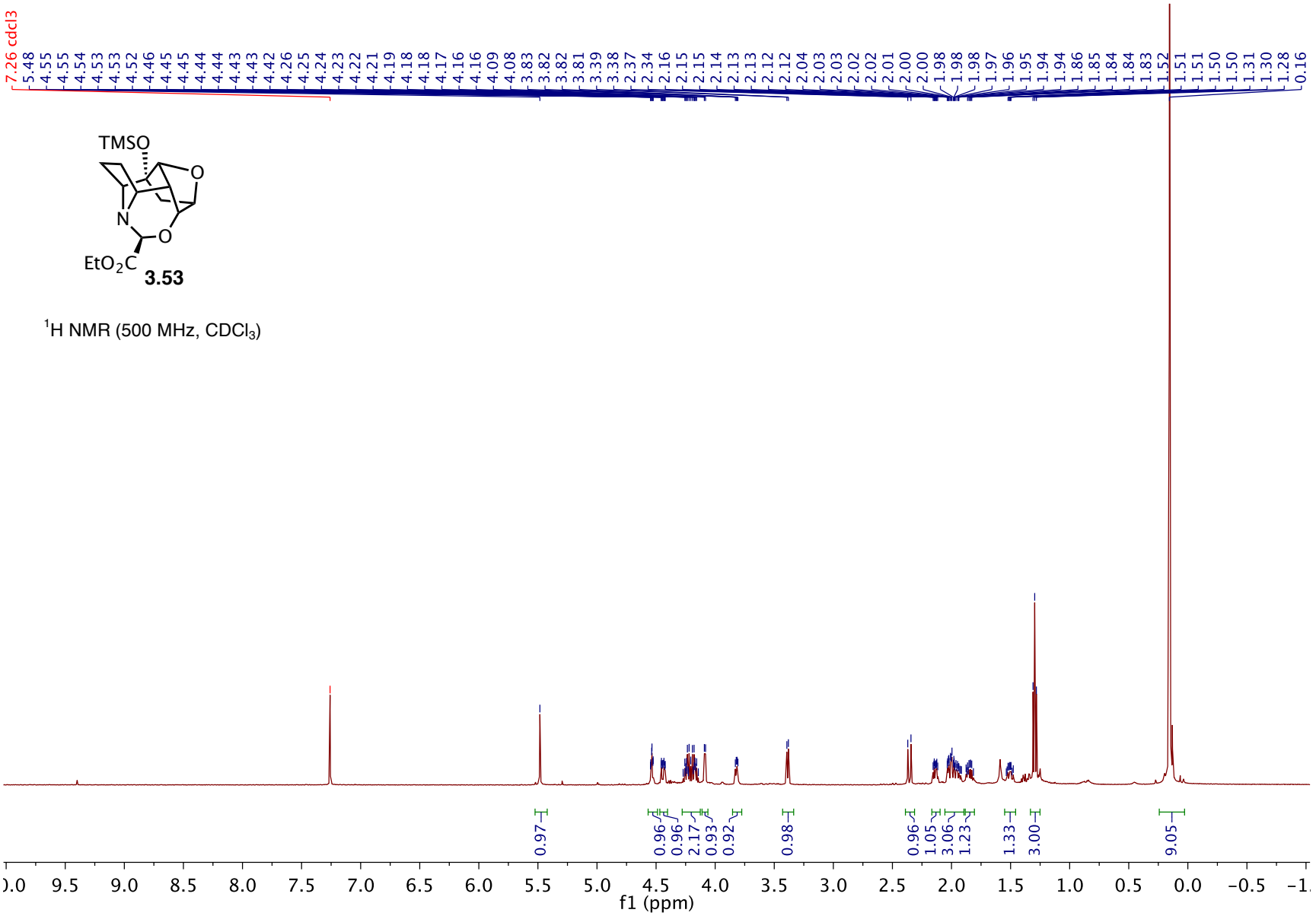
7.26 cdcl3
TMSO
O
N
O
EtO2C
3.53
1H NMR (500 MHz, CDCl3)
f1 (ppm)

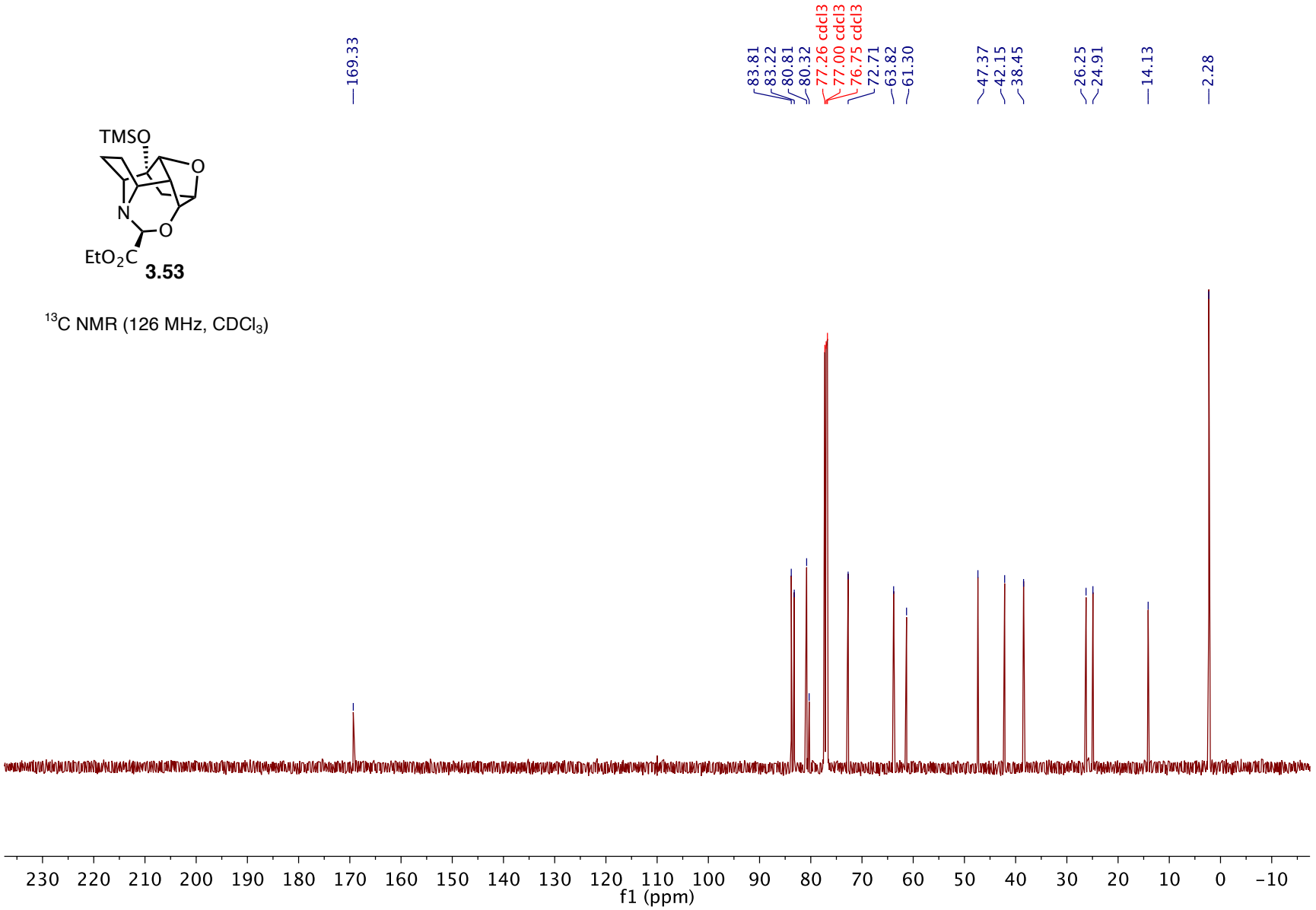
169.33
83.81
83.22
80.81
80.32
77.26 cdcl3
77.00 cdcl3
76.75 cdcl3
72.71
63.82
61.30
47.37
42.15
38.45
26.25
24.91
14.13
2.28
TMSO
O
N
O
EtO2C
3.53
13C NMR (126 MHz, CDCl3)
230 220 210 200 190 180 170 160 150 140 130 120 110 100 90 80 70 60 50 40 30 20 10 0 -10
f1 (ppm)

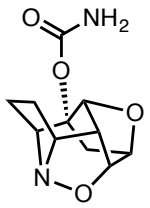

3.58

^{1}H NMR (400 MHz, $CDCl_3$)

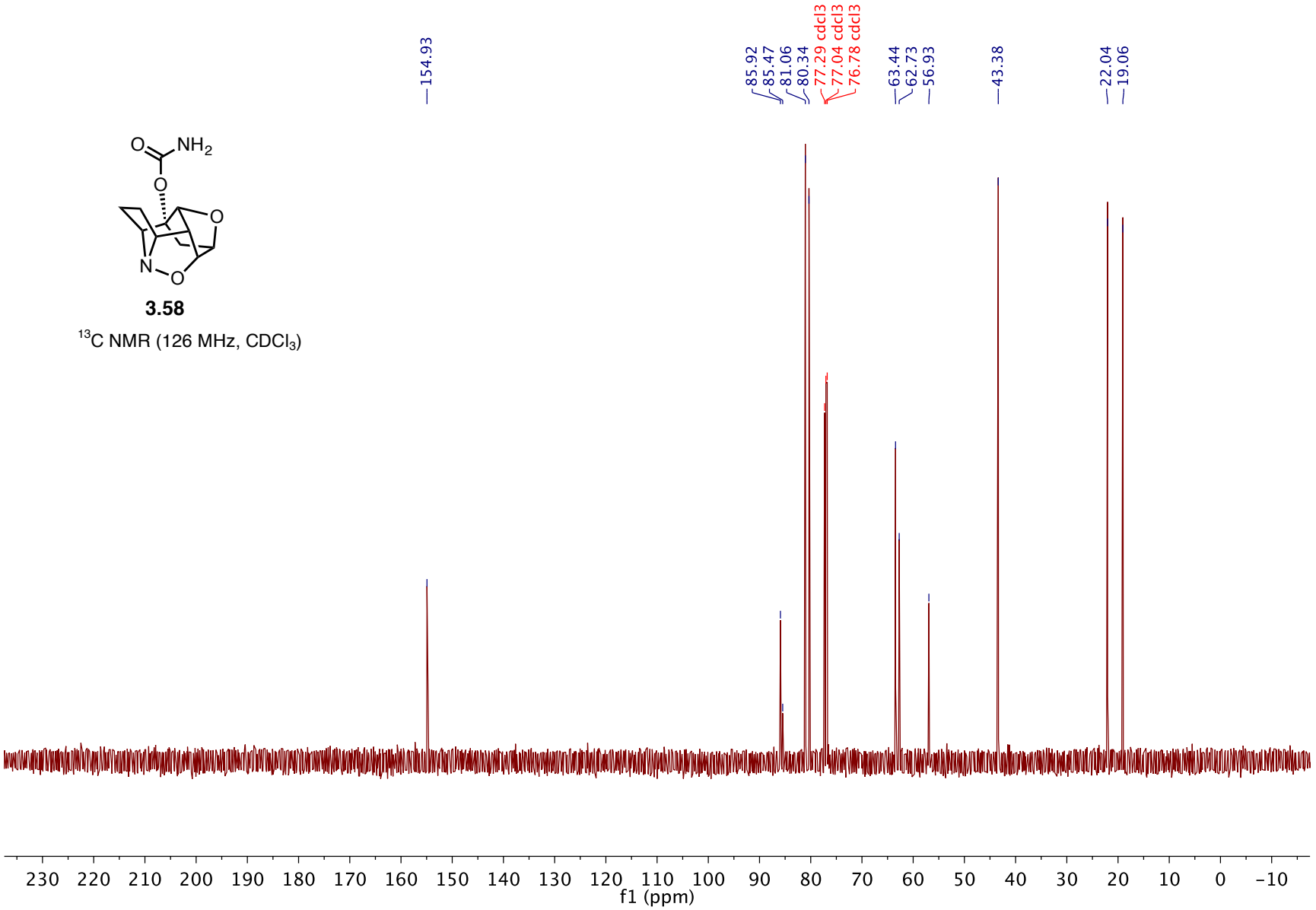
154.93
85.92
85.47
81.06
80.34
77.29 cdcl3
77.04 cdcl3
76.78 cdcl3
63.44
62.73
56.93
43.38
22.04
19.06
O
NH2
O
O
N
O
3.58
13C NMR (126 MHz, CDCl3)
230 220 210 200 190 180 170 160 150 140 130 120 110 100 90 80 70 60 50 40 30 20 10 0 -10
f1 (ppm)

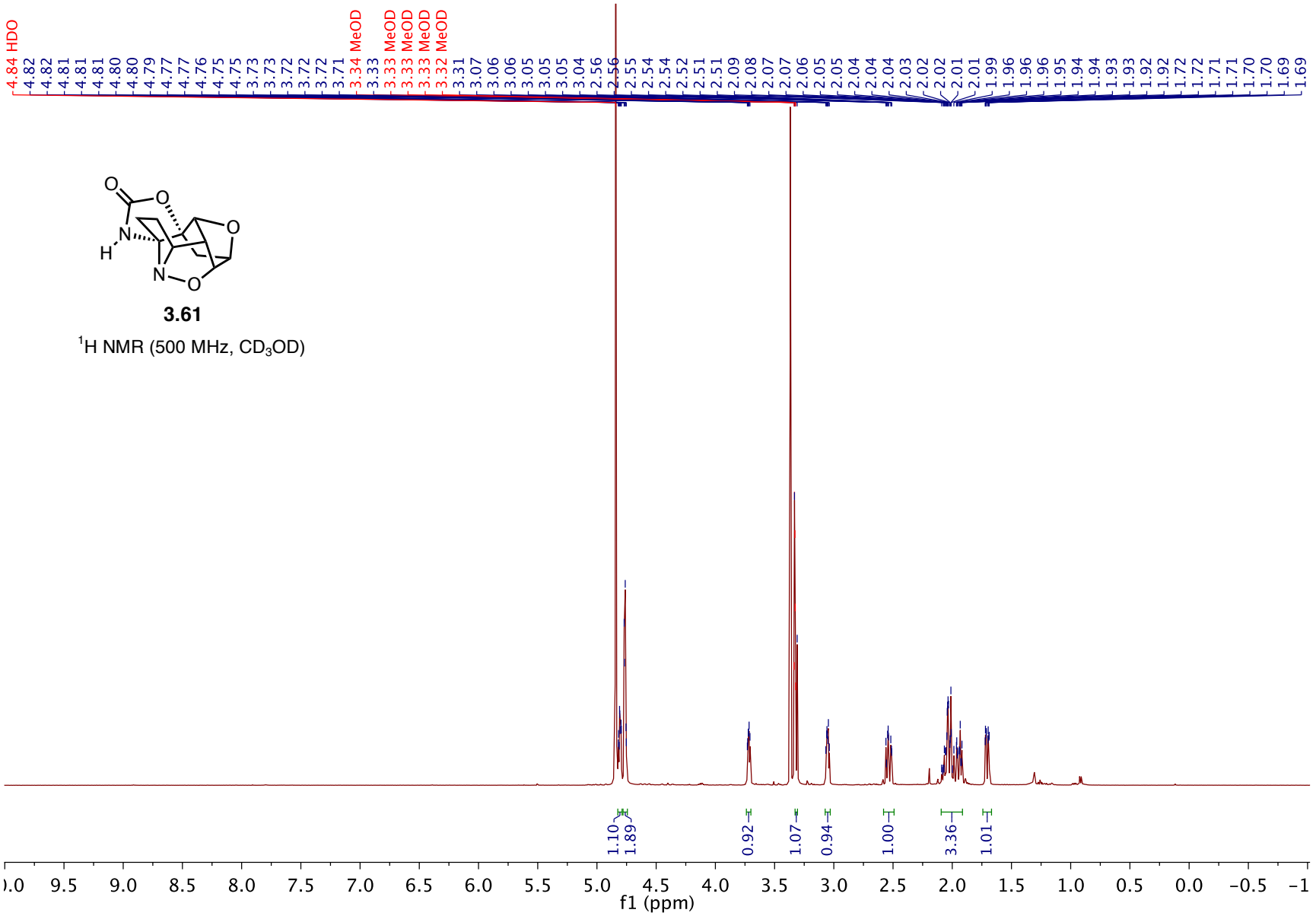

3.61

^{1}H NMR (500 MHz, CD_3OD)

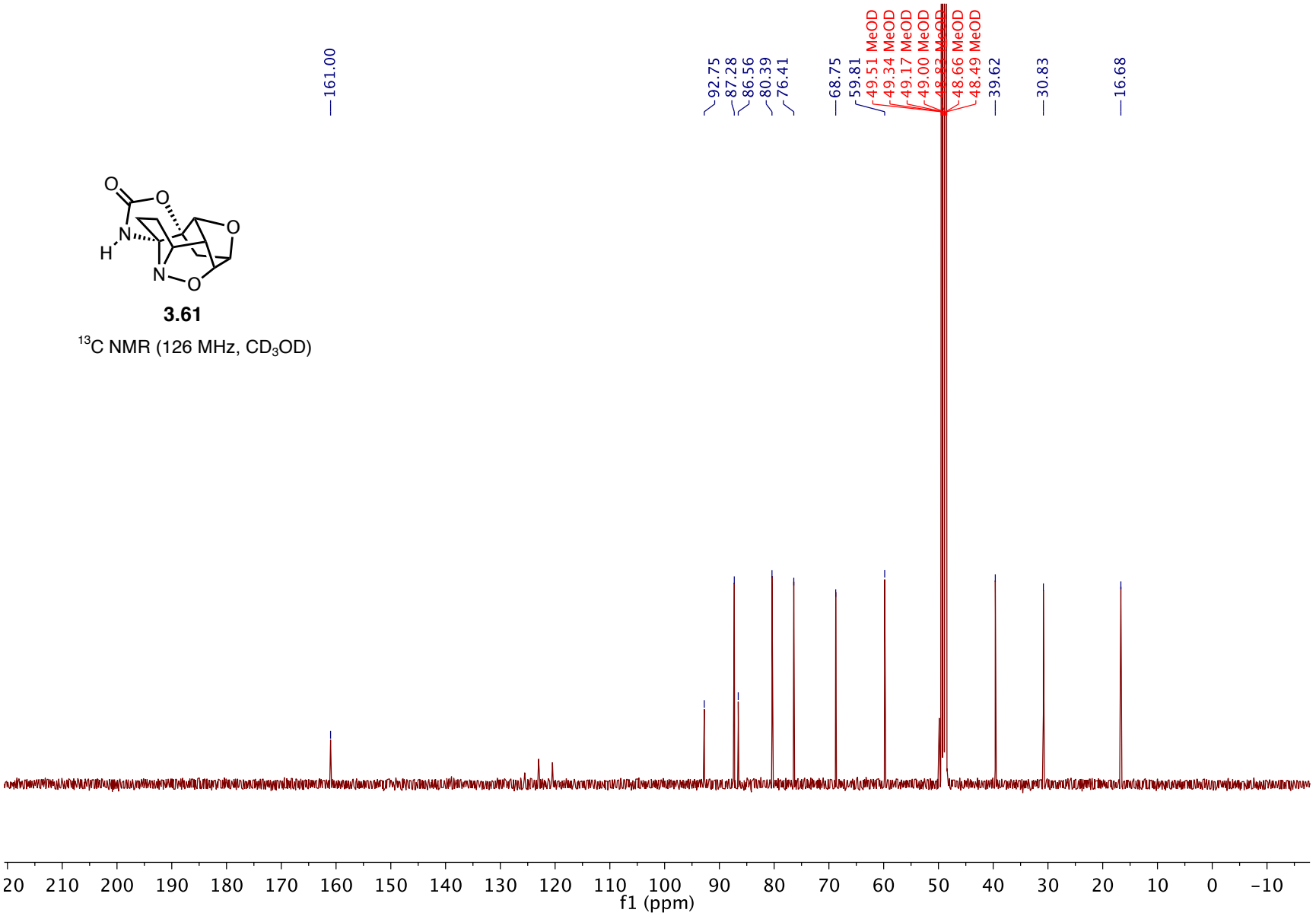

3.61

^{13}C NMR (126 MHz, CD_3OD)

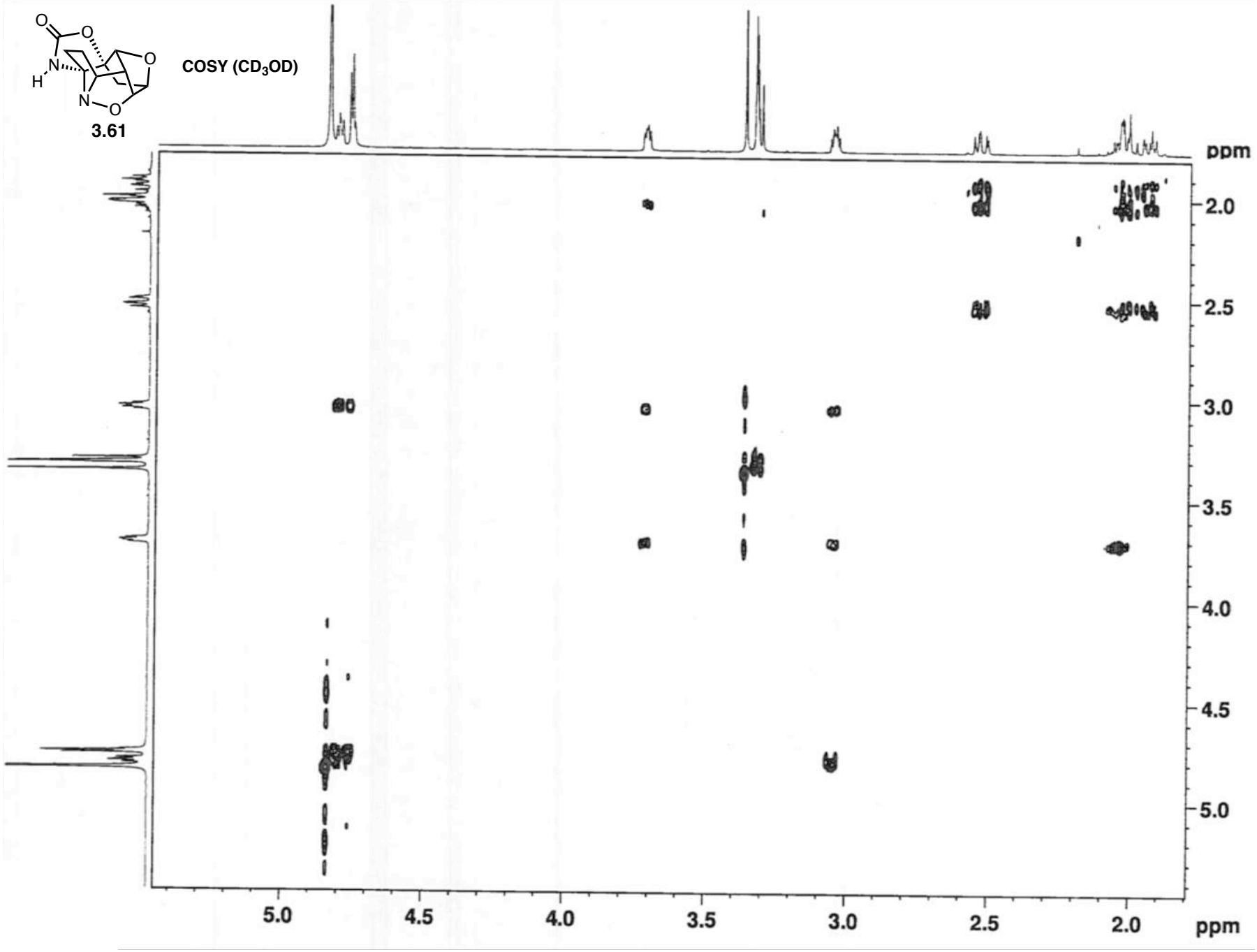
3.61
COSY (CD_3OD)
ppm
2.0
2.5
3.0
3.5
4.0
4.5
5.0
5.0
4.5
4.0
3.5
3.0
2.5
2.0
ppm

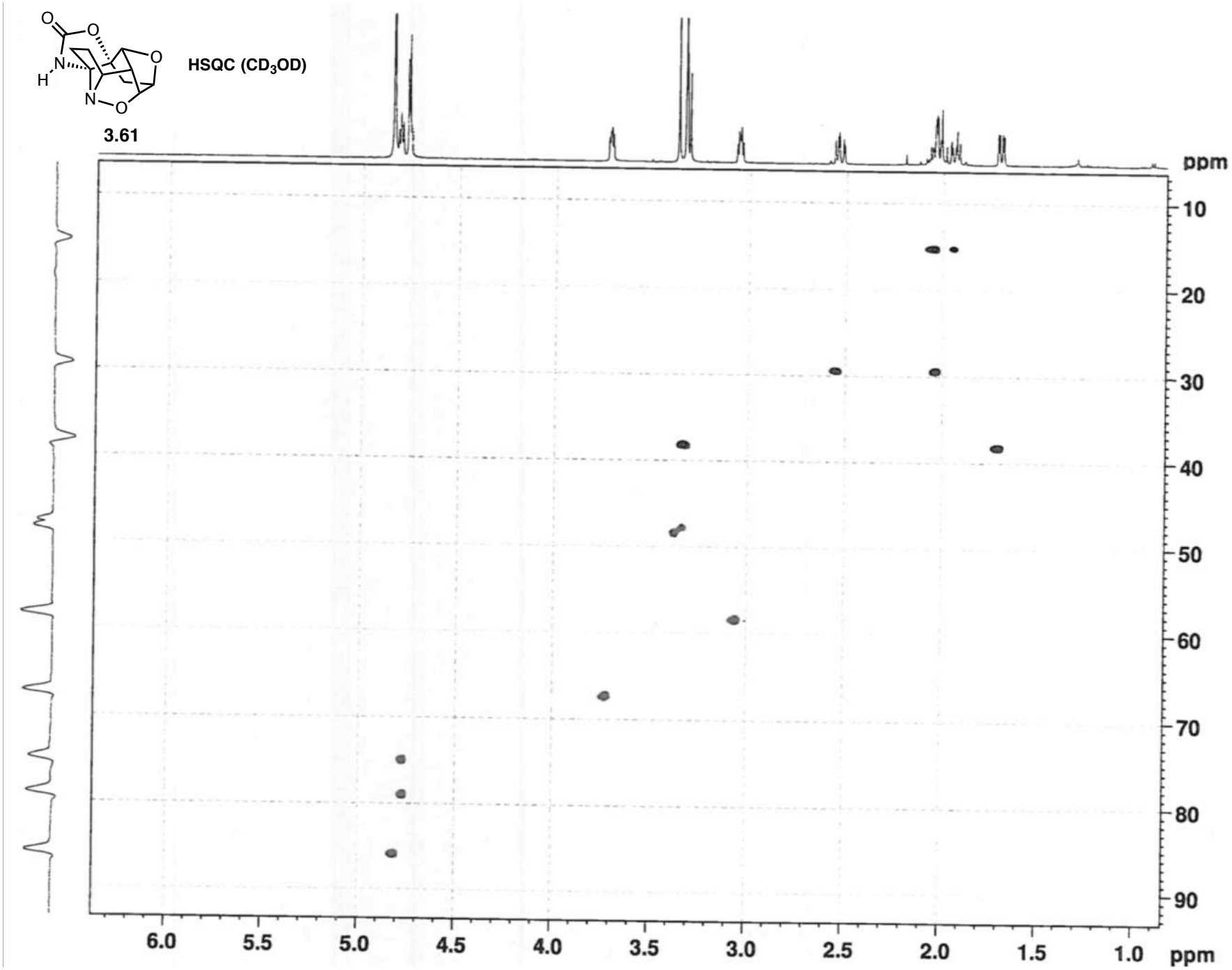
HSQC (CD_3OD)
3.61
ppm
10
20
30
40
50
60
70
80
90
6.0
5.5
5.0
4.5
4.0
3.5
3.0
2.5
2.0
1.5
1.0
ppm

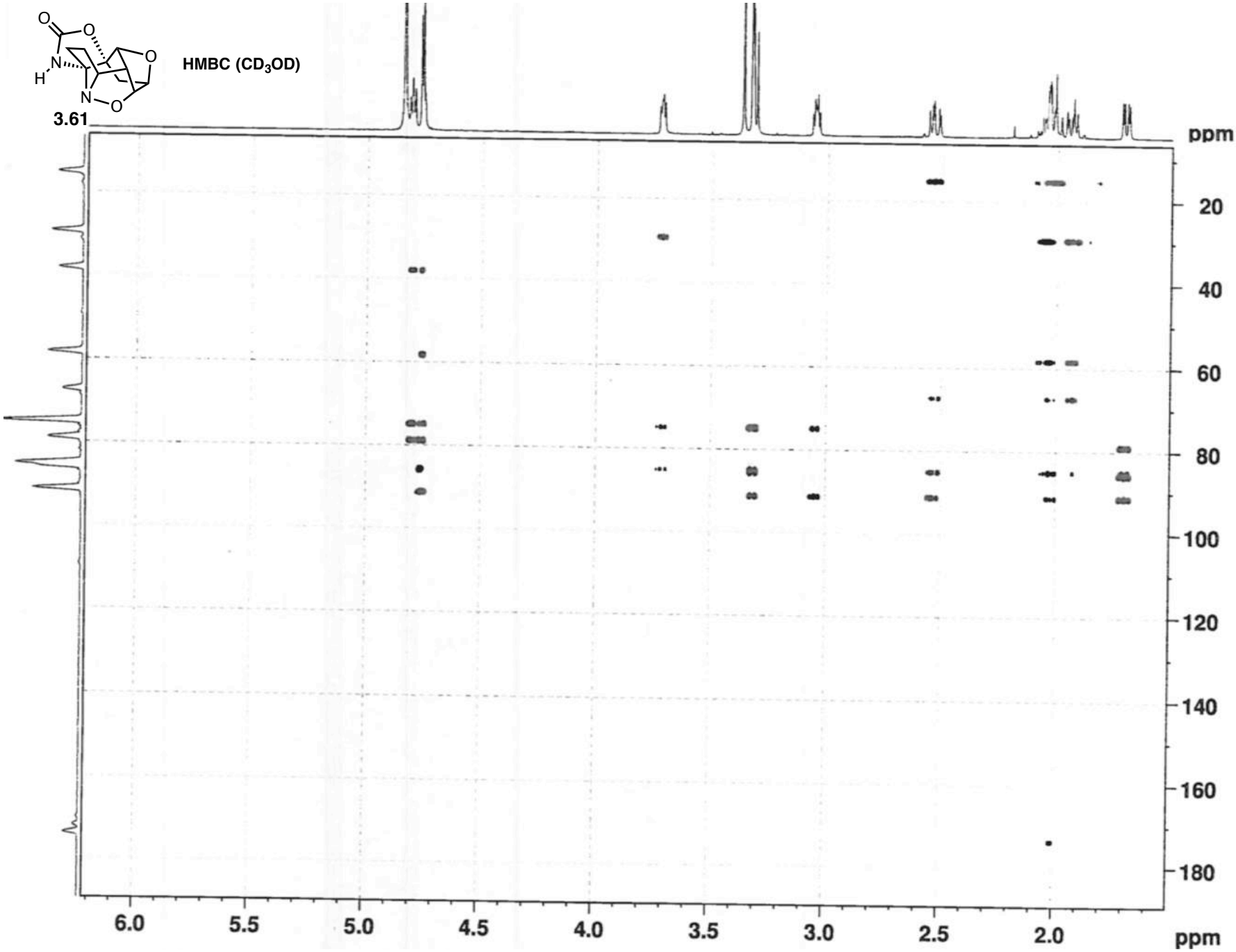
HMBC (CD_3OD)
3.61
ppm
20
40
60
80
100
120
140
160
180
6.0
5.5
5.0
4.5
4.0
3.5
3.0
2.5
2.0
ppm

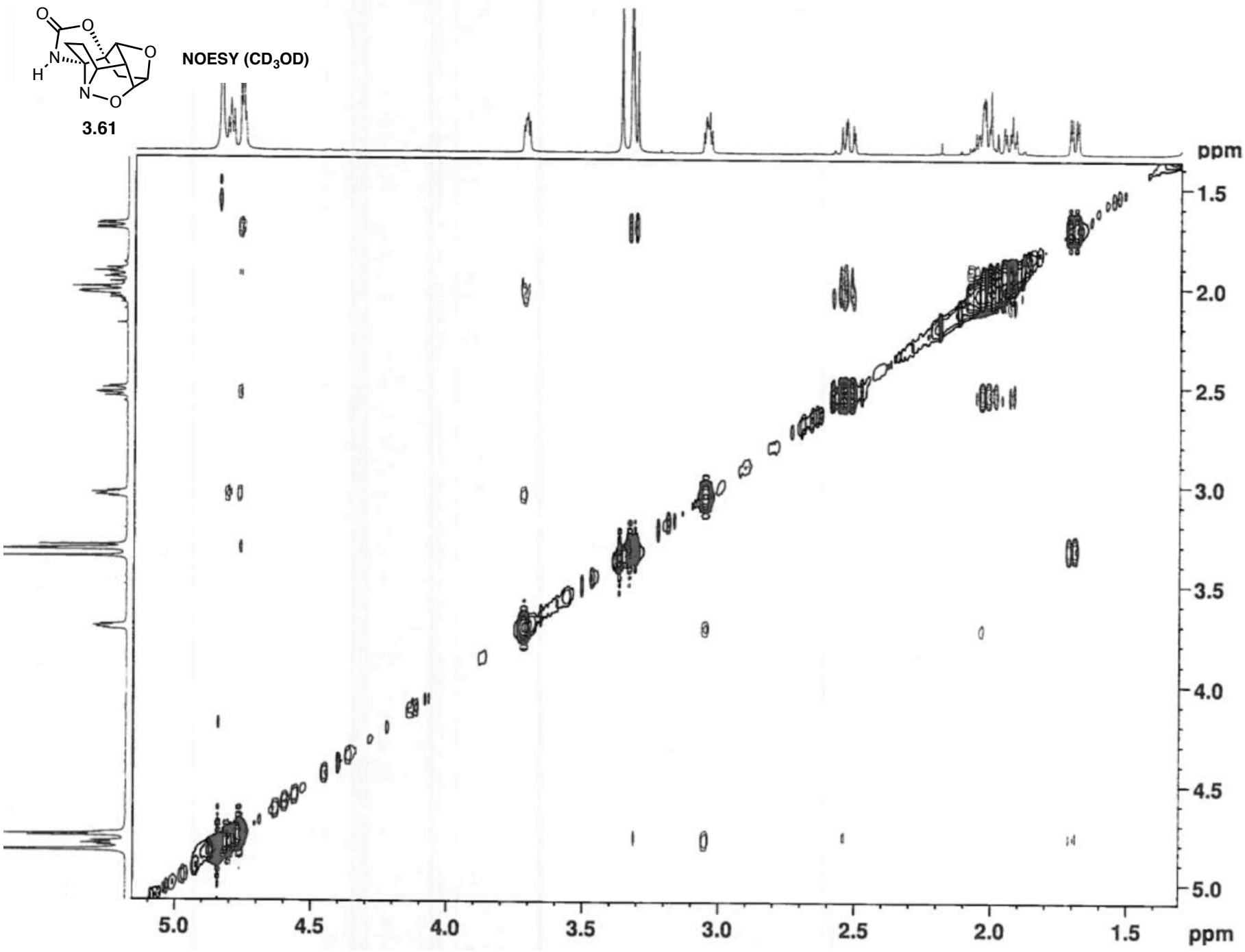
NOESY (CD_3OD)
3.61
ppm
1.5
2.0
2.5
3.0
3.5
4.0
4.5
5.0
5.0
4.5
4.0
3.5
3.0
2.5
2.0
1.5
ppm

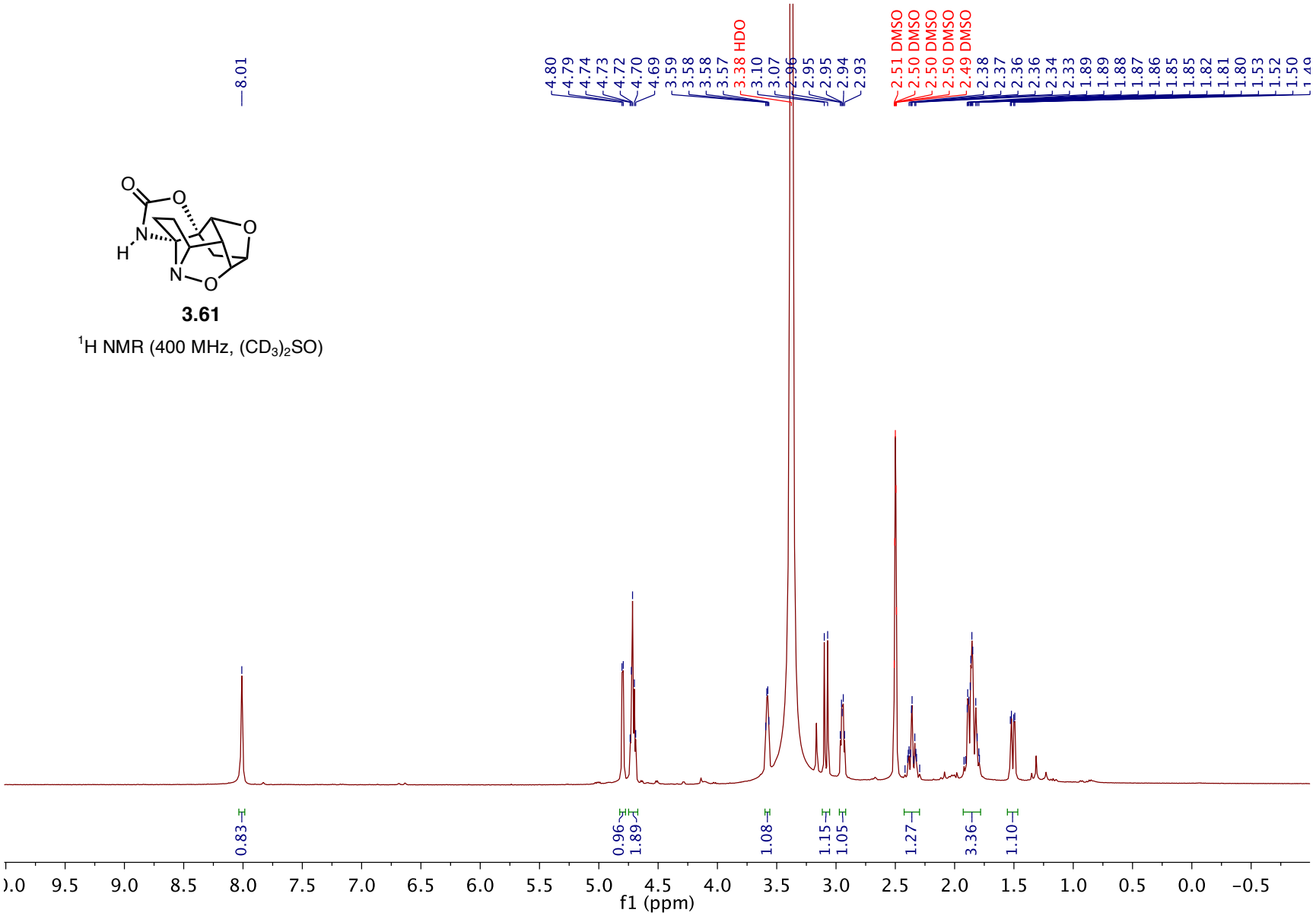

3.61

^{1}H NMR (400 MHz, $(CD_3)_2SO$)

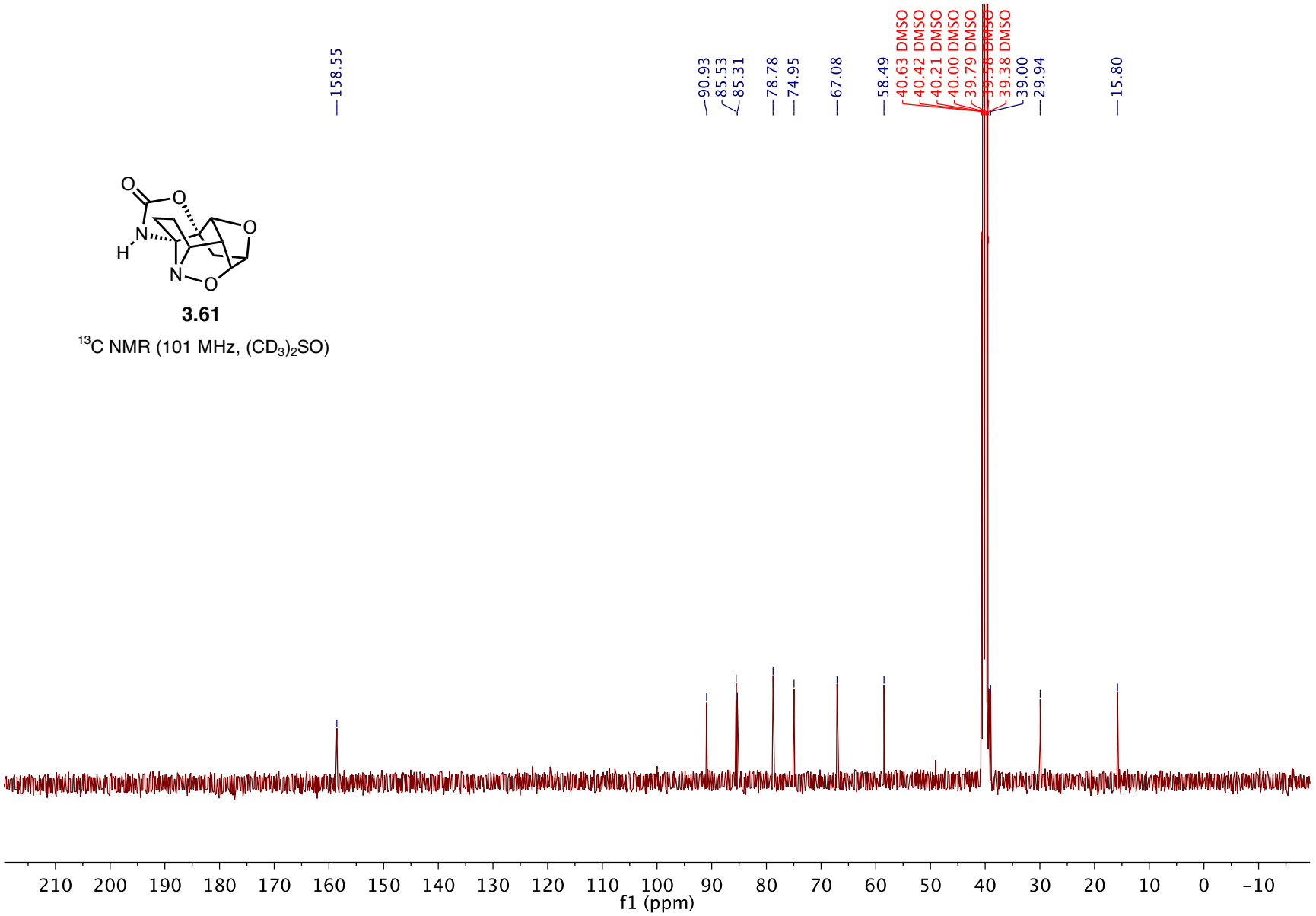

3.61

^{13}C NMR (101 MHz, $(CD_3)_2SO$)

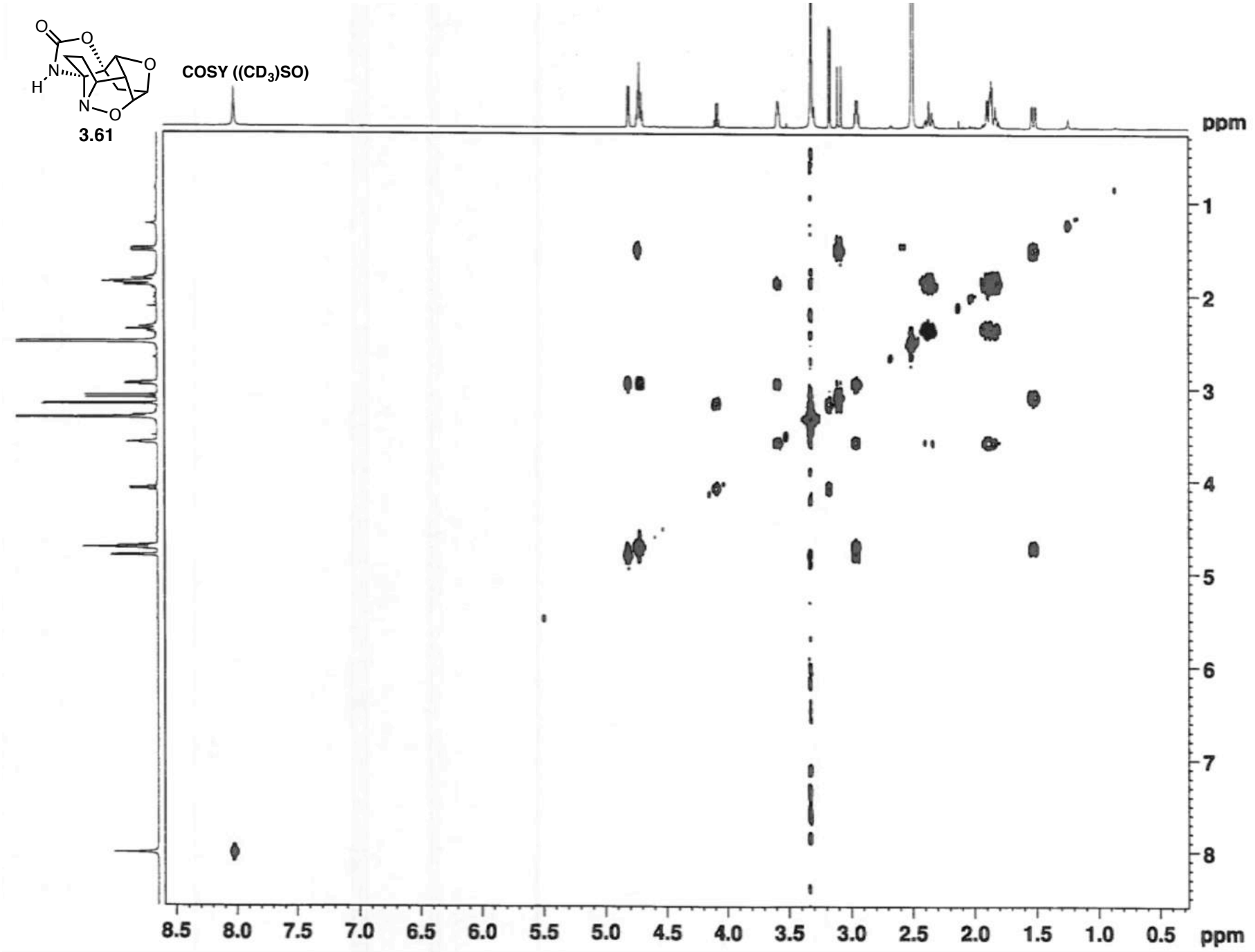
3.61
COSY ((CD3)SO)
ppm
1
2
3
4
5
6
7
8
8.5
8.0
7.5
7.0
6.5
6.0
5.5
5.0
4.5
4.0
3.5
3.0
2.5
2.0
1.5
1.0
0.5
ppm

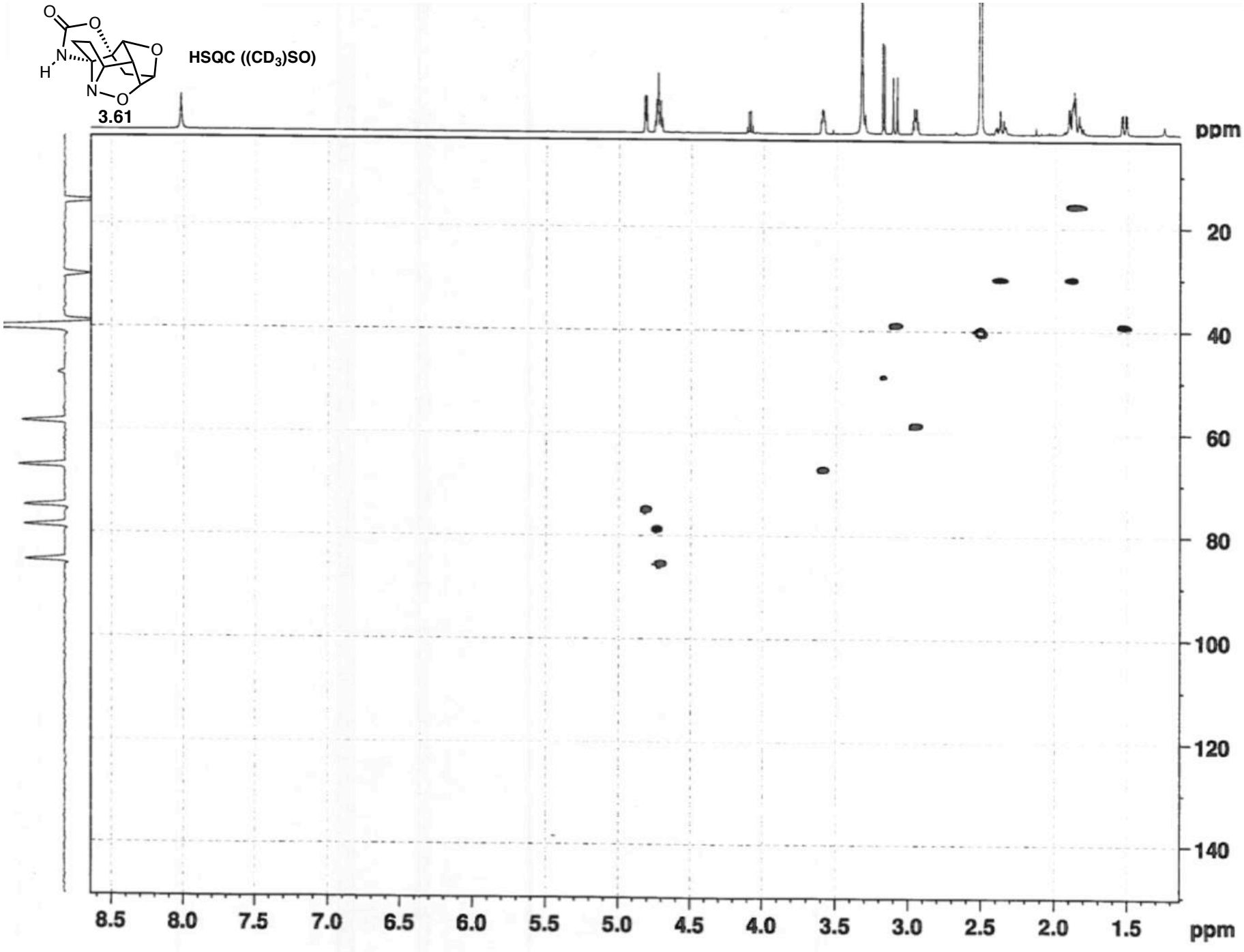
HSQC ((CD3)SO)
3.61
ppm
20
40
60
80
100
120
140
8.5
8.0
7.5
7.0
6.5
6.0
5.5
5.0
4.5
4.0
3.5
3.0
2.5
2.0
1.5
ppm

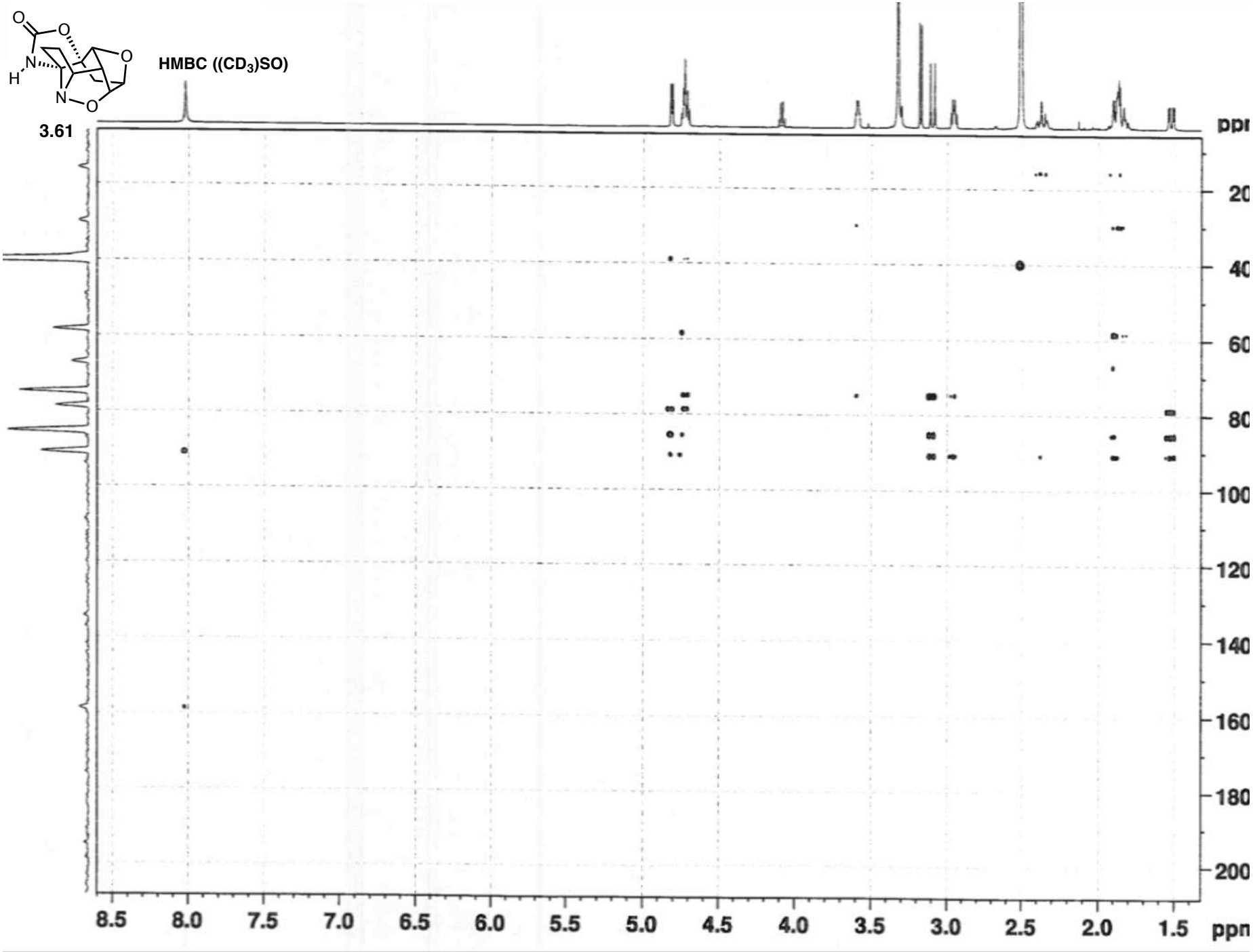
HMBC ((CD3)SO)
3.61
ppm
20
40
60
80
100
120
140
160
180
200
8.5
8.0
7.5
7.0
6.5
6.0
5.5
5.0
4.5
4.0
3.5
3.0
2.5
2.0
1.5
ppm

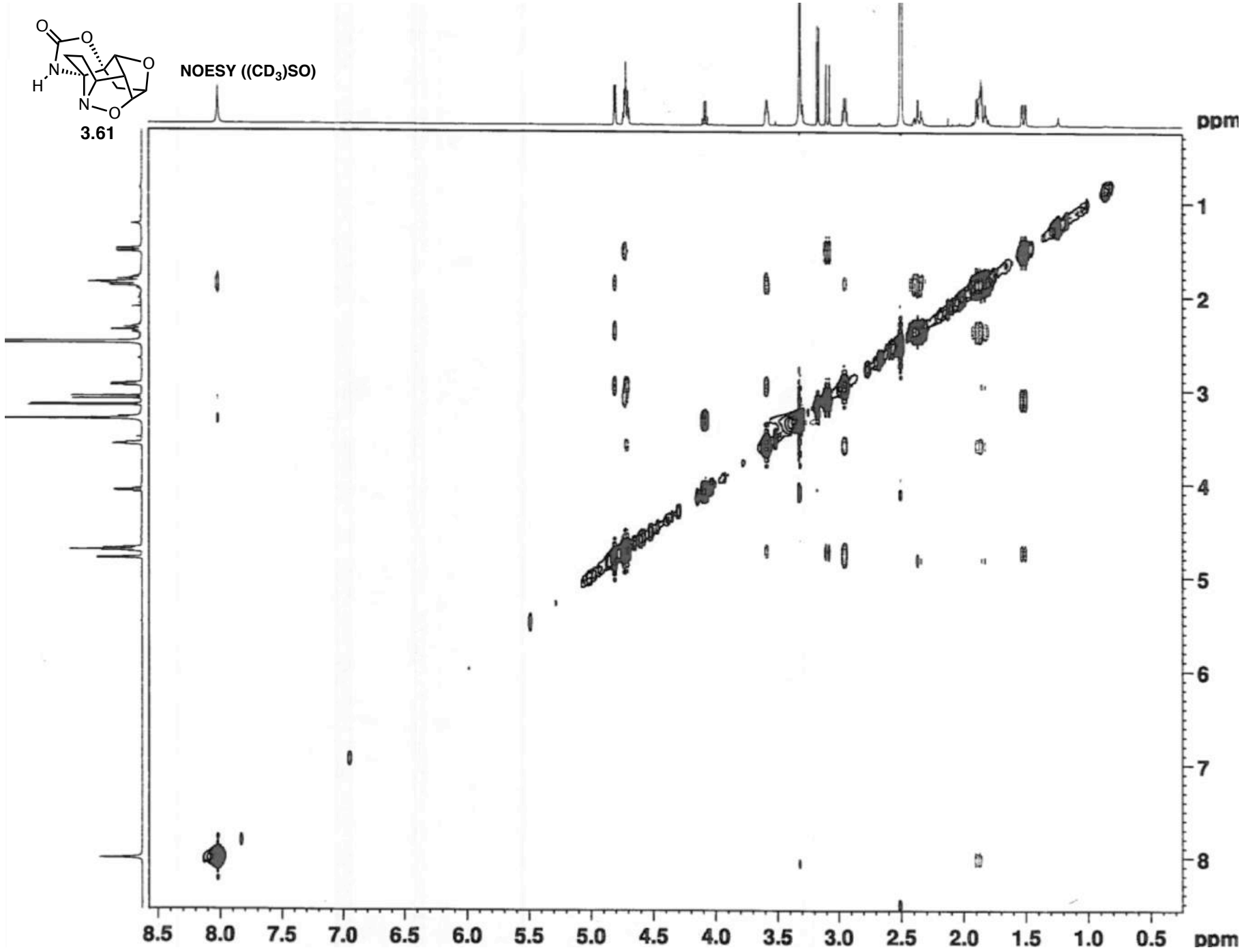
NOESY ((CD3)SO)
3.61
ppm
1
2
3
4
5
6
7
8
8.5
8.0
7.5
7.0
6.5
6.0
5.5
5.0
4.5
4.0
3.5
3.0
2.5
2.0
1.5
1.0
0.5
ppm

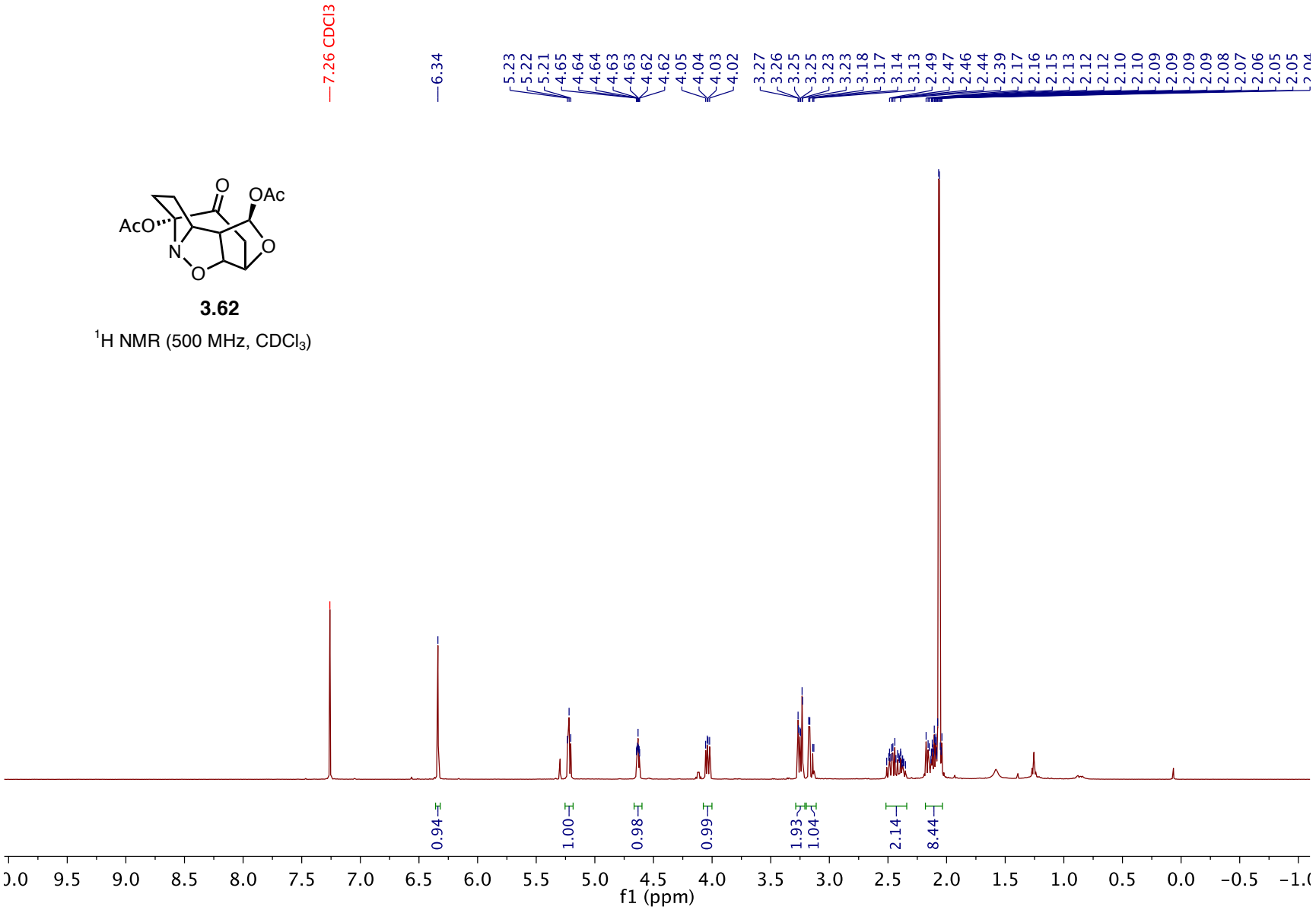

3.62

^{1}H NMR (500 MHz, $CDCl_3$)

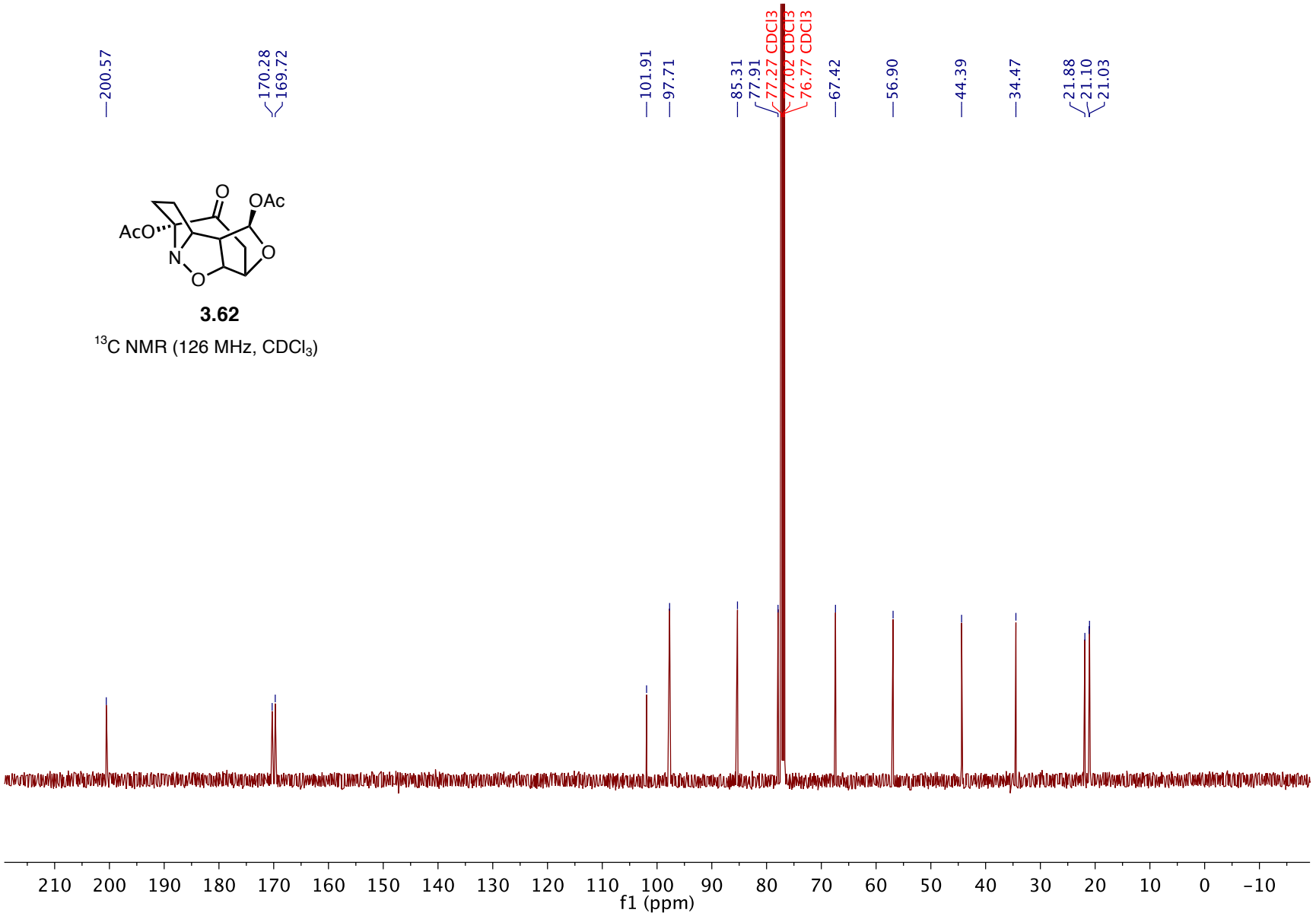
200.57
170.28
169.72
101.91
97.71
85.31
77.91
77.27 CDCl3
77.02 CDCl3
76.77 CDCl3
67.42
56.90
44.39
34.47
21.88
21.10
21.03
O
OAc
AcO
N
O
O
3.62
13C NMR (126 MHz, CDCl3)
210 200 190 180 170 160 150 140 130 120 110 100 90 80 70 60 50 40 30 20 10 0 −10
f1 (ppm)

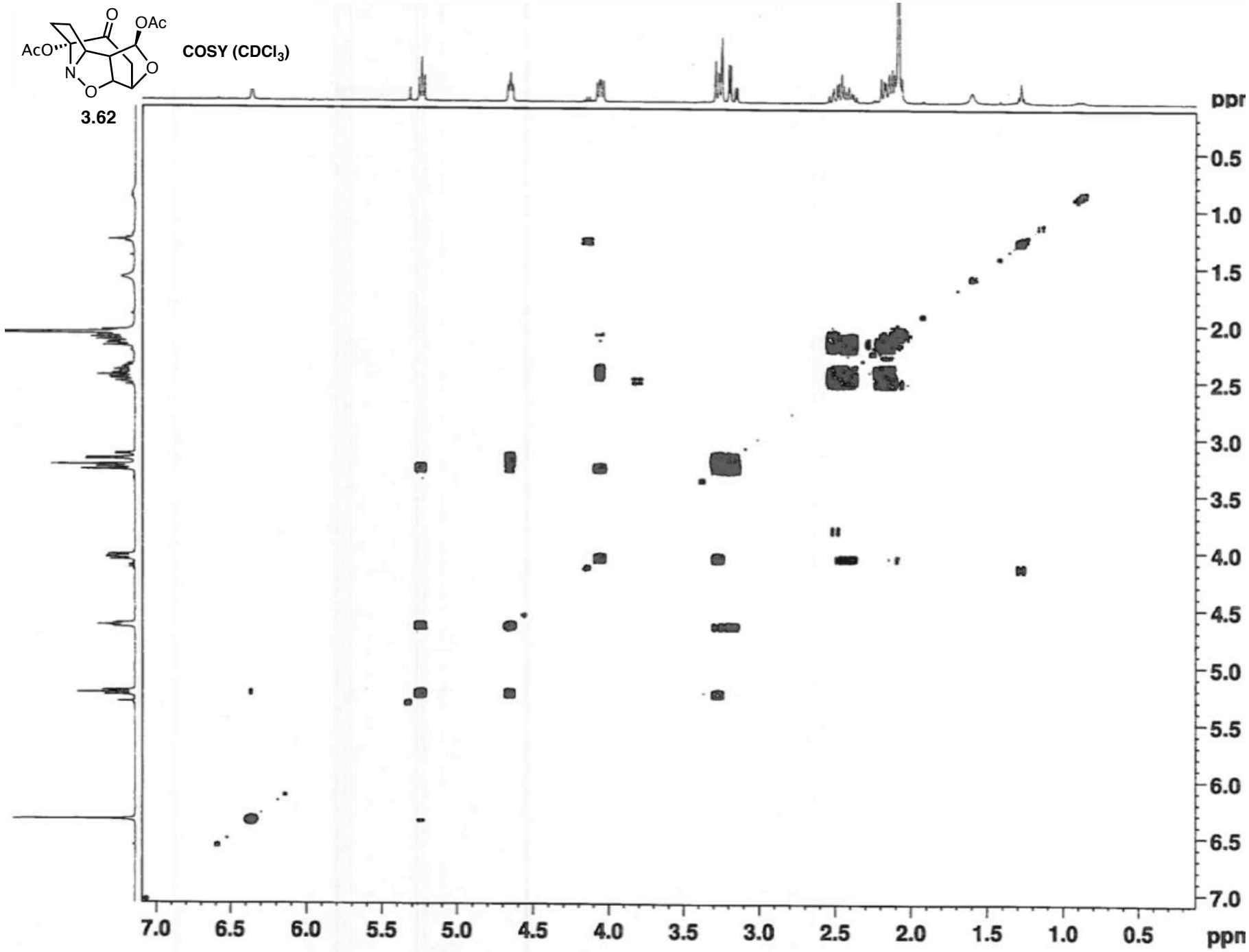
O
OAc
AcO
N
O
O
3.62
COSY ($CDCl_3$)
ppm
0.5
1.0
1.5
2.0
2.5
3.0
3.5
4.0
4.5
5.0
5.5
6.0
6.5
7.0
7.0
6.5
6.0
5.5
5.0
4.5
4.0
3.5
3.0
2.5
2.0
1.5
1.0
0.5
ppm

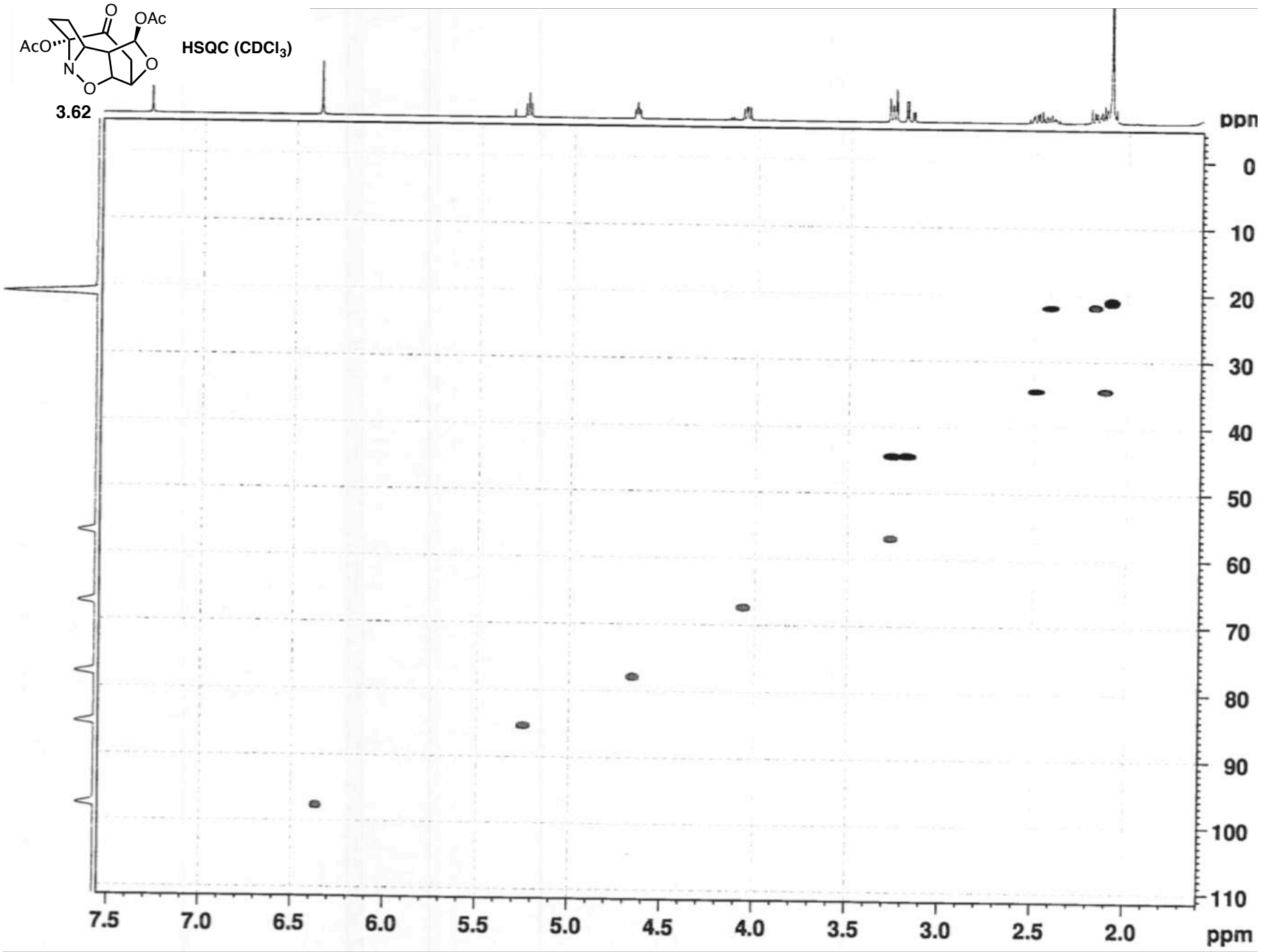
AcO
OAc
O
N
O
O
3.62
HSQC ($CDCl_3$)
ppm
0
10
20
30
40
50
60
70
80
90
100
110
7.5
7.0
6.5
6.0
5.5
5.0
4.5
4.0
3.5
3.0
2.5
2.0
ppm

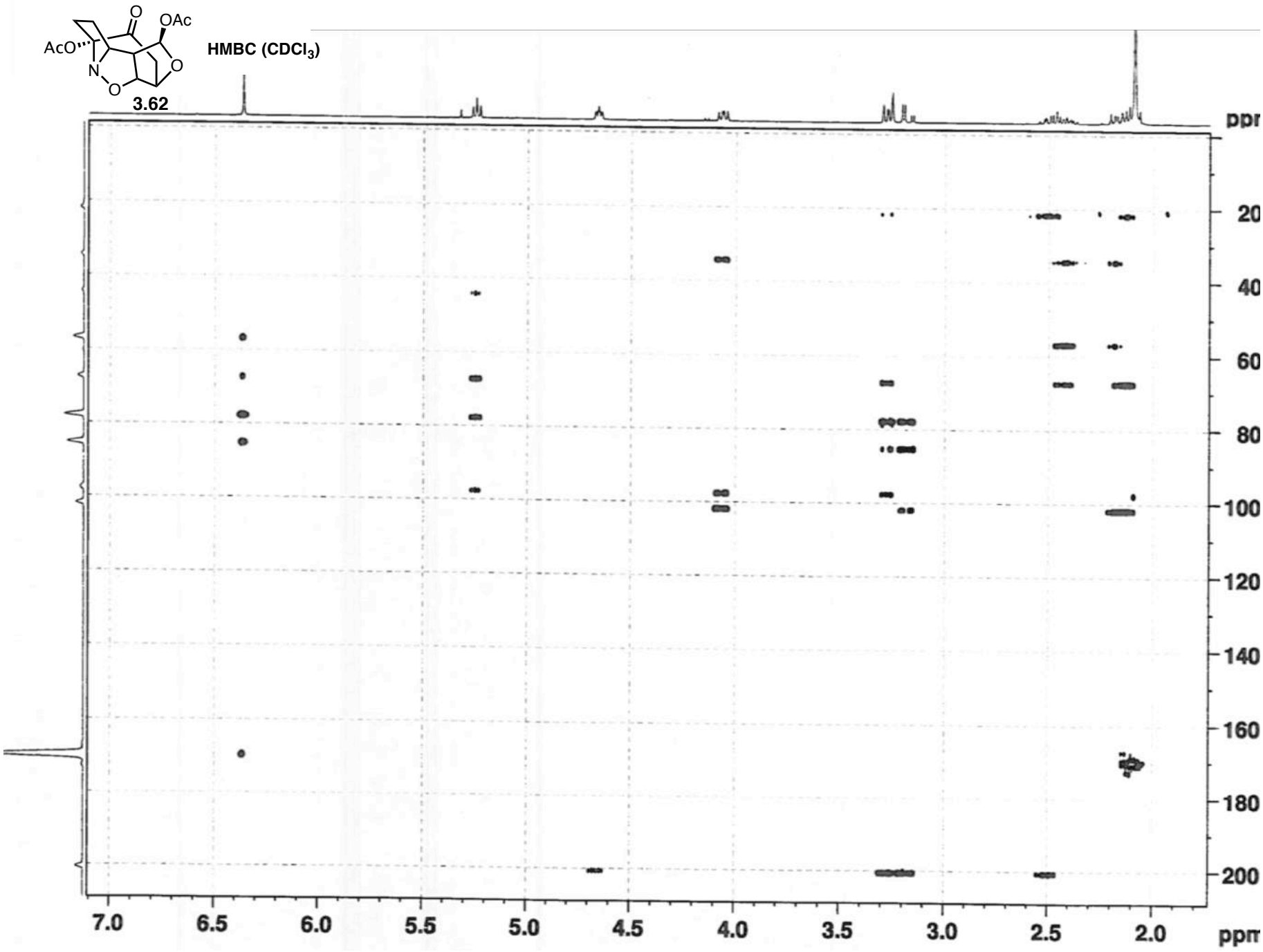
AcO
OAc
O
N
O
O
3.62
HMBC ($CDCl_3$)
ppm
20
40
60
80
100
120
140
160
180
200
7.0
6.5
6.0
5.5
5.0
4.5
4.0
3.5
3.0
2.5
2.0
ppm

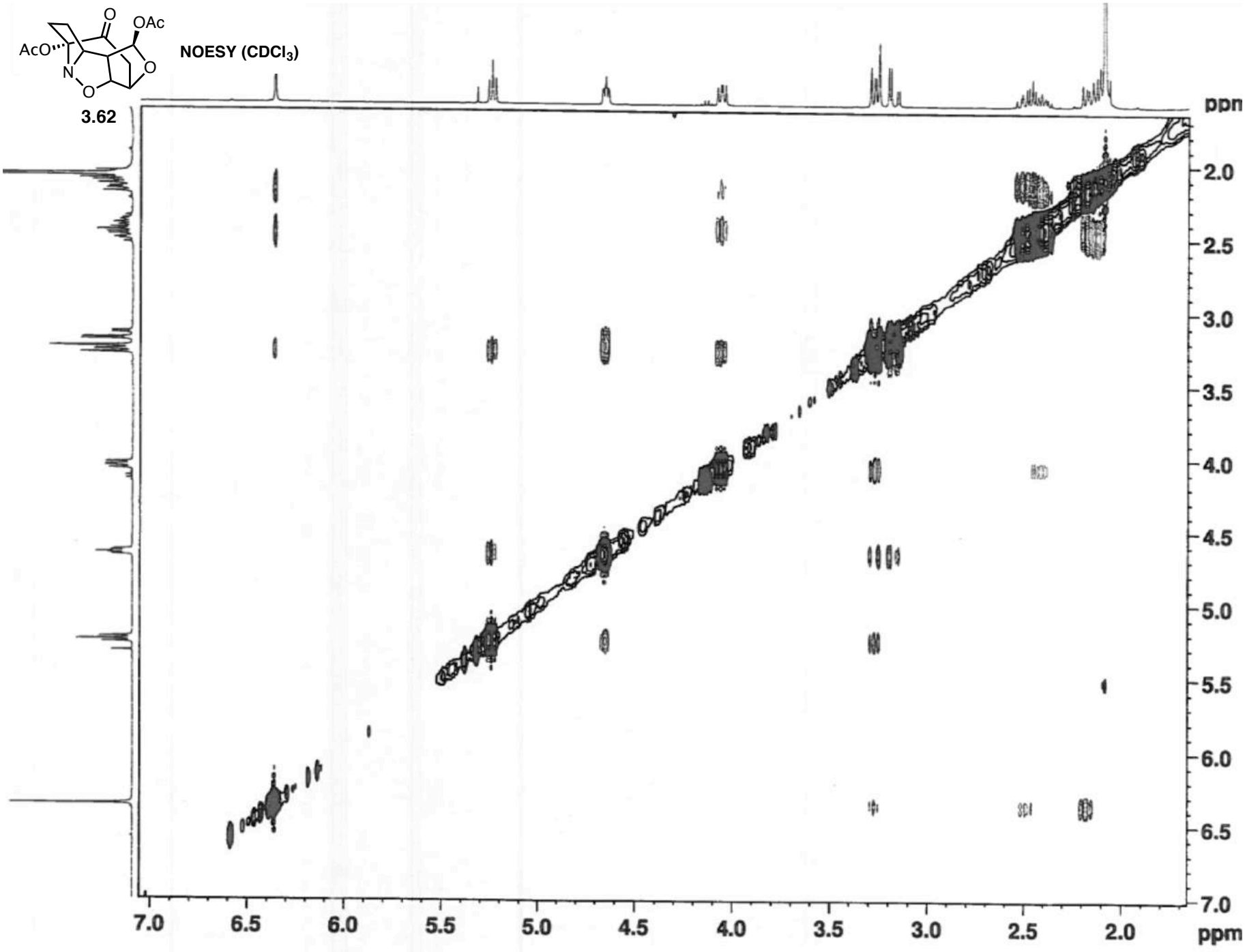
OAc
AcO
O
N
O
O
NOESY ($CDCl_3$)
3.62
ppm
2.0
2.5
3.0
3.5
4.0
4.5
5.0
5.5
6.0
6.5
7.0
7.0
6.5
6.0
5.5
5.0
4.5
4.0
3.5
3.0
2.5
2.0
ppm

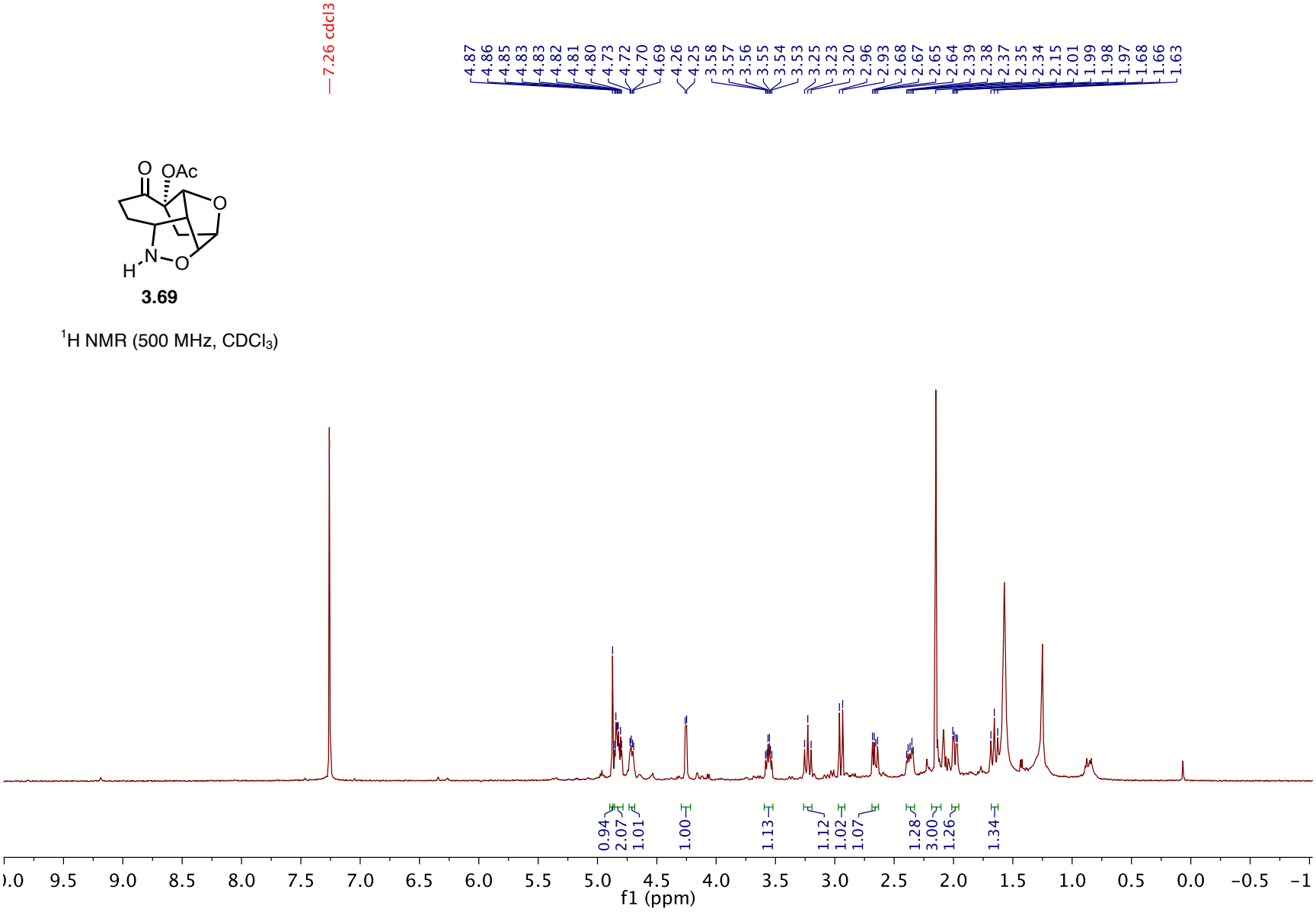

3.69

^{1}H NMR (500 MHz, $CDCl_3$)

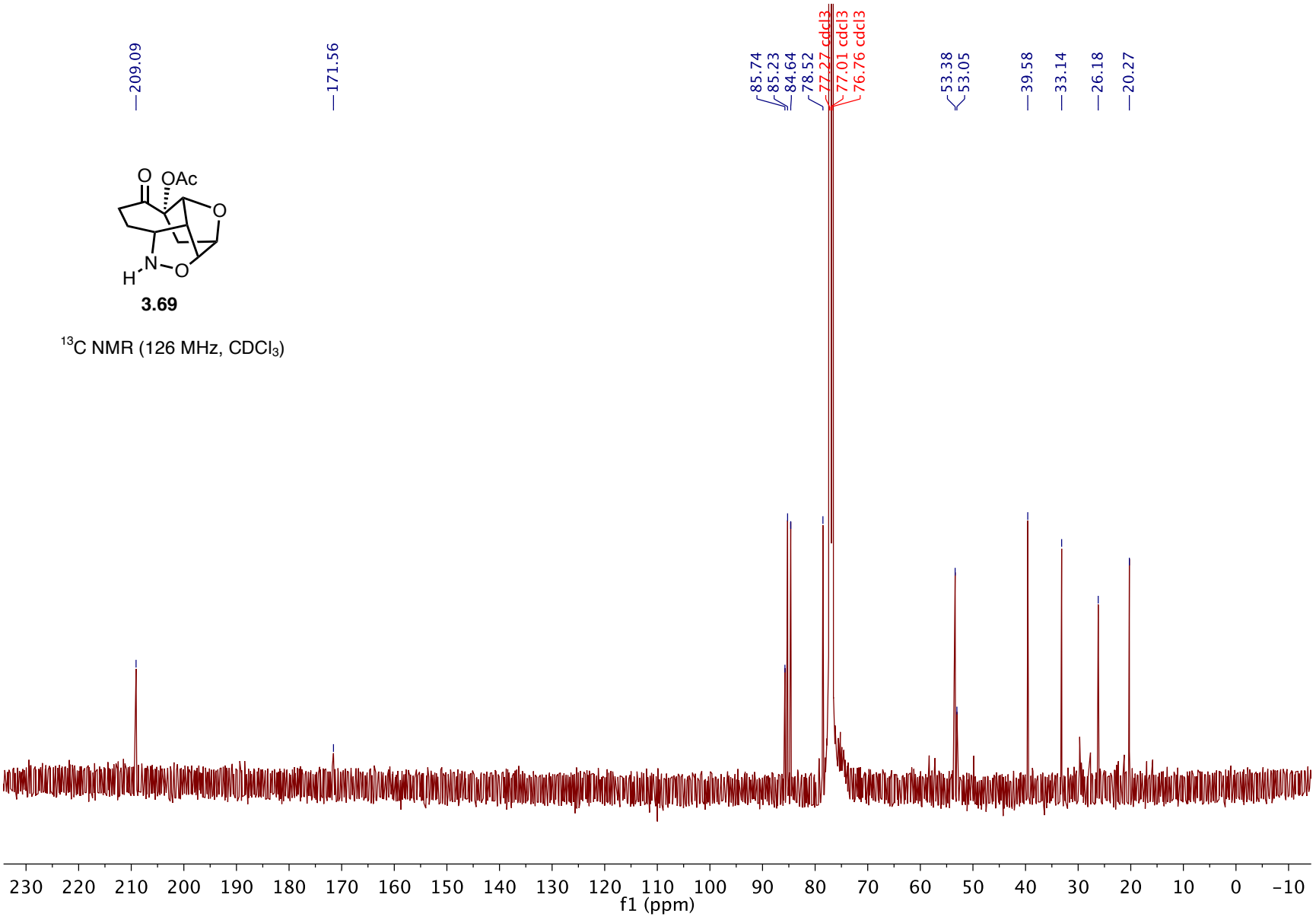
209.09
171.56
85.74
85.23
84.64
78.52
77.27 cdcl3
77.01 cdcl3
76.76 cdcl3
53.38
53.05
39.58
33.14
26.18
20.27
O
OAc
O
H
N
O
3.69
^{13}C NMR (126 MHz, $CDCl_3$)
230 220 210 200 190 180 170 160 150 140 130 120 110 100 90 80 70 60 50 40 30 20 10 0 -10
f1 (ppm)

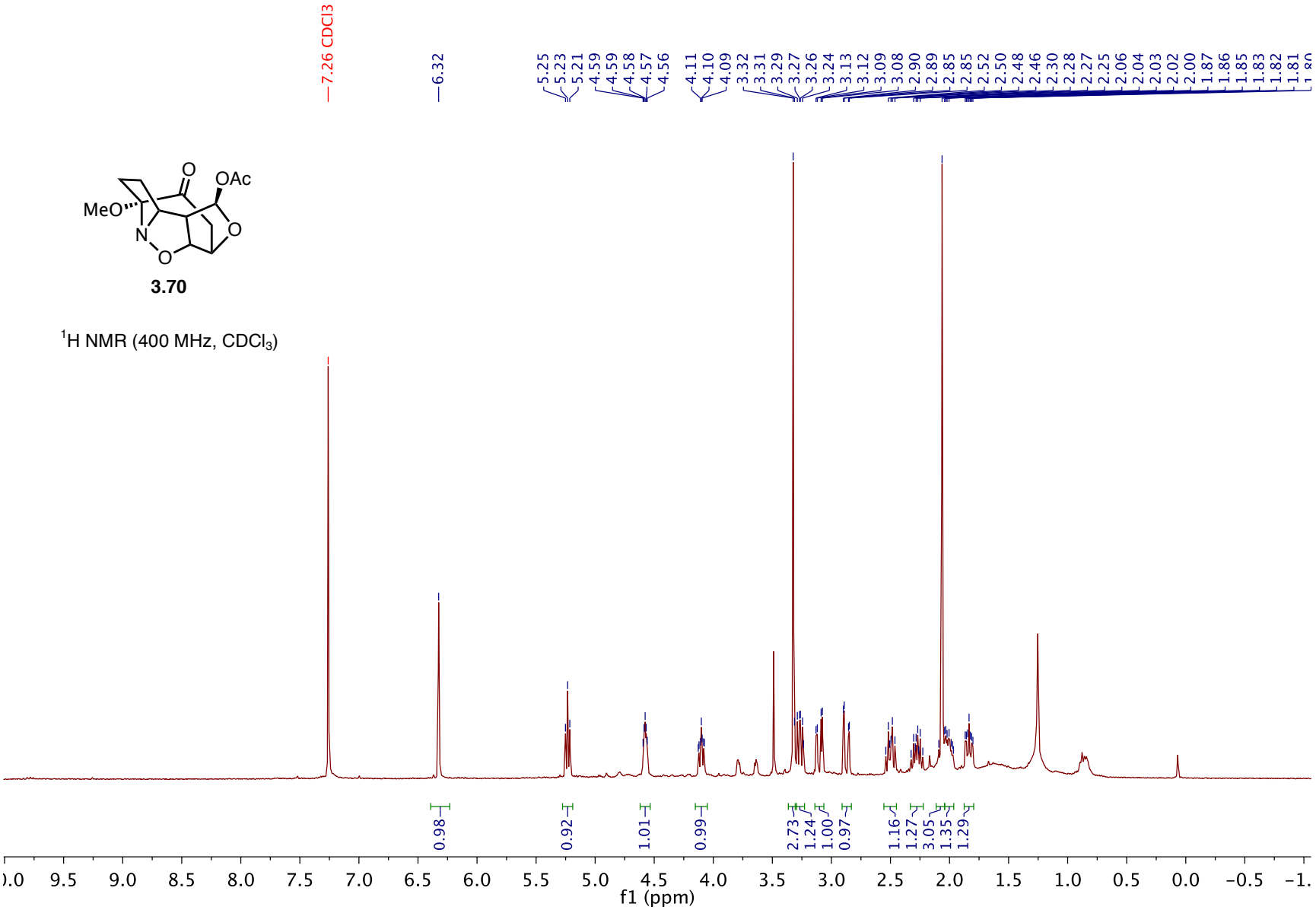

3.70

^{1}H NMR (400 MHz, $CDCl_3$)

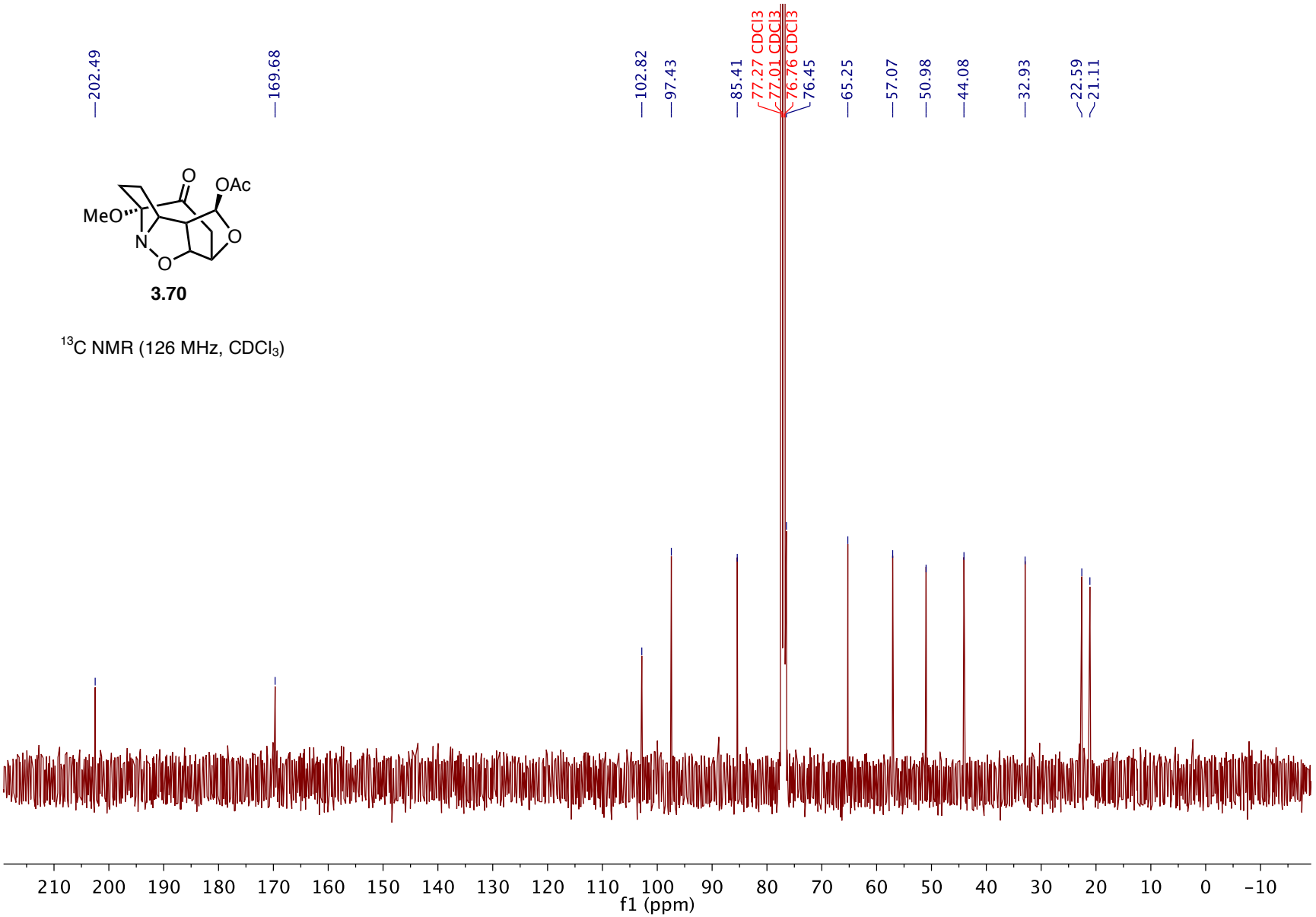
202.49
169.68
102.82
97.43
85.41
77.27 CDCl3
77.01 CDCl3
76.76 CDCl3
76.45
65.25
57.07
50.98
44.08
32.93
22.59
21.11
O
OAc
MeO
N
O
O
3.70
13C NMR (126 MHz, CDCl3)
210 200 190 180 170 160 150 140 130 120 110 100 90 80 70 60 50 40 30 20 10 0 -10
f1 (ppm)

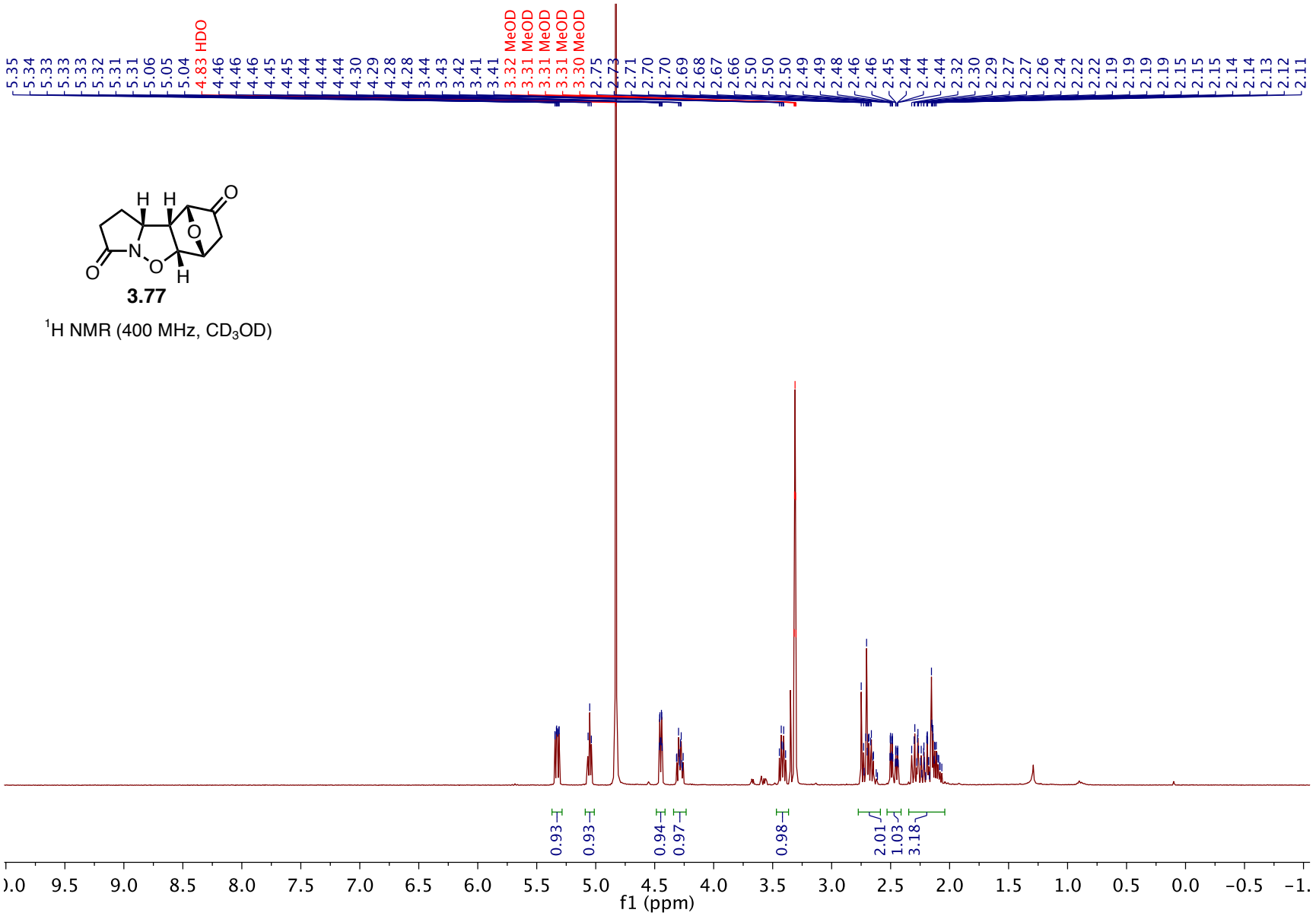

3.77

^{1}H NMR (400 MHz, CD_3OD)

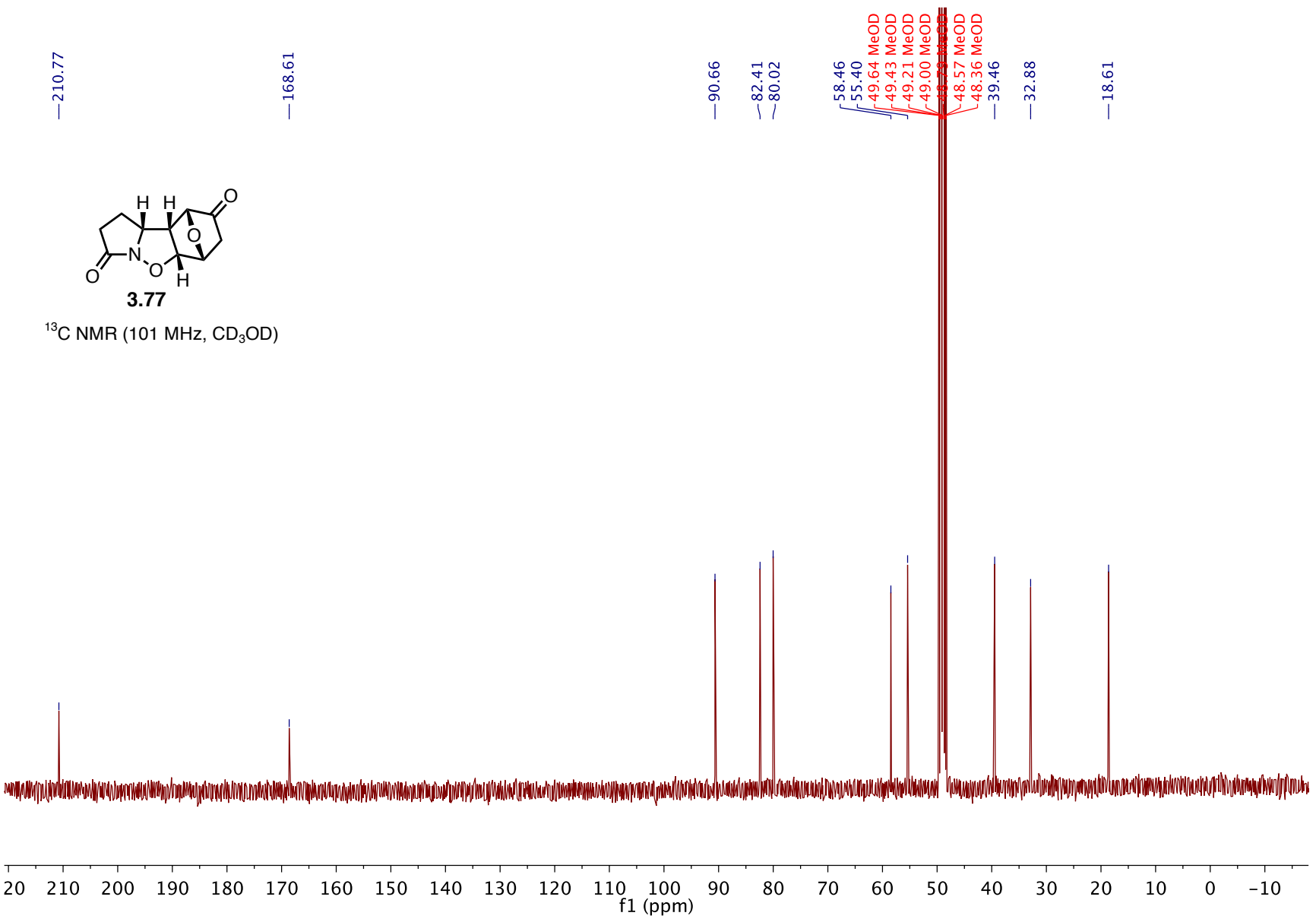
210.77
168.61
90.66
82.41
80.02
58.46
55.40
49.64 MeOD
49.43 MeOD
49.21 MeOD
49.00 MeOD
48.57 MeOD
48.36 MeOD
39.46
32.88
18.61
H
H
O
O
N
O
O
H
3.77
13C NMR (101 MHz, CD3OD)
20 210 200 190 180 170 160 150 140 130 120 110 100 90 80 70 60 50 40 30 20 10 0 -10
f1 (ppm)

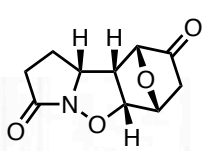

3.77

COSY (CD_3OD)

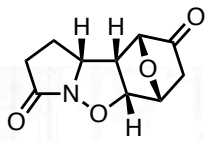

3.77

HSQC (CD_3OD)

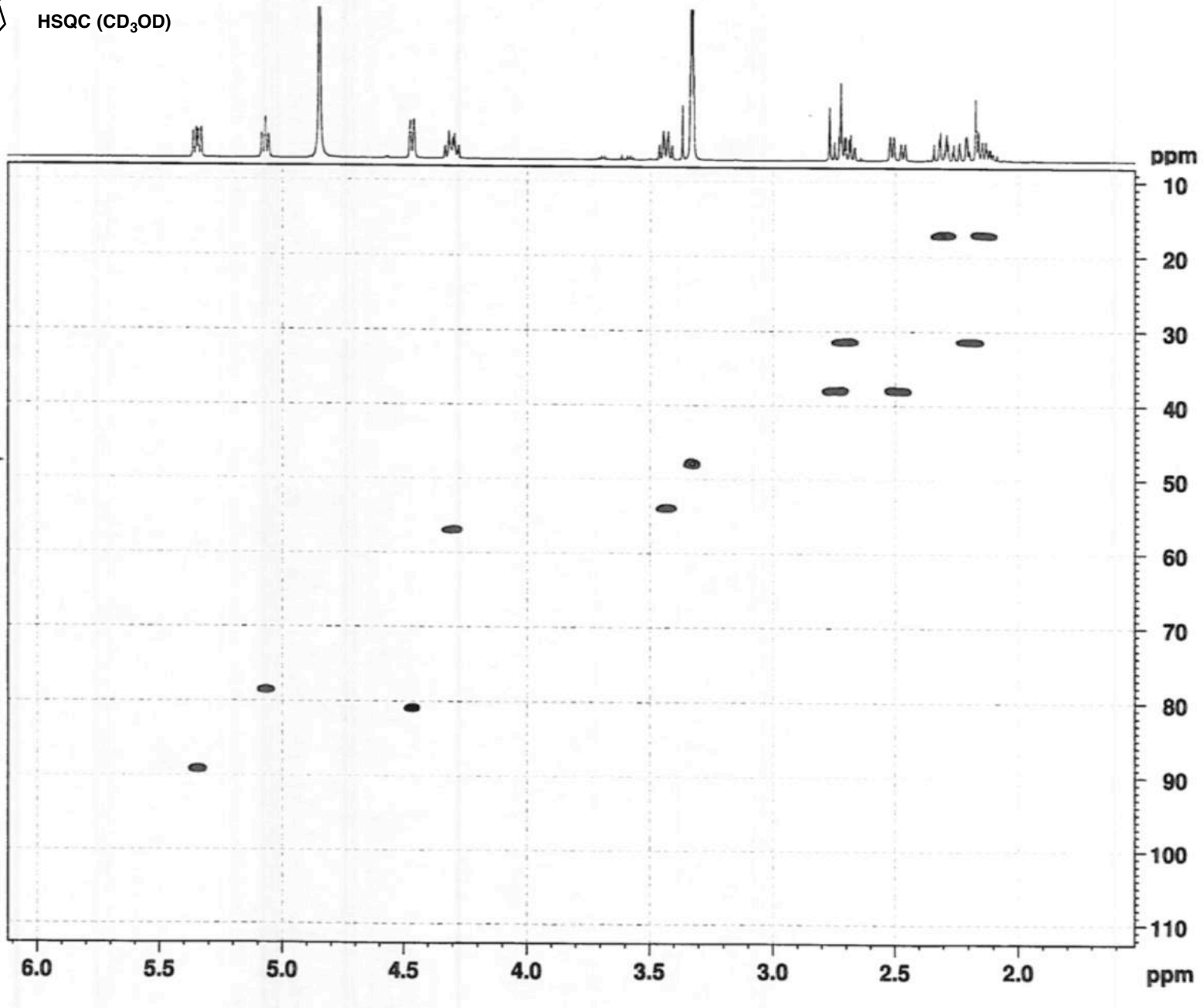

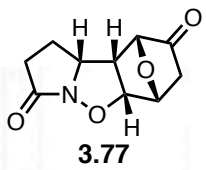

3.77

HMBC (CD_3OD)

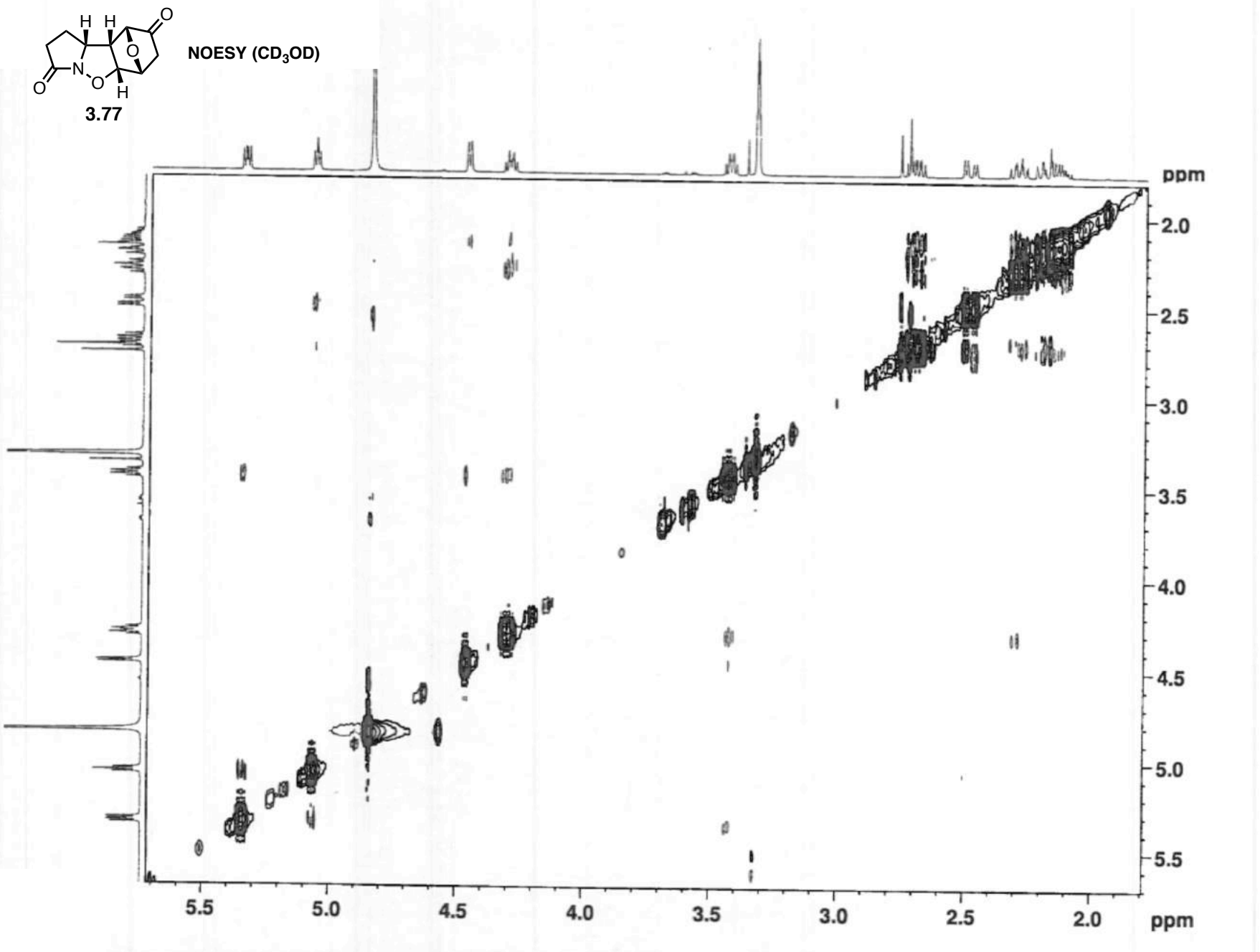
H H
O
O
N
O
H
3.77
NOESY (CD_3OD)
ppm
2.0
2.5
3.0
3.5
4.0
4.5
5.0
5.5
5.5
5.0
4.5
4.0
3.5
3.0
2.5
2.0
ppm

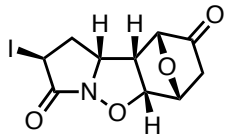

3.78

^{1}H NMR (400 MHz, $CDCl_3$)

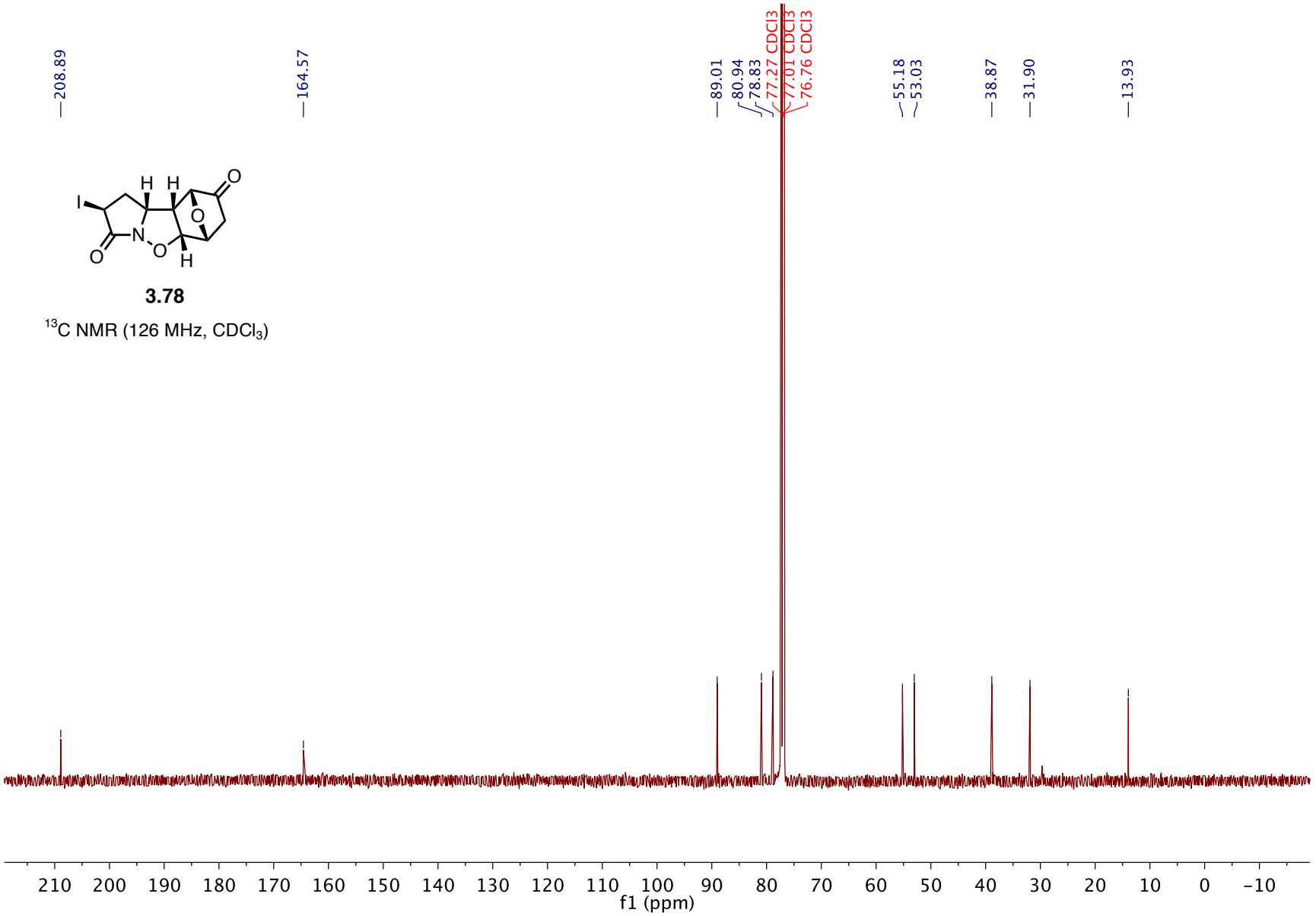

3.78

^{13}C NMR (126 MHz, $CDCl_3$)

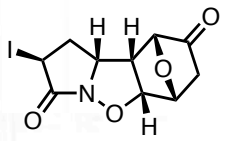

3.78

COSY ($CDCl_3$)

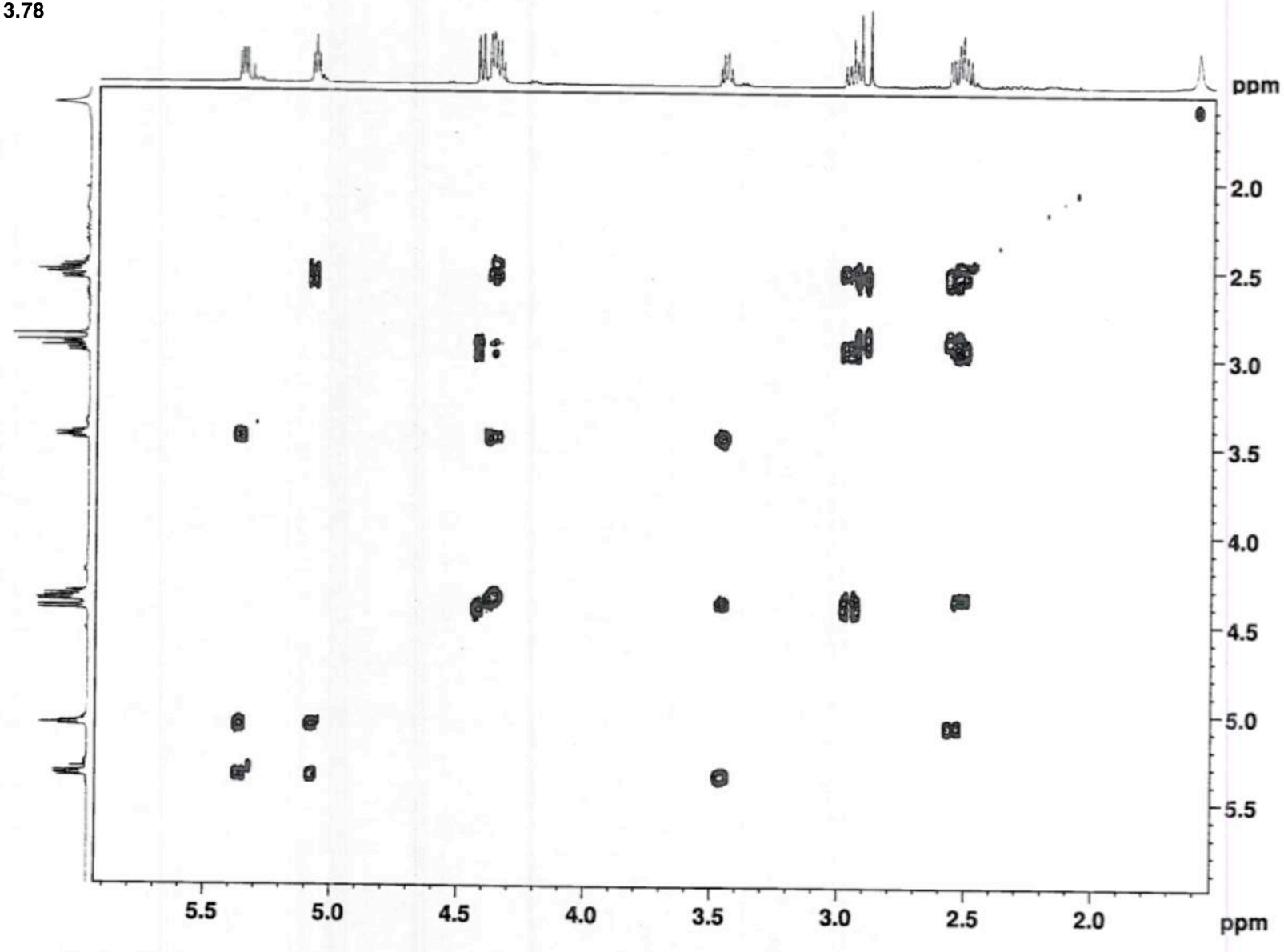

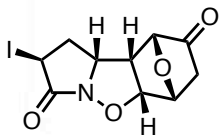

3.78

HSQC ($CDCl_3$)

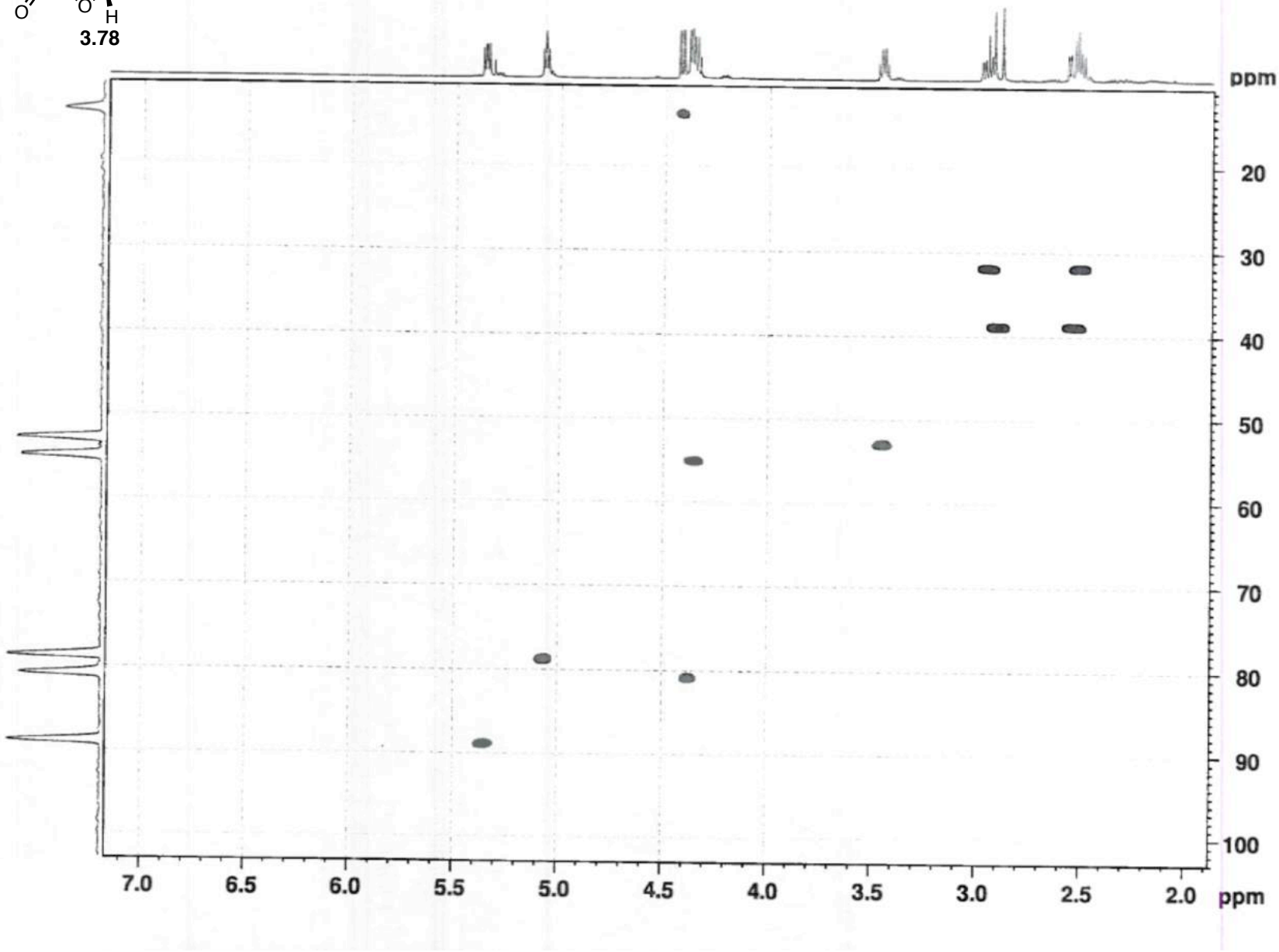

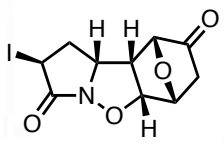

3.78

HMBC ($CDCl_3$)

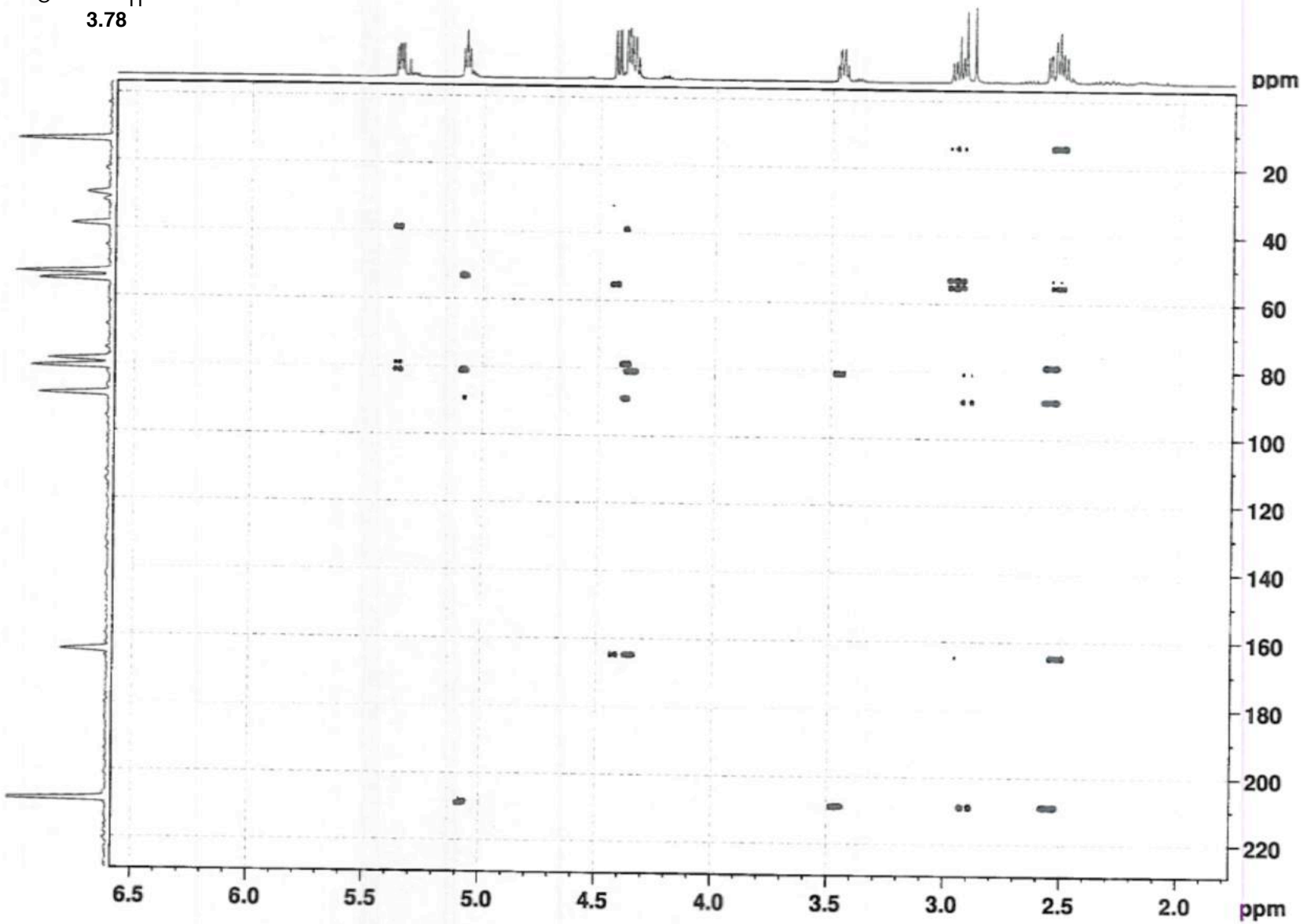

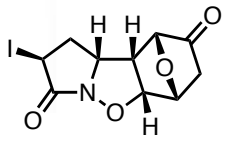

3.78

NOESY ($CDCl_3$)

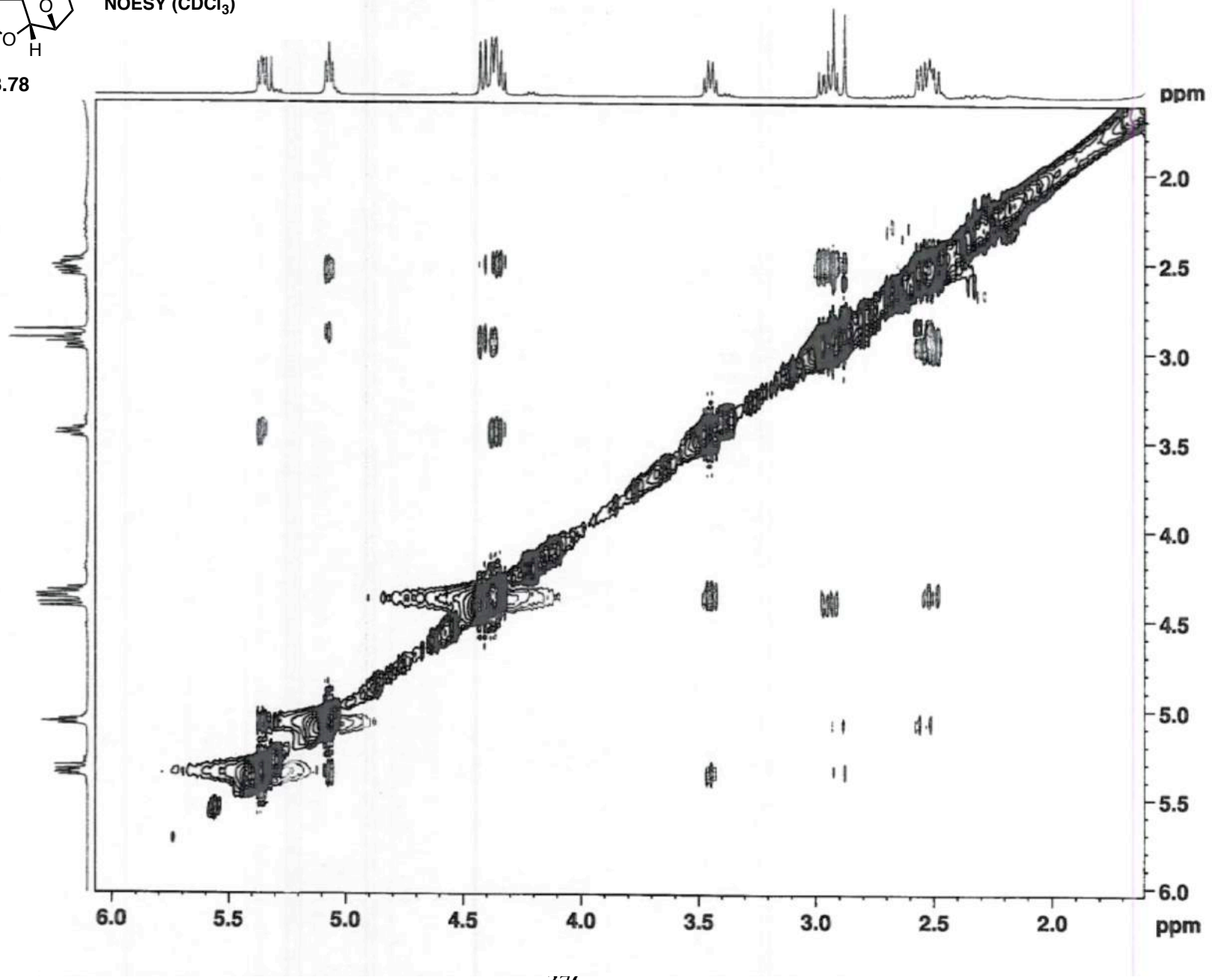

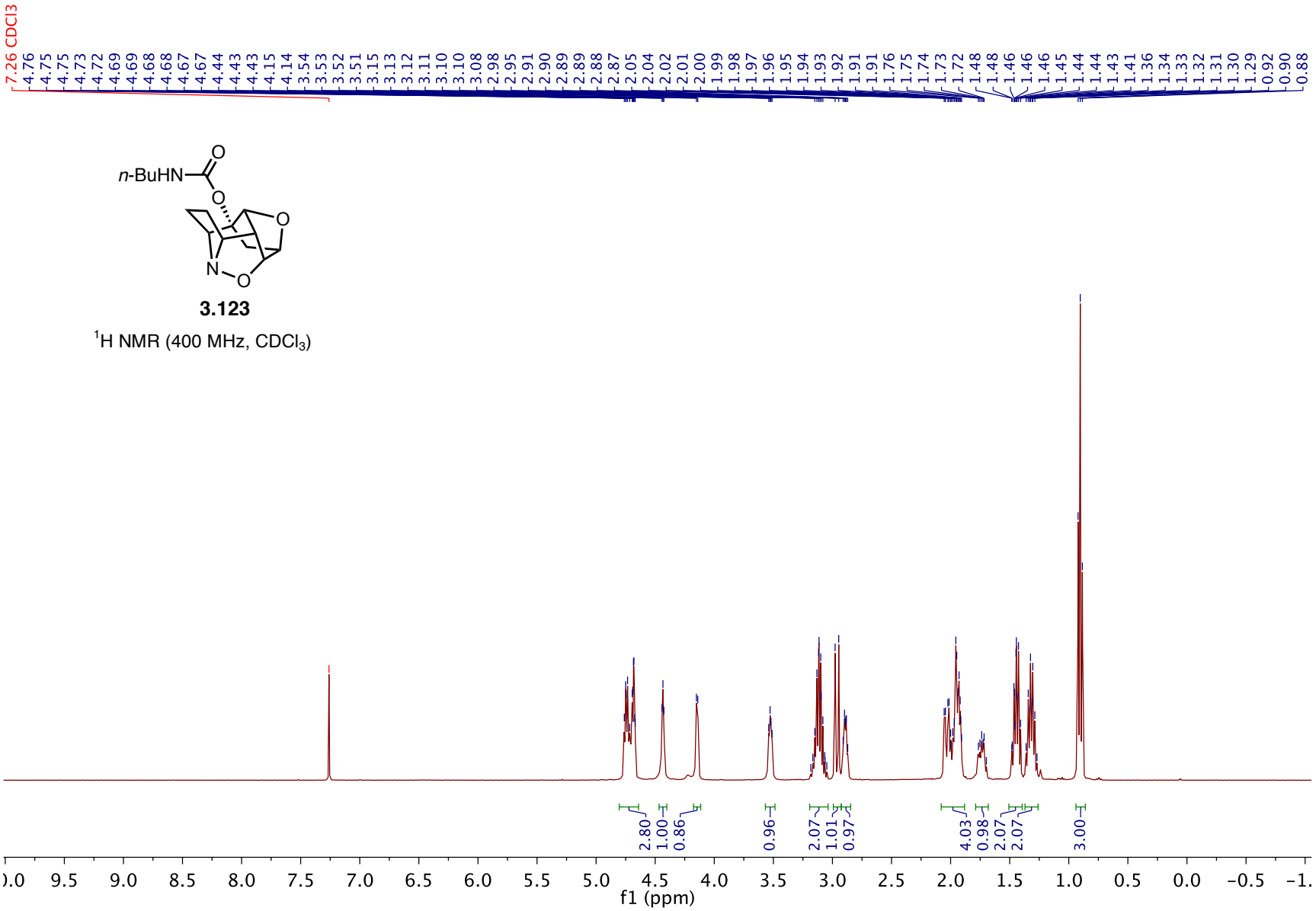

3.123

^{1}H NMR (400 MHz, $CDCl_3$)

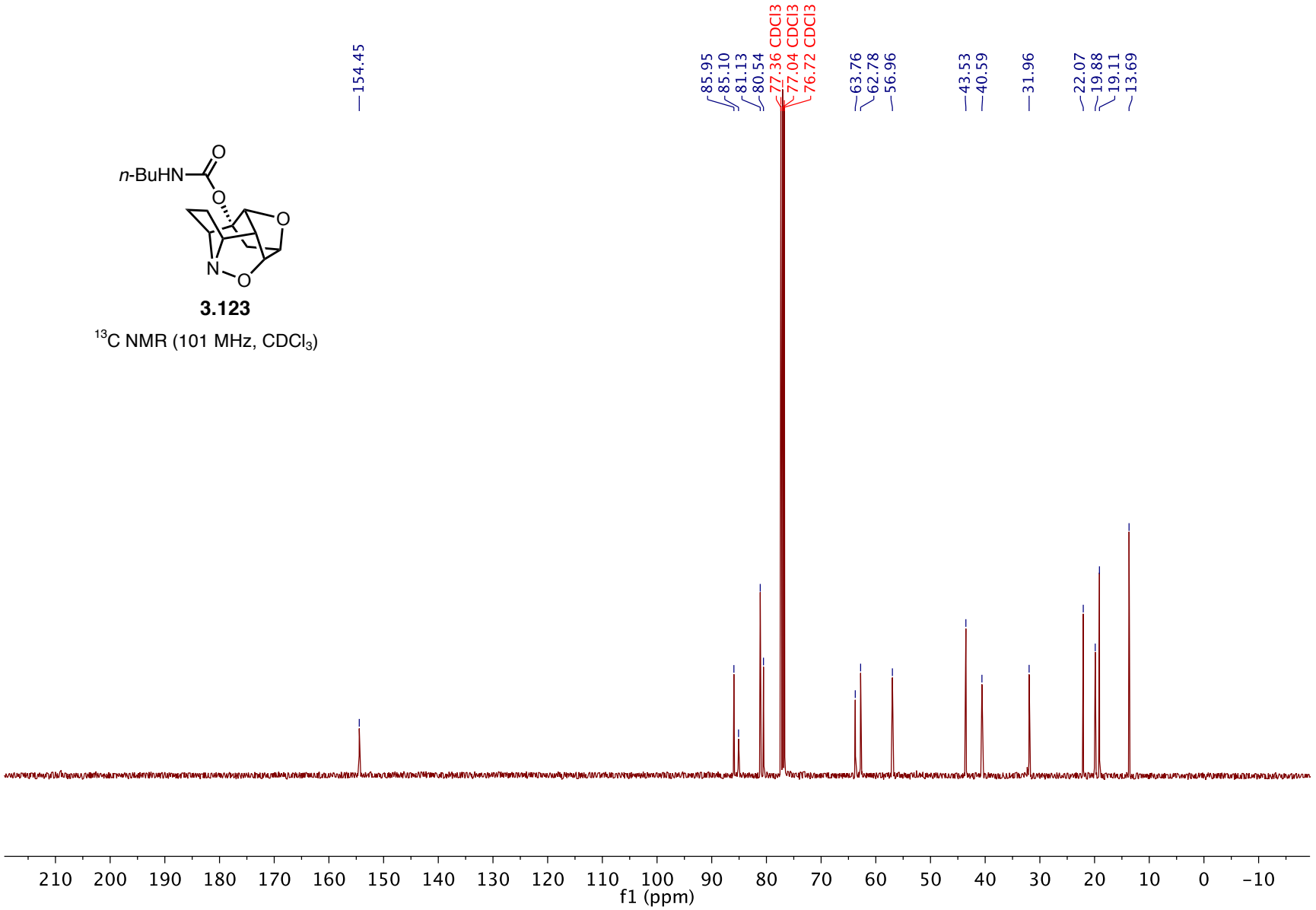

3.123

^{13}C NMR (101 MHz, $CDCl_3$)

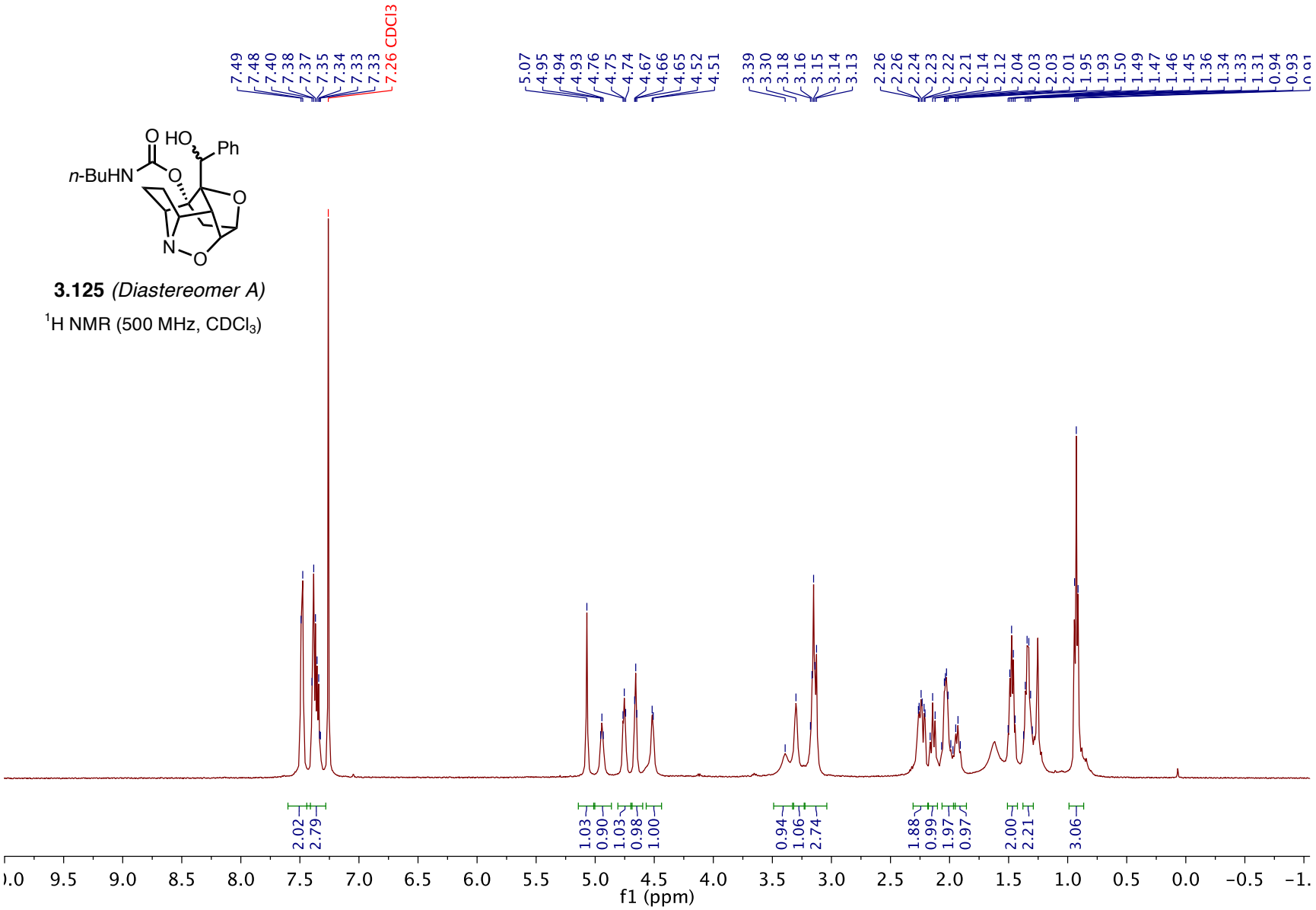
7.49
7.48
7.40
7.38
7.37
7.35
7.34
7.33
7.33
7.26 CDCl3
5.07
4.95
4.94
4.93
4.76
4.75
4.74
4.67
4.65
4.52
4.51
3.39
3.30
3.18
3.16
3.15
3.14
3.13
2.26
2.26
2.24
2.23
2.22
2.21
2.14
2.12
2.04
2.03
2.03
2.01
1.95
1.93
1.50
1.49
1.47
1.46
1.45
1.36
1.34
1.33
1.31
0.94
0.93
O
HO
Ph
n-BuHN
O
O
N
O
3.125 (Diastereomer A)
1H NMR (500 MHz, CDCl3)
2.02
2.79
1.03
0.90
1.03
0.98
1.00
0.94
1.06
2.74
1.88
0.99
1.97
0.97
2.00
2.21
3.06
f1 (ppm)

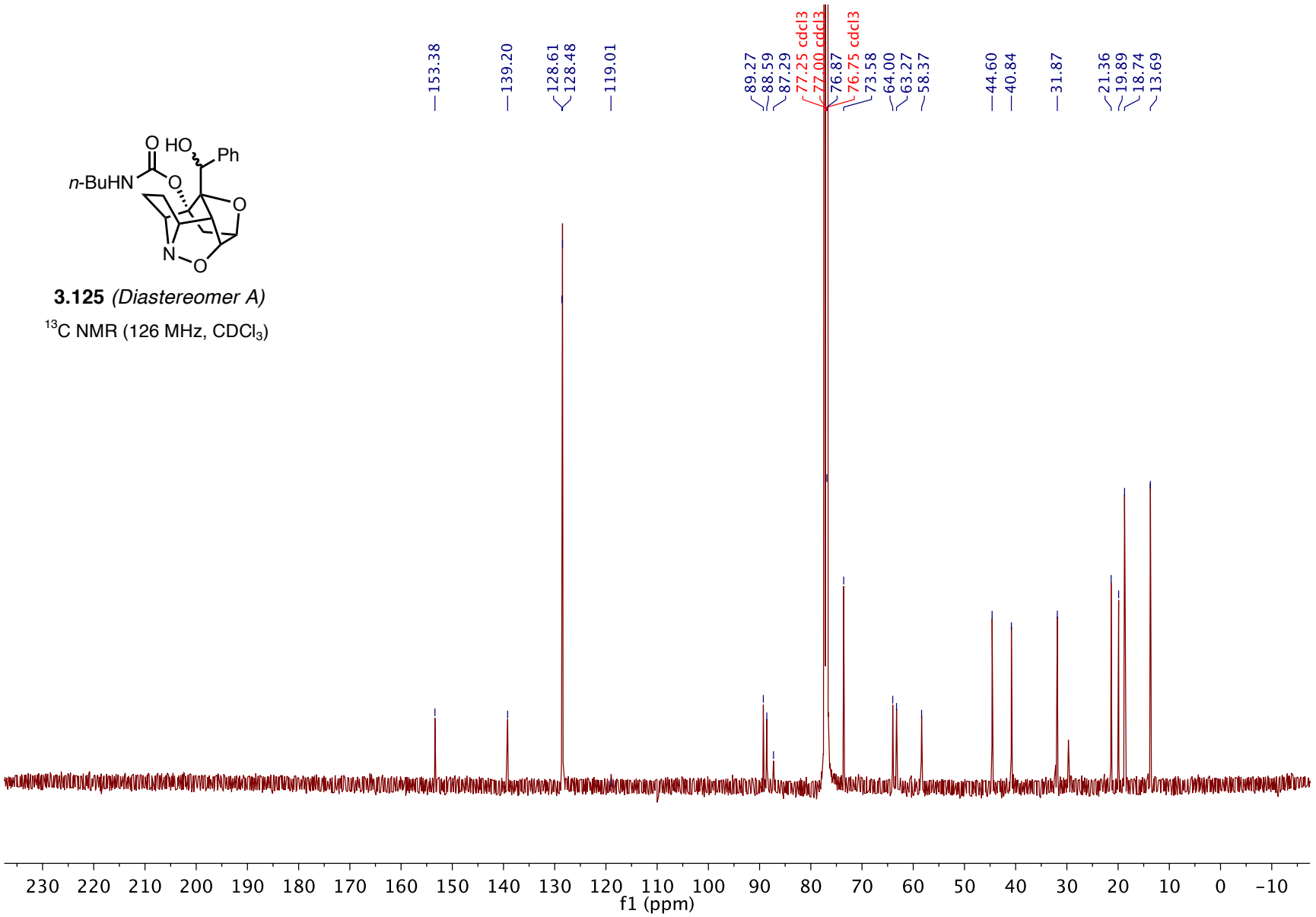

3.125 *(Diastereomer A)*

^{13}C NMR (126 MHz, $CDCl_3$)

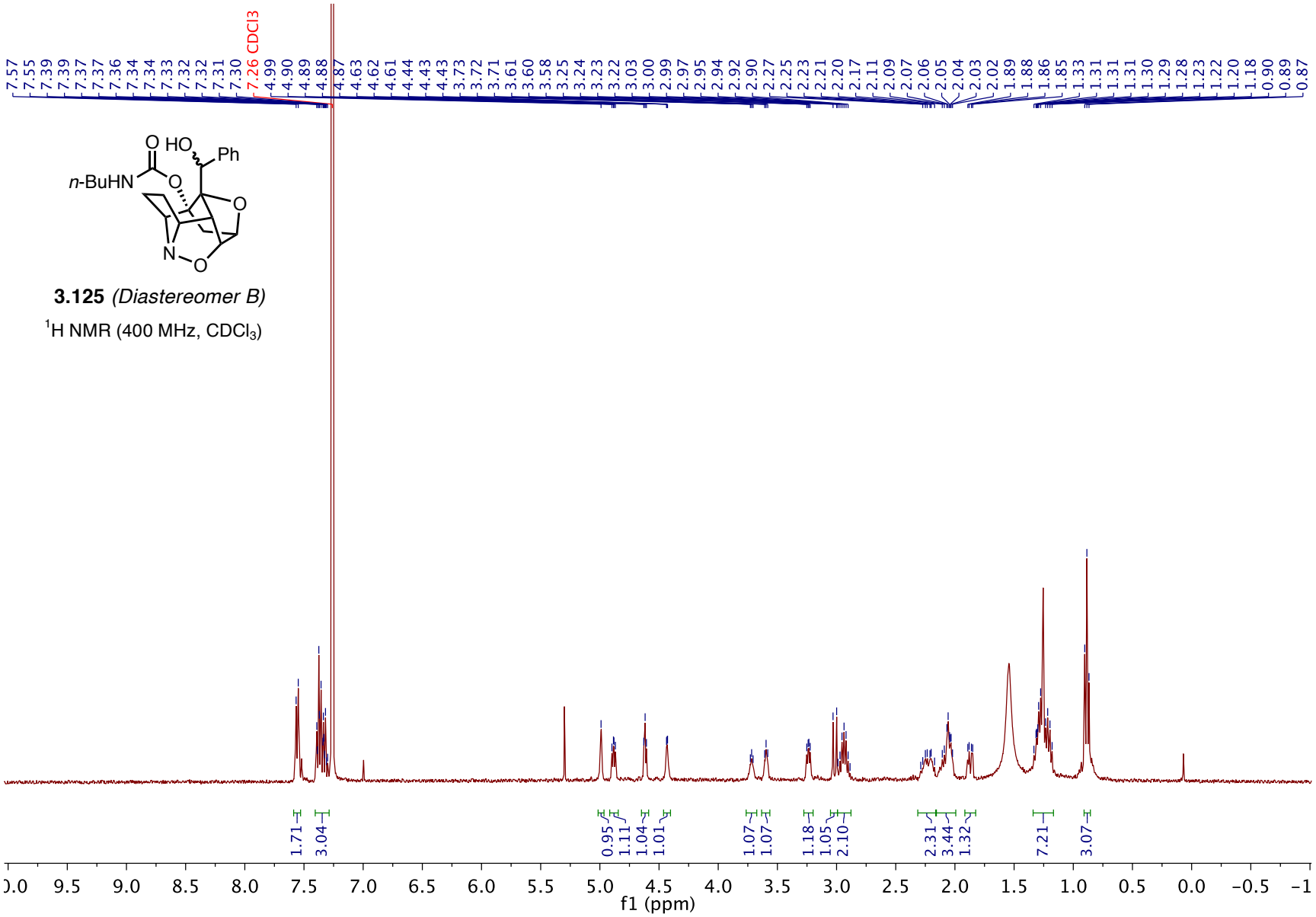

3.125 *(Diastereomer B)*

^{1}H NMR (400 MHz, $CDCl_3$)

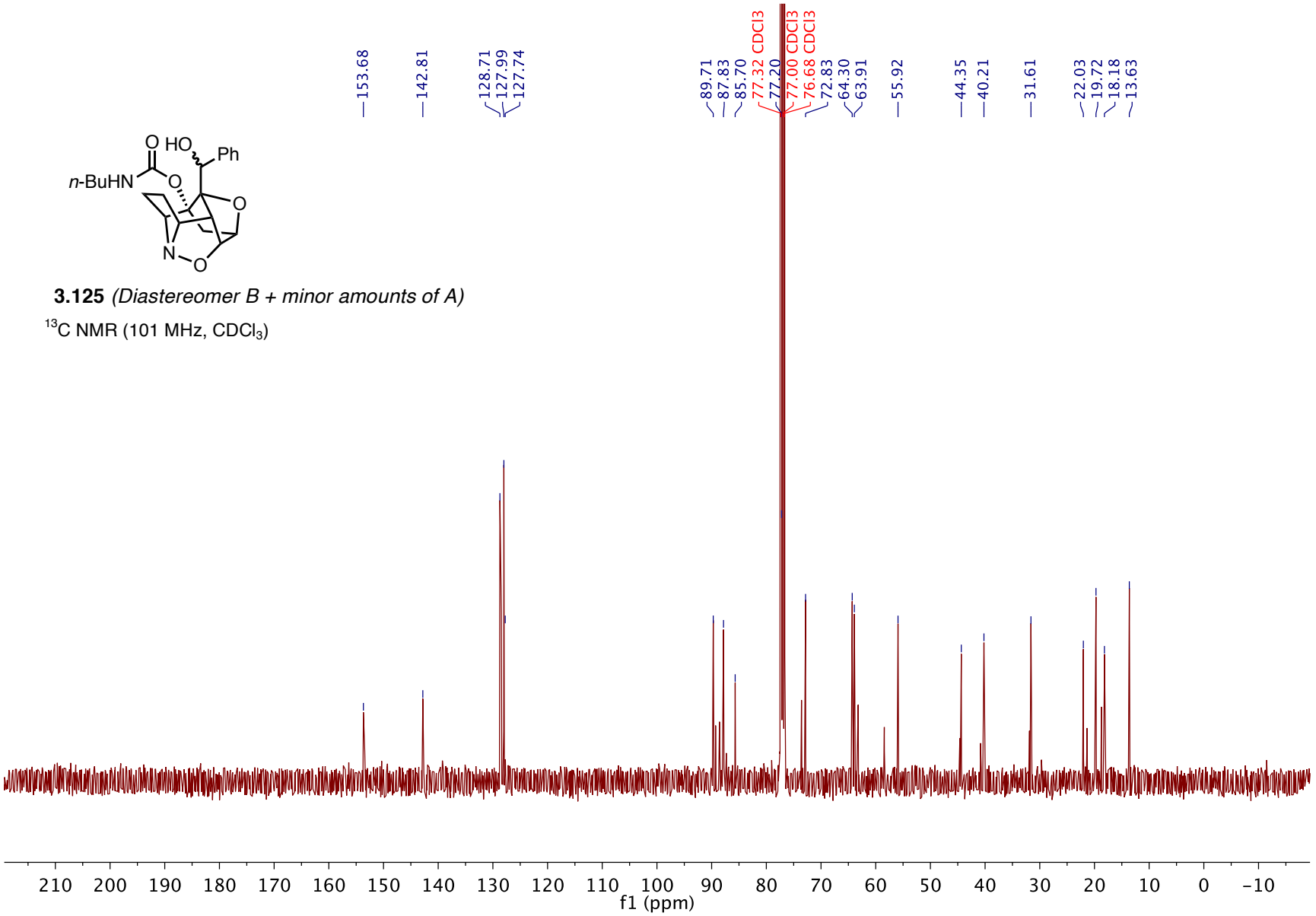

3.125 *(Diastereomer B + minor amounts of A)*

^{13}C NMR (101 MHz, $CDCl_3$)

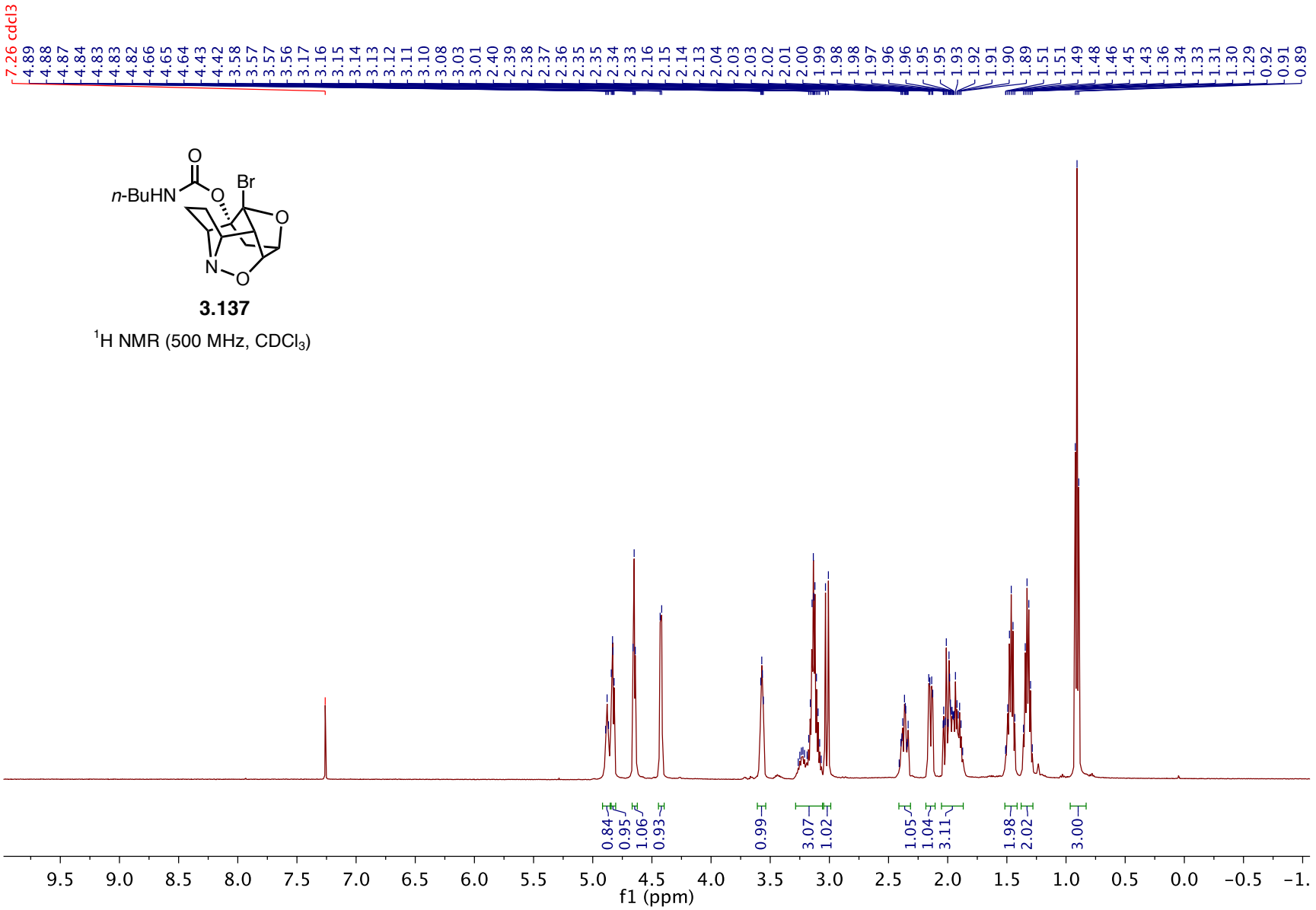

3.137

^{1}H NMR (500 MHz, $CDCl_3$)

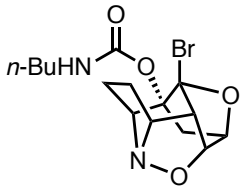

3.137

^{13}C NMR (126 MHz, $CDCl_3$)

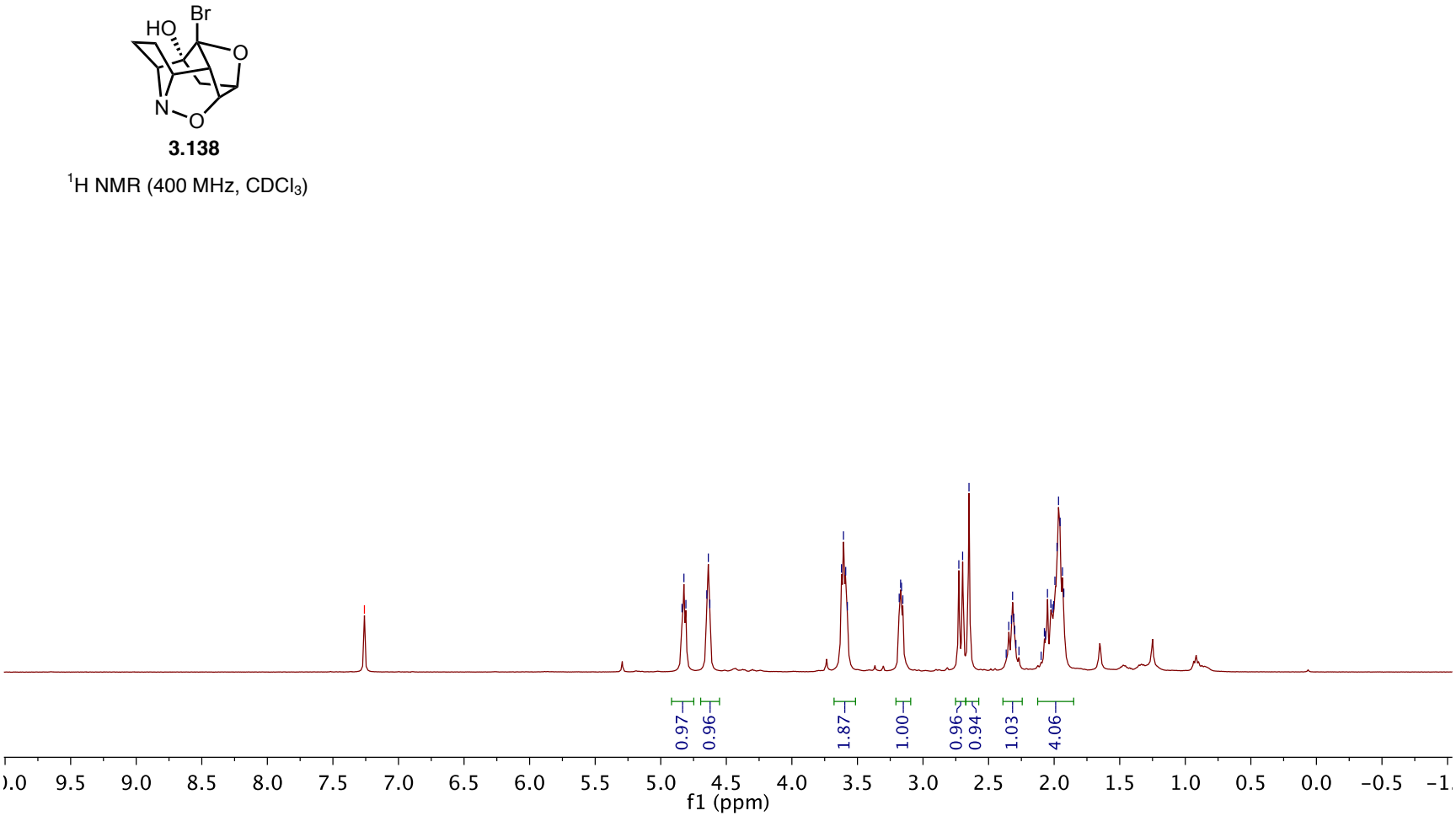

3.138

^{1}H NMR (400 MHz, $CDCl_3$)

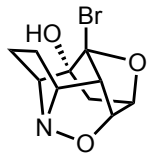

3.138

^{13}C NMR (101 MHz, $CDCl_3$)

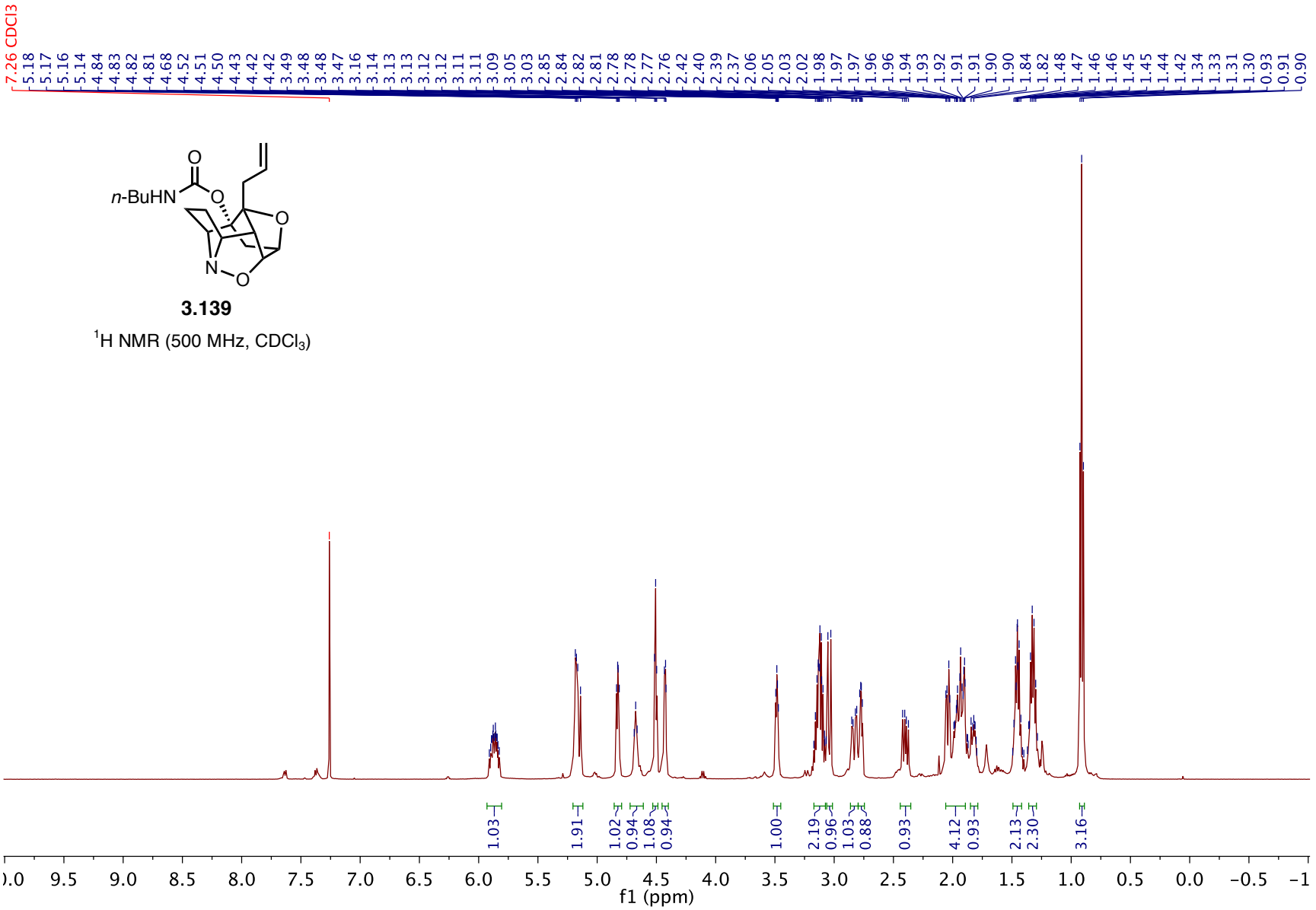

3.139

^{1}H NMR (500 MHz, $CDCl_3$)

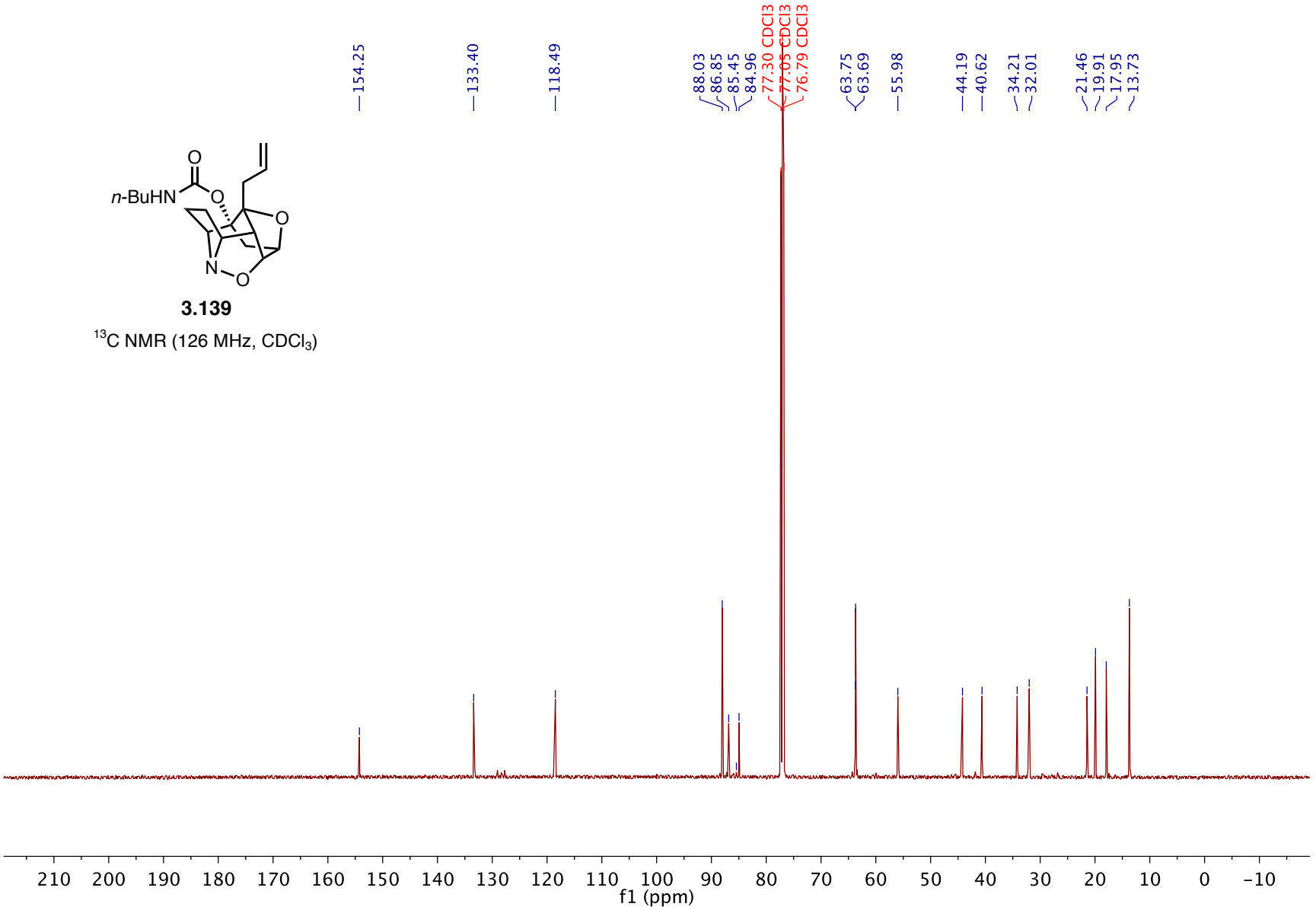

3.139

^{13}C NMR (126 MHz, $CDCl_3$)

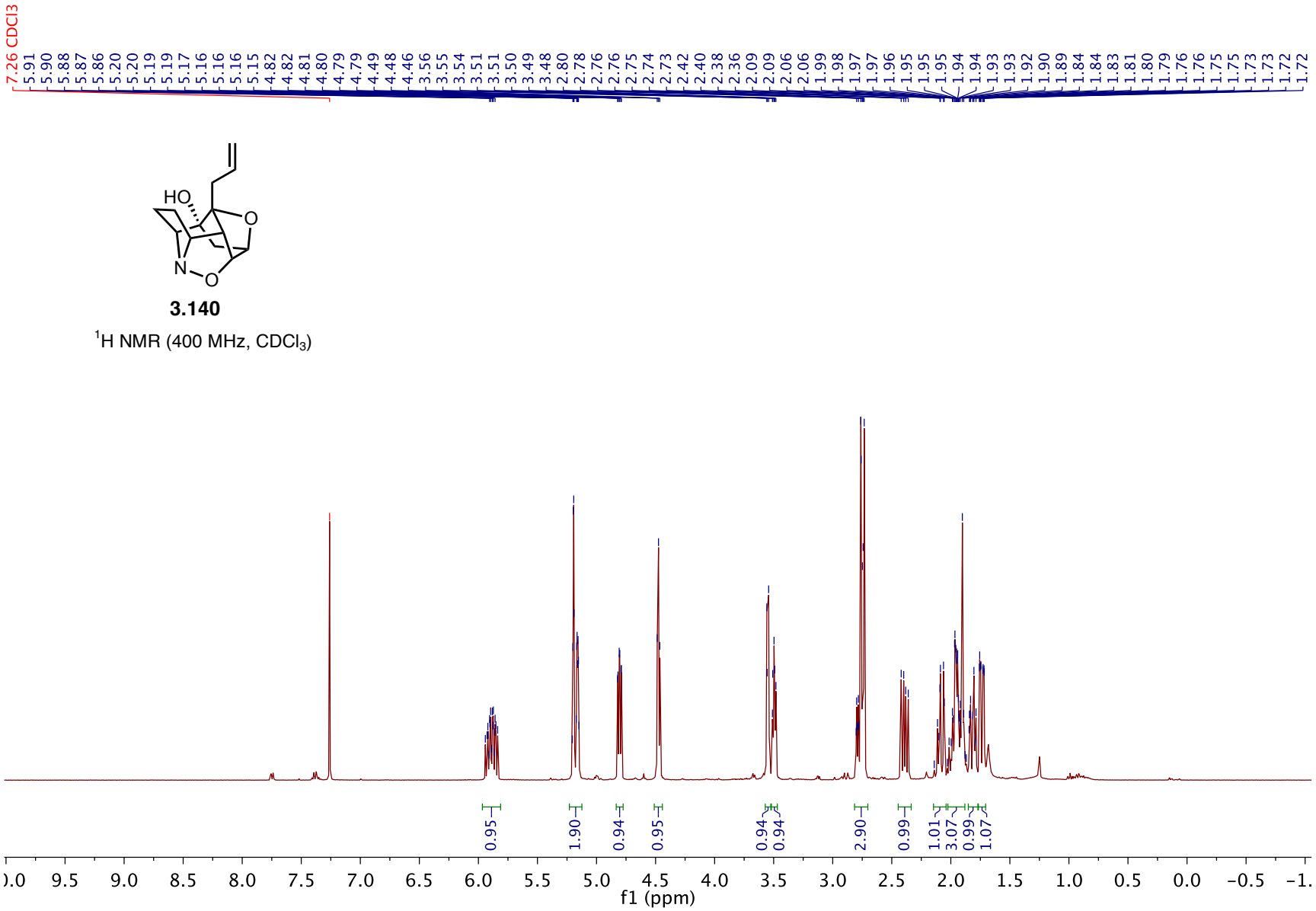

3.140

^{1}H NMR (400 MHz, $CDCl_3$)

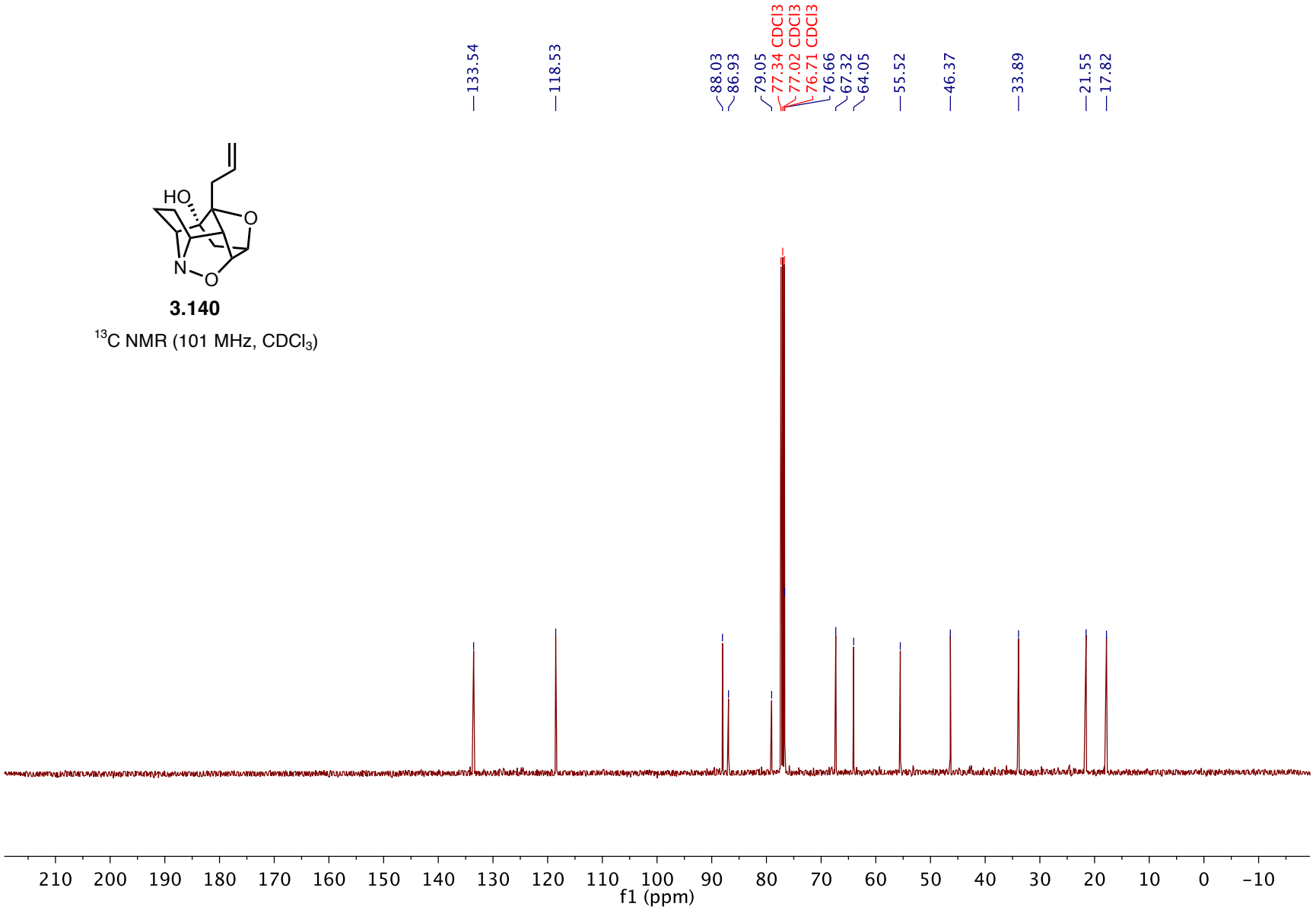

3.140

^{13}C NMR (101 MHz, $CDCl_3$)

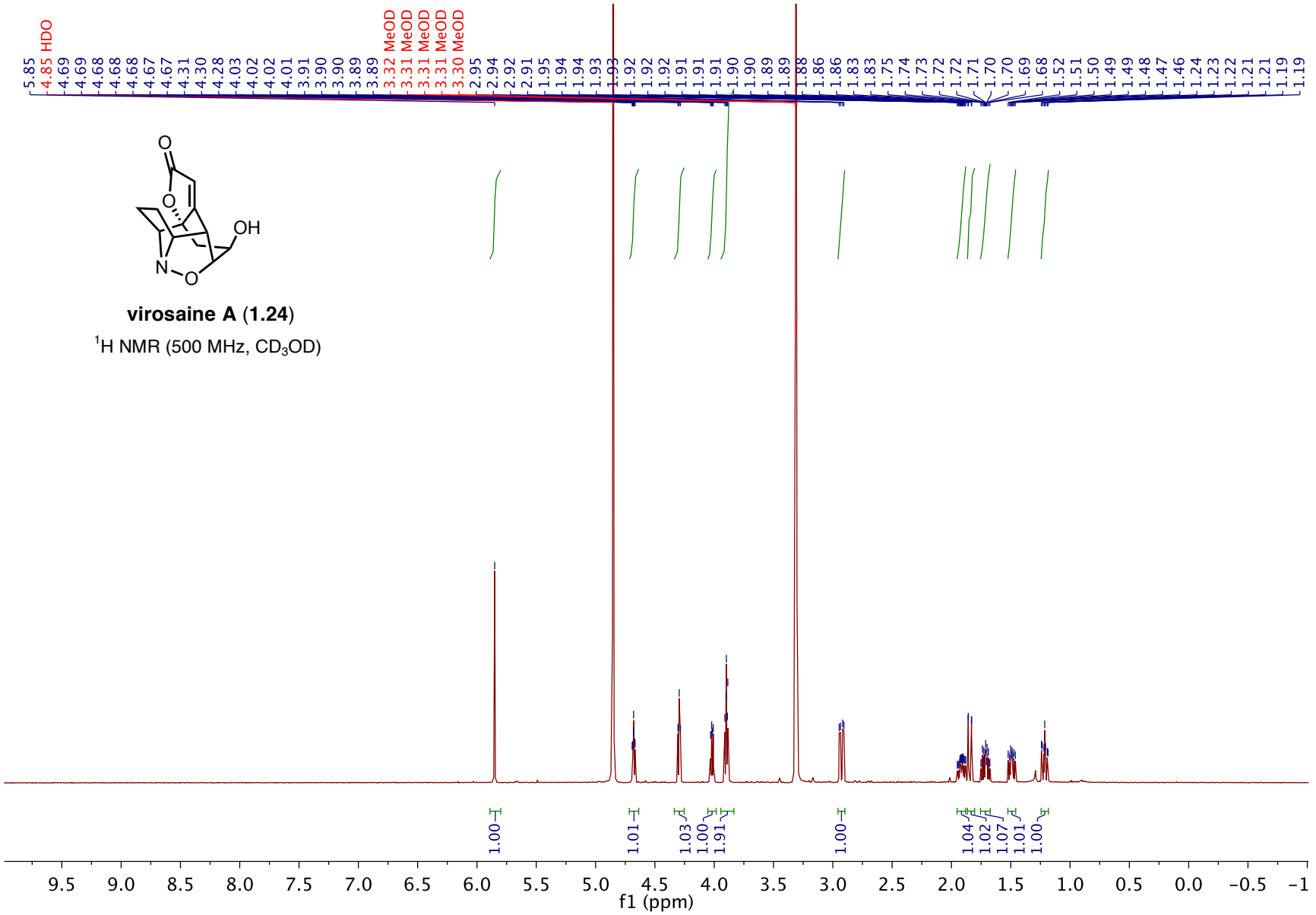
5.85 HDO
4.85 HDO
4.69
4.69
4.68
4.68
4.68
4.67
4.67
4.31
4.30
4.28
4.03
4.02
4.02
4.01
3.91
3.90
3.90
3.89
3.89
3.32 MeOD
3.31 MeOD
3.31 MeOD
3.31 MeOD
3.30 MeOD
2.95
2.94
2.92
2.91
1.95
1.94
1.94
1.93
1.93
1.92
1.92
1.92
1.91
1.91
1.91
1.90
1.90
1.89
1.89
1.88
1.86
1.86
1.83
1.83
1.75
1.74
1.73
1.72
1.72
1.71
1.70
1.70
1.69
1.68
1.52
1.51
1.50
1.49
1.49
1.48
1.47
1.46
1.24
1.23
1.22
1.21
1.21
1.19
1.19
O
O
OH
N
O
virosaine A (1.24)
1H NMR (500 MHz, CD3OD)
1.00
1.01
1.03
1.00
1.91
1.00
1.04
1.02
1.07
1.01
1.00
9.5
9.0
8.5
8.0
7.5
7.0
6.5
6.0
5.5
5.0
4.5
4.0
3.5
3.0
2.5
2.0
1.5
1.0
0.5
0.0
-0.5
-1
f1 (ppm)

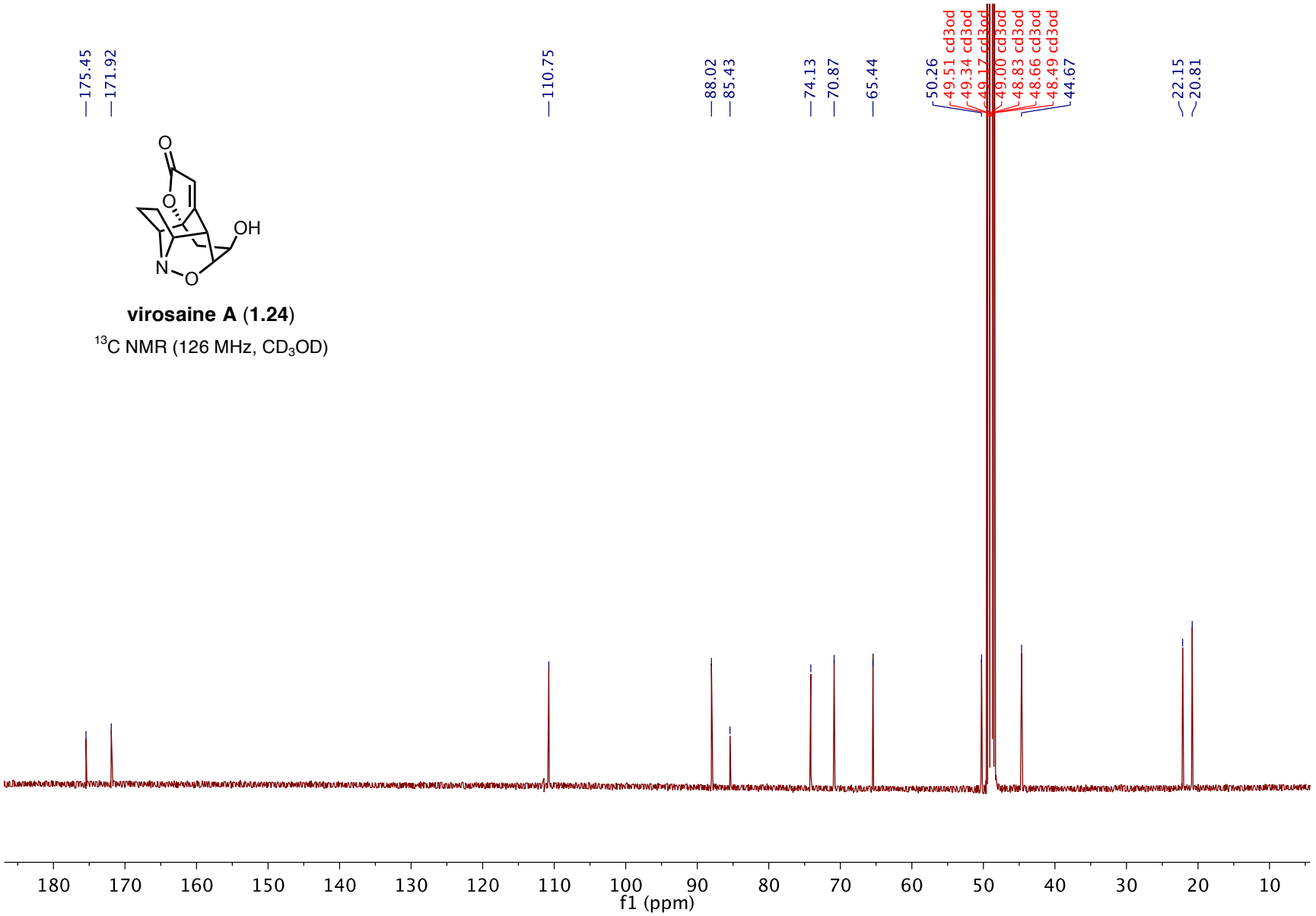
175.45
171.92
110.75
88.02
85.43
74.13
70.87
65.44
50.26
49.51 cd3od
49.34 cd3od
49.17 cd3od
49.00 cd3od
48.83 cd3od
48.66 cd3od
48.49 cd3od
44.67
22.15
20.81
O
O
OH
N
O
virosaine A (1.24)
13C NMR (126 MHz, CD3OD)
180
170
160
150
140
130
120
110
100
90
80
70
60
50
40
30
20
10
f1 (ppm)

^{1}H NMR comparison

Natural (300 MHz, CD_3OD)

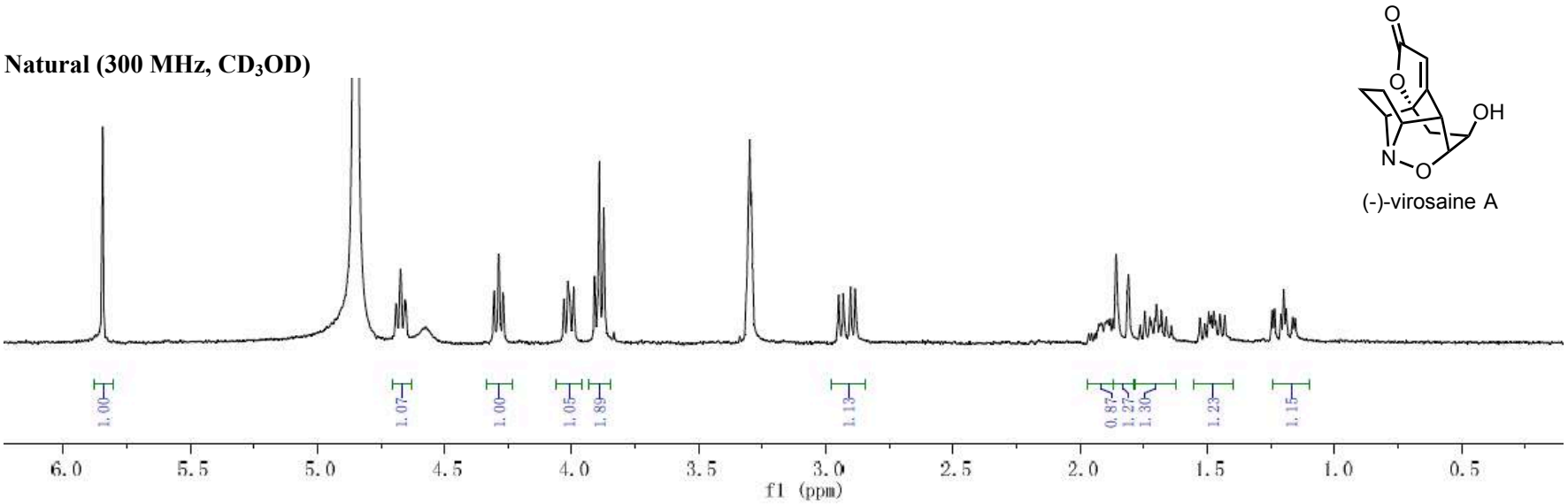

(-)-virosaine A

Synthetic (500 MHz, CD_3OD)

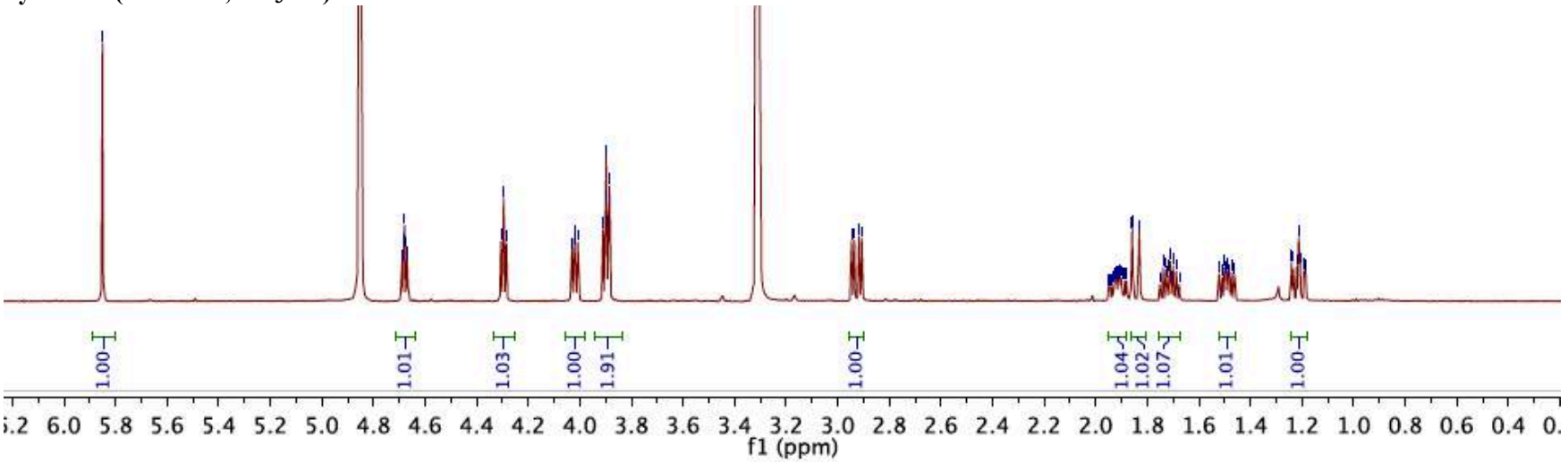

^{13}C NMR comparison

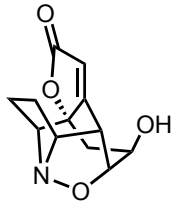

(-)-virosaine A

Natural (75 MHz, CD_3OD)

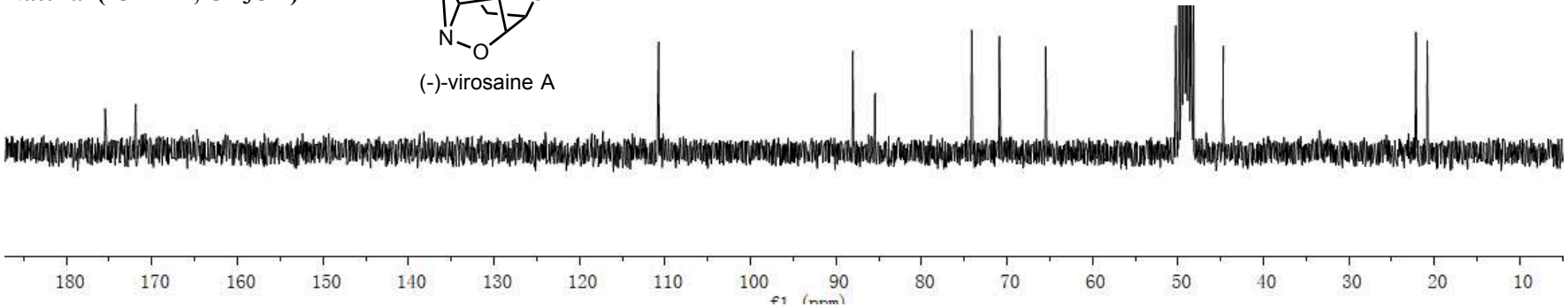

Synthetic (126 MHz, CD_3OD)

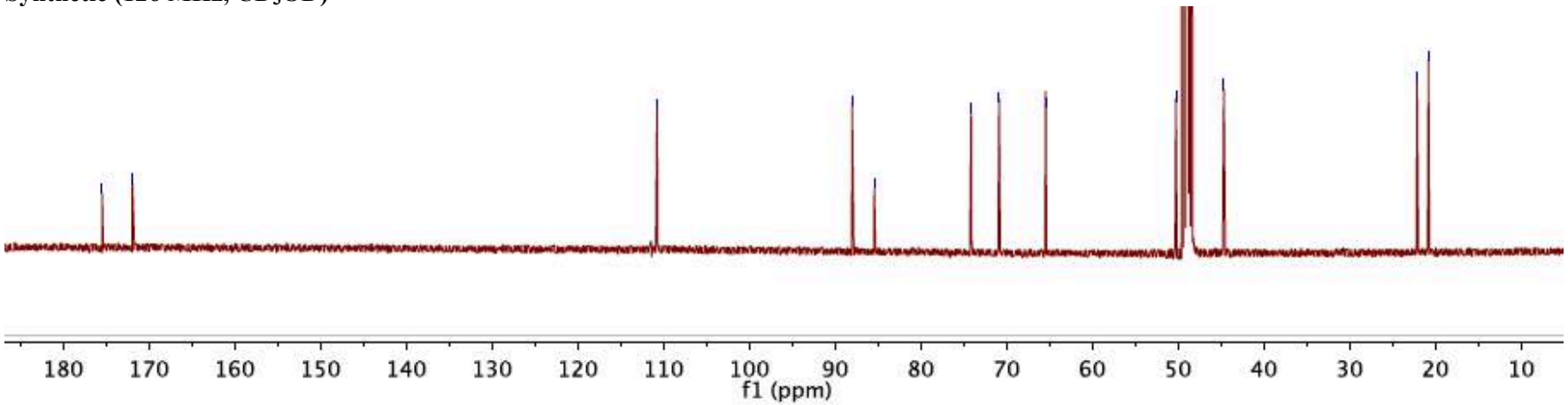

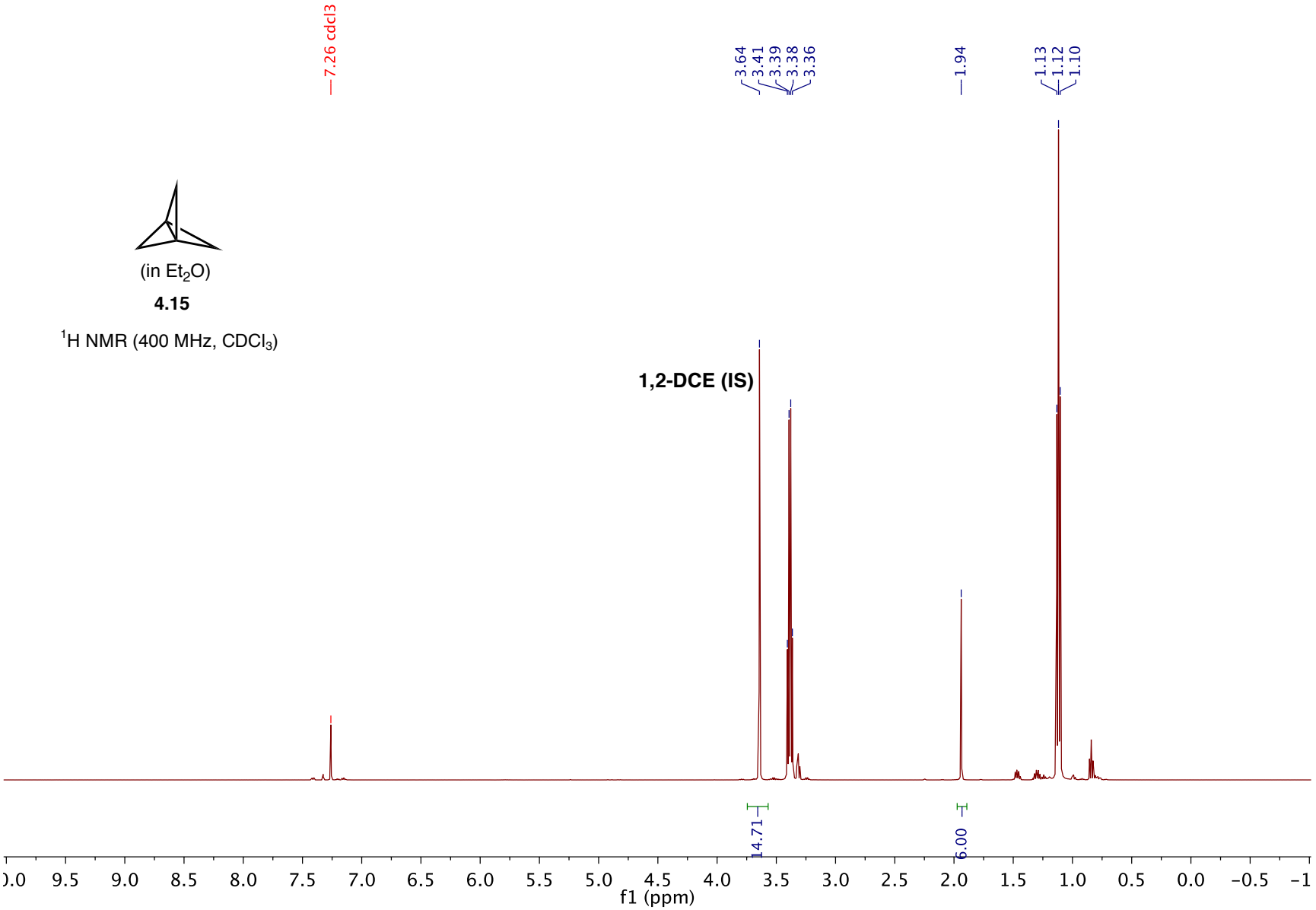
7.26 cdcl3
3.64
3.41
3.39
3.38
3.36
1.94
1.13
1.12
1.10
(in Et2O)
4.15
1H NMR (400 MHz, CDCl3)
1,2-DCE (IS)
14.71
6.00
f1 (ppm)

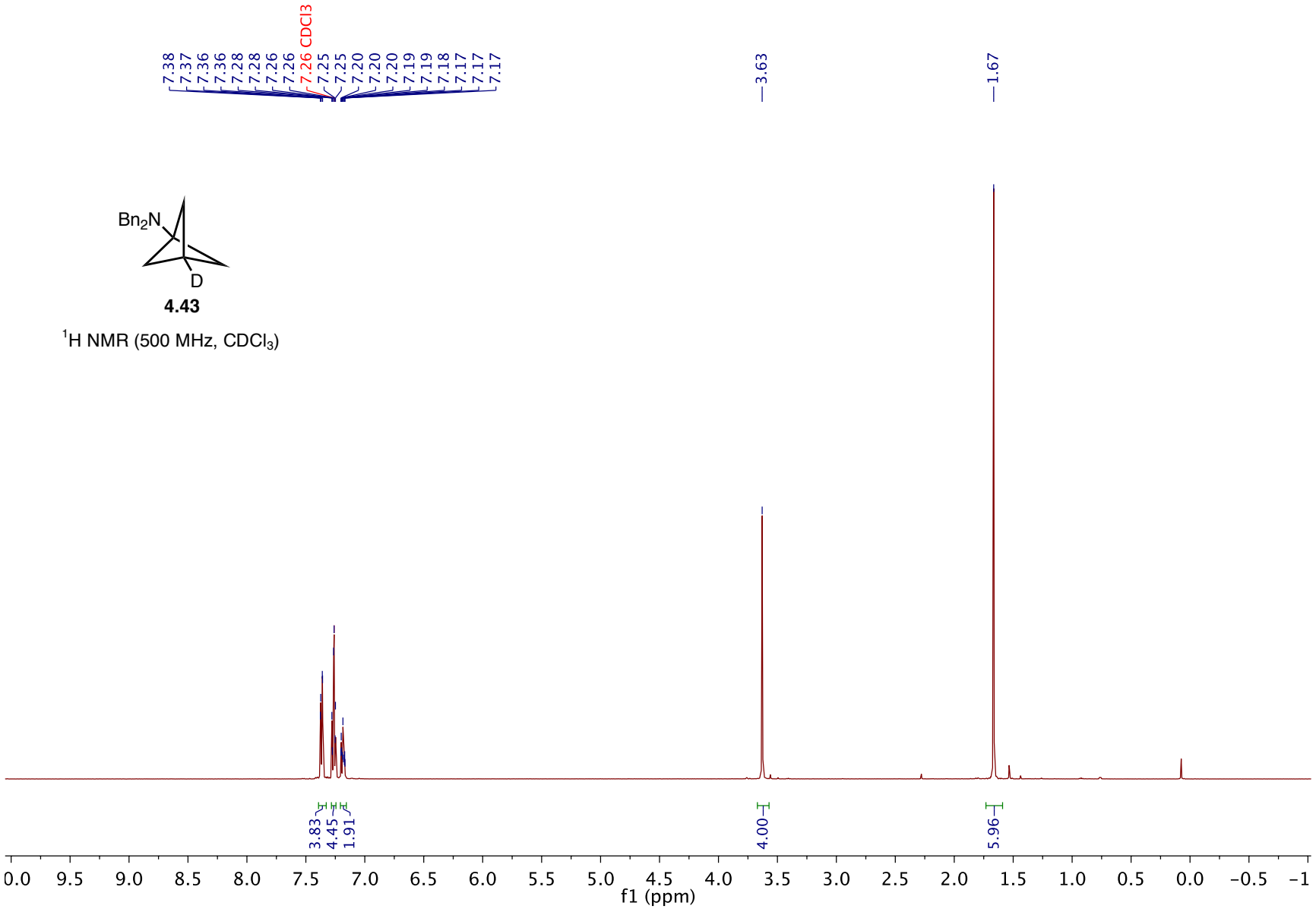

4.43

^{1}H NMR (500 MHz, $CDCl_3$)

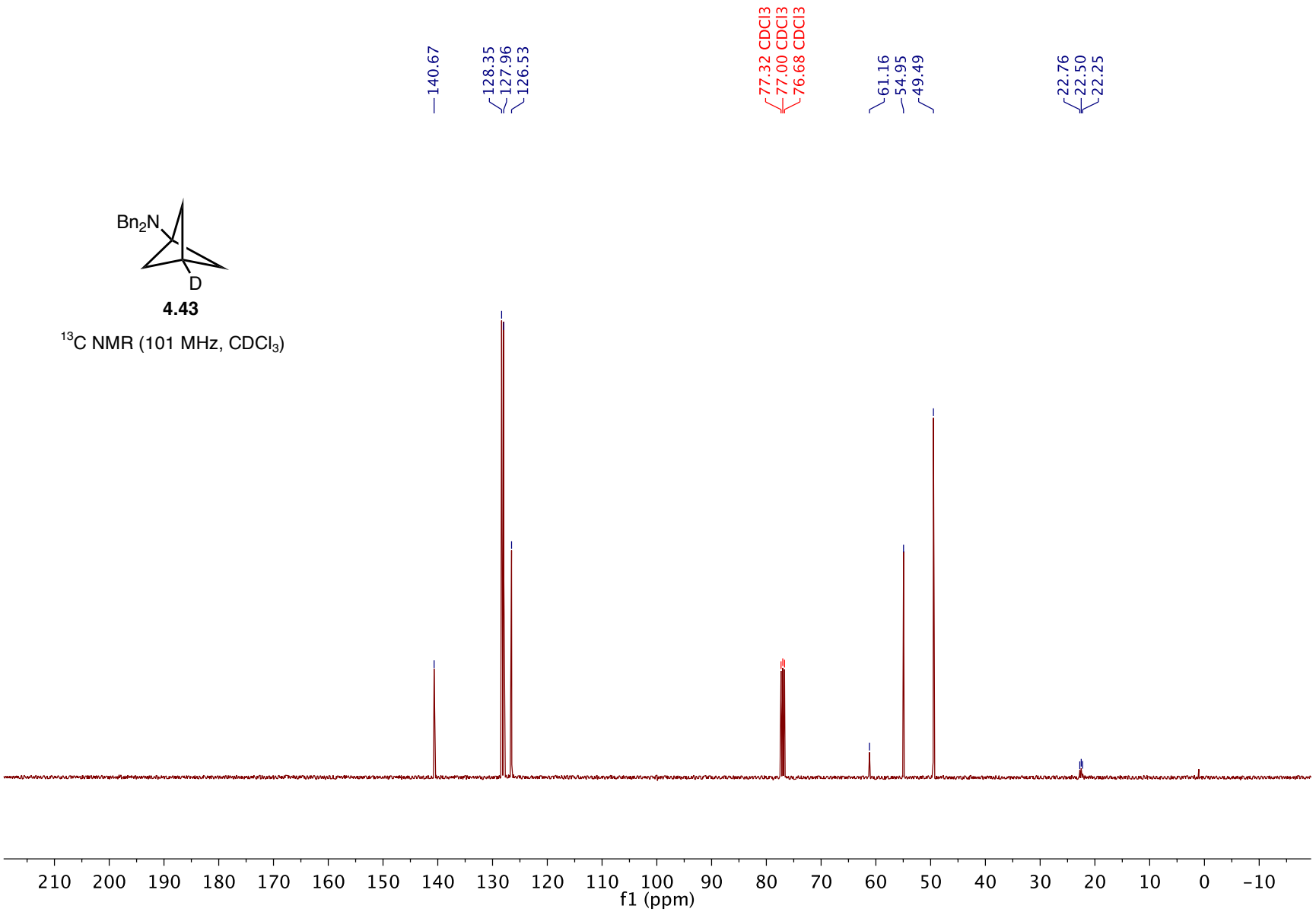
140.67
128.35
127.96
126.53
77.32 CDCl3
77.00 CDCl3
76.68 CDCl3
61.16
54.95
49.49
22.76
22.50
22.25
Bn2N
D
4.43
13C NMR (101 MHz, CDCl3)
210 200 190 180 170 160 150 140 130 120 110 100 90 80 70 60 50 40 30 20 10 0 −10
f1 (ppm)

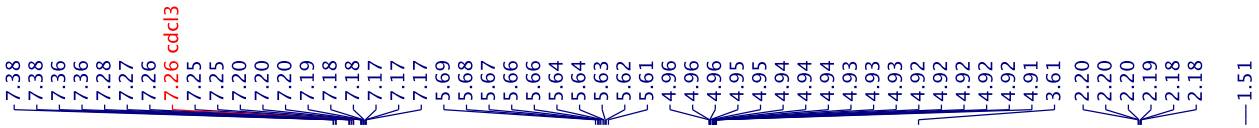

4.49

^{1}H NMR (500 MHz, $CDCl_3$)

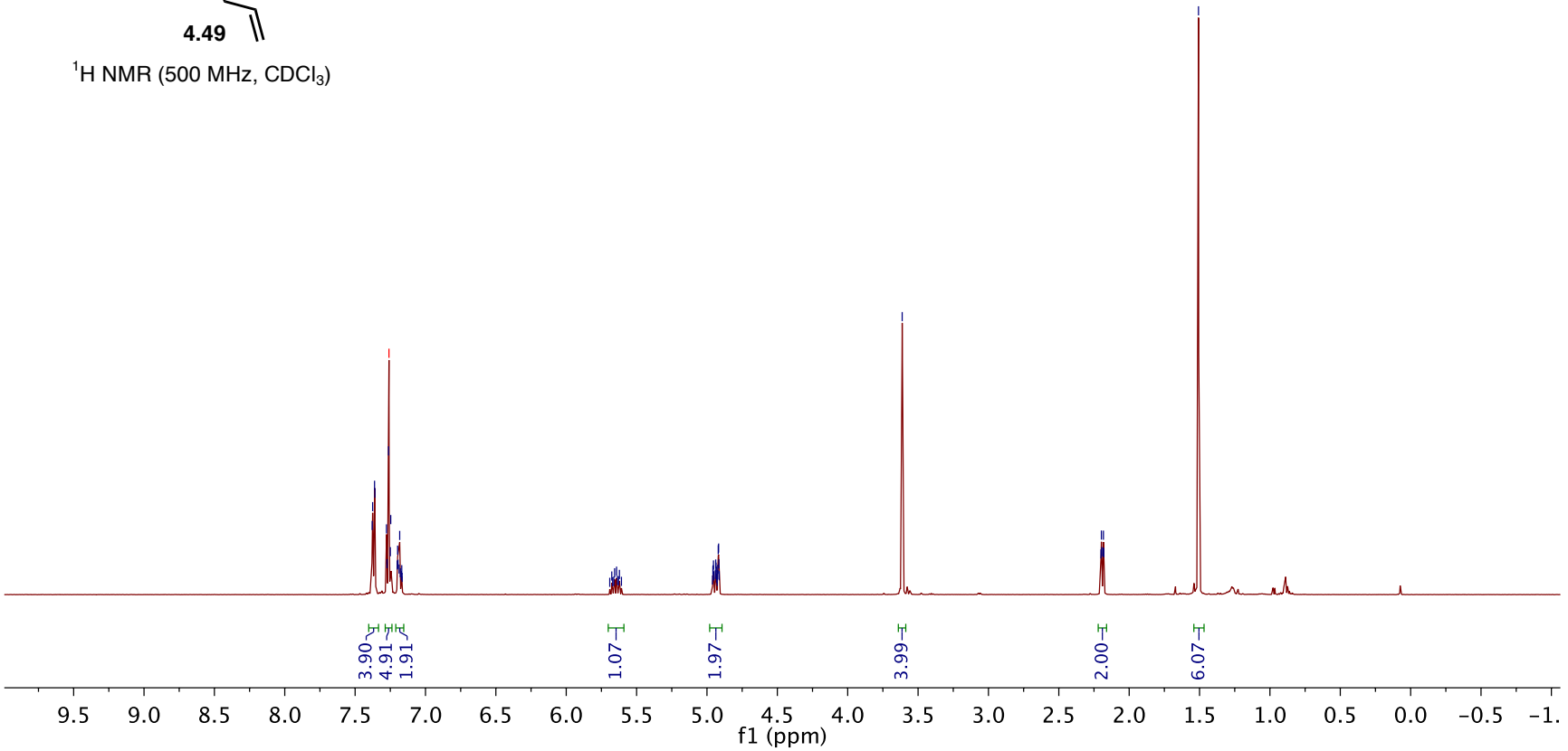

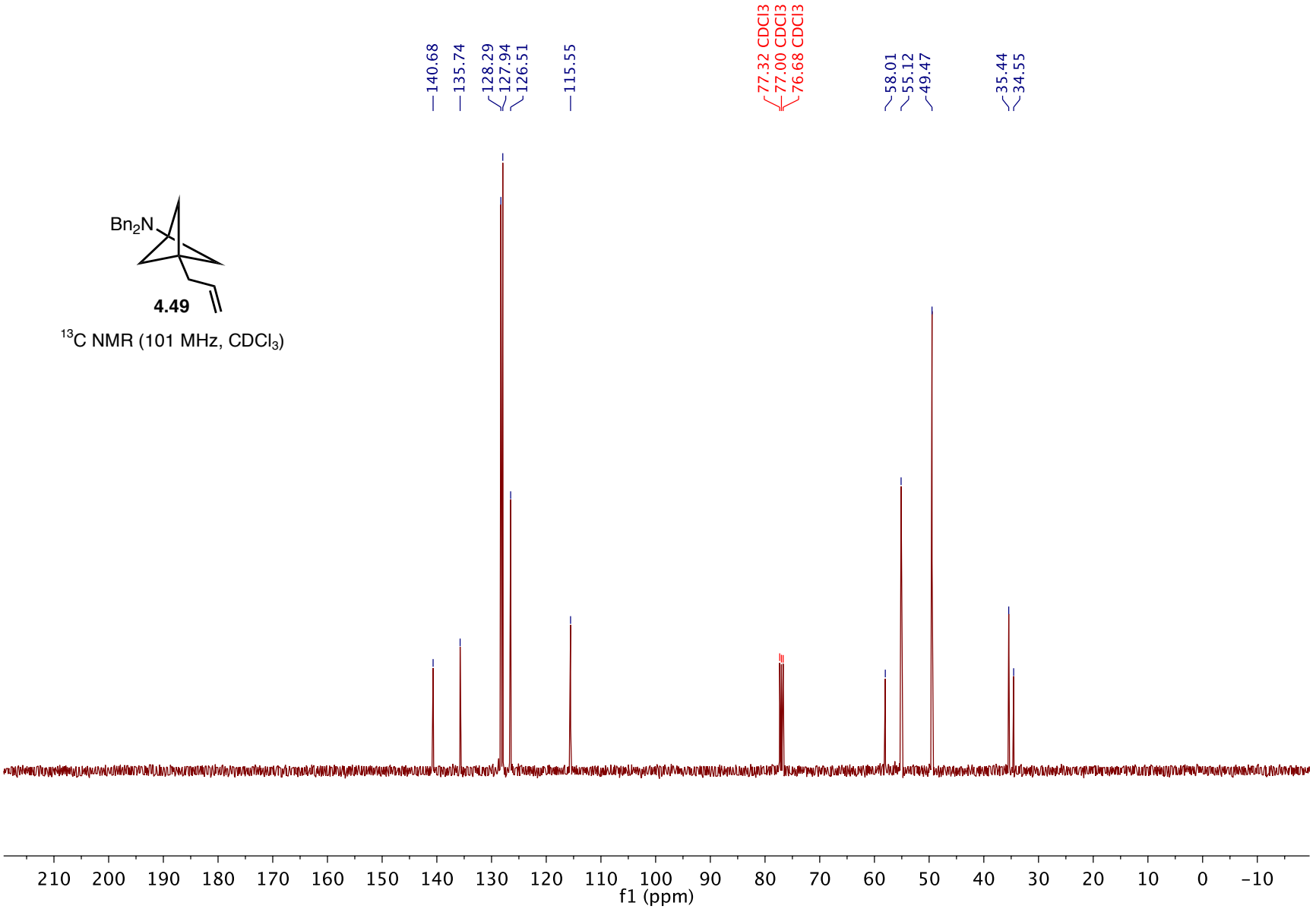
140.68
135.74
128.29
127.94
126.51
115.55
77.32 CDCl3
77.00 CDCl3
76.68 CDCl3
58.01
55.12
49.47
35.44
34.55
Bn2N
4.49
13C NMR (101 MHz, CDCl3)
210 200 190 180 170 160 150 140 130 120 110 100 90 80 70 60 50 40 30 20 10 0 -10
f1 (ppm)

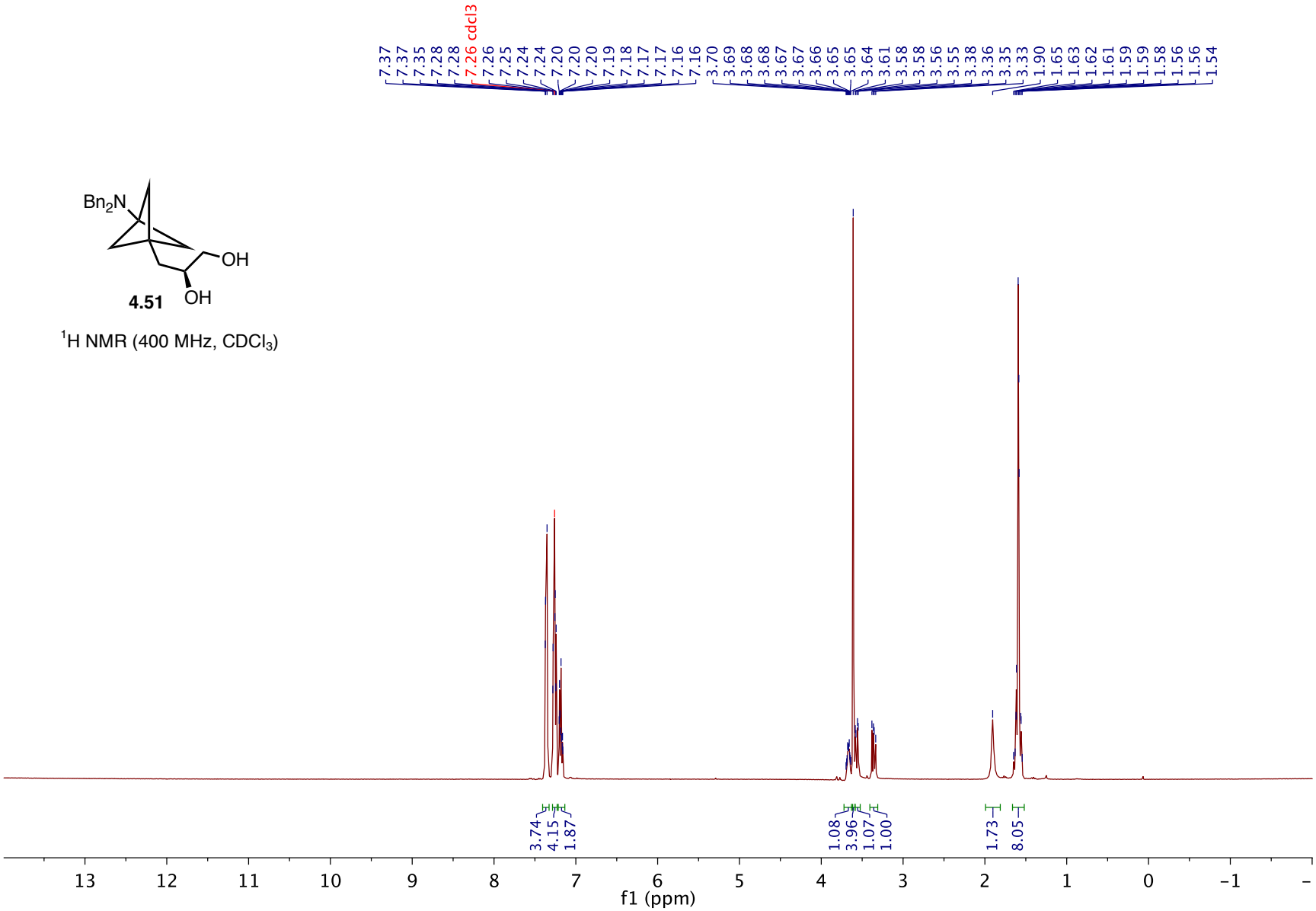
7.37
7.37
7.35
7.28
7.28
7.26 cdcl3
7.26
7.25
7.24
7.24
7.20
7.20
7.20
7.19
7.18
7.17
7.17
7.16
7.16
3.70
3.69
3.68
3.68
3.67
3.67
3.66
3.65
3.65
3.64
3.61
3.58
3.58
3.56
3.55
3.38
3.36
3.35
3.33
1.90
1.65
1.63
1.62
1.61
1.59
1.59
1.58
1.56
1.56
1.54
Bn2N
OH
OH
4.51
1H NMR (400 MHz, CDCl3)
3.74
4.15
1.87
1.08
3.96
1.07
1.00
1.73
8.05
13
12
11
10
9
8
7
6
5
4
3
2
1
0
−1
f1 (ppm)

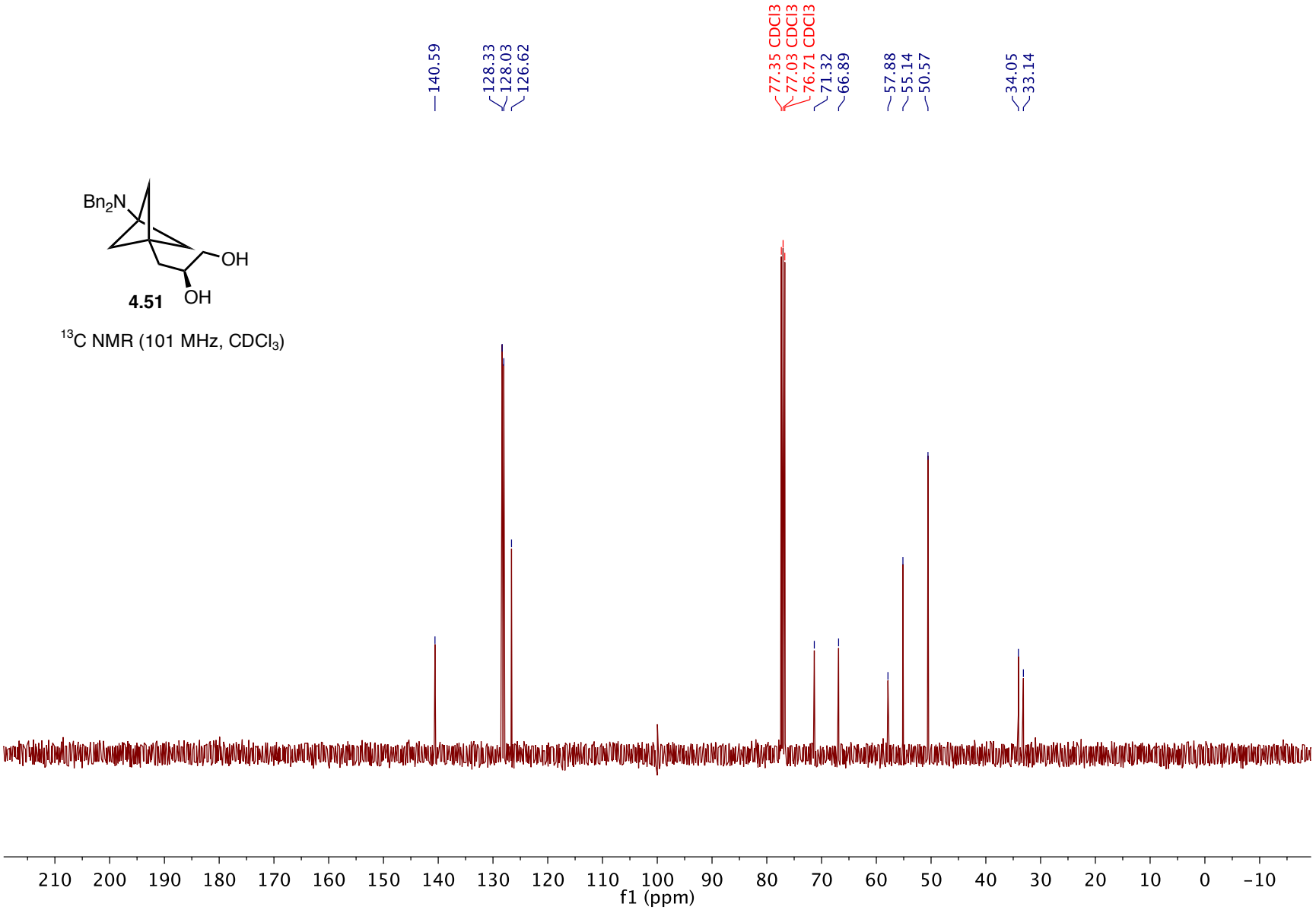
140.59
128.33
128.03
126.62
77.35 CDCl3
77.03 CDCl3
76.71 CDCl3
71.32
66.89
57.88
55.14
50.57
34.05
33.14
Bn2N
OH
OH
4.51
13C NMR (101 MHz, CDCl3)
210 200 190 180 170 160 150 140 130 120 110 100 90 80 70 60 50 40 30 20 10 0 -10
f1 (ppm)

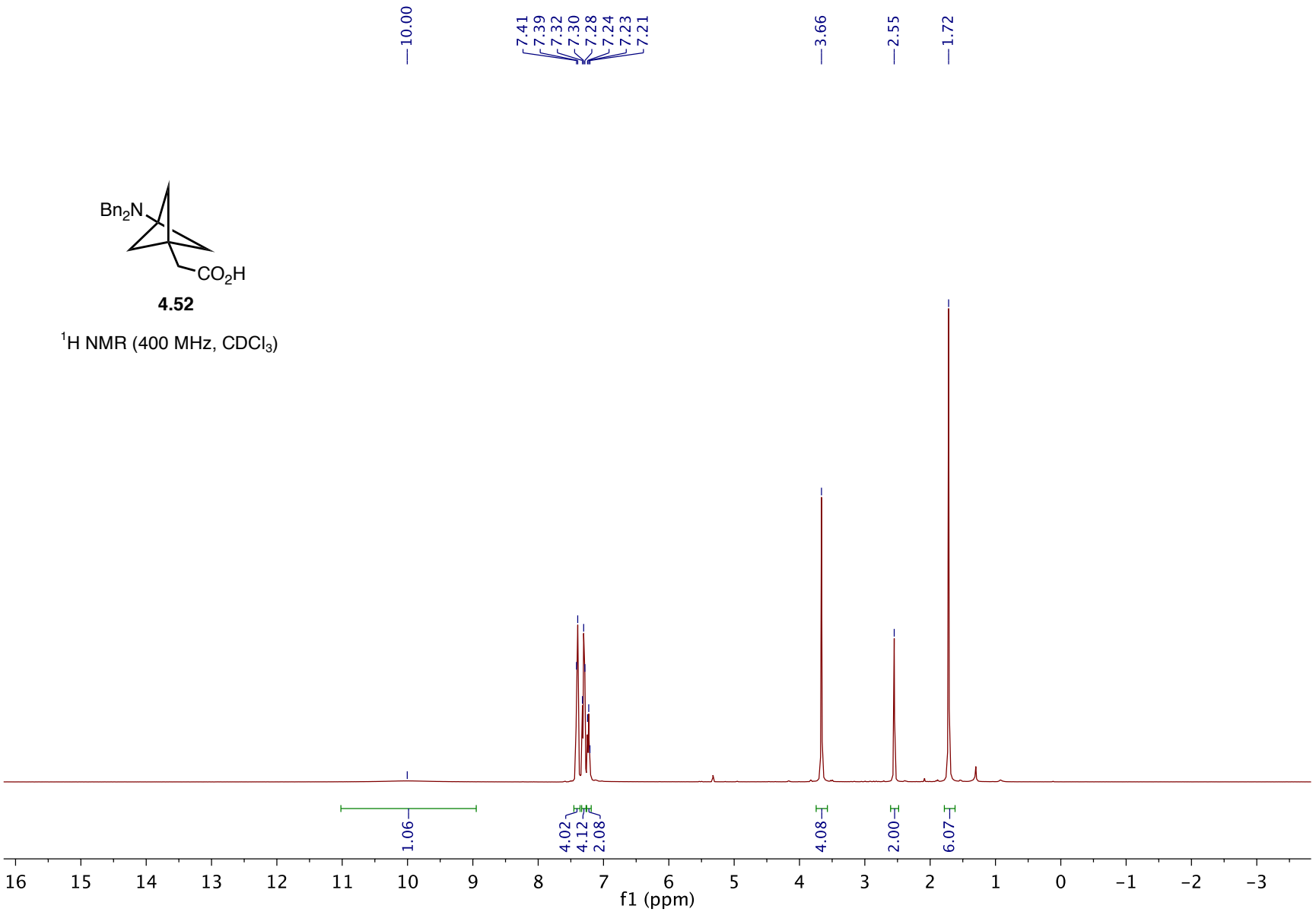
10.00
7.41
7.39
7.32
7.30
7.28
7.24
7.23
7.21
3.66
2.55
1.72
Bn2N
CO2H
4.52
1H NMR (400 MHz, CDCl3)
1.06
4.02
4.12
2.08
4.08
2.00
6.07
16 15 14 13 12 11 10 9 8 7 6 5 4 3 2 1 0 −1 −2 −3
f1 (ppm)

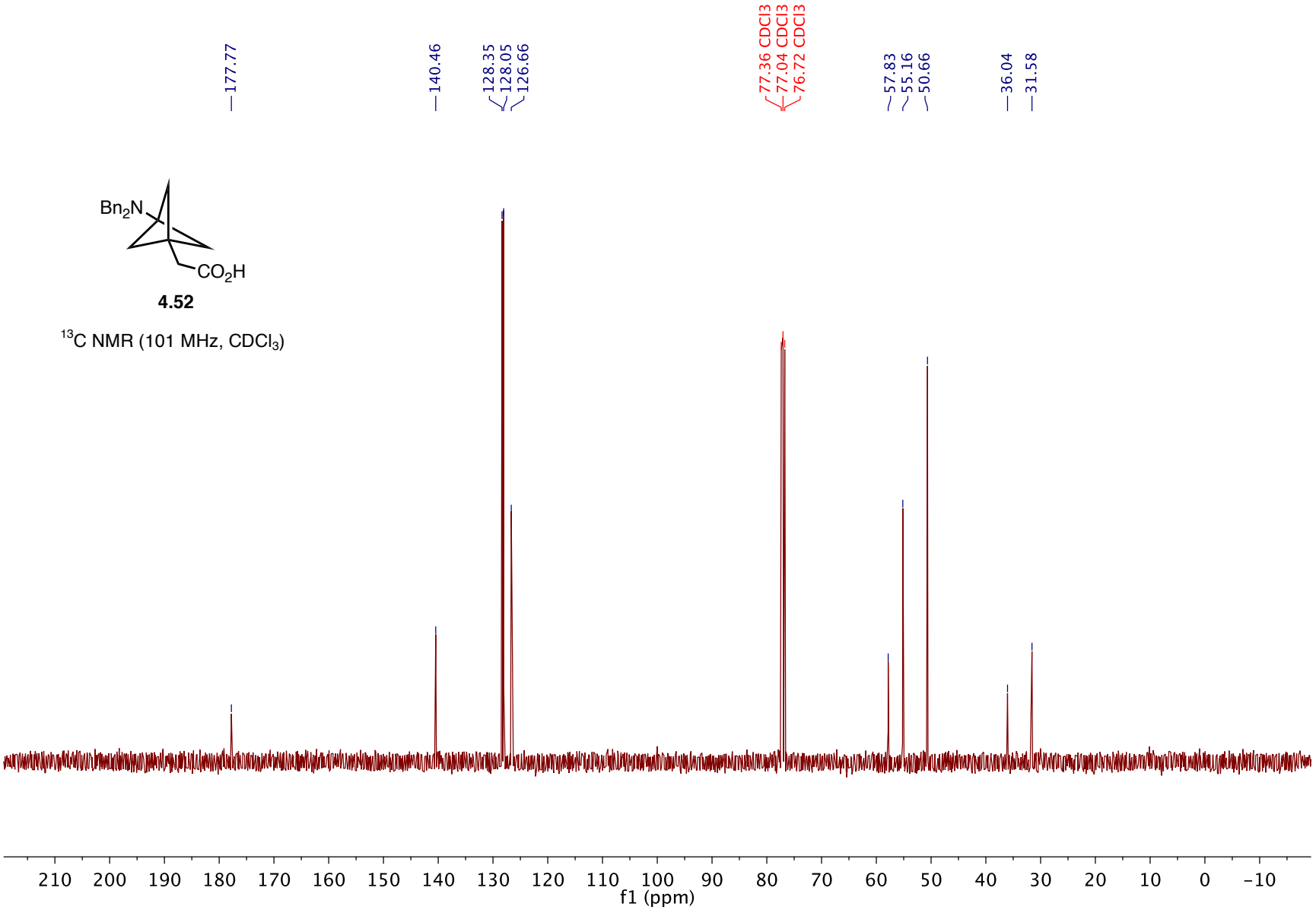
177.77
140.46
128.35
128.05
126.66
77.36 CDCl3
77.04 CDCl3
76.72 CDCl3
57.83
55.16
50.66
36.04
31.58
Bn2N
CO2H
4.52
13C NMR (101 MHz, CDCl3)
210 200 190 180 170 160 150 140 130 120 110 100 90 80 70 60 50 40 30 20 10 0 -10
f1 (ppm)

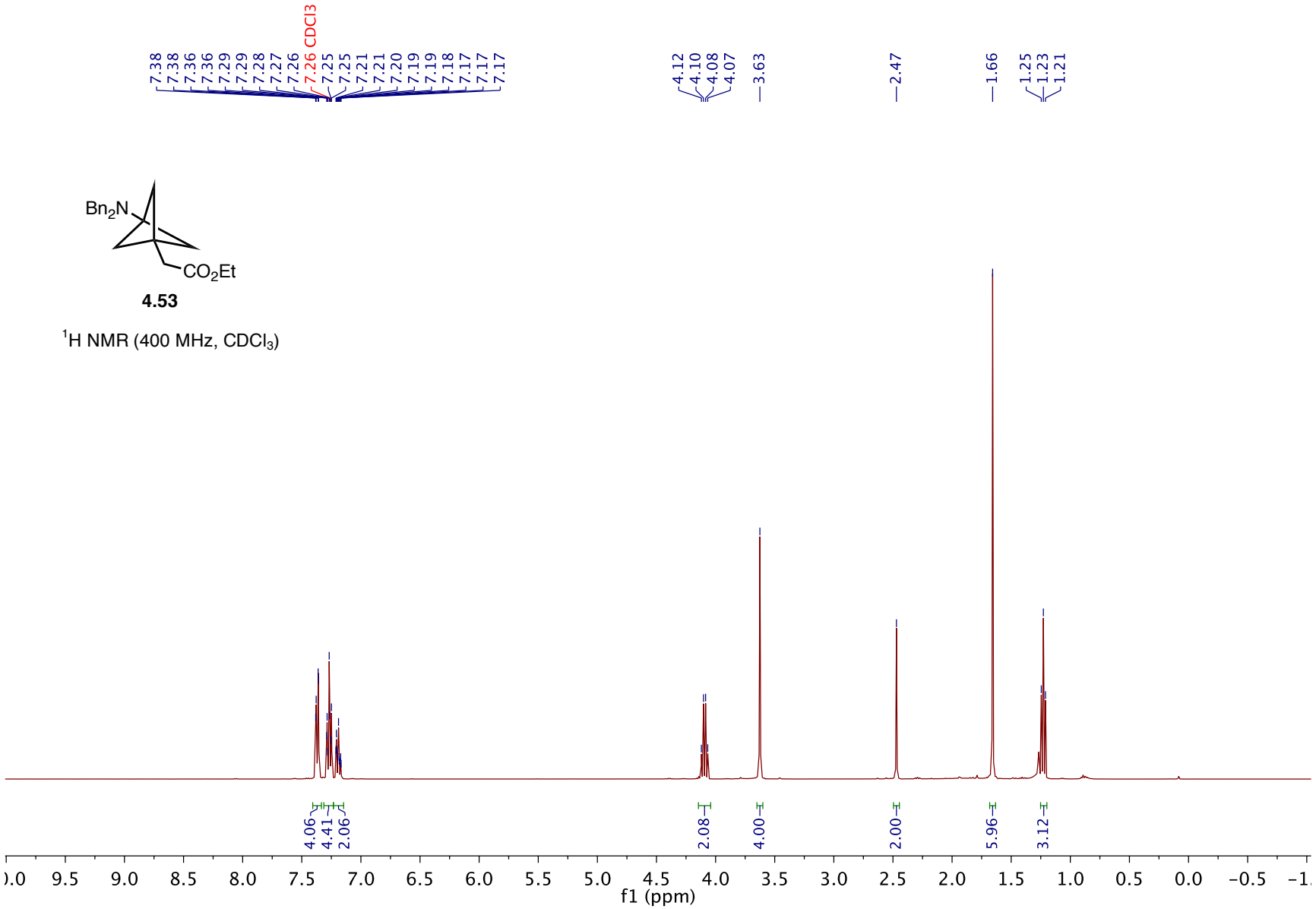

4.53

^{1}H NMR (400 MHz, $CDCl_3$)

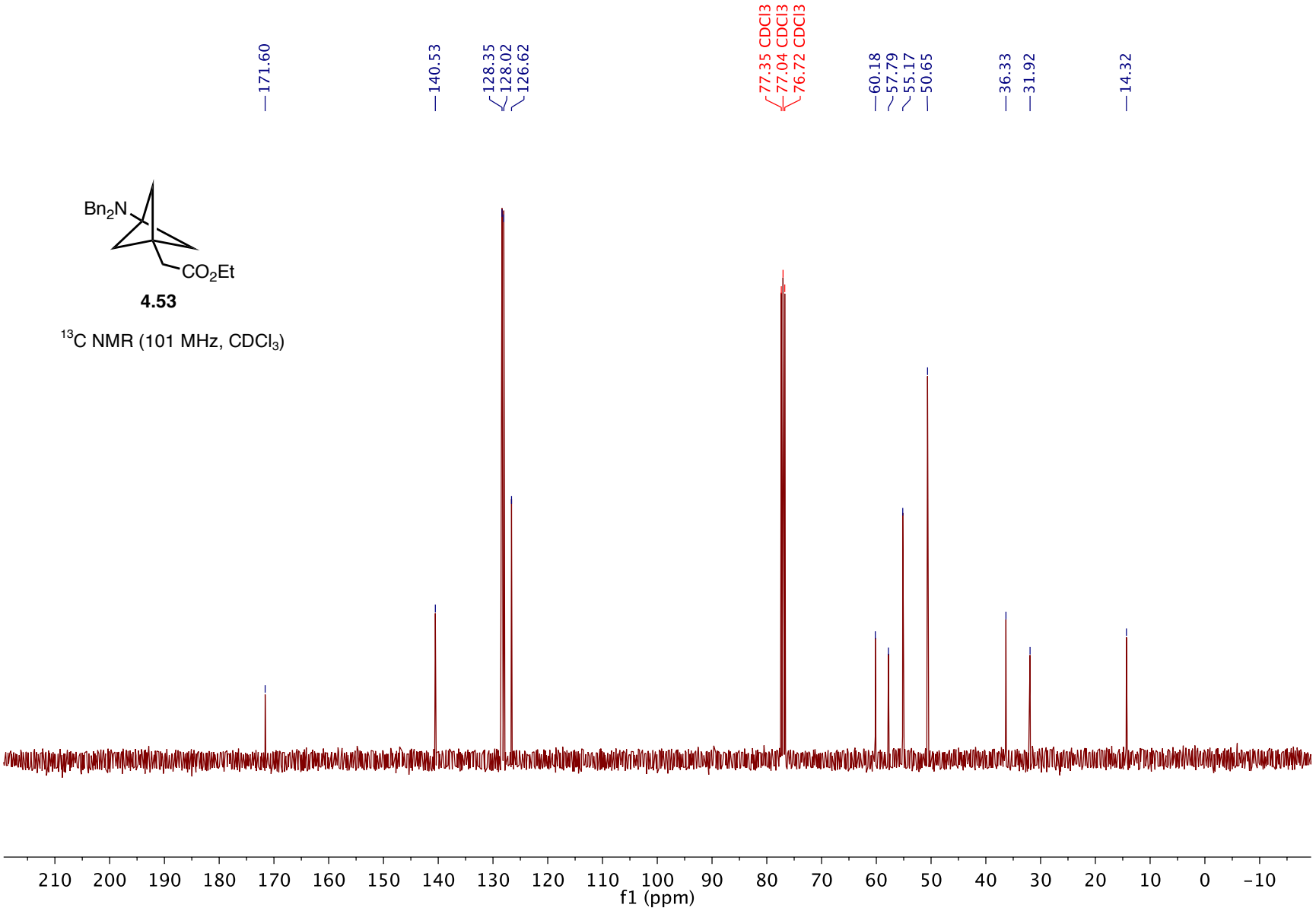
171.60
140.53
128.35
128.02
126.62
77.35 CDCl3
77.04 CDCl3
76.72 CDCl3
60.18
57.79
55.17
50.65
36.33
31.92
14.32
Bn2N
CO2Et
4.53
13C NMR (101 MHz, CDCl3)
210 200 190 180 170 160 150 140 130 120 110 100 90 80 70 60 50 40 30 20 10 0 -10
f1 (ppm)

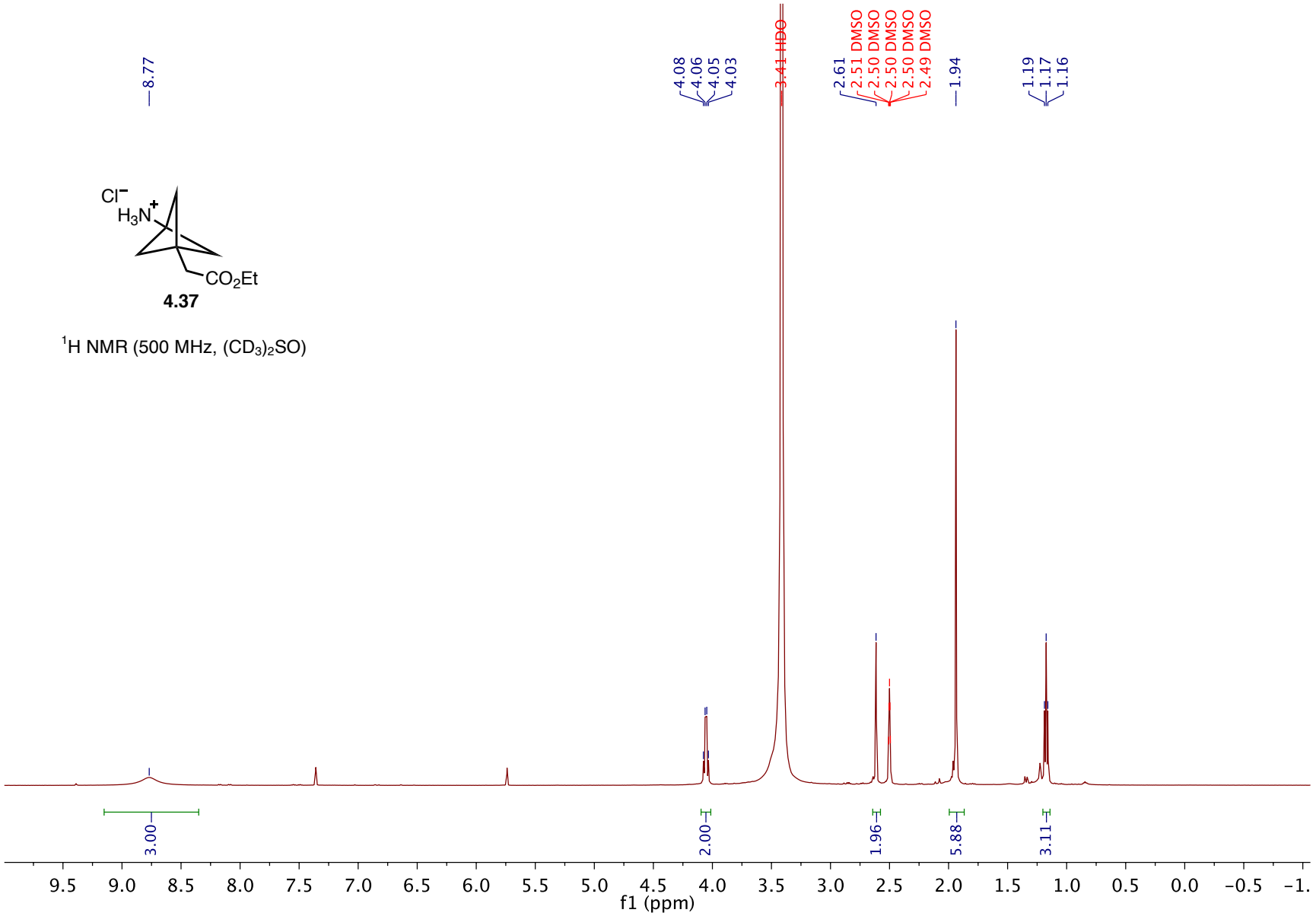
8.77
4.08
4.06
4.05
4.03
3.41 HDO
2.61
2.51 DMSO
2.50 DMSO
2.50 DMSO
2.50 DMSO
2.49 DMSO
1.94
1.19
1.17
1.16
Cl⁻
H3N+
CO2Et
4.37
1H NMR (500 MHz, (CD3)2SO)
3.00
2.00
1.96
5.88
3.11
9.5 9.0 8.5 8.0 7.5 7.0 6.5 6.0 5.5 5.0 4.5 4.0 3.5 3.0 2.5 2.0 1.5 1.0 0.5 0.0 -0.5 -1.
f1 (ppm)

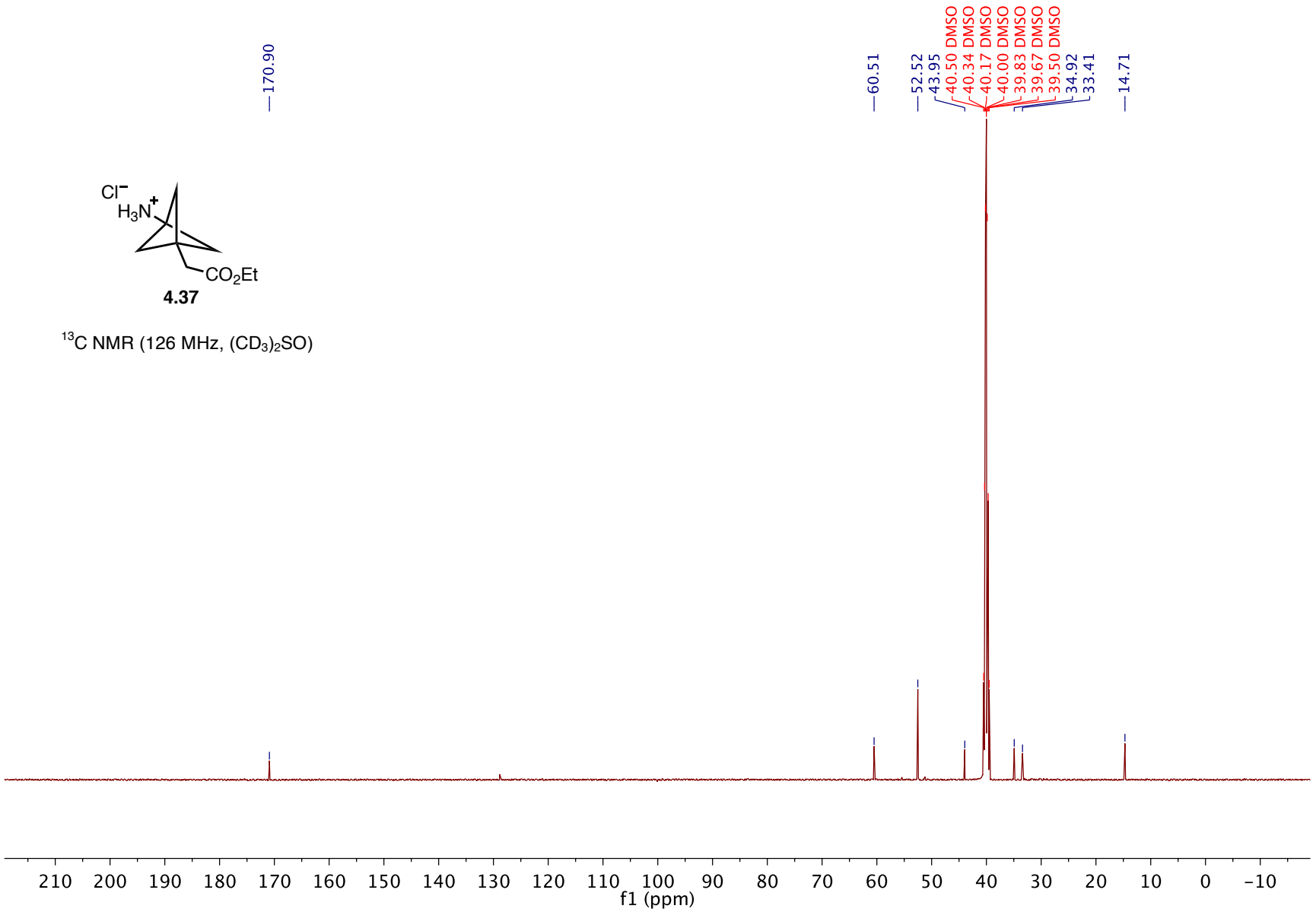

4.37

^{13}C NMR (126 MHz, $(CD_3)_2SO$)

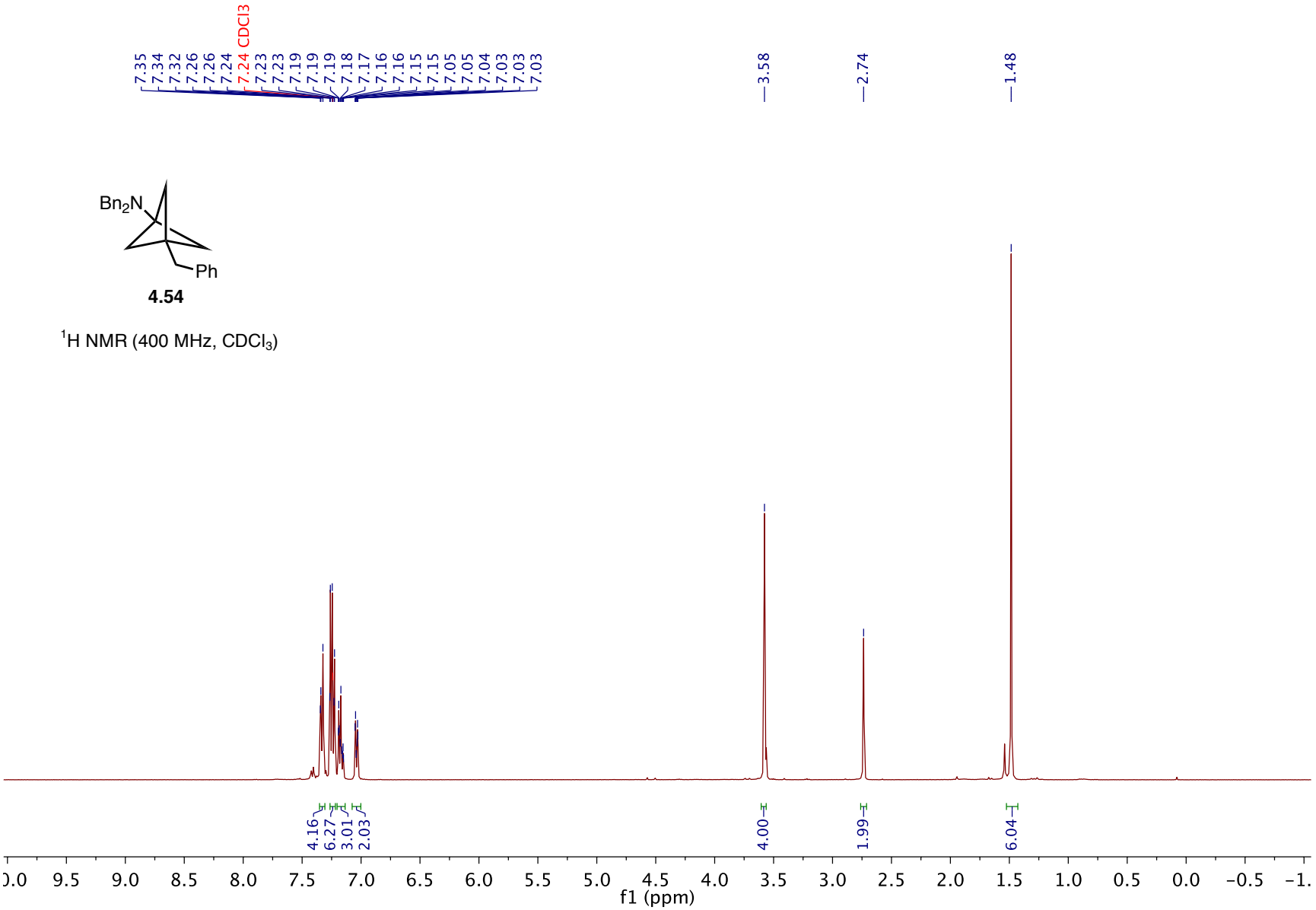

4.54

^{1}H NMR (400 MHz, $CDCl_3$)

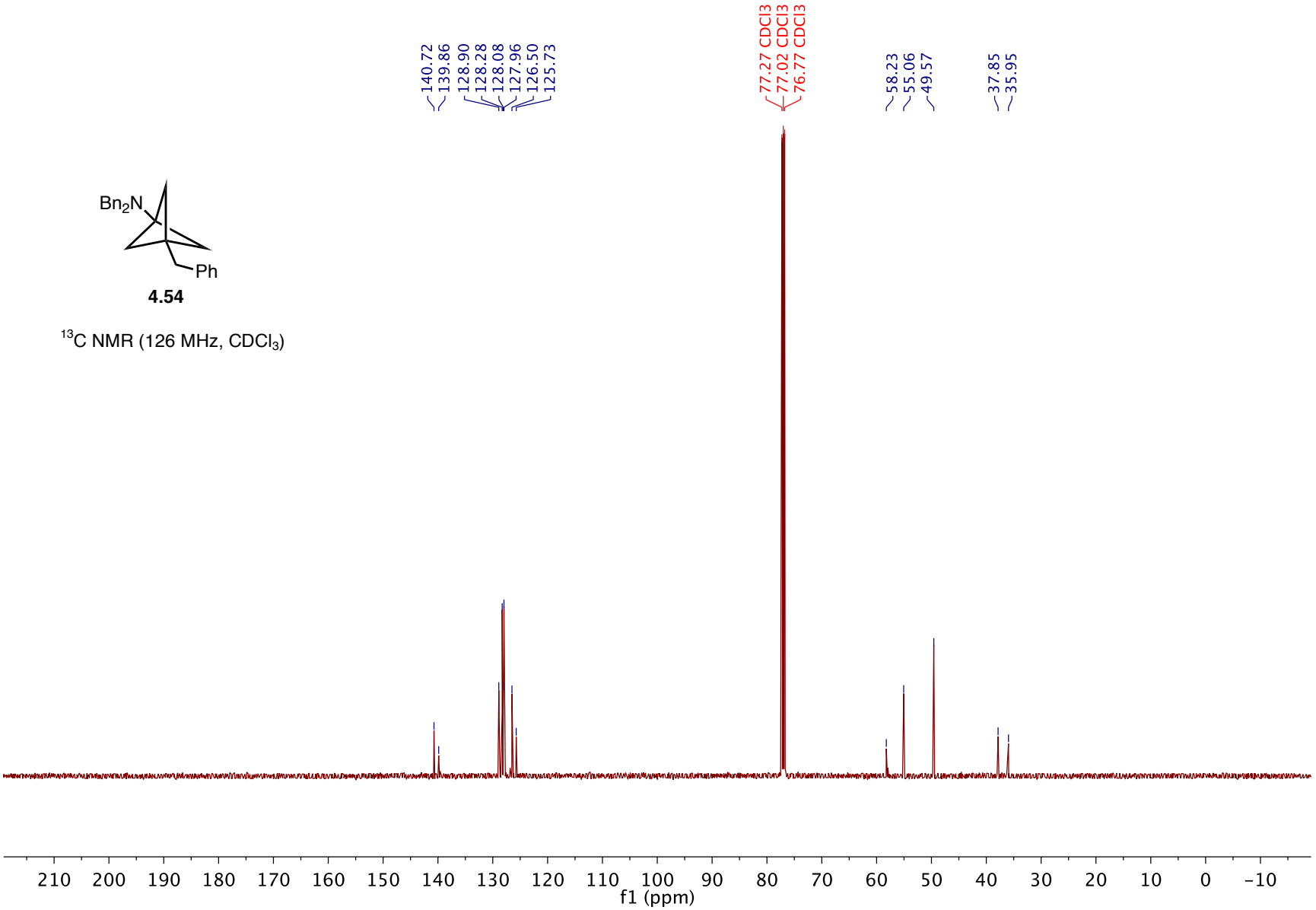

4.54

^{13}C NMR (126 MHz, $CDCl_3$)

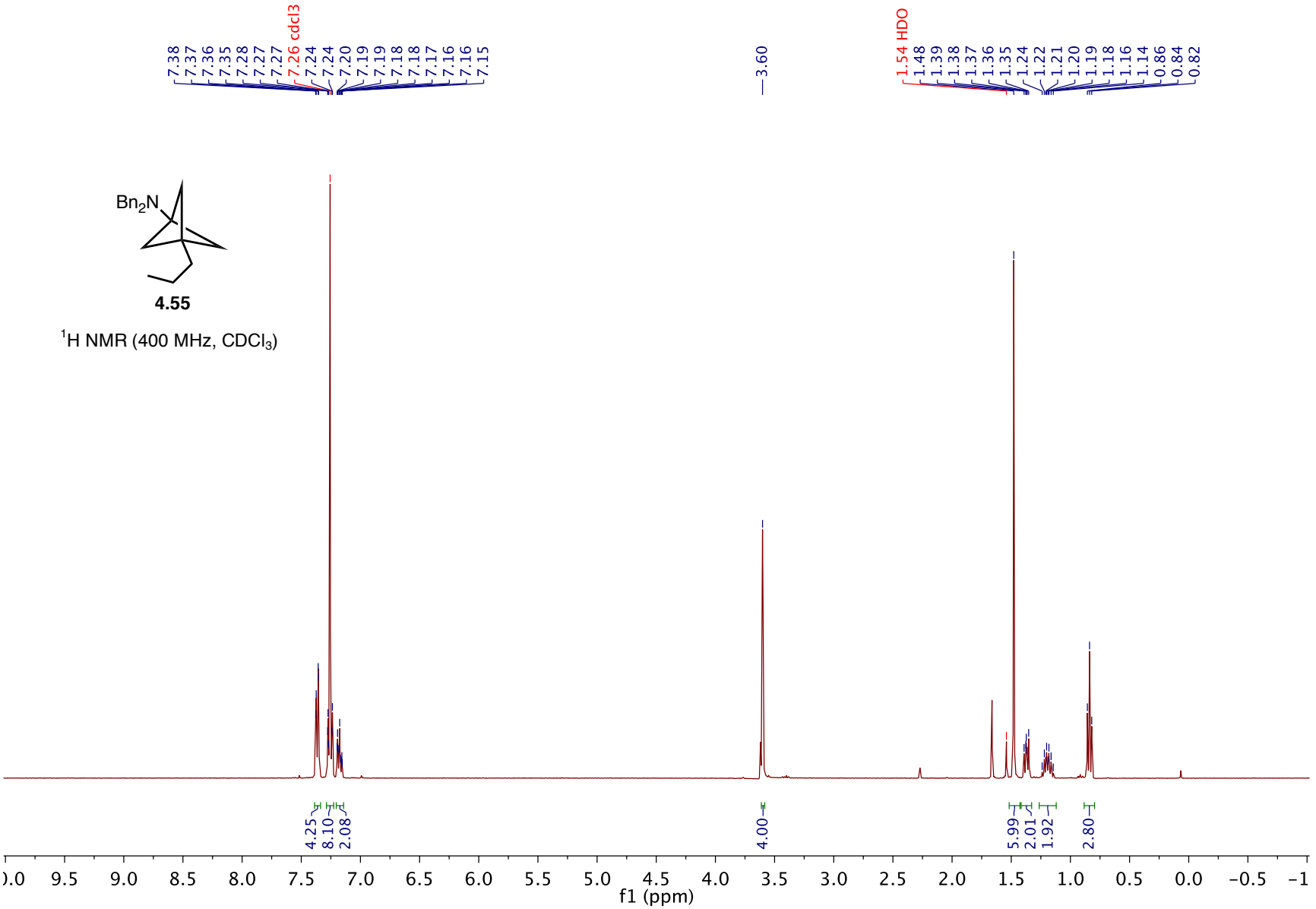
7.38
7.37
7.36
7.35
7.28
7.27
7.27
7.26 cdcl3
7.24
7.24
7.20
7.19
7.19
7.18
7.18
7.17
7.16
7.16
7.15
3.60
1.54 HDO
1.48
1.39
1.38
1.37
1.36
1.35
1.24
1.22
1.21
1.20
1.19
1.18
1.16
1.14
0.86
0.84
0.82
Bn2N
4.55
1H NMR (400 MHz, CDCl3)
4.25
8.10
2.08
4.00
5.99
2.01
1.92
2.80
f1 (ppm)

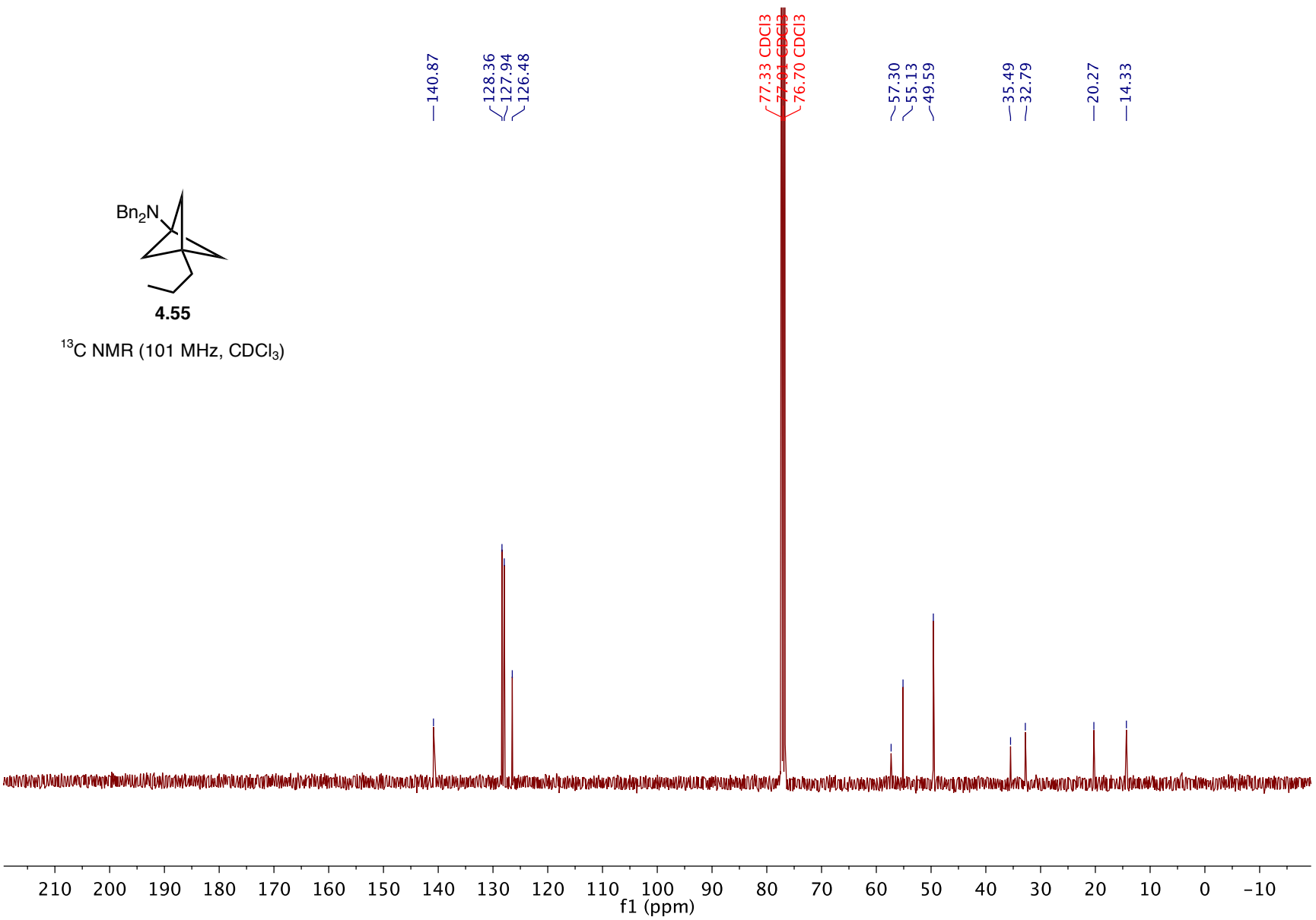

4.55

^{13}C NMR (101 MHz, $CDCl_3$)

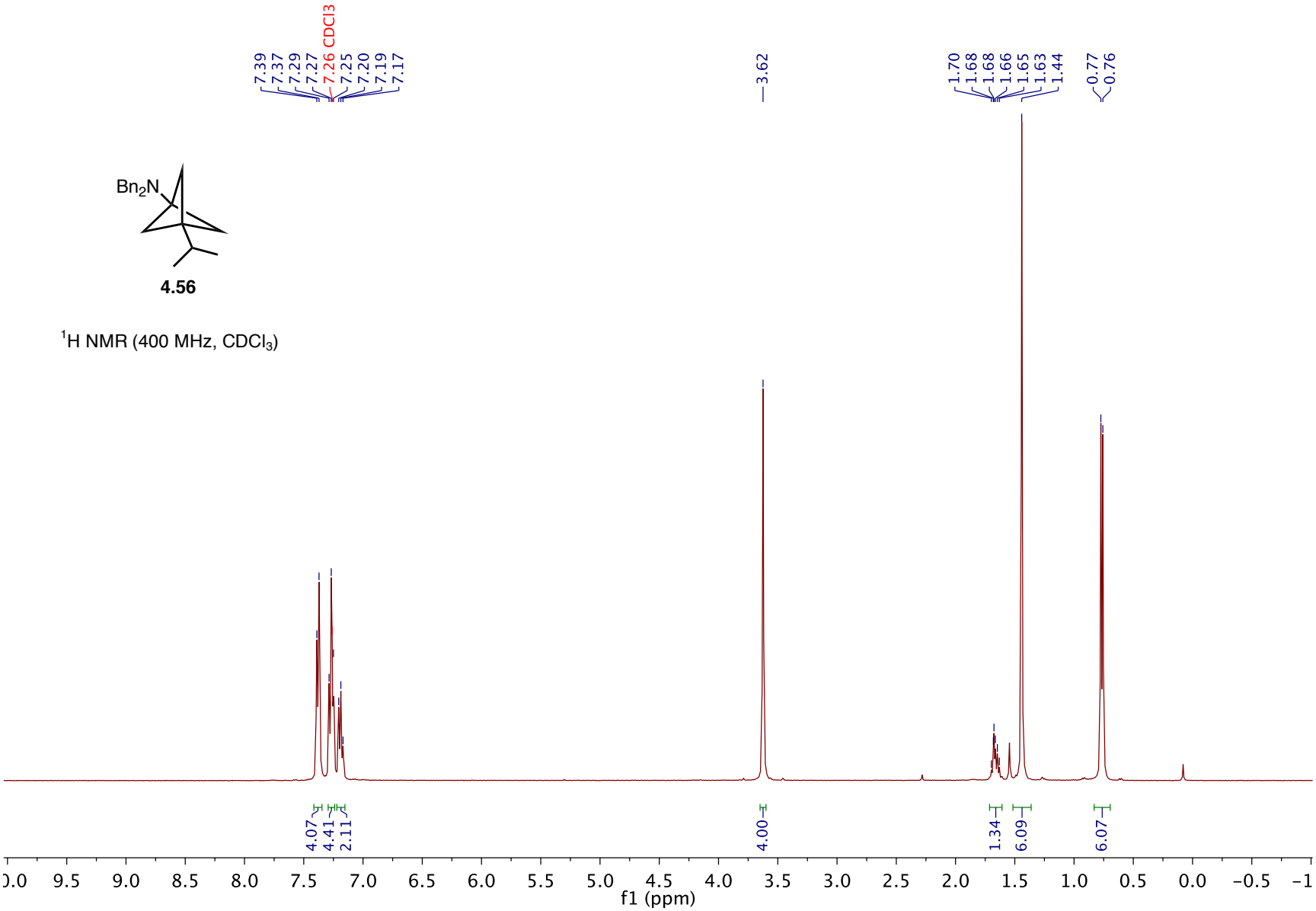

4.56

^{1}H NMR (400 MHz, $CDCl_3$)

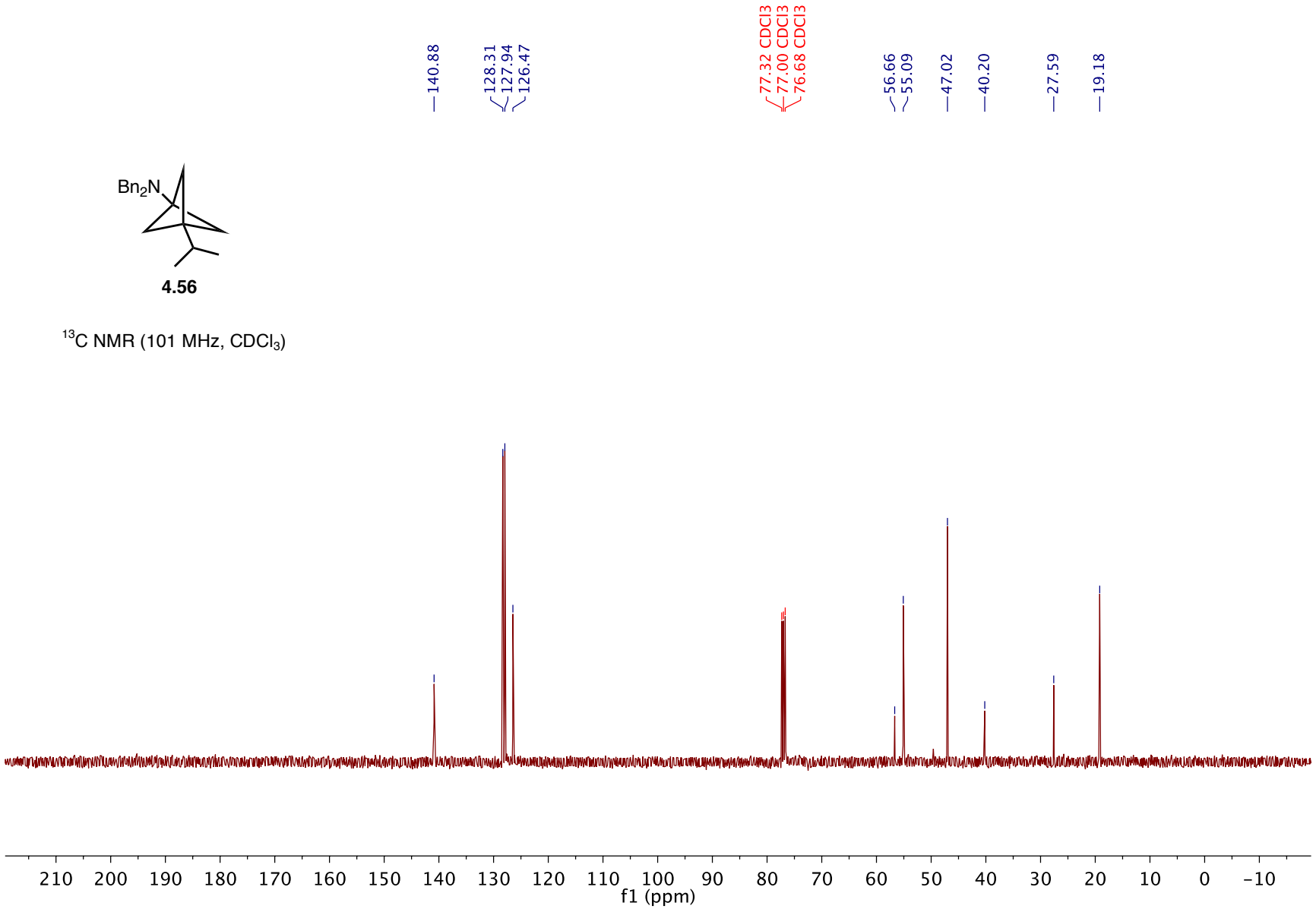
140.88
128.31
127.94
126.47
77.32 CDCl3
77.00 CDCl3
76.68 CDCl3
56.66
55.09
47.02
40.20
27.59
19.18
Bn2N
4.56
13C NMR (101 MHz, CDCl3)
210 200 190 180 170 160 150 140 130 120 110 100 90 80 70 60 50 40 30 20 10 0 −10
f1 (ppm)

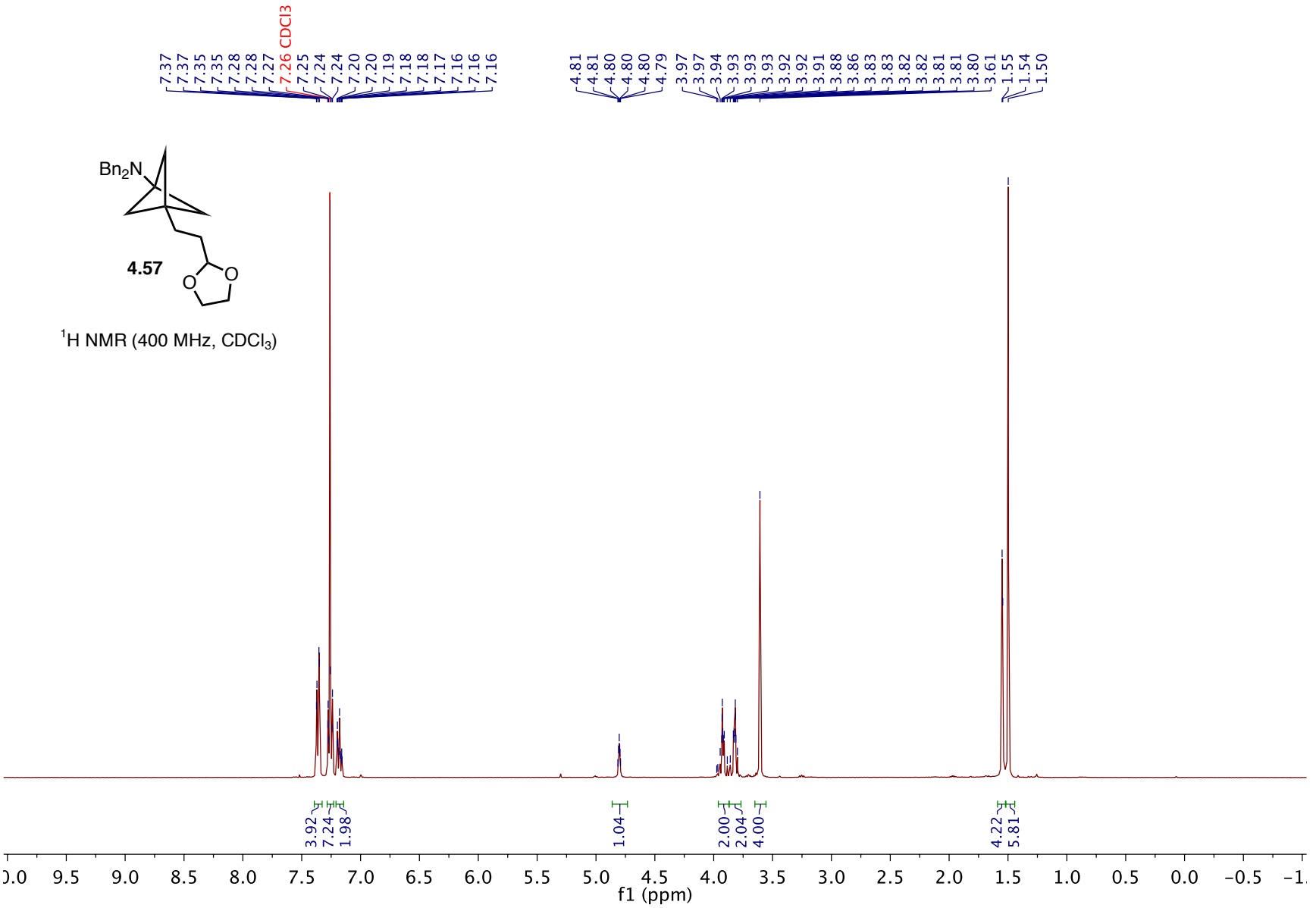
7.37
7.37
7.35
7.35
7.28
7.28
7.27
7.26 CDCl3
7.25
7.24
7.24
7.20
7.20
7.19
7.18
7.18
7.17
7.16
7.16
4.81
4.81
4.80
4.80
4.80
4.79
3.97
3.97
3.94
3.93
3.93
3.93
3.92
3.92
3.91
3.88
3.86
3.83
3.83
3.82
3.82
3.81
3.81
3.80
3.61
1.55
1.54
1.50
Bn2N
4.57
O
O
1H NMR (400 MHz, CDCl3)
3.92
7.24
1.98
1.04
2.00
2.04
4.00
4.22
5.81
f1 (ppm)

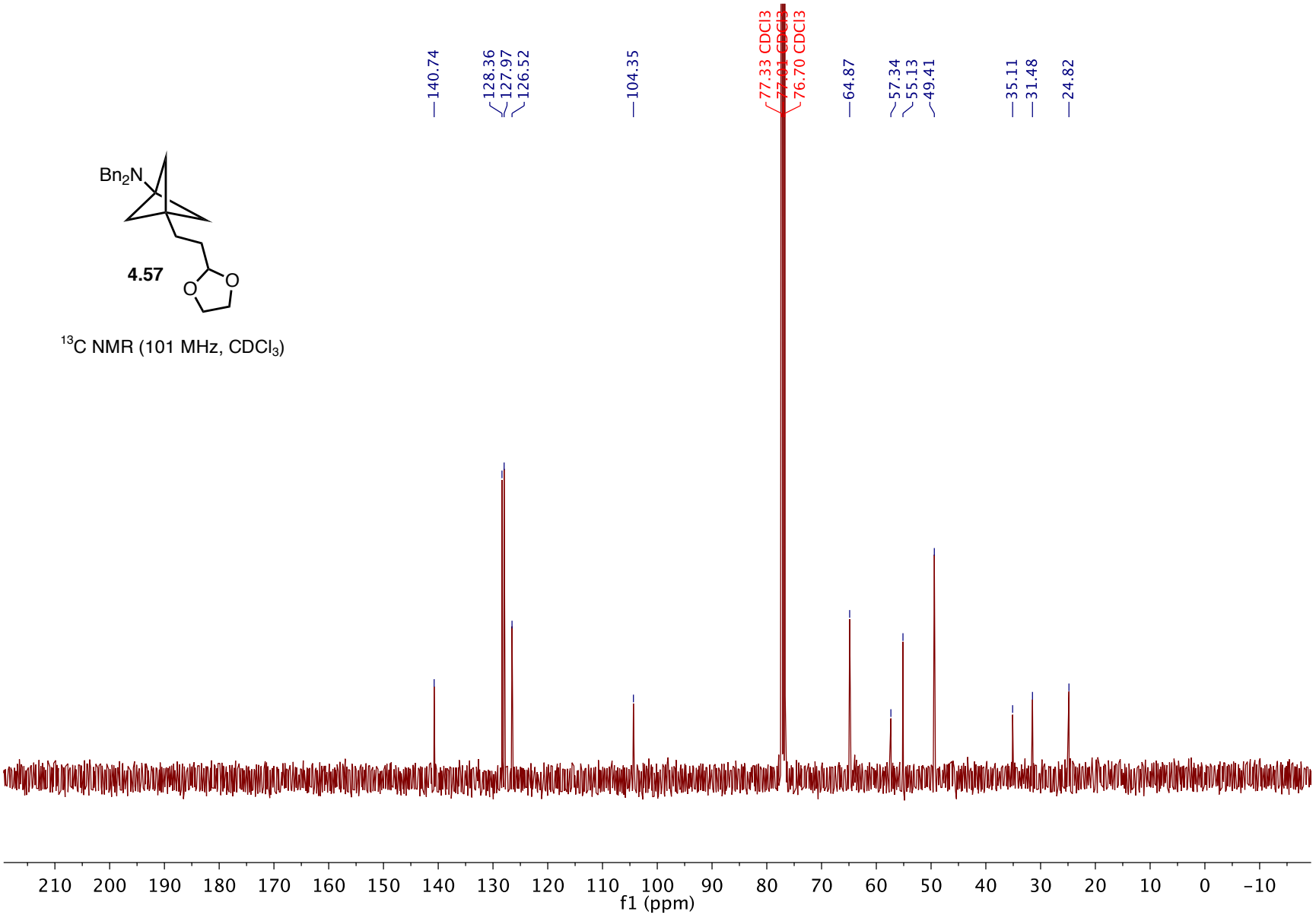
Bn2N
4.57
O
O
13C NMR (101 MHz, CDCl3)
140.74
128.36
127.97
126.52
104.35
77.33 CDCl3
77.01 CDCl3
76.70 CDCl3
64.87
57.34
55.13
49.41
35.11
31.48
24.82
210 200 190 180 170 160 150 140 130 120 110 100 90 80 70 60 50 40 30 20 10 0 -10
f1 (ppm)